

COPPER(I) CATALYZED EXO-SELECTIVE
[CN+C+CC] 1,3-DIPOLAR CYCLOADDITIONS
and
STUDIES TOWARDS THE TOTAL
SYNTHESIS OF KAITOCEPHALIN

by
JIEYU HU

Submitted in partial fulfillment of the requirements
for the degree of Doctor of Philosophy

Thesis Adviser: Prof. Anthony J. Pearson

Department of Chemistry
CASE WESTERN RESERVE UNIVERSITY

May 2010

CASE WESTERN RESERVE UNIVERSITY
SCHOOL OF GRADUATE STUDIES

We hereby approve the thesis/dissertation of

Jieyu Hu

candidate for the Doctor of Philosophy degree *.

(signed) John D. Protasiewicz
(chair of the committee)

Anthony J. Pearson

Gregory P. Tochtrop

Geneviève Sauvé

Yanming Wang

(date) March 15th 2010

*We also certify that written approval has been obtained for any proprietary material contained therein.

Contents

Contents	i
List of Tables	vi
List of Figures	vii
List of Schemes	ix
Acknowledgements	xv
Abbreviations and Nomenclature	xvii
Abstract	xxi
Section A	1
Chapter 1 Introduction to 1,3-Dipolar Cycloadditions	1
1.1 Copper(I) + Ligand – Directing the Stereoselectivity	1
1.2 Limitations of the Known Catalytic System	8
1.3 Our Approach	8
Chapter 2 [CN+C+CC] 1,3-Dipolar Cycloadditions	10
2.1 Initial Studies of the Catalytic System	10
2.1.1 Silver Catalysts	10
2.1.2 Copper Catalysts	11
2.2 Optimization of Reaction Conditions	13
2.2.1 Copper Catalyst Precursors	13
2.2.2 Best ratio between Cu(I) and dppf	15
2.2.3 Solvent and Temperature Selection	17
2.2.4 Catalyst Ligand	20
2.2.5 Preformation of the Imine	22
2.2.6 Reaction Time	23
2.2.7 Optimized Conditions	24
2.3 Exploring the Scope of the Cu(I)–Ligand Catalytic System	24
2.3.1 Asymmetric Dipolarophiles	24
2.3.2 Selectivity – Cu(I) vs. Ag(I)	26
2.3.3 Aldehyde Substrates	28
2.3.4 Configuration Assignment	29
2.4 Mechanism ⁴⁰	31
2.5 Applications	32
2.5.1 Synthesis of Multisubstituted Pyrrolidines	33
2.5.2 Disubstituted Pyrrolidines with Alternative Stereochemistry	34

2.5.3	Kaitocephalin Intermediates	35
2.6	Summary.....	37
2.7	Proposed Future Work.....	38
Chapter 3	Experimental	40
3.1	General Methods	40
3.2	Exo-Products	41
3.2.1	Reaction Procedures	41
3.2.2	Characterization of Compounds	42
3.3	Endo-Products	56
3.3.1	Reaction Procedures	56
3.3.2	Characterization of Compounds	56
Section B	61
Chapter 4	Introduction to Kaitocephalin	61
4.1	Biological Background.....	61
4.2	Characterization.....	62
4.3	Total Synthesis	64
4.3.1	Ma's Synthesis of (2 <i>S</i>)-Kaitocephalin.....	65
4.3.2	Kitahara's Synthesis of (2 <i>R</i>)-Kaitocephalin.....	68
4.3.3	Ohfuné's Synthesis of (2 <i>R</i>)-Kaitocephalin.....	70
4.3.4	Chamberlin's Synthesis of (2 <i>R</i>)-Kaitocephalin.....	74
4.3.5	Total Synthesis Summary	80
4.4	Summary.....	84
Chapter 5	Synthetic Analysis	85
5.1	Synthetic Planning.....	85
5.1.1	Electron Withdrawing Group Choice	86
5.1.2	The N-Acylalanine Moiety (C8-C10).....	88
5.1.3	Introduction of the C1-C3 Moiety	92
5.2	Evaluation of the Synthetic Route	95
5.2.1	Pyrrolidine Core with Stereochemical Diversity.....	95
5.2.2	Short route to C8-C10 moiety.....	97
5.3	Conclusions	98
Chapter 6	Aldehyde Formation	99
6.1	Retrosynthesis.....	99
6.2	Oxazolidine Formation from an Amide-Diol.....	100
6.2.1	A Specifically Protected Hydroxybenzoic Acid.....	101
6.2.2	N-Acyl Diol	102
6.2.3	Attempted Oxazolidine Preparation	103

6.2.4	Differential Protection	108
6.2.5	Aldehyde Formation	109
6.3	Oxazolidine Formation Followed by N-Acylation	110
6.3.1	Amino-Diol Synthesis	110
6.3.2	Cyclization to Oxazolidine	111
6.3.3	Acylation of Oxazolidine	116
6.3.4	Selective Ester Hydrolysis	122
6.3.5	Summary	124
6.4	A Fluorinated Alternative	124
Chapter 7	Cycloaddition	126
7.1	Catalytic Conditions	126
7.1.1	Exo or Endo Cycloadduct for Desulfonylation?	126
7.1.2	Comparing Reactivity	128
7.1.3	Cycloaddition Using Real Intermediates	129
7.1.4	Other Cycloadducts	132
7.2	Epimerization Experiment	134
7.3	Stereocontrol in Cycloaddition	135
7.4	Taking the Cycloaddition Product Towards Kaitocephalin	137
7.4.1	Aldol Reaction – With or Without Sultam?	138
7.4.2	Simultaneous Sultam Removal and Desulfonylation	139
7.4.3	Regioselective Influence of the Sulfone	141
7.4.4	Summary	142
Chapter 8	Sultam Removal	143
8.1	Literature	143
8.2	Basic Hydrolysis (Lithium Hydroxide)	144
8.3	Thiolate Mediate Cleavage	146
8.4	Titanate Mediate Cleavage	148
8.5	Reductive Cleavage	148
8.6	Base Catalyzed Cleavage Revisited (Methanolysis)	149
8.6.1	Magnesium Methoxide Mediation	149
8.6.2	Sodium Methoxide Mediation	151
Chapter 9	Desulfonylation	152
9.1	Literature	152
9.2	Unwanted Side Reactions	153
9.3	Sodium Amalgam Reductions	154
9.3.1	Initial tests	154
9.3.2	Model Compounds	155

9.3.3	Desulfonylation Conditions	156
9.3.4	Functional Group Stability	159
9.3.5	Testing on Real Intermediates	160
9.4	Alternative Reducing Conditions	161
9.4.1	Magnesium	162
9.4.2	Nickel – Aluminum	162
9.4.3	Samarium Iodide.....	163
9.5	Functional Group Stability to Samarium Iodide	165
9.5.1	Model Compound Testing	165
9.5.2	Real Intermediate Testing.....	166
9.5.3	Samarium Iodide Issues	167
9.5.4	Proposed Mechanism of Byproduct Formation	168
9.6	Alternative Protection Strategy	170
9.6.1	Model Compound Stability Testing.....	170
9.6.2	Testing with Real Substrates	170
9.6.3	Cbz Protection and SmI ₂	171
9.7	Alternative Sulfones	172
Chapter 10	Addition of C1-C3	173
10.1	Aldol Condensation	173
10.1.1	Stereochemistry – Ma and Chamberlin	173
10.1.2	Kitahara – Seebach’s Lactone	175
10.1.3	Reaction with <i>S</i> -Garner Aldehyde	176
10.1.4	Preferential Enolate Formation.....	178
10.2	Acylation	179
10.2.1	Acylation Reagent Synthesis	180
10.2.2	Model Reactions	180
10.2.3	Live Testing	181
10.2.4	Further Development.....	182
10.3	Alternative Synthetic Route	183
10.3.1	Lactone Preparation	184
10.3.2	Deprotection and Analysis.....	186
10.3.3	Summary	187
10.4	Proposed Future Work.....	188
Chapter 11	Experimental	191
11.1	General Methods	191
11.2	Reaction Procedures and Characterization.....	192
Appendix A	230

Appendix B	268
Bibliography	333

List of Tables

Table 1.1 Cycloaddition with different combinations of copper catalyst and dipolarophiles. ^a	7
Table 2.1 CuI / dppf (10 mol%) catalyzed cycloaddition in the different solvent.....	12
Table 2.2 Effect of copper precursors on cycloaddition. ^a	15
Table 2.3 Effect of ligand/metal ratio on cycloaddition. ^a	16
Table 2.4 Cu(I) / dppf (5 mol%) catalyzed cycloaddition ^a in the different solvents.	18
Table 2.5 Different ligands were investigated in the Cu(I) catalyzed cycloaddition. ^a	20
Table 2.6. Endo/exo selectivity in two catalytic systems with various dipolarophiles. ^a	27
Table 4.1 Comparison of ¹ H NMR spectral data of stereoisomers of kaitocephalin.	63
Table 4.2 Reported total syntheses of kaitocephalin and C2-epi-kaitocephalin	65
Table 6.1 Different cyclization conditions.....	113
Table 6.2 Different acylation conditions.	117
Table 7.1 NOE analysis of the endo-cycloadduct 7-14	131
Table 7.2 NOE analysis of the exo-cycloadduct 7-15	131
Table 8.1 NOE results of methanolysis product.	150
Table 9.1 Desulfonylation of model compound 7-2 using SmI ₂	164
Table 10.1 Aldol condensation between thioester 10-54 and aldehyde 10-18.	185

List of Figures

Figure 1.1 Transition states proposed to account for exo selectivity.....	2
Figure 1.2 Ligand library.....	6
Figure 1.3 Dipolarophile library.....	7
Figure 1.4 A model for chiral auxiliary-controlled facial selectivity and ligand controlled exo-selectivity.....	9
Figure 2.1 Ligands proposed for future testing.....	21
Figure 2.2 Cu(I)-Catalyzed enantioselective cycloaddition with various dipolarophiles.....	25
Figure 2.3 Variation of aldehyde for the cycloaddition with <i>tert</i> -butyl acrylate.....	28
Figure 2.4 X-ray crystal structure of adduct 2-30	30
Figure 2.5 X-ray crystal structure of the adduct formed from reaction with methyl acrylate.....	30
Figure 3.1 Substructure models indicating numbering and labelling used.....	41
Figure 4.1 The molecular structure of kaitocephalin.....	62
Figure 4.2 Compound 4-2 (left) a lactam derivative of 4-1 , and compound 4-3 (right) an MTPA ester of lactam 4-2	62
Figure 4.3 C2-epi-kaitocephalin 4-4 (left) and a protected derivative 4-5 (right).....	63
Figure 5.1 Candidates for “C” partner in [CN+C+CC] 1,3-dipolar cycloadditions.....	89
Figure 6.1 Aldehyde as a sub-component precursor of kaitocephalin.....	99
Figure 6.2 Approaches to oxazolidine aldehyde.....	100
Figure 6.3 NMR coupling constant evaluation for 6-34	115
Figure 6.4 By-products from the acylation reaction.....	118
Figure 7.1 Model compounds made by [CN+C+CC] 1,3-dipolar cycloadditions.....	132
Figure 7.2 X-ray crystal structure of adduct 2-14	135
Figure 7.3 X-ray crystal structure of adduct 2-30	136
Figure 7.4 Dipole and dipolarophile intermediates.....	136

Figure 7.5. The sulfonyl group shielding the Si face of the enolate 7-47	139
Figure 9.1 Model compounds for testing the effects of desulfonylation conditions.....	155
Figure 9.2 Real intermediates as substrates for testing the effects of desulfonylation conditions.....	161
Figure 10.1 Stereochemistry assignment of the compounds of mixture 10-58 / 10-59	187

List of Schemes

Scheme 1.1 Cu(II) / BINAP and Cu(II) / SEGPHOS catalyzed exo-selective azomethine ylide cycloadditions.	2
Scheme 1.2 CuClO ₄ / N,P ligand -catalyzed exo selective azomethine ylide cycloadditions.	3
Scheme 1.3 Cu(I) / N,P ligand -catalyzed azomethine ylide cycloadditions with nitroalkenes.	4
Scheme 1.4 Cu(I) -catalyzed exo-selective azomethine ylide cycloadditions with phenyl vinyl sulfone.	5
Scheme 2.1 Ag(I) and Ag(I) / dppf catalyzed [CN+C+CC] reactions.	11
Scheme 2.2 CuI / dppf (10 mol%) catalyzed [CN+C+CC] reaction.	11
Scheme 2.3 Comparison of cycloadduct formation with and without base.	13
Scheme 2.4 The cycloaddition was performed with preformed imine.	23
Scheme 2.5 CuX / dppf (5 mol%) catalyzed [CN+C+CC] reaction.	23
Scheme 2.6 Formation of the N-tosyl derivative of 2-28	29
Scheme 2.7. Dual mechanistic rationale for exo-selective asymmetric [CN+C+CC] coupling (Y = H or EWG).	32
Scheme 2.8 Cycloadducts prepared under different combination of auxiliary and catalyst.	33
Scheme 2.9 Disubstituted pyrrolidines prepared by removal of the EWG after ring formation.	34
Scheme 2.10 C2-epimer formation.	34
Scheme 2.11 Route to four isomers of 2,5 disubstituted pyrrolidines.	35
Scheme 2.12 A key intermediate of kaitocephalin can be prepared via one pot reaction.	36
Scheme 2.13 Potential for conversion to aldehyde.	36
Scheme 2.14 A possible route to a key intermediate of kaitocephalin in Chamberlin's synthesis. ³⁷	37
Scheme 2.15 Target directed cycloaddition.	39
Scheme 2.16. Possible synthesis of chiral substituted serine derived from azomethine ylide.	39

Scheme 4.1 Ma's retrosynthetic analysis of kaitocephalin.....	66
Scheme 4.2 Ma's synthesis of kaitocephalin.....	67
Scheme 4.3 Kitahara's retrosynthetic analysis of kaitocephalin.....	68
Scheme 4.4 Kitahara's synthesis of kaitocephalin.....	70
Scheme 4.5 Ohfuné's retrosynthetic analysis of kaitocephalin.....	71
Scheme 4.6 Ohfuné's synthesis of kaitocephalin.....	73
Scheme 4.7 Chamberlin's retrosynthetic analysis of kaitocephalin.....	74
Scheme 4.8 Chamberlin's synthesis of intermediate 4-40	75
Scheme 4.9 Aldol reaction of pyrrolidine trans- 4-40 with Garner's aldehydes.....	76
Scheme 4.10 Model reactions for the formation and hydrogenation of pyrrolidine dehydroamino esters.....	77
Scheme 4.11 Chamberlin's synthesis of kaitocephalin.....	79
Scheme 4.12 Construction of the substituted 4 <i>R</i> ,7 <i>R</i> -pyrrolidine core.....	81
Scheme 4.13 Incorporation of the hydroxyl group at C3.....	82
Scheme 4.14 Construction of the C8-C10 moiety.....	83
Scheme 4.15 Metal catalyzed one pot 1,3-dipolar cycloaddition.....	84
Scheme 5.1 Retrosynthetic analysis of kaitocephalin.....	86
Scheme 5.2 Cycloaddition with three EWG-based olefins.....	87
Scheme 5.3 Sulfone removal.....	88
Scheme 5.4 Aldol condensation precursor formation.....	89
Scheme 5.5 Possible sultam removal conditions.....	90
Scheme 5.6 Alternative methods to the introduce aryl chloride subunit.....	91
Scheme 5.7 Concomitant double deprotection followed by introduction of the desired group.....	91
Scheme 5.8 Proposed strategy for the introduction of the C1-C3 moiety.....	93
Scheme 5.9 Preparation of model compound 5-40	94

Scheme 5.10 Unsuccessful attempt to make a 2,2,4,5-tetrasubstituted pyrrolidine in one pot	94
Scheme 5.11 Construction of 5-39 an alternative precursor of tri-substituted pyrrolidines 5-33 ..	95
Scheme 5.12 Construction of the tri-substituted pyrrolidine core.	96
Scheme 5.13 Construction of the N-acylalanine moiety from different precursors.....	97
Scheme 5.14 C9-epi-kaitocephalin formation.	98
Scheme 5.15 Planned synthesis of kaitocephalin.....	98
Scheme 6.1 Synthetic plan from aminodiols to oxazolidine-alcohol.	101
Scheme 6.2 Synthesis of a specifically protected hydroxybenzoic acid.....	101
Scheme 6.3 N-Acyl diol formation.	103
Scheme 6.4 Attempted oxazolidine formation.....	104
Scheme 6.5 Mechanism for cyclizing of amino-1,4-diol.	104
Scheme 6.6 Conversion between five- and seven-membered ketal.	106
Scheme 6.7 The formation of model compound N-Cbz diol.	106
Scheme 6.8 Cyclizing of N-Cbz diol with DMP.	107
Scheme 6.9 Synthesis of oxazolidine aldehyde from N-acyl diol.	108
Scheme 6.10 Alternative method to prepared mono alcohol.	109
Scheme 6.11 Oxidation to the aldehyde.	109
Scheme 6.12 Synthetic plan from amino-diol to oxazolidine-alcohol.	110
Scheme 6.13 Preparation of 2-amino-1,4-butanediol 6-35	111
Scheme 6.14 Cyclizing from amino-diol.	111
Scheme 6.15 Acylation of the oxazolidine.	116
Scheme 6.16 Transformations from di-acyl oxazolidine 6-40	119
Scheme 6.17 Acylation of amino-diol.	120
Scheme 6.18 Control experiment showed no ring-opening product using TEA.	120

Scheme 6.19 Conversion of N,O-di-acyl oxazolidine 6-40 to N-acyl oxazolidine 6-16 with apparent yields.	123
Scheme 6.20 Acid catalysed ring opening and exchange.	123
Scheme 6.21 Synthetic routes to N-acyl oxazolidine 6-2	124
Scheme 6.22 Formation of new oxazolidine alcohol 6-48	125
Scheme 7.1. A 1,3-dipolar cycloaddition involving aldehyde 5-2 , sulfone 5-3 and sultam 4-80	126
Scheme 7.2 Model desulfonylation reactions.	127
Scheme 7.3 Cycloadducts as precursors for enolate 7-9	128
Scheme 7.4 Cycloaddition of model compounds under different conditions.	129
Scheme 7.5 Cycloaddition using oxazolidine 5-2 under different conditions.	130
Scheme 7.6 Boc protection of the endo-cycloadduct.	132
Scheme 7.7 Synthesis of an N-Cbz based cycloadduct.	133
Scheme 7.8 Synthesis of cycloadduct 7-18 bearing an aminoester group.	134
Scheme 7.9 Control experiment to test for C4 epimerization of cycloadducts.	135
Scheme 7.10 Possible transformations towards kaitocephalin from cycloadducts 7-1 and 7-16	138
Scheme 7.11 Testing for one pot removal of sulfone and sultam.	140
Scheme 7.12 Testing for one pot removal of sulfone and sultam with Boc protected substrate.	140
Scheme 7.13 Testing for one pot removal of sulfone and sultam with Boc protected substrate.	141
Scheme 7.14 Sequence towards kaitocephalin following pyrrolidine ring formation.	142
Scheme 8.1 Methods for removal of the sultam protecting group.	143
Scheme 8.2 Hydrolytic cleavage of auxiliary from a model compound.	145
Scheme 8.3 No sultam cleavage using lithium hydroxide.	146
Scheme 8.4 Thiolate mediate sultam removal.	147
Scheme 8.5 No sultam cleavage using titanium isopropoxide.	148
Scheme 8.6 Sultam removal under reductive conditions followed by conversion to an ester.	148

Scheme 8.7 Reductive sultam ring opening.....	149
Scheme 8.8 Sultam removal by magnesium methoxide.	149
Scheme 8.9 Magnesium methoxide mediated methanolysis of the model compound.....	150
Scheme 8.10 N-Boc protection of the methyl ester product after sultam removal.	151
Scheme 8.11 Sultam removal failure using sodium methoxide mediated methanolysis.	151
Scheme 9.1 Sulfone removal may lead to unwanted side reactions.....	153
Scheme 9.2 Desulfonylation of thiolate ester 8-16	154
Scheme 9.3 The preparation of model compound sulfone 7-2	156
Scheme 9.4 The preparation of model compound 6-33	156
Scheme 9.5 Desulfonylation of 7-2 using sodium-mercury amalgam.	157
Scheme 9.6 Carretero's desulfonylation.	157
Scheme 9.7 Possible mechanism for desulfonylation.....	158
Scheme 9.8 Desulfonylation conditions tested on 6-13 with production of unwanted side-products.....	159
Scheme 9.9 Mg mediated desulfonylation.....	162
Scheme 9.10 Attempted desulfonylation using Ni-Al-EtOH showing possible by-products.	163
Scheme 9.11 Attempted desulfonylation using Ni-Al-EtOH.....	163
Scheme 9.12 Desulfonylation using samarium iodide.	164
Scheme 9.13 Stability of model compound 6-33 to SmI ₂	165
Scheme 9.14 Stability of real intermediate 8-30 to SmI ₂	166
Scheme 9.15 Conversion of 9-20 to 8-30	167
Scheme 9.16 Possible mechanism for the formation of by-product alcohol 9-20	169
Scheme 9.17 Model reaction testing Cbz protected amine stability to Na-Hg reduction.	170
Scheme 9.18 Real reaction testing Cbz protected amine stability to Na-Hg reduction.	171
Scheme 9.19 Alternative approach to disubstituted pyrrolidines using different sulfones.....	172

Scheme 10.1 Insertion of C1-C3 in the synthesis of kaitocephalin using <i>S</i> -Garner aldehyde.....	173
Scheme 10.2 Aldol condensation of <i>R</i> -Garner aldehyde in the synthesis of kaitocephalin.....	174
Scheme 10.3 An aldol reaction with <i>R</i> -Garner aldehyde via a possible transition state.....	175
Scheme 10.4 Kitahara's aldol reaction of Seebach's lactone with modified <i>R</i> -Garner aldehyde.	175
Scheme 10.5 Kitahara's aldol reaction of Seebach's lactone with modified <i>S</i> -Garner aldehyde.	176
Scheme 10.6 Aldol condensation between substituted pyrrolidine 10-7 and <i>S</i> -Garner aldehyde.	177
Scheme 10.7 Aldol reactions with <i>S</i> -Garner aldehydes via possible transition states.	178
Scheme 10.8. Alternative route to the C3 <i>S</i> -isomer via E-enolate mediated aldol condensation.	178
Scheme 10.9 Preferential formation of E or Z enolates.	179
Scheme 10.10 Two approaches to the 3 <i>S</i> -isomer.	179
Scheme 10.11 Synthesis of acylation reagent 10-39	180
Scheme 10.12 Attempted acylation of model compound 10-40	181
Scheme 10.13 Using acylation to introduce the C1-C3 moiety.....	181
Scheme 10.14 Continuation to kaitocephalin.	183
Scheme 10.15 Alternative synthetic plan.....	184
Scheme 10.16 Synthesis of model compound 10-54	184
Scheme 10.17 Attempted one pot lactone formation.....	185
Scheme 10.18 Dioxane formation for stereo-identification.....	186
Scheme 10.19 Alternative synthetic plan.....	188
Scheme 10.20 Proposed retrosynthesis of lactam 10-60	189
Scheme 10.21 Alternative synthetic plan via intramolecular 1,3-dipolar cycloaddition.	189
Scheme 10.22 Alternative synthesis of disubstituted pyrrolidine 10-77	190

Acknowledgements

I'd like to thank anyone who has helped in any way with the research for and writing of this thesis. There are some people who deserve special mention.

Special thanks go to Dr. Anthony Pearson for his willingness to serve as my thesis adviser and to Dr. Barkley and Dr. Protasiewicz for their support for my Ph.D. defence.

To Dr. Garner, without whom none of this would be possible: I would like to record my gratitude for your several years' supervision, advice, guidance, and encouragement. Under your strict and systematic training, my work habit changed from "work hard" to "work smart, work carefully," which is useful in my whole life. I highly appreciate your giving me the opportunity to do total synthesis.

From my heart, I must thank my former committee chair Dr. Sayre. Thank you very much for your concern about my studies, project progress, and graduation. I wish Dr. Sayre be joyful forever in Heaven.

I would also like to thank all the members of my committee for agreeing to serve and for reviewing my thesis.

Many thanks to all the technical staff including Dr. Greg Helms, Dr. Bill, and Dr. Dale Ray for training me to use NMR instruments, James Faulk and Chongjie Zhu for the mass spectra, and Dr. Wiley Young's group for x-ray. Thanks also to Professor Rob Ronald for training me to use the optical rotation measuring instrument at WSU.

I would like to express my great appreciation to Dr. James Matthews. Thank you very much for your great help in proof reading my thesis. Thank you very much for your great help in proof reading my thesis and for the patient correction of my writing and page layout.

To all members of the Garner group, past and present: I really would like to thank them all for making my time in the group an interesting and enjoyable one. Special mentions must go to Chung-Min Park for being there both as a friend and comrade. A special mention for Özge for your getting me started when I first arrived in the lab; Nathan and Alper for being nice friends who brought happiness and laughter; Chris, Morgan and Regis for their technical assistance; Ümit and Valerie for the happy times we worked together in the lab.

Many thanks to Huanfeng, Wei Li, Yuming, and Shengying for your constant encouragement in my studies and life.

I would also like to thank the management within Organic Technologies at Corning Incorporated, including Dr. Glasgow, Dr. Winningham, Dr. Leslie and Dr. He, for their strong support for my Ph.D. defence.

Finally my deepest thanks are given to my family members, thanks for all your support throughout my education. Whenever and wherever, you are always standing behind me.

Thanks to my husband Songbo for your taking care of me. To me, you are like my “Friday” on a desert island.

Abbreviations and Nomenclature

Ac	acetyl
aq	aqueous
Ar	aryl
AIBN	2,2'-azobis(2-methylpropionitrile)
Boc	<i>tert</i> -butoxycarbonyl
Bz	benzoyl
Cal	calculated
Cbz	benzyloxycarbonyl
CAN	ceric ammonium nitrate
COSY	correlation spectroscopy
DBU	1,8-diazabicyclo[5.4.0]undec-7-ene
DCC	dicyclohexylcarbodiimide
DCM	dichloromethane
DDQ	2,3-dicyano-5,6-dichloro-parabenzoquinone
DIBAL-H	diisobutylaluminiumhydride
DMAP	4-dimethylaminopyridine
DMF	<i>N,N</i> -dimethylformamide
DMSO	dimethyl sulfoxide
DMP	Dess-Martin periodinane
dr	diastereomeric ratio
EDCI	1-ethyl-3-(3-dimethylaminopropyl)carbodiimide
ee	enantiomeric excess

EI	electron impact (ionization)
Equiv	equivalent
ESI	electrospray ionization
Et	ethyl
FAB	fast atom bombardment (in mass spectrometry)
HRMS	high resolution mass spectrum
h	hour(s)
HMPA	hexamethylphosphoramide
HMQC	heteronuclear multiple-quantum correlation
HWE	Horner–Wadsworth–Emmons
Hz	hertz
J	coupling constant (in NMR)
L	ligand
L*	chiral ligand
LAH	lithium aluminum hydride
LG	leaving group
LDA	lithium diisopropylamide
LHMDS	lithium hexamethyldisilazide
M	mol dm ⁻³
MALDI-ToF	matrix-assisted laser desorption ionization – time of flight
Me	methyl
min	minute(s)
mol	mole(s)

mmol	millimole(s)
μmol	micromole(s)
molec.	molecules
m.p.	melting point range
MS	molecular sieves
Ms	methanesulfonyl
NBS	<i>N</i> -bromosuccinimide
NMO	<i>N</i> -methylmorpholine- <i>N</i> -oxide
NMR	nuclear magnetic resonance
	br broad
	d doublet
	dt double triplet
	s singlet
	t triplet
	tq triple quartet
	tt triple triplet
NOE	nuclear overhauser effect
NOESY	nuclear overhauser enhancement spectroscopy
Nu ⁻	nucleophile
PCC	pyridinium chlorochromate
PE	petroleum ether
Ph	phenyl
PMB	<i>p</i> -methoxybenzyl

PPTS	pyridinium <i>p</i> -toluenesulfonate
pTsOH	<i>p</i> -toluenesulfonic acid
<i>i</i> -Pr	isopropyl
R	alkyl group
R _f	retention factor (in TLC)
sat. (sat'd)	saturated
rt	room temperature
TBAF	tetrabutylammonium fluoride
TBS (TBDMS)	<i>tert</i> -butyldimethylsilyl
TBSCl	<i>tert</i> -butyldimethylsilyl chloride
<i>t</i> -Bu	<i>tert</i> -butyl
TEA	triethylamine
Teoc	trimethylsilyl oxycarbonyl
TFA	trifluoroacetic acid
THF	tetrahydrofuran
TLC	thin layer chromatography
TMS	trimethylsilyl
TS	<i>p</i> -toluenesulfonyl
wt%	weight percent
X ^D	D-sultam
X ^L	L-sultam

Copper(I) Catalyzed Exo-Selective
[CN+C+CC] 1,3-Dipolar Cycloadditions
and
Studies Towards the Total
Synthesis of Kaitocephalin

Abstract

by

JIEYU HU

A novel exo-selective [CN+C+CC] 1,3-dipolar cycloaddition catalyzed by Cu(I)-phosphine ligand complex has been developed for ring formation using a chiral glycylic sultam exerting powerful stereochemical control with an aldehyde and an activated olefin. It is the best exo-selective condition so far reported that is suitable for use with a variety of aliphatic aldehydes. This method has great potential in natural product synthesis for the construction of tri- or tetra-substituted pyrrolidine rings bearing an α -aliphatic chain.

A new synthetic route to kaitocephalin, a glutamate receptor antagonist, has been designed featuring a disubstituted pyrrolidine as the key intermediate. An auxiliary-controlled [CN+C+CC] 1,3-dipolar cycloaddition followed by removal of auxiliary and sulfone was employed to synthesize 2,5-disubstituted pyrrolidines. The key intermediate disubstituted pyrrolidine was prepared in 10 steps and 4% overall yield. Acylation at C4 introduced the C1-C3 moiety and afforded an important precursor to kaitocephalin bearing a complete carbon skeleton in 8% unoptimized yield.

Section A

1 Introduction to 1,3-Dipolar Cycloadditions

Heterocyclic cores of pyrrolidine and proline are incorporated in many biologically active natural products¹ and organocatalysts.² 1,3-Dipolar cycloaddition of azomethine ylides with olefinic dipolarophiles is an efficient and convergent method for the construction of pyrrolidines.³ So far much attention has been devoted to endo-approach of the dipolarophile to the dipole.⁴ The exo-selective pyrrolidine formation has been relatively less explored. Among those reported results showing exo-selectivity, an amino ester was used for the cycloaddition.⁵

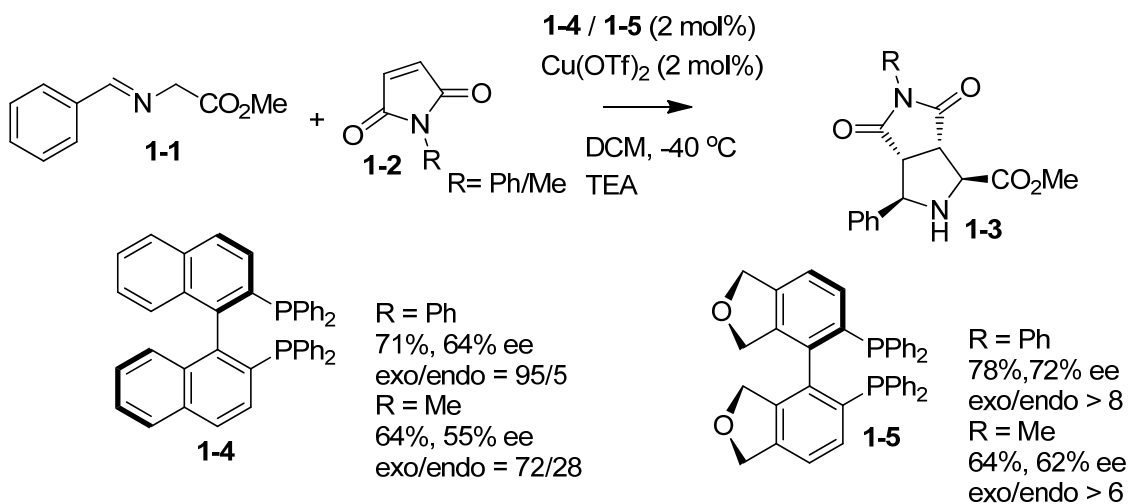
1.1 Copper(I) + Ligand – Directing the Stereoselectivity

It is known that Ag(I)-catalyzed azomethine ylide cycloadditions result in the selective formation of the *endo* pyrrolidine cycloadduct in high enantioselectivity.⁶ In addition, Zn(II)/chiral bis(oxazoline) complexes catalyze 1,3-dipolar cycloadditions with unsaturated aldehydes or acrylates and fumarates, also resulting in the formation of endo-cycloadducts.⁷

It has been reported that the combination of Cu(OTf)₂ and CuX (X = OAc, ClO₄⁻, PF₆⁻) with various bidentate ligands such as P,P-ligands (BINAP, SEGPHOS, ClickFerrophos), P,S-ligands (Fesulphos), N,P-ligands (ferrocene-derived phosphino-oxazoline ligands, Taniaphos) afforded the cycloadducts with middle to high exo-selectivities.⁸

Chapter 1: Introduction to 1,3-Dipolar Cycloadditions

In 2003, Komatsu⁹ reported the first highly exo-selective 1,3-dipolar cycloadditions between iminoesters such as **1-1**, derived from aromatic aldehydes and maleimides (**1-2**) using Cu(OTf)₂ / BINAP or Cu(OTf)₂ / SEGPHOS as the catalyst (Scheme 1.1).



Scheme 1.1 Cu(II) / BINAP and Cu(II) / SEGPHOS catalyzed exo-selective azomethine ylide cycloadditions.

They assumed in situ-generated Cu(II)-dipole complex (**1-4/1-5** + **1-7**) has a square geometry based on the calculation and proposed a transition state (Figure 1.1).

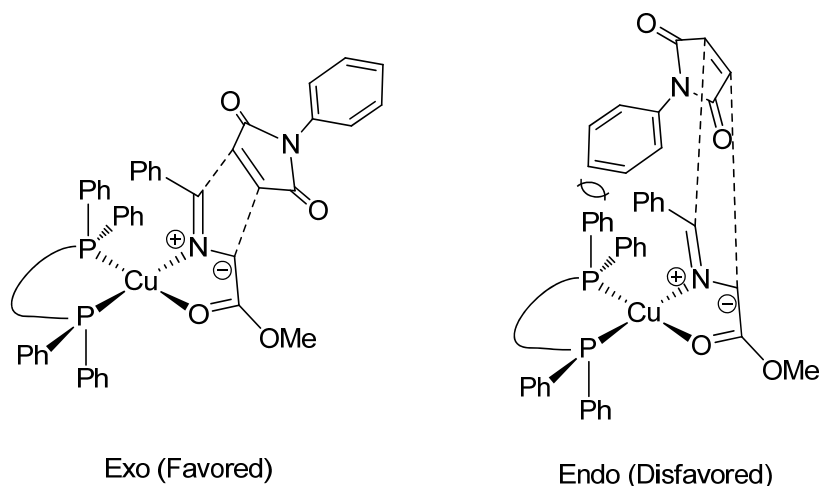
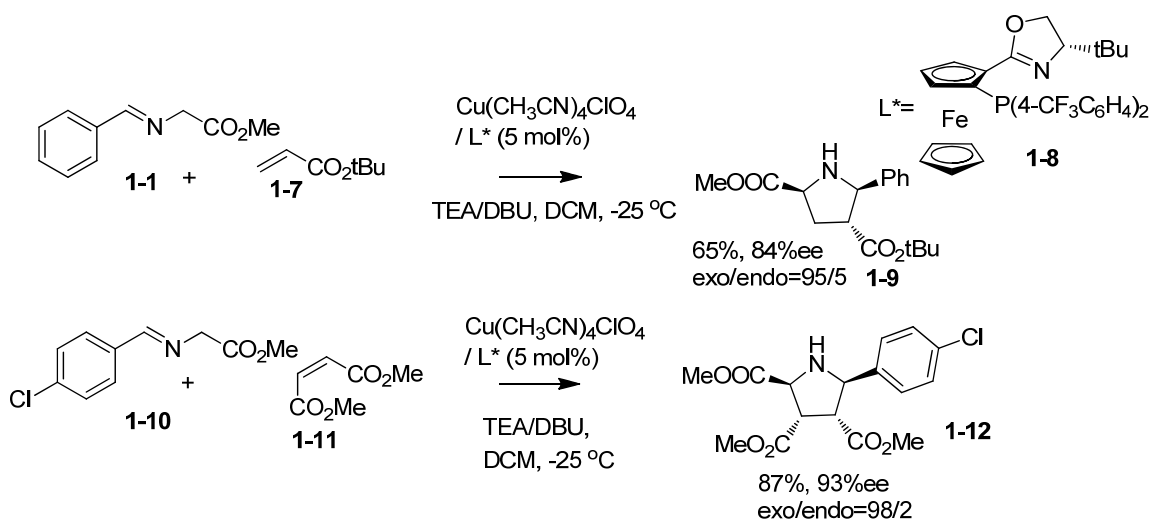


Figure 1.1 Transition states proposed to account for exo selectivity.

Chapter 1: Introduction to 1,3-Dipolar Cycloadditions

The preference for *exo*-cycloaddition was due to the steric repulsion between the *N*-substituent of maleimide **1-2** and the phenyl groups on the phosphorus atom of the chiral ligand (**1-4/1-5**) in the transition state. One drawback is that the *exo:endo* ratios decrease when acyclic dipolarophiles are used.

Zhang's combination of CuClO_4 and the ferrocene-derived phosphino-oxazoline ligand served to effectively address the limitation of Komatsu's low *exo* selectivity when using acyclic dipolarophiles.⁵ The cycloaddition of the azomethine ylide derived from **1-1** with acrylate and maleate dipolarophiles gave the pyrrolidine cycloadducts *exo* **1-9** and **1-12** in good yields with excellent diastereo- and enantio-selectivities (Scheme 1.2).



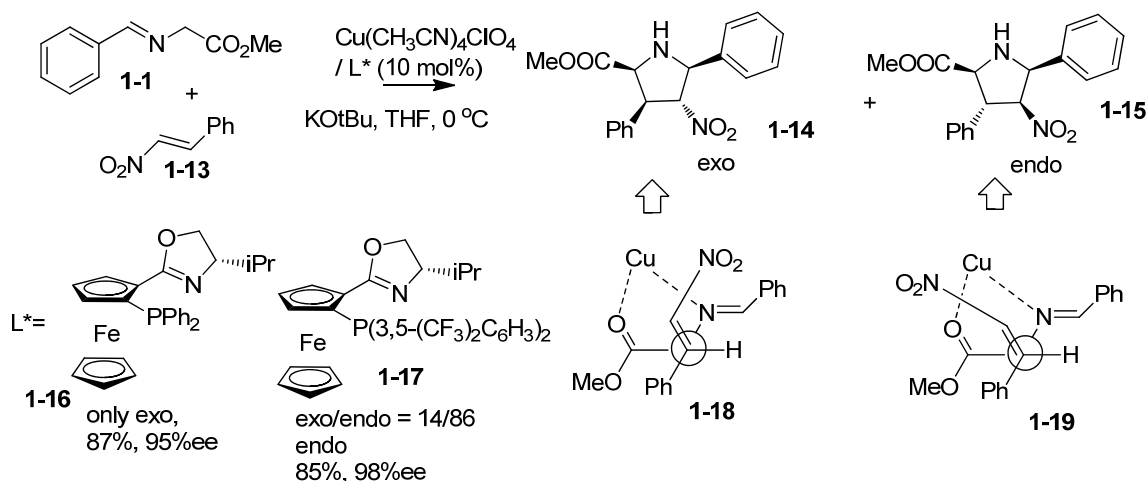
Scheme 1.2 CuClO_4 / N,P ligand -catalyzed *exo* selective azomethine ylide cycloadditions.

This was the first use of a copper(I) salt as the catalyst in the 1,3-dipolar cycloaddition reaction of azomethine ylides. They assumed that the dipole-Cu(I) complex adopted a tetrahedral geometry and the steric repulsion between the electron-withdrawing group of dipolarophiles and the substituent of the ligand governed the *endo/exo*

selectivity. They found that the bulky substituent bonding to the aryl groups of the ligand played an important role in controlling the exo-selectivity.

Interestingly, these reactions took place with excellent endo-selectivity using Zhou's AgOAc / N,P ligand catalyst, with a new N,P ligand formed by replacing *tert*-butyl groups of Zhang's ligand with the benzyl groups.¹⁰ This result indicated that ligands bound to a different metal ion afforded different exo/endo selectivity.

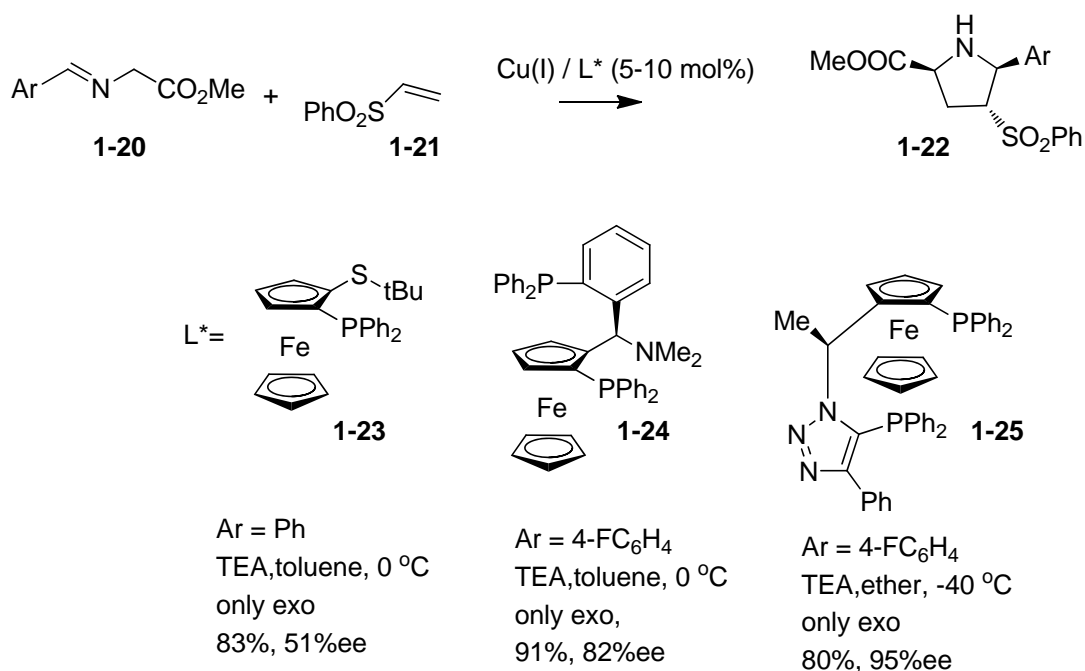
In 2008, Hou and co-workers¹¹ investigated the CuClO₄ / N,P-(ligand bearing ferrocene skeleton)-catalyzed cycloaddition of nitroalkenes such as **1-13**. They found that electron-rich aryl groups on the phosphorus atom (as in **1-16**) favored the exo-adduct, while the electron-deficient aryl group (as in **1-17**) promoted the formation of the endo-stereochemistry. Their results indicated that the electronic properties of ligands could control the endo/exo selectivity. They explained that the repulsion between the electron-rich aryl group on the phosphorus atom and the nitro group favored exo-cycloadduct formation (Scheme 1.3).



Scheme 1.3 Cu(I) / N,P ligand -catalyzed azomethine ylide cycloadditions with nitroalkenes.

Chapter 1: Introduction to 1,3-Dipolar Cycloadditions

Carretero and co-workers reported the first *exo* selective 1,3-dipolar cycloaddition with phenyl vinyl sulfone.¹² They found that the $\text{Cu}(\text{CH}_3\text{CN})_4\text{ClO}_4$ / Fesulphos (**1-23**) - catalyzed cycloaddition of *N*-benzylidene glycine methyl ester **1-20** to afforded *exo*-cycloadduct **1-22** in high yield, but with moderate enantioselectivity (Scheme 1.4).



Scheme 1.4 $\text{Cu}(\text{I})$ -catalyzed *exo*-selective azomethine ylide cycloadditions with phenyl vinyl sulfone.

When switching to the combination of $\text{Cu}(\text{CH}_3\text{CN})_4\text{ClO}_4$ and Taniaphos (**1-24**), *exo*-cycloadduct **1-22** was obtained with a better *exo/endo*- and enantio-selectivity. Recently, Fukuzawa's group¹³ reported that copper(I) / ClickFerrophos catalyzed the same cycloaddition at -40 °C resulting in an increase in ee to 99% with a complete *exo* selectivity. The copper(I) / ClickFerrophos also resulted in the *exo*-cycloadduct when dimethyl maleate and *tert*-butyl acrylate were used as dipolarophiles, but it induced the *endo*-cycloadduct when dimethyl fumarate was used. Similarly, the combination of $\text{Cu}(\text{CH}_3\text{CN})_4\text{ClO}_4$ and Fesulphos **1-23** lead to an *endo*-cycloadduct when utilizing

Chapter 1: Introduction to 1,3-Dipolar Cycloadditions

conjugated carbonyl dipolarophiles such as dimethyl maleate, fumaronitrile, methyl acrylate, and maleimides.

Table 1.1 outlines the results of the copper catalyzed 1,3-dipolar cycloaddition with different ligands (Figure 1.2) and different dipolarophiles (Figure 1.3). It can be seen that the catalyst complex with different ligands chelated to the copper showed different exo/endo selectivity. The same catalyst exhibited different exo/endo selectivity in the 1,3-dipolar cycloaddition with different dipolarophiles.

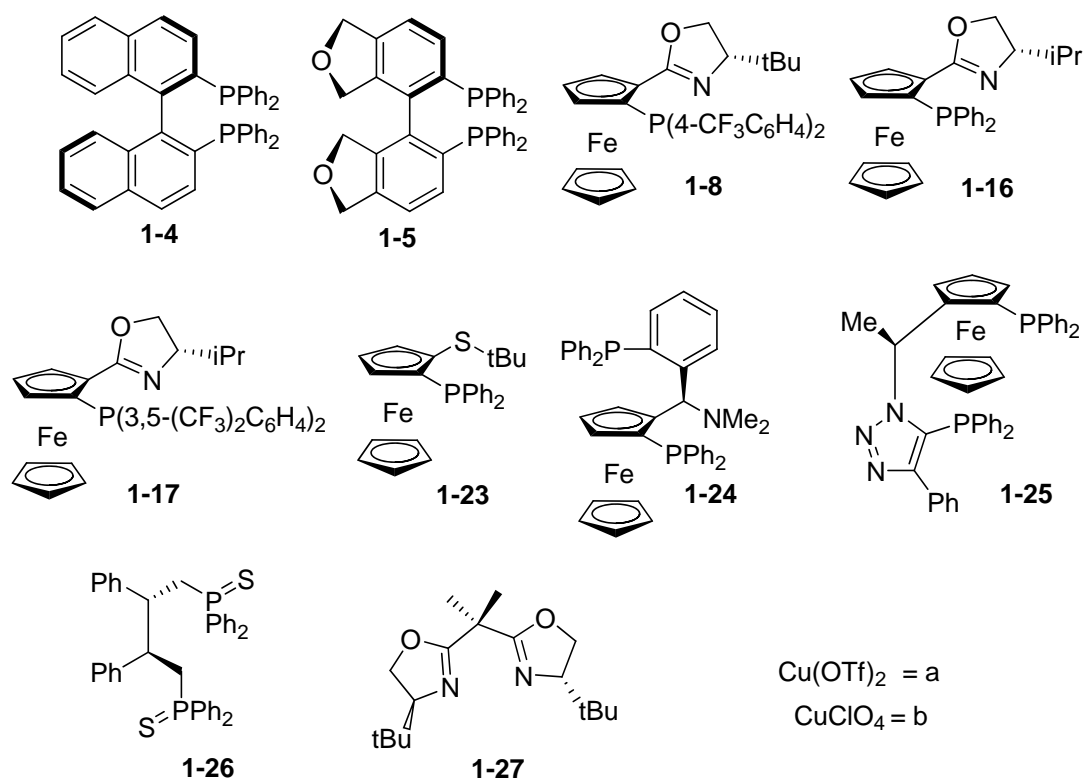


Figure 1.2 Ligand library.¹⁴

Chapter 1: Introduction to 1,3-Dipolar Cycloadditions

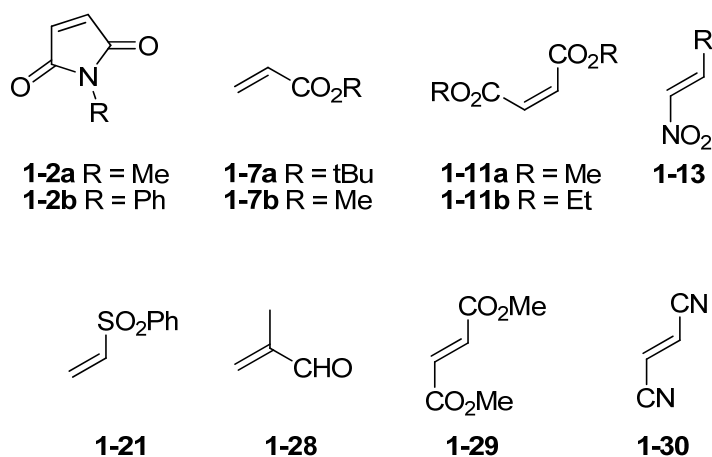


Figure 1.3 Dipolarophile library.

Table 1.1 Cycloaddition with different combinations of copper catalyst and dipolarophiles.^a

	L1-4	L1-5	L1-8	L1-16	L1-17	L1-23	L1-24	L1-25	L1-26 ¹⁵	L1-27
	+ a	+ a	+ b	+ b	+ b	+ b	+ b	+ b	+ b	+ a
1-2a	exo	exo								
1-2b									endo	
1-7a			exo					exo		endo
1-7b							7/3 ^b			
1-11a	endo		exo					exo		
1-11b										
1-13				exo	endo					
1-21						exo	exo	exo		
1-28						endo				
1-29						endo		endo		
1-30		63/37		49/51						

a The major product configuration is listed or the ratio of exo/endo is shown

b CuOAc was used

1.2 Limitations of the Known Catalytic System

The limitations of the above known catalysts used for the asymmetric synthesis of exo cycloadduct lie in the following:

1. A chiral phosphane ligand with a complex structure was used.
2. Only the azomethine ylides derived from aromatic aldehyde were reported and the exo-cycloadduct was given with moderate selectivity.
3. The azomethine ylide was formed from its precursor imine and base was required. (The preparation and isolation of imines especially derived from aliphatic aldehydes is challenging)
4. Most reactions were performed over long reaction times at low temperatures (-45 °C to 0 °C)

1.3 Our Approach

Our efforts were directed at a simple and efficient method for the asymmetric synthesis of pyrrolidines derived from aliphatic or aromatic aldehyde. In Garner's previous Ag catalyzed endo-selective [CN+C+CC] 1,3-dipolar cycloadditions, sultam incorporated into the "CN" partner was demonstrated to control the absolute stereochemistry of the cycloadduct independent of existing chirality.¹⁶

Sultam is an especially attractive auxiliary for testing [CN+C+CC] reactions because:

1. It dominates the diastereofacial selectivity of the 1,3-dipolar cycloaddition, and the opposite stereogenic center adjacent to nitrogen could be generated

Chapter 1: Introduction to 1,3-Dipolar Cycloadditions

employing the opposite stereogenic center adjacent to nitrogen could be generated employing the opposite chirality of the sultam.¹⁷

2. The presence of sulfoxide moiety increases the acidity of the α -H of the intermediate imine, and generates the azomethine ylide using glycylyl sultam. Furthermore, no extra base is needed, which avoids decomposition of the cycloadduct.
3. A side reaction such as Michael addition was avoided due to the low nucleophilicity of the sultam based amine.
4. The Garner group has developed a convenient scale-up synthesis of glycylyl sultam.¹⁸ Furthermore, it was easily prepared, removed and recovered.
5. The sultam moiety can become a new reaction site through chemoselective conversion of the acylsultam moiety.¹⁹

Since use of sultams leads to an excellent diastereocontrol of the stereogenic center adjacent to nitrogen, much attention was devoted to exo-approach of the dipolarophile to the dipole. Based on the analysis of reported results, it was reasoned that repulsion between the functional group on the ligand and an EWG group on the dipolarophile would lead to the exo-product (Figure 1.4).

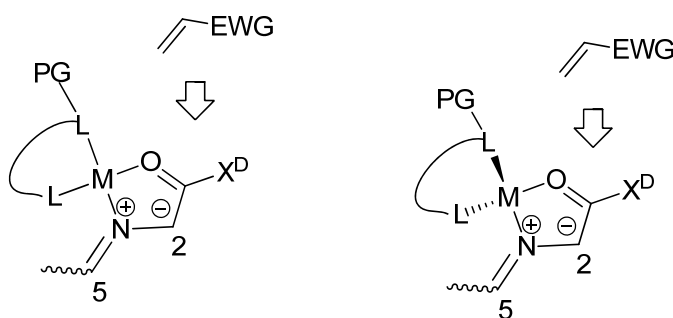


Figure 1.4 A model for chiral auxiliary-controlled facial selectivity and ligand controlled exo-selectivity.

2 [CN+C+CC] 1,3-Dipolar Cycloadditions

Auxiliary controlled 1,3-dipolar cycloadditions with hydrocinnamic aldehyde were carried out to screen the different combinations of metal and ligands. 1.3 Equivalents of Oppolzer's camphor sultam were added because it was used as both auxiliary and catalytic amount of base. 3 Equivalents of dipolarophile were required to inhibit the side reaction of Michael addition between glycyl sultam and the dipolarophile. The reaction was performed in a one pot procedure, and no extra base was utilized.

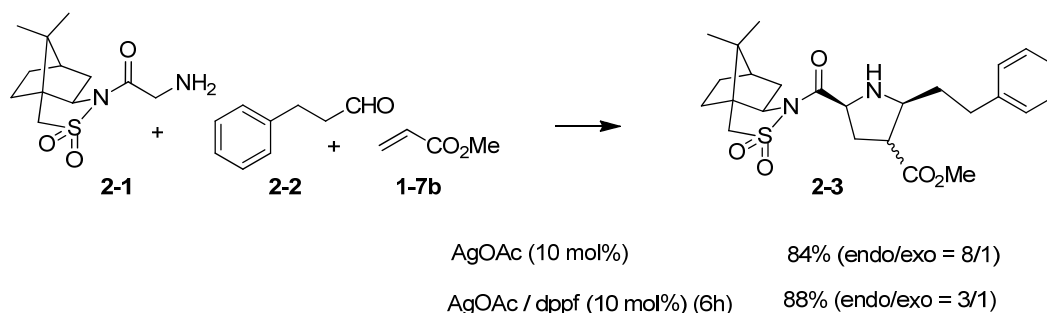
2.1 Initial Studies of the Catalytic System

The [CN+C+CC] reaction system yielded interesting results, which were highly dependent on the catalysts and conditions used.

2.1.1 Silver Catalysts

In previous research,²⁰ it was found that silver catalyzed cycloaddition of hydrocinnamic aldehyde (**2-2**) and methyl acrylate (**1-7b**) in the presence of Oppolzer's chiral glycyl sultam (**2-1**) gave an 8:1 ratio of endo- and exo-cycloadducts (**2-3**). The initial study undertaken was to perform the same [CN+C+CC] reaction employing 5% of AgOAc / dppf as a catalyst. The reaction was complete at room temperature after 6h, and a 3:1 mixture of endo:exo cycloadducts in 88% combined yield was obtained (Scheme 2.1). The initial experiments indicated that the AgOAc / dppf complex results in an increase of the exo/endo ratio of cycloadducts.

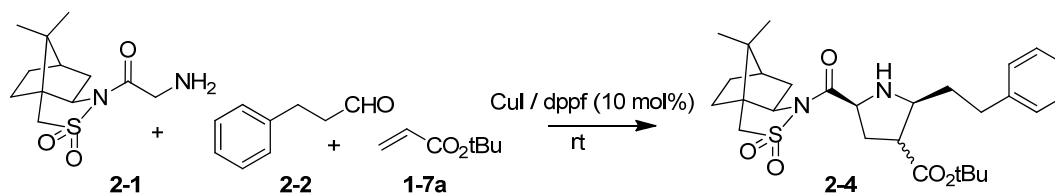
Chapter2: [CN+C+CC] 1,3-Dipolar Cycloadditions



Scheme 2.1 Ag(I) and Ag(I) / dppf catalyzed [CN+C+CC] reactions.

2.1.2 Copper Catalysts

Based on studies of reported result, it was noticed that the high exo-selectivity was achieved only employing copper catalysts. At first, CuI-dppf was used as the catalyst because, being an organic perchlorate-laden salt, $\text{Cu}(\text{MeCN})_4\text{ClO}_4$ is potentially explosive. The catalyst was prepared by stirring a mixture of CuI and dppf in THF at room temperature for 1h. To the heterogeneous catalyst solution, was added hydrocinnamic aldehyde, methyl acrylate and Oppolzer's chiral glycidyl sulfamate (Scheme 2.2). The reaction gave a 1:1 mixture of exo:endo cycloadducts in trace amounts (Table 2.1, Entry 1). Encouraged by the ratio of exo and endo cycloadduct, the reaction was investigated in different solvents (Table 2.1).



Scheme 2.2 CuI / dppf (10 mol%) catalyzed [CN+C+CC] reaction.

Table 2.1 CuI / dppf (10 mol%) catalyzed cycloaddition in the different solvent.

Entry	Solvent	Reaction time	Yield %	exo:endo
1	THF	17h	trace	1:1
2	MeCN	22h	trace	2:1
3	DCM	17h	19	3:1
4	DMSO	7h	24	3:1

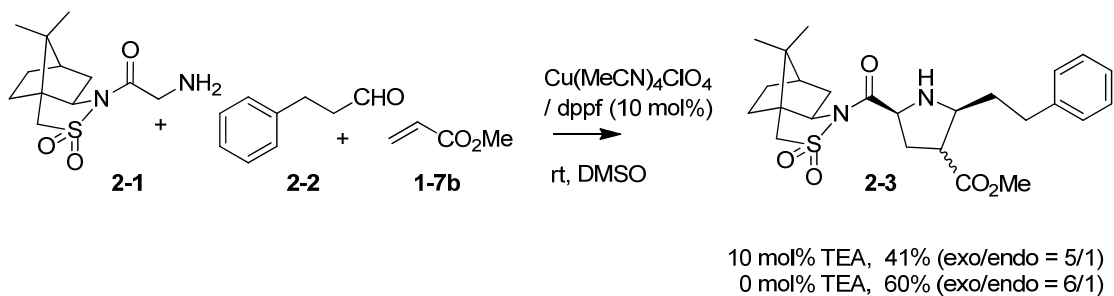
The results revealed that the reactions in DCM and DMSO gave a 3:1 mixture of exo- and endo-cycloadducts in a combined yield of 19% and 24% respectively (Entries 3 & 4). A 2:1 mixture of exo/endo cycloadduct was observed in MeCN, but the yield was very low (Entry 2).

Considering the possibility of ligand acceleration, we employed different achiral ligands (dppb, dppe, etc) for the CuI catalyzed cycloaddition. However, no ligand acceleration was observed, and the reactivity was still low. Most of Oppolzer's chiral glycylic sultam decomposed. Luckily, we found that the CuI-dppb system gave a 4:1 ratio of exo- and endo-cycloadducts.

The low reactivity might be ascribed to the poor solubility of the CuI / phosphane ligand complex in DCM. Also, CuI might be not a good catalyst precursor. Considering Cu(OTf)₂ is a good catalyst precursor and supposing exchanging the anion from a halide to a triflate would make it possible to promote the cycloaddition, Cu(OTf)₂ / dppf in DCM was employed as a catalyst in the cycloaddition. As anticipated, the exo/endo selectivity of the cycloaddition is enhanced (exo/endo = 5/1), however, the reactivity is still very low.

2.2 Optimization of Reaction Conditions

It was noticed that DMSO gave the highest yield in the CuI-dppf condition (Table 2.1). DMSO was therefore chosen as the solvent. However, a good catalyst system remained elusive until $\text{Cu}(\text{MeCN})_4\text{ClO}_4$ was prepared. The $\text{Cu}(\text{MeCN})_4\text{ClO}_4$ and dppf complex catalyzed the cycloaddition and gave a 6:1 mixture of exo- and endo-cycloadducts in combined yield of 60% (Scheme 2.3). It was also noticed that the addition of base tended to reduce both the yield and selectivity of the reaction.



Scheme 2.3 Comparison of cycloadduct formation with and without base

2.2.1 Copper Catalyst Precursors

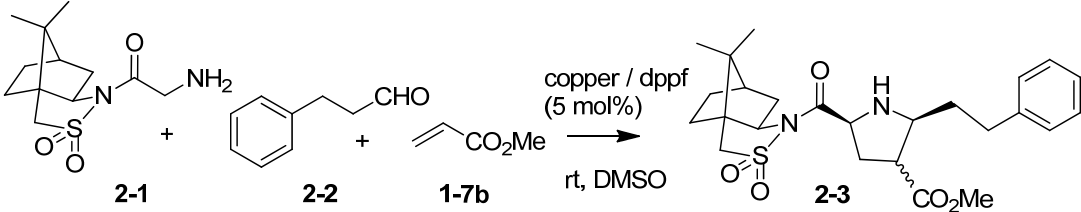
Intrigued by the effectiveness of $\text{Cu}(\text{MeCN})_4\text{ClO}_4$ in asymmetric cycloaddition, the effect of the counterions of copper on 1,3-dipolar cycloadditions was investigated.

$\text{Cu}(\text{MeCN})_4\text{PF}_6$, CuOAc , $\text{Cu}(\text{OAc})_2\cdot\text{H}_2\text{O}$ and $\text{Cu}(\text{OTf})_2$ were used in the cycloaddition of hydrocinnamic aldehyde, glycyl sultam, and methyl acrylate using Cu(I) / dppf-DMSO system at room temperature. Reactions were routinely performed in the dark to minimize degradation of the catalyst. Table 2.2. outlines the results of screening these copper precursors in the copper mediated [CN+C+CC] 1,3-dipolar cycloadditions reaction.

Chapter2: [CN+C+CC] 1,3-Dipolar Cycloadditions

The combination of dppf with copper(I) or copper(II) resulted in the exo-cycloadduct as the major product. CuClO_4 / dppf, CuOAc / dppf and CuPF_6 / dppf catalyzed 1,3-dipolar cycloadditions showed a similar exo/endo selectivity (Entries 1,2&3). Catalyst with CuOAc and CuPF_6 exhibited even higher reactivity. Comparison of results using Cu(II) / dppf showed that Cu(OTf)_2 / dppf exhibited a higher exo/endo selectivity, while $\text{Cu(OAc)}_2\text{-H}_2\text{O}$ / dppf catalyst resulted in a higher reactivity (Entries 4&5). Interestingly, $\text{Cu(OAc)}_2\text{-H}_2\text{O}$ catalyzed the cycloaddition to give the cycloadduct **2-23** in a 71% yield, which suggested that water existing in the $\text{Cu(OAc)}_2\text{-H}_2\text{O}$ did not affect the reactivity of the cycloadduct (Entry 5).

Based on these test reactions the best metal salts as catalyst precursors for this [CN+C+CC] 1,3-dipolar cycloadditions were $\text{Cu(MeCN)}_4\text{PF}_6$ and CuOAc .

Table 2.2 Effect of copper precursors on cycloaddition.^a


Entry	Catalyst: CuX-dppf	exo:endo ^b	Yield % ^c	Rxn time
1	Cu(MeCN) ₄ ClO ₄ -dppf	6/1	60%	16h
2	Cu(MeCN) ₄ PF ₆ -dppf	6/1	80%	12h
3	CuOAc-dppf	6/1	71-82%	2.5-12h
4	Cu(OAc) ₂ -H ₂ O-dppf(10%)	3/1	71%	9h
5	Cu(OTf) ₂ -dppf	5/1	31%	9h

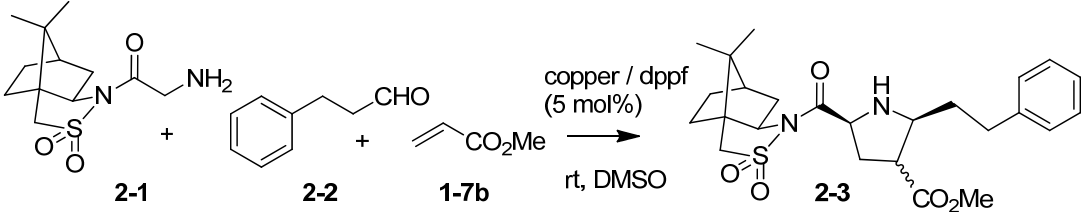
a Conditions: The catalyst was prepared by stirring the copper salt (Cu(I) or Cu(II) 5 mol %) and bisphosphine ligand (dppf, 5.5 mol %) in DMSO (1 mL) at rt for 1 h. To this mixture was added hydrocinnamic aldehyde (1.0 equiv), glycyl sultam (1.3 equiv), and methyl acrylate (3.0 equiv). After stirring at rt until complete (monitoring by NMR and TLC), the mixture was partitioned between sat. NH₄Cl(aq) and DCM. The combined organic layers were washed with brine, dried over MgSO₄, filtered and the solvent removed under vacuum to give the crude product. Further purification was accomplished using flash chromatography.

b Determined by ¹H NMR spectroscopic analysis of the crude product

c Isolated combined yields

2.2.2 Best ratio between Cu(I) and dppf

To find the most suitable catalytic species ligand/metal complexes were prepared using different ratios of copper precursor and dppf. The results are outlined in Table 2.3.

Table 2.3 Effect of ligand/metal ratio on cycloaddition.^a


Entry	Catalyst: CuX-dppf	exo:endo ^b	Yield % ^c	Rxn time
1	Cu(MeCN) ₄ ClO ₄ -dppf	6/1	60%	16h
2	Cu(MeCN) ₄ ClO ₄ -2dppf	6/1	82%	9h
3 ^d	2Cu(MeCN) ₄ ClO ₄ -dppf	2/1	61%	9h
4	CuOAc-dppf	6/1	71-82%	2.5-12h
5	CuOAc	1/6	34%	22h
6	Cu(MeCN) ₄ ClO ₄ -dppf	6/1	60%	16h

a Conditions: The catalyst was prepared by stirring the copper salt (Cu(I) 5 mol %) and bisphosphine ligand (dppf, 5.5 mol %) in DMSO (1 mL) at rt for 1 h. To this mixture was added hydrocinnamic aldehyde (1.0 equiv), glycyl sultam (1.3 equiv), and methyl acrylate (3.0 equiv). After stirring at rt until complete (monitoring by NMR and TLC), the mixture was partitioned between sat. NH₄Cl(aq) and DCM. The combined organic layers were washed with brine, dried over MgSO₄, filtered and the solvent removed under vacuum to give the crude product. Further purification was accomplished using flash chromatography.

b Determined by ¹H NMR spectroscopic analysis of the crude product

c Isolated combined yields

d 11 mol% of Cu(I) was used

CuClO₄-dppf ligand prepared from a 1:2 ratio of copper precursor and dppf showed the same exo/endo selectivity as that from a 1:1 ratio of metal and ligand, but resulted in the cycloadduct being produced in higher yield (Entries 1&2). It was reasoned that the same catalytic species was formed in these two systems based on the same exo/endo ratio. The higher yield may be due to the excess phosphine ligand which could be used as a base to generate azomethine ylide but would not lead to decomposition of the cycloadduct.

Chapter2: [CN+C+CC] 1,3-Dipolar Cycloadditions

A 2:1 ratio of copper precursor and dppf resulted in lower exo/endo selectivity but in the same yield as from the 1:1 ratio catalytic system (Entry 3). It was proposed that two catalytic species of Cu(I) and Cu(I) / dppf complex were in the reaction, in which Cu(I) favored formation of the endo-cycloadduct and the Cu(I) / dppf complex promoted the exo-cycloadduct. The control experiment revealed that Cu(I) (from CuOAc) gave a major endo-product in combined yield of 34%, while the Cu(I) / dppf complex (from CuOAc / dppf) resulted in the major exo cycloadduct (Entries 4&5). This result supported the assumption and also suggested that the ligand was the primary cause of exo selectivity in the [CN+C+CC] 1,3-dipolar cycloaddition. The same result was obtained in the initial Ag-ligand catalyzed [CN+C+CC] 1,3-dipolar cycloaddition. The effect of ligand acceleration in the [CN+C+CC] cycloadduct was also noticed by comparing the yield of Entries 4 and 5.

It was proposed that acetate could be used a base in 1,3-dipolar cycloaddition, thus a 1:1 ratio in the CuOAc / dppf as catalyst was chosen because of the issues associated with separation of excess phosphine ligands. Thus, it was concluded that a 1:1 ratio of copper precursor and dppf could form a suitable catalytic species in [CN+C+CC] 1,3-dipolar cycloaddition.

2.2.3 Solvent and Temperature Selection

Since the melting point of DMSO is 16 °C, the cycloaddition in DMSO can not be carried out at low temperature in this solvent. To get optimization of the solvent, the copper catalyzed cycloaddition was performed in different solvents (Table 2.4). Reagent grade DMSO was used and there was no need to dry it since an equivalent of water is

Chapter2: [CN+C+CC] 1,3-Dipolar Cycloadditions

formed during the reaction. The reactions were performed in air and carried out at ambient temperature without the need for base.

Table 2.4 Cu(I) / dppf (5 mol%) catalyzed cycloaddition^a in the different solvents.

Entry	Solvent	exo:endo ^b	Yield % ^c	Temp	Dielectric Constant
1 ^d	THF	3/1	47%	rt	7.6
2 ^e	DMF	3/1	34%	rt	36.7
3 ^e	MeOH	1/1	trace	rt	33
4 ^d	DMSO	6/1	72-82%	rt	46.7
5 ^d	DMSO/THF(1/8)	4/1	76%	rt	~36.7
6 ^d	DMSO/THF(1/8)	5/1	70%	0 °C	~36.7
7 ^d	DMSO/THF(1/1)	5/1	62%	0 °C	
8 ^d	MeOH/DMSO (1/20)	6/1	76%	rt	~46.7

a Conditions: The catalyst was prepared by stirring the copper salt (Cu(I) 5 mol %) and bisphosphine ligand (dppf, 5.5 mol %) in solvent (1 mL) at rt for 1 h. To this mixture was added hydrocinnamic aldehyde (1.0 equiv), glycyl sultam (1.3 equiv), and methyl acrylate (3.0 equiv). After stirring at rt until complete (monitoring by NMR and TLC), the mixture was partitioned between sat. NH₄Cl(aq) and DCM. The combined organic layers were washed with brine, dried over MgSO₄, filtered and the solvent removed under vacuum to give the crude product. Further purification was accomplished using flash chromatography.

b Determined by ¹H NMR spectroscopic analysis of the crude product

c Isolated combined yields

d CuOAc (5%) was used.

e Cu(MeCN)₄PF₆ was used.

An exo:endo ratio of 3:1 was observed in THF and DMF. The reaction in THF gave cycloadducts in 47% yield (Entry 1), while in DMF gave cycloadducts in 34% yield (Entry 2). Only trace amounts of cycloadducts were detected in methanol with an

Chapter2: [CN+C+CC] 1,3-Dipolar Cycloadditions

exo/endo ratio of 1:1 (Entry 3). The cycloaddition in reagent grade DMSO gave the cycloadduct with the highest exo/endo selectivity (Entry 4).

Next, the reaction was conducted in co-solvent systems of DMSO/THF. The reaction in the co-solvent of 1:8 DMSO-THF gave cycloadduct in 76% yield with an exo/endo ratio of 4:1 (Entry 5), and the ratio of exo- and endo-cycloadduct was increased to 5:1 when the reaction was performed at 0 °C. It is suggestive of a possible trend towards higher exo/endo ratios at lower temperature (Entry 6).

The reaction employing a 1:1 THF-DMSO serving as solvent at 0 °C gave the same ratio of exo- and endo-cycloadduct (Entry 7). Based on the above results, the co-solvent between THF and DMSO showed lower exo/endo selectivity. No further lower temperature reaction tests were investigated. The attempt to employ methanol as additive failed to result in a higher exo/endo selectivity (Entry 8). It was concluded that the best solvent is DMSO despite its lack of suitability for use below 16 °C.

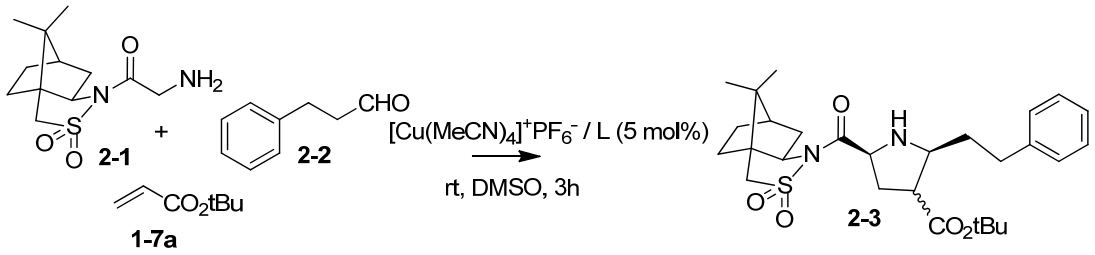
Since more polar solvent promoted the formation of the exo-cycloadduct, it was reasoned that a stepwise, more solvent-dependent cycloaddition can obviously compete with the concerted process. It was also reasoned that the transition state of exo-approach has a higher polarity. The high exo-selectivity and reactivity of the cycloaddition in DMSO may be ascribed to the following reasons:

1. The polar exo transition state is further stabilized by polar media.
2. The zwitterion is predicted to be strongly favored with the polar media.
3. The metal salt is dissociated completely in DMSO and the metal-ligand complex is dissolved in DMSO.

2.2.4 Catalyst Ligand

To optimize reaction conditions, catalysts derived from different ligands were investigated in the cycloaddition reaction. The results of this series of tests are outlined in Table 2.5.

Table 2.5 Different ligands were investigated in the Cu(I) catalyzed cycloaddition.^a



Entry	Ligand	exo:endo ^b	Yield ^c	<P-Cu-P ^d
1	PPh ₃ ^e	1.2/1	96%	121.0
2	dppe	1.1/1	54%	97.4
3	dppp	2.8/1	53%	104.3
4	dppb	6/1	81%	115.9
5	dppf	6/1	81%	

a Conditions: The catalyst was prepared by stirring the copper salt (Cu(I)5 mol %) and phosphine ligand (5.5 mol %) in DMSO (1 mL) at rt for 1 h. To this mixture was added hydrocinnamic aldehyde (1.0 equiv), glycyl sultam (1.3 equiv), and methyl acrylate (3.0 equiv). After stirring at rt until complete (monitoring by NMR and TLC), the mixture was partitioned between sat. NH₄Cl(aq) and DCM. The combined organic layers were washed with brine, dried over MgSO₄, filtered and the solvent removed under vacuum to give the crude product. Further purification was accomplished using flash chromatography.

b Determined by ¹H NMR spectroscopic analysis of the crude product.

c Isolated combined yields

d The binding angle was measured from the 3D structure.

e 11 mol% of PPh₃ were used.

dppe = 1,2-bis(diphenylphosphino)ethane; dppp = 1,2-bis(diphenylphosphino)propane

dppb = 1,4-bis(diphenylphosphino)butane; dppf = bis(diphenylphosphino)ferrocene

Chapter2: [CN+C+CC] 1,3-Dipolar Cycloadditions

The bidentate ligands dppb and dppf showed the highest exo/endo selectivity and reactivity (Entries 4&5). The reactivity and exo/endo selectivity was decreased when dppp was used (Entry 3). No exo/endo selectivity was observed when employing dppe or the bulky monodentate ligand PPh₃ (Entries 1&2). The PPh₃ promoted cycloaddition gave the product in 90% yield.

Thus, the increase in exo selectivity for the ligands is in the order dppb, dppf > dppp > dppe. It was noticed that the increase in bite angle for the ligand is in the order dppb > dppp > dppe, which was measured from the 3D structures of the metal dipole complexes derived from aminoacetamide and formaldehyde. The chelate ring size follows the order dppb > dppp > dppe. Considering the similar steric and electrostatic properties among dppe, dppp, and dppb, it was reasoned that the exo/endo selectivity depended on the chelate ring size and binding angle. Thus, the best ligands for the series tested are dppb and dppf.

It was reasoned by a inspiration from Hou's results that a better ligand would be developed through screening of phosphine based ligands with different electronic properties. Examples of possible ligands to test in the future are shown in Figure 2.1.

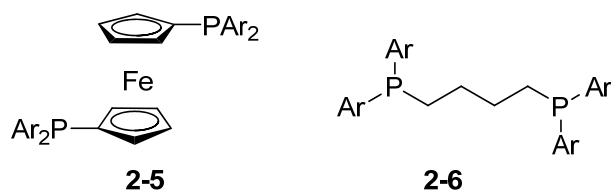
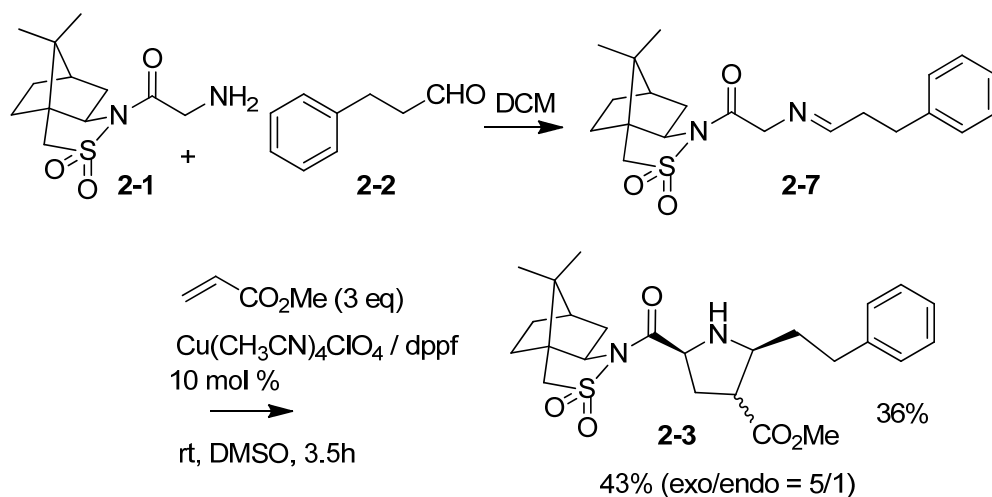


Figure 2.1 Ligands proposed for future testing.

2.2.5 Preformation of the Imine

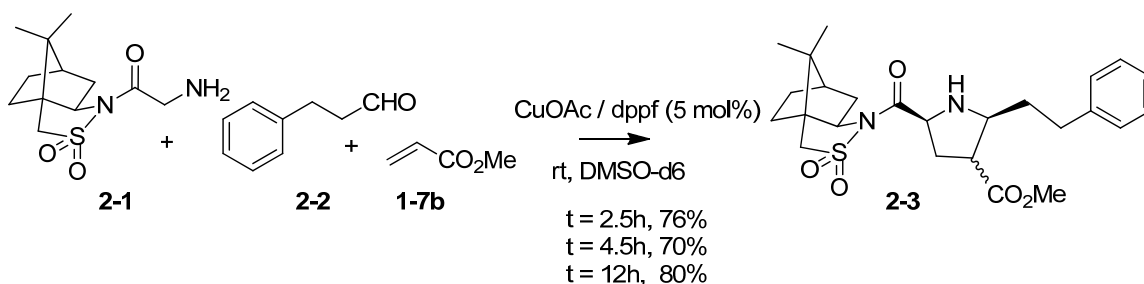
The cycloaddition was carried out in a one-pot procedure, where aldehyde, glycyll sultam and dipolarophile were combined in the same pot with catalyst complex. Imines were generated in situ from aldehydes and amine. NMR experiments indicated that imines were formed within 5 min when mixing aldehyde, glycyll sultam, and methyl acrylate in d6-DMSO; and the cycloadduct was produced within 10 min. The NMR experiments also confirmed that imines decomposed in 2h in the presence of Cu(I) / dppf-d6-DMSO. It is known that imines with α -protons commonly tautomerize to form enamines and imines are difficult to synthesize, isolate and further purify. It is also difficult to accurately measure the amount the imine in the cycloaddition when using crude imines without further purification. The one pot process from aldehyde offers a way to overcome the limitations related to the use of imines. In the reaction system, the cycloaddition between imines and dipolarophile in the presence of copper catalyst in DMSO, gave 41% yield with 5/1 of exo/endo ratio (Scheme 2.4). This might be ascribed to imines decomposing in the copper-DMSO system, because reagent grade DMSO contains some water.



Scheme 2.4 The cycloaddition was performed with preformed imine.

2.2.6 Reaction Time

It was also found that the cycloaddition gave similar results using longer reaction times (Scheme 2.5). In addition, almost no Michael addition of methyl acrylate to chiral glycylyl sultam or azomethine ylide occurred. Almost no cycloadduct imidazolidine and oxazolidine was isolated.



Scheme 2.5 CuX / dppf (5 mol%) catalyzed [CN+C+CC] reaction.

2.2.7 Optimized Conditions

Having conducted the tests outlined above, the optimized reaction conditions were established as 5 mol % of CuOAc (or Cu(MeCN)₄PF₆) and 5.5 mol% of dppb (or dppf), in reagent-grade DMSO at room temperature in ambient air.

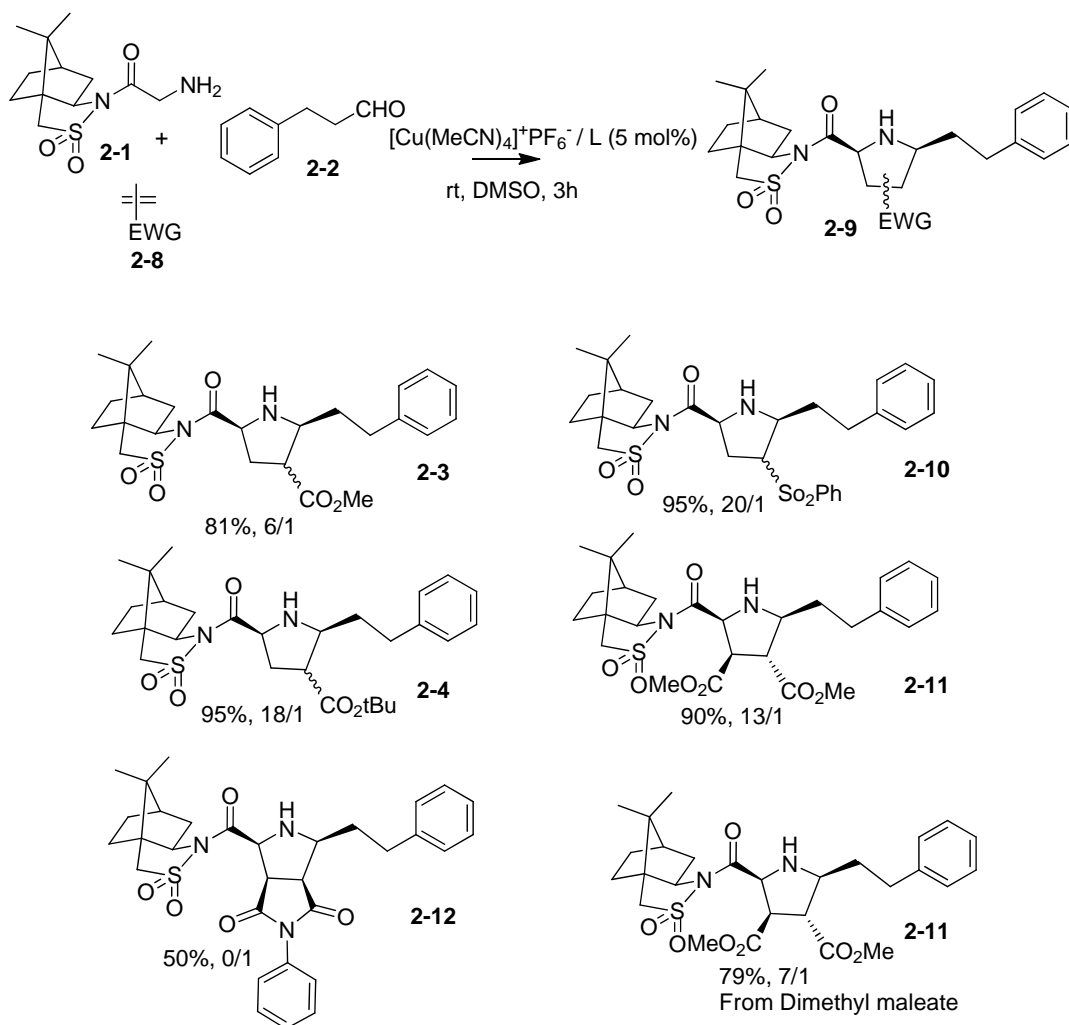
2.3 Exploring the Scope of the Cu(I)–Ligand Catalytic System

To explore the scope and generality of this novel Cu(I) catalyzed exo-selective [CN+C+CC] cycloaddition protocol, other dipolarophiles and different aldehydes were investigated.

2.3.1 Asymmetric Dipolarophiles

Figure 2.1 outlines the results in the Cu complex catalyzed [CN+C+CC] 1.3-dipolar cycloaddition with different dipolarophiles. The Cu(I) / P ligand catalyzed cycloaddition with methyl acrylate, *tert*-butyl acrylate, phenyl vinyl sulfone and fumarate gave high exo-selectivity with more than 80% yield. Using a bulky *tert*-butyl acrylate, much higher exo selectivity was observed as compared with methyl acrylate.

Chapter2: [CN+C+CC] 1,3-Dipolar Cycloadditions



The catalyst was prepared by stirring the copper salt ($\text{Cu}(\text{MeCN})_4\text{PF}_6$ or CuOAc , 5 mol %) and bisphosphine ligand (dppb or dppf, 5 mol %) in DMSO (6 mL/mmol aldehyde) at rt for 1 h. To this mixture was added hydrocinnamic aldehyde (1.0 equiv), glycyl sultam (1.3 equiv), and dipolarophile (3.0 equiv). After stirring at rt for 1-3 h (monitoring by NMR and TLC), the mixture was partitioned between sat. $\text{NH}_4\text{Cl}(\text{aq})$ and DCM. The combined organic layers were washed with brine, dried over MgSO_4 , filtered and the solvent removed under vacuum to give the crude product. Further purification was accomplished using flash chromatography. The yields specified are combined exo and endo yields. The ratios are exo / endo.

Figure 2.2 Cu(I) / Catalyzed enantioselective cycloaddition with various dipolarophiles.

However, in the case of the maleimide dipolarophiles, only one endo-cycloadduct was isolated. The strangest result is that cycloadducts using dimethyl maleate were the same as using fumarate, and a 7/1 mixture of exo and endo cycloadduct was obtained in a combined yield of 71%. A stepwise mechanism is probably responsible for the formation of the unexpected cycloadducts.

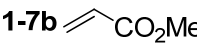
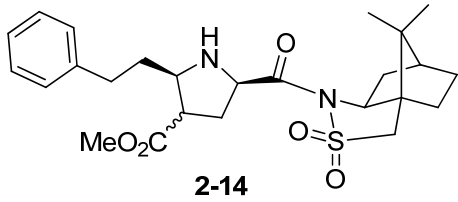
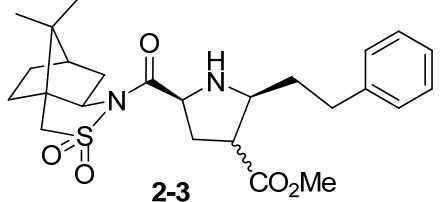
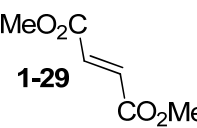
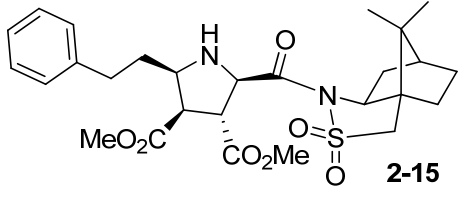
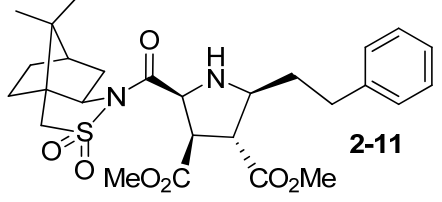
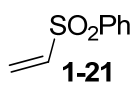
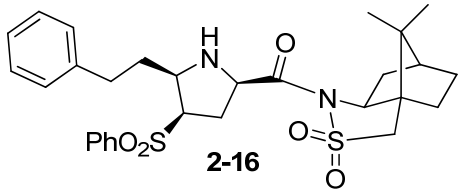
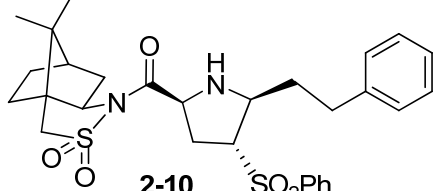
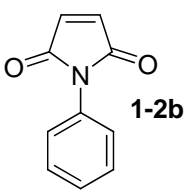
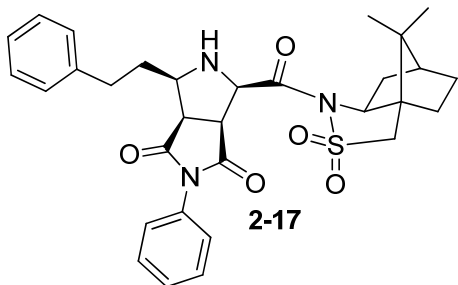
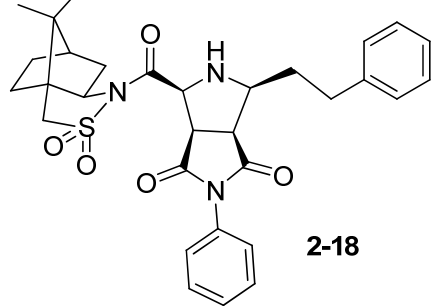
2.3.2 Selectivity – Cu(I) vs. Ag(I)

Table 2.6 outlines the results obtained when comparing silver and copper catalyzed 1,3-dipolar cycloadditions with different dipolarophiles. With Ag(I) catalytic conditions, the [CN+C+CC] 1,3-dipolar cycloaddition with methyl acrylate, phenyl vinyl sulfone and maleimide gave a more than 8:1 ratio of endo- to exo-cycloadducts. The endo/exo ratio was reduced when dimethyl fumarate was used. With Cu(I) catalytic conditions, the reaction with acyclic dipolarophiles afforded a higher ratio of exo- to endo-cycloadducts, while only endo cycloadduct was obtained when maleimide was used.

Comparing of the endo/exo ratio between two catalytic conditions, Cu(I) based catalyst showed better selectivity in the [CN+C+CC] 1,3-dipolar cycloadditions than silver based catalysts except with methyl acrylate. Both conditions gave the endo cycloadduct employing maleimide as dipolarophiles.

Chapter2: [CN+C+CC] 1,3-Dipolar Cycloadditions

 Table 2.6. Endo/exo selectivity in two catalytic systems with various dipolarophiles.^a

Olefin	AgOAc-THF ^b	Cu(I) / P,P-ligands-DMSO ^c
 1-7b	 2-14 82%, 1/8	 2-3 81%, 6/1
 1-29	 2-15 88%, 3/5	 2-11 90%, 13/1
 1-21	 2-16 94%, 1/8	 2-10 95%, 20/1
 1-2b	 2-17 83%, 1/10	 2-18 50%, 0/1

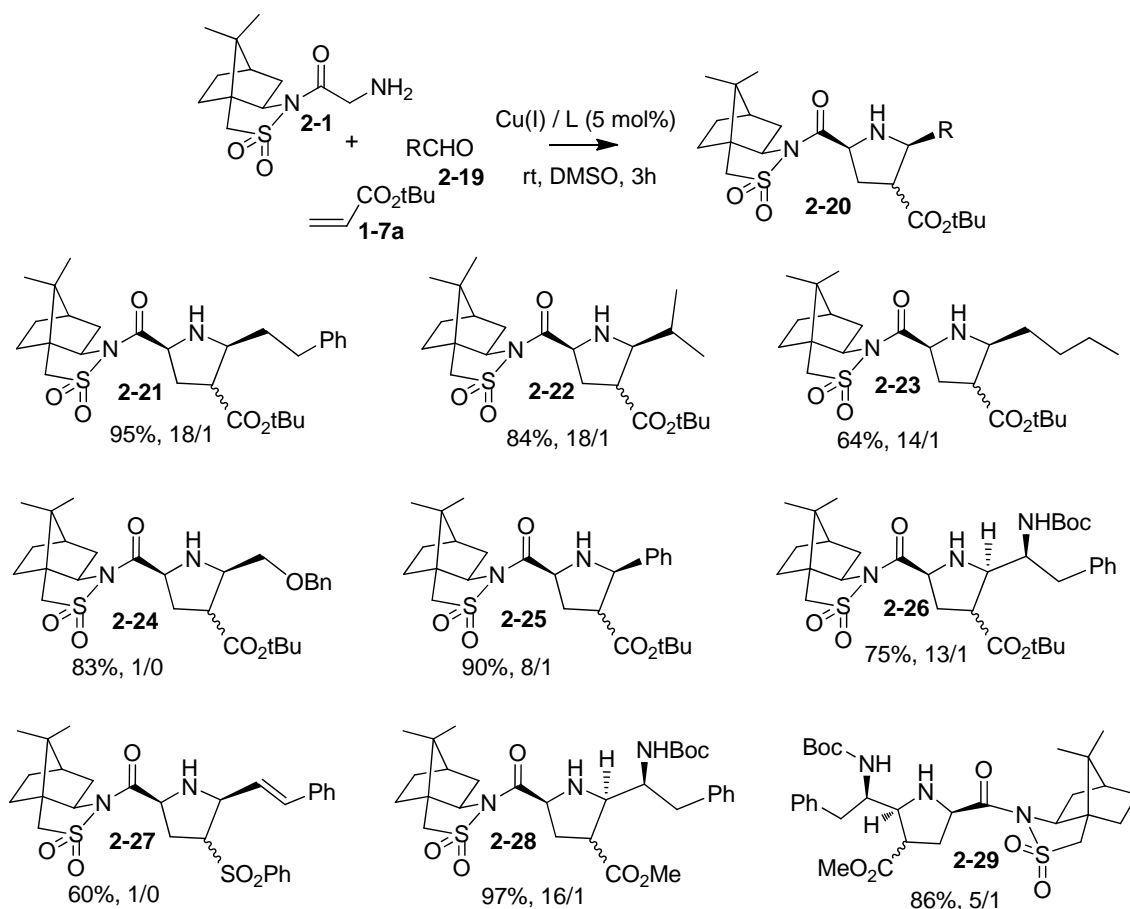
a. The catalyst, hydrocinnamic aldehyde (1.0 equiv), glycyl sultam (1.3 equiv), and dipolarophile (3.0 equiv) were mixed in solvent. After stirring at rt for 1-3 h (monitoring by NMR and TLC), the mixture was partitioned between sat. $\text{NH}_4\text{Cl}(\text{aq})$ and DCM. The combined organic layers were washed with brine, dried over MgSO_4 , filtered and the solvent removed under vacuum to give the crude product. Further purification was accomplished using flash chromatography. The yields specified are combined exo and endo yields. The ratios are exo / endo.

b. D-Sultam, Ag(I) and THF were used.

c. L-Sultam, Cu(I)-L and DMSO were used.

2.3.3 Aldehyde Substrates

Under the optimized conditions, cycloaddition utilizing a variety of aldehyde substrates with *t*-butyl acrylate and glycylic sultam was investigated (Figure 2.3).



The catalyst was prepared by stirring the copper salt ($\text{Cu}(\text{MeCN})_4\text{PF}_6$ or CuOAc , 5 mol %) and bisphosphine ligand (dppb or dppf, 5 mol %) in DMSO (6 mL/mmol aldehyde) at rt for 1 h. To this mixture was added hydrocinnamic aldehyde (1.0 equiv), glycylic sultam (1.3 equiv), and dipolarophile (3.0 equiv). After stirring at rt for 1-3 h (monitoring by NMR and TLC), the mixture was partitioned between sat. $\text{NH}_4\text{Cl}(\text{aq})$ and DCM. The combined organic layers were washed with brine, dried over MgSO_4 , filtered and the solvent removed under vacuum to give the crude product. Further purification was accomplished using flash chromatography.

The yields specified are combined exo and endo yields. The ratios are exo / endo.

Figure 2.3 Variation of aldehyde for the cycloaddition with *tert*-butyl acrylate.

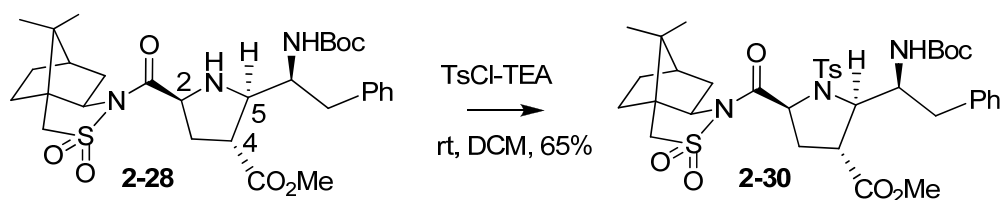
All the cycloadditions with both aliphatic and aromatic aldehydes afforded the corresponding cycloadducts with high reactivity and exo-selectivity. In the case of 2-(benzyloxy)acetaldehyde (forming 2-24) and cinnamaldehyde (forming 2-27), only the

exo products were observed. The cycloaddition with chiral aldehyde (*S*)-*tert*-butyl-1-oxo-3-phenylpropan-2-ylcarbamate in the presence of L-glycyl sultam, gave a higher ratio of exo- and endo-cycloadducts and the exo/endo selectivity was decreased when the D-glycyl sultam was used. The X-ray crystallographic analysis revealed that the absolute stereochemistry was controlled by the chirality of auxiliary, not by aldehyde (see section 2.3.4 below).

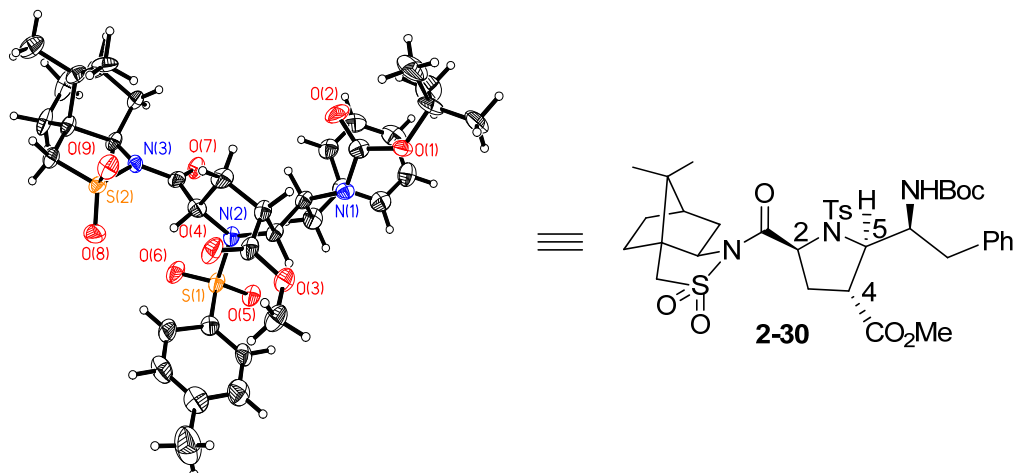
All the cycloaddition reactions lead to the cis-2,5-disubstituted cycloadducts indicating that EE dipole was formed before being trapped by the dipolarophile.

2.3.4 Configuration Assignment

Assignment of the major cycloadduct as endo or exo in Figure 2.2 and Figure 2.3 are based on a combination of J-coupling data and NOE experiments (see experimental section). The absolute stereochemistry of these cycloadducts is based on the X-ray crystallographic analysis of the corresponding tosylate derivative of exo-**2-28** (Scheme 2.6). This was assigned as 2*S*,4*S*,5*R* configuration (Figure 2.4).



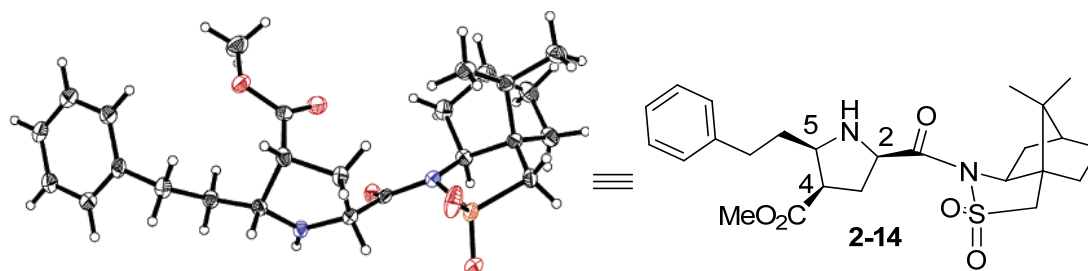
Scheme 2.6 Formation of the N-tosyl derivative of **2-28**.



CCDC-642220 (cycloadduct 2-30) contains the supplementary crystallographic data for this dissertation. These data can be obtained free of charge from the Cambridge Crystallographic Data Centre via www.ccdc.cam.ac.uk/datarequest/cif.

Figure 2.4 X-ray crystal structure of adduct **2-30**.

Assignment of the major cycloadduct as endo or exo in Table 2.6. are also based on a combination of J-coupling data and NOE experiments (see experimental section). The absolute stereochemistry of these cycloadducts is based on the X-ray crystallographic analysis of endo-**2-14**. This was assigned as *2R,4S,5R* configuration. (Figure 2.5).

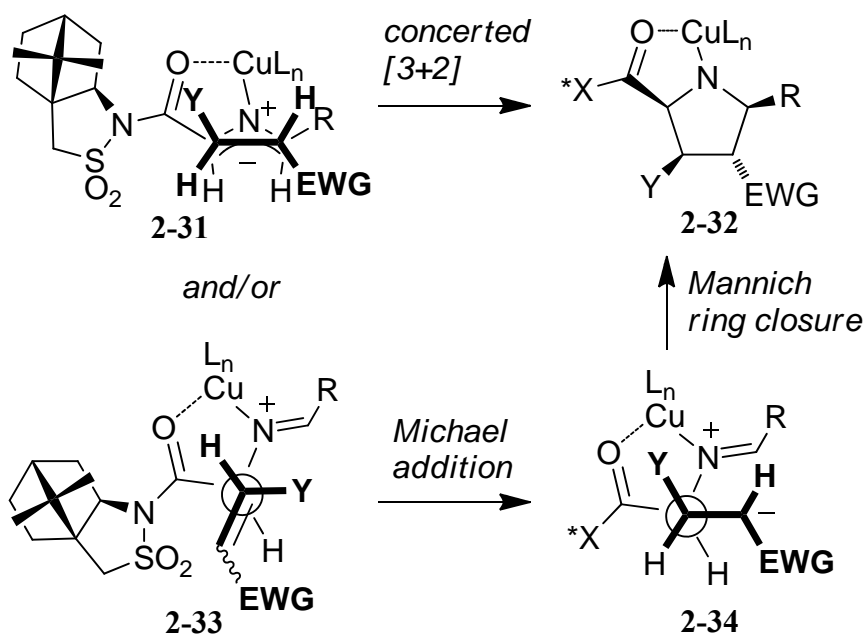


CCDC-614445 (cycloadduct 2-14) contains the supplementary crystallographic data for this dissertation. These data can be obtained free of charge from the Cambridge Crystallographic Data Centre via www.ccdc.cam.ac.uk/datarequest/cif.

Figure 2.5 X-ray crystal structure of the adduct formed from reaction with methyl acrylate.

2.4 Mechanism⁴⁰

These experimental results are consistent with either of the following two mechanistic hypotheses (Scheme 2.7). On one hand, the cycloaddition reaction may be concerted and proceed through an asynchronous [3+2] transition state (**2-31**→**2-32**). An unsymmetrical transition state — with C2–C3 bond formation (pyrrolidine numbering) being more advanced than C4–C5 bond formation — would be expected given the polarized nature of the metalated azomethine ylide. Alternatively, the reaction may also proceed in a step-wise manner via a zwitterionic intermediate such as **2-33**. If the alkene is β -substituted, the stereocenter at C3 would be set by an approach that places the smallest β -substituent above the chelate metallocycle. Rotation of the C2–C3 bond in **2-33** brings the enolate carbon toward the iminium carbon as in structure **2-34**. The 4,5-trans product results from the minimization of a steric clash between the dipolarophile activating group (EWG) and the azomethine ylide R group. Support for this step-wise mechanism is provided by the reaction with dimethyl maleate, which produced the same cycloadduct as the fumarate reaction. Both mechanistic schemes would account for DMSO being the optimal organic solvent for this reaction, since this high dielectric constant solvent ($\epsilon = 48$) would be expected to stabilize polar transition states.



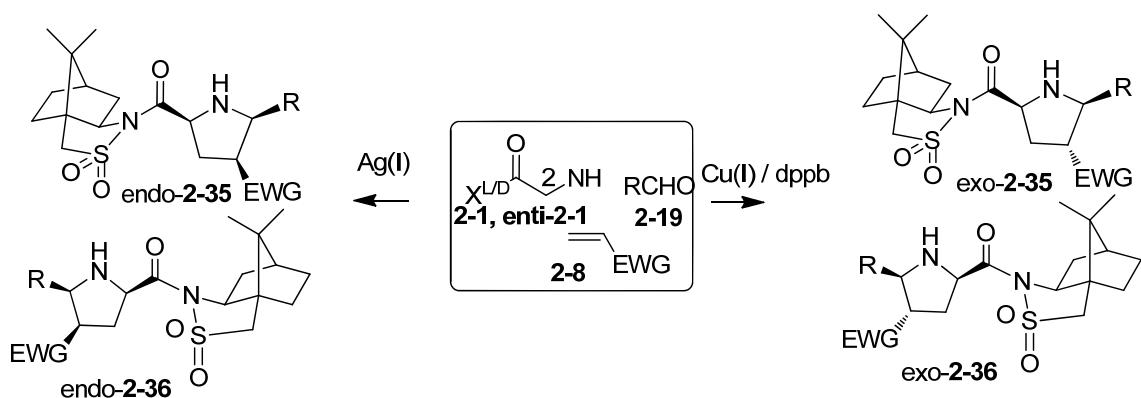
Scheme 2.7. Dual mechanistic rationale for exo-selective asymmetric [CN+C+CC] coupling (Y = H or EWG).

2.5 Applications

Having developed Ag(I) catalyzed endo selective [CN+C+CC] 1,3-dipolar cycloadditions, and Cu(I) / P ligand catalyzed exo-selective [CN+C+CC] 1,3-dipolar cycloadditions, a number of applications were explored.

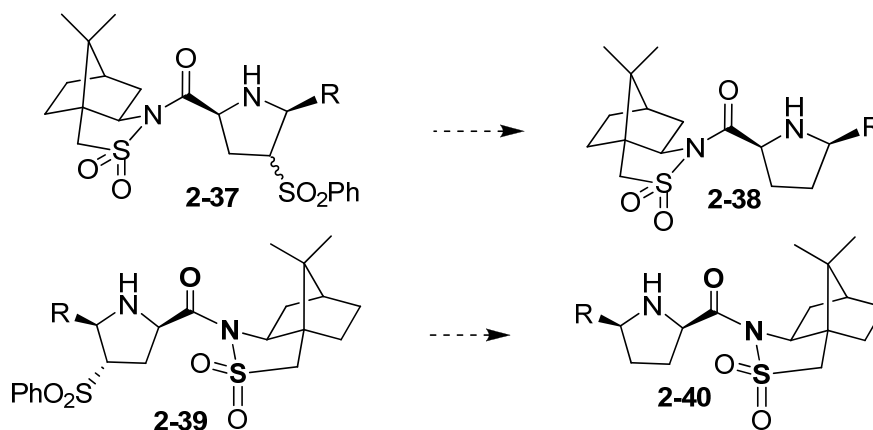
2.5.1 Synthesis of Multisubstituted Pyrrolidines

The chirality of the auxiliary glycylyl sultam controlled the stereochemistry of the cycloadduct. Thus, under the different combinations of catalyst and auxiliary, four kinds of tri-substituted cycloadducts (endo/exo-**2-35**, endo/exo-**2-36**) may be readily formed (Scheme 2.8).



Scheme 2.8 Cycloadducts prepared under different combination of auxiliary and catalyst.

Utilizing different dipolarophiles, di-, tri- and tetra-substituted pyrrolidines with different stereochemistries could be prepared. Di-substituted pyrrolidine may be converted from cycloadduct bearing sulfones through reductive desulfonation (Scheme 2.9). Use of other cleavable electron withdrawing groups may also be possible for the formation of disubstituted pyrrolidines. Tetrasubstituted pyrrolidines may be formed from dipolarophiles carrying two substituents.

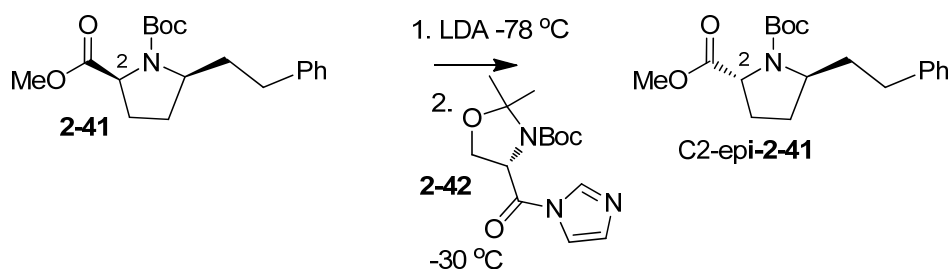


Scheme 2.9 Disubstituted pyrrolidines prepared by removal of the EWG after ring formation.

2.5.2 Disubstituted Pyrrolidines with Alternative Stereochemistry

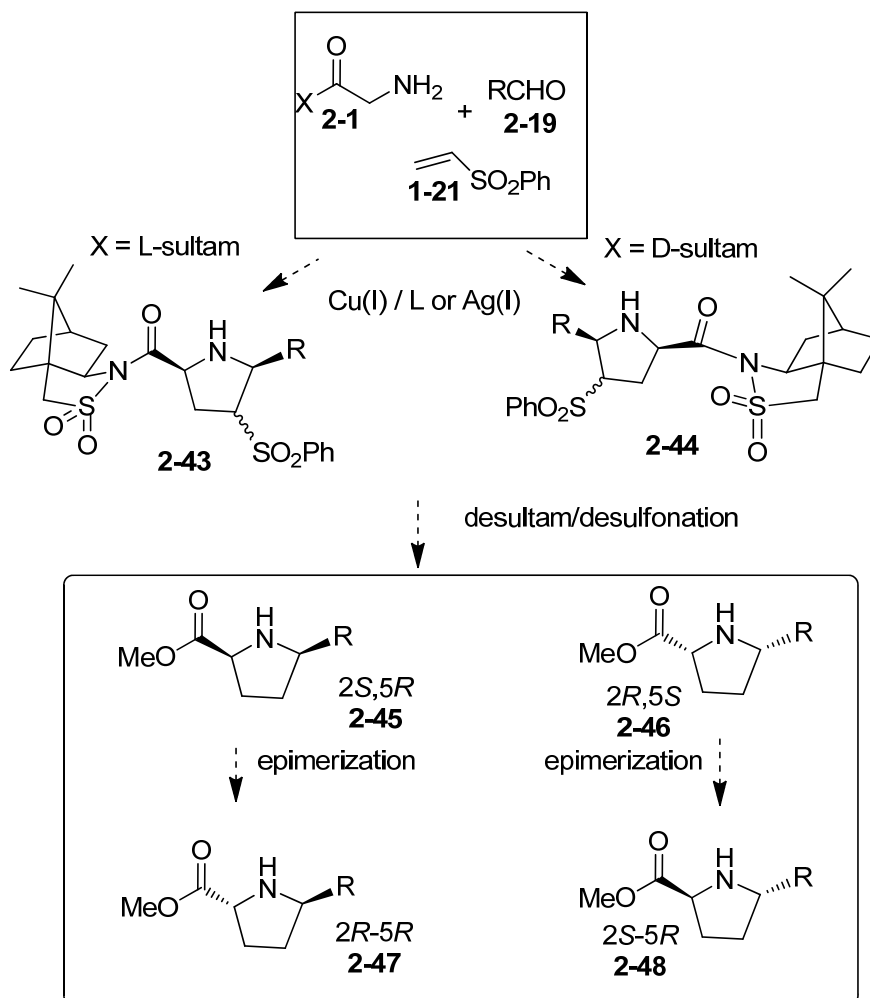
It was noticed that both *exo*- and *endo*-cycloadducts of a single compound bearing a sulfone are converted to the same 2,5-disubstituted pyrrolidines on desulfonylation.

While attempting another reaction, it was found that C2-*epi*-**2-41** could be prepared through lithium enolate formation of **2-41** (Scheme 2.10). Failing to trap the enolate, the C2-*epimer* was formed on work-up.



Scheme 2.10 C2-*epimer* formation.

Thus, 2,5-disubstituted pyrrolidines with different stereochemistry can be prepared through a metal catalyzed [CN+C+CC] 1,3-dipolar cycloaddition utilized glycol sultam with different chirality followed by epimerization (Scheme 2.11).

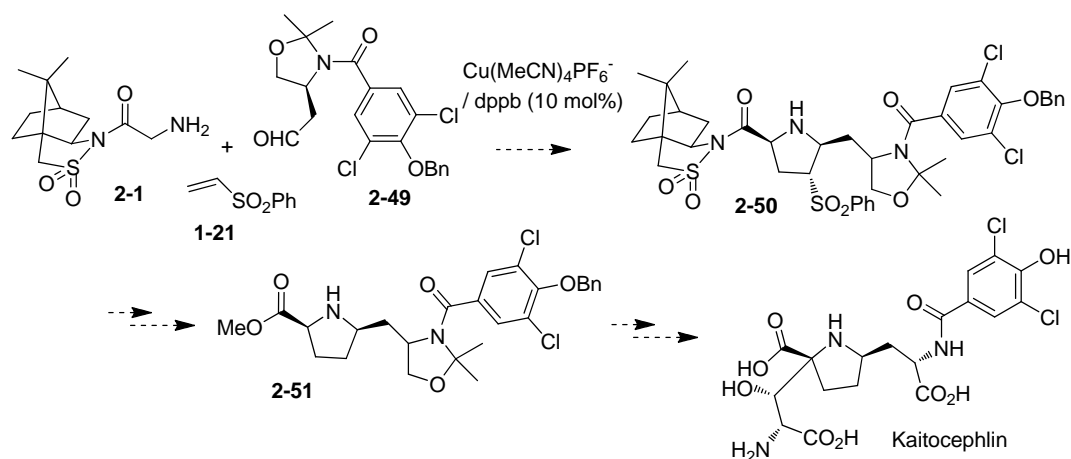


Scheme 2.11 Route to four isomers of 2,5-disubstituted pyrrolidines.

2.5.3 Kaitocephalin Intermediates

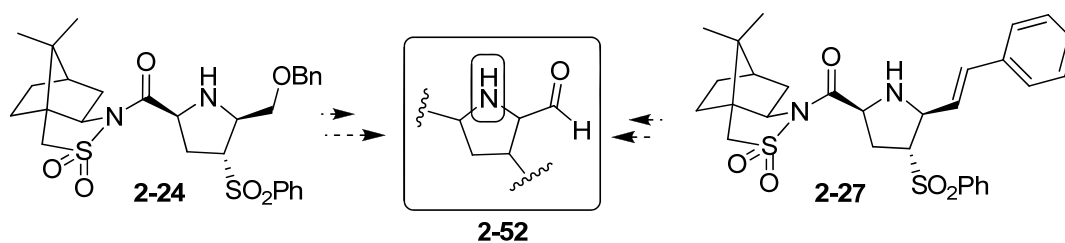
Encouraged by this result, it was planned to synthesize the key precursor of kaitocephalin, 2,5-disubstituted pyrrolidine **2-51** via a one pot cycloaddition followed by desulfonylation (Scheme 2.12).

Chapter2: [CN+C+CC] 1,3-Dipolar Cycloadditions



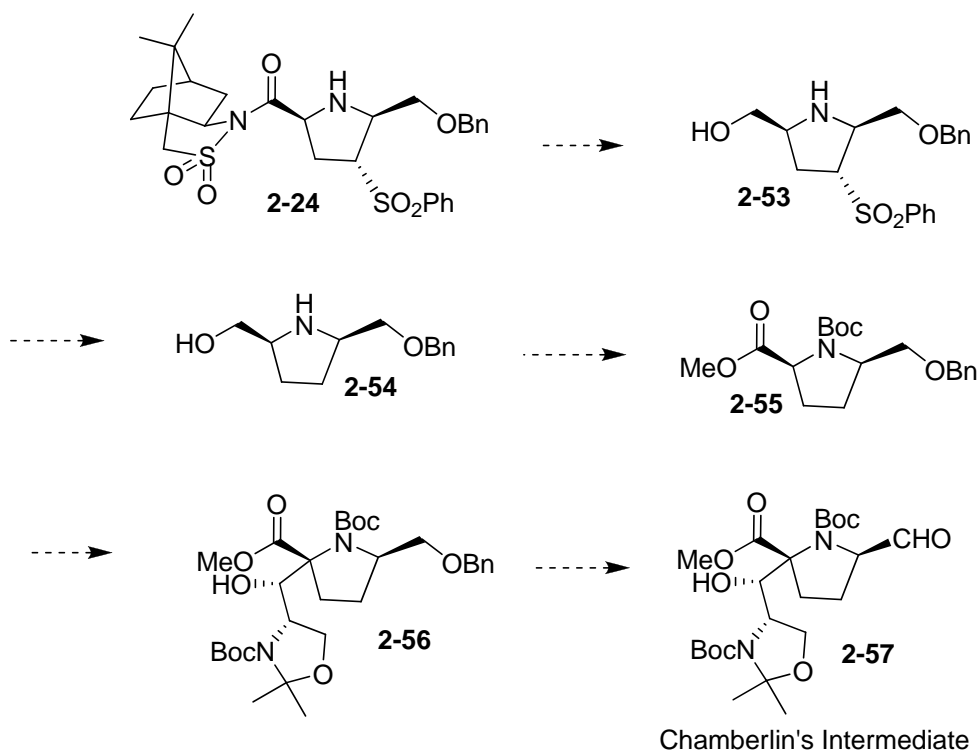
Scheme 2.12 A key intermediate of kaitocephalin can be prepared via one pot reaction.

It was observed that the substituent at C5 on both cycloadduct **2-24** and on **2-27** has the potential of conversion to aldehyde, which could be used as a new reaction site to introduce other functional groups (Scheme 2.13).



Scheme 2.13 Potential for conversion to aldehyde.

It was realized that a key intermediate (**2-55**) in Chamberlin's synthesis of kaitocephalin³⁷ could be prepared from cycloadduct **2-24** (Scheme 2.14).



Scheme 2.14 A possible route to a key intermediate of kaitocephalin in Chamberlin's synthesis.³⁷

2.6 Summary

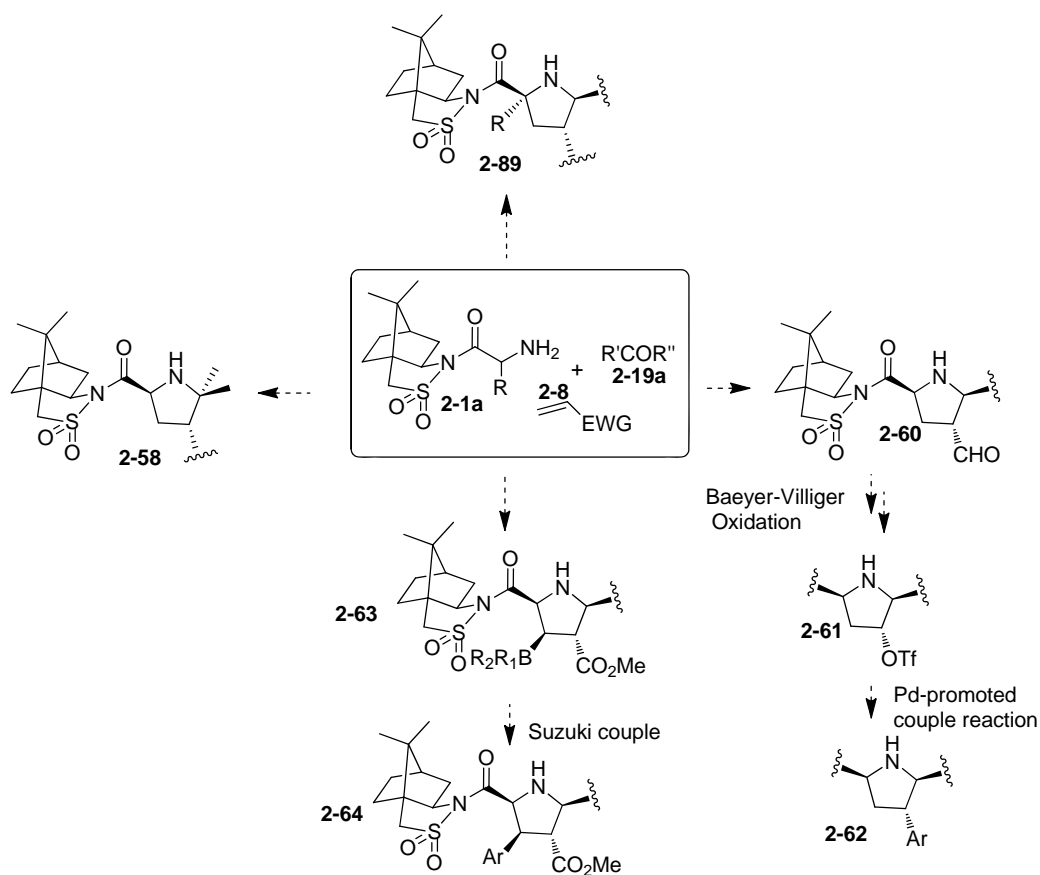
A good stereoselectivity in [3+2] cycloaddition reactions was achieved by employing a combination of chiral auxiliary and simple Cu(I)-achiral diphosphane ligand complexes. The reverse stereochemistry of the pyrrolidine ring was obtained using an auxiliary with opposite chirality.

The Cu(I)-catalyzed *exo*-selective [CN+C+CC] coupling reaction provides convenient access to 2,5-*trans* disubstituted pyrrolidines. The method is highlighted in the preparation of cycloadducts derived from aliphatic aldehydes.

2.7 Proposed Future Work

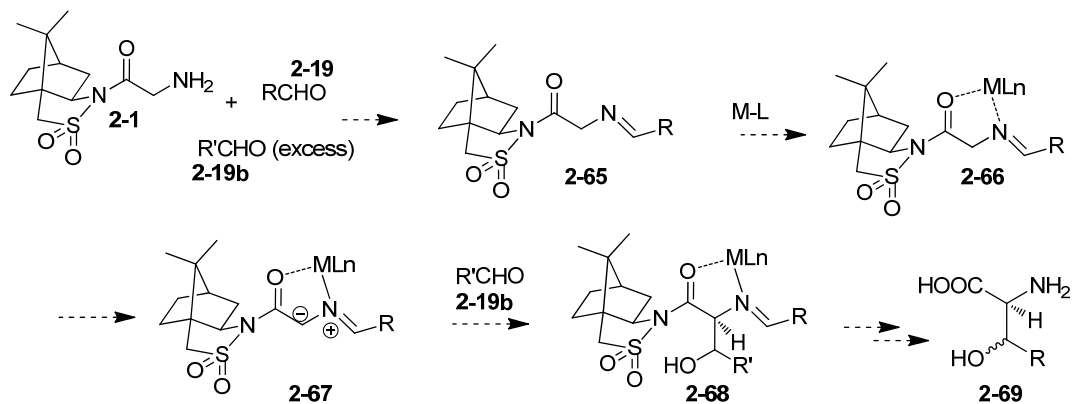
With the optimized reactions in hand, target directed cycloaddition should be investigated using suitable “CN”, “C” and “CC” partners.

When switching to ketone as the “C” partner, 2,4,5,5-tetrasubstituted pyrrolidines **2-58** would be prepared (Scheme 2.15). Employing α -substituted glycylyl sultam as the “CN” partner, 2,2,4,5-tetra-substituted pyrrolidine **2-59** would be constructed. Using olefin aldehyde²¹ as the “CC” partner, the aldehyde group would be introduced in the cycloadduct to form aldehyde **2-60**, which can be used as a new reaction site to install aromatic group at C4 (**2-62**). Using boron based acrylate²² as the “CC” partner, a boron group can be introduced in the cycloadduct **2-63**, which can furnish an aromatic substituent at C3 (**2-68**).



Scheme 2.15 Target directed cycloaddition.

Considering the possible stepwise mechanism,²³ aldehyde could be used to trap the azomethine ylide yield to generate α -hydroxyl substituted glycyl sultam **2-68**, which can lead to formation of substituted serines (Scheme 2.16).²⁴



Scheme 2.16. Possible synthesis of chiral substituted serine derived from azomethine ylide.

3 Experimental

3.1 General Methods

Cycloaddition reactions were performed in reagent grade DMSO in air. Reaction flasks were covered with Al foil to minimize light-mediated degradation of the catalyst. The progress of reactions was checked by ^1H NMR and analytical thin-layer chromatography (TLC). Plates were visualized first with UV illumination followed by charring with ninhydrin (0.3% (w/v) ninhydrin in 97/3 (v/v) EtOH-AcOH). Flash column chromatography was performed using silica gel (230-400 mesh). The solvent compositions reported for all chromatographic separations are on a v/v basis. ^1H NMR spectra were recorded at 400 MHz in the indicated solvent at rt and are reported in parts per million (ppm) on the δ scale relative to residual CHCl_3 (δ 7.24), $\text{C}_6\text{D}_5\text{H}$ (δ 7.16), and $\text{CD}_3\text{COCD}_2\text{H}$ (δ 2.09). Proton assignments are based on COSY experiments. Stereochemical assignments are based on the NOE difference data as indicated. The absolute stereochemistry of these cycloadducts is based on the X-ray crystallographic analysis of cycloadduct and tosylate derivative (Data was provided by the University of Akron collected on Bruker SMART Apex single crystal X-ray diffractometer). Unless otherwise stated, ^{13}C NMR spectra were recorded in CDCl_3 at 100 MHz and are reported in parts per million (ppm) on the δ scale relative to CDCl_3 (δ 77.00). High resolution mass spectra (HRMS) were recorded using fast atom bombardment (FAB) ionization.

The numbering and labeling system used corresponds to the IUPAC numbering system for substructures **i** - **v** shown in Figure 3.1 below.

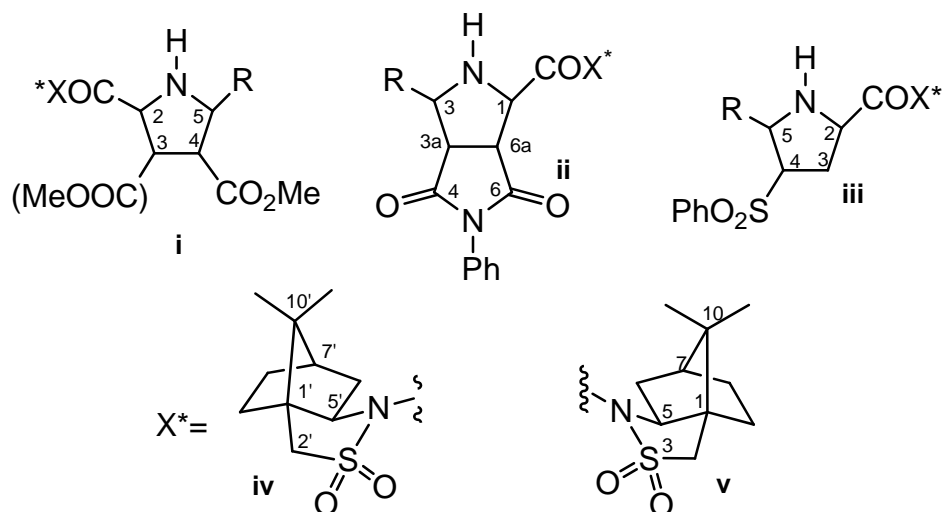


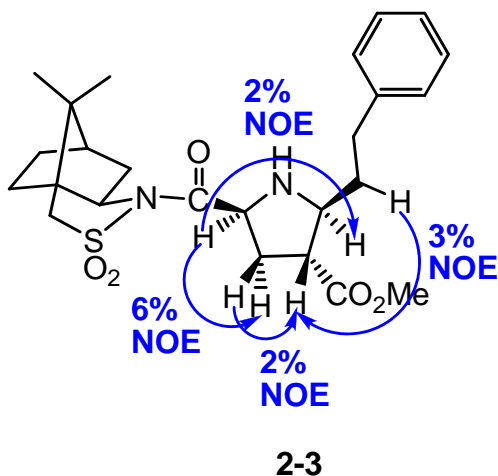
Figure 3.1 Substructure models indicating numbering and labelling used.

3.2 Exo-Products

3.2.1 Reaction Procedures

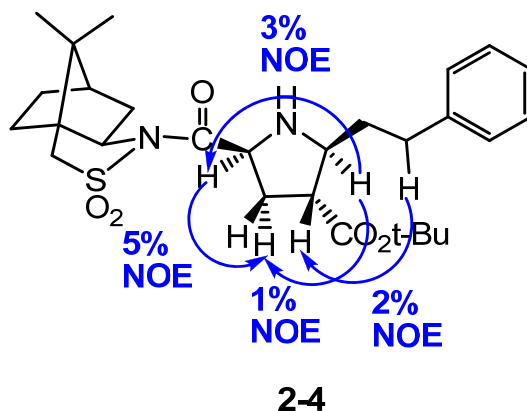
Exo-Selective [CN+C+CC] Coupling Conditions: A mixture of $\text{Cu}(\text{MeCN})_4\text{PF}_6$ (3.1 mg, 5 mol%, Aldrich) and dppb (4.0 mg, 5.5 mol%, Aldrich) in DMSO (2.0 mL) was stirred at rt for 1h. To the DMSO solution was added aldehyde (0.167 mmol, 1.0 equiv) followed by glycyI sultam (0.217 mmol, 1.3 equiv) and dipolarophile (0.501 mmol, 3.0 equiv) at room temperature. The reaction was stirred in the dark for the indicated time (monitored by ^1H NMR and/or TLC), at which point the mixture was partitioned between sat'd aq NH_4Cl (10 mL) and DCM (3×20 mL). The combined organic layers were washed with water (2×60 mL) and brine (60 mL), dried over MgSO_4 , filtered and concentrated under reduced pressure. The crude cycloadducts were purified by flash chromatography.

3.2.2 Characterization of Compounds



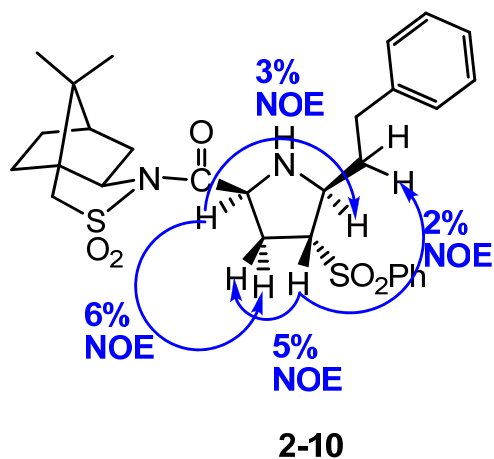
Methyl (2*S*,3*R*,5*S*)-5-[(10,10-dimethyl-3,3-dioxo-3 λ^6 -thia-4-azatricyclo[5.2.1.0^{1,5}]decan-4-yl)carbonyl]-2-(2-phenylethyl)pyrrolidine-3-carboxylate (2-3)

Pale yellow solid, total yield: 81% (dr = 6/1, minor component was characterized as endo by comparing its ¹H NMR data with that from: *Org. Lett.* **2006**, 8, 3647). m.p. 75-85 °C, (softens at 43 °C), R_f 0.42 in (1:1) hexanes/EtOAc. ¹H-NMR (CDCl₃) δ 7.29-7.16 (5H), 4.47 (dd, *J* = 9.0, 5.5 Hz, H2), 3.91 (t, *J* = 6.3 Hz, H5'), 3.67 (s, OMe), 3.51 (d, *J* = 13.9 Hz, ½ CH₂SO₂), 3.47 (d, *J* = 13.9 Hz, ½ CH₂SO₂), 3.29 (td, *J* = 8.3, 4.5 Hz, H5), 2.82 (ddd, *J* = 13.6, 10.9, 5.4 Hz, H7a), 2.67 (ddd, *J* = 13.9, 10.8, 5.9 Hz, H7b), 2.59 (td, *J* = 12.9, 8.9 Hz, H3 α), 2.51 (q, *J* = 8.4 Hz, H4), 2.15-1.96 (5H, H3 β + H6 + ?), 1.94-1.80 (4H), 1.46-1.34 (2H), 1.14 (s, Me), 0.98 (s, Me). ¹³C-NMR δ 173.9, 173.1, 141.7, 128.3, 128.2, 125.8, 65.1, 63.5, 59.8, 52.9, 51.9, 49.9, 48.7, 47.8, 44.5, 38.2, 36.4, 36.2, 33.2, 32.7, 26.3, 20.8, 19.8. HRMS (FAB) *m/z* (%) for C₂₅H₃₅N₂O₅S (MH⁺) calc. 475.2267, found 475.2252.



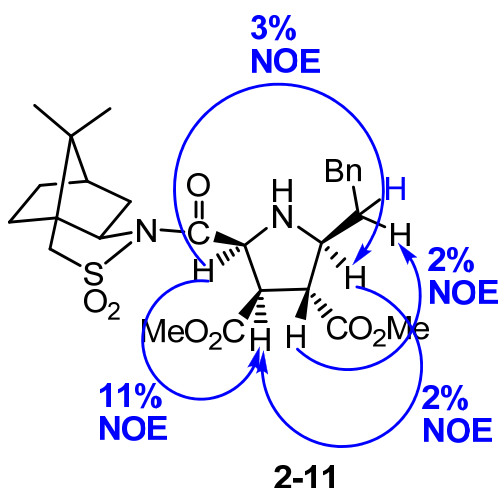
***tert*-Butyl (2*S*,3*R*,5*S*)-5-[(10,10-dimethyl-3,3-dioxo-3 λ^6 -thia-4-azatricyclo[5.2.1.0^{1,5}]decan-4-yl)carbonyl]-2-(2-phenylethyl)pyrrolidine-3-carboxylate (2-4)**

White solid, total yield: 95% (dr = 18/1), m.p. 73-90 °C (softens at 45 °C), R_f 0.56 in (1:1) hexanes/EtOAc. $^1\text{H-NMR}$ (CDCl_3) δ 7.29-7.15 (5H), 4.46 (dd $J = 9.1, 5.6$ Hz, H2), 3.90 (t, $J = 6.3$ Hz, H5'), 3.50 (d, $J = 13.8$ Hz, $\frac{1}{2}$ CH_2SO_2), 3.45 (d, $J = 13.8$ Hz, $\frac{1}{2}$ CH_2SO_2), 3.24 (td $J = 8.3, 4.7$ Hz, H5), 2.81 (ddd, $J = 13.5, 10.5, 5.4$ Hz, H7a), 2.70 (ddd, $J = 13.5, 10.1, 6.6$ Hz, H7b), 2.55 (dt, $J = 12.9, 8.6$ Hz, H3 α), 2.42 (q, $J = 8.6$ Hz, H4), 2.09-1.96 (3H), 2.04 (ddd, $J = 12.9, 8.7, 5.6$ Hz, H3 β), 1.93-1.81 (4H), 1.45 -1.33 (2H), 1.42 (s, 9H, *t*-Bu), 1.14 (s, Me), 0.96 (s, Me). $^{13}\text{C-NMR}$ δ 173.1, 172.6, 141.8, 128.3, 128.2, 125.7, 80.7, 65.0, 63.4, 60.0, 52.9, 51.5, 48.6, 47.7, 44.5, 38.2, 36.6, 36.1, 33.1, 32.6, 27.9, 26.3, 20.8, 19.8 HRMS (FAB) m/z (%) for $\text{C}_{28}\text{H}_{41}\text{N}_2\text{O}_5\text{S}$ (MH^+) calc. 517.2736, found 17.27319.



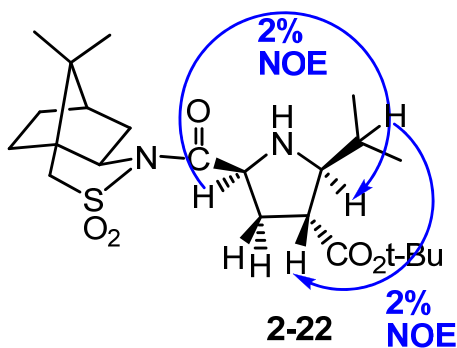
**4-{[(2*S*,4*R*,5*S*)-4-(Benzenesulfonyl)-5-(2-phenylethyl)pyrrolidin-2-yl]carbonyl}-
10,10-dimethyl-3λ⁶-thia-4-azatricyclo[5.2.1.0^{1,5}]decane-3,3-dione (2-10)**

White solid, yield: 90% yield, m.p. 110-125 °C (softens at 67 °C). R_f 0.65 in (1:1) hexanes/EtOAc. $^1\text{H-NMR}$ (C_6D_6) δ 7.69-6.85 (10H), 4.74 (t, $J = 7.5$ Hz, H2), 3.61-3.56 (H5), 3.47 (dd, $J = 7.7, 4.8$ Hz, H5'), 3.25 (dt, $J = 9.4, 6.4$ Hz, H4), 2.81 (ddd, $J = 13.8, 8.0, 6.0$ Hz, H3 α), 2.75-2.62 (H7a, CH_2SO_2), 2.52 (ddd, $J = 13.9, 9.4, 7.0$ Hz, H7b), 2.44 (NH), 2.15 (ddd, $J = 13.8, 9.3, 6.8$ Hz, H3 β), 1.95-1.86 (2H, H6a + ?), 1.80 (dd, $J = 13.7, 7.7$ Hz, 1H), 1.68 (ddd, $J = 13.7, 9.4, 4.9$ Hz H6b), 1.28-1.20 (2H), 1.07-0.98 (1H), 0.91 (s, Me), 0.72-0.66 (1H), 0.53-0.47 (1H), 0.37 (s, Me). $^{13}\text{C-NMR}$ δ 171.8, 141.1, 137.4, 133.8, 129.3, 128.8, 128.4, 128.3, 125.9, 68.6, 65.1, 59.5, 59.3, 52.8, 48.7, 47.7, 44.4, 38.1, 37.1, 33.4, 32.8, 32.7, 26.3, 20.7, 19.8. HRMS (FAB) m/z (%) for $\text{C}_{29}\text{H}_{37}\text{N}_2\text{O}_5\text{S}_2$ (MH^+) calc. 557.2144, found 557.21397.



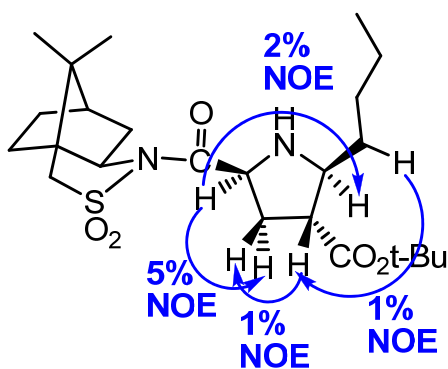
3,4-Dimethyl (2*S*,3*R*,4*R*,5*S*)-2-[(10,10-dimethyl-3,3-dioxo-3 λ^6 -thia-4-azatricyclo [5.2.1.0^{1,5}]decan-4-yl)carbonyl]-5- (2-phenylethyl)pyrrolidine-3,4-dicarboxylate (2-11)

White solid, total yield: 95% (dr = 20/1), m.p. 95-100 °C, (softens at 63 °C). R_f 0.59 in (1:1) hexanes/EtOAc. $^1\text{H-NMR}$ (CDCl_3) δ 7.29-7.15 (5H), 4.66 (d, $J = 8.2$ Hz, H2), 3.92 (dd, $J = 7.3, 5.4$ Hz, H5'), 3.80 (t, $J = 7.3$ Hz H3 α), 3.71 (s, OMe), 3.61 (s, OMe), 3.53 (d, $J = 13.8$ Hz, $\frac{1}{2}$ CH₂SO₂), 3.47 (d, $J = 13.7$ Hz, $\frac{1}{2}$ CH₂SO₂), 3.30 (td, $J = 7.8, 4.5$ Hz, H5), 3.14 (dd, $J = 8.0, 7.0$ Hz, H4), 2.80 (ddd, $J = 13.9, 10.4, 5.5$ Hz, H7a), 2.67 (ddd, $J = 13.9, 10.5, 6.1$ Hz, H7b), 2.13-2.02 (3H), 1.97-1.87 (4H), 1.45-1.33 (2H), 1.19 (s, Me), 0.98 (s, Me). $^{13}\text{C-NMR}$ δ 173.0, 171.7, 169.7, 141.6, 128.3, 128.2, 125.8, 65.2, 62.8, 62.1, 53.4, 52.9, 52.2, 52.1, 48.5, 47.7, 44.6, 37.7, 36.5, 32.9, 32.8, 26.4, 20.4, 19.9. HRMS (FAB) m/z (%) for C₂₇H₃₇N₂O₇S (MH⁺) calc. 533.2321, found 533.23070.



***tert*-Butyl (2*S*,3*R*,5*S*)-5-[(10,10-dimethyl-3,3-dioxo-3 λ ⁶-thia-4-azatricyclo
[5.2.1.0^{1,5}]decan-4-yl)carbonyl]-2-isopropylpyrrolidine-3-carboxylate (2-22)**

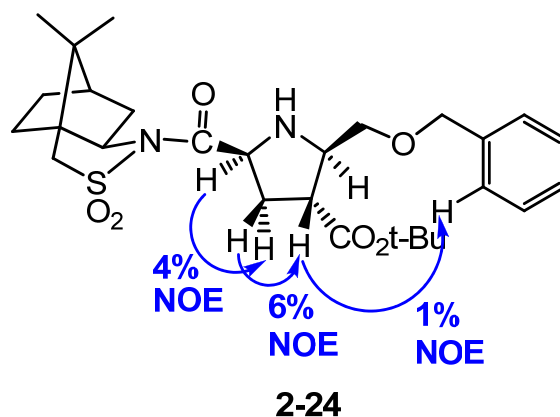
White solid, total yield: 84% yield (dr = 18/1), m.p. 80-85 °C (softens at 55 °C), R_f 0.60 in (1:1) hexanes/EtOAc. $^1\text{H-NMR}$ (CDCl_3) δ 4.42 (dd, $J = 8.0, 6.4$ Hz, H2), 3.88 (t, $J = 6.2$ Hz, H5'), 3.48 (d, $J = 13.9$ Hz, $\frac{1}{2}$ CH_2SO_2), 3.43 (d, $J = 13.9$ Hz, $\frac{1}{2}$ CH_2SO_2), 3.08 (t, $J = 7.2$ Hz, H5), 2.510-2.43 (H3 α , H4), 2.07-2.05 (2H), 2.02-1.95 (H3 β), 1.93-1.87 (3H), 1.81-1.73 (m, H6a) 1.43-1.36 (m, H6b), 1.43 (s, 9H, *t*-Bu), 1.42-1.32 (2H), 1.12 (s, Me), 1.00 (d, $J = 6.6$ Hz, 3H, $\text{CH}(\text{Me})_2$), 0.96 (s, Me), 0.95 (d, $J = 6.6$ Hz, 3H, $\text{CH}(\text{Me})_2$). $^{13}\text{C-NMR}$ δ 173.6, 173.1, 80.6, 69.6, 65.1, 60.1, 52.9, 48.9, 48.7, 47.8, 44.5, 38.2, 37.2, 32.7, 32.4, 27.9, 26.4, 20.8, 19.8, 19.6, 19.5. HRMS (FAB) m/z (%) for $\text{C}_{23}\text{H}_{39}\text{N}_2\text{O}_5\text{S}$ (MH^+) calc. 455.2580, found 455.2584.



2-23

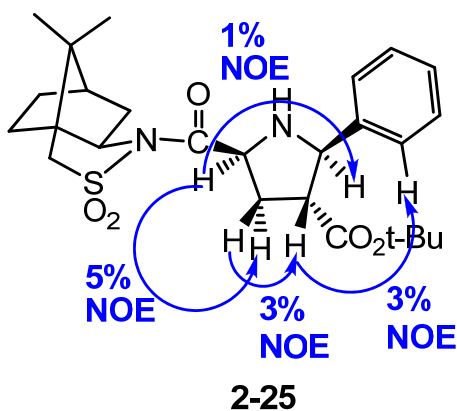
***tert*-Butyl (2*S*,3*R*,5*S*)-2-butyl-5-[(10,10-dimethyl- 3,3-dioxo-3 λ ⁶-thia-4-azatricyclo [5.2.1.0^{1,5}]decan-4-yl)carbonyl]pyrrolidine-3-carboxylate (2-23)**

White solid, yield: 60% yield, m.p. 97-99 °C, R_f 0.67 in (1:1) hexanes/EtOAc. ¹H-NMR (CDCl₃) δ 4.42 (dd, $J = 9.0, 5.9$ Hz, H2), 3.89 (t, $J = 6.3$ Hz, H5'), 3.49 (d, $J = 13.7$ Hz, $\frac{1}{2}$ CH₂SO₂), 3.44 (dd, d, $J = 13.9$ Hz, $\frac{1}{2}$ CH₂SO₂), 3.18 (td, $J = 7.8, 5.5$ Hz, H5), 2.53 (dt, $J = 12.9, 8.8$ Hz, H3 α), 2.33(q, $J = 8.8$ Hz, H4), 2.07-2.05 (2H), 2.00 (ddd, $J = 13.0, 9.0, 5.8$ Hz, H3 β), 1.93-1.88 (3H), 1.69-1.51 (2H, H6), 1.44(s, 9H, *t*-Bu), 1.46-1.24 (7H), 1.13 (s, Me), 0.96 (s, Me), 0.89 (t, $J = 7.1$ Hz, 3H, CH₂CH₃). ¹³C-NMR δ 173.2, 172.9, 80.6, 65.0, 63.9, 60.0, 52.8, 51.2, 48.6, 47.7, 44.4, 38.1, 36.4, 34.5, 32.6, 28.9, 28.0, 26.3, 22.6, 20.7, 19.7, 13.9. HRMS (FAB) m/z (%) for C₂₄H₄₁N₂O₅S (MH⁺) calc. 469.2736, found 469.2716.



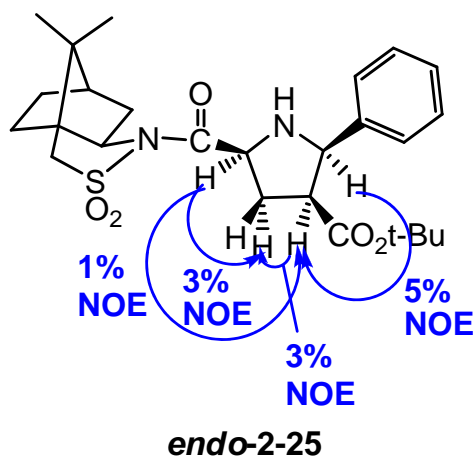
***tert*-Butyl (2*R*,3*R*,5*S*)-2-[(benzyloxy)methyl]-5- [(10,10-dimethyl-3,3-dioxo-3 λ ⁶-thia-4-azatricyclo[5.2.1.0^{1,5}]decan-4-yl)carbonyl]pyrrolidine-3-carboxylate (2-24)**

Yield: 83% yield, R_f 0.53 in (1:1) hexanes/EtOAc. ¹H-NMR (C₆D₆) δ 7.29-7.05 (5H), 4.97 (dd, J = 8.6, 6.4 Hz, H2), 4.33 (d, J = 12.4 Hz, $\frac{1}{2}$ OBn), 4.28 (d, J = 12.4 Hz, $\frac{1}{2}$ OBn), 3.66-3.57 (3H, H5, H6, and ?), 3.50 (dd, J = 7.6, 5.1 Hz, H5'), 3.06 (dt, J = 9.2, 7.4 Hz, H4), 2.86 (ddd, J = 12.9, 8.6, 7.8, Hz, H3 α), 2.72 (d, J = 13.8 Hz, $\frac{1}{2}$ CH₂SO₂), 2.66 (d, J = 13.7 Hz, $\frac{1}{2}$ CH₂SO₂), 2.24 (ddd, J = 12.6, 9.1, 6.2 Hz, H3 β), 1.92-1.85 (1H), 1.80 (dd, J = 13.9, 8.0 Hz, 1H), 1.36-1.23 (3H), 1.32 (s, 9H, *t*-Bu), 1.08-0.98 (1H), 0.93 (s, Me), 0.74-0.67 (1H), 0.55-0.50 (1H), 0.93 (s, Me). ¹³C-NMR δ 172.9, 172.6, 138.2, 128.3, 127.6, 127.5, 80.8, 73.1, 70.5, 65.1, 63.0, 60.1, 52.9, 48.7, 47.8, 47.1, 44.5, 38.2, 35.8, 32.7, 28.0, 26.4, 20.8, 19.8. HRMS (FAB) m/z (%) for C₂₈H₄₁N₂O₆S (MH⁺) calc. 533.2685, found 533.2665.



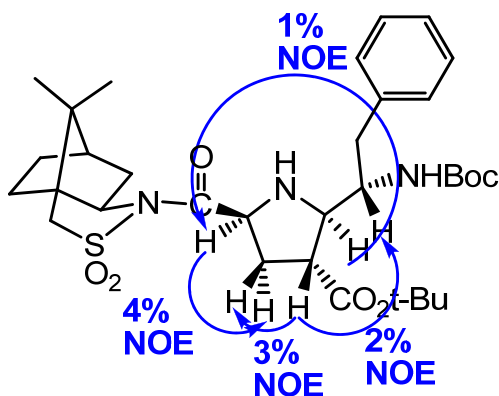
***tert*-Butyl (2*R*,3*R*,5*S*)-5-[(10,10-dimethyl-3,3-dioxo-3λ⁶-thia-4-azatricyclo[5.2.1.0]^{1,5}]decan-4-yl)carbonyl]-2-phenylpyrrolidine-3-carboxylate (2-25)**

White solid, yield: 80% yield, m.p. 75-80 °C (softens at 55 °C), R_f 0.68 in (1:1) hexanes/EtOAc. ¹H-NMR (CDCl₃) δ 7.47-7.24 (5H), 4.59 (dd, J = 9.4, 4.9 Hz, H₂) 4.31 (d, J = 9.0 Hz, H₅), 3.94 (t, J = 6.4 Hz, H_{5'}), 3.52 (d, J = 13.7 Hz, ½ CH₂SO₂), 3.46 (d, J = 13.7 Hz, ½ CH₂SO₂), 2.80 (q, J = 9.0 Hz, H₄), 2.62 (td, J = 13.3, 9.4 Hz, H_{3α}), 2.25 (ddd, J = 13.1, 8.4, 4.7 Hz, H_{3β}), 2.13-2.11 (2H), 1.94-1.87 (3H), 1.47-1.31 (2H), 1.34 (s, 9H, *t*-Bu), 1.17 (s, Me), 0.99 (s, Me). ¹³C-NMR δ 173.5, 172.1, 141.0, 128.4, 127.6, 127.1, 80.8, 67.3, 65.2, 59.5, 53.0, 52.9, 48.7, 47.8, 44.6, 38.3, 36.0, 32.8, 27.9, 26.4, 20.9, 19.9. HRMS (FAB) m/z (%) for C₂₆H₃₇N₂O₅S (MH⁺) calc. 489.2423, found 489.2412.



***tert*-Butyl (2*R*,3*S*,5*S*)-5-[(10,10-dimethyl-3,3-dioxo-3 λ ⁶-thia-4-azatricyclo[5.2.1.0^{1,5}]decan-4-yl)carbonyl]-2-phenylpyrrolidine-3-carboxylate (*endo*-2-25)**

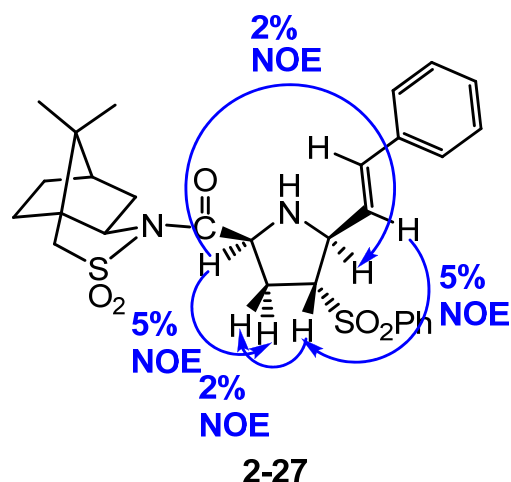
Yield: 10 %, R_f 0.61 in (1:1) hexanes/EtOAc. ¹H-NMR (CDCl₃) δ 7.37-7.21 (5H), 4.50 (d, J = 8.2 Hz, H5) 4.43 (t, J = 8.50 Hz, H2), 3.97 (t, J = 6.3 Hz, H5'), 3.52 (d, J = 13.8 Hz, $\frac{1}{2}$ CH₂SO₂), 3.48 (d, J = 13.8 Hz, $\frac{1}{2}$ CH₂SO₂), 3.30 (q, J = 7.8 Hz, H4), 3.14 (NH), 2.63(dt, J = 13.1, 8.0 Hz, H3 α), 2.18 (ddd, J = 13.1, 8.8, 6.8 Hz, H3 β), 2.14-2.12 (2H), 1.97-1.87 (2H), 1.47-1.31 (2H), 1.16 (s, Me), 1.00 (s, *t*-Bu), 0.98 (s, Me). ¹³C-NMR δ 171.8, 139.5, 128.1, 127.4, 127.3, 80.5, 65.3, 65.1, 60.9, 53.0, 50.8, 48.7, 47.8, 44.5, 38.2, 35.8, 32.7, 28.0, 26.4, 20.8, 19.9.



2-26

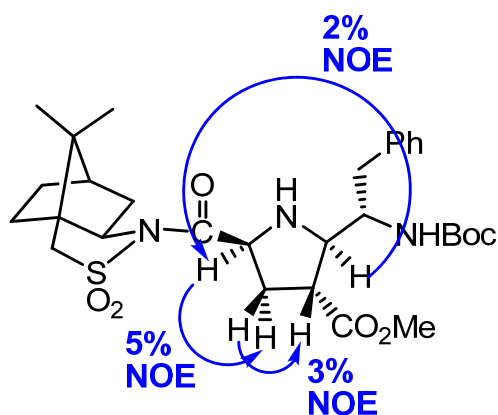
***tert*-Butyl (2*R*,3*R*,5*S*)-2-[(1*S*)-1-[[*tert*-butoxy]carbonyl]amino]-2-phenylethyl]-5-[(10,10-dimethyl-3,3-dioxo-3 λ^6 -thia-4-azatricyclo[5.2.1.0^{1,5}]decan-4-yl)carbonyl]pyrrolidine-3-carboxylate (2-26)**

Pale yellow solid, total yield: 75% (dr = 13/1), m.p. 108-120 °C (softens at 75 °C), R_f 0.58 in (1:1) hexanes/EtOAc. $^1\text{H-NMR}$ (C_6D_6) δ 7.35-6.95 (5H), 4.92(dd, $J = 8.3, 6.4$ Hz, H2), 4.39 (d, $J = 8.2$ Hz, NHBoc), 4.26 (br, H6), 3.53 (dd, $J = 7.2, 5.1$ Hz, H5'), 3.46 (br, H5), 3.25-3.22 (H7 α) 3.06-3.00 (H4), 2.72(d, $J = 13.8, \frac{1}{2} \text{CH}_2\text{SO}_2$), 2.66 (d, $J = 13.9$ Hz, $\frac{1}{2} \text{CH}_2\text{SO}_2$), 2.65-2.54 (2H, H3 α , H7b), 2.32-2.24 (H3 β), 1.90-1.78 (2H), 1.46-1.26 (3H), 1.37 (s, 3H, *t*-Bu), 1.36 (s, 6H, *t*-Bu), 1.11-1.01 (1H), 0.92 (s, Me), 0.75-0.69 (1H), 0.56-0.48 (1H), 0.37 (s, Me). $^{13}\text{C-NMR}$ δ 173.1, 172.6, 155.3, 137.5, 129.6, 128.2, 126.2, 81.0, 79.1, 65.4, 65.2, 60.1, 54.7, 53.0, 48.7, 48.3, 47.8, 44.5, 38.2, 36.0, 32.7, 28.3, 28.0, 26.4, 20.8, 19.9. HRMS (FAB) m/z (%) for $\text{C}_{33}\text{H}_{50}\text{N}_3\text{O}_7\text{S}$ (MH^+) calc. 632.3369, found 632.3370.



4-[(2*S*,4*R*,5*S*)-4-(Benzenesulfonyl)-5-[(*E*)-2-phenylethenyl]pyrrolidin-2-yl] carbonyl}-10,10-dimethyl-3 λ^6 -thia-4-azatricyclo[5.2.1.0^{1,5}]decane-3,3-dione (2-27)

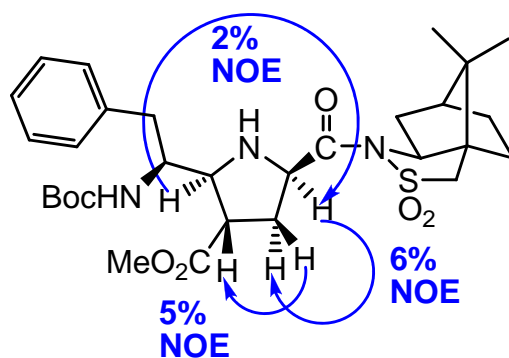
Pale yellow solid, yield: 60 %, m.p. 179-182 °C, R_f 0.42 in (1:1) hexanes/EtOAc. $^1\text{H-NMR}$ (CDCl_3) δ 7.90-7.14 (10H), 6.33 (d, $J = 15.8$ Hz, H7), 5.94 (dd, $J = 15.8, 7.4$ Hz, H₆), 4.50 (dd, $J = 8.2, 6.3$ Hz, H2), 4.15 (t, $J = 7.4$ Hz, H5), 3.88 (t, $J = 6.3$ Hz, H5'), 3.54 (dt, $J = 9.2, 7.4$ Hz, H4), 3.51 (d, $J = 13.8$ Hz, $\frac{1}{2}$ CH_2SO_2), 3.45 (d, $J = 13.98$ Hz, $\frac{1}{2}$ CH_2SO_2), 2.85 (ddd, $J = 13.9, 8.2, 7.4$ Hz, H3 α), 2.29 (ddd, $J = 13.9, 9.2, 6.2$ Hz, H3 β), 2.06-2.03 (2H), 1.94-1.87 (3H), 1.43-1.31 (2H), 1.10 (s, Me), 0.96 (s, Me). $^{13}\text{C-NMR}$ 172.0, 138.0, 136.1, 133.9, 132.8, 129.2, 128.8, 128.3, 127.8, 127.6, 126.5, 68.1, 65.2, 62.2, 58.9, 52.9, 48.8, 47.8, 44.5, 38.2, 32.7, 32.5, 26.3, 20.8, 19.8. HRMS (FAB) m/z (%) for $\text{C}_{29}\text{H}_{35}\text{N}_2\text{O}_5\text{S}_2$ (MH^+) calc. 555.1987, found 555.1957.



2-28

Methyl (2*R*,3*R*,5*S*)-2-[(1*S*)-1-[[*tert*-butoxy]carbonyl]amino]-2-phenylethyl]-5-[(10,10-dimethyl-3,3-dioxo-3 λ^6 -thia-4-azatricyclo[5.2.1.0^{1,5}]decan-4-yl)carbonyl]pyrrolidine-3-carboxylate (2-28)

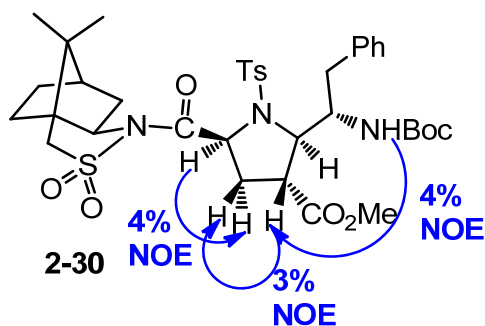
White solid, total yield: 95% (dr = 16/1), m.p. 95-105 °C, (softens at 72 °C), R_f 0.48 in (1:1) hexanes/EtOAc. $^1\text{H-NMR}$ (CDCl_3) δ 7.29-7.19 (5H), 4.53 (dd, $J = 8.9, 6.2$ Hz, H2), 4.40 (d, $J = 9.4$ Hz, NHBoc), 3.97-3.90 (H₆), 3.91 (t, $J = 6.25$ Hz, H5'), 3.65 (s, OMe), 3.51 (d, $J = 13.8$ Hz, $\frac{1}{2}$ CH₂SO₂), 3.46 (d, $J = 13.8$, $\frac{1}{2}$ CH₂SO₂), 3.35 (t, $J = 7.9$ Hz, H5), 3.10 (dd, $J = 13.9, 4.1$ Hz, H7a), 2.83 (q, $J = 7.8$ Hz, H4), 2.76 (dd, $J = 13.6, 8.0$ Hz, H7b), 2.50 (td, $J = 12.9, 8.4$ Hz, 1H, H3 α), 2.16 (ddd, $J = 13.2, 8.8, 6.1$ Hz, H3 β), 2.10-2.08(2H), 1.96-1.89(3H), 1.43(s, 6H, *t*-Bu), 1.32 (s, 3H, *t*-Bu), 1.46-1.18 (3H), 1.13 (s, Me), 0.97 (s, Me). $^{13}\text{C-NMR}$ δ 174.7, 172.7, 155.3, 137.4, 129.5, 128.3, 126.3, 79.1, 66.5, 65.2, 60.1, 54.6, 52.9, 52.0, 48.7, 47.7, 47.2, 44.5, 38.2, 36.0, 32.7, 29.6, 28.2, 26.3, 20.8, 19.8. HRMS (FAB) m/z (%) for C₃₀H₄₄N₃O₇S (MH⁺) calc. 590.2900, found 590.2909.



2-29

Methyl (2*S*,3*S*,5*R*)-2-[(1*S*)-1-{{(*tert*-butoxy)carbonyl}amino}-2-phenylethyl]-5-[(10,10-dimethyl-3,3-dioxo-3 λ^6 -thia-4-azatricyclo[5.2.1.0^{1,5}]decan-4-yl)carbonyl]pyrrolidine-3-carboxylate (2-29)

White solid, total yield: 60% (dr = 5/1), m.p. 110-125 °C (softens at 70 °C), R_f 0.54 in (1:1) hexanes/EtOAc. $^1\text{H-NMR}$ (CDCl_3) δ 7.28-7.16 (5H), 6.02 (d, $J = 9.2$ Hz, NHBoc), 4.52 (dd, $J = 8.6, 5.3$ Hz, H_2), 4.02 (q, $J = 8.4$ Hz, H_6), 3.92 (t, $J = 6.3$ Hz H_5), 3.61 (s, OMe), 3.50 (d, $J = 13.8$ Hz $\frac{1}{2}$ CH_2SO_2), 3.45 (d, $J = 13.7$ Hz $\frac{1}{2}$ CH_2SO_2), 3.48 (dd, $J = 7.2, 1.9$ Hz H_5), 2.95 (dd, $J = 13.7, 8.4$ Hz H_{7a}), 2.94 (q, $J = 7.8$ Hz H_4), 2.71 (dd, $J = 13.7, 8.4$ Hz, H_{7b}), 2.42 (ddd, $J = 13.1, 8.2, 7.8$ Hz, H_{3a}), 2.18 (ddd, $J = 13.3, 8.4, 5.3$ Hz, $\text{H}_{3\beta}$), 2.09-2.03 (2H), 1.93-1.87 (3H), 1.46-1.21 (3H), 1.40 (s, 9H, *t*-Bu), 1.13 (s, Me), 0.97 (s, Me). $^{13}\text{C-NMR}$ δ 174.0, 173.8, 156.0, 138.3, 129.1, 128.4, 126.2, 78.6, 65.3, 62.4, 59.3, 53.8, 53.0, 52.0, 48.6, 47.8, 45.6, 44.4, 40.1, 38.2, 34.3, 32.7, 28.4, 26.4, 20.8, 19.8. HRMS (FAB) m/z (%) for $\text{C}_{30}\text{H}_{44}\text{N}_3\text{O}_7\text{S}$ (MH^+) calc. 590.2900, found 590.2908.



Methyl (2*R*,3*R*,5*S*)-1-(toluene-4-sulfonyl)-2-[(1*S*)-1-[(tert-butoxy)carbonyl]amino]-2-phenylethyl]-5-[(10,10-dimethyl-3,3-dioxo-3 λ ⁶-thia-4-azatricyclo[5.2.1.0^{1,5}]decan-4-yl)carbonyl]pyrrolidine-3-carboxylate (2-30)

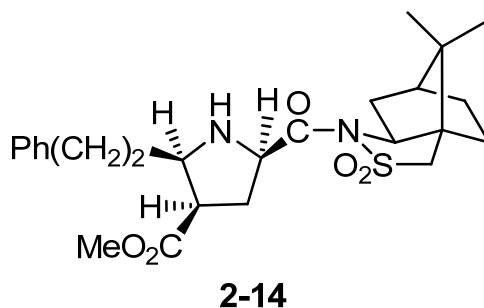
A mixture of **2-28** (110 mg, 0.187 mmol), TsCl (160 mg, 0.840 mmol – recrystallized from hexanes), and TEA (225 mL, 1.617 mmol) in DCM (1 mL) was stirred at rt for 16 h. The reaction mixture was partitioned between DCM (3 x 10 mL) and H₂O (5 mL). The combined organic extracts were washed with brine (20 mL), dried with MgSO₄, filtered and concentrated to give the crude product, which was purified by flash chromatography (hexanes-EtOAc) to give 118 mg of **2-30** as a white solid (85% yield). m.p. 225-227 °C (dec), R_f 0.64 in (1:1) hexanes/EtOAc. ¹H-NMR (CD₃COCD₃) δ 7.76 (d, J = 8.2 Hz, 2H), 7.41-7.14 (7H), 6.12 (d, J = 7.6 Hz, NHBoc), 5.07 (t, J = 8.8 Hz, H₂), 4.20 (d, J = 9.4 Hz, H₅), 4.03 (t, J = 6.0, Hz, H_{5'}), 3.82 (d, J = 13.9 Hz, $\frac{1}{2}$ CH₂SO₂), 3.81-3.78 (H₆), 3.72 (d, J = 13.9 Hz, $\frac{1}{2}$ CH₂SO₂), 3.25 (s, OMe), 3.10 (d, J = 6.8 Hz, H₄), 2.85-2.75 (6H), 2.44 (s, MeAr), 2.15-1.89 (4H), 1.68-1.63 (1H), 1.46-1.40 (1H), 1.21 (s, 9H, *t*-Bu) 1.16 (s, Me), 1.05 (s, Me). ¹³C-NMR (CD₃COCD₃), δ 173.3, 172.0, 157.8, 145.6, 142.1, 137.2, 131.5, 131.3, 129.8, 129.7, 127.5, 79.8, 70.7, 66.9, 63.8, 58.1, 54.2, 53.3, 50.8, 49.4, 48.0, 46.5, 39.8, 39.6, 34.0, 33.8, 29.4, 27.8, 22.4, 22.3, 21.0. HRMS (FAB) m/z (%) for C₃₇H₅₀N₃O₉S₂ (MH⁺) calc. 744.2988, found 744.2979.

3.3 Endo-Products

3.3.1 Reaction Procedures

Endo-Selective [CN+C+CC] Coupling Conditions: To a stirred mixture of glycyll sultam (0.37 mmol, 1.1 equiv) and AgOAc (5 mol %) in dry THF (1 mL) was added aldehyde (0.33 mmol, 1.0 equiv) followed by dipolarophile (3.0 equiv) at room temperature. The reaction was stirred in the dark under Ar for the indicated time (TLC monitoring of aldehyde and/or ^1H NMR monitoring of imine), at which point the mixture was partitioned between sat'd aq NH_4Cl (5 mL) and DCM (4×10 mL). The combined organic layers were dried over Na_2SO_4 , filtered and concentrated under reduced pressure. The crude cycloadducts were purified by flash chromatography.

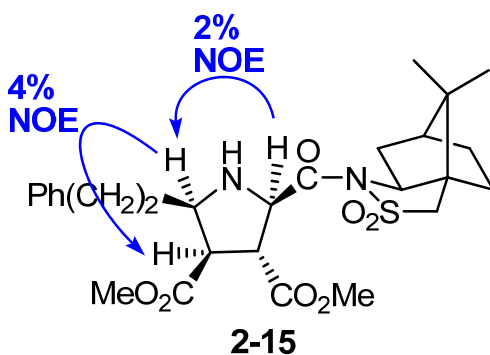
3.3.2 Characterization of Compounds



Methyl (2*R*,3*R*,5*R*)-5-[(10,10-dimethyl-3,3-dioxo-3 λ ⁶-thia-4-azatricyclo[5.2.1.0]^{1,5}] decan-4-yl)carbonyl]-2-(2-phenylethyl)pyrrolidine-3-carboxylate (2-14)

Pale yellow solid, yield: 82%, m.p. 147-150 °C (decomp), R_f 0.51 (1:1 hexanes/EtOAc). ^1H -NMR (600 MHz) δ 7.28-7.18 (m, 5H), 4.34 (d,d $J = 9.5, 6.8$ Hz, 1H), 3.94 (dd, $J = 7.2, 5.2$ Hz, 1H), 3.65 (s, 3H), 3.49 (d, $J = 13.7$ Hz, 1H), 3.45 (d, $J =$

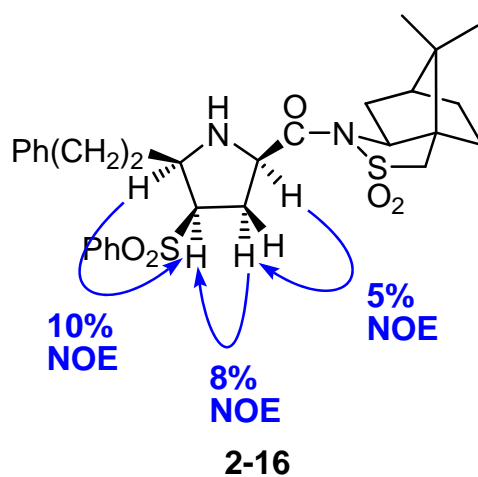
13.7 Hz, 1H), 3.28 (q, $J = 6.8$ Hz), 3.00 (dt, $J = 7.6, 3.9$ Hz, 1H) 2.86-2.72 (m, 2H), 2.58 - 2.52 (m, 1H), 2.14-2.08 (m, 3H), 1.95-1.87 (m, 3H), 1.80 (q, $J = 7.6$ Hz 2H), 1.46-1.35 (m, 2H), 1.14 (s, 3H), 0.97 (s, 3H). ^{13}C -NMR (50 MHz) δ 174.2, 171.9, 141.6, 128.3, 125.8, 65.0, 62.6, 60.8, 51.5, 48.6, 47.8, 47.4, 44.4, 38.0, 36.0, 33.6, 33.1, 32.5, 26.4, 20.6, 19.8. HRMS (FAB) m/z (%) for $\text{C}_{25}\text{H}_{35}\text{N}_2\text{O}_5\text{S}$ (MH^+) calc. 475.2267, found 475.2257.



3,4-Dimethyl (2*R*,3*R*,4*R*,5*R*)-2-[(10,10-dimethyl-3,3-dioxo-3 λ ⁶-thia-4-azatricyclo [5.2.1.0^{1,5}]decan-4-yl)carbonyl]-5-(2-phenylethyl)pyrrolidine-3,4-dicarboxylate (2-15)

White solid, total yield: 88 % (49% major, 29% minor, 10% another minor isomer was not fully characterized), R_f 0.59 (1:1 hexanes/EtOAc). ^1H -NMR (400 MHz) δ 7.25-7.13 (m, 5H), 4.63 (d, $J = 8.1$ Hz, 1H, minor), 4.45 (d, $J = 7.3$ Hz, 1H, **2-15**), 3.94 (dd, $J = 7.6, 4.9$ Hz, 1H, **2-15**), 3.89 (dd, $J = 7.5, 5.3$ Hz, 1H, minor), 3.77 (t, $J = 7.4$ Hz, 1H, minor), 3.68 (s, 3H, minor), 3.66 (s, 3H, **2-15**), 3.64 (s, 3H, **2-15**), 3.59 (s, 3H, minor), 3.65-3.62 (m, 1H, **2-15**), 3.50 (d, $J = 13.7$ Hz, 1H, minor), 3.48 (d, $J = 13.8$ Hz, 1H, **2**), 3.45 (d, $J = 13.8$ Hz, 1H, **2-15**), 3.44 (d, $J = 13.7$ Hz, 1H, **2**), 3.43 (dd, $J = 8.4, 5.3$ Hz, 1H, **2**), 3.29 (dd, $J = 7.6, 5.9$ Hz, 1H, **2**), 3.27 (dd, $J = 8.2, 4.6$ Hz, 1H, minor), 3.12 (t, $J = 7.5$ Hz, 1H, minor), 2.81-2.75 (m, 1H), 2.68-2.61 (m, 1H), 2.16-1.98 (m, 3H), 1.93-1.85 (m,

3H), 1.78-1.67 (m, 1H), 1.43-1.33 (m, 2H), 1.17 (s, 3H, minor), 1.16 (s, 3H, **2-15**), 0.96 (s, 3H, **2-15**), 0.95 (s, 3H, minor). ^{13}C -NMR (100MHz) δ 172.9 (minor), 172.2 (**2-15**), 172.0 (**2-15**), 171.5 (minor), 170.7 (**2-15**), 169.5 (minor), 141.4 (**2-15**), 128.2, 128.1, 125.7, 65.2 (**2-15**), 65.0 (minor), 63.0 (**2-15**), 62.6 (minor), 62.0 (minor), 61.6 (**2-15**), 53.4 (minor), 53.2 (**2-15**), 52.8 (**2-15**), 52.7 (minor) 52.3 (**2-15**), 52.1 (**2-15**), 52.0 (minor), 51.8 (**2-15**), 51.4, 48.4 (**2-15**), 47.6 (**2-15**), 44.5 (**2-15**), 38.0 (minor), 37.6 (minor), 36.4 (minor), 33.2 (**2-15**), 33.1 (**2-15**), 32.8 (minor), 32.7 (minor), 32.6, 26.2, 20.5 (**2-15**), 20.2 (minor), 19.8 (minor) 19.7 (**2-15**). HRMS (FAB) m/z (%) for $\text{C}_{27}\text{H}_{37}\text{N}_2\text{O}_7\text{S}$ (MH^+) calc. 533.2321, found 533.2317.

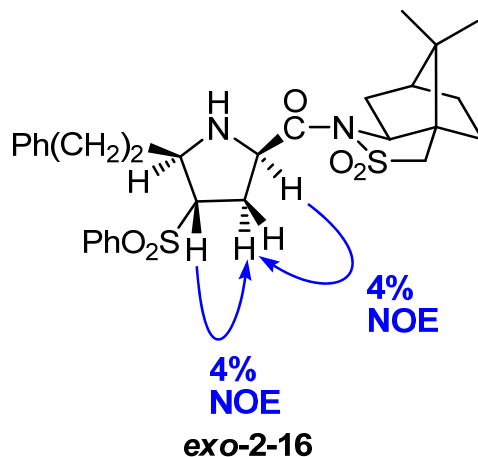


**4-[[*(2R,4R,5R)*-4-(Benzenesulfonyl)-5-(2-phenylethyl)pyrrolidin-2-yl]carbonyl]-
10,10-dimethyl-3 λ^6 -thia-4-azatricyclo[5.2.1.0 1,5]decane-3,3-dione (**2-16**)**

Pale yellow solid, yield: 83 %, m.p. 156-159 °C (decomp), R_f 0.42 (1:1 hexanes/EtOAc). ^1H -NMR (600 MHz) δ 7.81 (d, $J = 7.3$, 2H), 7.62 (t, $J = 7.6$, 1H), 7.52 (t, $J = 7.6$, 2H), 7.28-7.16 (m, 5H), 4.27 (t, $J = 8.3$ Hz, 1H), 3.94 (dd, $J = 7.6$, 4.9 Hz, 1H), 3.59 (q, $J = 8.3$, 6.2 Hz, 1H), 3.44 (s, 2H), 3.32 (ddd, $J = 10.0$, 6.4, 4.4 Hz, 1H), 2.95 (ddd, $J = 13.7$, 9.0, 5.4 Hz, 1H), 2.76 (dt, $J = 13.7$, 8.0, 1H), 2.48 (dt, $J = 14.4$, 8.6,

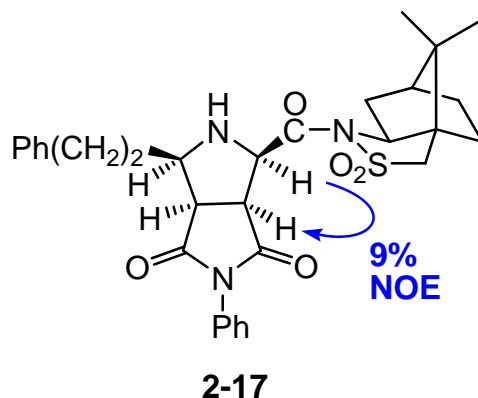
Chapter 3: Experimental

¹H) 2.44-2.38 (m, 1H), 2.35-2.29 (m, 1H), 2.18-2.08 (m, 3H), 1.95-1.88 (m, 3H), 1.46-1.37 (m, 2H), 1.04 (s, 3H), 0.96 (s, 3H). ¹³C-NMR (50 MHz) δ 170.6, 141.4, 139.8, 133.5, 129.2, 128.6, 128.2, 128.0, 125.8, 65.6, 65.1, 62.0, 59.7, 52.8, 48.7, 47.7, 44.4, 38.1, 34.7, 33.7, 32.5, 31.8, 26.3, 20.6, 19.8. HRMS (FAB) *m/z* (%) for C₂₉H₃₇N₂O₅S₂ (MH⁺) calc. 557.2144, found 557.2140.



4-[(2*R*,4*S*,5*R*)-4-(Benzenesulfonyl)-5-(2-phenylethyl)pyrrolidin-2-yl]carbonyl]-10,10-dimethyl-3λ⁶-thia-4-azatricyclo[5.2.1.0^{1,5}]decane-3,3-dione (*exo*-2-16)

Minor isomer: Pale yellow solid, yield: 11 %, *R_f* 0.50 (1:1 hexanes/EtOAc). ¹H-NMR (600 MHz) δ 7.78 (d, *J* = 7.5 Hz, 2H), 7.64 (t, *J* = 7.5 Hz, 1H), 7.52 (t, *J* = 7.8 Hz, 2H) 7.29- 7.12 (m, 5H), 4.30 (t, *J* = 7.7 Hz, 1H), 3.88 (dd, *J* = 6.8, 5.8 Hz, 1H), 3.50 (d, *J* = 13.7 Hz, 1H) 3.48-3.45 (m, 1H), 3.44 (d, *J* = 13.7 Hz, 1H), 3.31 (dt, *J* = 9.7, 6.4 Hz, 1H), 2.78 (ddd, *J* = 13.6, 9.5, 5.0 Hz, 1H), 2.71 (ddd, *J* = 14.0, 8.0 Hz, 1H), 2.62 (dt, *J* = 13.9, 8.2 Hz 1H), 2.11 (ddd, *J* = 14.1, 9.7, 7.3 Hz 1H), 2.07-2.05 (m, 2H), 1.95-1.87 (m, 4H), 1.80-1.74 (m, 1H), 1.44-1.34 (m, 2H), 1.08 (s, 3H), 0.97 (s, 3H). HRMS (FAB) *m/z* (%) for C₂₉H₃₇N₂O₅S₂ (MH⁺) calc. 557.2144, found 557.2120.



4-{{(1*R*,3*R*,3*aR*,6*aS*)-4,6-dioxo-5-phenyl-3-(2-phenylethyl)-tetrahydro-1*H*-pyrrolo[3,4-*c*]pyrrol-1-yl}carbonyl}-10,10-dimethyl-3λ⁶-thia-4-azatricyclo[5.2.1.0^{1,5}]decane-3,3-dione (2-17)

White solid, total yield: 83%, m.p. 286-289 °C (decomp), R_f 0.42 (24:1 CH₂Cl₂/MeOH). ¹H-NMR (600 MHz) δ 7.45-7.17 (m, 10H), 4.53 (t, $J = 8.5$ Hz, 1H), 3.96 (dd, $J = 7.7, 4.8$ Hz, 1H), 3.90 (t, $J = 7.5$ Hz, 1H), 3.56 (d, $J = 13.7$ Hz, 1H) 3.51 (d, $J = 13.7$ Hz, 1H), 3.42 (t, $J = 7.8$ Hz, 1H), 3.40-3.33 (m, 1H), 2.89(dt, $J = 9.0, 6.6$ Hz, 2H), 2.53-2.48 (m, 1H), 2.27-2.20 (m, 2H), 2.01 (dd, $J = 13.9, 7.9$ Hz, 1H), 1.96-1.85 (m, 4H), 1.45-1.34 (m, 2H), 1.30 (s, 3H), 0.96 (s, 3H). ¹³C-NMR (50 MHz) δ 174.9, 174.6, 167.8, 141.2, 131.6, 129.1, 128.7, 128.5, 128.4, 126.6, 126.0, 65.5, 63.4, 61.1, 53.1, 50.7, 49.1, 48.7, 47.9, 44.5, 37.3, 33.6, 32.9, 32.7, 26.6, 20.3, 20.1. HRMS (FAB) m/z (%) for C₃₁H₃₆N₃O₅S (MH⁺) calc. 562.2376, found 562.2376.

Section B

4 Introduction to Kaitocephalin

As the first natural glutamate receptor antagonist, kaitocephalin (Figure 4.1) protects against neuronal death resulting from NMDA and AMPA/KA glutamate receptors. Its potent biological activities have sparked renewed interest in the systematic synthesis and study of the structure-property relationships.

4.1 Biological Background

In 1997, kaitocephalin was isolated from *Eupenicillium Shearii* PF 1191 by Seto and Shin-ya *et al.*²⁵ A screening test for glutamate receptor antagonists to treat brain strokes indicated that kaitocephalin was the first (*S*)-amino-3-hydroxy-5-methyl-4-isoxazolepropionic acid (AMPA) and kainic acid (KA) antagonist isolated from nature. It protected chick primary telencephalic and rat hippocampal neurons from kainate, AMPA, and *N*-methyl-daspartic acid (NMDA) excitotoxicity, and inhibition of the Ca²⁺ influx elicited by AMPA and NMDA.²⁶ Based on the EC50 value, kaitocephalin has almost the same degree of efficacy as AMPA/KA antagonist CNQX bearing a quinoxalinedione skeleton. However, CNQX exhibited cytotoxicity, while kaitocephalin showed no cytotoxic effect.²⁷

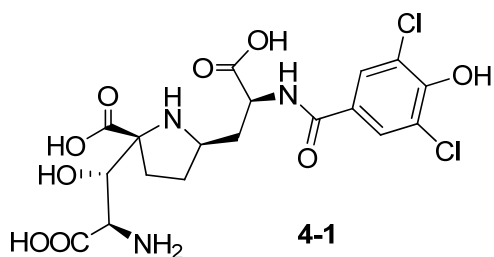


Figure 4.1 The molecular structure of kaitocephalin.

Since AMPA/KA antagonist showed potency in preventing neuronal death, kaitocephalin has promising potential as a lead compound for developing therapeutic drugs for use in treating ischemic stroke.²⁸

4.2 Characterization

Kaitocephalin was characterized by the Kazuo Shin-ya group.²⁹ It possesses a tri-substituted proline skeleton assembled by serine and N-acylalanine moieties at the α -position. In 2001, kaitocephalin was converted to a protected lactam **4-2** via Boc protection and methylation (Figure 4.2). The absolute structure of kaitocephalin was assigned as *2S,3S,4R,7R,9S* based on the assignment of **4-2** and its diastereomeric MTPA esters **4-3** (Figure 4.2).³⁰

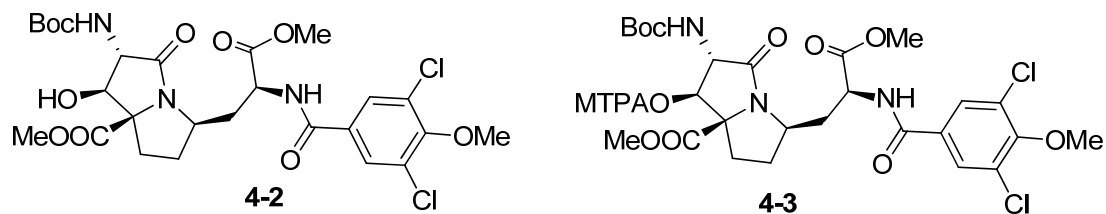


Figure 4.2 Compound **4-2** (left) a lactam derivative of **4-1**, and compound **4-3** (right) an MTPA ester of lactam **4-2**.

In 2001, Ma's group synthesized what was thought to be kaitocephalin with the $2S,3S,4R,7R,9S$ configuration (Figure 4.3).³¹ The absolute stereochemistry was established as $2S,3S,4R,7R$ by single-crystal X-ray analysis compound **4-5** (Figure 4.3).

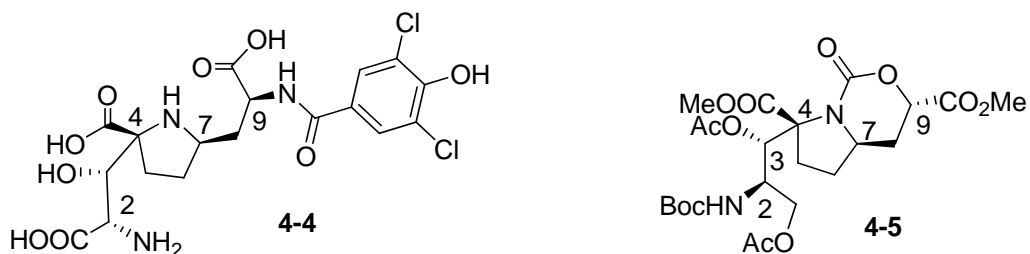


Figure 4.3 C2-epi-kaitocephalin **4-4** (left) and a protected derivative **4-5** (right).

Ma failed to notice his spectra were different from those of natural kaitocephalin, thus he lost the chance to point out the previous incorrect assignment for C2 of isolated natural kaitocephalin. Later, Ma explained that racemization in the last step gave a 1:1 mixture of $(2R,3S,4R,7R,9S)$ - and $(2S,3S,4R,7R,9S)$ -isomers.³²

In 2002, the Kitahara group also prepared $(2S,3S,4R,7R,9S)$ -Kaitocephalin.³³ They found that the retention time on HPLC separation and ¹H NMR spectra of their synthetic “kaitocephalin” were not identical with those of natural kaitocephalin.³⁴ Table 1.1. outlines the different chemical shifts of C2- and C3- protons and their coupling constants (³J_{C₂H-C₃H}) in ¹H NMR between the synthetic and natural kaitocephalin.

Table 4.1 Comparison of ¹H NMR spectral data of stereoisomers of kaitocephalin.

	2H	3H
Synthesized Kaitocephalin ($2S,3S,4R,7R,9S$)	3.81 (d), J = 4.3 Hz	4.3 (d), J = 4.3 Hz
Natural Kaitocephalin	4.16 (s), J = 0 Hz	4.41 (s), J = 0 Hz

In order to assign the stereochemistry unambiguously, Kitahara's group prepared (2*S*,3*R*)-kaitocephalin, (2*S*,9*R*)-Kaitocephalin, and analogues of kaitocephalin with the absence of C8-C10 moiety. As a result, they correctly assigned the configurations of kaitocephalin as 2*R*,3*S*,4*R*,7*R*,9*S* through comparing their ¹H NMR spectra data with that of natural kaitocephalin. They confirmed their assignment of the configurations by preparing (2*R*,3*S*,4*R*,7*R*,9*S*)-kaitocephalin. The prepared (2*R*,3*S*,4*R*,7*R*,9*S*)-kaitocephalin has the same ¹H NMR spectral data, retention time on HPLC and specific rotation as those of natural kaitocephalin, as expected.³⁵

From their deuteration model experiment, they suspected that a possible epimerization at C-2 of natural kaitocephalin occurred during the derivatization to lactam **4-2** for structure assignment.²⁹

4.3 Total Synthesis

The availability of extremely small amounts from natural sources and promising bio-reactivity makes kaitocephalin an attractive synthetic target. Up to now, four synthetic groups have finished the synthesis of kaitocephalin (**4-1**) and C2-epi-kaitocephalin (**4-4**) (Table 4.2). As mentioned earlier, Ma's and Kitahara's groups have done a total synthesis of (2*S*)-kaitocephalin due to the wrong stereochemistry assignment. Kitahara's synthesis of (2*S*)-kaitocephalin led to the correct assignment of kaitocephalin. Later, the Kitahara,³⁵ Ohfuné³⁶ and Chamberlin³⁷ groups separately published novel routes for the synthesis of (2*R*)-kaitocephalin. Up to now, no biosynthesis of kaitocephalin has been reported.

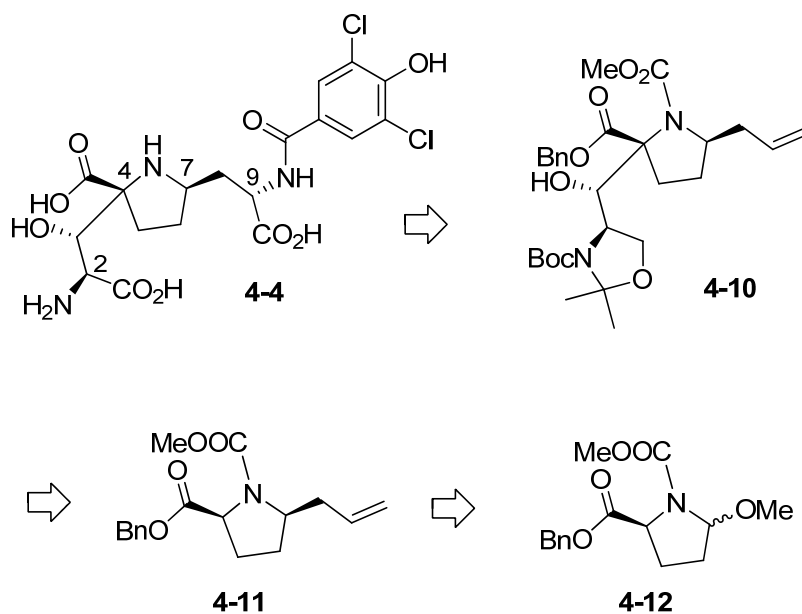
Table 4.2 Reported total syntheses of kaitocephalin and C2-epi-kaitocephalin

(2 <i>R</i>)-Kaitocephalin (4-1)	(2 <i>S</i>)-Kaitocephalin (4-4)		
(2 <i>S</i>)-Kaitocephalin (4-4)			
2001 / Ma / 25 steps / 1.1% / from (<i>S</i>)-pyroglutamic acid (4-6)			
2002 / Kitahara / 15 steps / 0.21% / from (<i>S</i>)-proline (4-7)			
(2 <i>R</i>)-Kaitocephalin (4-1)			
2002 / Kitahara / 15 steps / 0.8% / from (<i>S</i>)-proline (4-7)			
2005 / Ohfuné / 25 steps / 0.1% / from (<i>R</i>)-hydroxymethylglutamate (4-8)			
2008 / Chamberlin / 22 steps / 2.08% / from (<i>R</i>)-pyroglutamic Acid (4-9)			
4-6	4-7	4-8	4-9

4.3.1 Ma's Synthesis of (2*S*)-Kaitocephalin

In 2001, the first total synthesis of (2*S*)-kaitocephalin was described by the Ma group.³¹ In Ma's synthetic plan, allyl proline **4-10** was used as the key intermediate. The C8-C10 N-acylalanine subunit of (2*S*)-kaitocephalin was planned to be prepared from the allyl group of **4-10** via the reaction sequence involving the Sharpless catalytic asymmetric dihydroxylation, oxidation of primary alcohols to carboxylic acids, conversion of protected C8-hydroxy group hydroxyl groups into azides, hydrogenation and acylation of the resultant amine. The C1-C3 serine subunit was planned to be

introduced through stereoselective aldol condensation between an enolate of cis disubstituted pyrrolidines **4-11** and (*R*)-Garner aldehyde. Steric hindrance from the allyl group would dictate the preferred *Si*-face attack on the enolate, which would generate an expected (*R*)-C4 quaternary stereocenter. The 3*R* stereocenter could be predicted with the Felkin-Anh model, and it can be converted to the correct 3*S* stereocenter via oxidation of the C3 alcohol followed by selective reduction of the resulting ketoester. Cis-2,5-disubstituted pyrrolidine **4-11** can be obtained from amina **4-12** through Lewis acid promoted allylation (Scheme 4.1).

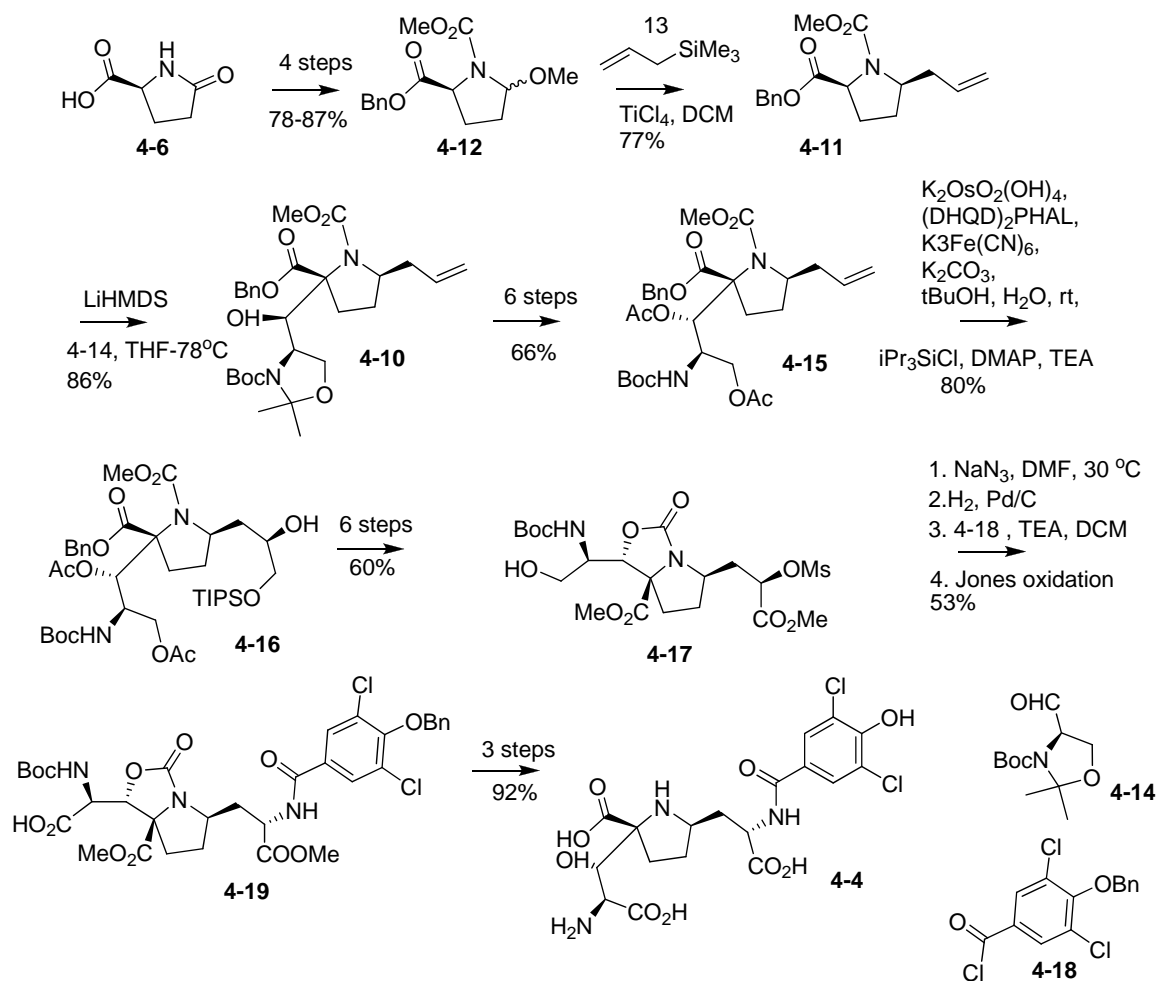


Scheme 4.1 Ma's retrosynthetic analysis of kaitocephalin.

The amina **4-12** was prepared from (*S*)-pyroglutamic acid in 4 steps in 78-87% overall yield. Ti(IV) induced allylation of the amina **4-12** to afford a cis disubstituted pyrrolidine **4-11** as the major product along with a small amount of the trans isomer. Lithiation of **4-11** followed by aldol condensation between enolate of **4-11** and (*R*)-Garner aldehyde exclusively gave trisubstituted pyrrolidines C3-epi-**4-10** in 86% yield.

Chapter 4: Introduction to Kaitocephalin

After correcting the wrong stereochemistry at C3, allyl **4-10** underwent dihydroxylation and monosilylation to give a 6.8:1 ratio of the desired (*9R*) alcohol **4-16** and (*9S*) isomer. Through protecting group adjustment, bicyclic compound **4-17** was obtained from (*9R*) alcohol **4-16** in 6 steps in 60% total yield, which introduced amino group at C9 via azidation of **4-17**, reduction and acylation of the resultant amino group. After oxidation of C1 alcohol into carboxylic acids, a protected kaitocephalin **4-19** was constructed. Finally, after Boc removal and hydrogenolytic and hydrolytic deprotection, the desired (*2S*)-kaitocephalin was generated from **4-19** (Scheme 4.2).



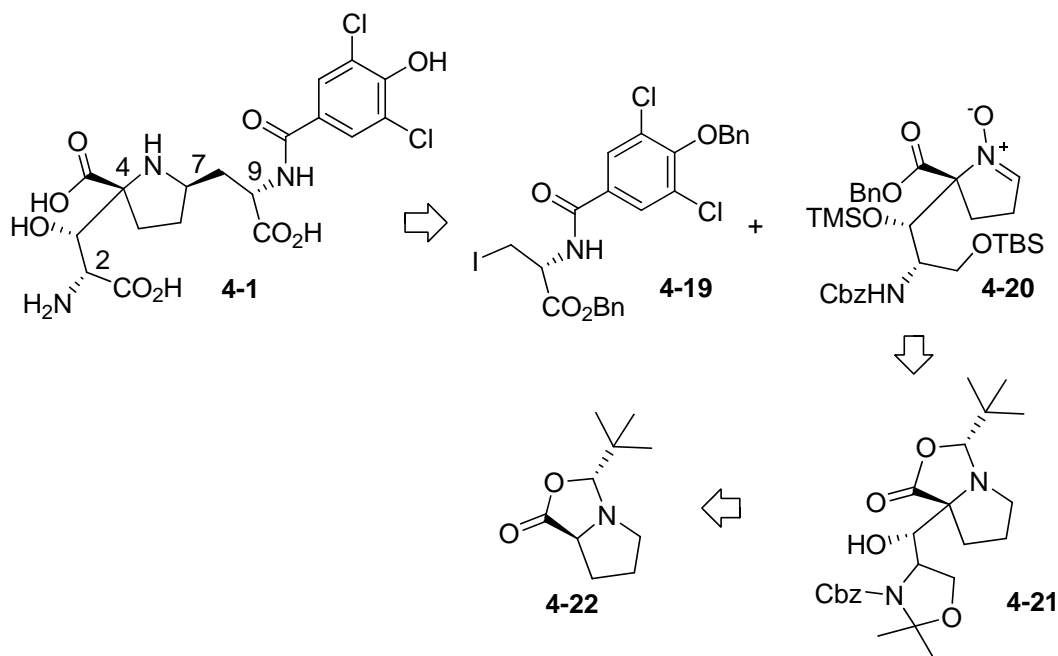
Scheme 4.2 Ma's synthesis of kaitocephalin.

(2*S*)-Kaitocephalin was synthesized by Ma's group in 25 steps in 8% total yield.

The synthesis was highlighted by high stereoselectivity in every asymmetric reaction.

4.3.2 Kitahara's Synthesis of (2*R*)-Kaitocephalin

In 2002, the first total synthesis of (2*R*)-kaitocephalin was reported by the Kitahara group.³⁵ In Kitahara's synthesis, α -substituted proline derivative **4-21** was employed as the key intermediate. The C8-C10 N-acyl alanine subunit of kaitocephalin was planned to be installed through C-C bond connection of N-acyl alanine iodide **4-19** and pyrrolidine oxide **4-20** which was derived from aldol product **4-21**. The steric bulk of the C1-C3 moiety allowed stereospecific introduction of the new chiral centers at C4. Stereoselectively introducing a substituent into the α -position of protected proline **4-22** could be realized through the Seebach principle of self-regeneration of stereocenters³⁸ (Scheme 4.3).

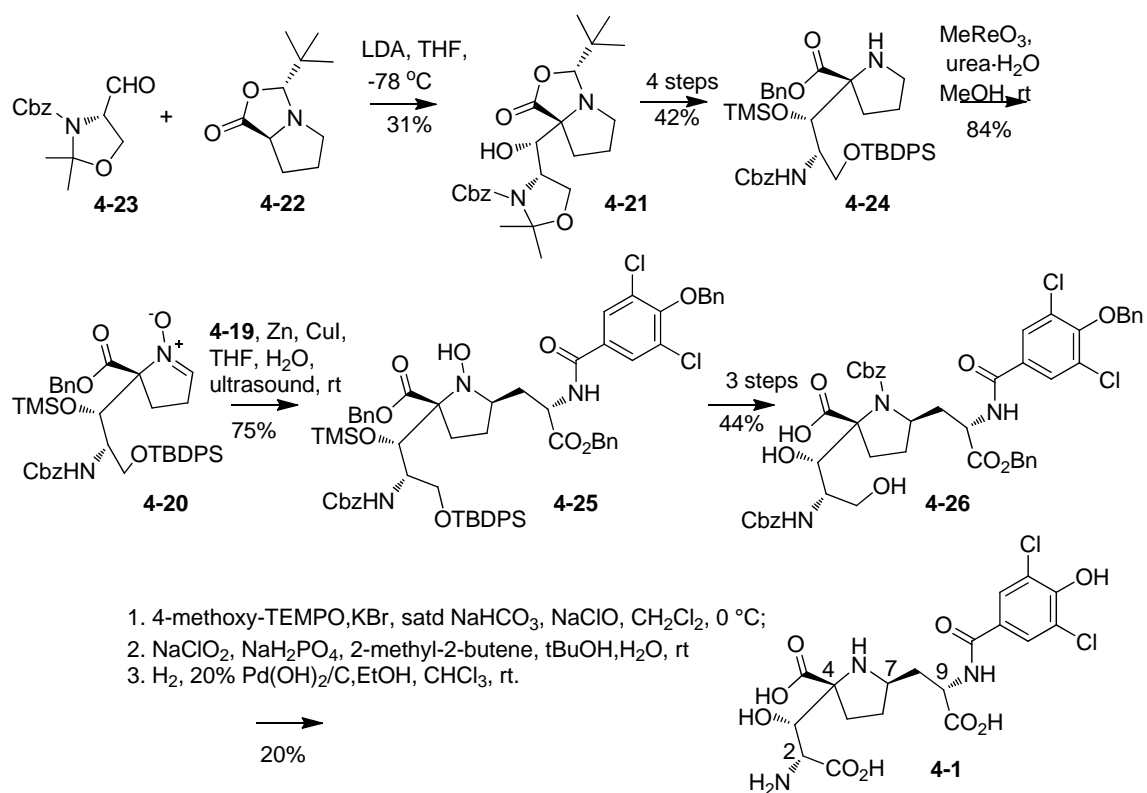


Scheme 4.3 Kitahara's retrosynthetic analysis of kaitocephalin.

Chapter 4: Introduction to Kaitocephalin

Protected proline **4-22** was prepared from L-proline using Seebach's method. The enolate of **4-22** was reacted with (*S*)-Garner aldehyde to give a 3:2 ratio of the desired aldol product (*3R*)-, and (*3S*)-**4-21** in a combined yield of 53%. The unexpected (*3R*)-**4-21** could be converted into the (*3S*)-**4-21** by oxidation of the 3-hydroxyl group followed by stereoselective reduction of the resultant ketoester. After removal of the acetal and ketal groups, proline ester **4-24** was converted into pyrrolidine oxide **4-20** through $\text{MeReO}_3 - \text{urea} \cdot \text{H}_2\text{O}_2$ mediated oxidation of the secondary amine. Oxazolone **4-20** was employed in the nucleophilic additions with N-acyl alanine iodide using a copper(I)-activated organozinc reagent to give a single desired pyrrolidinol (*7R*)-**4-25** in 75% yield. Reduction of the pyrrolidinol **4-25** into a pyrrolidine followed by protecting group adjustment generated amino diol **4-26** which was then converted into kaitocephalin (**4-1**) through the selective oxidation of primary alcohol to carboxylic acid and hydrogenolysis of the benzyl ether and Cbz group of the intermediate (Scheme 4.4).

Chapter 4: Introduction to Kaitocephalin



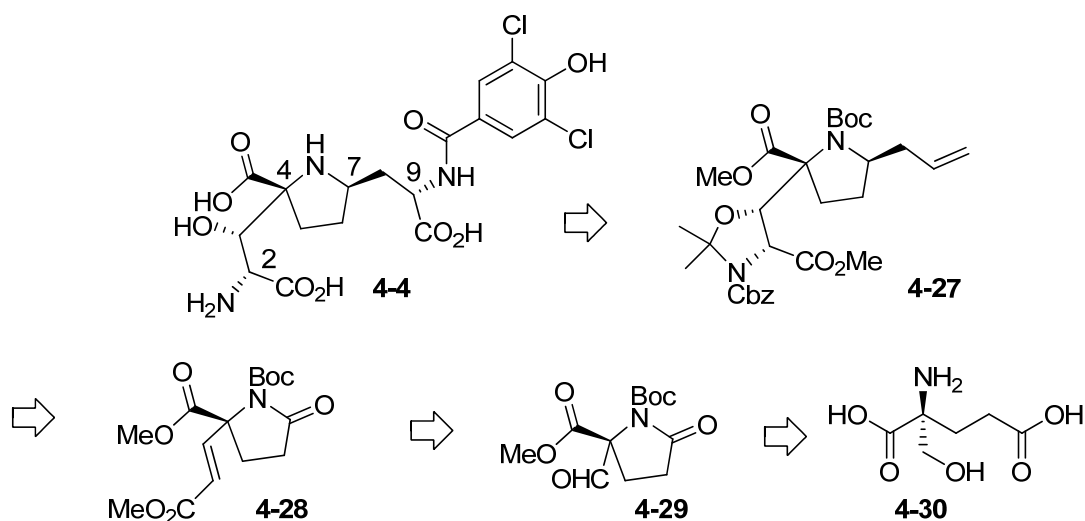
Scheme 4.4 Kitahara's synthesis of kaitocephalin.

(2*R*)-Kaitocephalin was synthesized from L-proline by Kitahara's group in 14 steps in 0.5% total yield. The synthesis was highlighted by the efficient way they introduced the C8-C10 moieties. Three natural amino acids were employed in the construction of three amino-moieties in kaitocephalin.

4.3.3 Ohfuné's Synthesis of (2*R*)-Kaitocephalin

In 2005, Ohfuné's group finished the total synthesis of (2*R*)-kaitocephalin.³⁶ Ohfuné's group developed a methodology for highly enantioselective synthesis of (2*R*)- α -hydroxymethylglutamate **4-30** with a latent quaternary stereocenter, that of C4 in kaitocephalin.³⁹ In Ohfuné's synthesis, a trisubstituted pyrrolidine **4-27** was utilized as the key intermediate. The C8–C10 N-acylalanine side chain in kaitocephalin was planned

to be built from an allyl group which was anticipated to be introduced stereoselectively from the same face as the methoxycarbonyl group using an allylcopper reagent. Utilizing an (E)- α,β -unsaturated ester group as a precursor, the C1-C3 serine subunit was expected to be introduced through stereoselective dihydroxylation and S_N2 azidation of a thionocarbonate. The formyl lactam **4-29** would be required to introduce an α,β -unsaturated ester group for the C1-C3 serine subunit (Scheme 4.5).



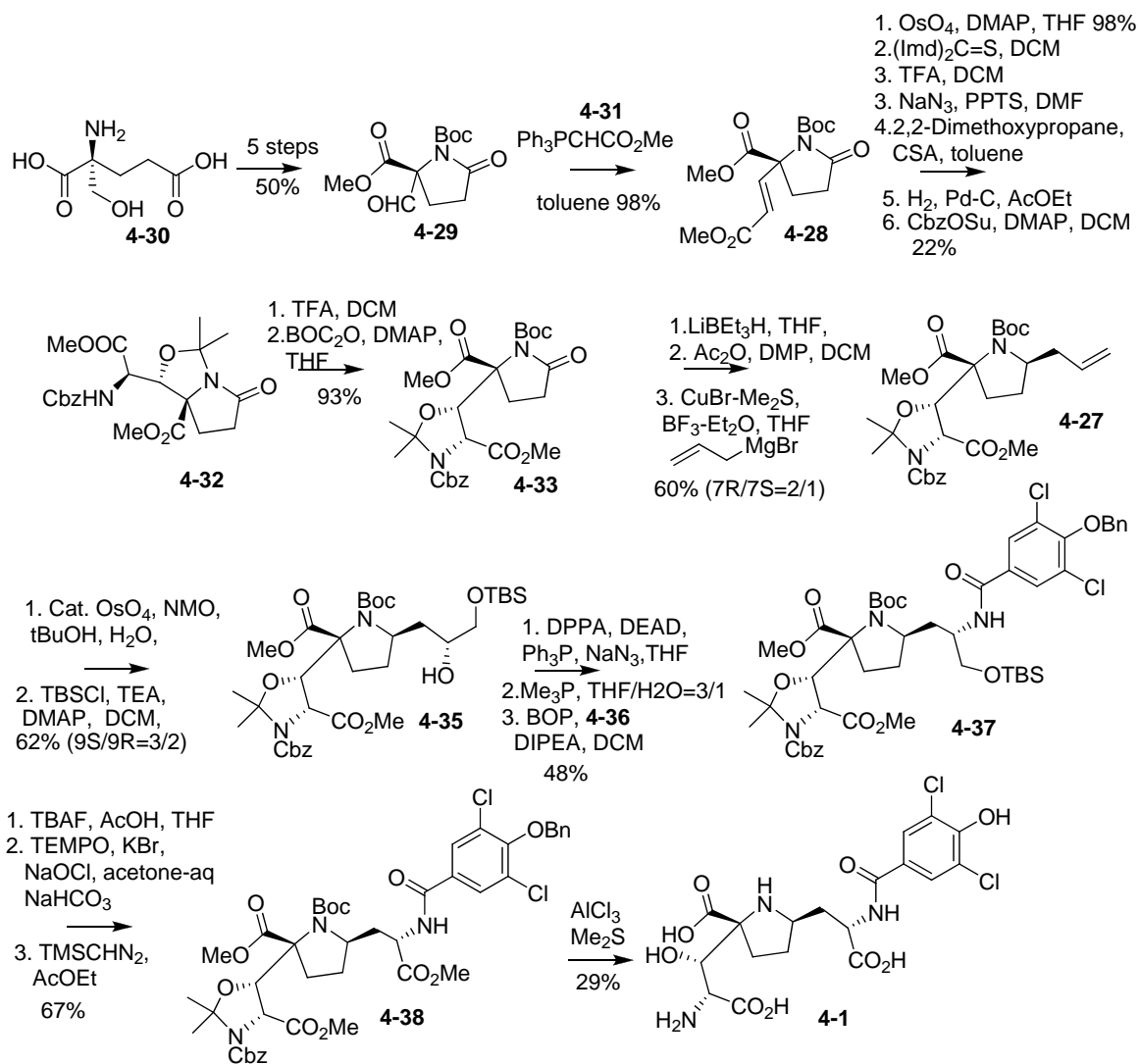
Scheme 4.5 Ohfuné's retrosynthetic analysis of kaitocephalin.

The aldehyde **4-29** was prepared from (2*R*)- α -hydroxymethylglutamate **4-30** in 5 steps in 50% total yield. E-selective Horner–Wadsworth–Emmons (HWE) reactions of phosphonoacetate **4-31** with aldehyde **4-29** furnished the (E)- α,β -unsaturated ester **4-28**. A dihydroxylation of (E)- α,β -unsaturated ester **4-28** afforded the desired (2*S*,3*S*) diol in 98% yield in a highly stereoselective manner. Next, S_N2 azidation of the thionocarbonate of the intermediate, reduction of the azide and then protecting group adjustment of the intermediate generated lactam bearing protected C1-C3-moiety **4-33**. Reduction of the lactam **4-33** by LiBET₃H yielded an aminal which was subjected to the BF₃ mediated

Chapter 4: Introduction to Kaitocephalin

allylation with allylmagnesium bromide in the presence of CuBr-Me₂S to give an unseparated 2:1 mixture of the desired (7*R*)- allyl **4-27** and (7*S*)-isomer of **4-27** in a combined yield of 60%. Dihydroxylation of **4-27** followed by silyl etheration afforded the corresponding mono alcohol (9*R*) and (9*S*)-**4-35** in a combined yield of 62% which were converted into azides using Mitsunobu conditions. Reduction of the azide group with PMe₃ provided the (9*S*) amine. After BOP-mediated acylation, the dichlorohydroxybenzoate subunit was introduced. Kaitocephalin was prepared through a sequence of removal of the TBS group, oxidation of primary alcohol to carboxylic acid and the simultaneously removal of all the protecting groups using AlCl₃-Me₂S (Scheme 4.6).

Chapter 4: Introduction to Kaitocephalin

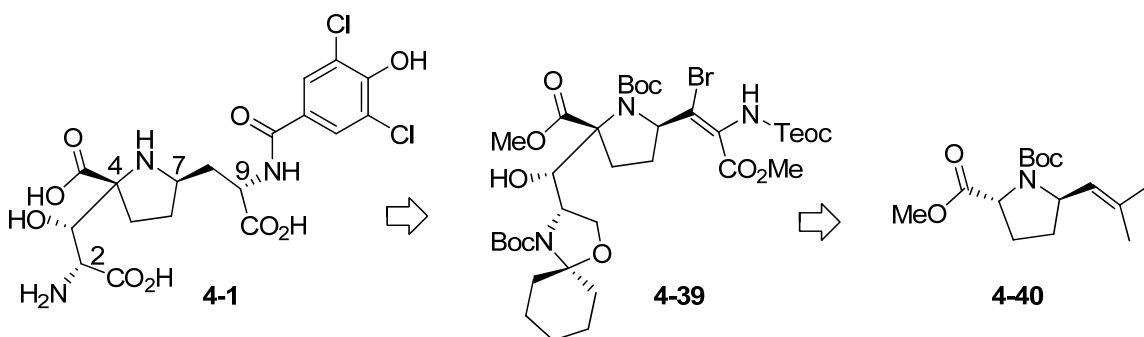


Scheme 4.6 Ohfuné's synthesis of kaitocephalin.

(2*R*)-Kaitocephalin was synthesized from (2*R*)-*R*-hydroxymethylglutamate **4-30** by Ohfuné's group in 25 steps in 0.1% overall yield. The highlight of Ohfuné's synthesis is the stereoselective introduction of the asymmetric centers C2, C3 and C4 and the efficient removal of protecting groups using of AlCl₃/Me₂S.

4.3.4 Chamberlin's Synthesis of (2*R*)-Kaitocephalin

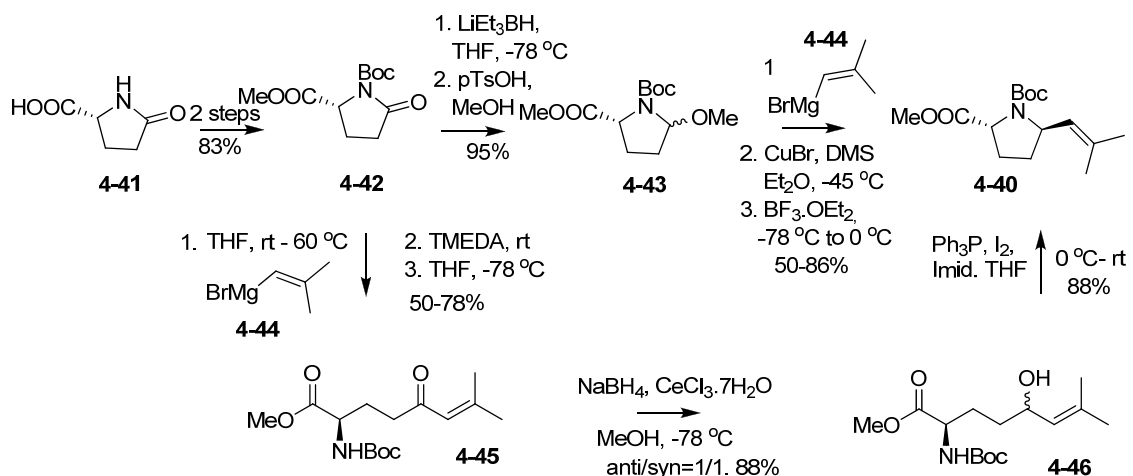
In Chamberlin's synthesis, 4,7-*trans*-disubstituted **4-40** was used as the key intermediate. The C1-C3 serine subunit was planned to be introduced through enolate acylation with *N*-acyl imidazole derived from *L*-serine, followed by reduction of the ketone group into a (3*S*) hydroxyl group. A methylpropenyl group would act as an effective steric block to the *Re*-face approach of an enolate of **4-40**. The C8-C10 alanine subunit was planned to be obtained through hydrogenation of bromo-dehydroamino ester **4-39**. The methylpropenyl group was used as a latent aldehyde function and would be converted to the dehydroamino ester through ozonolysis of the methylpropenyl into an aldehyde followed by Horner–Wadsworth–Emmons (HWE) olefination of the pyrrolidine aldehyde (Scheme 4.7).



Scheme 4.7 Chamberlin's retrosynthetic analysis of kaitocephalin.

Chamberlin's group designed a four step synthetic route for *trans*-disubstituted pyrrolidines **4-40** (Scheme 4.8). The preparation to give the pyrrolidines **4-40** commenced with esterification of *R*-pyroglutamic acid **4-41** followed by *N*-Boc protection to furnish lactam-ester **4-42** in 83% overall yield. The resultant fully protected lactam-ester **4-42** was then reduced to methoxy amination **4-43** with LiBEt_3H in 95% yield.

Next, Lewis-acid promoted olefination of methoxy aminal **4-43** with 2-methylpropenylmagnesium bromide **4-44** in the presence of CuBr produced the desired **4-40** in 69-78% yield with diastereomeric ratios ranging from 15/1 to 20/1 of trans to cis with 5-10% of side products (Scheme 4.8). However, it is very difficult to separate **4-40** from side products.

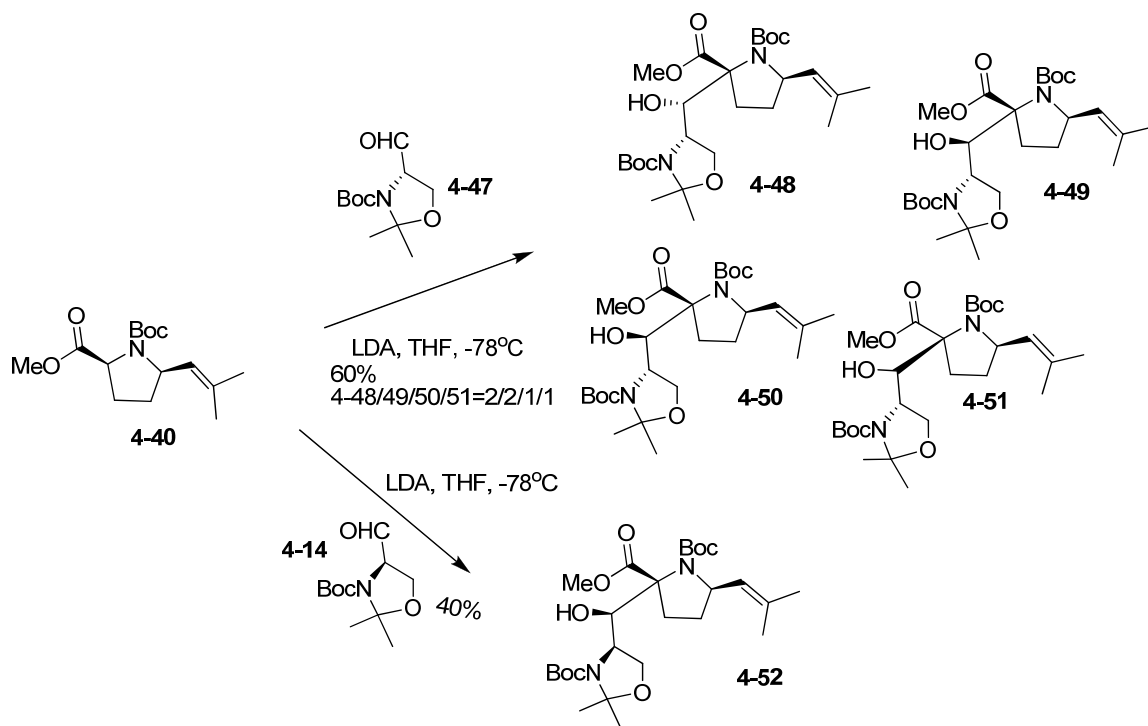


Scheme 4.8 Chamberlin's synthesis of intermediate **4-40**.

Considering the difficulty in the purification, Chamberlin's group developed another synthetic route to prepare the 4,7-trans-disubstituted pyrrolidine **4-40**. The new synthesis of pyrrolidine **4-40** commenced with the chemoselective ring opening of lactam-ester **4-42** utilizing 2-methylpropenylmagnesium bromide **4-44** in the presence of TMEDA to provide enone **4-45** in 50-78% yield. Next, **4-45** was subjected to reduction with $\text{NaBH}_4/\text{CeCl}_3\cdot 7\text{H}_2\text{O}$ to produce a 1:1 (anti-/syn-) mixture of diastereomers of allylic alcohols **4-46** in 88% yield, which furnished the major 4,7-trans-disubstituted pyrrolidine **4-40** with trans/cis ratio 14/1 in a combined yield of 74% yield by cyclizing via treatment with Ph_3P , I_2 , and imidazole (Scheme 4.8).

Chapter 4: Introduction to Kaitocephalin

Next, Chamberlin's group investigated the aldol condensation of trans-disubstituted pyrrolidine **4-40**. Four aldol-adducts in a ratio of 2:2:1:1 were obtained in a combined yield of 60% in the aldol condensation with (*S*)-Garner-aldehyde; while one diastereomer of the aldol product was formed in an unoptimized yield of 40% using (*R*)-Garner aldehyde. He realized that the desired aldol reaction was a case of mismatched double stereodifferentiation (Scheme 4.9).



Scheme 4.9 Aldol reaction of pyrrolidine trans-**4-40** with Garner's aldehydes.

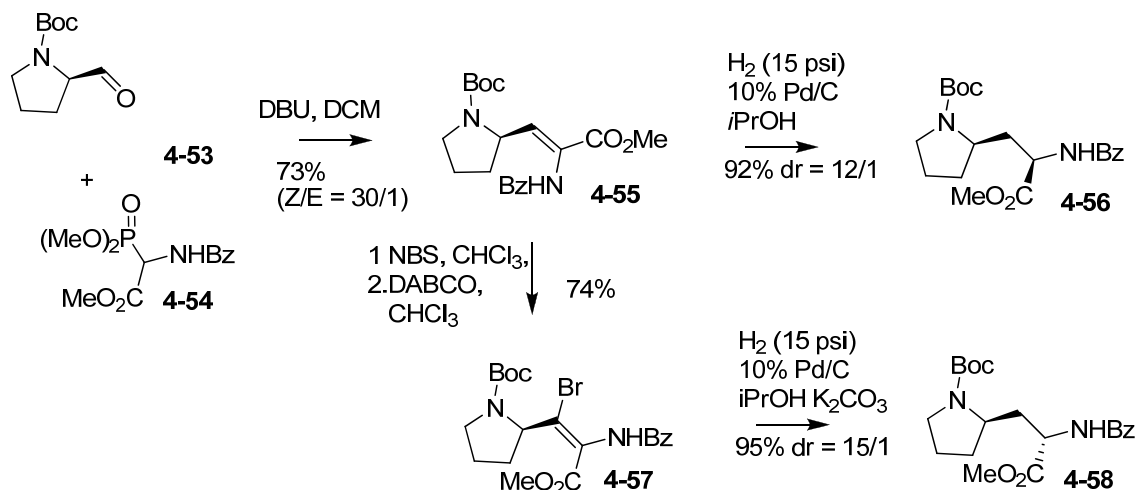
An alternative approach for the construction of the C1-C3 serine subunit involved the C-acylation of the **4-40** enolate followed by reduction of keto ester. Acylation of **4-40** derived enolates was carried out with serine-derived N-acylimidazole **4-59** and generated β -keto ester **4-60** in 40-50% yield. Chemoselective reduction using DIBAL-H gave the

desired (3*S*)- α -hydroxy ester **4-61** as a single diastereomer in 86-93% yield. Ozonolysis of the olefin group in **4-61** afforded the corresponding aldehyde **4-62** (Scheme 4.11).

Chamberlin's group employed the aldehyde as the reaction site to introduce C8-C10 moiety. They planned to install the N-benzoylalanine moieties via hydrogenation of pyrrolidine dehydroamino esters which were derived from aldehyde **4-62**. However, they found that attempts to convert the dehydroamino esters bearing the benzoyl protection at amino group to the corresponding N-benzoylalanine moieties failed.

Their alternative approach was to form N-Teoc-alanine followed by switching to N-benzoyl-alanine. The Horner-Wadsworth-Emmons olefination of phosphonate **4-63** with aldehyde **4-62** furnished the dehydroamino ester **4-39** with an E:Z ratio of 1:1.

Their model reaction revealed that hydrogenation of (*Z*)-dehydroamino esters **4-55** provided corresponding aminoester with the wrong stereocenter at C9 **4-56** (Scheme 4.10). (*Z*)-Bromo-dehydroamino ester (*Z*)-**4-57** was used as the equivalent of (*E*)-**4-55** which furnished the desired (9*S*)-amino ester **4-58** through hydrogenation.

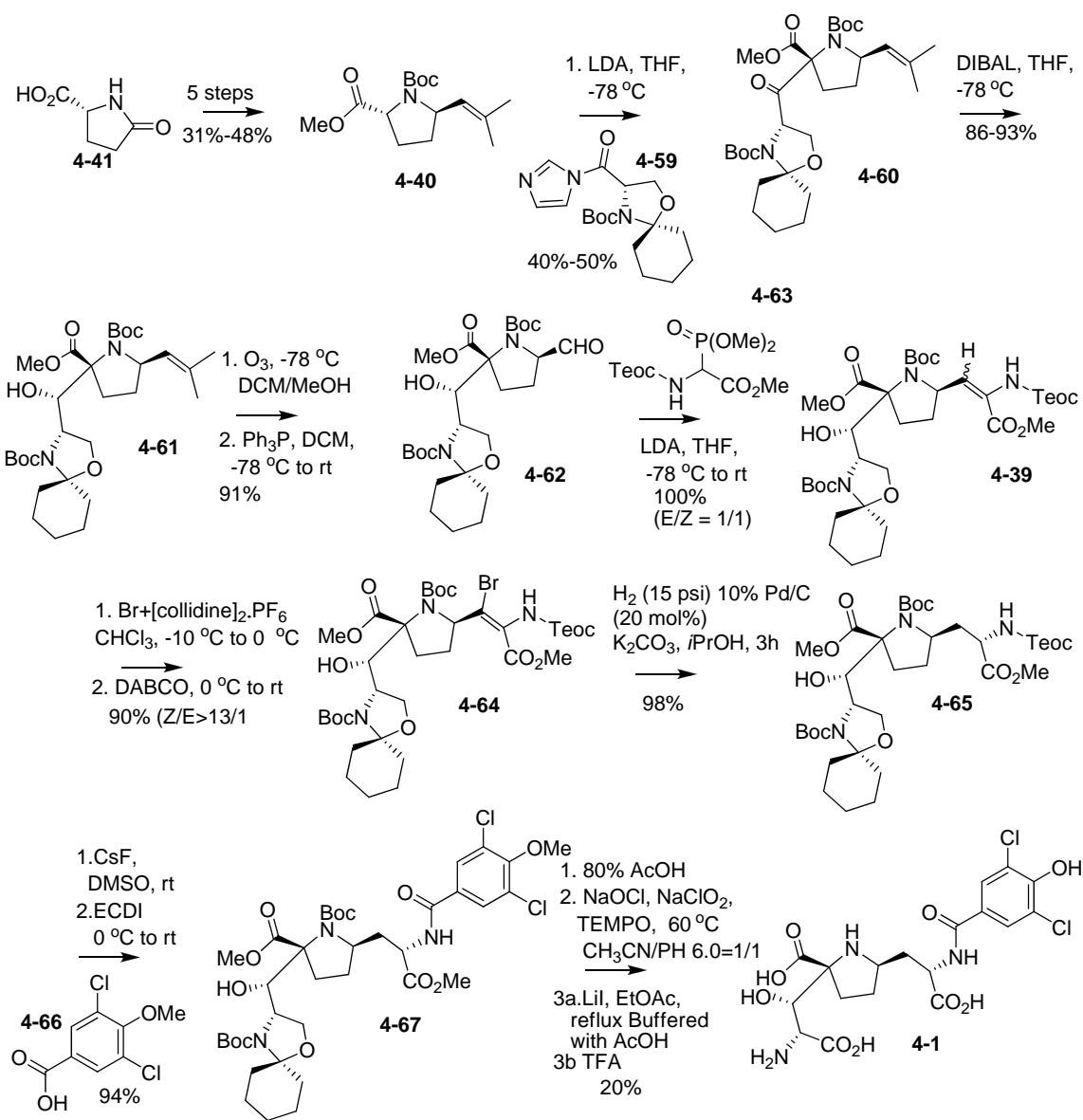


Scheme 4.10 Model reactions for the formation and hydrogenation of pyrrolidine dehydroamino esters.

Chapter 4: Introduction to Kaitocephalin

Next, the 1:1 (E-/Z-) mixture of dehydroamino esters **4-39** was exposed to $\text{Br}^+[\text{collidine}]_2\text{PF}_6^-$ followed by the addition of DABCO to furnish the (Z)-Br-**4-64** in 90% yield along with a small amount of (E)-Br-**4-64**. The bromovinyl group at **4-64** was hydrogenated over Pd/C in the presence of K_2CO_3 to give a single desired diastereomer **4-65** in 98% yield. Removal of the Teoc protecting group followed by EDCI-mediated amide coupling with 4-methoxy-3,5-dichlorobenzoic acid **4-66** generated alanine-proline ester **4-67** in 94% yield over two steps (Scheme 4.11).

Chapter 4: Introduction to Kaitocephalin



Scheme 4.11 Chamberlin's synthesis of kaitocephalin.

Ultimately, kaitocephalin was synthesized from **4-67** via hydrolysis of the cyclohexylidene N,O-acetal, chemoselective oxidation of primary hydroxyl into carboxylic acid, LiI promoted cleavage of the methyl ether, and removal of N-Boc protection (Scheme 4.11).

(2*R*)-Kaitocephalin was synthesized by Chamberlin's group in 22 steps in 2.08% overall yield. The synthesis was highlighted by a stereocontrolled construction of the asymmetric centers of C3,C4,C7, and C9.

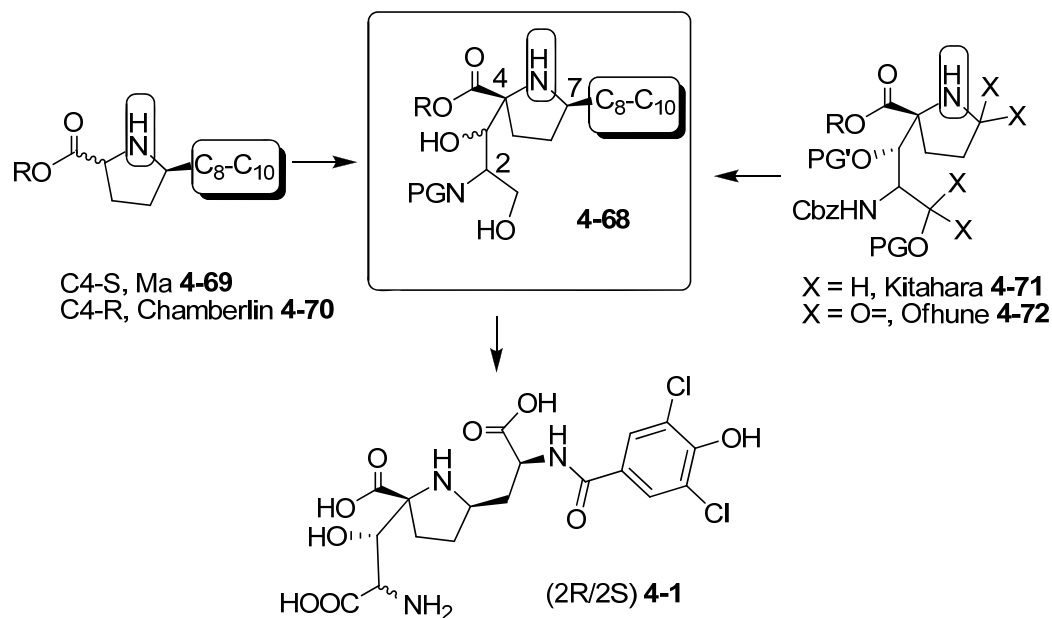
4.3.5 Total Synthesis Summary

Kitahara developed a 15-step synthesis of kaitocephalin in 0.8% total yield. Ofhune and Chamberlin both described more than 20-step syntheses of kaitocephalin. Ma prepared (2*S*)-kaitocephalin in 25 steps in 8% total yield, with the highest average yield, but of the wrong compound.

4.3.5.1 Tri-Substituted Pyrrolidine Core

Kaitocephalin possesses three amino acid subunits. It can be visualized as α -substituted L-proline with N-acylalanine and serine moieties in positions 2 and 5 respectively, and containing a quaternary carbon at C4. One of the most challenging aspects in the synthesis of kaitocephalin is constructing the trisubstituted pyrrolidine core bearing carbon quaternary stereogenic centers (**4-68**) (Scheme 4.12).

The Ma³¹ and Chamberlin³⁷ groups built the trisubstituted pyrrolidines via lithiation of 4,7-disubstituted pyrrolidines **4-69/4-70** followed by introducing the equivalent of C1-C3 moiety. The construction of stereocenter C4 was dictated by the substituent at C7. Ma's cis disubstituted pyrrolidine bearing desired stereocenter C4 (**4-69**), was installed through titanium promoted allylation of the aminal. Chamberlin's trans-disubstituted pyrrolidine possessing stereocenter C4 (**4-70**) was constructed through a cyclization reaction of an allylic alcohol bearing an amino acid group.

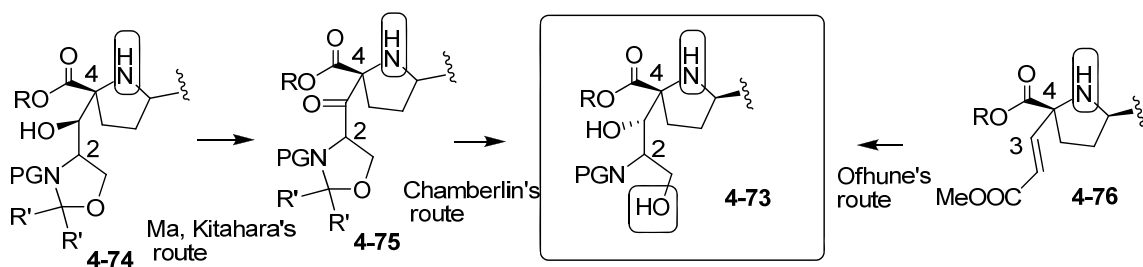


Scheme 4.12 Construction of the substituted $4R,7R$ -pyrrolidine core.

Synthetic approaches in Kitahara's and Ofhune's group were started by generating the intermediates bearing two substituents at C4 (**4-71**, **4-72**). A sequence of aldol reaction between Seebach's lactone and *S*-Garner's aldehyde afforded Kitahara's 4,4-disubstituted pyrrolidine **4-71**, which exclusively converted to ($7R$)-tri-substituted pyrrolidine core **4-68** through oxazoline formation followed by Zn promoted couple reaction of the resultant pyrrolidine oxide with an alkyl halide derived from serine. In Ofhune's synthesis, an intramolecular version of the Strecker synthesis gave the key precursor ($2R$)-*R*-hydroxymethylglutamate which provided 4,4,-disubstituted lactam **4-72** and constructed the C4 stereocenter. The aldehyde group became a reaction site to introduce the C1-C3 moiety. The trisubstituted pyrrolidine core was then furnished through a copper mediated allylation of amination derived from lactam **4-72** with a ratio of $7R$ - to $7S$ -**4-68** being 2:1.

4.3.5.2 The C3 Stereocenter

In Ma, Kitahara, and Chamberlin's synthetic strategy, the hydroxyl group was incorporated at C3 with *S* configuration through stereoselective reduction of ketone **4-75** (Scheme 4.13). Chamberlin's group obtained the ketoester **4-75** through C-acylation at C4 of 4,7-disubstituted pyrrolidines, while Ma and Kitahara's groups obtained the ketoester from aldol product C3-epi-**4-73**. Ohfuné's group introduced a C3S-hydroxyl group through asymmetric hydroxyamination of olefin **4-76**.

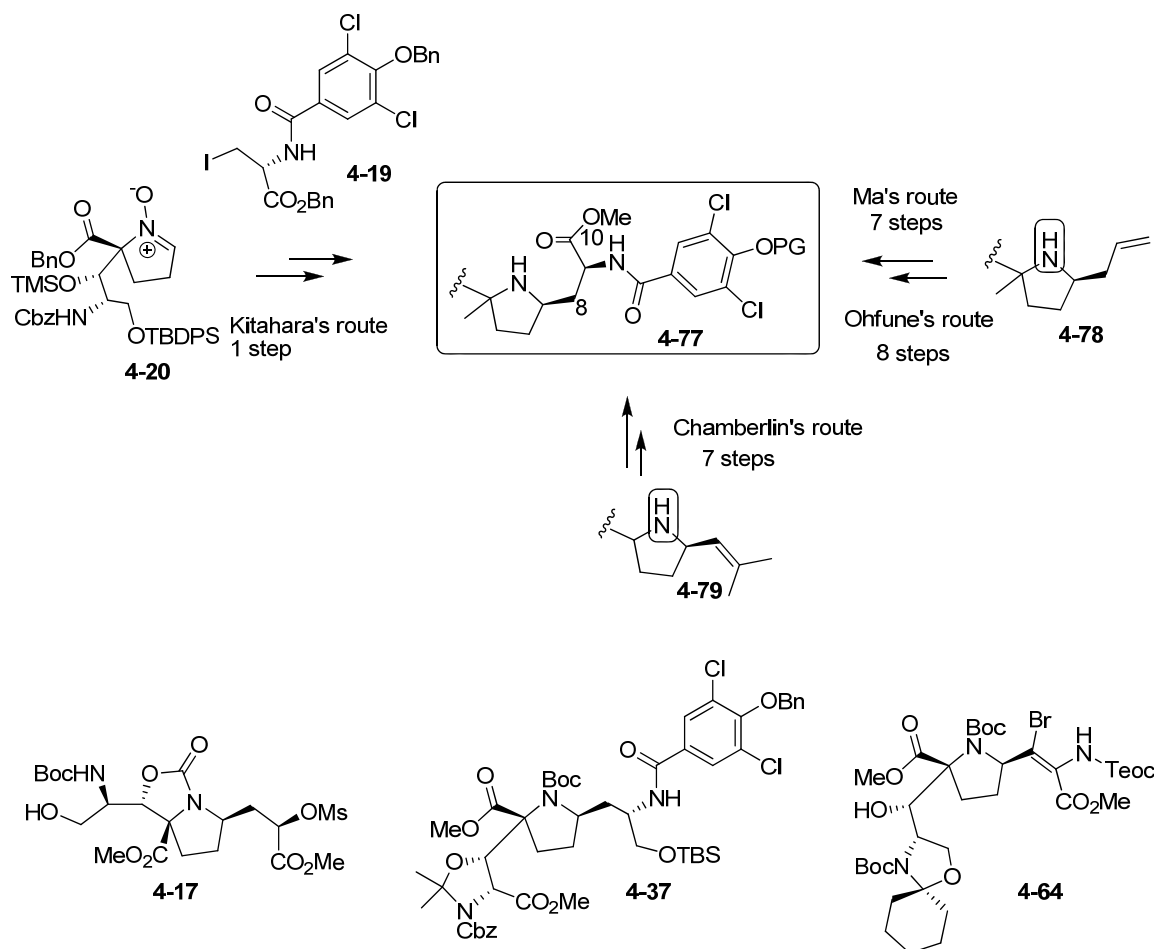


Scheme 4.13 Incorporation of the hydroxyl group at C3.

4.3.5.3 The C8-C10 Moiety

The C8-C10 moiety in Kitahara's synthesis was introduced in one step through a Zn promoted coupling reaction between an alkyl halide derived from serine **4-19** and pyrrolidine oxide **4-20**. In both Ma and Ohfuné's syntheses, an allyl group was used as the precursor of the C8-C10 moiety. Ma's seven-step conversion to the C8-C10 moiety was realized using amino formation via azidation of intermediate **4-17** followed by reduction, while Ohfuné's group furnished the C8-C10 moiety using protected aminoalcohol **4-37** as an intermediate whose amine was formed through Mitsunobu reaction followed by reduction of the resultant azide (Scheme 4.14).

Chapter 4: Introduction to Kaitocephalin



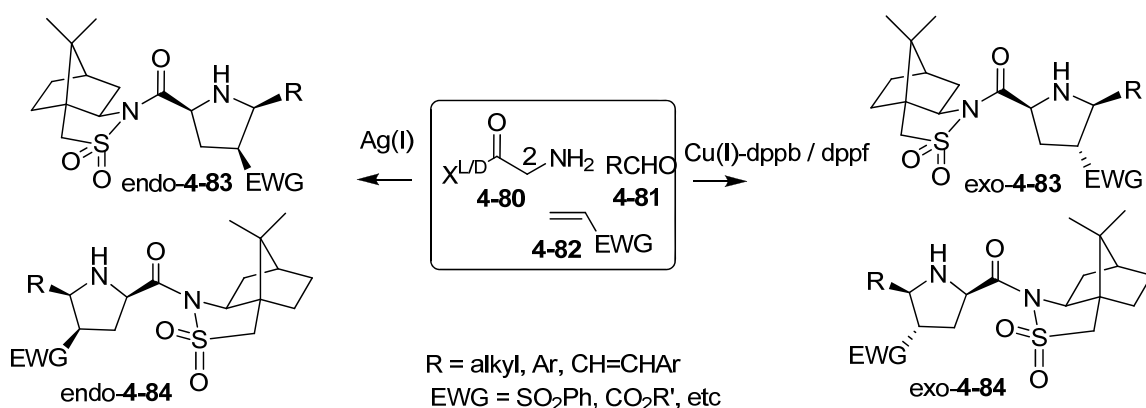
Scheme 4.14 Construction of the C8-C10 moiety.

Chamberlin's seven-step synthesis to construct the C8-10 moiety employed olefin **4-79** as the equivalent of an aldehyde which was transformed to the key intermediate dehydroamino ester **4-64** through a HWE reaction.

Kitahara's shortest synthesis is due to an efficient route for installing the C8-C10 moiety and the utilization of three natural amino acids to build the three amino acid subunits in kaitocephalin.

4.4 Summary

It is known that 1,3-dipolar cycloaddition can provide highly functionalized pyrrolidines. Most of these reactions have proven effective using imines derived from aromatic aldehydes. The application of this chemistry to the synthesis of pyrrolidine cores is limited by this substrate scope. In an effort to expand the substrate scope, the Garner group developed metal catalyzed one pot 1,3-dipolar cycloadditions for which both aromatic and aliphatic aldehyde undergo the 1,3-dipolar cycloaddition (Scheme 4.15).



Scheme 4.15 Metal catalyzed one pot 1,3-dipolar cycloaddition.

It is anticipated that the Garner one pot 1,3-dipolar cycloaddition can become an important synthesis tool to build multi substituted pyrrolidine cores appended by aliphatic tails. As a challenging practical test of this hypothesis kaitocephalin was chosen as a target compound.

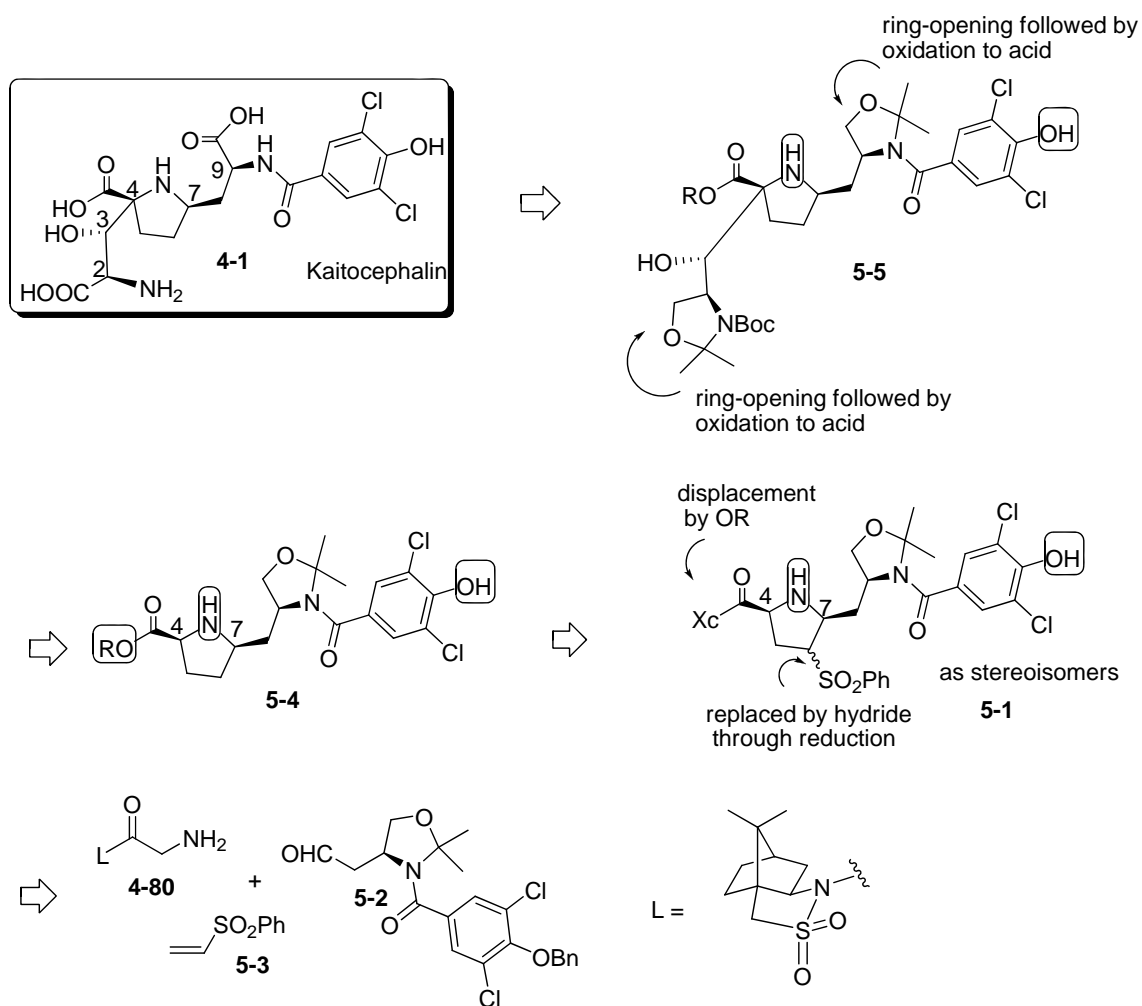
5 Synthetic Analysis

Retrosynthesis is an important starting point in the development of a new synthetic route to kaitocephalin.

5.1 Synthetic Planning

The Garner group has developed stereospecific syntheses for 4,6,7-tri-substituted pyrrolidines **5-1** via a one pot [CN+C+CC] 1,3-dipolar cycloaddition between EWG-based olefins and dipoles derived from an aldehyde **5-2** and L-glycyl sultam **4-80**.⁴⁰ It is expected the substituent at the 6-position may be removed to afford a 4,7-disubstituted pyrrolidine **5-4**. The C1-C3 moiety can be introduced through aldol condensation or acylation at C4 of **5-4**. The 4,6,7-tri-substituted pyrrolidine formation and the removal the EWG group from pyrrolidines is a key part in the synthetic strategy. The retrosynthetic analysis is shown in Scheme 5.1.

In the metal catalyzed one pot [CN+C+CC] 1,3-dipolar cycloaddition, an oxazolidine aldehyde derived from aspartic acid was used as a “C” partner and L-Oppolzer’s glycyl sultam was utilized as the “CN” partner. It was anticipated that the dipole generated from aldimines (prepared in situ via condensation between aldehyde **5-2** and amine **4-80**) would be trapped by phenyl vinyl sulfone to furnish a sulfone-substituted pyrrolidine **5-1**.



Scheme 5.1 Retrosynthetic analysis of kaitocephalin.

5.1.1 Electron Withdrawing Group Choice

Since the removal of the EWG (electron withdrawing group) is one of the two key reactions in the synthetic strategy, choice of a suitable EWG is very important. A suitable EWG group should induce a high reactivity towards dipolarophiles for cycloaddition reactions and be easily removed from cycloadducts in the synthesis of kaitocephalin. The choice of phenyl sulfone as the EWG is based on literature searches and control experiments. Since the EWG group would be removed in the synthesis of kaitocephalin,

the regioselectivity and endo/exo selectivity in the cycloaddition with EWG based olefin are not of significant importance. In the literature search for 1,3-dipolar cycloaddition reactions, it was found that CO₂R, SO₂Ph and NO₂Ph- based olefins were mostly employed to perform 1,3-dipolar cycloadditions, while B, Si and halogen based olefins were seldom utilized.⁴¹

As for the removal of the EWG group, the aromatic sulfone moiety could be removed by reduction with sodium amalgam in methanol,⁴² a carboxylic acid group could be removed via the Barton decarboxylation⁴³ and halogen substituents are frequently removed by hydrogenation.⁴⁴

Control experiments employing different EWG-based olefins in the [CN+C+CC] 1,3-dipolar cycloaddition were carried out. Hydrocinnamic aldehyde and L-glycyl sultam were treated with different EWG based olefins in the presence of silver. The results are shown in Scheme 5.2.

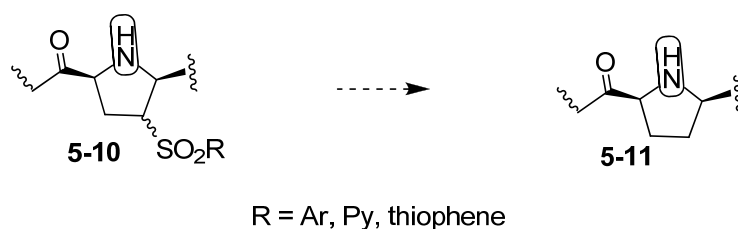


Scheme 5.2 Cycloaddition with three EWG-based olefins.

The reaction with phenyl vinyl sulfones afforded the desired cycloadduct mixture **5-8** in 94% yield with an exo:endo ratio of 8:1, while with methyl acrylate gave the desired cycloadduct **5-9** mixture in 82% with an exo:endo ratio of 8:1. However, no

reaction occurred with 1,1,2-trichloroethene. Since only combined yields were considered, phenyl vinyl sulfone olefin was chosen as the “CC” partners in one pot reactions.

However, because phenyl sulfone has a typical reduction potential of -2.3 V, harsh reduction conditions were anticipated for removal of the sulfone. This may possibly lead to a decomposition of other incompatible functional groups. A backup strategy is to employ a different sulfone bearing a substituent with a lower electron density, such as a pyridine substituted sulfone (Scheme 5.3).



Scheme 5.3 Sulfone removal.

5.1.2 The N-Acylalanine Moiety (C8-C10)

In the [CN+C+CC] 1,3-dipolar cycloaddition reaction, phenyl vinyl sulfones are commercially available reagents and the Garner group has developed a convenient method to prepare glycyl sultam on 30 g scale.¹⁸ The synthesis of starting material was focused on the aldehyde (**5-2**) formation.

5.1.2.1 Oxazolidine as a latent α -amino acid group

A ketal was chosen as the protecting group for the amino alcohol because the C1-C3 moiety would be installed employing Garner aldehyde or its derivative. It was planned to convert both sides to amino acids in one reaction. Through considering the

basic nature of the deprotection strategies for the other groups involved in the synthesis, such as LiOH mediated desultamization, Na-Hg promoted desulfonylation and lithiation for the aldol reaction, it was believed to be acceptable to choose an acid labile protecting group. Furthermore, oxazolidine compounds show good solubility in most organic solvents and it is easy to convert oxazolidines to amino-alcohols under weak acid conditions.

The use of an aldehyde bearing amino benzyl ester was considered as the “C” partner in [CN+C+CC] reaction (Figure 5.1).

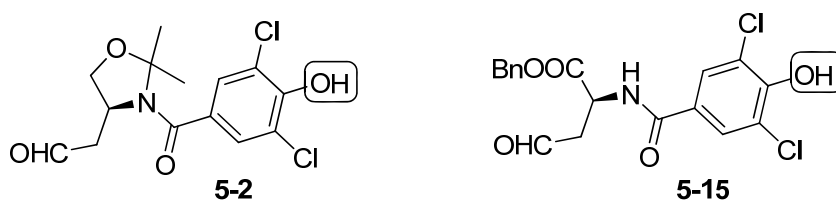
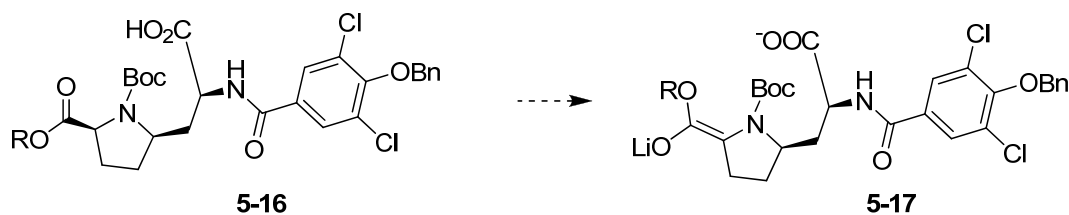


Figure 5.1 Candidates for “C” partner in [CN+C+CC] 1,3-dipolar cycloadditions.

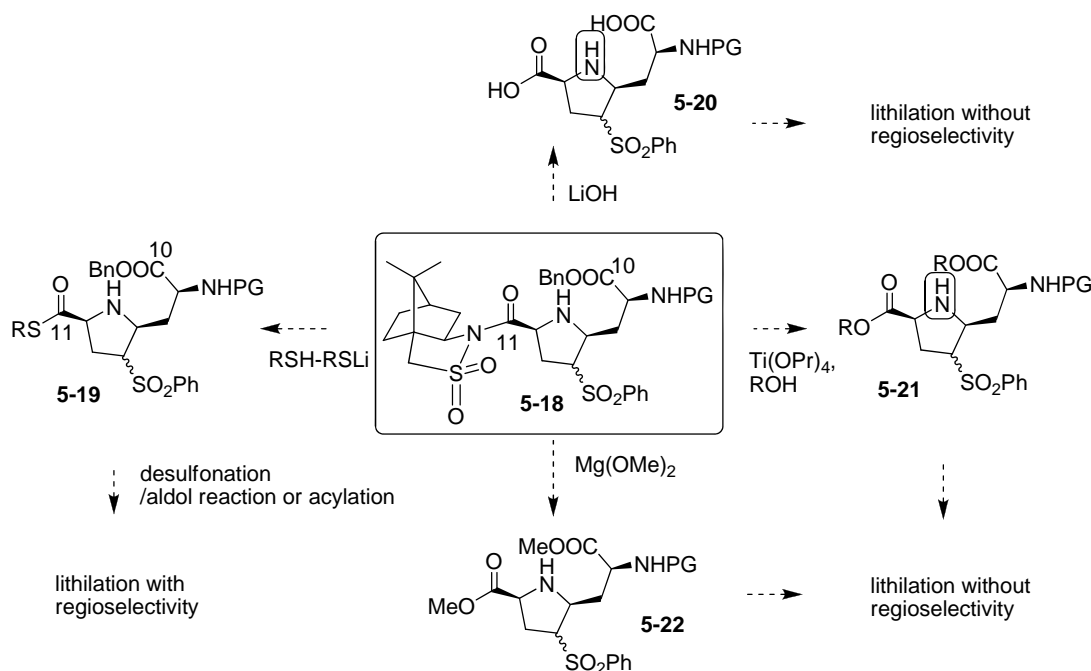
To avoid lithiation at C9 in the aldol reaction, it was planned to convert the benzyl ester to an acid which would be used as the precursor for the aldol condensation (Scheme 5.4).



Scheme 5.4 Aldol condensation precursor formation.

However, the benzyl ester might suffer from the desultamization reaction conditions and lead to no regioselectivity in lithiation with the exception of the thioester **5-19** mediated desultamization reaction (Scheme 5.5). Furthermore, epimerization at C9

would occur in the basic conditions if the aldehyde bearing amino ester were used as a “C” partner in a one pot reaction.



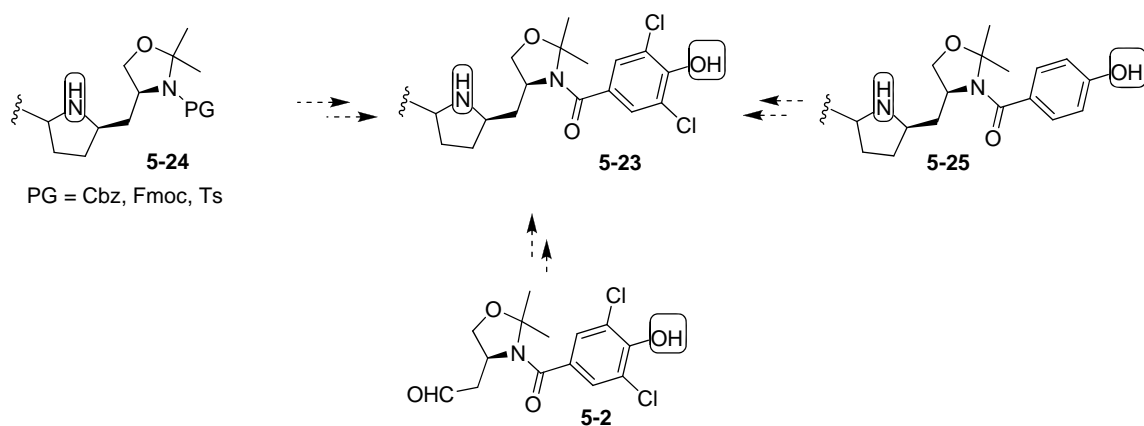
Scheme 5.5 Possible sultam removal conditions.

It is known that aminoalcohol derivatives bearing stereogenic centers afford the corresponding product with complete retention of the original configuration. Thus, an amino alcohol group used as the equivalent of the amino acid has no epimerization under basic condition and no regioselectivity problem in the lithiation. In the later step, the amino alcohol would be oxidized into an amino acid using KMnO_4 or PtO_2 . A similar reaction reported in the literature was shown to proceed with retention of stereochemistry.⁴⁵

5.1.2.2 Amine Protection

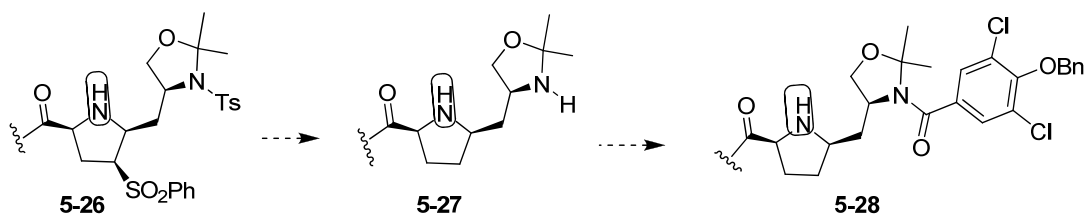
In pursuit of a short and efficient synthesis of kaitocephalin, it was decided to install the aryl chloride group (as shown in Scheme 5.4) in the early stage.

Typical problems associated with benzamide (**5-23**) shown in Scheme 5.6. (basically the natural group present in kaitocephalin) as the protecting groups were anticipated, such as cleavage of aryl chloride bonds and reduction of amide group under the harsh desulfonylation conditions. It was reasoned that mild desulfonylation conditions could be developed and that the chloro groups could be reintroduced using NCS (no hv) if cleavage of the aryl-chloride occurs.



Scheme 5.6 Alternative methods to the introduce aryl chloride subunit.

Alternatively, the aryl chloride group can be introduced in a later step via removal of a protecting group from the amine (such as Cbz and Fmoc) and acylation of the released free amine (Scheme 5.6). It is attractive employing tosyl as the protecting group because of the possibility of removal of sulfone and tosyl groups in one reaction (Scheme 5.7).



Scheme 5.7 Concomitant double deprotection followed by introduction of the desired group.

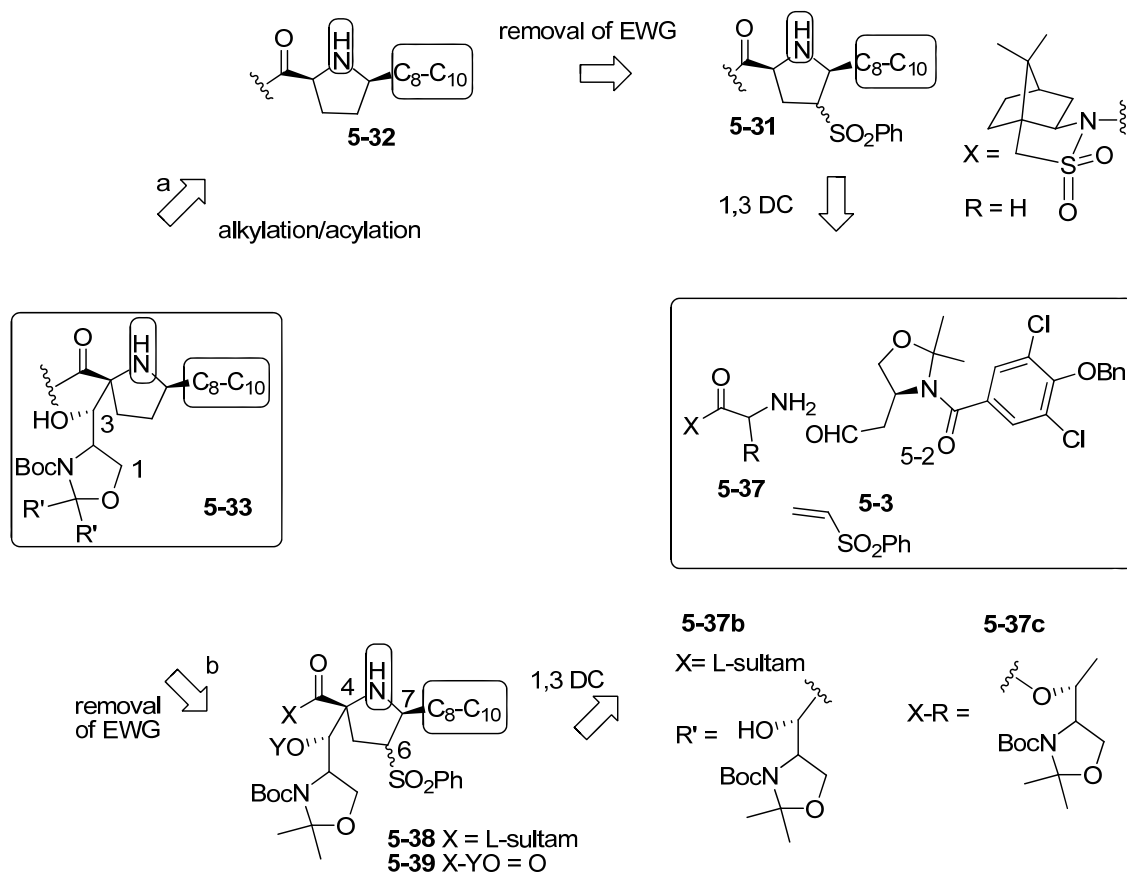
A non-chloro substituted benzoyl can be used as the protection group, and aryl chloride could be introduced on the desulfonylation product via chlorination.

5.1.2.3 Phenol Protection

Next, the appropriate protection group for the phenol was considered. In the known syntheses to kaitocephalin, the phenol group was already reported to be protected as a methyl or benzyl ether. Initially benzyl ether was chosen as the protecting group. However, later experiments revealed that benzyl ether cleavage occurred in the desulfonylation. It was thought that desulfonylation could be arranged in a later step, and it is appealing to remove the sulfone and benzyl in one reaction. Thus, benzyl ether was chosen as the protecting group.

5.1.3 Introduction of the C1-C3 Moiety

The C1-C3 moiety was planned to be introduced into the C4 position of disubstituted **5-32** via alkylation or acylation. (Route a, Scheme 5.8).



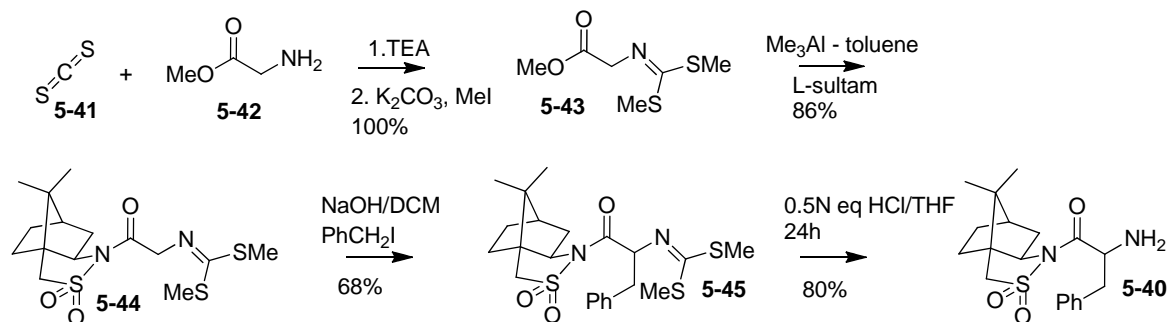
Scheme 5.8 Proposed strategy for the introduction of the C1-C3 moiety.

5.1.3.1 Alternative Introduction of the C1-C3 Moiety

It was suggested that the C1-C3 moiety could also be incorporated into the “CN” partner to form an α -substituted glycyI-sultam **5-37b** whose 1,3-dipolar cycloaddition would generate a 4,4,6,7 tetrasubstituted pyrrolidine **5-38/5-39**. Removal of the sulfone group would lead to the formation of the key intermediate trisubstituted pyrrolidine **5-33** (route b, Scheme 5.8)

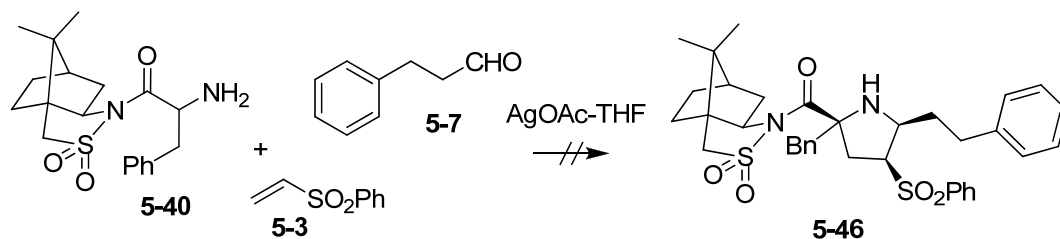
The challenge lies in the synthesis of the α -substituted glycyI-sultam **5-37b** and its application in a one pot [CN+C+CC] 1,3-dipolar cycloaddition. α -Benzyl-substituted glycyI-sultam (**5-40**) was chosen as a model compound to investigate its reactivity in one

pot 1,3-dipolar cycloadditions (Scheme 5.9). Following Oppolzer's procedure,⁴⁶ model compound **5-40** was prepared from glycine ester **5-42** in 4 steps in 47% overall yield.



Scheme 5.9 Preparation of model compound **5-40**.

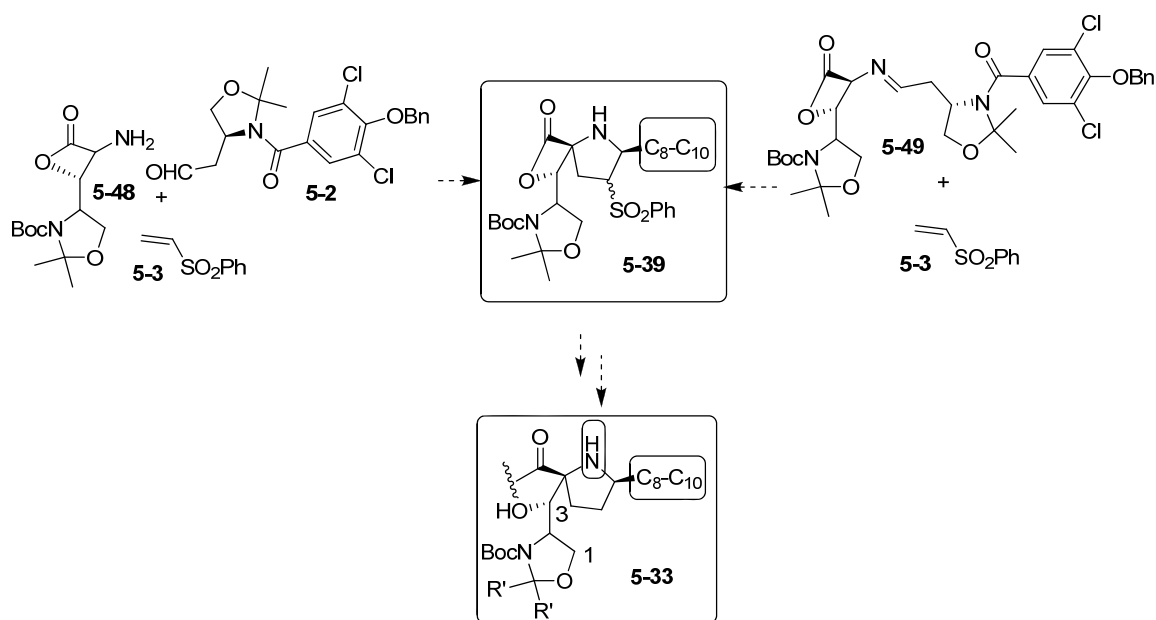
After preparing the α -benzyl substituted glycine-sultam, a one pot reaction was carried out. However, no desired tetra-substituted pyrrolidine was obtained (Scheme 5.10).



Scheme 5.10 Unsuccessful attempt to make a 2,2,4,5-tetrasubstituted pyrrolidine in one pot.

5.1.3.2 A Second Alternative for the Introduction of the C1-C3 Moiety

The failure of the cycloaddition using α -benzyl-substituted glycyl-sultam might be due to the “CN” partner being too bulky. A lactone **5-48** was designed presenting less steric hindrance as the “CN” partner. It was anticipated that the 1,3-dipolar cycloaddition with amine **5-48** would afford the corresponding 4,4,6,7-tetrasubstituted pyrrolidines and that the alkyl substituent at the 4-membered lactone ring would be predicted to control the stereochemistry of the pyrrolidine core (Scheme 5.11).



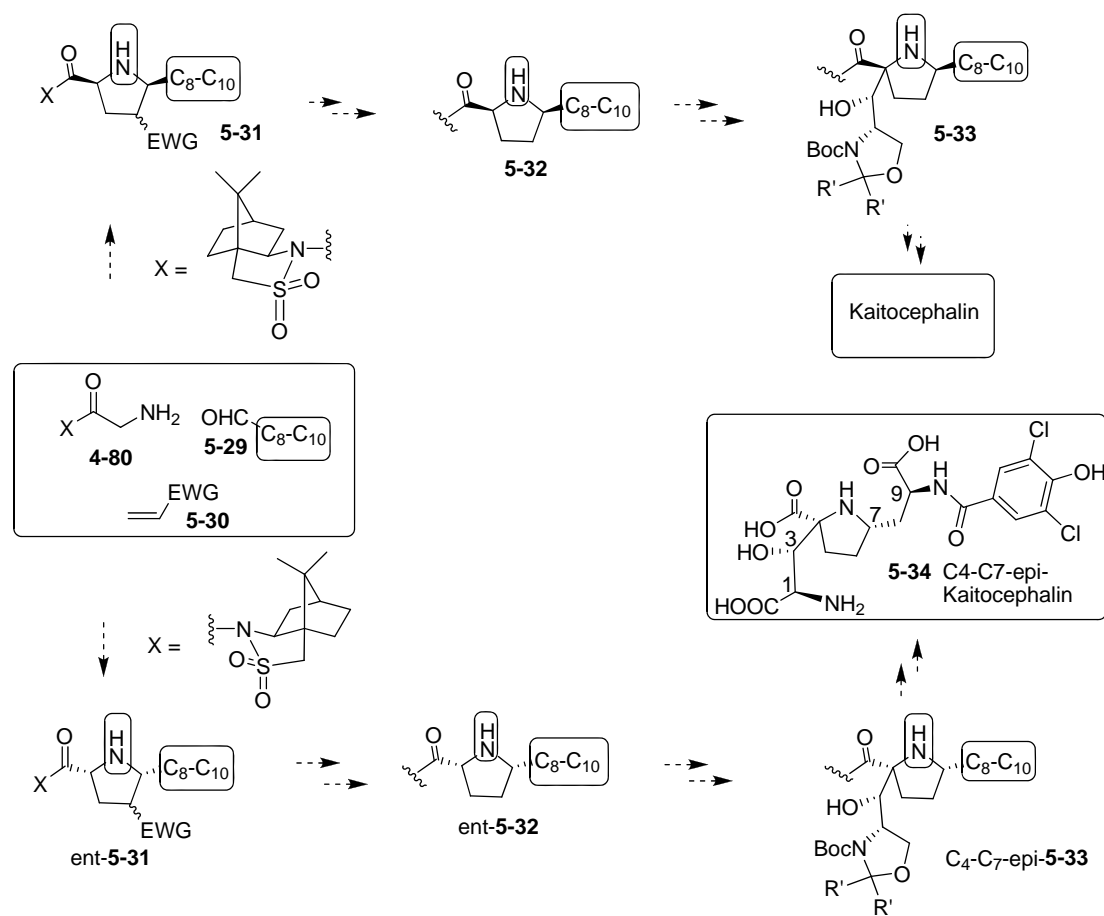
Scheme 5.11 Construction of **5-39** an alternative precursor of tri-substituted pyrrolidines **5-33**.

5.2 Evaluation of the Synthetic Route

A novel approach to the synthesis of *cis*-4,7-disubstituted pyrrolidine core and C₈-C₁₀ side chain has been designed. It is predicted that this synthetic route is also suitable for the synthesis of derivatives of kaitocephalin using different combination of (*R/S*)- glycyl sultam and (*R/S*)-aspartic acid, (*R/S*)-Garner aldehyde or (*R/S*)-chlorocarbonyl-oxazoline.

5.2.1 Pyrrolidine Core with Stereochemical Diversity

The distinguishing aspect of the synthetic strategy is to build 4,7-disubstituted pyrrolidine (**5-32**) via a one pot [CN+C+CC] 1,3-dipolar cycloaddition involving simultaneous creation of the C₄ and C₇ stereocenters, followed by removal of the EWG group (Scheme 5.12).



Scheme 5.12 Construction of the tri-substituted pyrrolidine core.

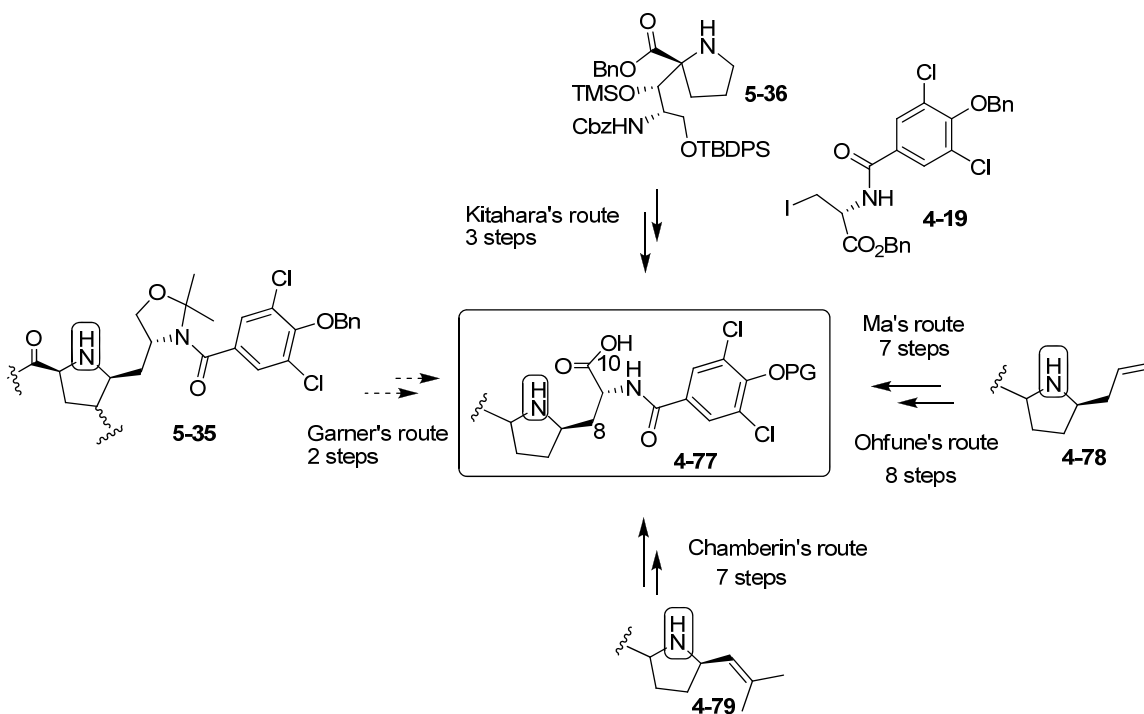
With the same strategy as Ma and Chamberlin, aldol condensation or acylation of enolate derived from disubstituted pyrrolidines **5-32** is anticipated to afford the corresponding tri-substituted pyrrolidines **5-33**.

An appealing strategy for auxiliary mediated one pot [CN+C+CC] 1,3-dipolar cycloaddition involves the possibility of generating the enantiomer of the disubstituted pyrrolidine (**ent-5-32**) which could result in the synthesis of C₄-C₇-epi-kaitocephalin under the same procedure.

5.2.2 Short route to C8-C10 moiety

The synthetic plan is attractive because the N-acylalanine C8-C10 moiety was anticipated to be installed from amino alcohols through ring-opening followed by oxidation.

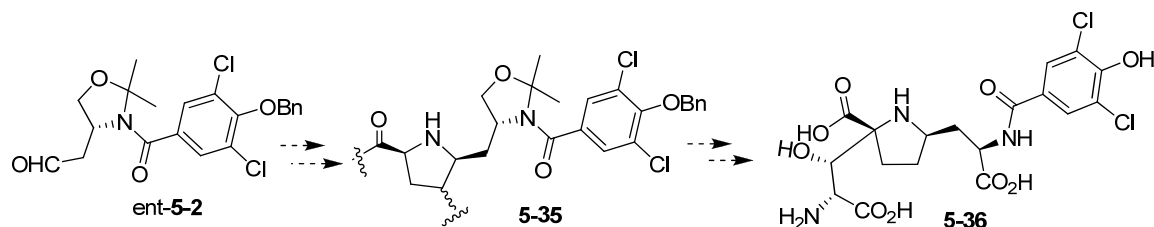
In Ma and Ohfuné's synthesis, C8-C10 was installed from an allyl group of **4-78** in 7-8 steps. Chamberlin's group employed an olefin as the latent aldehyde, which would be converted to the C8-C10 moiety in 7 steps. Only Kitahara's group gave the N-acylalanine moieties in three steps through pyrrolidine oxide formation followed by coupling with a halide **4-19** (Scheme 5.13).



Scheme 5.13 Construction of the N-acylalanine moiety from different precursors.

Since the auxiliary controlled the stereochemistry of the pyrrolidine core in the one pot [CN+C+CC] 1,3-dipolar cycloaddition, it was felt that a C9-epi-kaitocephalin could

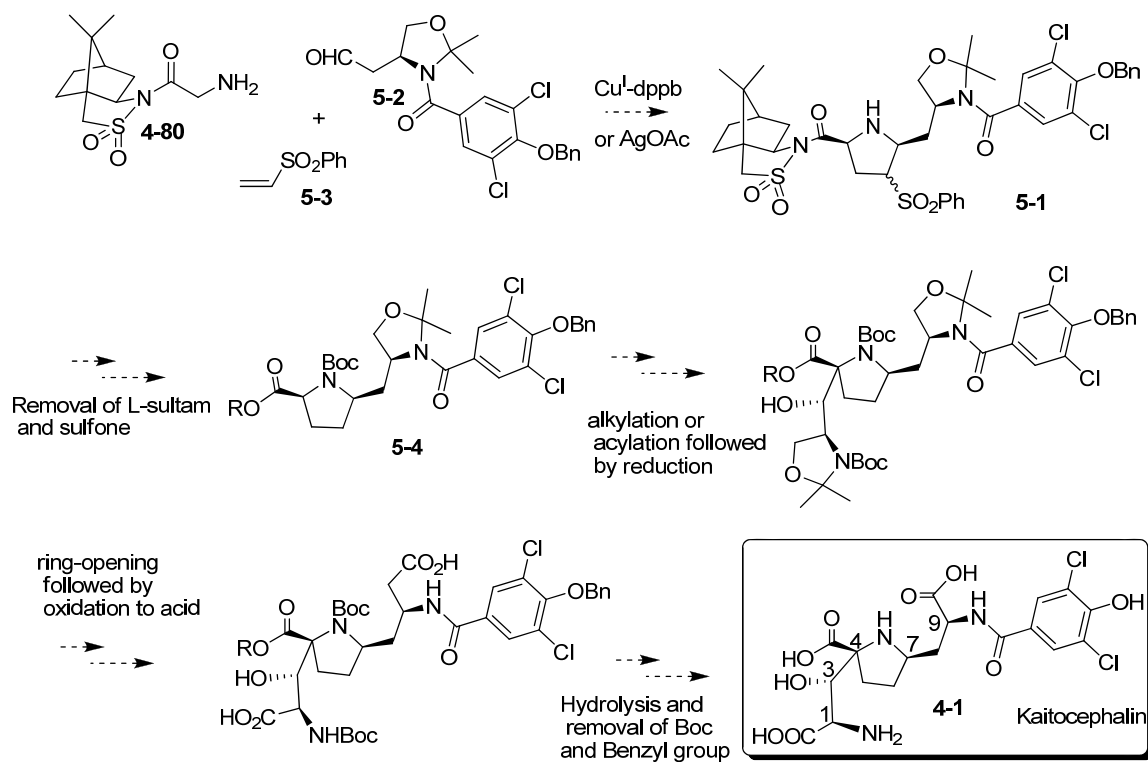
be synthesized using *S*-aldehyde (ent-**5-2**) via the same procedure as for synthesis kaitocephalin (Scheme 5.14).



Scheme 5.14 C9-epi-kaitocephalin formation.

5.3 Conclusions

Based on the retrosynthetic analysis and above further detailed analysis, the synthetic plan towards the synthesis of kaitocephalin is outlined below in Scheme 5.15.



Scheme 5.15 Planned synthesis of kaitocephalin.

6 Aldehyde Formation

The retrosynthetic analysis presented in the previous chapter, combined with other factors, lead to the conclusion that introduction of C7-C9 and its N-substituted benzamide into kaitocephalin would be best accomplished by formation of a suitable aldehyde (Figure 6.1) and incorporation using a [CN+C+CC] 1,3-dipolar cycloaddition.

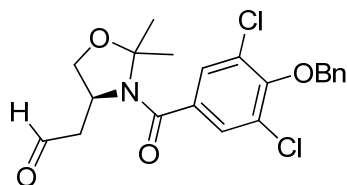


Figure 6.1 Aldehyde as a sub-component precursor of kaitocephalin.

6.1 Retrosynthesis

Aldehydes **6-1** can be prepared via a number of pathways including: oxidation of primary alcohols **6-2**,⁴⁷ reduction of the CN group of nitriles **6-3**,⁴⁸ oxidative cleavage of olefins,⁴⁹ and nucleophilic attack at a protected alcohol derived from serine by thioacetals followed by converting the thioacetals **6-4** into aldehyde (Figure 6.2).

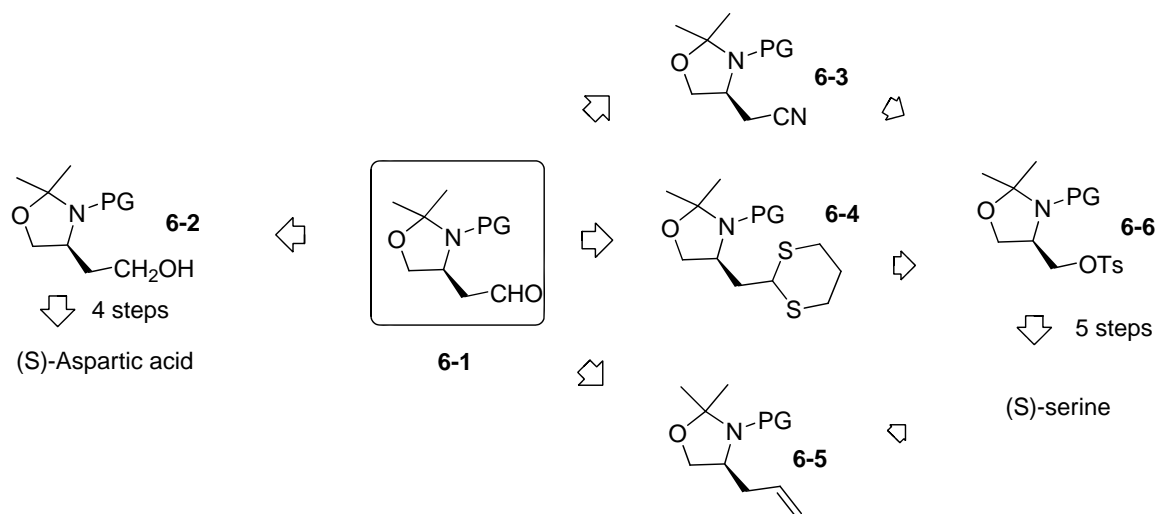


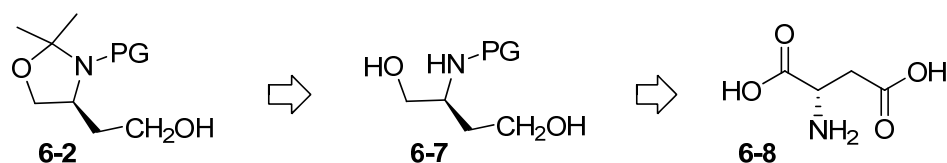
Figure 6.2 Approaches to oxazolidine aldehyde.

Following Ribes' procedure,⁵⁰ aldehyde precursor alcohol **6-2** can be prepared from L-aspartic acid in four steps. Based on retrosynthetic analysis of precursors **6-3**, **6-4**, and **6-5**, it is predicted that all of them could be provided from the tosylate **6-6**, which could be prepared from (S)-serine in 5 steps.⁵¹

The shortest practicable route to the desired aldehyde **6-1** was chosen for investigation first. Furthermore, it is known that the conversion of alcohols to aldehydes is very easy to accomplish, and with fairly high yields. Alcohol **6-2** was predicted as a useful precursor of aldehydes because of its long shelf life.

6.2 Oxazolidine Formation from an Amide-Diol

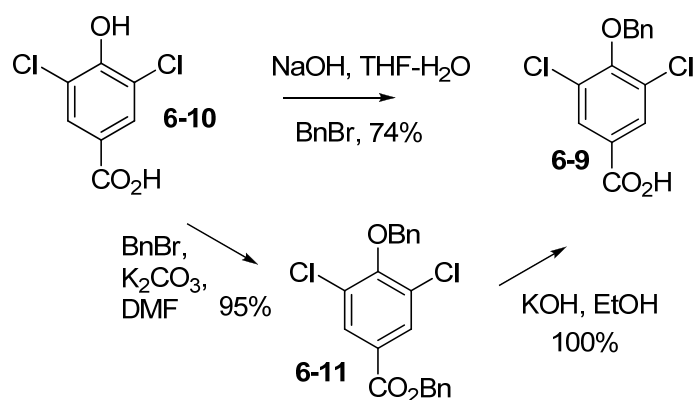
As seen in the retrosynthetic analysis above, the initially favored route to the desired oxazolidine-alcohol **6-2** was via amide functionalization of an amino-diol **6-7** followed by oxazolidine ring formation (Scheme 6.1).



Scheme 6.1 Synthetic plan from aminodiol to oxazolidine-alcohol.

6.2.1 A Specifically Protected Hydroxybenzoic Acid

The synthesis started with the preparation of a benzyl ether carboxylic acid **6-9**. The reaction of phenol acid **6-10** with benzyl bromide and NaOH in refluxing THF-water⁵² gave the desired benzyl ether acid in 74% yield, but some starting material **6-10** remained, and it is difficult to remove the residual starting material **6-10** from reaction products (Scheme 6.2). By analyzing the reaction conditions, we found that an intermediate benzyl ether ester was formed and then the ester was hydrolyzed with NaOH in this one-pot conversion of phenol acid into benzyl ether acid. The product acid was difficult to separate from the starting material acid, but it is extremely easy to separate acid from the intermediate benzyl ether ester by extraction (water/ether).



Scheme 6.2 Synthesis of a specifically protected hydroxybenzoic acid.

Chapter 6: Aldehyde Formation

It was planned to isolate the intermediate benzyl ether ester **6-11**, which would give the desired benzyl ether acid **6-9** via subsequent base hydrolysis.

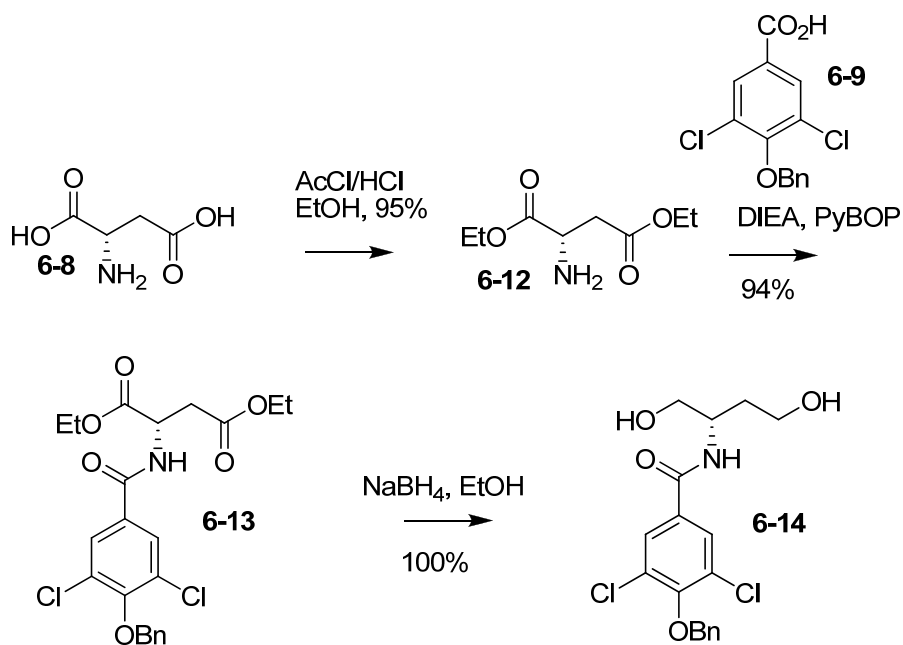
Thus, the hydroxybenzoic acid **6-10** was treated with benzyl bromide in the presence of K_2CO_3 to afford the benzyl ether ester **6-11**. A liquid/liquid extraction was sufficient to remove the hydroxybenzoic acid sodium salt. The benzyl ether ester **6-11** was then hydrolyzed with KOH/EtOH solution to give the expected benzyl ether acid **6-9** in 95% overall yield (Scheme 6.2).

The optimized two-step process from phenol acid **6-8** to benzyl ether acid **6-9** required neither distillation nor chromatographic purification. This procedure to prepare acid has been performed on a 100 g scale.

With the acid in hand, the synthesis toward the oxazolidine based aspartic aldehyde **5-2** was started.

6.2.2 N-Acyl Diol

Following Paintner's procedure, aspartic acid **6-8** was treated with acetyl chloride in ethanol to give diester **6-12** in 95% (Scheme 6.3). A mild PyBOP mediated coupling reaction of the prepared benzyl ether acid **6-9** with amino diester **6-12** afforded the desired N-acyl diester **6-13** in high 94% yield. Treatment of the resulting N-acyl diester **6-13** with sodium borohydride, gave nearly quantitative yield of N-acyl diol **6-14**.

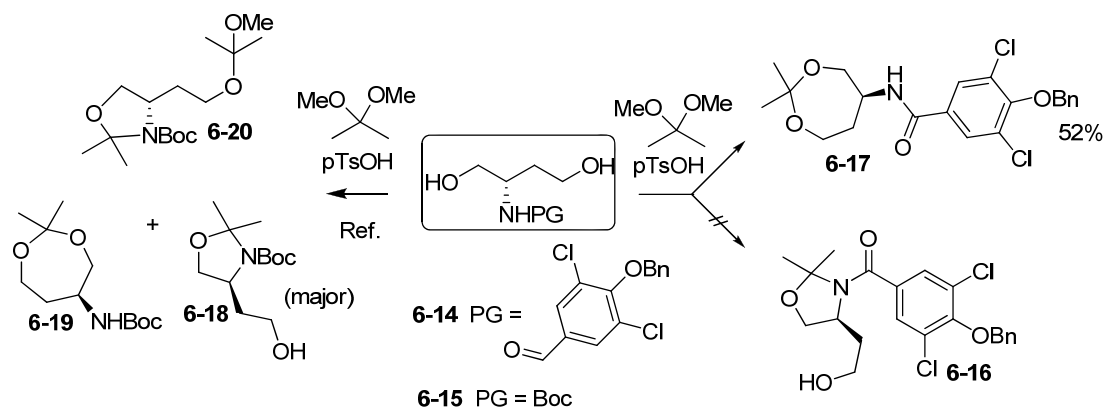


Scheme 6.3 N-Acyl diol formation.

6.2.3 Attempted Oxazolidine Preparation

With the N-acyl diol **6-14** in hand, the oxazolidine preparation by intramolecular cyclization of the N-acyl diol **6-14** was investigated. Following Paintner's cyclizing procedure,⁵³ N-acyl diol **6-14** was first treated with 2,2-dimethoxypropane (DMP) with a catalytic amount of pTsoH in DCM, but no desired oxazolidine compound **6-16** was formed. We found that the reaction ran smoothly to yield the unexpected 7-membered ring **6-17** (Scheme 6.4). This is in sharp contrast to the cyclization of N-Boc protected diol **6-15** where an excellent yield of the corresponding oxazolidine **6-18** was obtained.

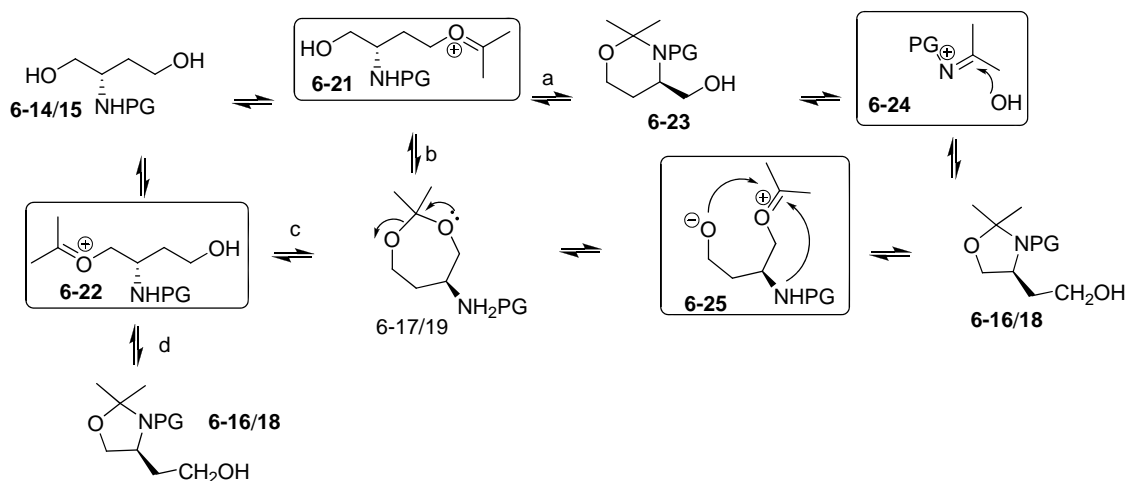
Chapter 6: Aldehyde Formation



Scheme 6.4 Attempted oxazolidine formation.

Different reaction conditions varying the Lewis acids (BF_3/PPTS , and pTsOH), the acetalization reagent (acetone, dimethoxypropane, and 2-methoxypropene), the solvents (cyclohexane, toluene, DCM, and THF) and the temperatures were tried, but no expected N-acyl oxazolidine **6-16** formation was observed. Under the DMP- pTsOH -DCM conditions, neither substrate (**6-14** nor **6-15**) gave six-membered cyclic N,O-ketal.

To understand the different reactivity between the two substrates (**6-14** and **6-15**), a mechanism was proposed for the formation of seven- and five-membered ketals (Scheme 6.5).



Scheme 6.5 Mechanism for cyclizing of amino-1,4-diol.

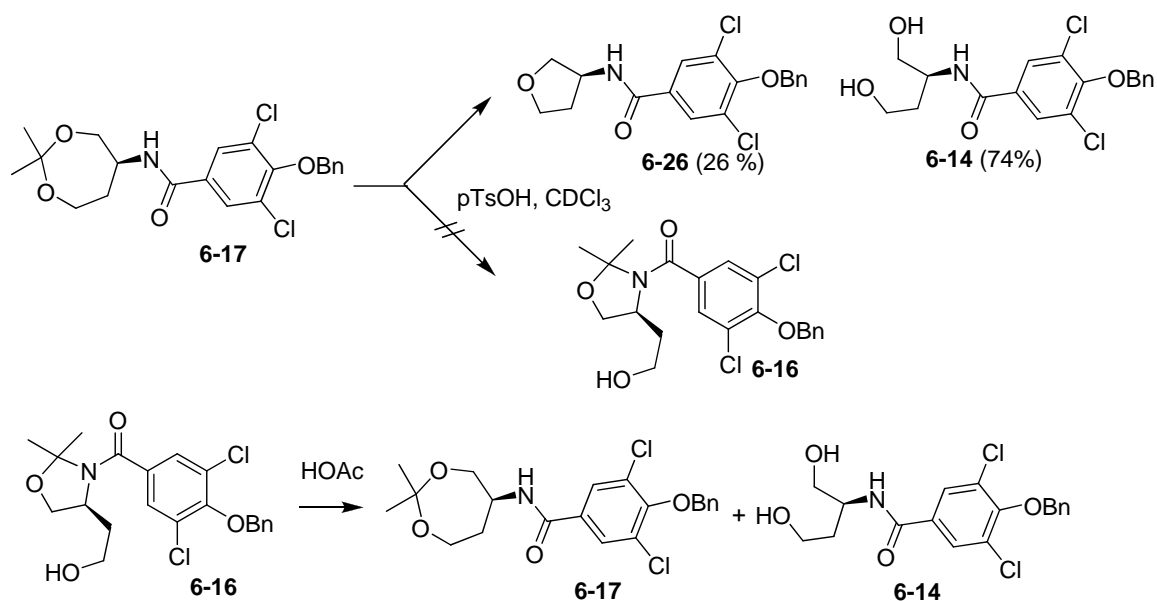
Chapter 6: Aldehyde Formation

In this equilibrium reaction, condensation between hydroxyl groups of diol (**6-14** and **6-15**) and acetone gives the corresponding oxocarbenium ion **6-21** and **6-22** then undergoes intramolecular attack by hydroxyl and amino separately followed by loss of a proton to give the 1,3-oxazinane **6-23**, O,O ketal **6-17/19** and 1,2-oxazolidine **6-16/18** respectively. The reverse process of ketalization from ketals **6-23** and **6-17/19** produced an immonium cation **6-24** and oxocarbenium ion **6-25** separately, both of which would afford 1,2 ketal **6-16/18** via intramolecular nucleophile attack.

Obviously, the result indicated that the subject favors seven-membered ketal formation, while in the case of the N-Boc diol, it is greatly in favor of the oxazolidine formation.

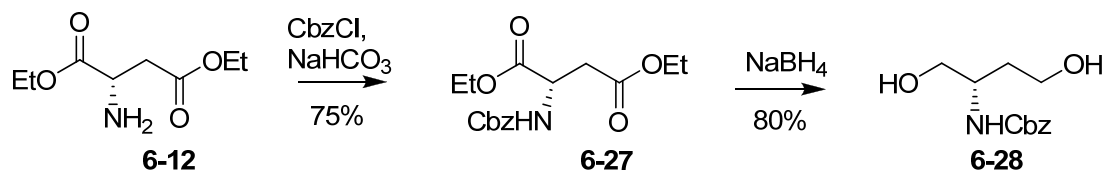
It has been reported that the seven-membered ketal may be converted into five-membered ketal under appropriate reaction conditions.⁵³

As a control experiment, seven-membered ketal **6-17** was treated with pTsOH in CDCl₃ at 80 °C, and produced ring cleavage N-acyl diol **6-14** (76%) and N-acyl ether bearing tetrahydrofuran ring **6-26** (24%). Later, on preparation of N-acyl 1,2-oxazolidine **6-16** through another method, it was found that N-acyl 1,2-oxazolidine **6-16** was easy to convert to seven-membered ketal **6-17** using AcOH (Scheme 6.6). These results indicated that equilibrium favors the seven-membered ketal formation **6-17**.



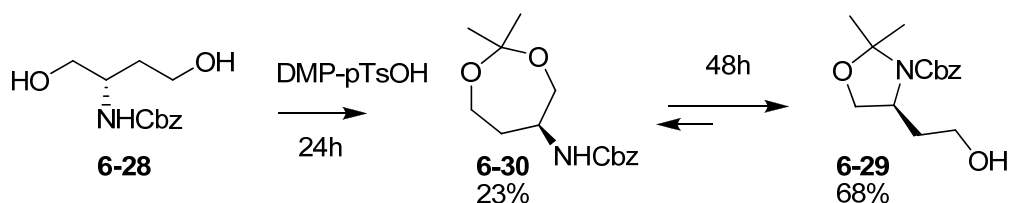
Scheme 6.6 Conversion between five- and seven-membered ketal.

Comparison of the two different protecting groups on the amine, shows that one is a carbamate compound while the other is an amide compound. It was doubted the result of the equilibrium disfavoring the desired five-member ring formation was due to the direct connection between carbonyl and benzene. To test this assumption, a model reaction was carried out. N-Cbz diol **6-28** was chosen as a model compound, since benzyloxycarbonyl (Cbz) shows similar steric and electronic effects on the amino group as those with a trisubstituted benzoyl group. Followed the same procedure as for the diol **6-15**, the N-Cbz diol **6-28** was prepared from the aspartic diester **6-12** in two steps in 60% overall yield (Scheme 6.7).



Scheme 6.7 The formation of model compound N-Cbz diol.

While switching the protective group to Cbz and proceeding via the same transformation (cyclization), the five-membered oxazolidine **6-29** was isolated in 68% yield and the seven-membered ketal **6-30** in 23% yield (Scheme 6.8).



Scheme 6.8 Cyclizing of N-Cbz diol with DMP.

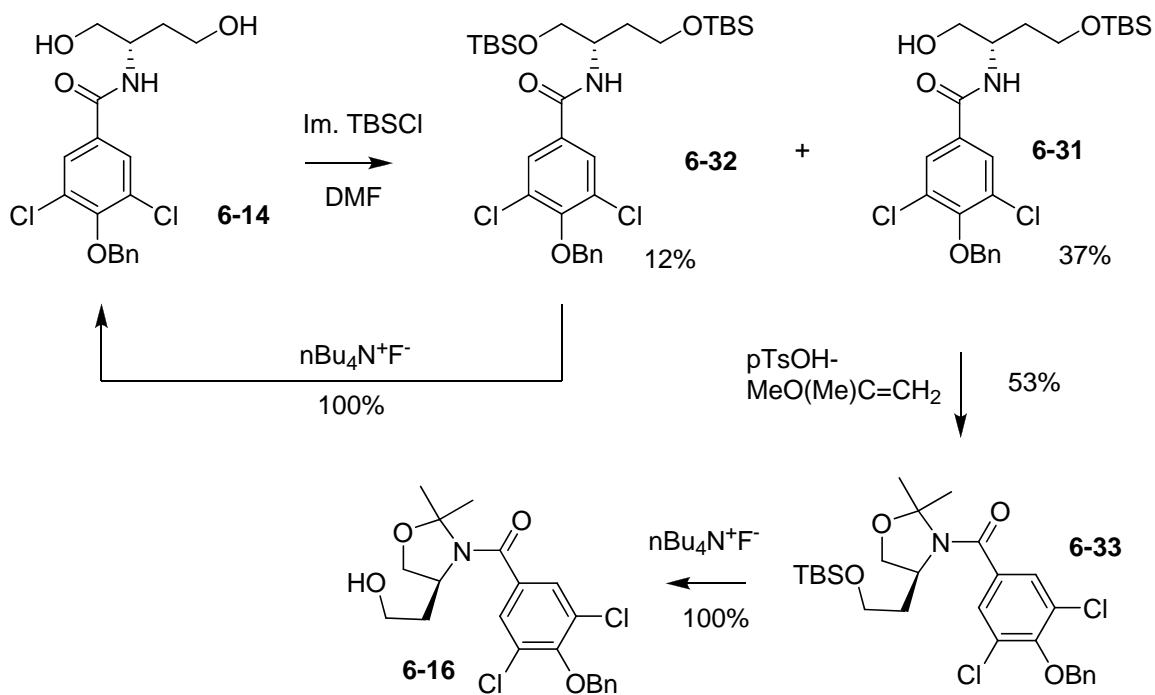
The reaction process showed that seven-membered ketal **6-30** was prepared in 24h, which was converted to N-Cbz oxazolidine **6-29** in 48h. This factor suggested that N-Cbz five-membered ketal **6-29** was formed under thermodynamic control. Based on this result, it was concluded that the presence of the amine protecting group (Cbz and Boc) lead to the kinetic formation of the seven-membered ketal in the cyclizing N-acyl diol.

Evidence for the structure of the seven-membered cyclic N,O-ketal **6-17** was based on proton and carbon NMR spectra. Both ^{13}C NMR spectra of the quaternary carbon at O,O-ketalization and ^1H NMR spectra of NH should be diagnostic. The structure of five-membered ether **6-26** was confirmed by NMR analysis. Remarkably, the NMR spectra at room temperature of amide **6-17** and **6-26** showed that both amides exist as only one rotamer in CDCl_3 solution.

It was hypothesized that the N-acyl oxazolidine **6-2** could be formed through protection of the 4-hydroxy group followed by the deprotection of the resultant oxazolidine compound, or via a sequence of cyclization from free aminodiols and acylation on the monoalkyl substituted amine.

6.2.4 Differential Protection

With the N-acyl diol in hand, interest was directed to selective protection of the C4-hydroxy group. Considering the strong acid lability of the oxazolidine ring products, the hydroxyl group was chosen to be protected by TBSCl for the resulting silyl ether can be easily removed under non-acidic conditions. Treatment of the N-acyl diol **6-14** with TBSCl and imidazole in DMF afforded the desired mono protection product **6-31** as the major product in 37% yield, together with 12% di-protection product **6-32**. The di-protected silyl ether was exposed to TBAF to give the diol **6-14** in 100% yield (Scheme 6.9).



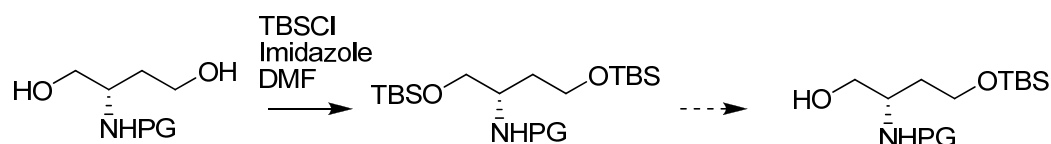
Scheme 6.9 Synthesis of oxazolidine aldehyde from N-acyl diol.

Obviously, the N-acyl group played a central role in the regioselective synthesis of TBSCl ether, as almost no mono protection of C4-hydroxyl was observed.

Chapter 6: Aldehyde Formation

Next, the silyl-protected N-acyl amino alcohol **6-31** was treated with 2-methoxyprop-1-ene in the presence of pTsOH to give silyl ether oxazolidine **6-33** in 53% yield. Subsequent cleavage of the silyl ether with TBAF provided the oxazolidine alcohol **6-2** as an oil in 100% yield (Scheme 6.9).

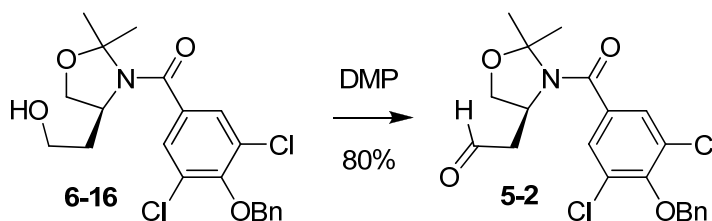
Alternatively, simultaneous protection of two primary hydroxy groups as TBDMS ethers followed by selective removal of the TBDMS group from the primary alcohol at C4 would give the mono protected amino alcohol (Scheme 6.10).



Scheme 6.10 Alternative method to prepared mono alcohol.

6.2.5 Aldehyde Formation

With the desired alcohol **6-16** in hand, the aldehyde intermediate **5-2** was readily obtained in 80% yield by oxidation using DMP (Scheme 6.11). The aldehyde was purified through a short column of silica gel, and this compound was stored in the refrigerator for several weeks.



Scheme 6.11 Oxidation to the aldehyde.

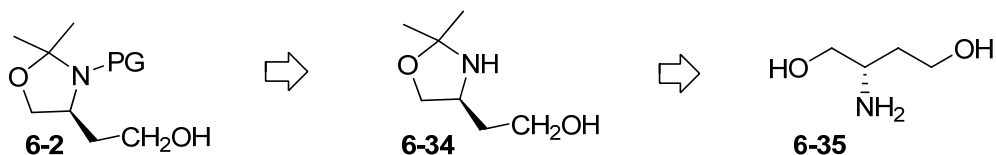
Evidence for the structure of the aldehyde bearing five-membered cyclic N,O-ketal is based on the HH COSY experiment which showed a correlation between the aldehyde

proton and two protons at C3. This indicated that the C4 hydroxyl group was selectively protected as the silyl ether, otherwise an aldehyde bearing a six-membered ring would be obtained.

The syntheses of aldehydes featuring selective protection of primary hydroxyl groups at C4 followed by cyclization and deprotection was accomplished from aspartic acid in seven steps in 14% total yield. Though deprotection afforded an alcohol in near quantitative yield, it is not thought this synthetic route should to be further investigated due to the low isolated yield of monosilyl ether **6-31**.

6.3 Oxazolidine Formation Followed by N-Acylation

An alternative to the formation of the oxazolidine alcohol **6-2** from the amide-diol **6-14** is to form the oxazolidine **6-34** first from the amino-diol **6-35** and then to introduce the acyl group to form the amide **6-2** (Scheme 6.12).

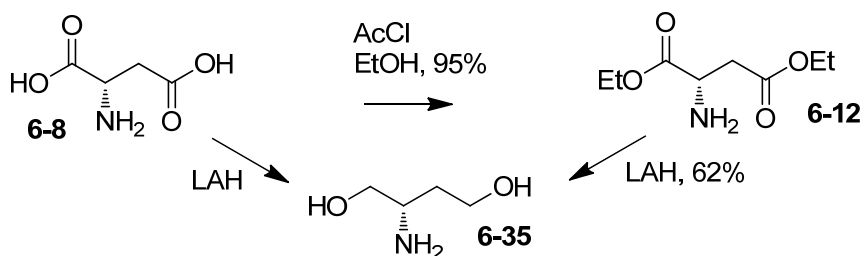


Scheme 6.12 Synthetic plan from amino-diol to oxazolidine-alcohol.

6.3.1 Amino-Diol Synthesis

The synthesis of **6-35** was carried out as outlined in Scheme 6.13. Starting from the L-aspartic acids **6-8**, in the presence of acetyl chloride and ethanol, the corresponding diethyl ester **6-12** was readily prepared in high yield (95%). This was then subjected to LAH reduction to afford the aminodiol in 62% yield. Amino diol **6-35** could be prepared

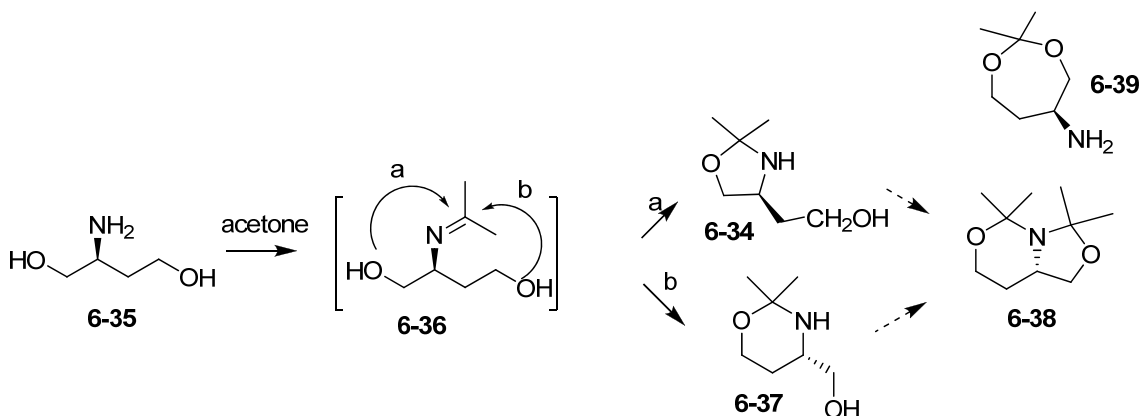
from aspartic acid, but low solubility of L-aspartic acid in THF resulted in recovery of mostly L-aspartic acid.



Scheme 6.13 Preparation of 2-amino-1,4-butanediol **6-35**.

6.3.2 Cyclization to Oxazolidine

With the amino diol **6-35** in hand, the construction of the N-acyl oxazolidine alcohol **6-2** via a ketalization followed by acylation was next investigated. However, problems associated with ketalization from amino diol **6-35** were anticipated, such as regioselectivity of ketalization. The formation of both 5- and 6-membered rings could be rationalized as shown in Scheme 6.14.



Scheme 6.14 Cyclizing from amino-diol.

Chapter 6: Aldehyde Formation

Condensation between amine **6-35** and acetone would produce imine **6-36** and water. The nucleophilic addition of diol onto this electrophilic species would produce two expected products separately. Luckily, a literature survey indicated that no example of N-acyl ketal bearing 6-membered rings had been reported to be synthesized through ketalization followed by acylation. It was hoped that any 6-membered ketal could be converted into an oxazolidine through protective group adjustment under the condition of one pot ketalization followed by acylation.

The possibility that the amino-alcohol might produce an undesired O,O-ketalization compound **6-39** and / or bicyclic compounds **6-38** (Scheme 6.14), was still of concern. The ketal compounds were unstable towards water and silica gel and could not be isolated. The ^{13}C NMR signal of the quaternary carbon at O,O-ketalization should be most diagnostic. The formation of bicyclic compound **6-38** can be deduced by comparison of the proton integration between the methyl groups and other protons in the ^1H NMR spectra.

6.3.2.1 Solvent Evaluation

Ketalization of the amino-diol with acetone was investigated under different conditions with different solvents. The results are shown in Table 6.1.

Table 6.1 Different cyclization conditions.

Entry	Solvent / Additive	Temp. (°C)	Time (h)	Product Ratio 5-:6-:other
1	Toluene	130	48	1.6:1
2	Toluene	130	58	1.88:1
3	Toluene	130	120	2:1:x
4	Benzene	100	48	1.67:1
5	DMSO	rt	2	2:1
6	d7-DMF	rt	2	1.78:1
7	d6-Pyridine	rt	2	1.4:1
8	Acetone	rt	2	1.7:1
9	d6-Acetone	80	24	3:1:0.3:0.3
10	Acetone / MgSO ₄	rt	12	1.68:1
11	Acetone / Na ₂ SO ₄	rt	12	1.64:1
12	Acetone / 4Å mol. sieves	rt	12	1.64:1

The condensation between amino diol and acetone under refluxing toluene gave a 1.88:1 ratio of 1,2-oxazolidine and 1,3-oxazinane (Entry 2). The reaction gave the similar result in refluxing benzene (Entry 4). In these reactions the amino-diol was treated with a co-solvent mixture of acetone-toluene (1:10) at room temperature for 30 min, until the amino-diol was dissolved. The reaction was then carried out in boiling toluene with azeotropic distillation of water. Since acetone has a lower boiling point than the azeotrope, it would accumulate in the Dean–Stark stillhead. Acetone should be introduced into the reaction in a large excess. However, large scale preparation of oxazolidine under refluxing acetone-toluene with a Dean-Stark trap needed a long

Chapter 6: Aldehyde Formation

reaction time. Crude NMR indicated that bicyclic compound **6-38** was formed when ketals were heated for one week (Entry 3).

Next, the reaction with excess acetone was performed in different solvents at room temperature, and gave the highest ratio of 1,2 oxazolidine to 1,3-oxazinane (2:1) using DMSO. The lowest regioselectivity was achieved in pyridine (1.44/1). In acetone and DMF, both condensation reactions produced a 1.7:1 mixture of 5- and 6-membered rings. In all these reactions, only two ring compounds were generated based on the ^1H NMR spectra (Entries 5, 6, 7 & 8).

Similar results were found when samples were prepared from amino-diol and acetone using different deuterated NMR solvents. The ratio of 1,2-oxazolidine to 1,3-oxazinane under DMSO- d_6 , DMF- d_7 , acetone- d_6 and pyridine- d_5 was 2:1, 1.7:1, 1.7:1 and 1.4:1 respectively.

When a 1.7:1 mixture of 1,2 oxazolidine and 1,3-oxazinane was heated in refluxing acetone, it converted to a 3:1 mixture, indicating that 1,2-oxazolidines are thermodynamically more stable. However, ^1H NMR spectra in d_6 -acetone solution revealed two new cyclization compounds were formed at the same time, thus, we abandoned further testing of the thermodynamic control of 1,2 oxazolidine formation.

In this condensation reaction, water was formed and it is known that oxazolidines are sensitive toward water. Water should be removed before acylation. Our control experiment indicated that the 1.7:1 mixture of oxazolidine and oxazinane started to decompose in d_6 -DMSO with 5% D_2O in only 1h, and no oxazolidine remained after two days, while in d_5 -pyridine with 5% D_2O , only 20% of the oxazolidine and oxazinane underwent ring cleavage. Based on these results and the properties of DMSO, such as

being a highly hygroscopic liquid and having a high boiling point, acetone was chosen as the reaction solvent, even though 1,2-oxazolidine formation showed the highest regioselectivity in DMSO.

This condensation reaction using acetone as solvent was always with retention of less than 1% amino-diol remaining in this reaction. Additives such as MgSO_4 , Na_2SO_4 , and molecular sieves were tried to remove the water from the reaction, however, the same ratio of oxazolidine mixture was observed as that achieved without them (Entries 10, 11 & 12).

6.3.2.2 NMR Evidence

Evidence for the 1,2-oxazolidine was obtained from the coupling constant between H1b and H1a in 1,2-oxazolidine ($J_{1a-1a'}$ 7.5 Hz). (Figure 6.3) 1,2-oxazolidine was deduced from the desired N-acyl 1,2-oxazolidine **6-2** as the major product when trapped by acyl chloride. Direct evidence for the 6-membered oxazolidine formation such as ^{13}C NMR spectra of the quaternary carbon at O,N-ketalization was not obtained. Based on proton ratios between the methyls and the protons at C2, it was reasoned that the other unknown compound was a one ring system. The fact that acylation of condensation product failed to give any N-acyl 7 membered ring compound indicated that no O,O ketalization was formed.

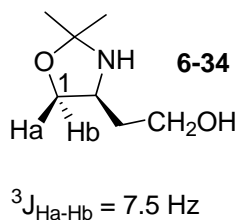
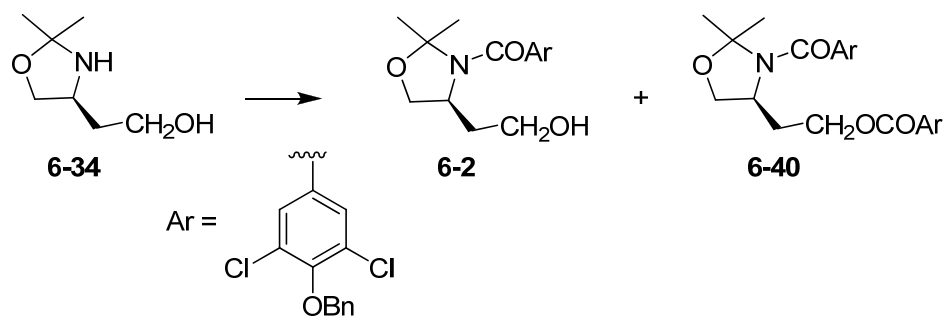


Figure 6.3 NMR coupling constant evaluation for **6-34**.

Thus, the simplest method to prepare oxazolidine was to stir the aminodiol in acetone for 2h at room temperature. Under the developed conditions, products arising from dialkylation of amine were not observed. Presumably the hindrance of cyclization leads to decrease in nucleophilicity of the product amine.

6.3.3 Acylation of Oxazolidine

With the convenient synthetic method in hand, next, the acylation with the oxazolidine **6-34** was explored. Since oxazolidines are unstable towards water and silica gel, they were immediately converted to N-acyl oxazolidine without further purification or delay (Scheme 6.15).



Scheme 6.15 Acylation of the oxazolidine.

6.3.3.1 Acylation Conditions

Different acylation conditions varying the base [TEA, pyridine and K₂CO₃ PPTS], the solvents (DCM, acetone-DCM, DCM-DMSO), and acylating reagents were used (Table 6.2).

Chapter 6: Aldehyde Formation

Table 6.2 Different acylation conditions.

Entry	Base	Acyating		Yield
		Reagent (1.1 eq)	Solvent	N-acylation : N,O-diacylation
1	TEA (1.2 eq)	ArCOCl	DCM (dried)	34% : 10.5%
2	TEA (1.2 eq)	ArCOCl	DCM	37% : 4.5%
3	TEA (2 eq)	ArCOCl	DCM	32% : 8.5%
4	TEA (2 eq)	ArCOCl	DCM	20% : 30%
5	TEA (5 eq)	ArCOCl	DCM	15% : 18%
6	DIEA (1.2 eq)	ArCOOH	DCM	0% : 10%
7	Na ₂ CO ₃	ArCOCl	DMF	trace
8	TEA (1.2 eq)	ArCOCl	DCM:Acetone 1:1	-
9	Pyridine (excess)	ArCOCl	DCM:Acetone 1:1	-
10	K ₂ CO ₃	ArCOCl	DCM:Acetone 1:1	trace
11	TEA (1.2 eq)	ArCOCl	DCM:DMSO 10:1	35% : 3.2%
12	TEA (1.8 eq)	ArCOCl	DCM:DMSO 10:1	29% : 15%

It was found that the best condition for acylation was utilizing ArCOCl with TEA (1.2 eq) in DCM (Table 6.2, Entries 1 & 2). The N-acylated oxazolidine formed from this reaction was unambiguously identified as the same as the N-acylated oxazolidine prepared via a sequence of silyl-protected oxazolidine formation followed by deprotection, through comparison of physical data such as VT NMR, mass spectrometry and R_f on TLC. In these reactions, N,O-diacylation product was always isolated. Both

employing more equivalents of TEA (Entries 3&5) and adding oxazolidine to the acyl chloride in the presence of TEA (Entry 4) lead to N,O-diacylation in higher yield. To suppress the amount of N,O-diacylation formed an attempt at acylation under Schotten-Baumann conditions failed to generate the desired oxazolidine compound in high yield due to the hydrolysis of oxazolidine (Entries 7 & 9).

6.3.3.2 Byproducts

Large numbers of ring cleavage byproducts such as **6-40/41/42/43/44**, **6-8** and **6-14** were isolated (Figure 6.4), which indicated the presence of water in the solvent influenced the reaction result. Among these byproduct, N-acyl diol **6-14** and mono-alcohol **6-42** were the major byproducts. No product bearing 6-membered rings was observed. It is highly likely the 6-membered ring compound decomposed under the acylation conditions.

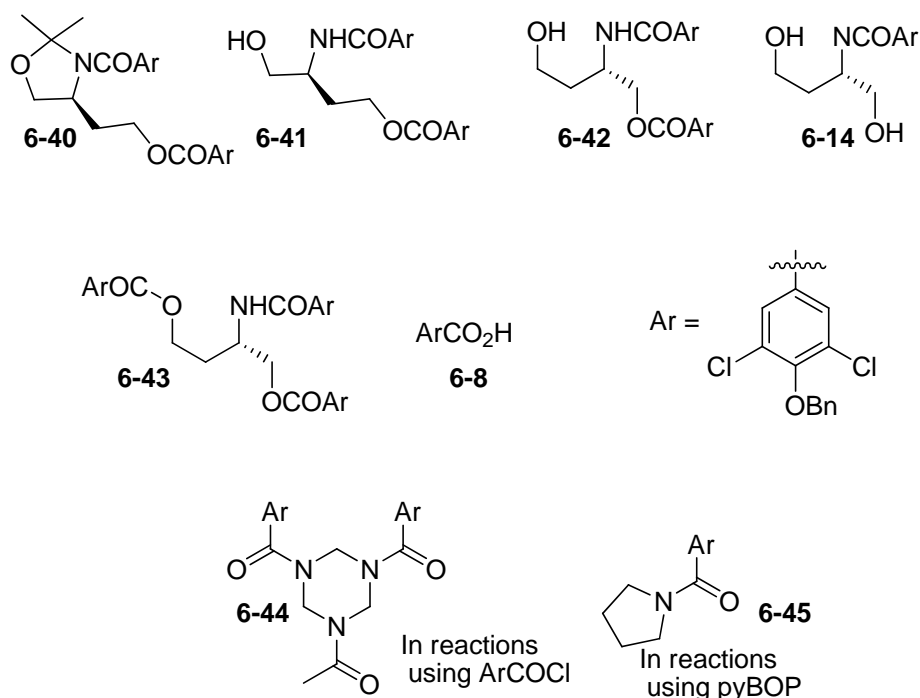
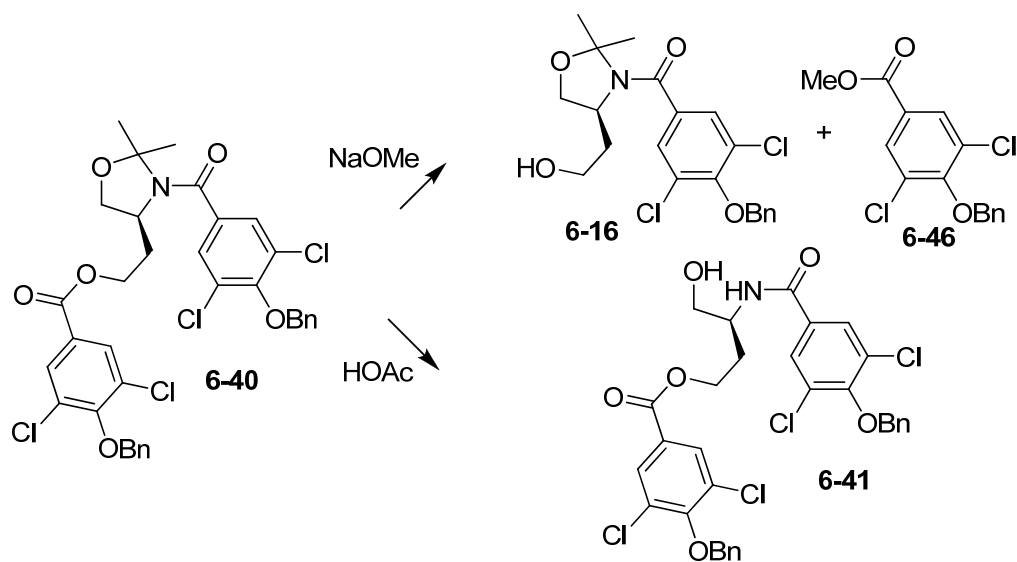


Figure 6.4 By-products from the acylation reaction.

Evidence for the diacyl oxazolidine **6-40** was obtained from its conversion to oxazolidine alcohol **6-15** by treatment with NaOMe. The structure of mono alcohol **6-41** was deduced from the result that cleavage of the oxazolidine ring of compound **6-40** under acidic conditions afforded the mono alcohol **6-41** (Scheme 6.16).



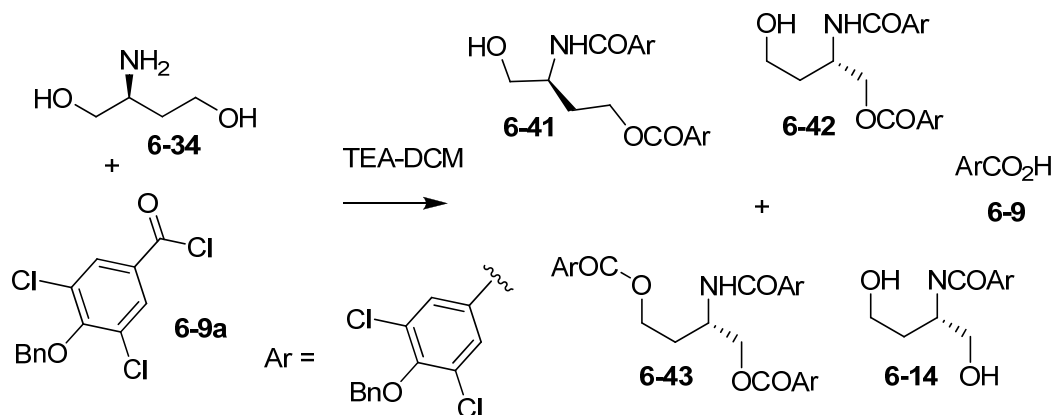
Scheme 6.16 Transformations from di-acyl oxazolidine **6-40**.

6.3.3.3 Diagnosing Byproduct Reactions

Since the control experiment using d_5 -pyridine with 5% D_2O suggested a slow hydrolysis of oxazolidine, it was believed that byproducts might be formed from 6-membered ring compounds via an acylation followed by ring cleavage.

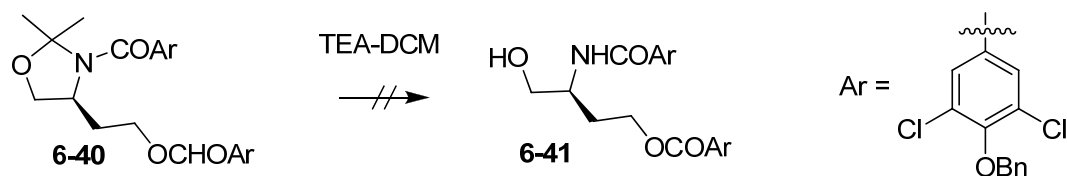
Under the same optimizing acylation conditions (Table 6.2., Entries 1&2), amino-diol was treated with $ArCOCl$ with TEA in DCM. This produced four acylation products **6-41/42/43** and **6-14** (Scheme 6.17). Among these products, di-acylation products (**6-41** and **6-42**) were the major compounds produced. However, the acylation with stringent water free conditions gave a large amount of N-acyl diol and a small amount of

diacylation product **6-41**. This result indicated that byproducts were mostly formed through acylation followed by hydrolysis.



Scheme 6.17 Acylation of amino-diol.

Next, a control experiment was carried out to test the stability of diacyl oxazolidine **6-40** under the reaction conditions. N,O-diacylated 1,2-oxazolidine **6-40** was treated with TEA-DCM, and no hydrolysis compound **6-41** was detected (Scheme 6.18). This result indicated that mono alcohol **6-41** was produced from amino diol **6-34**, which suggested that amino diol **6-34** was formed under acylation conditions.



Scheme 6.18 Control experiment showed no ring-opening product using TEA.

Thus, the ring cleavage of parent oxazolidine **6-34**, 1,3-oxazinane **6-37** and its acylation products led to the byproducts formation.

6.3.3.4 Avoiding Byproducts

On a small scale, acylation using parent 1,2-oxazolidine after removal of water gave similar results to that utilizing oxazolidine with water remaining in the reaction system (Table 6.2, Entries 1 & 2). However, on a large scale, water (wet solvent) dramatically influenced the reaction outcome.

It was felt that acylation employing K_2CO_3 and pyridine would lead to a higher yield considering that they could be used as a base and drying reagent in this reaction, however, the use of K_2CO_3 or pyridine gave inferior results (Table 6.2, Entries 9 & 10). When oxazolidine was quenched with acyl chloride solution in pyridine, no desired N-acyl ketal **6-2/40** was detected, and a large amount of N-acyl diol **6-14** was observed.

After keeping oxazolidine in acetone for at least one week, NMR spectra revealed that no hydrolysis was detected. This observation prompted the choice of the co-solvent mixture of DCM and acetone (1:1) as solvent for acylation, but no desired acylated oxazolidine **6-2/40** was formed. (Table 6.2, Entry 8).

When parent 1,2-oxazolidine **6-34** was treated with acid **6-9** (1.1 eq) under a mild condition using PyBop as activating agent, N,O-diacyl oxazolidine **6-40** was obtained in 10% yield along with acyclic di-acyl **6-41** (14%) and triacyl **6-43** (14%) (Table 6.2, Entry 6).

Next, acylation employing anhydride with Na_2CO_3 in DMF was investigated, but this gave a mixture of an unknown major compound and the desired N-acyl oxazolidine **6-2** in a very low yield (Table 6.2, Entry 7).

Attempts to use the solvent effects on this competition between acylation and ring cleavage failed to afford acylation product in a higher yield. The acylation performed

in co-solvent of anhydrous DMSO and DCM (1:10) afforded the desired acyl oxazolidine **6-2** and the diacylated product **6-40** in a combined yield of 44% (Table 6.2, Entry 11).

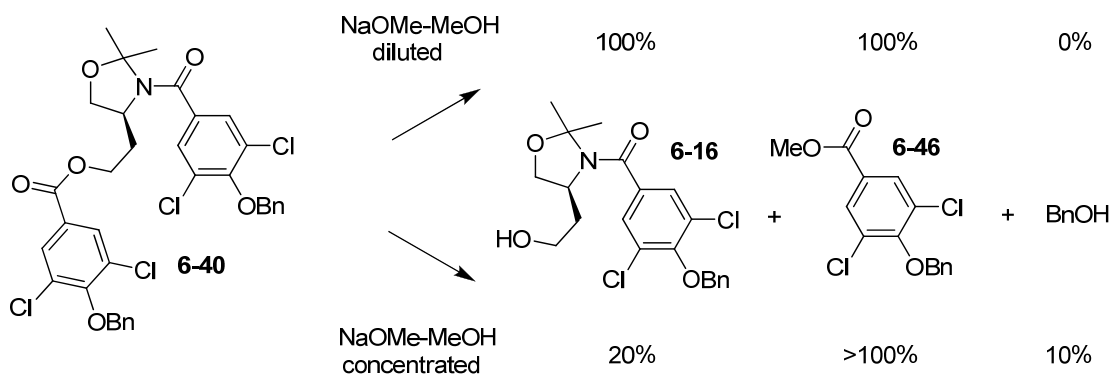
Thus, using a tandem two-step procedure involving oxazolidine formation followed by acylation, N-acyl oxazolidine **6-2** was prepared from amino diol **6-34** in 37% overall yield.

Considering the mass equilibrium of acyl chloride **6-9a** and amino diol **6-14**, it was reasoned that a large amount of amino diol **6-35** must remain in the reaction which was lost in the extraction process with the bi-phase system $\text{CH}_2\text{Cl}_2\text{-H}_2\text{O}$. Attempts to use excess acyl chloride **6-9a** failed to give acyl ketals **6-2/40** in a high overall yield.

6.3.4 Selective Ester Hydrolysis

Work was next focused on the conversion of N,O-di-oxazolidine **6-40** into N-acyl oxazolidine **6-2** (Scheme 6.19). Basic cleavage of the ester **6-40** with dilute NaOMe solution in MeOH followed by a sequence of desalting gave oxazolidine alcohol **6-2** exclusively in 100% yield,⁵⁴ while using excess NaOMe and in a concentrated solution⁵⁵ afforded the oxazolidine **6-2** in 20% yield along with methyl ester **6-46** in more than 100% apparent yield, which suggested amides had undergone cleavage. ^1H NMR of crude compound indicated that a small amount of benzyl alcohol was produced. Fortunately, no de-chloro compound was observed based on the crude NMR spectra.

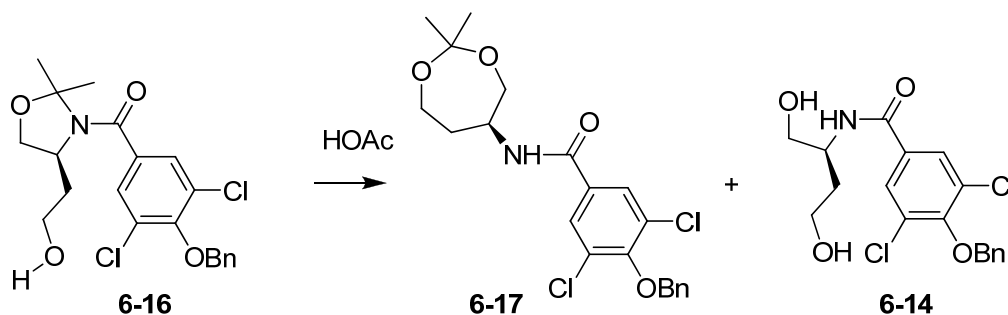
Chapter 6: Aldehyde Formation



Scheme 6.19 Conversion of N,O-diacyl oxazolidine **6-40** to N-acyl oxazolidine **6-16** with apparent yields.

Hydrolysis of N,O-diacyl ketal **6-40** was also performed using KOH in hot EtOH-H₂O. This gave the desired hydroxyl oxazolidine **6-2** but also gave a large amount of unknown by-products.

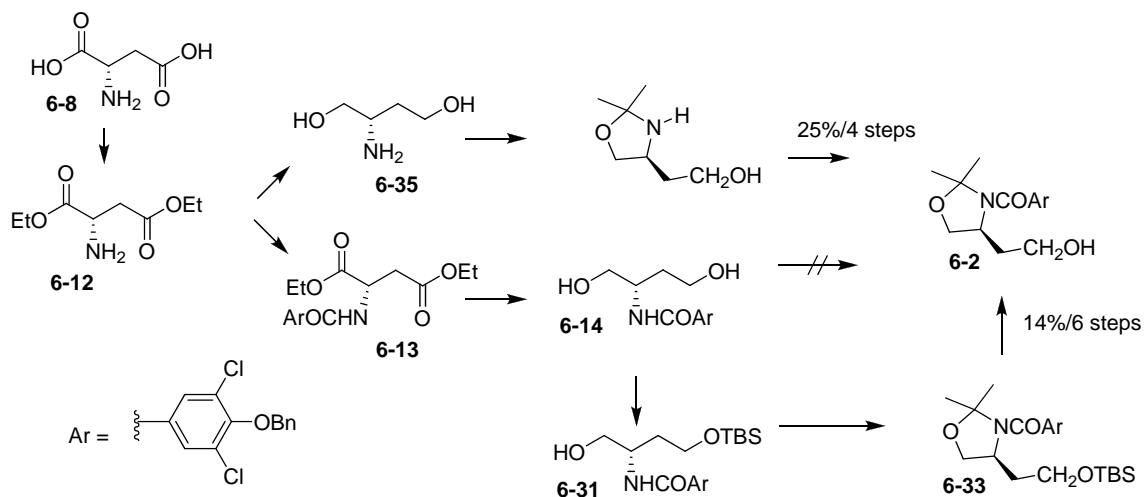
The fast conversion of N-acyl oxazolidine **6-16** to a mixture of 7-membered ring ketal **6-17** and N-acyl diol **6-14** when exposed to acetic acid, (Scheme 6.20) suggested that N-acyl oxazolidine **6-16** should be stored in non-acidic conditions or used without delay.



Scheme 6.20 Acid catalysed ring opening and exchange.

6.3.5 Summary

A four-step process from L-aspartic acid **6-8** to N-acyl oxazolidine alcohol **6-2** did not require chromatographic purification, except in the last step, and gave the desired oxazolidine alcohol **6-2** in 25% overall yield (Scheme 6.21). In spite of the modest yield, this procedure was found to be superior to the original synthesis featuring with mono protected silyl ether **6-31** as an intermediate due to its shorter route and higher overall yield.

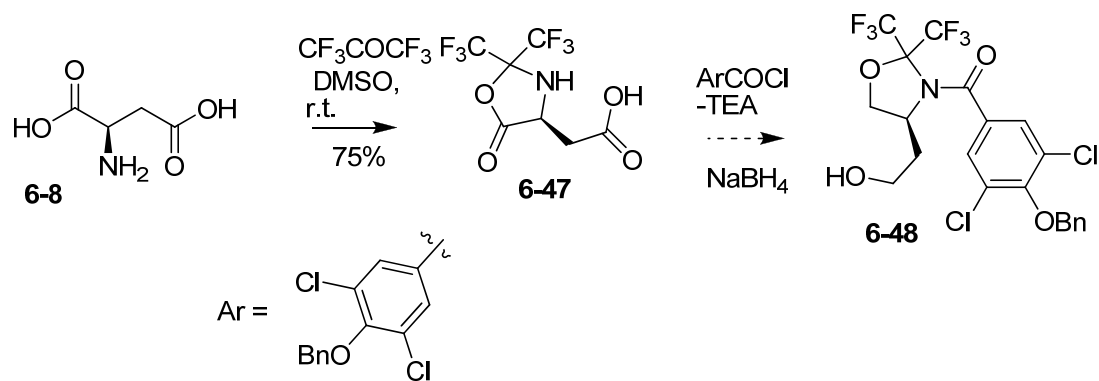


Scheme 6.21 Synthetic routes to N-acyl oxazolidine **6-2**.

6.4 A Fluorinated Alternative

Obviously, a different order to the introduction of the carbonyl group and isopropene mask group lead to different results. An approach featuring a key regioselective ketalization step will be more attractive if a higher regioselective five-membered ketal can be developed. In 2004 year, the Burger group reported that using perfluorinated acetone and aspartic acid, regioselectively provided oxazolidine **6-47** in

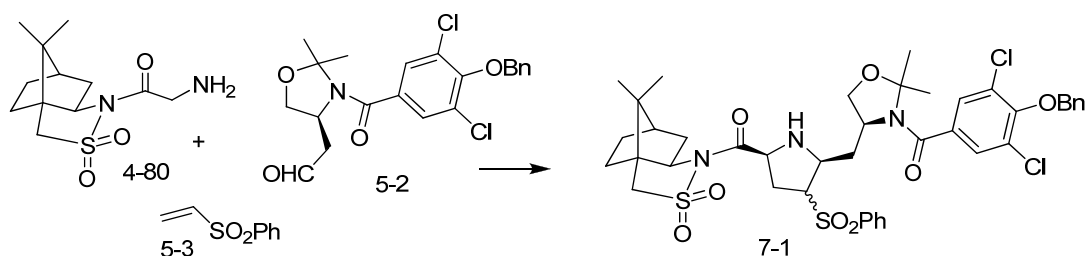
75% yield (Scheme 6.22).⁵⁶ Based on this result, it is predicted that oxazolidine alcohol **6-48** could be generated through acylation of **6-47** with ArCOCl followed by reduction of the resultant compound's acid and ester groups with NaBH₄.



Scheme 6.22 Formation of new oxazolidine alcohol **6-48**.

7 Cycloaddition

With the aldehyde **5-2** in hand, next, the 1,3-dipolar cycloaddition was tested with this aldehyde (Scheme 7.1). The plan is for the preparation of 4,7-disubstituted pyrrolidines from 4,6,7-trisubstituted pyrrolidines.⁵⁷ It is therefore very important to investigate the formation of trisubstituted pyrrolidines in [CN+C+CC] 1,3-dipolar cycloadditions of aldehyde **5-2**. It is also important to control potential epimerization of the desired stereocenters at C4 and C7.



Scheme 7.1. A 1,3-dipolar cycloaddition involving aldehyde **5-2**, sulfone **5-3** and sultam **4-80**.

7.1 Catalytic Conditions

The Garner group has developed two different catalytic conditions for 1,3-dipolar cycloaddition reactions. Ag catalyzed endo-selective [CN+C+CC] cycloadditions and CuI-dppb mediated exo-selective [CN+C+CC] cycloadditions.

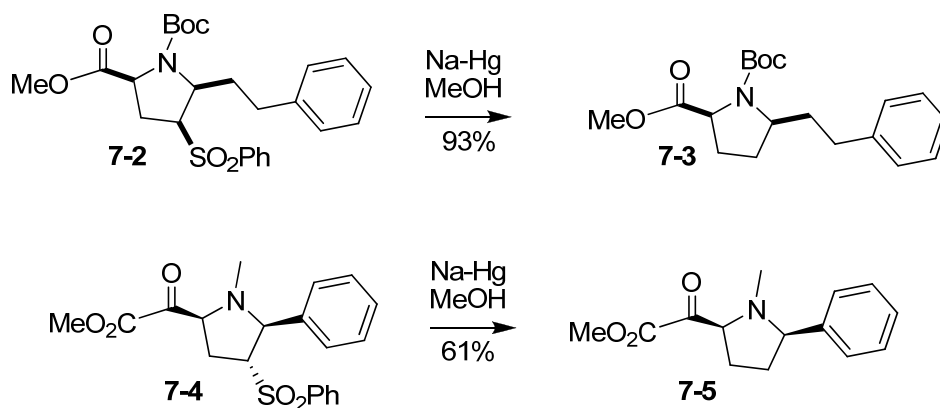
7.1.1 Exo or Endo Cycloadduct for Desulfonylation?

The question is which isomer (the exo or endo cycloadduct) is the most suitable precursor for desulfonylation? Considering the mechanism of desulfonylation proceeds through a sequence of forming a radical anion followed by fragmenting to an anion

section and a radical section,⁵⁸ it was reasoned that both endo- and exo-species could form desulfonylation products. (The regioisomers should also give the desulfonylation product, though no regioisomers were observed in either the silver or copper mediated reactions).

7.1.1.1 Sodium Amalgam Desulfonylation

Desulfonylation of model compound **7-2** indicated that endo sulfone pyrrolidines gave the desulfonylation product in 93% yield by treatment with Na-Hg (Scheme 7.2). In 2006 Carretero's group reported that exo-sulfone pyrrolidines afforded the corresponding desulfonylation product in 60% yield under the same reducing conditions.⁵⁹ Based on these results, it was presumed that both endo- and exo-species could form desulfonylation products.

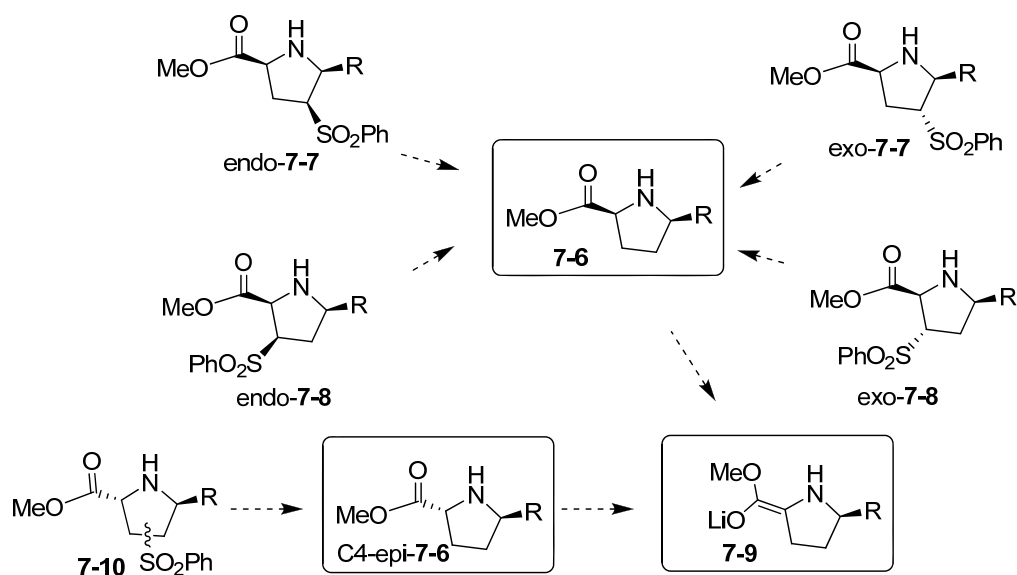


Scheme 7.2 Model desulfonylation reactions.

Thus, the synthetic plan to use 1,3 dipolar cycloaddition to form the pyrrolidine ring was attractive because all the isomers, such as, regioisomers, exo/endo isomers, and C4-epi-isomers can be used as efficient intermediates for the synthesis of kaitocephalin.

7.1.1.2 Isomer Equivalence

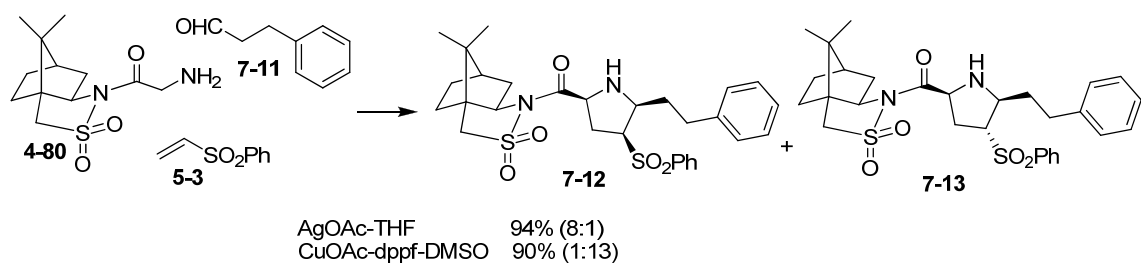
Since all the isomers (except C4-epimers) would convert to one compound after desulfonylation, and all the isomers would be transformed to the same lithium enolate via a sequence of desulfonylation and lithiation (Scheme 7.3), separation of all of the individual isomers was not necessary. Thus, the choice for the cycloaddition catalytic conditions was based on the combined yield of the cycloadducts.



Scheme 7.3 Cycloadducts as precursors for enolate 7-9.

7.1.2 Comparing Reactivity

Model compound reactions indicated that the [CN+C+CC] one pot 1,3-dipolar cycloadditions using Ag(I) gave the cycloadduct endo- and exo-isomers in an 8:1 ratio with a combined yield of 94%, while the reaction using Cu(I) gave a similar yield of the cycloadduct (90%) but with a very different endo:exo ratio (1:13) (Scheme 7.4).



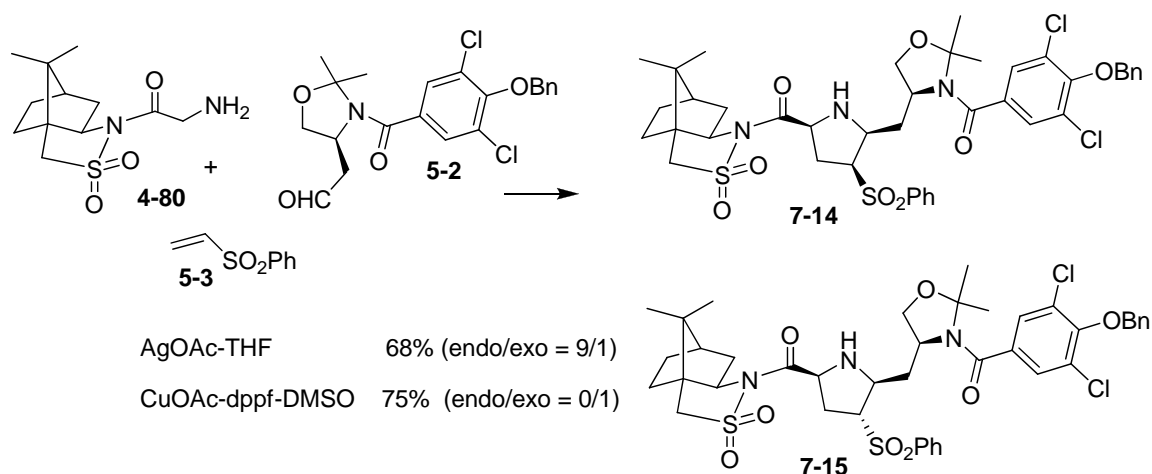
Scheme 7.4 Cycloaddition of model compounds under different conditions.

Both Ag and Cu catalytic systems generated endo- and exo-isomers with no regioisomeric adducts. The regiochemistries of these adducts were easily deduced from the splitting pattern of ^1H at C4 in the NMR.

Based on these results, the two catalytic conditions exhibited similar reactivity. Both the silver and copper catalytic conditions could be used to prepare sulfone pyrrolidines using an oxazolidine aldehyde.

7.1.3 Cycloaddition Using Real Intermediates

Following the procedure previously reported by the Garner group,⁴⁰ a mixture of aldehyde **5-2** and glycylyl sultam **4-80** was treated with phenyl vinyl sulfone **5-3** in the presence of different catalytic reagents. It was found that the AgOAc catalyzed cycloaddition gave the product in 68% yield as a 9:1 mixture of endo- to exo-cycloadduct, while copper-dppf afforded exclusively exo-product in 75% yield (Scheme 7.5).

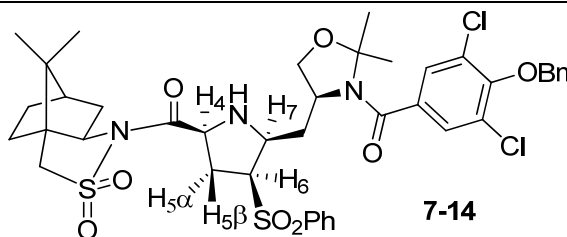


Scheme 7.5 Cycloaddition using oxazolidine **5-2** under different conditions.

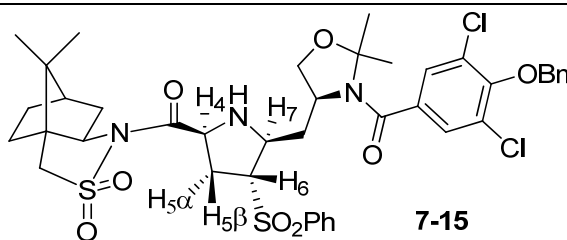
Clearly, the Cu-dppf promoted cycloaddition provided a convenient method as chromatographic separation of endo and exo-isomers was difficult, due to close R_f values, though the mixture of endo- and exo-isomers could be used directly for desulfonylation.

7.1.3.1 NMR Analysis

Assignment of the endo- and exo-structures was based on the proton and carbon NMR spectra. The stereochemistry of the cycloadduct was established by NOE-spectra. The correlation between H₄ and H₇ and between H₆ and H₇ indicated an endo-structure for **7-14** (Table 7.1). The correlation between H₄ and H₅ α and between H₅ α and the aromatic protons of the SO₂Ph indicated an exo-structure for **7-15** (Table 7.2).

Table 7.1 NOE analysis of the endo-cycloadduct **7-14**.

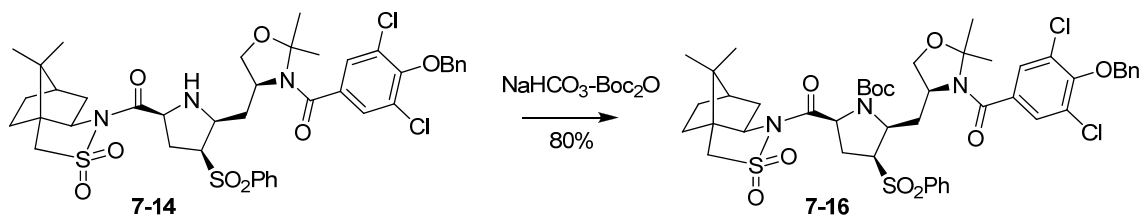
Irradiated Hydrogen	Enhancement%				
	H4	H5 α	H5 β	H6	H7
H4	-	0.8%	-%	0.4%	0.4%
H5 α	2.7%	-	11.5%	1.80%	0.04%
H7	2.4%		-	2.10%	-

Table 7.2 NOE analysis of the exo-cycloadduct **7-15**.

Irradiated Hydrogen	Enhancement%				
	H4	H5 α	H5 β	H7	SO ₂ Ph
H4	-	2.1%	-	0.4%	-
H5 α	4.2%	-	16%	-	1.80%
H7	0.42%	-	-	-	0.63%

7.1.3.2 Cycloadduct Protection

Next, the N-Boc protected compound of the endo-cycloadduct was prepared in 80% yield using NaHCO₃-Boc₂O in THF-H₂O (Scheme 7.6).



Scheme 7.6 Boc protection of the endo-cycloadduct.

7.1.4 Other Cycloadducts

It was predicted that choice of a suitable reductive desulfonylation method will heavily depend on the other functionalities present in the molecule. To investigate the relationship between substrate and desulfonylation condition, different cycloadducts were prepared using [CN+C+CC] 1,3-dipolar cycloadditions (Figure 7.1).

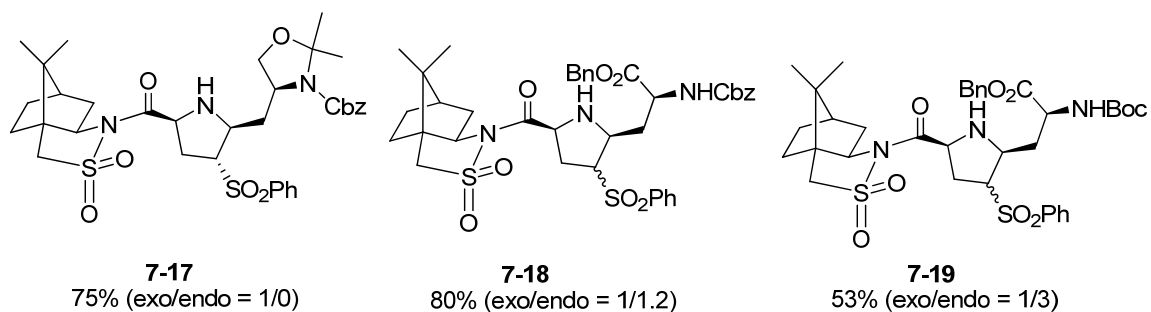
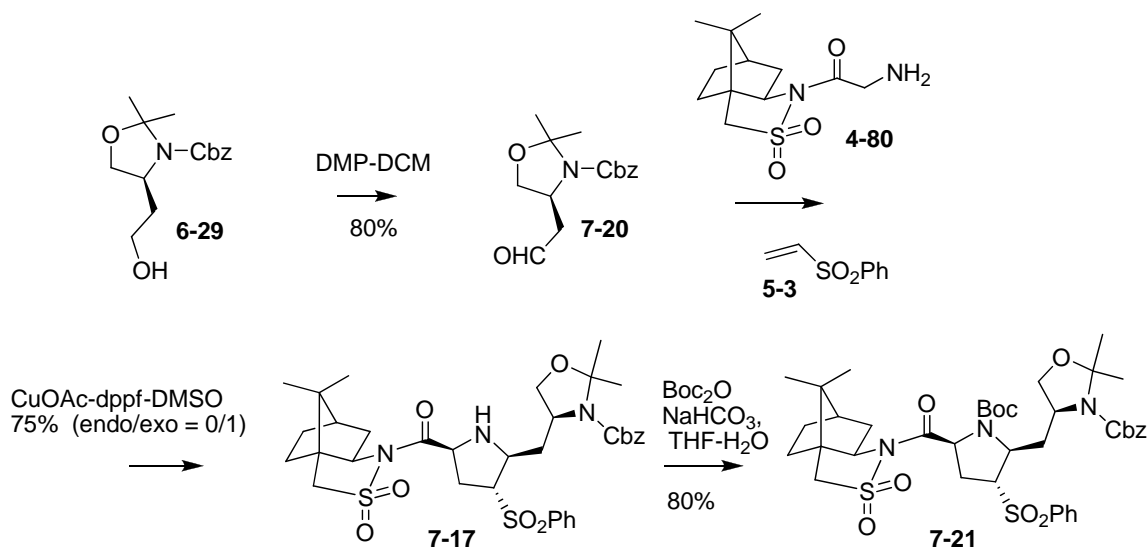


Figure 7.1 Model compounds made by [CN+C+CC] 1,3-dipolar cycloadditions.

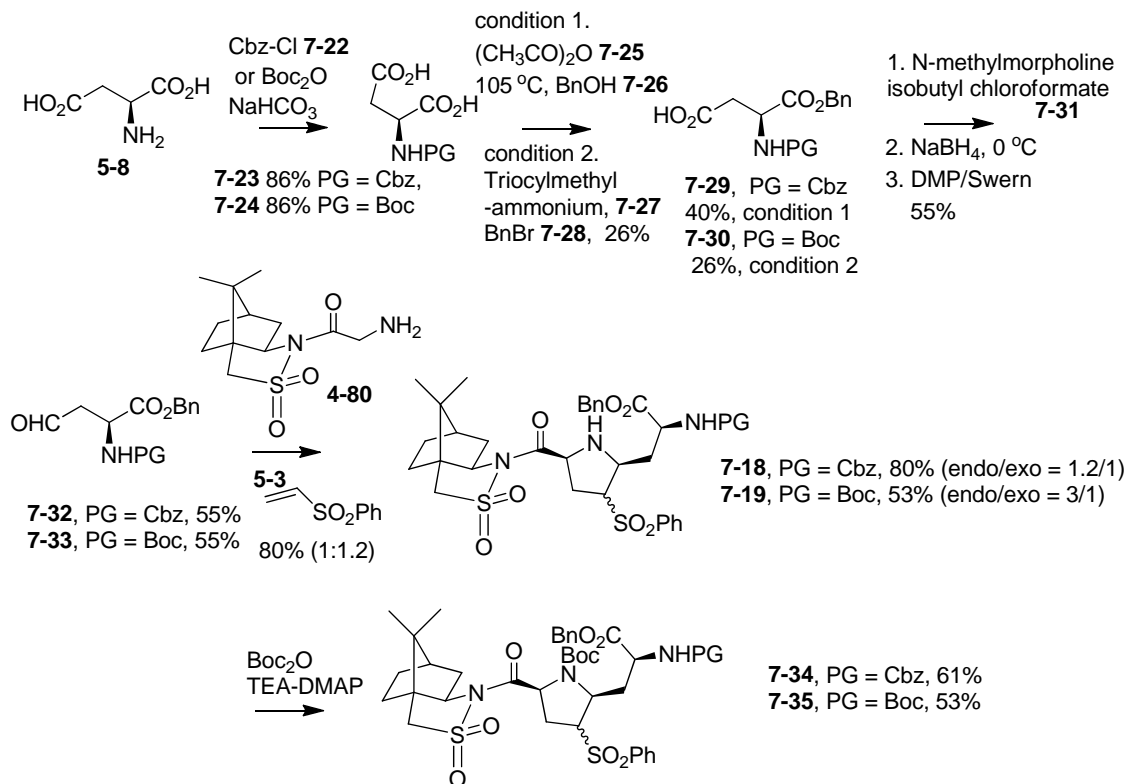
Cbz-based cycloadduct **7-17** was prepared from the corresponding alcohol precursor **6-29** in two steps in 60% total yield, and was further converted to the Boc-protected product **7-21** in 80% yield (Scheme 7.7).



Scheme 7.7 Synthesis of an N-Cbz based cycloadduct.

The N-Cbz based cycloadduct bearing an aminoester group at C9 (**7-18**) was synthesized from L-aspartic acid in four steps in 10.4% overall yield. The corresponding Boc protected product **7-35** was obtained in 53% yield using TEA-DMAP-Boc₂O (Scheme 7.8). N-Cbz based cycloadduct was chosen as a model compound. Aspartic acid was treated with CbzCl in the presence of NaHCO₃ in THF-H₂O to generate the N-Cbz diacid in 86% yield. Monoacid was prepared through anhydride formation followed by regioselective phenylmethanolysis in 43% yield. A sequence of anhydride generation followed by reduction using NaBH₄ converted the acid to aldehyde in 55% yield. The resulting aldehyde was treated with glycine sultam and phenyl vinyl sulfone, and two cycloadducts were obtained in 80% yield in a ratio 1.2:1.

Chapter 7: Cycloaddition

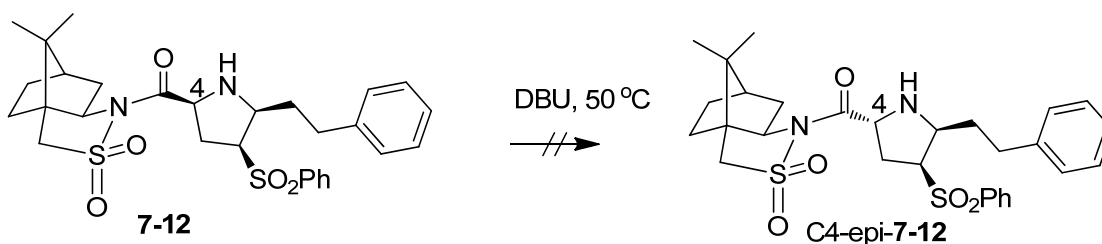


Scheme 7.8 Synthesis of cycloadduct **7-18** bearing an aminoester group.

The Boc protected equivalent reactions to make **7-19** (and subsequently **7-35**) were also carried out with similar results (Scheme 7.8).

7.2 Epimerization Experiment

It was felt necessary to test whether epimerization at C4 would occur under likely reaction conditions. A control experiment designed to be a stringent test of the stability of the C4 stereocenter was carried out (Scheme 7.9).

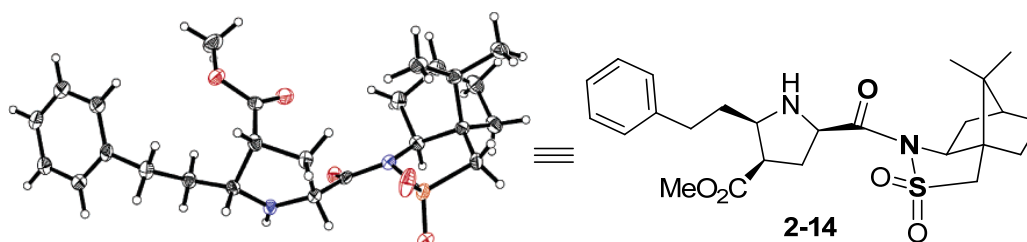


Scheme 7.9 Control experiment to test for C4 epimerization of cycloadducts.

The control experiment indicated no epimerization of cycloadduct occurred even when treated with DBU at 50 °C for 2 days, indicating that no epimerization would occur in the reaction system.

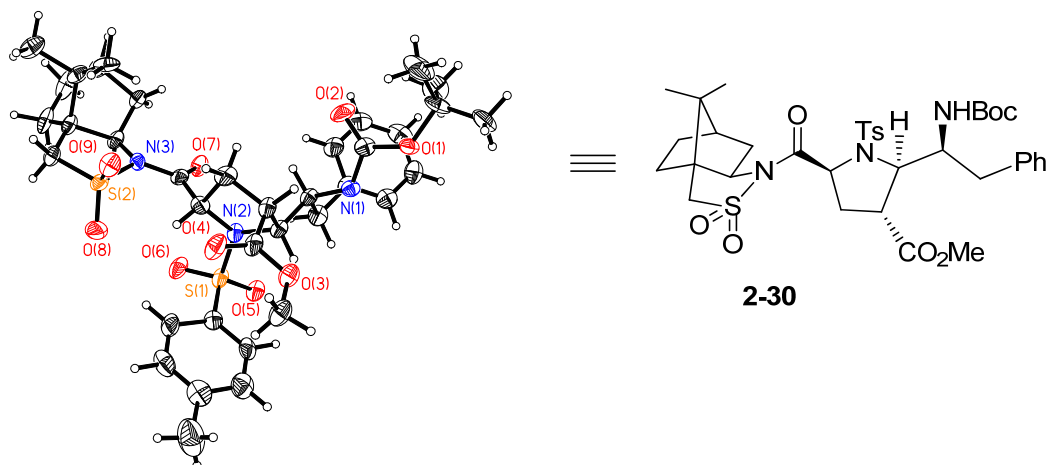
7.3 Stereocontrol in Cycloaddition

The strategy for the generation and control of stereocenters at C4 and C7 was to employ one pot cycloaddition with a chiral-sultam to produce the desired 7*R*-configuration which was expected to control the stereochemistry at C4 in any aldol condensation or acylation. Thus, the generation of C7*R* configuration is very important in our synthetic plan. The absolute stereochemistry of each of the cycloadducts produced using both catalytic systems (Ag(I) and Cu(I)-dppf) was determined by structure analysis of the X-ray diffraction of crystals of compound **2-14** (Figure 7.2) and **2-30** (Figure 7.3).



CCDC-614445 (cycloadduct **2-14**) contains the supplementary crystallographic data for this dissertation. These data can be obtained free of charge from the Cambridge Crystallographic Data Centre via www.ccdc.cam.ac.uk/datarequest/cif.

Figure 7.2 X-ray crystal structure of adduct **2-14**.



CCDC-642220 (cycloadduct 2-30) contains the supplementary crystallographic data for this dissertation. These data can be obtained free of charge from the Cambridge Crystallographic Data Centre via www.ccdc.cam.ac.uk/datarequest/cif.

Figure 7.3 X-ray crystal structure of adduct **2-30**.

Since no epimerization occurred under the reaction conditions, a model for addition reactions can be made based on the stereochemical outcome of the cycloaddition reaction, assuming starting materials are converted to products with only small changes in geometry.

In theory, azomethine ylides **7-36** may exist in several conformations through bond rotation of amide and carbon-carbon bond (Figure 7.4).

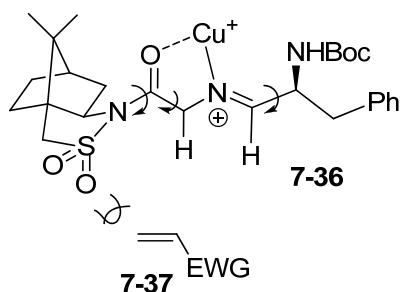


Figure 7.4 Dipole and dipolarophile intermediates.

The X-ray analysis showed Oppolzer's sultam exhibited the conformation with the carbonyl and sulfonyl groups opposed, which is dominated by dipolar interactions. The s-

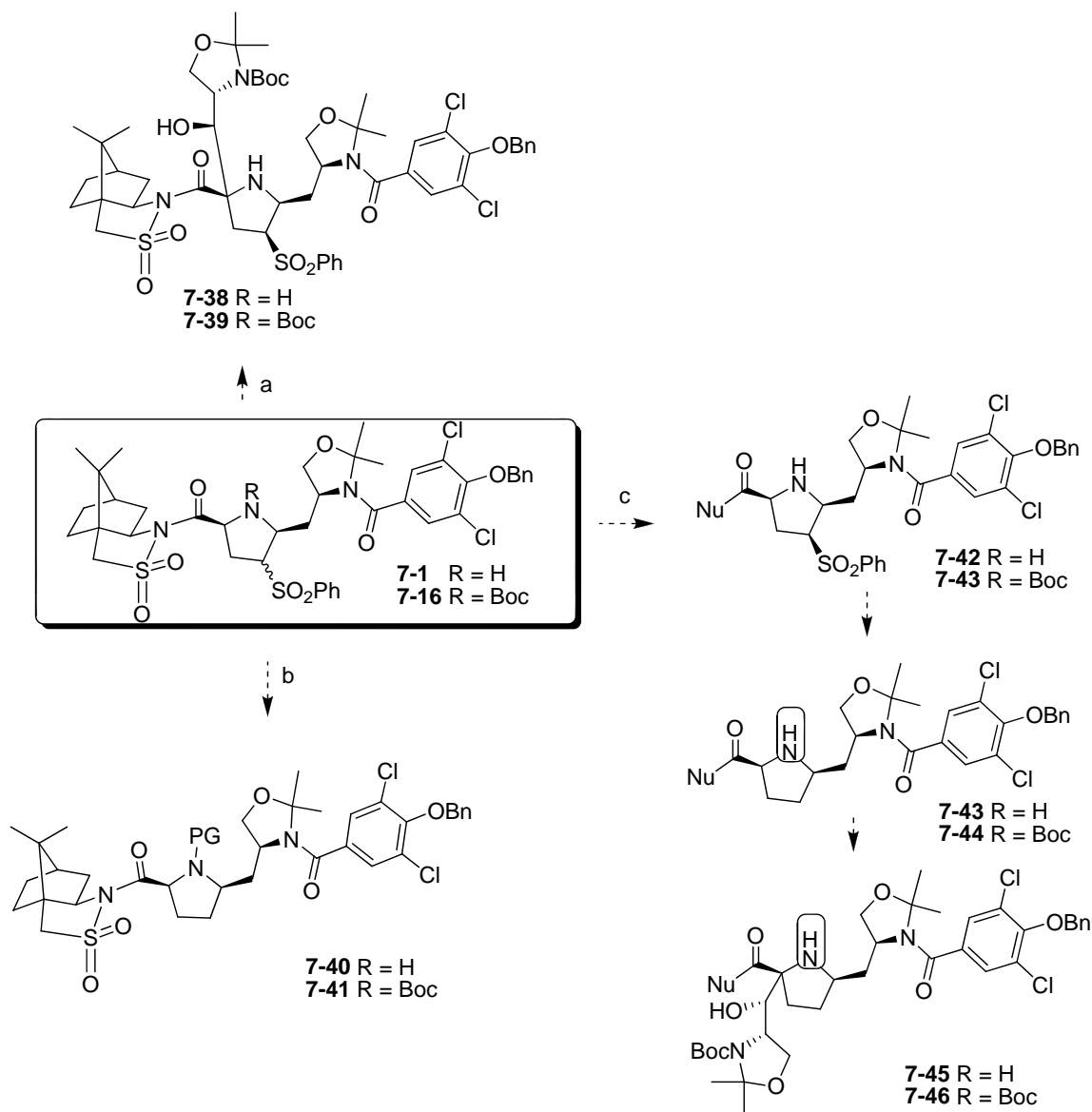
Chapter 7: Cycloaddition

cis conformation of the dipole was preferred to form the metal chelate compounds with amino-amide and to avoid the interactions between the sulfonyl group and the dipole moiety. The W-shaped conformation of the dipole was favored to avoid repulsion between the proton at C4 and the substituent at C7. It can be reasoned that all steric interactions and electrostatic repulsion resulted in the s-cis coplanar arrangements of the dipole. Dipolarophiles approach the dipole from the upper (α -Si) side, due to the sulfonyl group shielding the lower face.

Thus, it is understood that diastereofacial control in the cycloaddition was from the sultam, and not from the aldol partner. L-Oppolzer's sultam would lead to a desired 4*R*, 7*R*-isomer. D-Oppolzer's sultam would lead to a 4*S*, 7*S*-isomer. Thus, we reasoned that kaitocephalin and C4,C7-epi-Kaitocephalin could be synthesized through [CN+C+CC] 1,3-dipolar cycloadditions employing L- and D-glycyl sultam respectively.

7.4 Taking the Cycloaddition Product Towards Kaitocephalin

With the key intermediate cycloadducts (**7-1** and **7-16**) in hand, several synthetic approaches to kaitocephalin were considered (Scheme 7.10).



Scheme 7.10 Possible transformations towards kaitocephalin from cycloadducts **7-1** and **7-16**.

7.4.1 Aldol Reaction – With or Without Sultam?

In the case of aldol condensation with a cycloadduct, the substituent at C7 was expected to direct the lithium enolate to attack the aldehyde from the opposite face of the pyrrolidine ring at C4. Thus, cycloadducts bearing a sultam should not be utilized for aldol condensation due to the sulfonyl group shielding the opposite face of the ring at C4

(Figure 7.5). Thus, the sultam should be removed before introducing the C1-C3 side chain using aldol condensation.

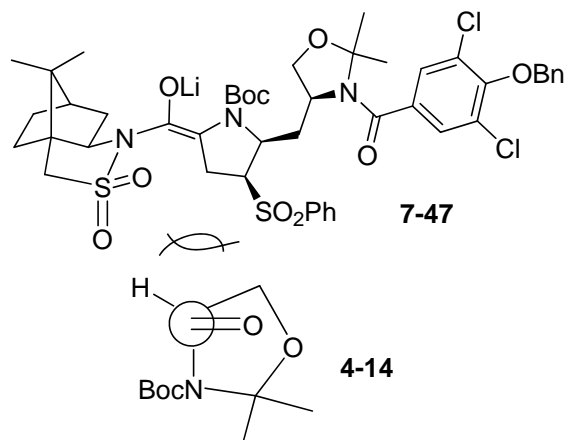


Figure 7.5. The sulfonyl group shielding the Si face of the enolate **7-47**.

7.4.2 Simultaneous Sultam Removal and Desulfonylation

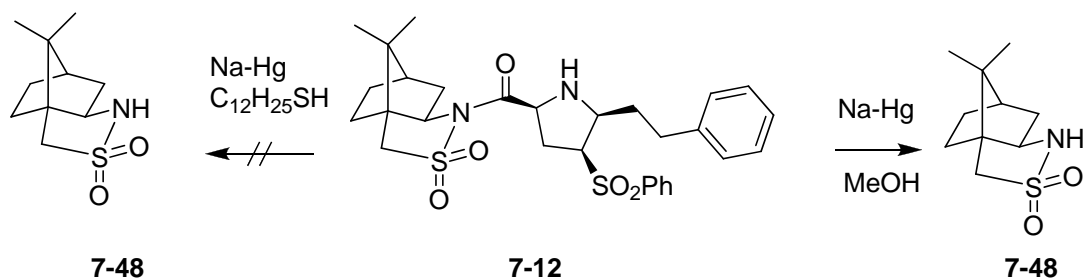
Since the sultam can be used as a leaving group, it was envisaged that the sultam would be replaced by methoxide under the Na-Hg mediated desulfonylation.

Such a strategy would be particularly attractive if a single method of desulfonylation could be exploited to remove both the sulfone and the sultam. Since the sultam contained a sulfone group, it was also suspected that the sultam would be degraded under the same desulfonylation conditions (Na-Hg).

A control experiment with Na-Hg was carried out. When the cycloadduct **7-12** was treated with Na-Hg in $\text{HSC}_{12}\text{H}_{25}$ no reaction occurred. Treatment of the model compound **7-12** with 6% Sodium amalgam in methanol in the presence of four equivalents of disodium hydrogen phosphate gave the free sultam (Scheme 7.11). However, no desired methyl ester and no desulfonylation compound were isolated. This result suggested that

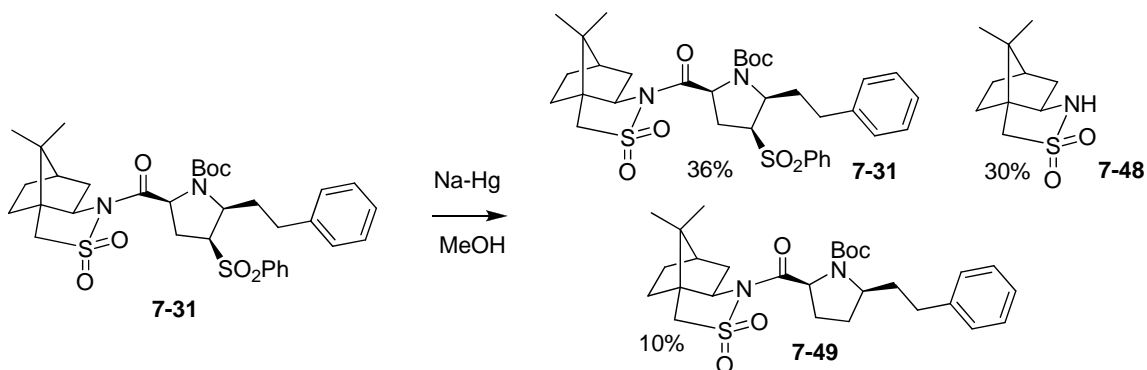
Chapter 7: Cycloaddition

under sodium amalgam conditions, free sultam is stable, though the free sultam possesses a sulfone moiety.



Scheme 7.11 Testing for one pot removal of sulfone and sultam.

Under the same conditions (Na-Hg, MeOH), the N-Boc cycloadduct gave the desulfonated compound in 10% yield with a mixture of starting material (36%) and sultam (30%) (Scheme 7.12). The steric hindrance imposed by Boc may potentially hamper the nucleophilic attack of NaOMe onto the carbonyl moiety. Thus, the sultam should be removed before desulfonylation.

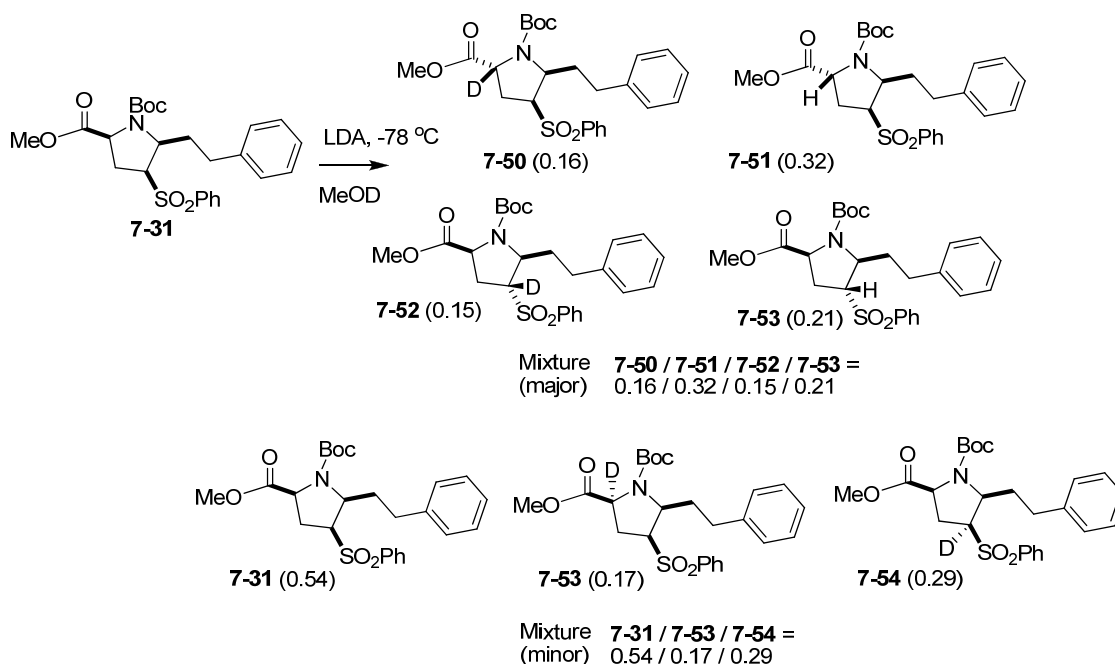


Scheme 7.12 Testing for one pot removal of sulfone and sultam with Boc protected substrate.

7.4.3 Regioselective Influence of the Sulfone

Since the cycloadducts that possess a sulfone group have a secondary site to form the sulfonate equivalent of an enolate, which is at α - position of sulfone, the base should be carefully readjusted to for regioselective lithiation.

To test the regioselectivity of the lithiation of the pyrrolidine ester bearing a sulfone group, a control experiment was carried out. Model compound **7-31** was treated with LDA at $-78\text{ }^{\circ}\text{C}$ to generated the lithium enolate, which was trapped with MeOD (Scheme 7.13).⁶⁰



Scheme 7.13 Testing for one pot removal of sulfone and sultam with Boc protected substrate.

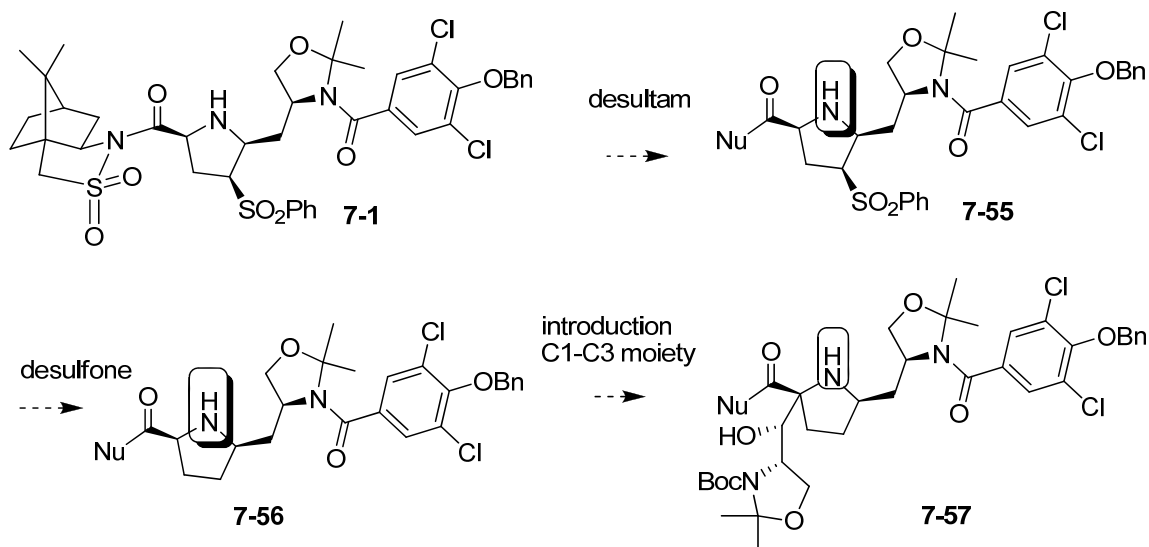
Two unseparated mixtures were isolated, and VT-NMR studies in CDCl_3 at $50\text{ }^{\circ}\text{C}$ indicated that the major mixture contained four compounds with a 0.16/0.32/0.15/0.21 ratio of **7-50 / 7-51 / 7-52 / 7-53**. Based on the product ratios, the ratio of deprotonation at C4 to that at C6 may be calculated as being 1.3:1. VT-NMR studies in d_6 -benzene at

50 °C showed the minor mixture consisted of starting material **7-31**, **7-53** and **7-54** (0.54 : 0.17 : 0.29), but the ratio of deprotonation at C4 and C6 could not be calculated because of lack of data for C2-H-pyrrolidine and C4-H-pyrrolidine.

The control experiment indicated that lithiation occurred at both α - position of sulfone and the pyrrolidine ester, which suggested that the sulfone should be removed before lithium enolate formation.

7.4.4 Summary

Based on the above results, it was decided that the preparation of 4,4,7-trisubstituted pyrrolidines should be via a sequence of sultam removal, desulfonylation, then aldol condensation or acylation (Scheme 7.14).



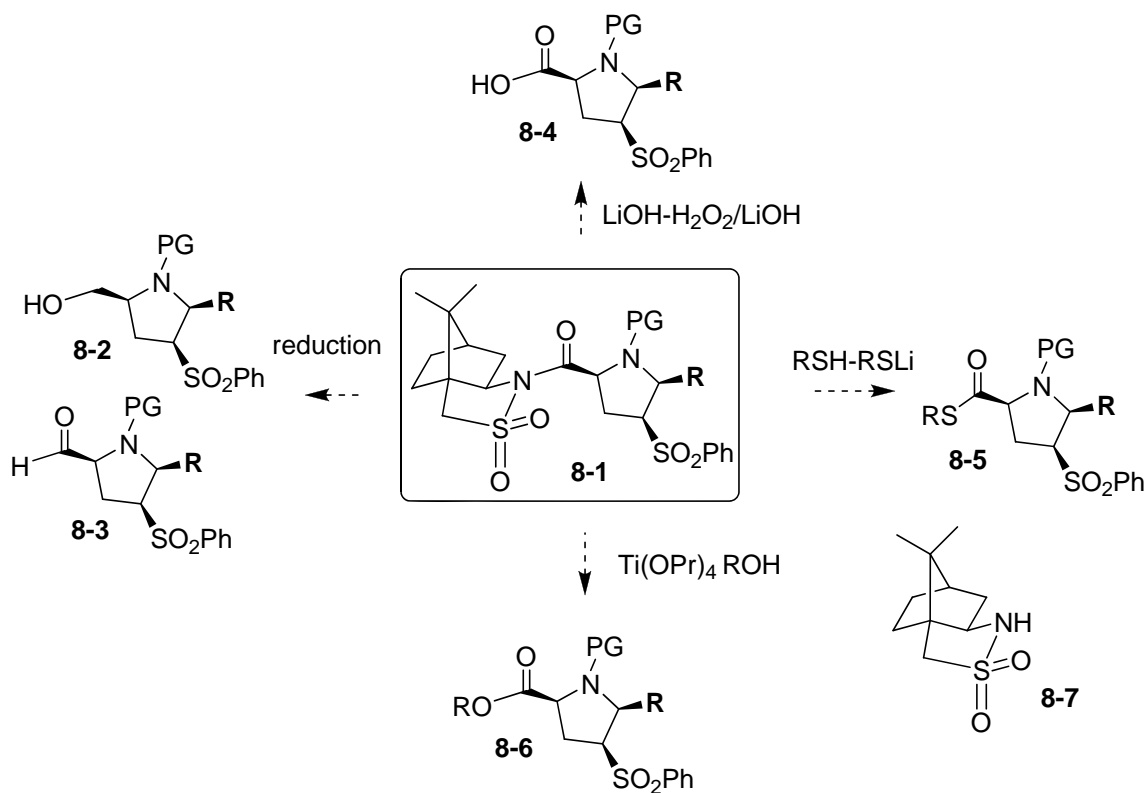
Scheme 7.14 Sequence towards kaitocephalin following pyrrolidine ring formation.

8 Sultam Removal

Having made use of the sultam functionality as both a protecting group and as a stereo- and regio-selectivity directing group, in the end it is necessary to remove the sultam group to progress with the synthetic pathway.

8.1 Literature

A literature search for the de-sultamation of sultam derivatives indicated that several methods were reported to remove the sultam group (Scheme 8.1).



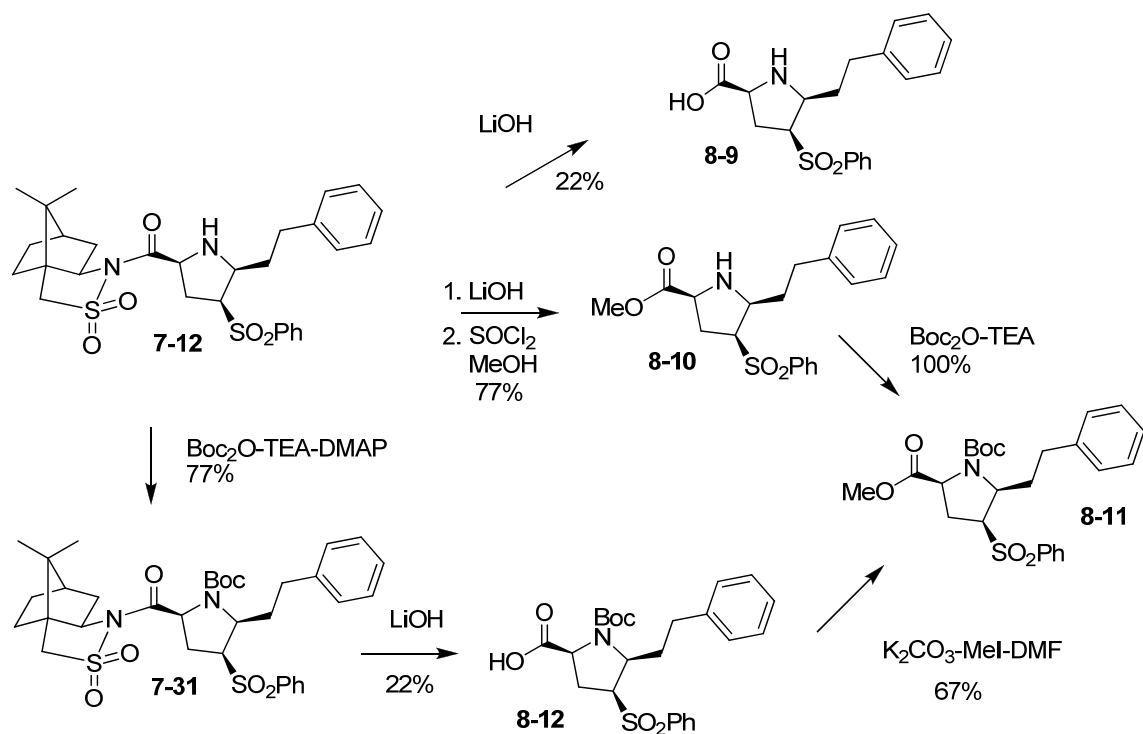
Scheme 8.1 Methods for removal of the sultam protecting group.

Reduction of sultam derivative **8-1** with LAH and NaBH_4 generated alcohol **8-2** and it afforded aldehyde **8-3** on treatment with DIBAL-H.⁶¹ Direct hydrolytic cleavage of

the camphorsultam auxiliary with LiOH or under basic hydroperoxide conditions followed by acidification gave the corresponding acid **8-4**,⁶² but it usually provided another undesired fragment owing to the reagents (LiOH, LiOOH) attacking the sulfoxide moiety preferentially. Thiolate-mediated cleavage of the chiral auxiliary employing RSH-RSLi gave the corresponding thioester **8-5**, however, the resulting thioester was contaminated with amounts of free sultam **8-7** as chromatographic separation of the mixture of thioester products and sultam was difficult, due to close Rf values.⁶³ A titanate-mediated transesterification of sultam derivatives with alcohol afforded the corresponding ester **8-6** showing that the sultam group may be removed in a facile manner.⁶⁴ In addition to all these methods, recycling of the auxiliary after removal is often practical using these conditions.

8.2 Basic Hydrolysis (Lithium Hydroxide)

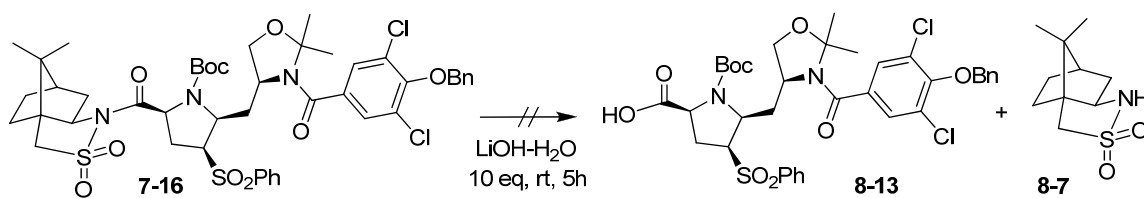
Model compound sultam pyrrolidine **7-12** gave the acid **8-9** using LiOH in 22% (Scheme 8.2). The low yield may be attributed to the low liquid-liquid extraction yield. When the hydrolyzed product was trapped by methylation conditions, sultam pyrrolidine **7-12** afforded the corresponding ester **8-10** in 77% yield, from which Boc protected methyl ester **8-11** was obtained in 100% yield.



Scheme 8.2 Hydrolytic cleavage of auxiliary from a model compound.

An alternative pathway involving Boc protection prior to sultam removal was also explored. The sultam pyrrolidine **7-12** was converted into N-Boc cycloadduct **7-31** in 77% yield. However, under LiOH promoted hydrolysis, Boc protected pyrrolidine **7-31** gave the acid **8-12** in only 22% yield. This was converted to the corresponding methyl ester **8-11** in 67% yield.

Considering that the oxazolidine ring is unstable to $\text{SOCl}_2\text{-MeOH}$, it was planned to choose Boc-protected pyrrolidine **7-16** as the substrate for hydrolysis. However, when Boc-protected sultam intermediate **7-16** was treated with LiOH (10 eq), no free sultam **8-7** was detected (Scheme 8.3). Many new compounds were produced when using more LiOH and longer time. Thus, further investigation using LiOH promoted hydrolysis was abandoned.

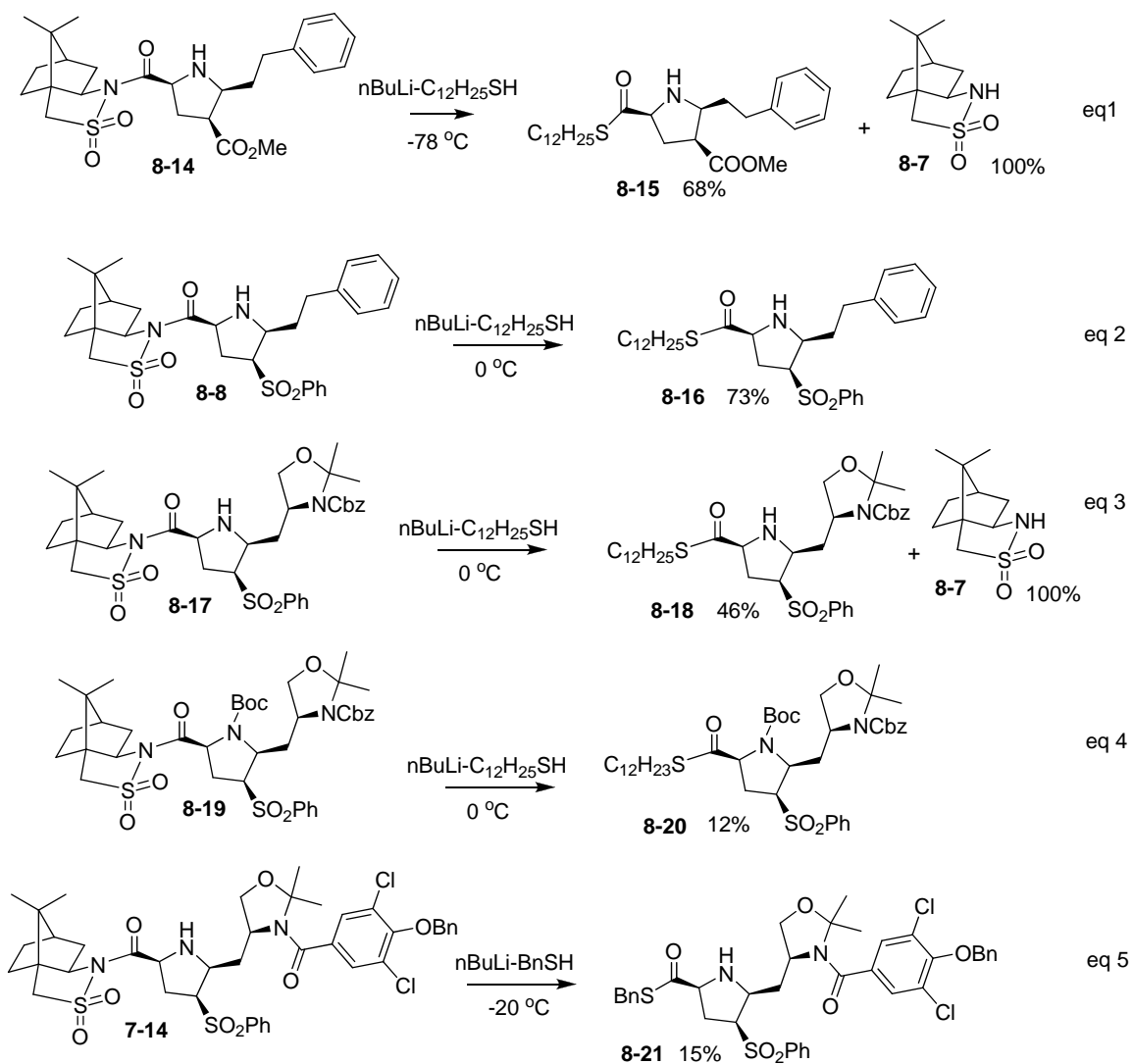


Scheme 8.3 No sultam cleavage using lithium hydroxide.

8.3 Thiolate Mediate Cleavage

Sultam removal from different substrates by thiolate-mediated cleavage of the chiral auxiliary was examined (Scheme 8.4). It was found that cycloadduct **8-14** bearing methyl ester at C4 gave the best desultamization result at -78 °C (eq 1); while C4-sulfone substituted cycloadduct **8-8** afforded the best desultamization result at 0 °C (eq 2). Under the same condition, Cbz-based cycloadduct **8-17** was subjected to the buffer RSLi-RSH to generate the corresponding desultamization product **8-18** in 46% yield and sultam **8-7** was recovered in 100% (eq 3). However, Boc protection of the Cbz based cycloadduct **8-19** lead to a significant decrease in yield, to 12% (eq 4). It was reasoned that the steric effect from the Boc group would lead to a decrease in the thiolysis yield.

Chapter 8: Sultam Removal

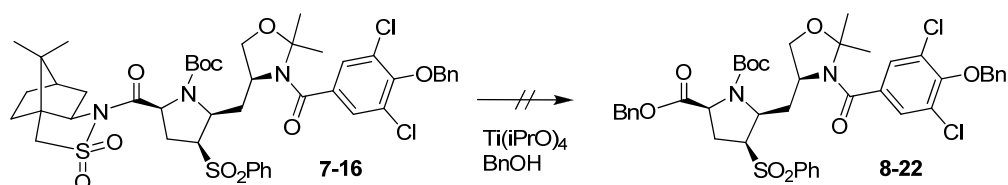


Scheme 8.4 Thiolate mediate sultam removal.

Upon treating the kaitocephalin intermediate **7-14** with the lithium buffer at $0\text{ }^\circ\text{C}$, TLC analysis revealed many spots. At $-20\text{ }^\circ\text{C}$ these reaction conditions gave the desired desultamization product in 15% along with a large amount of unknown byproduct (eq 5). It was noticed that the separation of the resultant desultamization **8-21** compound and sultam **8-7** is very difficult. Both the low yield of this reaction and the purification problems prompted investigation of another method of removing the sultam.

8.4 Titanate Mediate Cleavage

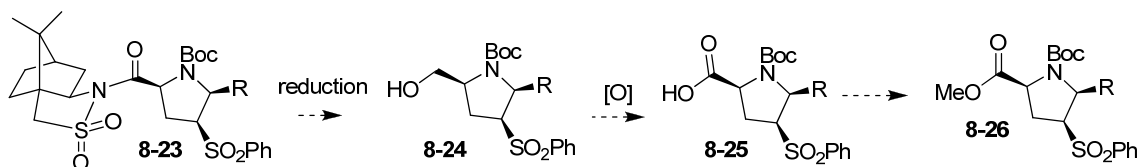
Tetraisopropyl titanate catalyzed transesterifications of Boc-protected intermediate **7-16** with BnOH was carried out, but no reaction occurred and starting material was recovered in 85% yield (Scheme 8.5).



Scheme 8.5 No sultam cleavage using titanium isopropoxide.

8.5 Reductive Cleavage

Considering the limitation of thiolate-mediated cleavage and hydrolytic removal of the sultam, it was planned to remove the sultam under reductive conditions followed by reoxidation and esterification to give the ester **8-26** (Scheme 8.6).

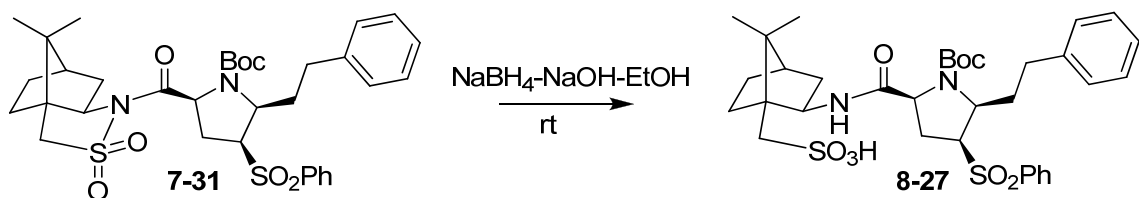


Scheme 8.6 Sultam removal under reductive conditions followed by conversion to an ester.

Furthermore, since the cycloadduct did not afford a suitable single crystal for X-ray diffraction analysis, it was hoped that the alcohol **8-24** derived from cycloadduct **8-23** could give a single crystal, though 1D-NOE NMR experiments could be used to determine the structure of endo- and exo-cycloadducts.

Chapter 8: Sultam Removal

The N-acyl diol formation using NaBH_4 suggested that the amide bond was stable to this reducing reagent. Thus, the model compound was subjected to $\text{NaBH}_4\text{-NaOH}$ in EtOH to give the ring opened product **8-27** which was formed via NaOH attacking the sulfoxide moiety (Scheme 8.7). The reduction product is easily identified by the NMR splitting pattern of ^1H at C4, and the crude NMR spectrum revealed that no desired reduced product was formed.



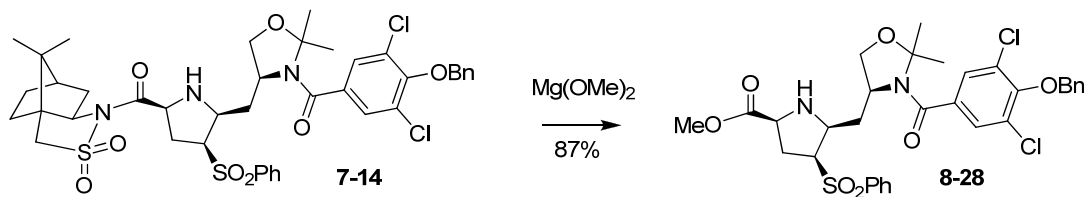
Scheme 8.7 Reductive sultam ring opening.

8.6 Base Catalyzed Cleavage Revisited (Methanolysis)

A serendipitous discovery in the lab involving methoxide prompted re-examination of based catalyzed cleavage as an option.

8.6.1 Magnesium Methoxide Mediation

The sultam was successfully removed through $\text{Mg}(\text{OMe})_2$ -mediated methanolysis, and the corresponding methyl ester **8-28** was formed in 87% yield (Scheme 8.8).



Scheme 8.8 Sultam removal by magnesium methoxide.

Chapter 8: Sultam Removal

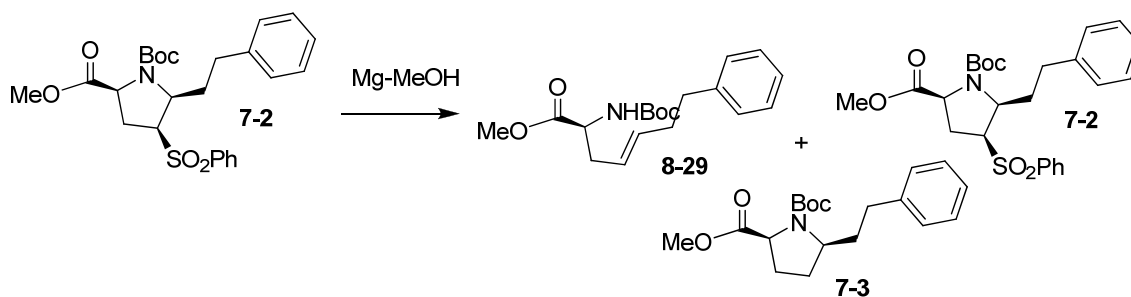
Assignment of the stereochemistry of the methyl ester was based on the proton and carbon NMR spectra. The stereochemistry of cycloadduct **8-28** was established by analysis of NOE-spectra (Table 8.1).

Table 8.1 NOE results of methanolysis product.

8-28

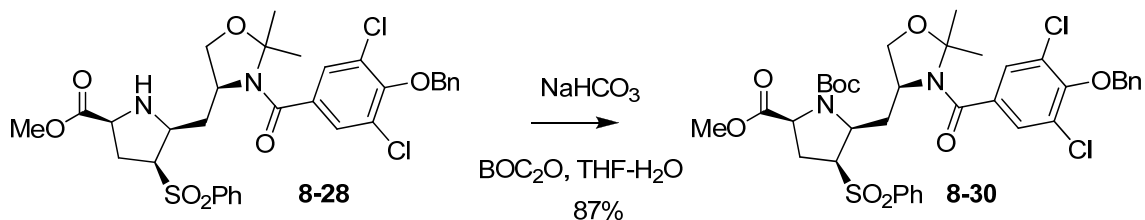
Irradiated Hydrogen	Enhancement%				
	H2	H3 α	H4	H5	SO ₂ Ph
H4	-	2.6%	-	3.4%	1.9%
H5	1.2%	-	4.2%	-	0.63%

¹H-¹H correlations between H4 and H7 and between H4 and H5 in the NOE spectra indicated that no epimerization occurred during Mg(OMe)₂ mediated methanolysis. The control experiment also indicated no epimers were detected when Boc-protected pyrrolidine **7-31** was treated with Mg(OMe)₂ (Scheme 8.9).



Scheme 8.9 Magnesium methoxide mediated methanolysis of the model compound.

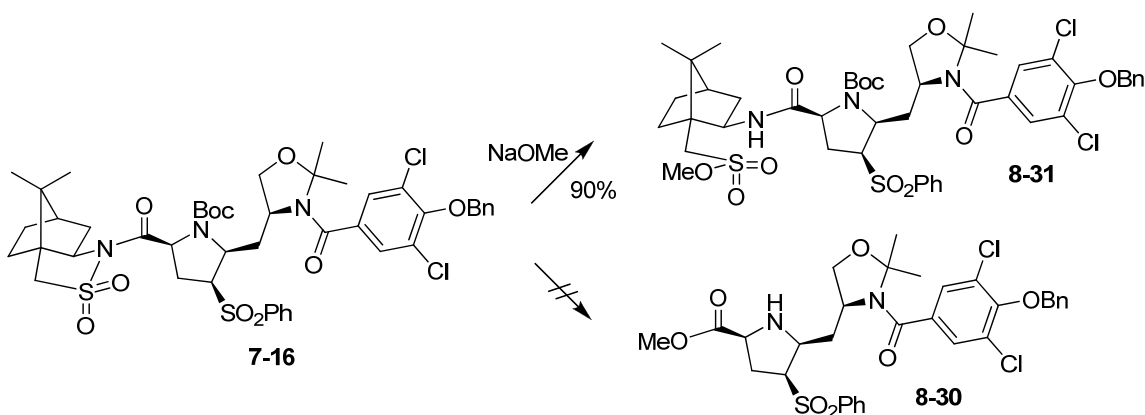
Thus, sultam intermediate **7-14** was converted into methyl ester **8-28** in high yield using $\text{Mg}(\text{OMe})_2$. The methyl ester **8-28** was subsequently converted to the N-Boc protected product **8-30** in 87% yield (Scheme 8.10).



Scheme 8.10 N-Boc protection of the methyl ester product after sultam removal.

8.6.2 Sodium Methoxide Mediation

Interestingly, crude NMR spectra revealed that no free sultam **8-7** was formed when Boc-protected pyrrolidine **7-16** was treated with NaOMe. It was somewhat surprising to find that the NaOMe mediated methanolysis with the N-Boc cycloadduct led to a sultam ring-opening product in 90% yield, and failed to produce even trace amounts of the desired N-Boc methyl ester **8-30** (Scheme 8.11).



Scheme 8.11 Sultam removal failure using sodium methoxide mediated methanolysis.

9 Desulfonylation

It was envisaged that the cycloaddition between azomethazine ylide and phenyl vinyl sulfone could in theory be applicable to build the pyrrolidine core of kaitocephalin. This idea was attractive because all the regio- and stereo-isomers at the sulfone position would converge to a single compound and because it is possible to remove the phenyl sulfone moiety from a cycloadduct using mild reductive conditions. Thus, the success of the plan for employing phenyl vinyl sulfones as a synthetic equivalent of ethene depends critically on the desulfonylation step.

9.1 Literature

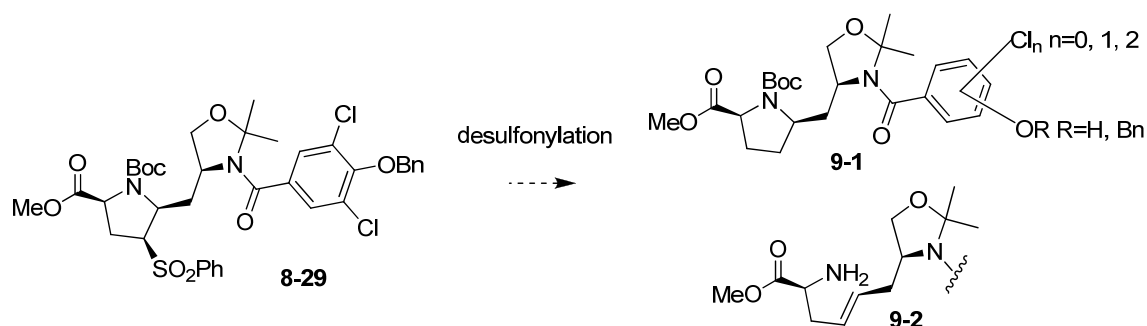
Before starting the synthesis towards kaitocephalin, a literature search was done to look for desulfonating conditions. It was found that in sulfone-mediated syntheses, several reducing reagents were reported for reductive desulfonylation. These reagents included dissolving metals and amalgams (sodium amalgams, aluminum amalgam),⁶⁵ lithium or sodium in liquid ammonia,⁶⁶ sodium naphthalenide, lithium naphthalenide,⁶⁷ magnesium in methanol,⁶⁸ magnesium in the presence of a catalytic amount of mercury(II) chloride (1 mol%) in methanol (or ethanol),⁶⁹ Raney nickel,⁷⁰ zinc and ammonium chloride in THF,⁷¹ sodium dithionite in DMF, samarium diiodide, and tributylstannane hydrides.⁷²

All these reduction methods are mediated by highly aggressive metal-containing reducing agents. Among these conditions, the Na-Hg-mediated reduction is the most popular and general procedure for the reduction of all types of alkyl sulfones and has

been used extensively in the reduction of β -amino sulfone derivatives.⁷³ Mg metal in methanol and sodium naphthalenide were also reported as reducing reagents for the desulfonylation of a β -amino sulfones compound. However, the choice of a suitable reductive desulfonylation method will heavily depend on the other functionalities present in the molecule.

9.2 Unwanted Side Reactions

When analyzing the structure of the precursor, it was anticipated that dechlorination, debenzylation, and elimination may occur under the desulfonylation conditions, because aryl sulfones typically have a reduction potential of -2.3 V, while chloride possess lower reduction potentials. This raises the possibility of desulfonylation conditions adversely affecting other groups in the substrate (Scheme 9.1). Finding an effective chemoselective desulfonylation might be challenging in the target system, en route to kaitocephalin. Thus, desulfonylation was investigated using various reducing agents and conditions on a variety of substrates, in the hope of finding a suitable combination.



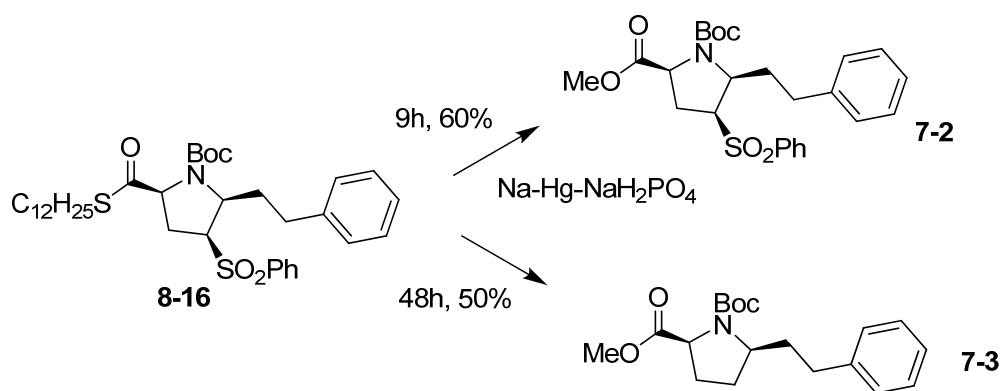
Scheme 9.1 Sulfone removal may lead to unwanted side reactions.

9.3 Sodium Amalgam Reductions

As the most popular method of reducing sulfones, sodium amalgam was considered the most appropriate starting point for testing reducing conditions for desulfonylation.

9.3.1 Initial tests

Since the Garner group has developed a mild thiolate-mediated cleavage of sultams to afford thioesters, attention was drawn to testing the desulfonylation conditions with thioesters. Thioester **8-16**, prepared from **8-8**, was subjected to sodium amalgam at rt for 9h, to give methyl ester **7-2** through catalyzed transesterifications, but no desulfonylation product was detected. Fortunately, it was found further reaction time lead to significant desulfonylation. A one pot transesterifications followed by reductive desulfonylation gave the desired di-substituted pyrrolidine **7-3** in 50% yield (Scheme 9.2).



Scheme 9.2 Desulfonylation of thiolate ester **8-16**.

This result suggested converting the sultam-derivatives to methyl esters for the removal of the sulfone group. This prompted a reexamination of the sultam removal conditions. This was part of the inspiration that led to the discovery of methanolysis as a good means of sultam deprotection (see section 8.6)

9.3.2 Model Compounds

Four compounds were chosen as the model substrates on which to test desulfonylation conditions (Figure 9.1). Sulfone **7-2** was used for the optimization of desulfonylation condition. The other three model compounds **6-33**, **6-13**, and **6-27** were employed to investigate the stability of the functional groups under the optimized desulfonylation conditions.

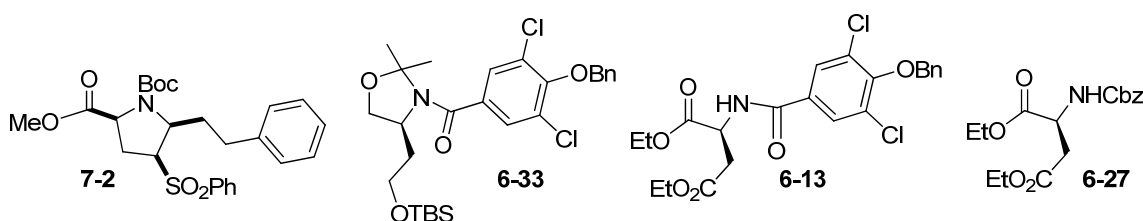
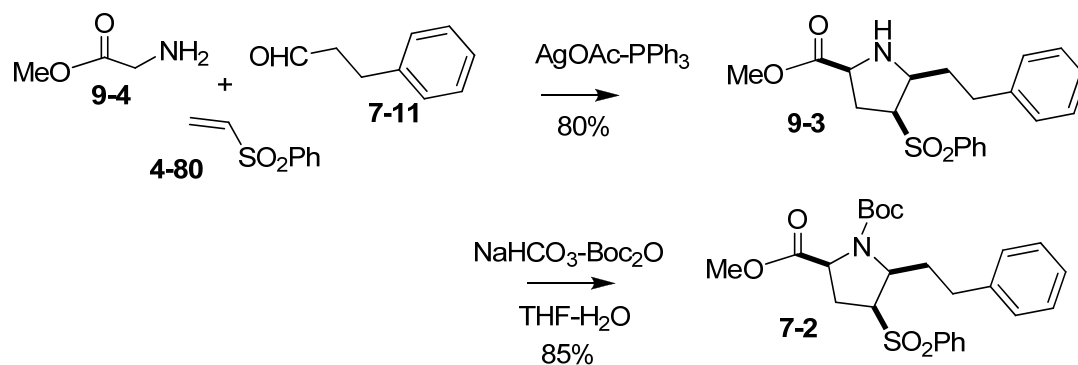


Figure 9.1 Model compounds for testing the effects of desulfonylation conditions.

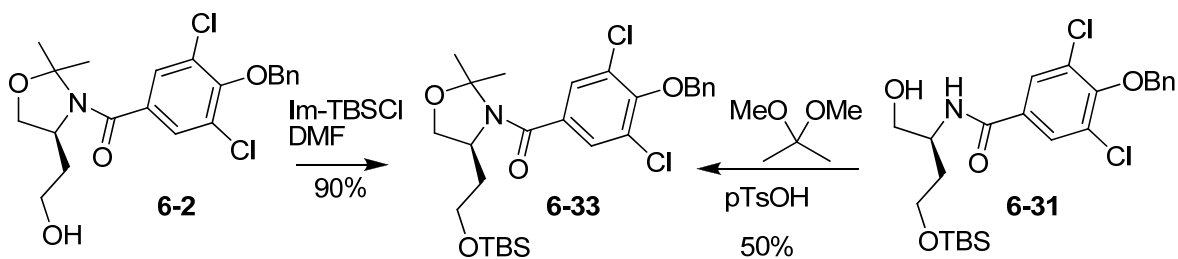
9.3.2.1 Model Compound Preparation

Model compound **7-2** was prepared via a AgOAc-PPh₃ catalyzed one pot cycloaddition reaction (Scheme 9.3). PhCH₂CH₂CHO was reacted with glycine and phenyl vinyl sulfone in the presence of AgOAc-PPh₃ in THF at room temperature to give the methyl ester cycloadduct **9-3** in 80% yield. N-Boc protection using Boc₂O-NaHCO₃ in THF-H₂O gave the desired racemic N-Boc cycloadduct **7-2** in 85% yield.



Scheme 9.3 The preparation of model compound sulfone **7-2**.

Treatment of oxazolidine alcohol with TBSCl in the presence of imidazole afforded the model compound silyl ether **6-33** in 90% yield (Scheme 9.4). Alternatively, the oxazolidine ring may be formed after silyl ether protection of the alcohol **6-31**.



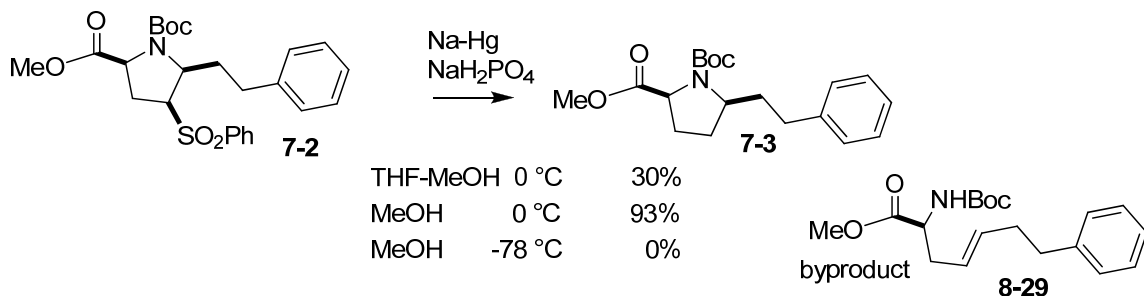
Scheme 9.4 The preparation of model compound **6-33**.

The preparation of compound **6-13** and **6-27** was described in chapter six (Sections 6.2.2 and 6.2.3 respectively).

9.3.3 Desulfonylation Conditions

With the model sulfone compounds in hand, different desulfonylation conditions were investigated. Sulfone derivative **7-2** was subjected to sodium amalgam (6%) in methanol-THF (1:4) in the presence of four equivalents of disodium hydrogen phosphate

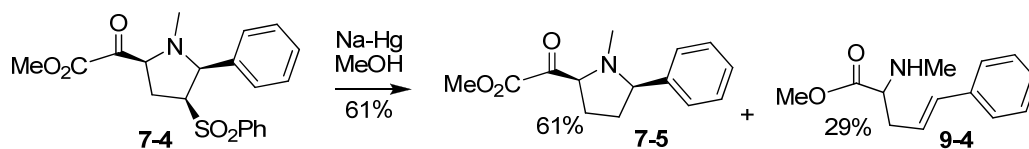
and gave the desulfonylation product **7-3** in 30% (Scheme 9.5). The yield was increased to 93% by using pure methanol as solvent at 0 °C.



Scheme 9.5 Desulfonylation of **7-2** using sodium-mercury amalgam.

By carefully analyzing the ^1H NMR spectrum, we found that the desulfonylation product was contaminated with small amounts of elimination product **8-29** involving the cleavage of the C-N bond. It is extremely difficult to use chromatography to separate these two compounds because they have almost the same R_f value. On further decreasing the reaction temperature to -78 °C, elimination product **8-29** was detected, but no desulfonylation product was observed.

It was noticed that in Carretero's desulfonylation, elimination product **9-4** was isolated in 29%. It was reasoned that the driving force for this conversion is the formation of a conjugated olefin structure (Scheme 9.6).

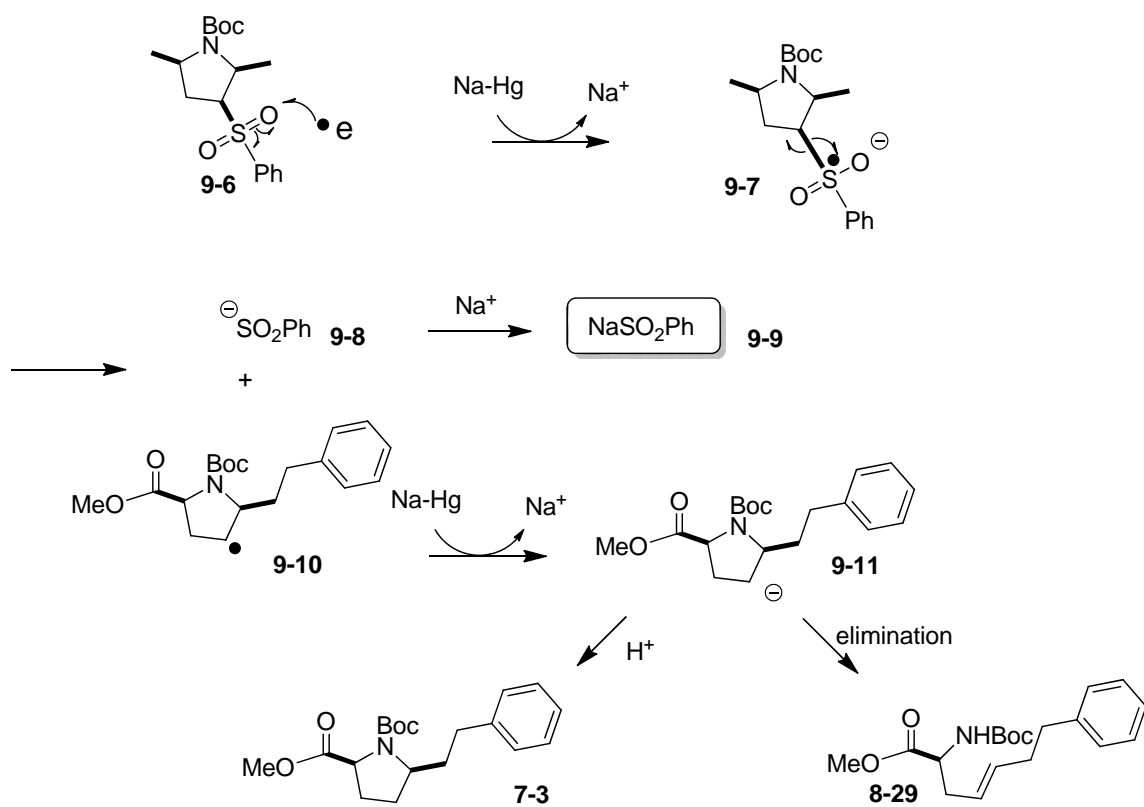


Scheme 9.6 Carretero's desulfonylation.

To explain the elimination product, the following mechanism was proposed (Scheme 9.7). An electron-transfer from the single-electron donor (Na-Hg) to the phenyl

Chapter 9: Desulfonylation

sulfonyl group of **9-6** generated Na^+ and radical-anion **9-7**. The radical-anion **9-7** then fragmented to radical **9-10** and anion **9-8**, which subsequently forms anion- Na^+ complex **9-9**. Meanwhile, radical **9-9** is converted to anion **9-11** through another one-electron reduction. Protonation of the anion **9-11** gives the desired product **7-3**. The olefin **8-29** was produced through anion elimination. Since the sulfonyl group was converted to NaSO_2Ph **9-9**, which would be extracted into the aqueous layer in subsequent workup, the phenyl group will not be detected in the proton NMR spectrum after desulfonylation, thus ^1H NMR could be used to see whether the desulfonylation was complete.



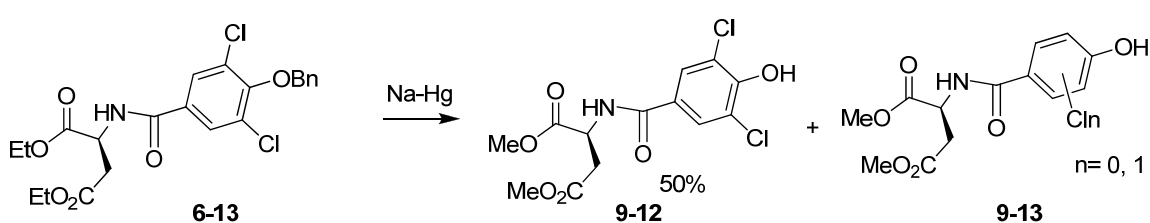
Scheme 9.7 Possible mechanism for desulfonylation.

9.3.4 Functional Group Stability

With the optimized desulfonylation conditions in hand, the model compounds synthesized for the purposes of testing reducing desulfonylation conditions were used to test the stability of various functional groups.

9.3.4.1 Aryl Chlorides and Benzyl Ethers

The model compound **6-13** was selected to test the stability of both aryl chloride and benzyl ether groups to the reducing desulfonylation conditions previously developed (Scheme 9.8).



Scheme 9.8 Desulfonylation conditions tested on **6-13** with production of unwanted side-products.

Under the developed conditions, model compound N-acyl diester **6-13** was treated with Na-Hg. Examination of the crude ^1H NMR reveals the formation of methyl ester **9-12** (50%) and de-chloro compounds which can be inferred by comparison of proton numbers between the methoxy groups and aromatic protons. It was found that the benzyl group was also removed under these conditions. This result was consistent with the less negative redox potentials of halides and it seemed that chemoselectivity of desulfonylation of this intermediate is particularly challenging. It presented particular problems for using cycloaddition followed by desulfonylation sequence to generate the desired 2,5-disubstituted pyrrolidines. In the synthesis of kaitocephalin, [CN+C+CC]

cycloaddition is employed to synthesize the pyrrolidine core, due to the practicality of formation of functionalized pyrrolidines in one step. Unfortunately, this control experiment showed that aryl chloride and benzyl ether groups were unstable under Na-Hg reducing conditions.

9.3.4.2 Oxazolidine Ring Stability

Next, the stability of oxazolidine rings to sodium amalgam was further investigated because an oxazolidine bearing other protecting groups could undergo Na-Hg mediated desulfonylation. Model compound oxazolidine silyl ether **7-3** was treated with sodium amalgam. Analysis by TLC showed numerous new compounds to have been formed. However, the ^1H NMR signals between 1.6 and 1.8 ppm indicated the presence of the methylene peak of oxazolidine, which suggested that the oxazolidine ring itself was stable under Na-Hg.

9.3.5 Testing on Real Intermediates

Having tested certain functional groups for susceptibility to the reducing desulfonylation conditions using model compounds, it proved more efficient to test the susceptibility of other groups using real intermediates. With the sulfone cycloadducts **8-28**, **8-30**, and **8-31** in hand (Figure 9.2), desulfonylation with these intermediates was performed.

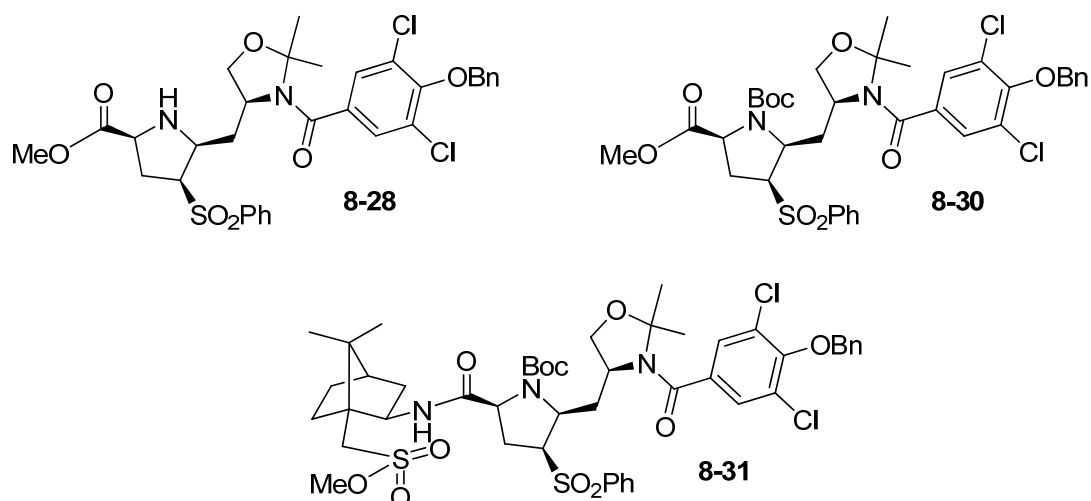


Figure 9.2 Real intermediates as substrates for testing the effects of desulfonylation conditions.

It was found, by monitoring using TLC, that desulfonylation under different reaction conditions, varying the percentage of sodium in the amalgam (100%, 10%, 0%), the buffer (Na₂HPO₄, NaH₂PO₄, Na₂HPO₄-NaH₂PO₄, no buffer), the solvent (MeOH, MeOH-THF), the temperature (0 °C, rt), yielded many new compounds.

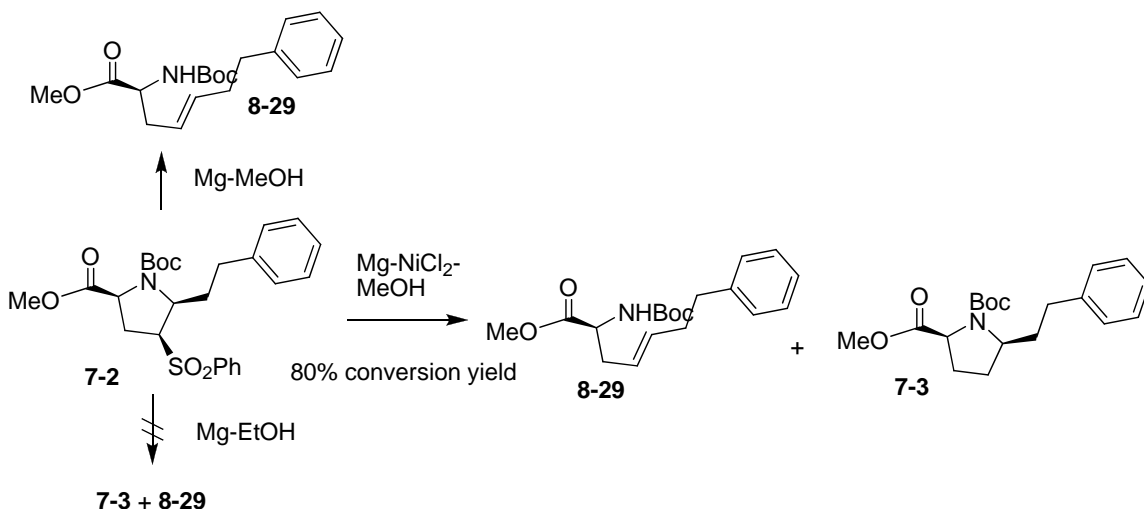
Based on the control experiment result, we reasoned that radical anions from halide and sulfones were formed in this reaction and underwent further complex reactions from radical anions (such as coupling reaction) which led to the formation of many new compounds.

9.4 Alternative Reducing Conditions

Next the work was focused on robust and selective methods and reagents for chemoselectivity in favor of the sulfonation reduction. At the same time, other protecting groups for the amine, such as Cbz and benzoyl groups were considered.

9.4.1 Magnesium

Mg metal in methanol was reported as a reducing reagent for the desulfonylation of β -amino sulfone compounds.⁷⁴ Model compound sulfone **7-2** was subjected to desulfonylation using Mg in methanol (Scheme 9.9). None of the desired desulfonylation product **7-2** was detected, however, elimination product **8-29** was detected. When NiCl₂ was used as an additive in the Mg-MeOH system, the reaction produced a 1:1 mixture of the desired desulfonylation product **7-3** and elimination products **8-29**. Starting material **7-2** was also recovered in 20% yield. No desulfonylation product was formed using Mg in ethanol.

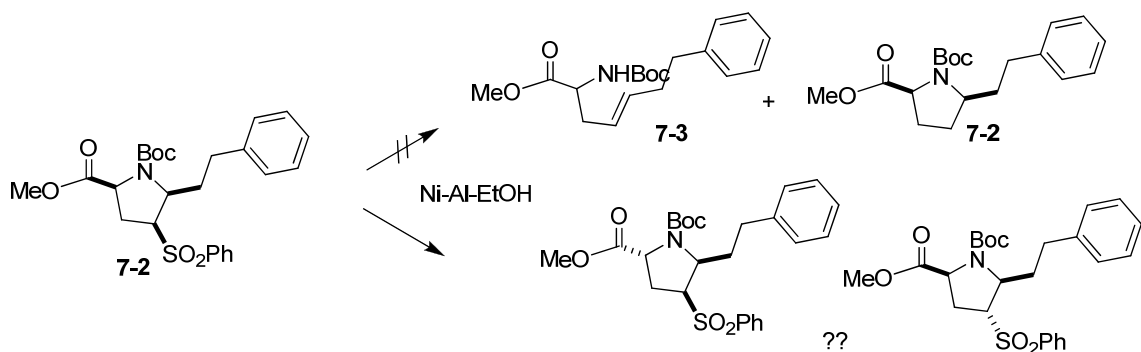


Scheme 9.9 Mg mediated desulfonylation.

9.4.2 Nickel – Aluminum

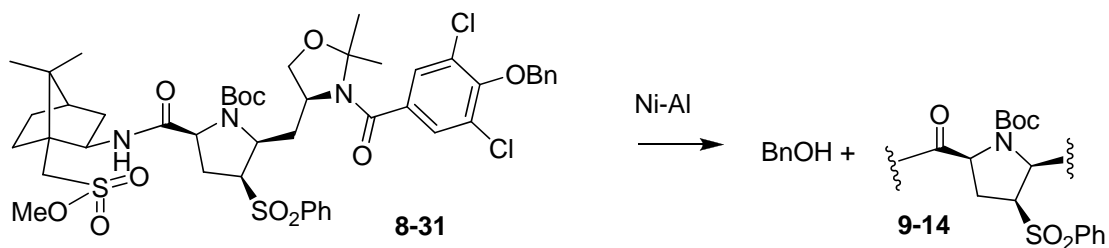
Model compound **7-2** was subjected to the Ni-Al in refluxing MeOH, but no desired desulfonylation **7-3** or elimination products **8-29** were observed based on TLC

analysis (Scheme 9.10). The starting material was found to be converted into a new compound with R_f value close to that of the starting material.



Scheme 9.10 Attempted desulfonylation using Ni-Al-EtOH showing possible by-products.

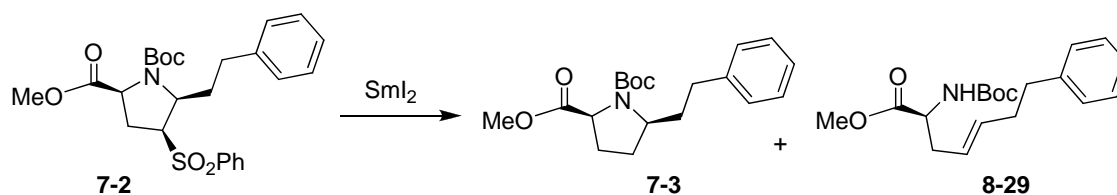
Under the same condition, the sulfone intermediate **8-30** was treated with Ni-Al in refluxing EtOH (Scheme 9.11). ¹H NMR spectra of crude compound indicated that debenzylation and oxazolidine-ring-opening occurred, but no desulfonylation product was detected.



Scheme 9.11 Attempted desulfonylation using Ni-Al-EtOH.

9.4.3 Samarium Iodide

After unsuccessful attempts with many other reducing agents, SmI₂ was tested for the desulfonylation (Scheme 9.12).



Scheme 9.12 Desulfonylation using samarium iodide.

Initial attempt to effect SmI_2 -mediated desulfonylation (SmI_2 -THF) with model compound **7-2** failed to obtain any desired desulfonylation product (Table 9.1, Entry 1) with 100% recovery of the starting material. A literature search revealed a report that the electrochemical properties of SmI_2 were found to be very sensitive to the nature of the solvents and the reducing properties increased by going from THF to HMPA.⁵⁸

Table 9.1 Desulfonylation of model compound **7-2** using SmI_2 .

Entry	Conditions	Results
1	SmI_2 – THF – rt	-
2	SmI_2 – THF – rt – HMPA	49% 8-29
3	SmI_2 – THF – 0 °C – HMPA	34% 7-3
4	SmI_2 – THF – -78 °C – HMPA	-
5	SmI_2 – THF – 0 °C – HMPA – MeOH	74% 7-3 + small amount of 8-29
6	SmI_2 – THF – rt – HMPA – MeOH	92% 7-3

The addition of HMPA to the SmI_2 -mediated desulfonylation at rt resulted in the fast consumption of starting material (20 min) but generated the undesired elimination product in 49% (Entry 2). When the reaction was performed at 0 °C, the elimination product was isolated in 34%. Based on the proposed mechanism (Scheme 9.7) it is believed that a proton source may solve the elimination problem. To test this assumption, MeOH was added to the SmI_2 -THF-HMPA promoted desulfonylation. This gave the desired product in 74% yield at 0 °C along with a small amount of starting material

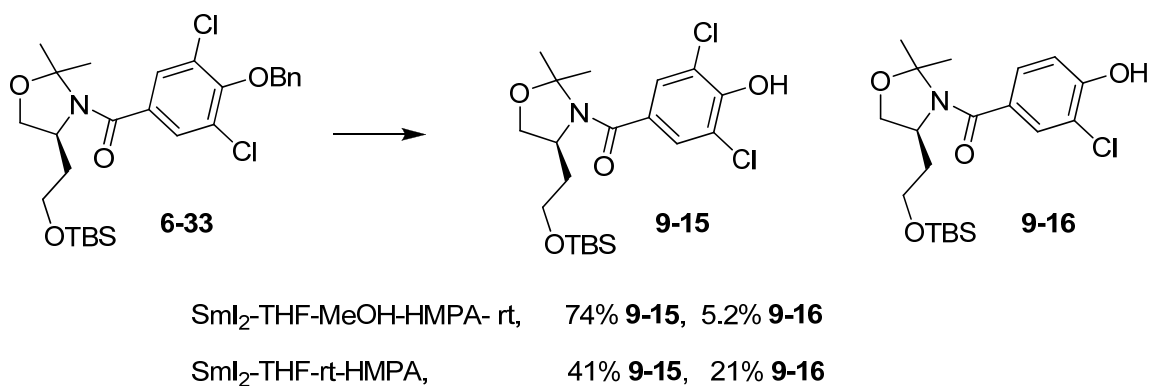
(Entry 5). When the reaction was performed at rt the desired desulfonylation product **7-3** was obtained in 92% yield (Entry 6). Thus, optimized desulfonylation conditions were finally obtained, using samarium iodide.

9.5 Functional Group Stability to Samarium Iodide

Having developed and optimized the new samarium iodide desulfonylation conditions it was necessary to test the stability of vulnerable functional groups present on intermediates towards kaitocephalin.

9.5.1 Model Compound Testing

Model compounds were subjected to SmI_2 desulfonylation conditions to test the stability of the functional groups on the sulfone intermediates (Scheme 9.13).



Scheme 9.13 Stability of model compound **6-33** to SmI_2 .

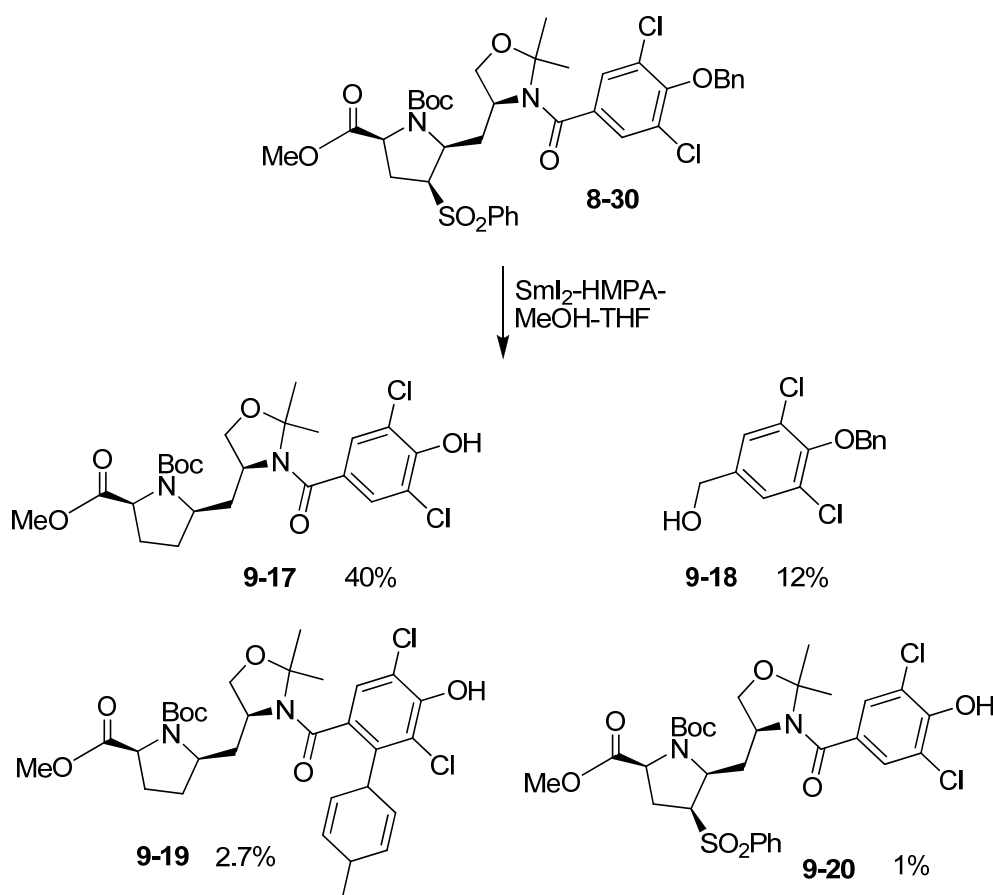
Model compound **6-33** was treated with SmI_2 -MeOH-HMPA and generated a mixture of de-benzyl dichloro product **9-15** (75%) and de-benzyl monochloro product **9-16** (5%). Without the methanol the reaction afforded a mixture of de-benzyl dichloro product **9-15** (41%) and de-benzyl monochloro product **9-16** (21%). These results

revealed that MeOH plays an important role not only in the desulfonylation itself, but also in “protecting” the chloro groups of the aryl chloride.

The control experiment for testing the stability of functional group indicated that chemocontrolled desulfonylation is possible employing SmI₂-MeOH-HMPA.

9.5.2 Real Intermediate Testing

Using the same conditions, the key intermediate **8-30** was treated with the SmI₂-HMPA-MeOH. The debenzyl-desulfonylation product **9-17** was isolated in 40% yield (Scheme 9.14).

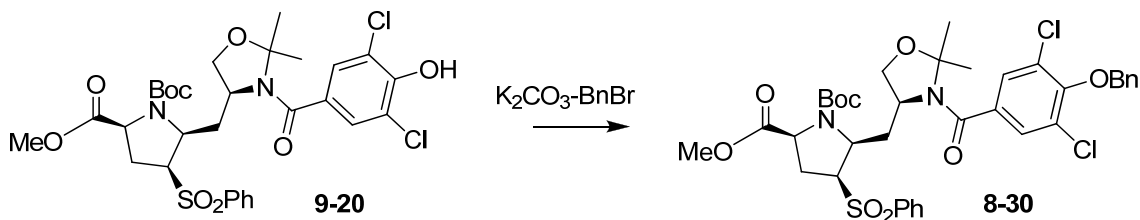


Scheme 9.14 Stability of real intermediate **8-30** to SmI₂.

Chapter 9: Desulfonylation

A known compound, alcohol **9-18** was the major byproduct of this reaction in 12% yield, along with another two by-products **9-19** and **9-20**. From analyzing the structure of the isolated compounds, it was found that the chloro groups seemed stable, but the amide bond seemed unstable under these radical reaction conditions.

The assignment of desulfonylation products was based on the vt NMR spectra. The evidence for the structure of alcohol **9-18** was from D₂O exchange- ¹H NMR spectra and by comparing ¹H NMR spectra of isolated **9-18** with reported data for this compound.⁷⁵ The structure of compound **9-20** was deduced via its conversion to starting material **8-29** using benzyl bromide (Scheme 9.15). The structure of byproduct **9-19** was inferred from analysis of ¹H NMR spectra, unfortunately, without further corroborating evidence.



Scheme 9.15 Conversion of **9-20** to **8-30**.

9.5.3 Samarium Iodide Issues

This reaction provided the desired desulfonylation product in an unoptimized yield of 40%, indicating chemoselective removal of sulfone with the intermediate in the synthesis of kaitocephalin can be obtained. However, the 40% yield is unsatisfactory and, it suffered from issues such as:

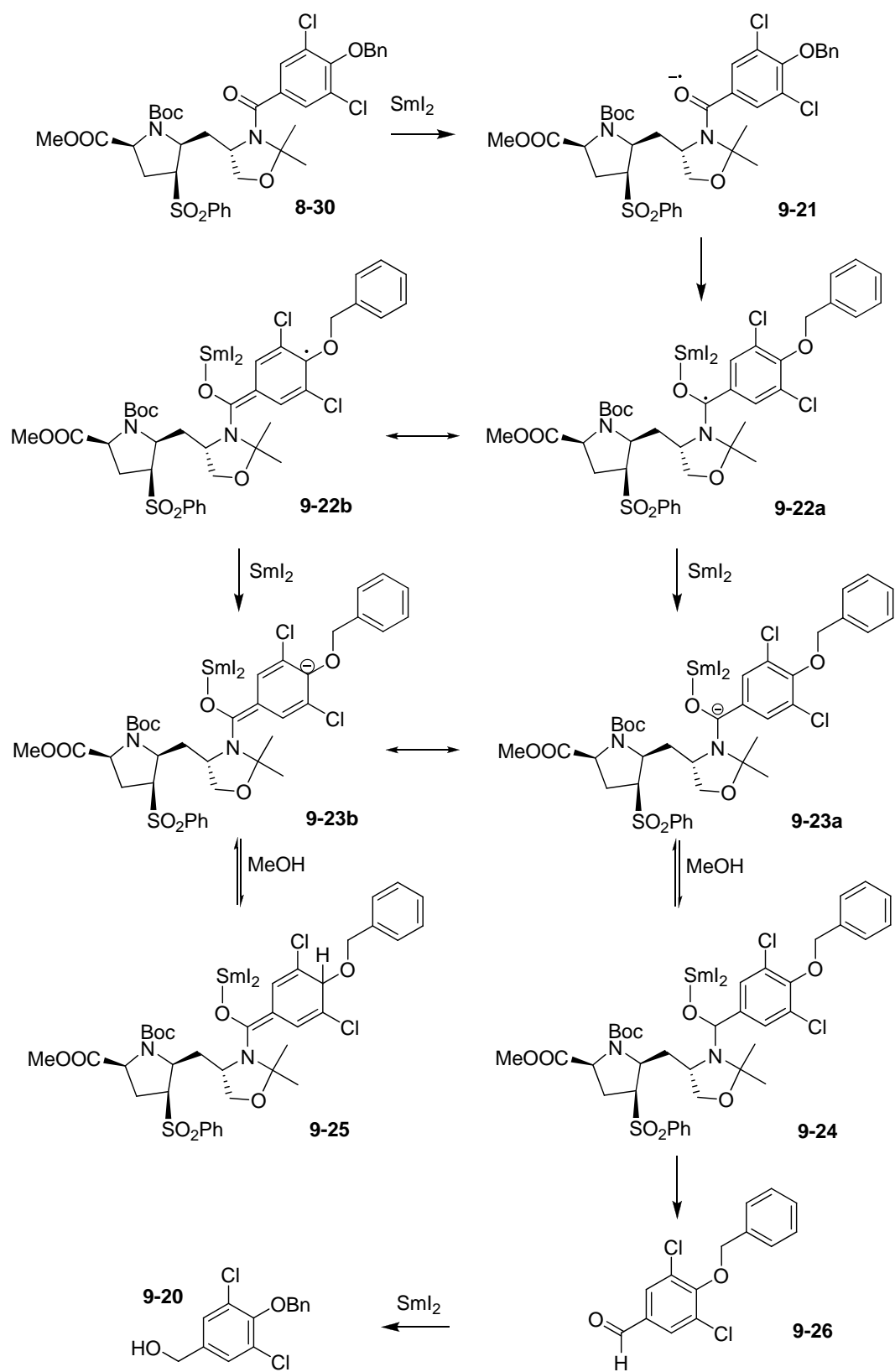
1. Unknown functional group tolerance.
2. Reagent instability and air sensitivity (SmI₂) which made scale up difficult.

3. Reagent toxicity (HMPA).
4. What accounts for about 45% of the remaining mass?

9.5.4 Proposed Mechanism of Byproduct Formation

A proposal for the mechanism of alcohol formation is shown in Scheme 9.16. Electron-transfer from single-electron donor (SmI_2) to the amide oxygen generates the radical-anion **9-21** which could trap the Sm(III) afford radical **9-22**. This species is more stable due to the delocalization of the radical onto several possible resonance structures. A second electron reduction gives anion **9-23**, also resonance stabilized. This may pick up a proton to give either **9-24** or **9-25**. Compound **9-24** may eliminate an amide anion (or be protonated and eliminate an amine) to give aldehyde **9-26**. This may be further reduced by the samarium iodide to give alcohol **9-20**.

Chapter 9: Desulfonylation



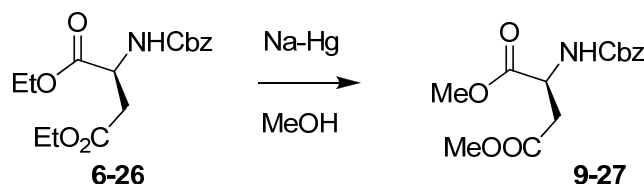
Scheme 9.16 Possible mechanism for the formation of by-product alcohol **9-20**.

9.6 Alternative Protection Strategy

Through reasoning the mechanism of byproduct alcohol formation, it was predicted that protecting the amine with a group such as Cbz might avoid reduction of the amide bond and might give the desulfonylation product using Na-Hg. The correct aryl-chloride group may be introduced after desulfonylation.

9.6.1 Model Compound Stability Testing

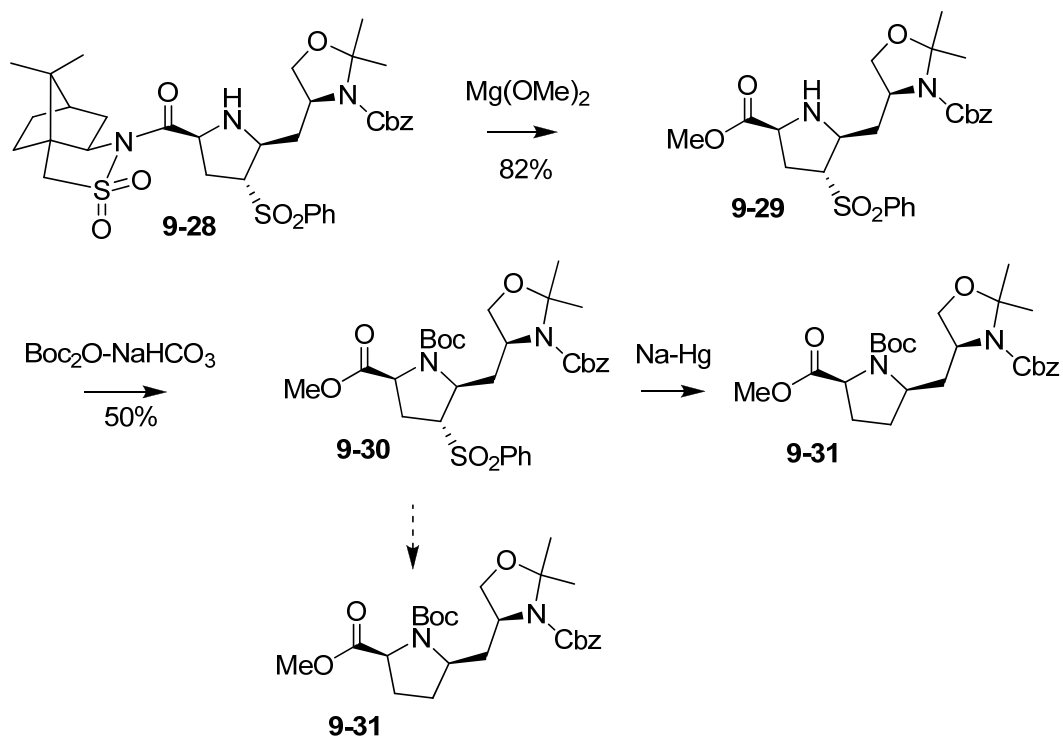
The model compound N-Cbz diester **6-26** was subjected to Na-amalgam mediated desulfonylation and generated the corresponding methyl ester **9-27** (Scheme 9.17). This result indicated that the Cbz protected amine tolerated the relatively harsh Na-Hg mediated desulfonylation conditions.



Scheme 9.17 Model reaction testing Cbz protected amine stability to Na-Hg reduction.

9.6.2 Testing with Real Substrates

Next, N-Cbz cycloadduct was converted to the precursor for the desulfonylation via a sequence of desultamization and Boc protection (Scheme 9.18). The desulfonylation with Cbz compound **9-30** was performed using Na-Hg.



Scheme 9.18 Real reaction testing Cbz protected amine stability to Na-Hg reduction.

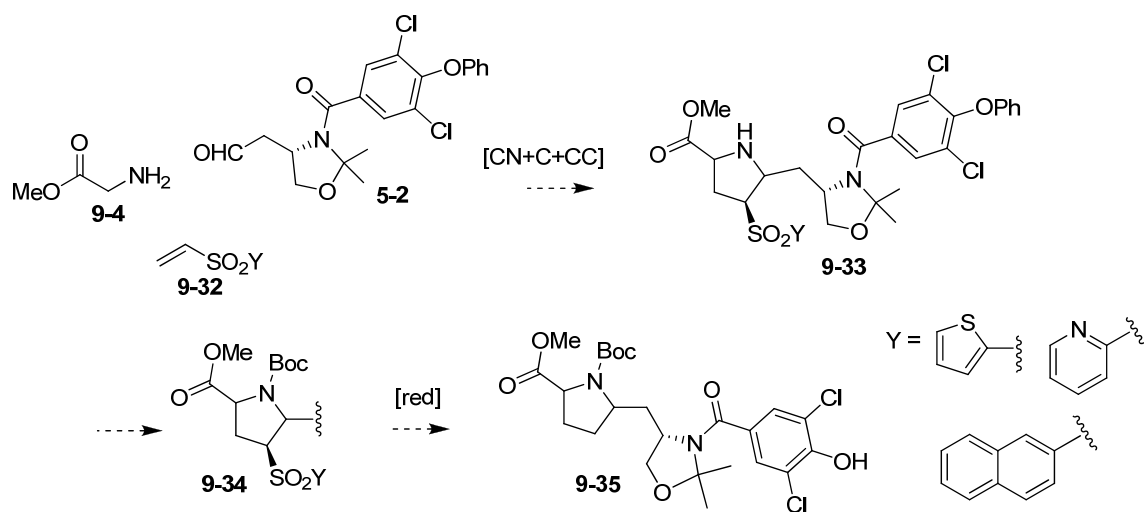
The crude NMR indicated that the sulfone group was removed (inferred from comparison of the proton signals between the methoxy group and aromatic protons). The ^1H NMR signals between 5.0-5.4 ppm indicated the presence of a CH_2O on the Cbz group, which suggested that Cbz group was stable under Na-Hg reducing conditions.

9.6.3 Cbz Protection and SmI_2

Though the desulfonylation with the N-Cbz cycloadduct **9-30** was not carried out using SmI_2 -HMPA-MeOH, it is anticipated SmI_2 mediated desulfonylation of this compound would afford the desired product. Based on the results of a literature search for SmI_2 -HMPA-MeOH mediated reactions, many substrates subjected to samarium iodide reductions possessed the Cbz protecting group.⁵⁸

9.7 Alternative Sulfones

Considering the mechanism of 1,3-dipolar cycloaddition and desulfonylation, it was predicted that [CN+C+CC] 1,3-dipolar cycloadditions with a vinyl sulfone bearing substituent with lower electronic density should give the corresponding cycloadduct, which may be removed using milder conditions (Scheme 9.19).



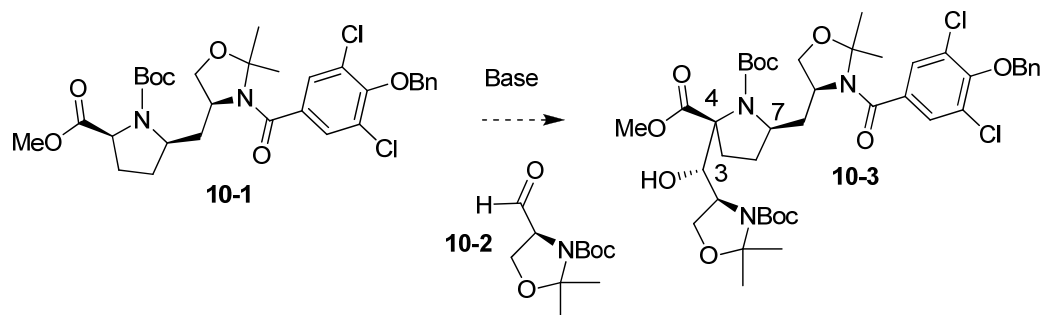
Scheme 9.19 Alternative approach to disubstituted pyrrolidines using different sulfones.

10 Addition of C1-C3

Installation of the C1-C3 branch of the kaitocephalin molecule is a key step. Appropriate use of chiral directing functionality may be used to control the stereochemistry at the new chiral center created in the reaction as well as maintaining the appropriate stereochemistry at all existing stereocenters.

10.1 Aldol Condensation

With the 4,7-disubstituted pyrrolidine **10-1** in hand,⁵⁷ installation of the C1-C3 moiety of kaitocephalin on C4 was anticipated to be achieved using an aldol condensation with *S*-Garner aldehyde, derived from *S*-serine. The configuration of C3-*S* and C4-*R* was envisioned to be constructed simultaneously (Scheme 10.1).

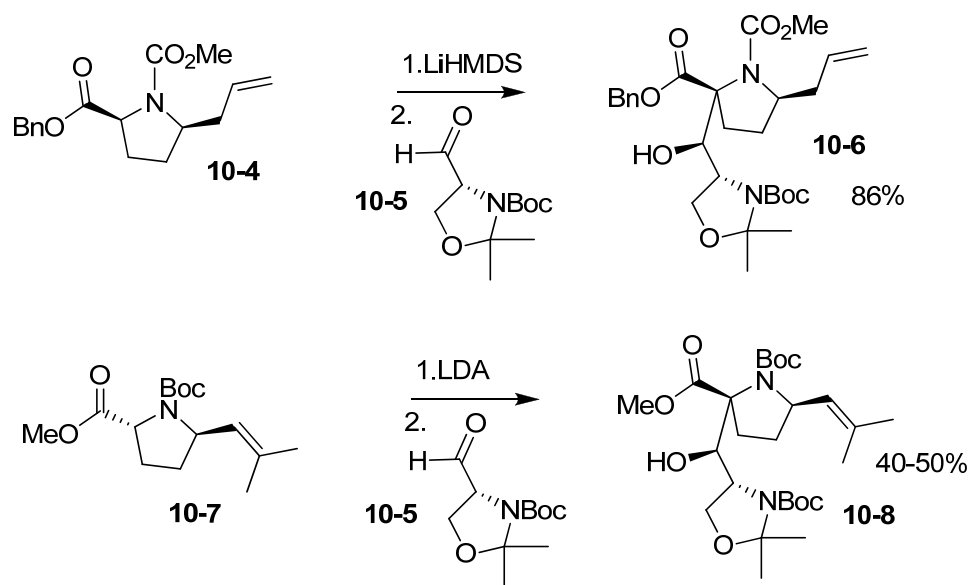


Scheme 10.1 Insertion of C1-C3 in the synthesis of kaitocephalin using *S*-Garner aldehyde.

10.1.1 Stereochemistry – Ma and Chamberlin

In the synthesis of kaitocephalin, aldol condensation between pyrrolidine intermediate and Garner aldehyde was performed in Ma, Chamberlin, and Kitahara's group. The aldol reaction between *R*-Garner aldehyde **10-5** and Ma's cis disubstituted

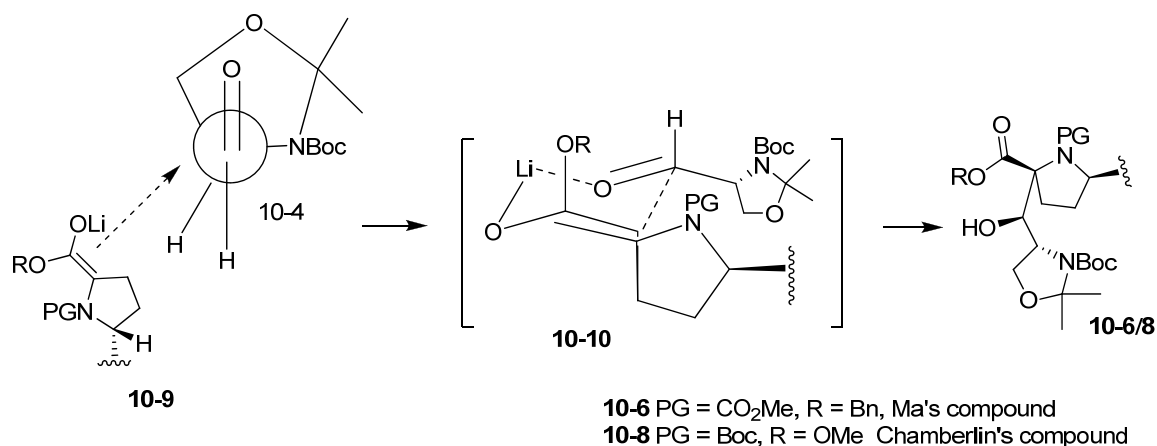
pyrrolidine **10-4** exclusively afforded one diastereomer of aldol product **10-6** with a $2R,3R$ configuration in 86% yield (Scheme 10.2). With the aldehyde **10-5**, Chamberlin's trans-disubstituted pyrrolidine **10-7** also exclusively produced the same single diastereomer ($2R,3R$) but in lower yield.



Scheme 10.2 Aldol condensation of *R*-Garner aldehyde in the synthesis of kaitocephalin.

10.1.1.1 Analysis

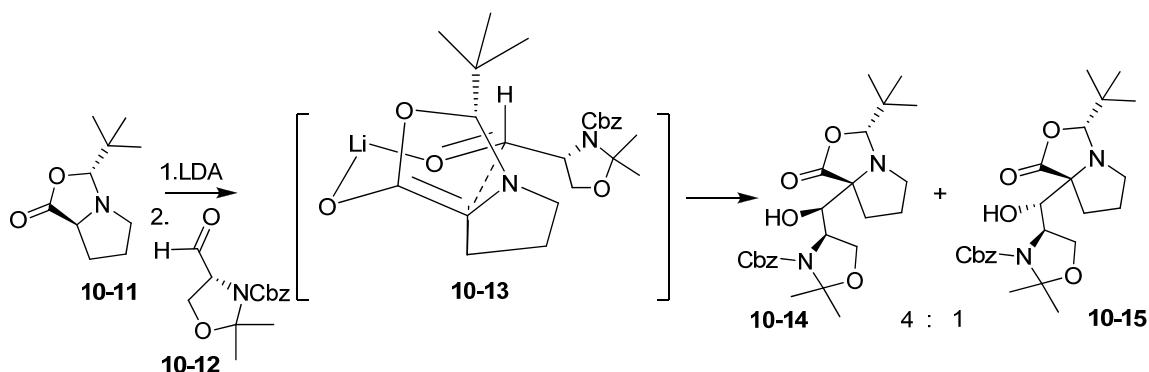
Analysis of the addition product indicates that the Si face of *Z*-enolate **10-9** adds to the Si face of the aldehyde **10-5** (as expected by the Anh model) via a chelated chair conformation (Scheme 10.3).



Scheme 10.3 An aldol reaction with *R*-Garner aldehyde via a possible transition state.

10.1.2 Kitahara – Seebach's Lactone

In Kitahara's synthesis, the aldol reaction between Seebach's lactone **10-11** and the modified *R*-Garner aldehyde bearing a Cbz group **10-12** gave the predicted (3*R*)-isomer as the major product (Scheme 10.4).

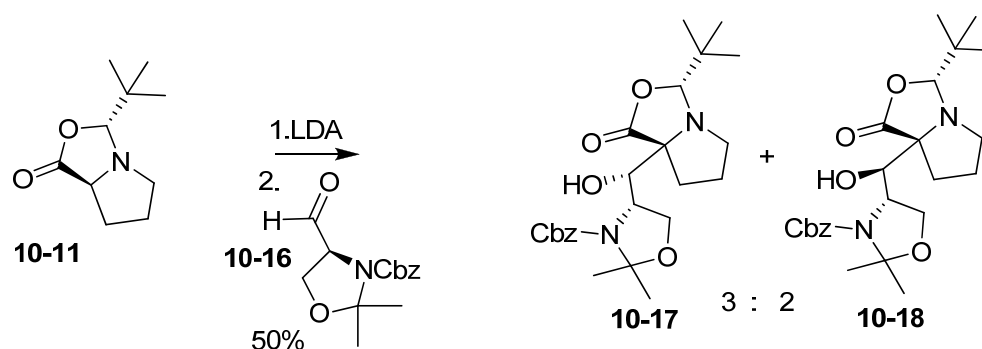


Scheme 10.4 Kitahara's aldol reaction of Seebach's lactone with modified *R*-Garner aldehyde.

The fused ring system makes it impossible to form the *Z* isomer of the enolate. This reduces the flexibility of this reaction to adopt a conformation that minimizes steric clash between groups. Again, the oxazolidine stereochemistry dictates the face of the aldehyde most easily approached. Without the fused ring constraint the bulky *t*-butyl group would

dictate that the *Z*-enolate would react preferentially, but the fused ring prevents this. As only the *E*-enolate can form, the bulky *t*-butyl group is forced towards the aldehyde, thus raising the energy of the transition state. That is why there is a mixture of diastereomers produced as the oxazolidine and *t*-butyl group compete for steric influence.

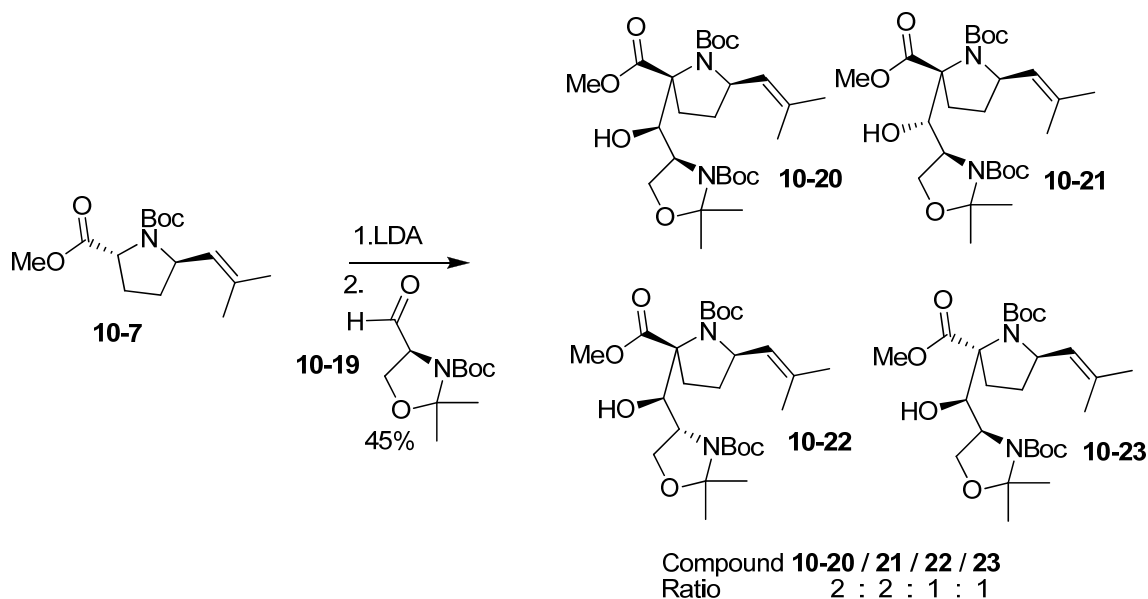
In contrast, while *S*-Garner aldehyde was investigated in the aldol condensation, the reaction with Seebach's lactone afforded a 3:2 mixture of (*3R*)- and (*3S*)- aldol products (Scheme 10.5).



Scheme 10.5 Kitahara's aldol reaction of Seebach's lactone with modified *S*-Garner aldehyde.

10.1.3 Reaction with *S*-Garner Aldehyde

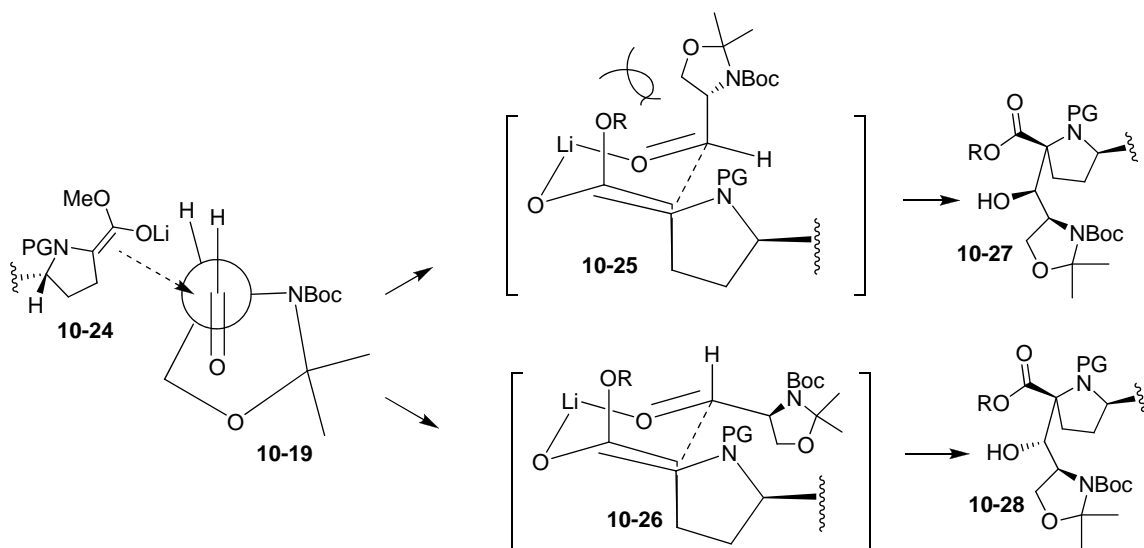
Use of Chamberlin's *trans*-disubstituted pyrrolidine **10-7** as the precursor for the aldol condensation reaction with *S*-Garner aldehyde gave four isomers in a ratio of 2:2:1:1 (Scheme 10.6).



Scheme 10.6 Aldol condensation between substituted pyrrolidine **10-7** and *S*-Garner aldehyde.

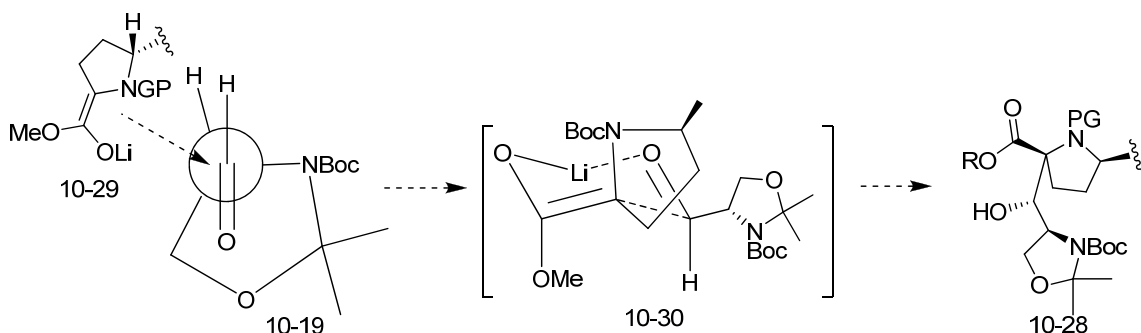
10.1.3.1 Analysis

Felkin-Anh chair transition state models may be used to analyze the possible products and predict which are more likely. The $3R$ aldol product **10-27** may be produced if the structure in a chelated chair model has the oxazolidine located in an axial position. The 1,3-diaxial interaction in **10-25** renders the conformer higher in energy than **10-26**. In order to obtain the $3S$ product using the model presented in Scheme 10.7 the Si face of *Z*-enolate **10-24** must add to the Si face of the aldehyde **10-19** (by an anti Felkin-Anh chair transition model) via a chelated chair conformation. This result indicated that *Z*-lithium enolate is unlikely to be the source of the $3S$ isomer as this would require a mismatched double asymmetric induction.



Scheme 10.7 Aldol reactions with *S*-Garner aldehydes via possible transition states.

It was postulated that the *E*-enolate **10-29** adds to the *Re* face of the aldehyde **10-19** (by a Felkin-Anh chair transition model) leading to an alternative axial and equatorial arrangement in the chelated chair with the oxazolidinone located on the equatorial position and therefore lacking the 1,3-diaxial interaction (Scheme 10.8).

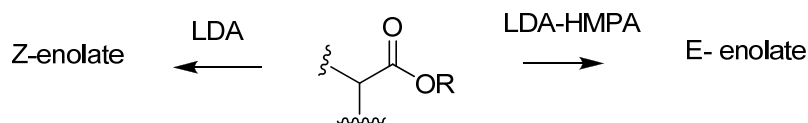


Scheme 10.8. Alternative route to the C3*S*-isomer via *E*-enolate mediated aldol condensation.

10.1.4 Preferential Enolate Formation

It is known that reactions of esters with LDA in THF in the presence of HMPA predominantly give *E*-enolates (Scheme 10.9).⁷⁶ However, after one failed HMPA

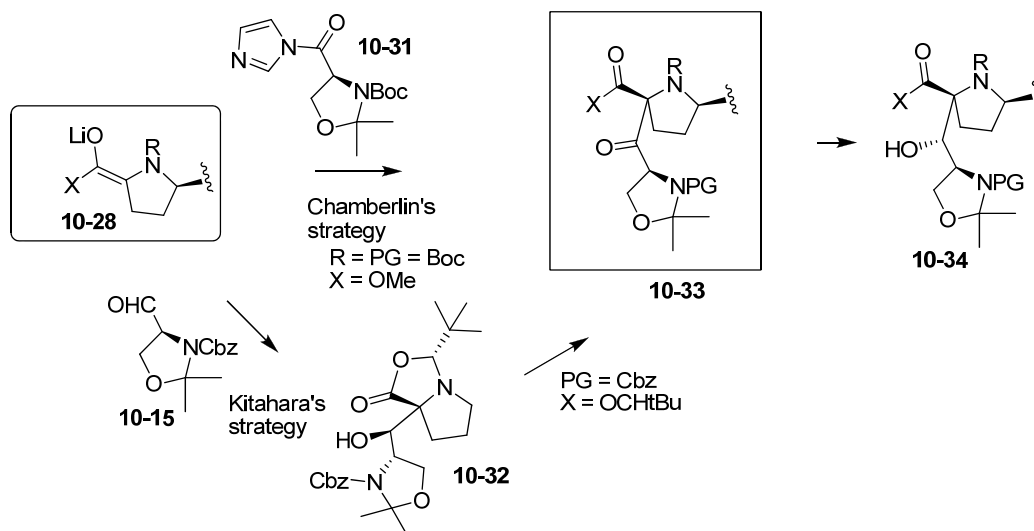
mediated aldol condensation, it was decided not to continue with HMPA mediated reaction tests due to its high hygroscopic nature, toxicity, and high boiling point.



Scheme 10.9 Preferential formation of E or Z enolates.

10.2 Acylation

In Kitahara's synthesis, the 3*S*-isomer **10-34** was generated by conversion of 3*R*-isomer **10-32** through oxidation to ketoester **10-33** followed by reduction (Scheme 10.10).

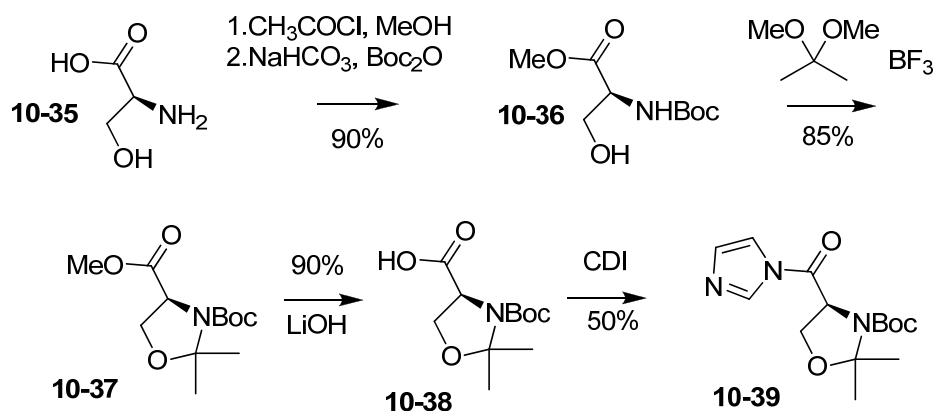


Scheme 10.10 Two approaches to the 3*S*-isomer.

It was felt Chamberlin's strategy was reasonable to form ketoester **10-33** directly through acylation of enolate **10-28** (Scheme 10.10).

10.2.1 Acylation Reagent Synthesis

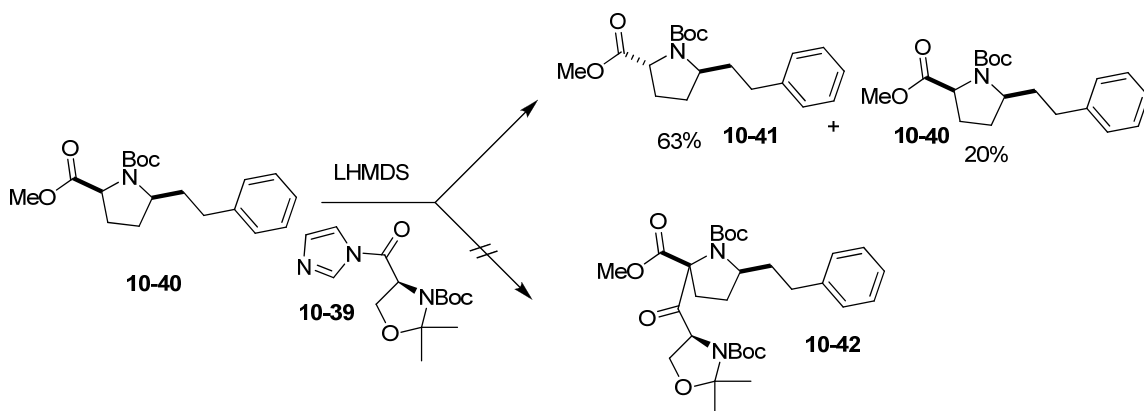
Following Chamberlin's procedure, *S*-*N*-acylimidazole **10-39** was prepared from L-serine **10-35** in five steps in 35% overall yield (Scheme 10.11).



Scheme 10.11 Synthesis of acylation reagent **10-39**.

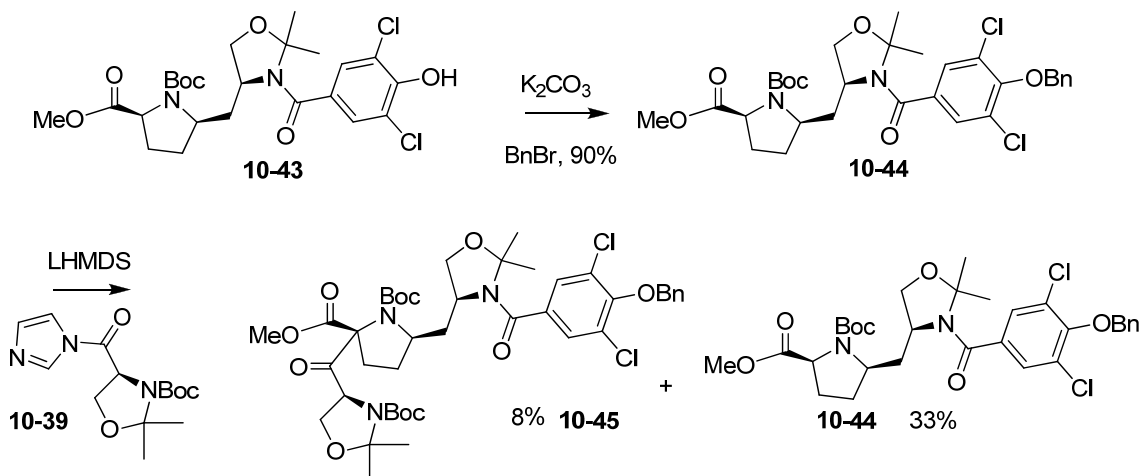
10.2.2 Model Reactions

Attempts to use the lithium enolate of model compound **10-40** formed using LHMDS at $-78\text{ }^\circ\text{C}$ to be trapped by *S*-*N*-acylimidazole **10-39** at $30\text{ }^\circ\text{C}$ failed to give the desired C-acylation product **10-42** (Scheme 10.12). The C2-epimer **10-41** was isolated in 63% and the starting material **10-40** was recovered in 20% yield. No further control experiments were investigated because of time limitations.

Scheme 10.12 Attempted acylation of model compound **10-40**.

10.2.3 Live Testing

The desulfonylation product **10-43** was protected as benzyl ether in 90% yield, and the resultant key intermediate **10-44** was subjected to lithiation using LDA at 0 °C followed by trapping with *S*-*N*-acylimidazole **10-39** at 0 °C (Scheme 10.13). The desired C-acylation product **10-45** was obtained in 8% yield with recovery of 33% of the starting material **10-44**.

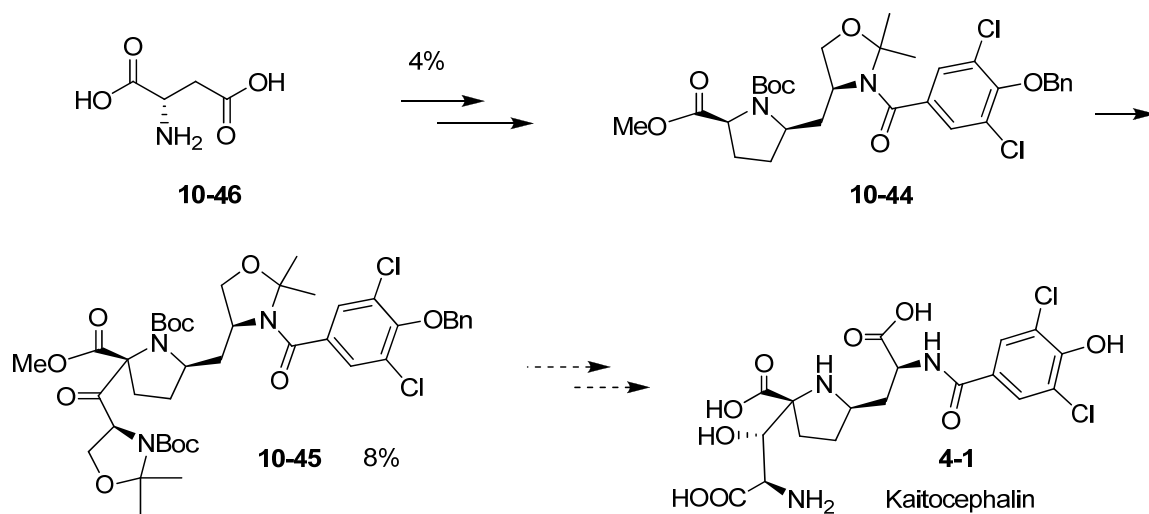


Scheme 10.13 Using acylation to introduce the C1-C3 moiety.

The evidence for the structure of **10-45** was from the ^1H NMR analysis and mass spectrometry data. No further evidence for desired stereochemistry was obtained. It was assumed that the substituent at C7 controlled stereochemistry at C4. This is easily rationalized as the C7 substituent is extremely large in comparison to all other groups in the molecule. A transition state geometry will therefore be adopted to place this very large C7 substituent angled away from the reaction center. It is much more favorable for the aldehyde to approach the C4 center from the opposite side of the pyrrolidine ring to that of the C7 substituent, thus ensuring a predominance of C4*R* isomer.

10.2.4 Further Development

Based on all the reports of construction of the C3*S* configuration employing oxidation/reduction procedures in the prior syntheses of kaitocephalin, it was reasoned that the stereocenter at C3 in the intermediate could be formed through diastereoselective reduction. Thus, the key intermediate 4,7-disubstituted pyrrolidine **10-44** was prepared from aspartic acid **10-46** in 10 steps in 4% overall yield. This was converted to the trisubstituted pyrrolidine **10-45** in an unoptimized 8% yield (Scheme 10.14).

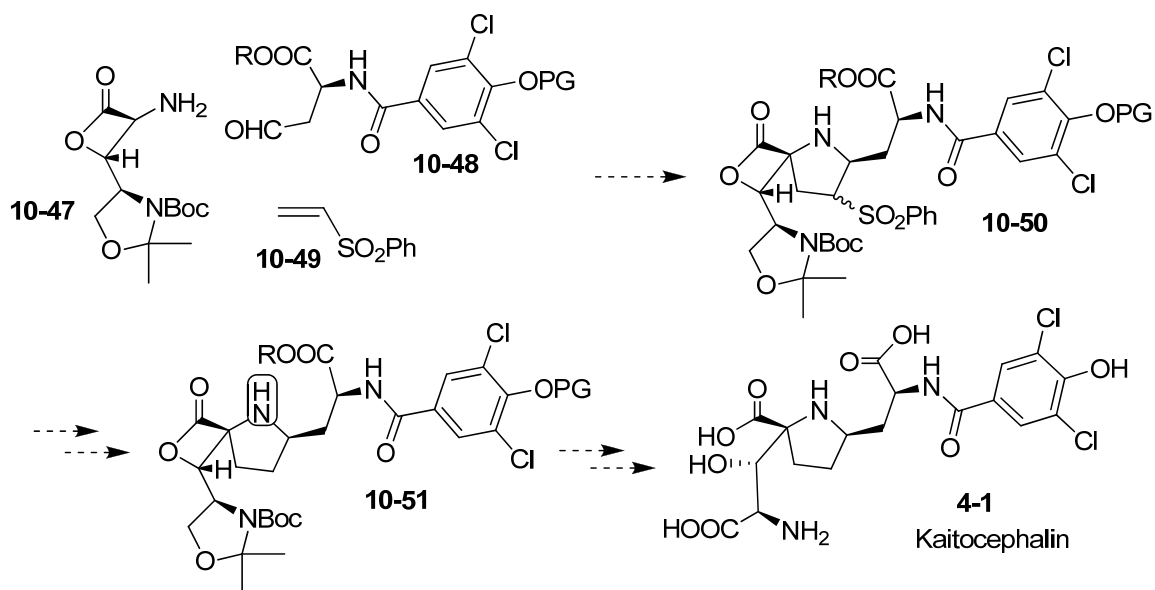


Scheme 10.14 Continuation to kaitocephalin.

Kaitocephalin would be prepared from the ketoester **10-45** via a sequence of ring-opening, oxidation, then Al_2S_3 mediated removal of benzyl ether, Boc and methyl ester (Scheme 10.14).

10.3 Alternative Synthetic Route

It was also proposed that kaitocephalin may be synthesized via lactone-sulfone intermediate **10-50**. This might be achieved with substrate-controlled reactions via [CN+C+CC] 1,3-dipolar cycloaddition or with a 1,3-dipolar cycloaddition between an imine and a phenyl vinyl sulfone (Scheme 10.15).



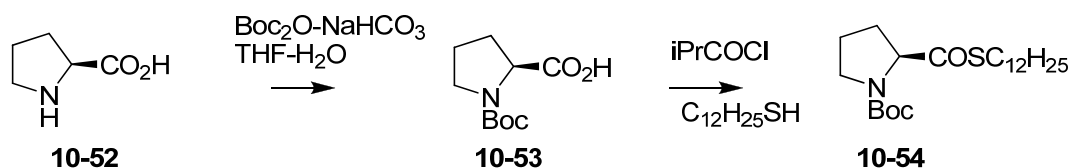
Scheme 10.15 Alternative synthetic plan.

10.3.1 Lactone Preparation

It was planned to prepare the lactone through tandem aldol condensation followed by intramolecular transesterification.

10.3.1.1 Model Compound Precursor

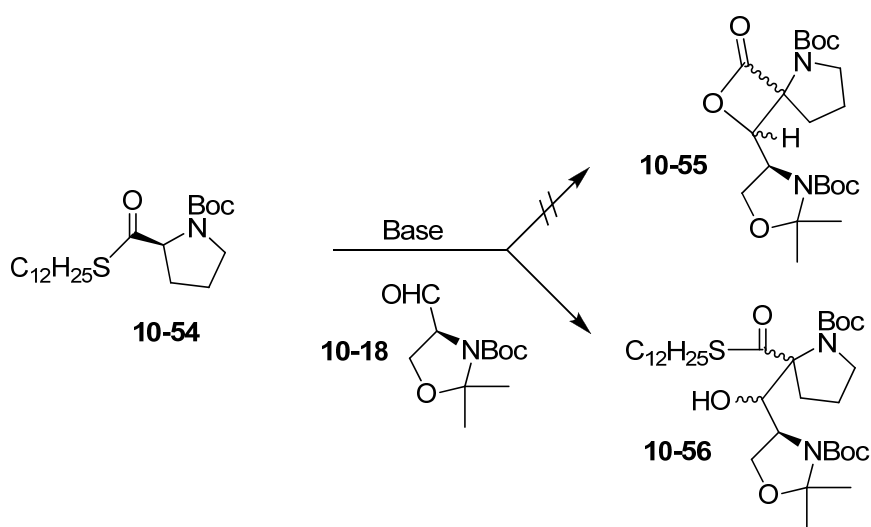
The model compound thiolate **10-54** was prepared from proline via Boc protection and thioester formation in 50% overall yield (Scheme 10.16).



Scheme 10.16 Synthesis of model compound 10-54.

10.3.1.2 Attempted Lactonization

Next, following Ma's procedure to form the lactone lithium enolate this was trapped by *S*-Garner aldehyde at -78 °C. The temperature of the aldol reaction mixture was then raised from -78 °C to -40 °C. However, mass spectrometric analysis of the crude product mixture indicated that no desired 4 membered lactone was formed, but aldol condensation product was detected (Scheme 10.17).



Scheme 10.17 Attempted one pot lactone formation.

Table 10.1. outlines the results of this aldol condensation attempted under different conditions.

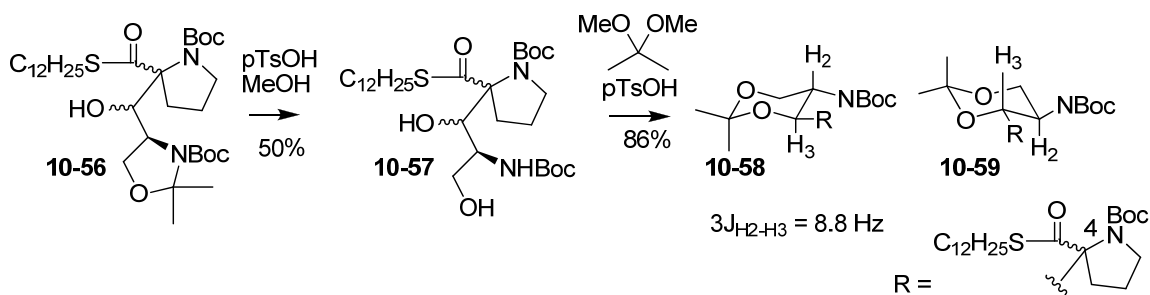
Table 10.1 Aldol condensation between thioester **10-54** and aldehyde **10-18**.

Entry	Base	Equivalents of Aldehyde	Yield
1	<i>s</i> -BuLi	3	67%
2	NaHMDS	3	48%
3	LiHMDS	3	80%
4	NaHMDS	1.6	8%

Lithiation of thioester with *s*BuLi at $-78\text{ }^{\circ}\text{C}$ followed by trapping the resulting anion with (*S*)-Garner aldehyde afforded a chromatographically inseparable mixture of α -hydroxy ester isomers in 67% yield (Entry 1). Employing NaHMDS as the base gave the isomers in 48% yield (Entry 2). Switching the base to LiHMDS lead to produce the isomers in 80% yield (Entry 3). Three equivalents of aldehyde were required to achieve respectable yields. The yield decreased to 8% when 1.6 eq of aldehyde were used to trap the lithium enolate derived from NaHMDS (Entry 4).

10.3.2 Deprotection and Analysis

With the alcohol **10-56** in hand, *p*TsOH catalyzed acetone cleavage of this alcohol mixture in methanol gave the corresponding N-Boc diols **10-57** in 52% yield (Scheme 10.18). Examination of the ^1H NMR of the mixture of unseparated isomers revealed three aldol products were formed in a ratio of 2.3:1.6:1 based on comparison of the integration values for the proton at C3 with a doublet peak. The stereochemistry was established by converting the mixture of isomers of N-Boc amino diol **10-57** into its respective mixture of 1,3-dioxanes **10-58** in 86% yield using DMP-*p*TsOH (Scheme 10.18). Analysis of the vicinal coupling constants between the protons at C3 and C2 centers indicated that the corresponding anti diastereomer of **10-58** was formed.



Scheme 10.18 Dioxane formation for stereo-identification.

10.3.2.1 Interpretation

Considering the Felkin-Anh transition-state model, chair-like transition state and anti diastereomers deduced from coupling constants, it was rationalized that the structures of the isomers of **10-58** were the *2S,3S,4R*-isomer (Felkin-Anh product), *2S,3S,4S*-isomer (mismatched), and *2R,3R,4R*-isomers (Felkin-Anh product) (Figure 10.1).

The aldehyde was freshly prepared to use in the aldol condensation, so this indicates that epimerization occurred under these reaction conditions. Chamberlin obtained the same results.³⁷

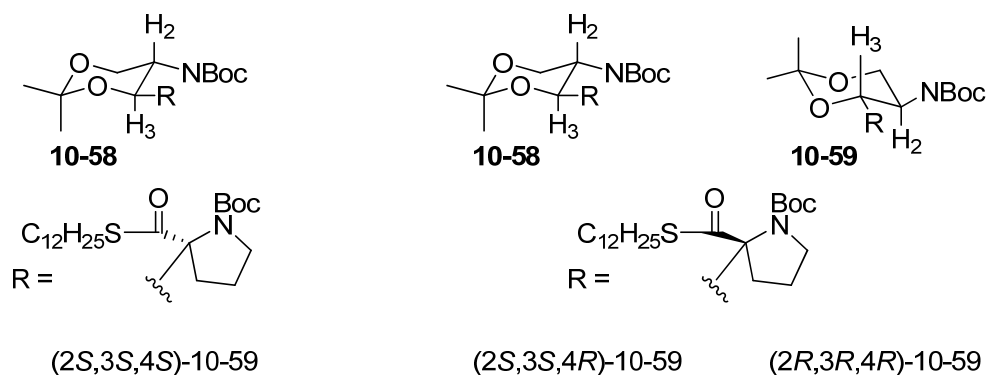


Figure 10.1 Stereochemistry assignment of the compounds of mixture **10-58** / **10-59**.

An alternative method to assign the stereochemistry of the isomers was sought, such as removing all the protecting groups to facilitate crystallization. However, up to now, no positive results have been obtained.

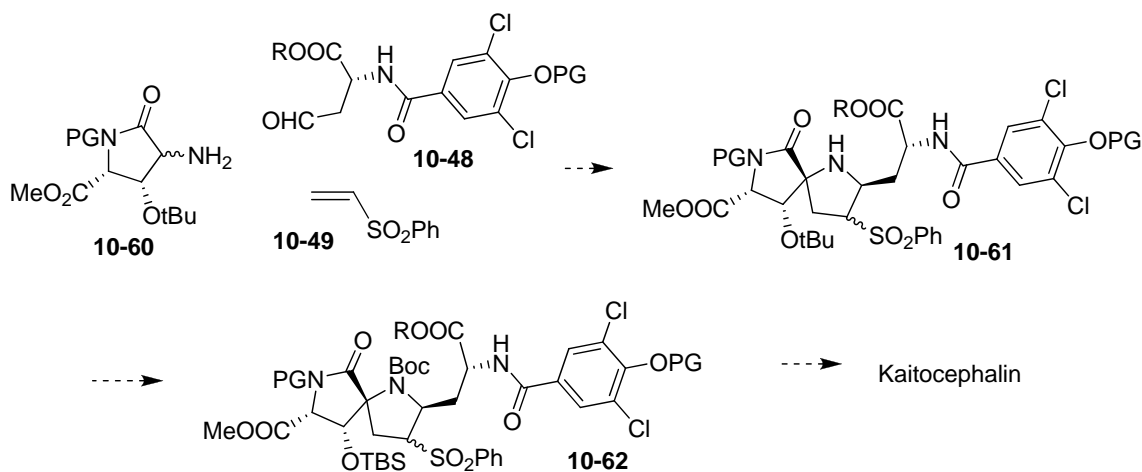
10.3.3 Summary

Though the model reaction did not afford the lactone, we obtained some useful information about aldol condensations with *S*-aldehydes.

Though the C1-C3 moiety could be installed via acylation at C4, both our and Chamberlin's substrates generated the corresponding trisubstituted pyrrolidine in low to moderate yields.

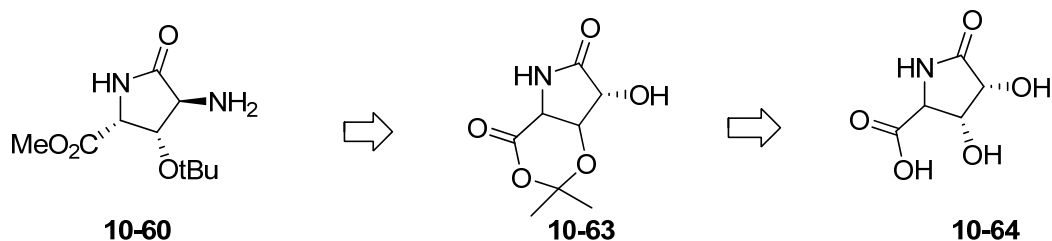
10.4 Proposed Future Work

It was also proposed that kaitocephalin may be synthesized via lactam-sulfone intermediate **10-61** bearing a (C3*R*)-hydroxyl group. This might be achieved with substrate-controlled reactions via [CN+C+CC] 1,3-dipolar cycloaddition or with a 1,3-dipolar cycloaddition between an imine and a phenyl vinyl sulfone (Scheme 10.19).



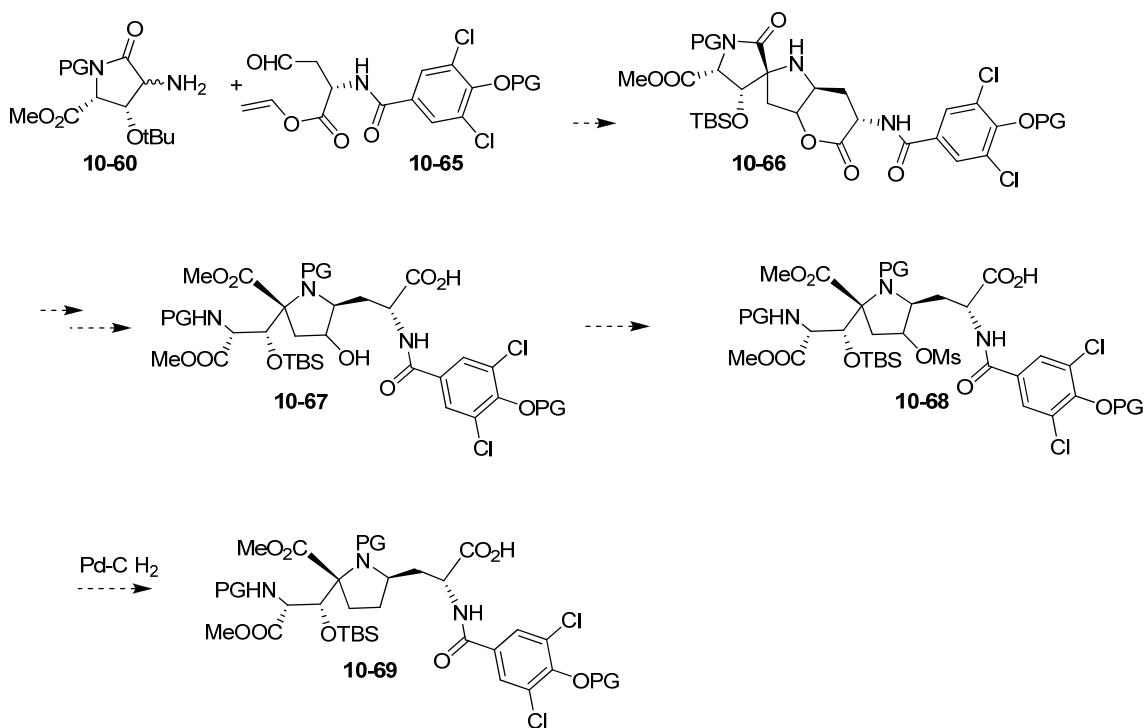
Scheme 10.19 Alternative synthetic plan.

Based on the successful conversion of C3*R*-hydroxyl group to C3*S* hydroxyl in the synthesis of kaitocephalin,⁷⁷ it is believed that the most challenging steps would be the [CN+C+CC] 1,3-dipolar cycloaddition with α -substituted amine and desulfonation. The lactam can be prepared from known diol **10-64** via a sequence of selective mono protection of alcohol, Mitsunobu reaction with azides, and reduction of the resultant azide (Scheme 10.20).⁷⁸



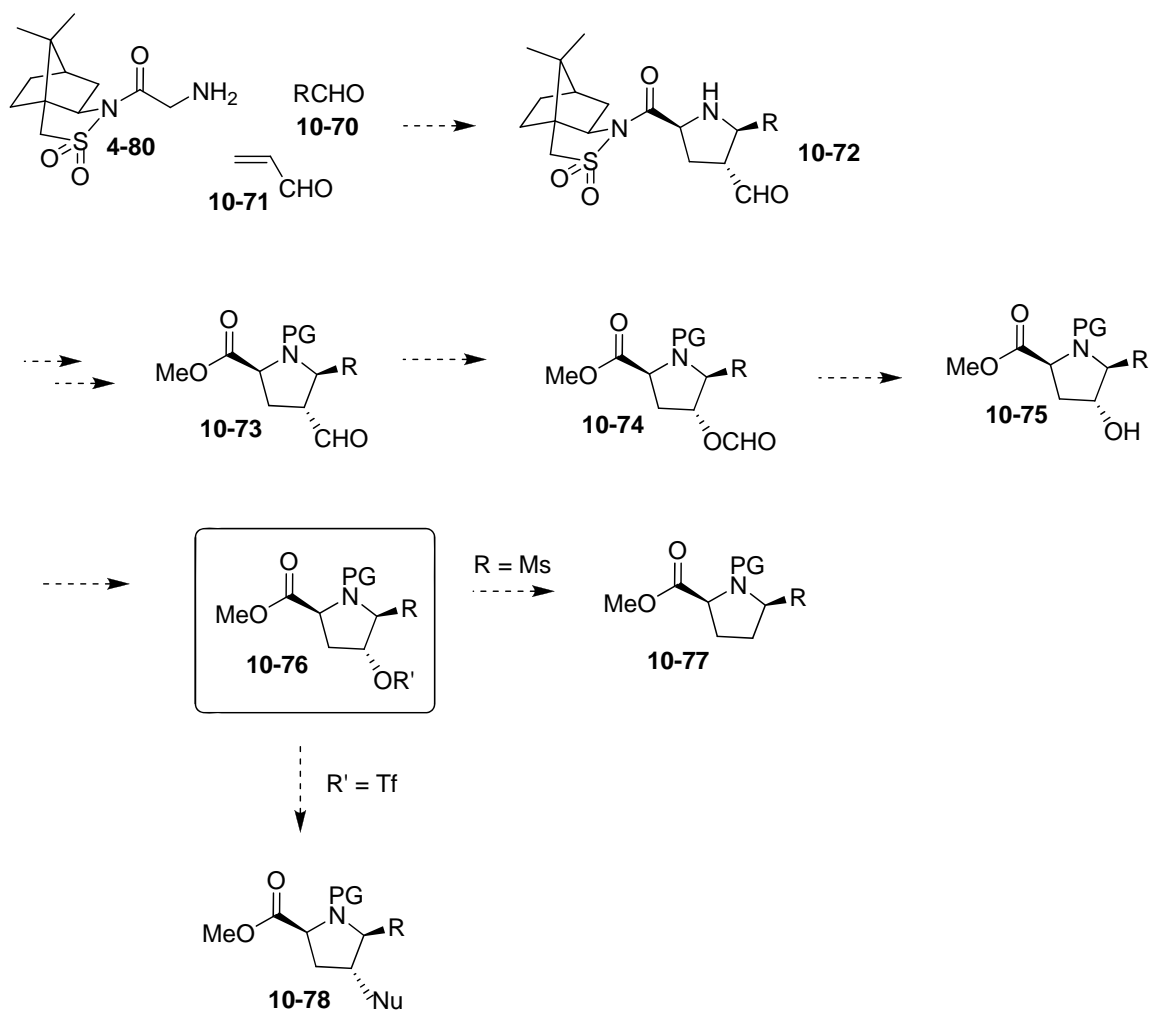
Scheme 10.20 Proposed retrosynthesis of lactam **10-60**.

If an olefin were attached onto the acid of the C8-C10 moiety, an intramolecular 1,3-dipolar cycloaddition could provide a new possibility to install 4,4,7-trisubstituted pyrrolidines without using a sulfone based olefin. The key 1,3-dipolar cycloaddition would be anticipated to afford a hydroxy-substituted pyrrolidine. The hydroxyl group could be removed by conversion to a Ms ester followed by hydrogenation (Scheme 10.21)⁷⁹



Scheme 10.21 Alternative synthetic plan via intramolecular 1,3-dipolar cycloaddition.

It was felt that auxiliary promoted [CN+C+CC] 1,3-dipolar cycloaddition employing an acrylaldehyde⁸⁰ as “CC” partner could generate 2,5-disubstituted pyrrolidines via Baeyer-Villiger oxidation, esterification, and hydrogenation. It also provides a reaction site to introduce the side chain at C6 if so desired (Scheme 10.22).



Scheme 10.22 Alternative synthesis of disubstituted pyrrolidine **10-77**.

11 Experimental

11.1 General Methods

All the reactions were carried out in anhydrous solvents and under argon atmosphere. All anaerobic and moisture-sensitive reactions were performed in flame-dried flasks fitted with a glass stopper under a positive pressure of argon, unless otherwise noted. Air- and moisture-sensitive liquids and solutions were transferred via syringe or cannula through rubber septa.

All reagents were purchased from commercial sources. Reagent grade solvents were used for extraction and flash chromatography. THF and benzene were freshly distilled from sodium/benzophenone under argon; dichloromethane (DCM, methylene chloride) was distilled from CaH₂ under argon and methanol from magnesium. Acetone was distilled from KMnO₄; DMSO, triethylamine (NEt₃) and NH(iPr)₂ from CaH₂; and all were stored over microwave-activated 4Å molecular sieves. Dimethylformamide was obtained from commercial suppliers as anhydrous (99.98%) and used directly.

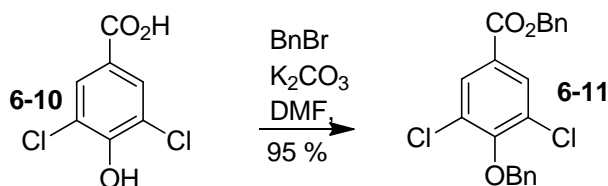
Melting points were determined in open-end capillary tubes on a GallemKamp apparatus, and are uncorrected. Optical rotation data were measured on a Perkin- Elmer 241 polarimeter at $\lambda = 589$ nm (Na D line) at room temperature and were reported $[\alpha]_D^{25}$ concentration ($c = \text{g}/100\text{mL}$). High resolution mass spectra (HRMS) were recorded on a Kratos MS25RFA mass spectrometer using Matrix-assisted laser desorption ionization (MALDI). NMR spectra were recorded at 300 MHz (¹H), 75 MHz (¹³C) on a Varian 300 spectrometer. Experiments were carried out at high temperature using hexadeuterio-

dimethyl-sulfoxide (d6-DMSO (δ H 2.50, δ C (central line of t) 39.50)) unless otherwise stated and chemical shifts are reported in parts per million (ppm). Coupling constants J are reported in Hertz (Hz). COSY and DEPT were used to aid spectral assignments. Stereochemical assignments are based on the NOE difference data. The absolute stereochemistry of intermediates is based on the X-ray crystallographic analysis of cycloadduct and tosylate derivative (Data was provided by the University of Akron collected on Bruker SMART Apex single crystal X-ray diffractometer).

The progress of reactions was monitored by analytical thin-layer chromatography and NMR spectra; Thin-layer chromatography (analytical and preparative) was performed using glass plates pre-coated to a depth of 0.25 mm with 230-400 mesh silica gel impregnated with a fluorescent indicator (254 nm). The plates were visualized first with UV illumination followed by charring with ninhydrin (0.3% ninhydrin (w/v), 97:3 EtOH-AcOH) or Verghn's reagent (10 g ammonium molybdate(VI), 5 g cerium(IV) sulfate, 1 L 10% aq. H₂SO₄). Flash column chromatography was performed employing 230-400 mesh silica gel. The solvent compositions reported for all chromatographic separations are on a volume/volume (v/v) basis.

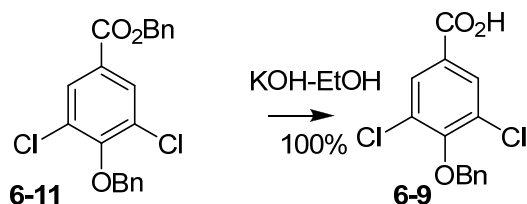
For simplicity reasons, in the compounds named in this section the sulfone moiety has been always considered as substituent.

11.2 Reaction Procedures and Characterization



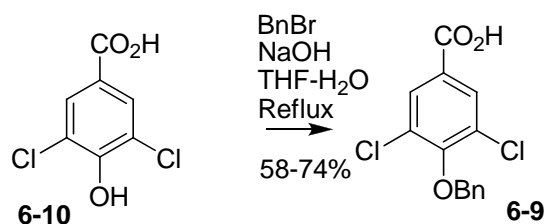
Benzyl 4-(benzyloxy)-3,5-dichlorobenzoate (6-11)

A mixture of 3,5-dichloro-4-hydroxybenzoic acid 6-10 (4.90 g, 23.0 mmol), benzyl bromide (4.44 g, 26.0 mmol), and K_2CO_3 (6.34g, 45.0 mmol) in DMF (50 mL) was stirred for 18 h at room temperature and then diluted with EtOAc (100 mL) and water (50 mL). The organic layer was separated, washed with water (2×50 mL) and brine (30 mL) and dried (Na_2SO_4). Concentration in vacuo gave a white solid residue. Recrystallization from CH_2Cl_2/n -hexane gave 3b as colorless needles (8.43 g, 95%): white solid, m.p. 64-66 °C, R_f 0.77 (6:1 hexanes/EtOAc); 1H -NMR ($CDCl_3$, rt) δ 8.01 (s, 2H, Ar), 7.55-7.34 (m, 10H, Ph), 5.09 (s, 2H, $PhCH_2O$), 5.34 (s, 2H, $PhCH_2O$); ^{13}C -NMR ($CDCl_3$, rt), δ 163.9 (CO_2), 154.8 ($C^*(Ar)$), 135.7, 135.3, 130.3, 129.9, 128.7, 128.6, 128.5, 128.4, 128.3, 127.3, 67.4 (OCH_2Ph); HRMS (MALDI) m/z (%) for $C_{21}H_{17}Cl_2O_3$ (MH^+) calc. 387.0555, found 387.0555.

**4-(Benzyloxy)-3,5-dichlorobenzoic acid (6-9)**

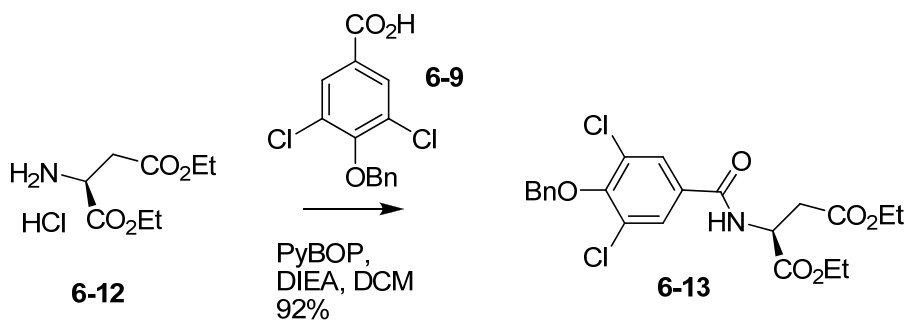
KOH (1.5 g, 27 mmol) was added to a stirred solution of **6-11** (2.3 g, 5.4mmol) in water (20 mL) and ethanol (80 mL). The mixture was refluxed for 1 h until it became homogeneous and then concentrated in vacuo. The residue was poured into water (100 mL) and washed with diethyl ether (2×50 mL). The organic phases were discarded, and the aqueous phase acidified with concentrated H_2SO_4 until the formation of a white solid in suspension. The mixture was extracted with diethyl ether (3×100 mL) and ethyl

acetate (2×100 mL). The combined organic layers were washed with a solution of 1.5% HCl (100 mL), dried (Na_2SO_4), filtered, and concentrated in vacuo to give 1.6 g (98%) of **6-9** as a white solid. white solid, m.p. 214-217 °C, R_f 0.61 (3:1 EA/EtOH); $^1\text{H-NMR}$ (DMSO, rt) δ 7.94 (s, 2H, Ar), 7.52-7.37 (m, 5H, Ph), 5.06 (s, 2H, PhCH_2O); $^{13}\text{C-NMR}$ (DMSO, rt) δ 164.8 (CO_2), 153.8 (CO_2), 135.7, 130.0, 129.1, 128.7, 128.6, 128.5, 74.9 (OCH_2Ph).



4-(Benzyloxy)-3,5-dichlorobenzoic acid (**6-9**)

To a solution of 4-hydroxyphthalic acid **6-10** (5.60 g, 27.5 mmol) in 1.7 mol/l aqueous NaOH (80 mL, 138 mmol) was added benzyl bromide (3.80 g, 30.0 mmol). The reaction mixture was stirred at 120 °C for 18 h. After the reaction mixture had cooled, 2.0 mol/L aqueous HCl was added to it until the product precipitated. The precipitate was collected by filtration and washed with toluene twice, affording **6-9** (6.0 g, 74%) as a white solid. This was used for the next reaction without purification.



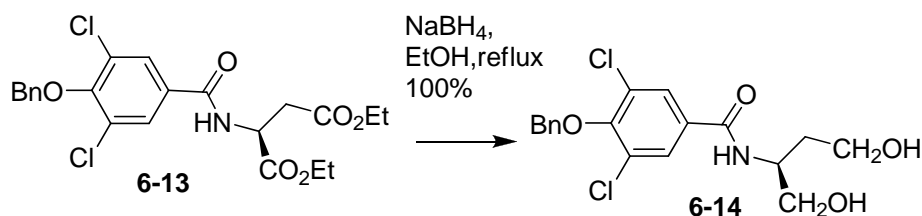
1,4-Diethyl (2S)-2-aminobutanedioate hydrochloride (6-12)

Prepared from aspartic acid according to procedure of Coward *et al.*⁸¹ in 95% yield without chromatographic separation. The spectral data matches to the reported values.

1,4-Diethyl (2S)-2-{{4-(benzyloxy)-3,5-dichlorophenyl}formamido}butanedioate (6-13)⁸²

To a solution of the aminodiester **6-12** in CH₂Cl₂ (35 mL) was added 4-benzyloxy-3,5 dichlorobenzoic acid (2.83g, 9.43 mmol), PyBOP reagent (4.9g, 9.4 mmol) and DIPEA(2.03 mL, 11.6 mmol) at 0 °C. The reaction mixture was stirred at room temperature under argon for 29 h, The residue is partitioned between water (60 mL) and DCM (60 mL). The aqueous layer is separated and extracted with DCM (2 × 60 mL). The combined organic layers are dried (magnesium sulfate) and concentrated on a rotary evaporator to give a residue. The chromatographic separation gives 156 mg (37%) of **6-2** as a slight yellow oil, along with 43 mg (5%) of **6-40** as a white solid. The residue was purified by column (developed with hexane/EtOAc = 12:1 to 5:1) to give 3g (94%) of **6-13** as a pale solid. White solid, yield: 92% yield, m.p. 79-81 °C; R_f 0.30 (4:1 hexanes/EtOAc); [α]_D²⁵ = + 33.8 (*c* 1.13, CHCl₃). ¹H-NMR (CDCl₃, rt) δ 7.77 (s, 2H, Ar), 7.57-7.33 (m, 5H, Ph), 7.19 (d, *J* = 7.7 Hz, NH), 5.10 (s, 2H, OCH₂Ph), 4.99 (dt, *J* = 8.1, 4.2 Hz, NHCH), 4.27 (qd, *J* = 6.9, 3.5 Hz, 2H, CHCO₂CH₂CH₃), 4.17 (qd, *J* = 7.3, 1.5 Hz, 2H, CH₂CO₂CH₂CH₃), 3.13 (dd, *J* = 17.3, 4.2 Hz, 1H, CH₂CH), 2.94 (dd, *J* = 17.3, 4.2 Hz, 1H, CH₂CH), 1.28 (q, *J* = 7.3 Hz, 6H, CH₂CH₃); ¹³C-NMR (CDCl₃, rt) δ 171.1 (CO₂), 170.4 (CO₂), 164.2 (CON), 153.8 (C*(Ar)), 130.9, 128.6, 128.5 (3), 127.9, 75.1

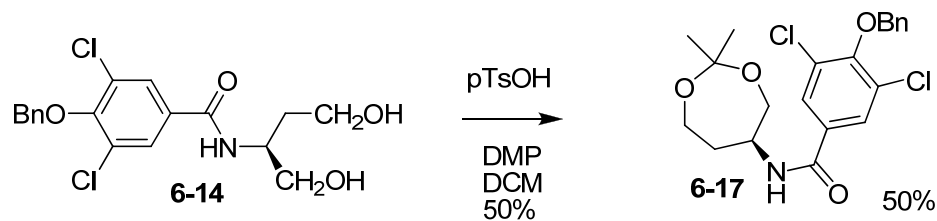
(OCH₂Ph), 62.1 (OCH₂), 61.2 (OCH₂), 49.1 (NCH), 36.1(CH₂), 14.1 (Me) HRMS (MALDI) *m/z* (%) for C₂₂H₂₄Cl₂NO₆ (MH⁺) calc. 468.0981, found 468.0947.



4-(Benzyloxy)-3,5-dichloro-N-[(2S)-1,4-dihydroxybutan-2-yl]benzamide (6-14)⁵³

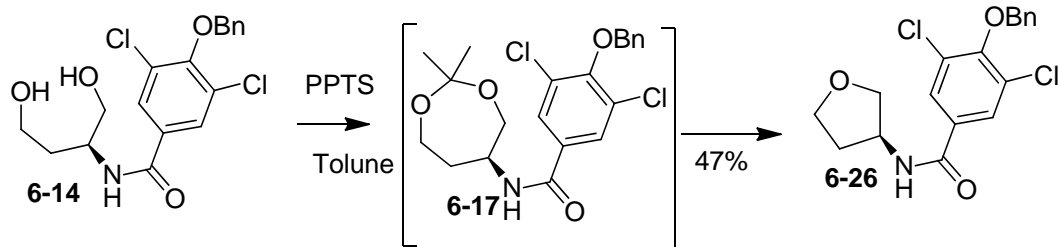
To a stirred mixture of **6-13** (17 g, 36 mol) in absolute EtOH (587 mL) at 0 °C was added sodium borohydride (13.6 g, 360 mol) in three portions. The cooling bath was removed when the reaction subsided, and the reaction mixture was heated slowly to reflux for 4 h at which point TLC analysis indicated complete consumption of the starting material. The reaction mixture was cooled to 25 °C, and the lumps that formed were broken up to give a slurry that was poured into brine (450 mL). The mixture was concentrated to give the white solid which was extraction by soxhlet with EtOAc for 2 days. The combined organic extracts were dried over MgSO₄, filtered, and concentrated to give **6-14** as a white solid (13.3g g, 100%), which can be crystallized with ethanol). White solid, yield: 100%; m.p. 144-146 °C; R_f 0.16 (1:7 hexanes/EtOAc);); [α]²⁵_D = -7.53 (*c* 0.93, DMSO). ¹H-NMR (DMSO, 90 °C) δ 8.13 (d, , *J* = 8.1 Hz, NH), 7.96 (s, 2H, Ar), 7.53-7.36 (m, 5H, Ph), 5.09 (s, 2H, OBn), 4.56 (br, OH), 4.26 (br, OH), 4.08-3.97 (m, 1H, NHCH), 3.53-3.38 (m, 4H, CH₂OH), 1.83-1.57 (m, 2H, CH₂); ¹³C-NMR ((DMSO, 70 °C) δ 163.0 (CO), 152.1 (C*(Ar)), 135.6(C*(Ar)), 132.1 (C*(Ar)), 128.3 (C*(Ar)), 128.2, 128.1, 128.0, 74.7 (OCH₂Ph), 63.0 (OCH₂), 58.9 (OCH₂), 49.4

(NHCH₂), 33.8 (CH₂); HRMS (MAUDI) *m/z* (%) for C₁₈H₂₀Cl₂NO₄ (M⁺) calc. 384.0764, found 384.0769.



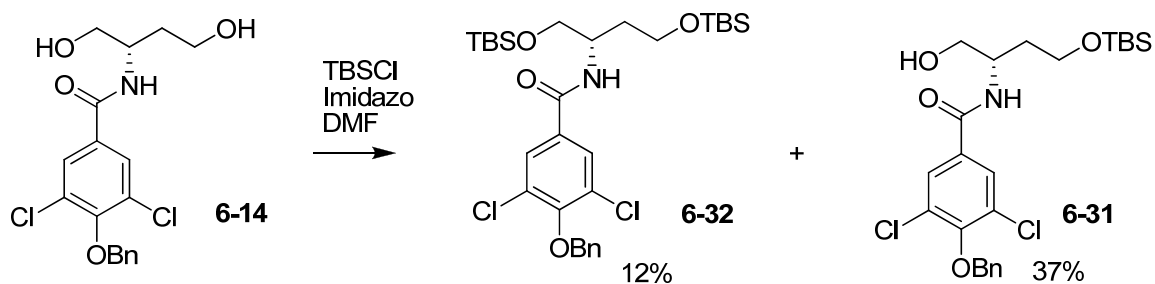
4-(Benzyloxy)-3,5-dichloro-N-[(5S)-2,2-dimethyl-1,3-dioxepan-5-yl]benzamide (**6-17**)

To 1,1-dimethoxypropane (8.7 mL, 0.0707 mol) and *p*-toluenesulfonic acid monohydrate (5.4mg, 2.76 mmol) were added to a stirred solution of the diol **6-14** (1.06 g, 2.76 mmol) in CH₂Cl₂ (319 mL) at 25 °C. The reaction was monitored by TLC (EtOAc/hexanes 2:1) until complete (90 h). The solution was poured into cold saturated aqueous NaHCO₃ (38 mL). The reaction mixture was extracted with EtOAc (5 × 20 mL) then washed with aqueous NaHCO₃ (5%, 2 × 25 mL) and brine (25 mL), dried (MgSO₄), and concentrated. Flash column chromatography of the residue yielded slight yellow solid (580 mg, 52%). m.p. 144-147 °C; R_f 0.19 (3:1 hexanes/EtOAc); [α]_D²⁵ = -5.38 (*c* 1.15, CHCl₃). ¹H-NMR (CDCl₃, rt) δ 7.73 (s, 2H, Ar), 7.56-7.34 (m, 5H, Ph), 6.61 (d, *J* = 7.7 Hz, NH), 5.09 (s, 2H, OCH₂Ph), 4.30-4.21 (m, NHCH), 3.96 (dd, *J* = 12.2, 1.2 Hz, 1H, CHCH₂O), 3.76 (dt, *J* = 12.2, 6.1 Hz 1H, OCH₂CH₂), 3.63 (dd, *J* = 12.3, 3.6 Hz, 1H, CHCH₂O), 1.90-1.85 (m, 2H, CH₂CH₂O), 1.40 (s, CH₃), 1.38 (s, CH₃); ¹³C-NMR (CDCl₃, rt) δ 164.1 (CO), 153.7 (C*(Ar)), 136.0, 132.1, 130.3, 128.8 (2), 128.7, 127.9, 101.9 (OCO), 75.4 (OCH₂Ph), 63.7 (OCH₂) 58.2 (OCH₂), 48.6 (NHCH), 35.3 (CH₂), 25.1 (CH₃), 24.9 (CH₃); HRMS (MALDI) *m/z* (%) for C₂₁H₂₄Cl₂NO₄ (MH⁺) calc. 424.1082, found 384.0837 (-Me₂C, -H₂O, calc. 384.0764).



4-(Benzyloxy)-3,5-dichloro-N-[(3S)-oxolan-3-yl]benzamide (6-26)

2-Methoxypropene (0.31 mL, 3.19 mmol) was added to a stirred solution of **6-14** (122.5 mg, 0.319 mmol) in dry toluene (7 mL) under Ar. Pyridinium p-toluenesulfonate (PPTS) (3 mg) was added to the mixture, which was refluxed under Ar. TLC (3:1 hexanes/EtOAc) indicated that **6-17** was formed, after refluxing overnight. The reaction mixture was quenched with aqueous NaHCO₃ and the aqueous phase was extracted with Et₂O (3 × 10). The combined organic layers were dried over anhydrous MgSO₄ and filtered. The filtrate was concentrated under reduced pressure. The crude residue was purified by flash column chromatography to give **6-26** (55 mg, 47%). Decomposed at 250 °C. ¹H-NMR (CDCl₃, rt) δ 7.73 (s, 2H, Ar), 7.55-7.36(m, 5H, Ph), 6.56 (d, *J* = 7.3 Hz, NH), 4.73-4.65 (m, 1H, NHCH), 4.00 (q, *J* = 7.8 Hz, 1H, OCH₂CH), 3.86 (dt, *J* = 5.0, 9.6 Hz, 2H, OCH₂CH), 3.80 (td, *J* = 8.9, 2.7 Hz, OCH₂CH), 2.42-2.30 (m, 1H, OCH₂CH₂), 1.98-1.88 (m, 1H, OCH₂CH₂); ¹³C-NMR (CDCl₃, rt) δ 164.7 (CO), 153.8 (C*(Ar)), 136.0, 131.6, 130.3, 128.9, 128.8, 128.7, 128.0, 75.4 (OCH₂Ph), 73.5 (OCH₂), 67.1(OCH₂), 51.4 (NCH), 33.4 (CH₂); HRMS (MALDI) *m/z* (%) for C₁₈H₁₈Cl₂NO₃ (MH⁺) calc. 366.0664, found 366.0562.

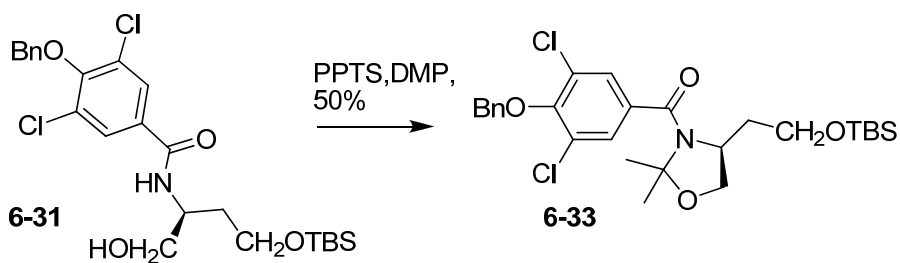


4-(Benzyloxy)-N-[(2S)-4-[(tert-butyldimethylsilyl)oxy]-1-hydroxybutan-2-yl]-3,5-dichlorobenzamide (6-31)

To a solution of **6-14** (217mg, 0.568 mmol) in DMF (3 mL) was added TBDMS-Cl (95mg, 0.626 mmol) and then imidazole (86 mg, 1.26 mmol) at 0 °C. After 2 h at 0 °C saturated NH_4Cl and EtOAc were added. The aqueous layer was extracted with EtOAc (3 × 30 mL). The organic layer was dried (MgSO_4) and evaporated and the residue purified by flash chromatography (Hexanes-EtOAc 9:1) to give **6-31** (42 mg, 12.4%), followed by **6-32** (102 mg, 36.4%). **6-31**, slight yellow oil, R_f 0.58 (1:1 hexanes/EtOAc); $[\alpha]_D^{25} = -4.63$ (c 0.475, CHCl_3). $^1\text{H-NMR}$ (DMSO, 90 °C) δ 8.04 (d, $J = 8.1$ Hz, NH), 7.92 (s, 2 H, Ar), 7.52-7.35 (m, 5H, Ph), 5.10 (s, 2H, OCH_2Ph), 4.10-3.99 (m, NHCH), 3.65 (t, $J = 6.5$ Hz, CH_2OTBS); 3.51-3.42(m, 2H, CH_2OH), 1.89-1.62 (m, 2H, $\text{TBSOCH}_2\text{CH}_2$), 0.84 (s, 9H, ^tBu), 0.00 (s, 6H, Me); $^{13}\text{C-NMR}$ (DMSO, 90 °C) δ 162.8 (CO), 152.0 ($\text{C}^*(\text{Ar})$) 135.5 ($\text{C}^*(\text{Ar})$), 132.2 ($\text{C}^*(\text{Ar})$), 128.2 ($\text{C}^*(\text{Ar})$), 128.1 ($\text{CH}(\text{Ar})$), 128.0 ($\text{CH}(\text{Ar})$), 127.9 ($\text{CH}(\text{Ar})$), 127.8($\text{CH}(\text{Ar})$), 74.6 (OBn), 64.3 (OCH_2 , minor), 62.9 (OCH_2 , major), 59.7 (OCH_2 , major), 57.7 (OCH_2 , minor), 49.0 (NCH), 33.6 (CH_2 , major), 33.4 (CH_2 , major), 25.4 (^tBu), 25.3 (^tBu , minor), 17.5 (Me); HRMS (MALDI) m/z (%) for $\text{C}_{24}\text{H}_{34}\text{Cl}_2\text{NO}_4\text{Si}^+$ (MH^+) calc. 498.1634, found 498.1683.

4-(Benzyloxy)-3,5-dichloro-N-[(6S)-2,2,3,3,10,10,11,11-octamethyl-4,9-dioxa-3,10-disiladodecan-6-yl]benzamide (6-32)

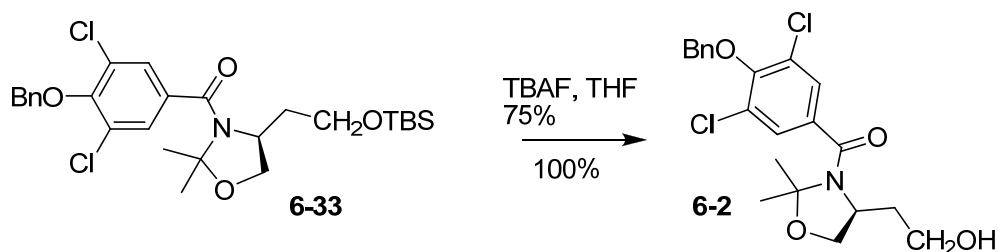
Slightly yellow oil (42 mg, 12.4%). R_f 0.34 (15:1 hexanes/EtOAc); $[\alpha]_D^{25} = -8.81$ (c 0.635, CHCl_3). $^1\text{H-NMR}$ (CDCl_3 , rt) δ 7.69 (s, 2H, Ar), 7.56-7.36 (m, 5H, Ph), 7.00 (d, $J = 7.3$ Hz, NH), 5.08 (s, 2H, OCH_2Ph), 4.30-4.18 (m, NHCH), 3.91 (td, $J = 5.7, 10.2$ Hz, 1H, $\text{CH}_2\text{CH}_2\text{O}$), 3.82-3.673 (m, 2H, CHCH_2O , $\text{CH}_2\text{CH}_2\text{O}$), 3.67 (dd, $J = 6.1, 10.0$ Hz, 1H, CHCH_2O), 1.92 (q, $J = 5.6$ Hz, 2H, OCH_2CH_2), 0.90 (s, 9H, ^tBu), 0.88 (s, 9H, ^tBu), 0.08 (s, Me), 0.079 (s, Me), 0.06 (s, 6H, Me); $^{13}\text{C-NMR}$ (CDCl_3 , rt) δ 164.4 (CO), 153.5 ($\text{C}^*(\text{Ar})$), 136.1 ($\text{C}^*(\text{Ar})$), 132.5 ($\text{C}^*(\text{Ar})$), 130.2 ($\text{C}^*(\text{Ar})$), 128.8 ($\text{CH}(\text{Ar})$), 128.7 ($\text{CH}(\text{Ar})$), 127.9 ($\text{CH}(\text{Ar})$), 75.3 (OCH_2Ph), 63.5 (CH_2O), 61.1 (CH_2O), 50.5 (NCH), 32.9 (CH_2), 26.1 (^tBu), 26.0 (^tBu), 18.6 (CH_3), 18.4 (CH_3); HRMS (MALDI) m/z (%) for $\text{C}_{30}\text{H}_{48}\text{Cl}_2\text{NO}_4\text{Si}_2^+$ (MH^+) calc. 612.2499, found 612.2450.



(4S)-3-{{4-(Benzyloxy)-3,5-dichlorophenyl}carbonyl}-4-{2-[(tert-butyldimethylsilyl)oxy]ethyl}-2,2-dimethyl-1,3-oxazolidine (6-33)

2-Methoxypropene (0.3 mL, 2.78 mmol) was added to a stirred solution of **6-31** (69.3 mg, 0.1395 mmol) in dry toluene (3 mL) under Ar. Pyridinium p-toluenesulfonate (PPTS) (1.3 mg) was added to the mixture, which was stirred at rt for 22 h under Ar. The reaction mixture was quenched with aqueous NaHCO_3 and the aqueous phase was

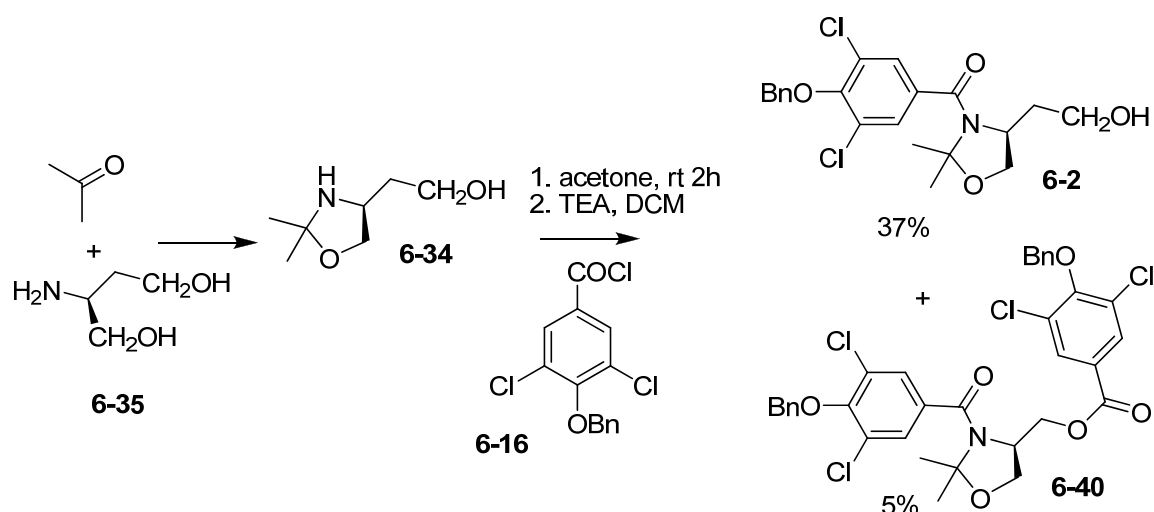
extracted with EtOAc. The combined organic layers were dried over anhydrous MgSO_4 and filtered. The filtrate was concentrated under reduced pressure. The crude residue was purified by flash column chromatography (12:1 hexanes: EtOAc) to give **6-33** as a slight yellow oil (37 mg, 50%): R_f 0.58 (4:1 hexanes/EtOAc); $[\alpha]_D^{25} = +30.7$ (c 1.08, CHCl_3). $^1\text{H-NMR}$ (DMSO, 90 °C) δ 7.69 (s, 2H, Ar), 7.62-7.45 (m, 5H, Ph), 5.17 (s, 2H, OCH_2Ph), 4.18-4.11 (m, 2H, OCH_2CHNH), 3.97-3.92 (m, 1H, OCH_2CHN), 3.58-3.45 (m, 2H, TBSOCH_2), 1.79-1.51 (m, 2H, $\text{CH}_2\text{CH}_2\text{OTBS}$), 1.72 (s, Me), 1.65 (s, Me), 0.87 (s, 9H, ^tBu), 0.02 (s, Me), 0.00 (s, Me); $^{13}\text{C-NMR}$ (DMSO, 90 °C) δ 163.4 (NCO), 150.8 ($\text{C}^*(\text{Ar})$), 135.6, 135.3, 128.5, 128.0, 127.9, 126.8, 94.1 (OC^*N), 74.4 (OBn), 66.3 (OCH_2), 59.2 (OCH_2), 55.7 (NCH), 36.1 (CH_2), 26.1 (Me), 25.3 (^tBu), 23.1 (Me), 17.3 (Me) HRMS (MALDI) m/z (%) for $\text{C}_{27}\text{H}_{38}\text{Cl}_2\text{NO}_4\text{Si}$ (MH^+) calc. 538.1947, found 538.1877.



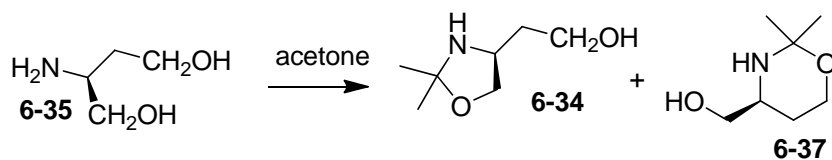
2-[(4S)-3-[[4-(Benzyloxy)-3,5-dichlorophenyl]carbonyl]-2,2-dimethyl-1,3-oxazolidin-4-yl]ethanol (6-2)

TBAF (0.123 mL, 1M in THF) was added to a solution of **6-33** (32 mg, 0.0614 mmol) in THF (3 mL) at 0 °C. The reaction mixture was left to warm gradually to RT over 12h. The reaction mixture was then concentrated, dissolved in DCM and the residue was purified by flash chromatography on silica gel (1: 2 Hexane/EtOAc) to provide **6-2** as slight yellow oil (26 mg, 100%). **6-2**, Oil, R_f 0.46 (1:1 hexanes/EtOAc); $[\alpha]_D^{25} = +46.3$

(*c* 0.95, CHCl₃). ¹H-NMR (DMSO, 90 °C) δ 7.58 (s, 2H, Ar), 7.52-7.35 (m, 5H, Ph), 5.09 (s, 2H, OCH₂Ph), 4.14 (t, *J* = 5.0 Hz, 1H, CH₂OH), 4.07-4.02 (m, 2H, OCH₂CHNH), 3.87-3.82 (m, 1H, OCH₂CHNH), 3.28-3.17 (m, 2H, CH₂OH), 1.65-1.50 (m, 1H, CH₂CH₂OH), 1.62 (s, Me), 1.54 (s, Me), 1.49-1.37 (m, 1H, CH₂CH₂OH) ¹³C-NMR (DMSO, 90 °C) δ 163.4 (NCO), 150.7 (C*(Ar)), 135.6 (C*(Ar)), 135.2 (C*(Ar)), 128.4 (C*(Ar)), 128.1 (CH(Ar)), 128.0 (CH(Ar)), 127.9 (CH(Ar)), 126.9 (CH(Ar)), 94.0 (NC*O), 74.5 (OBn), 66.9 (OCH₂), 57.4 (OCH₂), 56.1 (NCH), 36.5 (CH₂), 26.1 (Me), 23.3 (Me); HRMS (MALDI) *m/z* (%) for C₂₁H₂₄Cl₂NO₄ (MH⁺) calc. 424.1083, found 424.1079.



(2S)-2-Aminobutane-1,4-diol (6-35) was prepared from (S)-2-aminosuccinic acid according to procedure of Coward *et al.*⁸³ in 59% yield without chromatographic separation. The spectral data matches to the reported values.



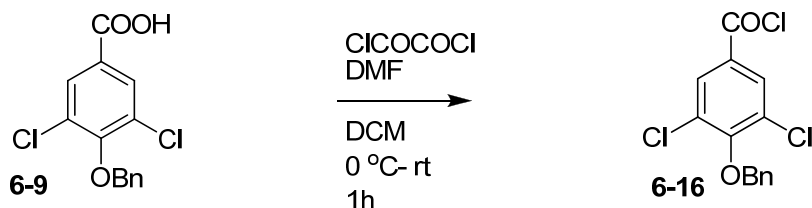
2-[(4S)-2,2-Dimethyl-1,3-oxazolidin-4-yl]ethanol (6-34)

Method 1— (acetone served as solvent)

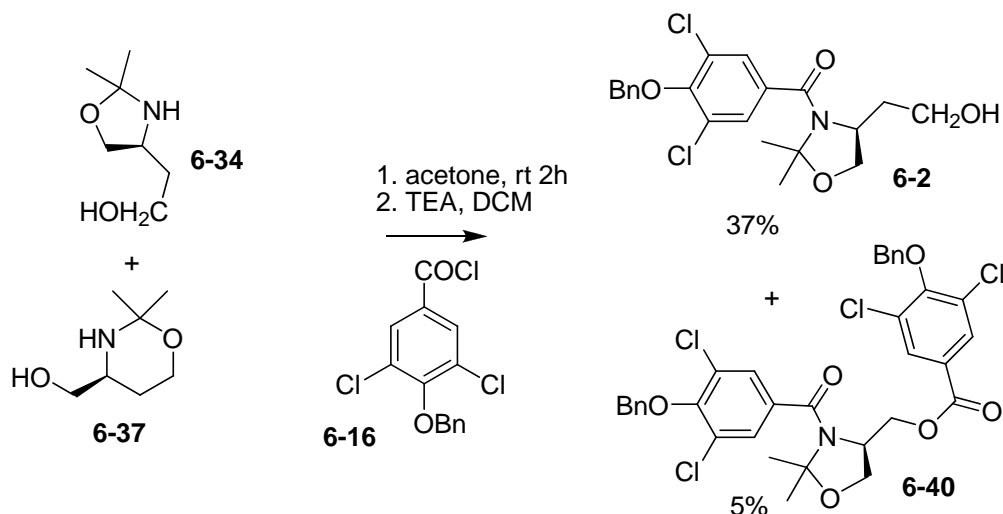
To amino diol **6-35** (121mg, 1 mmol) was added acetone (2 mL) (distilled under KMnO_4). The homogeneous solution was stirred for 2 h at room temperature. Azeotropic removal of water in benzene in the presence of acetone gives the yellow residue (oxazolidine alcohol **6-34**). The crude products were used in the next step without purification due to their chromatographic instability.

Method 2— (toluene as solvent)

To amino diol **6-35** (121mg, 1 mmol) solution in toluene (10 mL) was added acetone (2 mL) (distilled under KMnO_4). The homogeneous solution was stirred for 0.5 h at room temperature, and heated to reflux under argon with azeotropic removal of water for 48 hr. The reaction mixture is cooled, concentrated on a rotary evaporator to give the brown residue. (oxazolidine alcohol **6-34**). The crude products were used in the next step without purification due to their chromatographic instability.

**4-(Benzyloxy)-3,5-dichlorobenzoyl chloride (6-16)**

To the heterogeneous solution of acid **6-9** (325 mg, 1.1 moles) in DCM (10 mL) at 0 °C, is added oxalyl chloride (150 mg, 1.2 mmol) dropwise and anhydrous DMF (cat. about 1 drop), With stirring at 0 °C for 30 min, and at rt for 1h, concentrated on a rotary evaporator to give a pale solid (**6-16**).



2-[(4S)-3-{4-(Benzyloxy)-3,5-dichlorophenyl}carbonyl]-2,2-dimethyl-1,3-oxazolidin-4-yl]ethanol (6-2)

Method 1.

To the solution of crude oxazolidinone **6-34** and Et₃N (0.16 mL, 1.2 mmol) in DCM (20 mL) at 0 °C, was slowly added acyl chloride **6-16** (1.1 mmol).

The reaction mixture was then allowed to stir at 0 °C for 45 min. and at rt for 1h. The mixture was then washed with saturated aq. NaHCO₃ (20 mL). The residue is partitioned between water (40 mL) and DCM (40 mL). The aqueous layer is separated and extracted with DCM (2 × 40 mL). The combined organic layers are dried (magnesium sulfate) and concentrated on a rotary evaporator to give a residue. The chromatographic separation gives 156 mg (37%) of **6-2** as a slightly yellow oil, along with 43 mg (5%) of **6-40** as a white solid.

Method 2.

To the solution of acyl chloride **6-16** and Et₃N (0.16 mL, 1.2 mmol) in DCM (20 mL) at 0 °C, was slowly added freshly prepared crude oxazolidinone **6-34**. The reaction

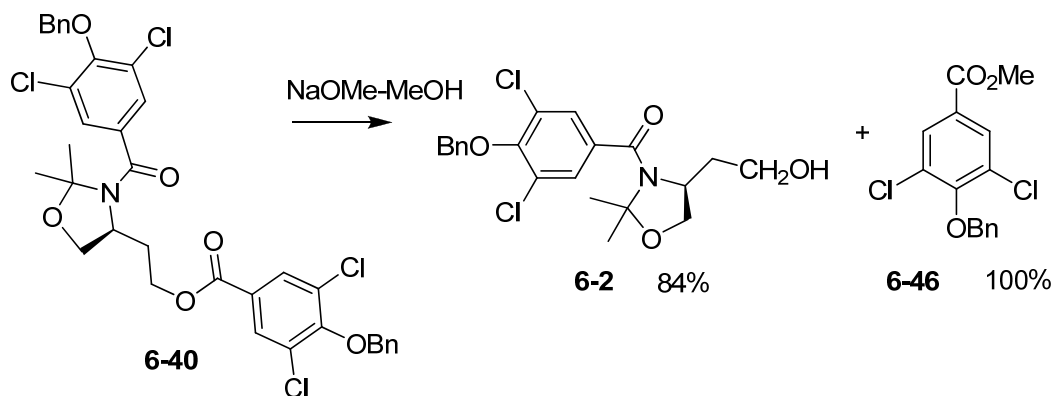
mixture was then allowed to stir at 0 °C for 45 min. and at rt for 1h. The mixture was then washed with saturated aq. NaHCO₃ (20 mL). The residue is partitioned between water (40 mL) and DCM (40 mL). The aqueous layer is separated and extracted with DCM (2 × 40 mL). The combined organic layers are dried (magnesium sulfate) and concentrated on a rotary evaporator to give a residue. The chromatographic separation gives 127 mg (30%) of **6-2** as a slight yellow oil, along with 137 mg (20%) of **6-40** as a white solid.

Alternatively: Crude oxazolidine (**6-34**) in one portion, was slowly added (4.35 mmol). The reaction mixture was then allowed to stir at 0 °C for 45 min. and at rt for 1h. The mixture was then washed with saturated aq. NaHCO₃ (20 mL). The residue is partitioned between water (40 mL) and DCM (40 mL). The aqueous layer is separated and extracted with DCM (2 × 40 mL). The combined organic layers are dried (magnesium sulfate) and concentrated on a rotary evaporator to give a residue. The chromatographic separation gives 156 mg (37%) of **6-2** as a slight yellow oil, along with 43 mg (5%) of **6-40** as a white solid.

[(4R)-3-{[4-(benzyloxy)-3,5-dichlorophenyl]carbonyl}-2,2-dimethyl-1,3-oxazolidin-4-yl]methyl 4-(benzyloxy)-3,5-dichlorobenzoate (6-40**)**

White solid, yield: 5% yield, m.p. 145-148 °C; R_f 0.48 (3:1 hexanes/EtOAc); [α]_D²⁵ = +3.96 (c 0.97, CHCl₃). ¹H-NMR (DMSO, 90 °C) δ 7.78 (s, 2H, Ar), 7.55 (s, 2H, Ar), 7.46-7.29 (m, 10H, Ph), 4.99 (d, *J* = 10.8 Hz, 1H, PhCH₂O), 4.94 (d, *J* = 10.8 Hz, 1H, PhCH₂O), 4.88 (s, 2H, OCH₂Ph), 4.22-4.05 (m, 2H, CHNHCH₂CH₂OCOAr), 4.17 (d, *J* = 7.3 Hz, 1H, OCH₂CHNH), 3.92 (d, *J* = 7.7 Hz, 1H, OCH₂CHNH), 1.92-1.76 (m, 2H, CH₂CH₂O), 1.65 (s, Me), 1.56 (s, Me); ¹³C-NMR (DMSO, 90 °C) δ 163.6 (NCO), 162.5

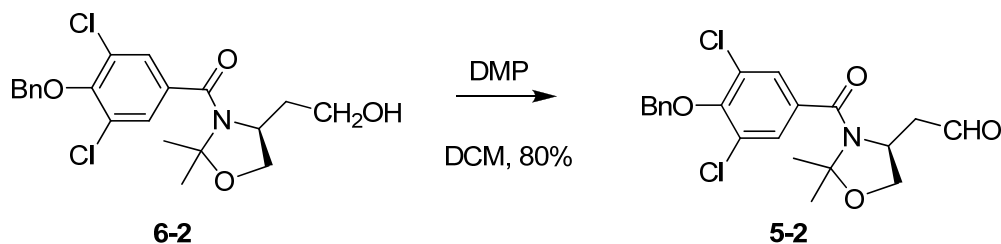
(NCO), 154.0 (C*(Ar)), 150.7 (C*(Ar)), 135.5 (C*(Ar)), 135.4 (C*(Ar)), 134.9 (C*(Ar)), 129.3 (CH(Ar)), 128.9 (C*(Ar)), 128.5 (C*(Ar)), 128.0 (CH(Ar)), 127.9 (CH(Ar)), 127.8 (CH(Ar)), 126.9 (CH(Ar)), 126.5 (C*(Ar)), 94.4 (OC*N), 74.5 (OBn), 74.3 (OBn), 66.6 (OCH₂), 61.8 (OCH₂), 55.2 (NCH) 32.5 9 (CH₂), 26.4 (Me), 23.1 (Me); HRMS (MALDI) *m/z* (%) for C₃₅H₃₂Cl₄NO₆ (MH⁺) calc. 702.0984, found 702.0908.



Methyl 4-(benzyloxy)-3,5-dichlorobenzoate (6-46)

To a solution of **6-40** (132 mg, 0.192 mmol) in dry MeOH (2 mL) is added sodium methoxide (NaOMe) (20.7 mg, 0.384 mmol) methanol (prepared by the addition of 9 mg of sodium to 0.5 mL of methanol). The solution is stirred for 20 mins and provided a homogeneous solution. Sat. ammonium chloride (NH₄Cl, sat.) was added to the solution until the pH reached 8. Remove MeOH on a rotary evaporator to afford a white solid. The residue is partitioned between water (buffer Ph=7, 20 mL) and DCM (20 mL). The aqueous layer is separated and extracted with DCM (2 × 20 mL). The combined organic layers are dried (magnesium sulfate) and concentrated on a rotary evaporator to give a pale solid. The chromatographic separation gives 68 mg (84%) of **6-2** as a slight yellow oil, along with 59 mg (100%) of methyl ester **6-46** as a slight yellow solid. methyl ester white solid, m.p. 102-104 °C, R_f 0.92 (6:1 hexanes/EtOAc); ¹H-NMR (CDCl₃, rt) δ 7.99

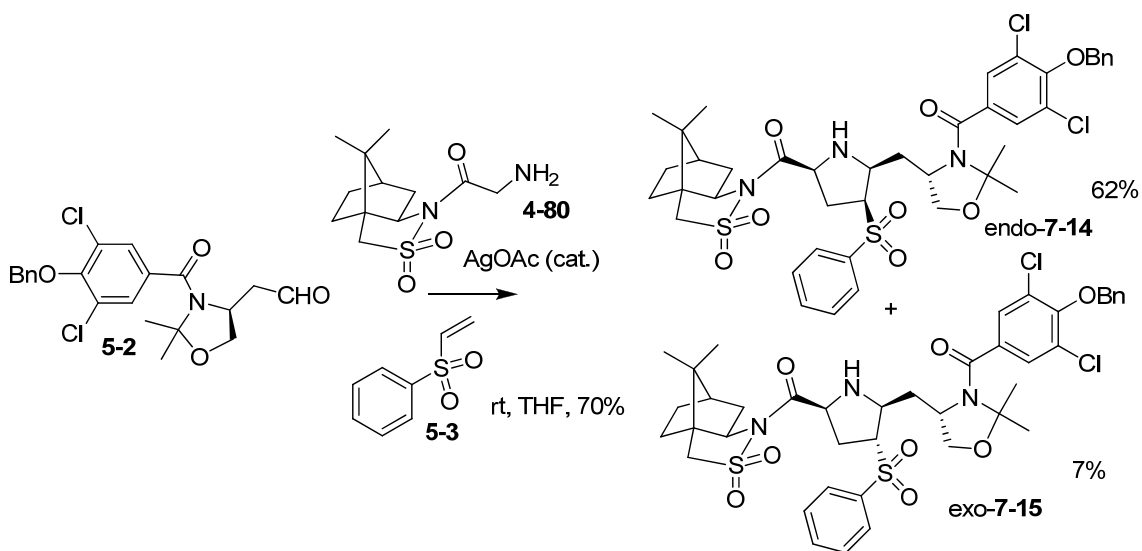
(s, 2H, Ar), 7.66-7.34 (m, 5H, Ph), 5.10 (s, 2H, PhCH₂O), 3.91 (s, OMe); ¹³C-NMR (CDCl₃, rt), δ 164.6 (CO) 154.8 (C*(Ar)), 135.7, 130.2, 129.9, 128.6, 128.5, (2), 127.3, 75.1 (OCH₂Ph), 52.6 (OMe).



2-[(4S)-3-{4-(Benzyloxy)-3,5-dichlorophenyl}carbonyl]-2,2-dimethyl-1,3-oxazolidin-4-yl]acetaldehyde (5-2)

To a solution of **6-2** (28 mg, 0.0658 mmol) in DCM (0.5 mL) at rt was added Dess-Martin periodinane (DMP) (31mg 0.0732mmol). The reaction mixture was allowed to stir at the same temperature for 1 h. TLC indicated no starting material remained. Then a 1N solution of Na₂S₂O₃ in sat. aq NaHCO₃ (15 mL) was added. The aqueous phase extracted with DCM (2 × 15 mL). The combined DCM layer was washed with water (3 × 40) and dried over MgSO₄ and concentrated. The residue was purified by flash chromatography on silica gel (1:1 Hexane/EtOAc) yielded slight yellow soft solid. (22.4 mg, 80%); R_f 0.36 (5:2 hexanes/EtOAc); [α]_D²⁵ = +18.73 (c 0.74, CHCl₃). ¹H-NMR (DMSO, 70 °C) δ 9.45 (s, br, CHO), 7.63 (s, 2H, Ar), 7.53-7.37 (m, 5H, Ph), 5.10 (s, 2H, OCH₂Ph), 4.43-4.33 (m, COCH), 4.16 (dd, *J* = 5.4, 8.9 Hz, 1H, OCH₂CHN), 3.76 (dd, *J* = 1.9, 8.9 Hz, 1H, OCH₂CHN), 2.71 (ddd, *J* = 1.4, 8.8, 17.4 Hz, 1H, CH₂CHO), 2.55-2.48 (m, 1H, CH₂CHO), 1.60 (s, Me), 1.53 (s, Me); ¹³C-NMR (DMSO, 70 °C) δ 200.4 (CHO), 163.6 (NCO), 150.8 (C*(Ar)), 135.6 (C*(Ar)), 134.9 (C*(Ar)), 128.7 (C*(Ar)), 128.2 (CH(Ar)), 128.1 (CH(Ar)), 128.0 (CH(Ar)), 127.0 (CH(Ar)), 94.4 (OC*N), 74.6 (OCH₂),

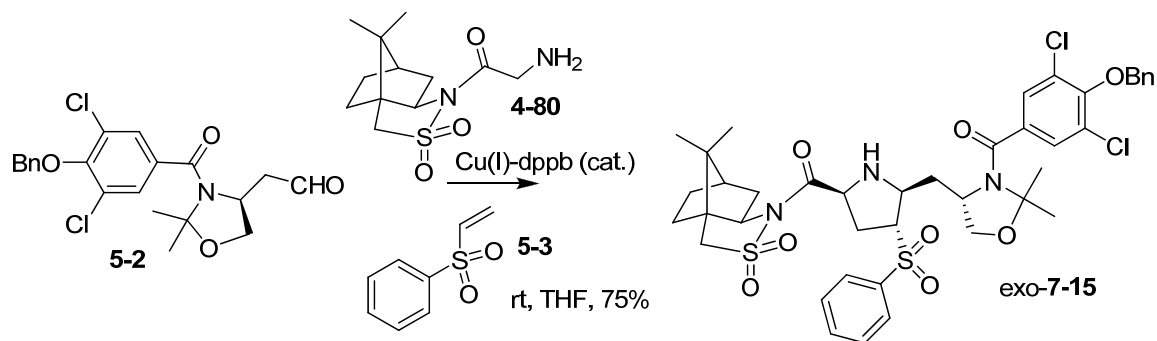
67.4 (OCH₂), 52.9 (NCH), 47.1 (CH₂), 26.1 (Me), 23.4 (Me); HRMS (MALDI) *m/z* (%) for C₂₁H₂₂Cl₂NO₄ (MH⁺) calc. 422.0926, found 422.0948.



4-{{(2*S*,4*S*,5*S*)-5-{{(4*S*)-3-{{[4-(Benzyloxy)-3,5-dichlorophenyl]carbonyl}-2,2-dimethyl-1,3-oxazolidin-4-yl]methyl}-4-(benzenesulfonyl)pyrrolidin-2-yl]carbonyl}-10,10-dimethyl-3λ⁶-thia-4-azatricyclo[5.2.1.0^{1,5}]decane-3,3-dione endo-(7-14)

To a stirred mixture of glycyl sultam (390 mg, 1.4 mmol, 1.1 equiv) and AgOAc (18.4mg, 10 mol %) in dry THF (7 mL) was added aldehyde (466 mg, 1.104 mmol) followed by phenyl vinyl sulfone(556 mg, 3.0 eq) at room temperature for 5.5h. The mixture was partitioned between sat'd aq NH₄Cl (17 mL) and DCM (4 × 25 mL). The combined organic layers were dried over Na₂SO₄, filtered and concentrated under reduced pressure. The crude cycloadducts were purified by flash chromatography. The chromatographic separation of this residue yielded white solid, **7-14** (523 mg, 62%) along with **exo-7-15** (57 mg, 6.86%). m.p. soften at 104 °C, liquidity (108-144 °C) R_f 0.33 (1:1 hexanes/EtOAc); [α]_D²⁵ = -1.72 (c 1.28, CHCl₃). ¹H-NMR (DMSO, 80 °C) δ 7.76-7.60 (m, 5H, PhSO₂), 7.51-7.35 (m, 5H, PhCH₂O), 7.46 (s, 2H, Ar), 5.05 (s, 2H,

PhCH₂O), 4.07-3.99 (m, 4H, CHCO, NCHCH₂O), 3.82 (t, *J* = 7.3 Hz, SO₂NHCH), 3.82-3.76 (m, 1H, CHCHSO₂Ph), 3.74 (d, *J* = 14.2 Hz, 1H, SO₂CH₂), 3.60 (d, *J* = 14.2 Hz, 1H, SO₂CH₂), 3.07-2.92 (m, 1H, CHSO₂Ph), 2.57 (t, *J* = 10.7 Hz, 1H, SO₂CHCH₂), 2.25 (dt, *J* = 8.4, 13.5 Hz, 1H, CH₂CHCH₂O), 1.99-1.79 (m, 7H, CH₂CHSO₂Ph, CH₂CHCH₂O, 5H in sultam), 1.60 (s, Me), 1.52 (s, Me), 1.46-1.23 (m, 2H, sultam), 0.93 (s, Me), 0.90 (s, Me); ¹³C-NMR (DMSO, 90 °C) δ 170.5 (NCO), 163.8 (NCO), 150.9 (C*(Ar)), 139.6 (C*(Ar)), 135.7 (C*(Ar)), 134.9 (C*(Ar)), 133.4 (CH(Ar)), 129.1 (CH(Ar)), 128.5 (C*(Ar)), 127.9 (CH(Ar)), 127.1 (C*(Ar)), 126.9 (C*(Ar)), 93.9 (NC*O), 74.5 (OBn), 67.8 (OCH₂), 64.9 (NCH), 64.0 (NCH), 58.5 (NCH), 58.6 (NCH), 57.8 (CHSO₂), 51.9 (CH₂SO₂Ph), 48.2 (C*), 46.9 (C*), 43.9 (CH), 37.3 (CH₂), 35.0 (CH₂), 32.8 (CH₂), 31.5 (CH₂), 26.1 (Me), 25.4 (CH₂), 23.4 (Me), 20.0 (Me), 19.2 (Me)
 HRMS (MALDI) *m/z* (%) for C₄₁H₄₈Cl₂N₃O₈S₂ (MH⁺) calc. 844.2260, found 844.2287.

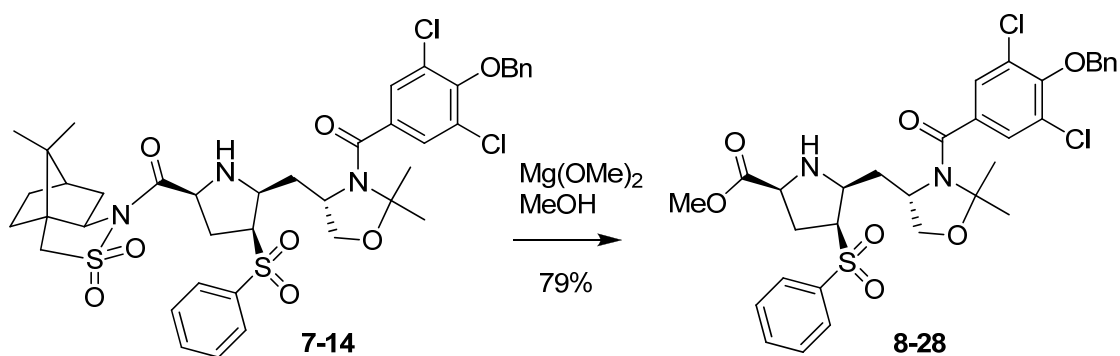


4-[[[(2*S*,4*R*,5*S*)-5-[[[(4*S*)-3-[[4-(Benzyloxy)-3,5-dichlorophenyl]carbonyl]-2,2-dimethyl-1,3-oxazolidin-4-yl]methyl]-4-(benzenesulfonyl)pyrrolidin-2-yl]carbonyl]-10,10-dimethyl-3λ⁶-thia-4-azatricyclo[5.2.1.0^{1,5}]decane-3,3-dione *exo*-(7-15)

CuClO₄ (5%) and dppb (5%) in DMSO (2.0 mL) was stirred at rt for 1h. To the DMSO solution was added aldehyde **5-2** (91 mg, 0.217 mmol) followed by glycyl sultam **4-80** (76 mg, 1.3 equiv) and dipolarophile **5-3** (109 mg, 3.0 equiv) at room temperature.

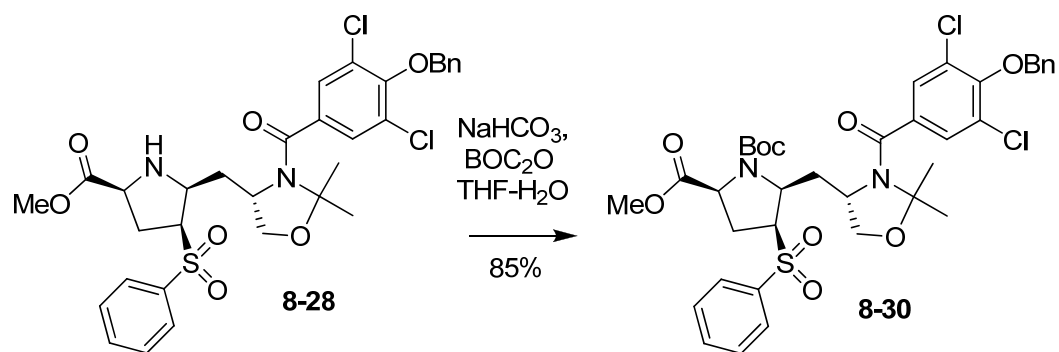
Chapter 11: Experimental

The mixture was stirred for 5h at rt. the mixture was partitioned between sat'd aq NH₄Cl (10 mL) and DCM (5 × 30mL). The combined organic layers were washed with water (2 × 60 mL) and brine (60 mL), dried over MgSO₄, filtered and concentrated under reduced pressure. The crude cycloadducts were purified by flash chromatography. Column chromatography of this residue yielded white solid (137 mg, 75%) m.p. soften at 110 °C, liquidity (120-162 °C) R_f 0.27 (1:1 hexanes/EtOAc); [α]_D²⁵ = -0.084 (c 1.48, CHCl₃). ¹H-NMR (DMSO, 90 °C) δ 7.77-7.35 (m, 10H, Ph), 7.58 (s, 2H, Ar), 5.00 (s, 2H, PhCH₂O), 4.06 (t, *J* = 8.5 Hz, 1H, CHCO), 4.03-3.90 (m, OCH₂NCH), 3.99 (d, *J* = 7.6 Hz, 1H, OCH₂), 3.91 (d, *J* = 7.0 Hz, 1H, OCH₂), 3.78 (t, *J* = 6.2 Hz, SO₂NCH), 3.74 (d, *J* = 14.1 Hz, 1H, CH₂SO₂), 3.58 (d, *J* = 14.1 Hz, 1H, CH₂SO₂), 3.22-3.07 (m, 2H, SO₂CHCH), 2.56 (t, *J* = 9.1 Hz, 2H, CH₂CHSO₂), 2.32 (ddd, *J* = 4.4, 8.0, 13.5 Hz, 1H, CH₂CHNCH₂O), 1.87-1.68 (m, 7H, CH₂CHSO₂, CH₂CHNCH₂O, 5H in sultam group), 1.60 (s, Me), 1.52 (s, Me), 1.43-1.20 (m, 2H in sultam group); 0.92 (s, Me), 0.90 (s, Me); ¹³C-NMR (DMSO, 90 °C) δ 170.7 (CO₂Me), 163.5 (NCO), 151.0 (C*(Ar)), 137.5, 135.7, 135.1, 133.7, 129.2, 128.6, 127.9, 127.8, 127.7, 126.9, 94.1 (OC*N), 74.5 (OBn), 67.5, 67.2, 63.9, 59.2, 56.7, 56.5, 51.9, 48.2, 46.9, 43.9, 37.3, 32.7, 31.2, 26.1 (Me), 25.4 (CH₂), 23.2 (Me), 19.9 (Me), 19.0 (Me); HRMS (MALDI) *m/z* (%) for C₄₁H₄₈Cl₂N₃O₈S₂ (MH⁺) calc. 844.2260, found 786.1851 (M-58).



Methyl (2*S*,4*S*,5*S*)-4-(benzenesulfonyl)-5-[[*(4S)*-3-[[4-(benzyloxy)-3,5-dichlorophenyl]carbonyl]-2,2-dimethyl-1,3-oxazolidin-4-yl]methyl]pyrrolidine-2-carboxylate (8-28)

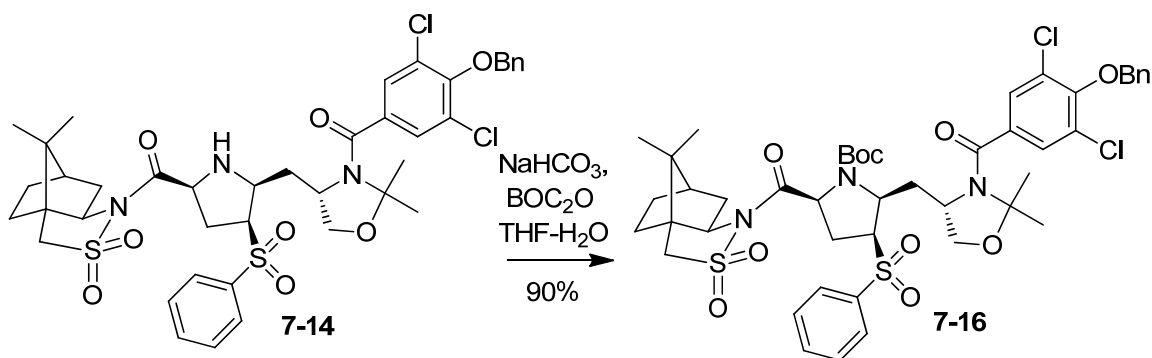
The mixture of Mg (780 mg) in MeOH was refluxed for 3h. To the solution of Mg(OMe)₂, was added 7-14 (3.96 g, 4.695 mmol) at 0 °C. The mixture was stirred for 8h from 0 °C to rt. Evaporated MeOH, the mixture was partitioned between sat'd aq NH₄Cl (100 mL) and DCM (5 × 50 mL). The combined organic layers were washed with water (2 × 60 mL) and brine (60 mL), dried over MgSO₄, filtered and concentrated under reduced pressure. The crude cycloadducts were purified by flash chromatography and gave **8-28** (2.7g, 87%) m.p. soften at 61 °C, liquid (79 °C-90 °C) R_f 0.18 (1:1 hexanes/EtOAc); [α]_D²⁵ = + 0.14 (c 1.67, CHCl₃). ¹H-NMR (DMSO, 90 °C) δ 7.80-7.35 (m, 10H, Ph), 7.50 (s, 2H, Ar), 5.05 (s, 2H, PhCH₂O), 4.11-4.02 (m, 1H, OCH₂NCH), 4.08 (t, *J* = 5.9 Hz, 1H, CH₂O), 4.04 (d, *J* = 5.9 Hz, 1H, OCH₂), 3.72 (q, *J* = 8.0 Hz, 1H, PhSO₂CH), 3.64-3.56 (m, 1H, COCH), 3.62 (s, OMe), 3.08-2.95 (m, 1H, SO₂CHCH), 2.58-2.50 (m, NH), 2.10 (t, *J* = 8.4 Hz, 2H, CH₂CHSO₂), 1.99-1.89 (m, 1H, CH₂CHNH), 1.88-1.77 (m, 1H, CH₂CHNH), 1.59 (s, Me), 1.53 (s, Me) ¹³C-NMR (DMSO, 90 °C) δ 173.0 (CO₂Me), 164.1 (NCO), 151.1 (C*(Ar)), 139.8 (C*(Ar)), 136.0 (C*(Ar)), 135.4 (C*(Ar)), 133.8 (CH(Ar)), 129.5 (CH(Ar)), 128.9 (C*(Ar)), 128.4 (CH(Ar)), 128.3 (CH(Ar)), 127.6 (CH(Ar)), 127.3 (CH(Ar)), 94.2 (OC*N), 74.7 (OBn), 68.2 (OCH₂), 65.0 (OMe), 58.3 (NCH), 58.0 (NCH), 57.7 (NCH), 51.9 (CHSO₂Ph), 35.2 (CH₂), 31.2(CH₂), 26.6 (Me), 23.1 (Me); HRMS (MALDI) *m/z* (%) for C₃₂H₃₅Cl₂N₂O₇S (MH⁺) calc. 661.1542, found 661.1579



1-*tert*-Butyl 2-methyl (2*S*,4*S*,5*S*)-4-(benzenesulfonyl)-5-{[(4*S*)-3-{[4-(benzyloxy)-3,5-dichlorophenyl]carbonyl}-2,2-dimethyl-1,3-oxazolidin-4-yl]methyl}pyrrolidine-1,2-dicarboxylate (8-30)

To a solution of the **8-28** (2.27g, 3.44 mmol) in THF (26 mL) were added aq NaHCO_3 and di-*tert*-butyl-dicarbonate (1.473 g, 7.9 mmol) at room temperature. After being stirred for 7h. The THF was evaporated then the mixture was partitioned between sat'd aq NH_4Cl (30 mL) and EtOAc (5 × 50 mL). The reaction mixture was extracted with EtOAc. The organic layer was successively washed with water, brine, dried over MgSO_4 , and concentrated in vacuo. The resulting residue was purified by silica gel chromatography to yield **8-30** (2.282 g, 87%) as white film. m.p. (108 °C-111 °C) R_f 0.47 (3:2 hexanes/EtOAc); $[\alpha]_D^{25} = +17.1$ (c 1.66, CHCl_3). $^1\text{H-NMR}$ (DMSO, 95 °C) δ 7.82-7.72 (m, 5H, SO_2Ph), 7.55-7.36 (m, 5H, Ph), 7.54 (s, 2H, Ar), 5.10 (s, 2H, PhCH_2O), 4.45-4.30 (m, 1H, COCH), 4.26 (d, $J = 7.9$ Hz, 1H, NCHCH_2O), 4.18 (t, $J = 8.9$ Hz, 1H, CHCHSO_2), 4.04 (q, $J = 7.0$ Hz, 1H, CHSO_2Ph), 4.02-3.88 (m, 2H, NCHCH_2O), 2.16 (t, $J = 9.1$ Hz, 2H, $\text{PhSO}_2\text{CHCH}_2$), 2.00 (t, $J = 8.8$ Hz, 2H, $\text{PhSO}_2\text{CHCH}_2$), 1.84 (s, 9H, Boc) 1.62 (s, Me), 1.57 (s, Me); $^{13}\text{C-NMR}$ (DMSO, 95 °C) δ 171.4 (CO_2Me), 163.6 (NCO), 152.7 (Boc), 150.9 ($\text{C}^*(\text{Ar})$), 138.8 ($\text{C}^*(\text{Ar})$), 135.7 ($\text{C}^*(\text{Ar})$), 135.0 ($\text{C}^*(\text{Ar})$),

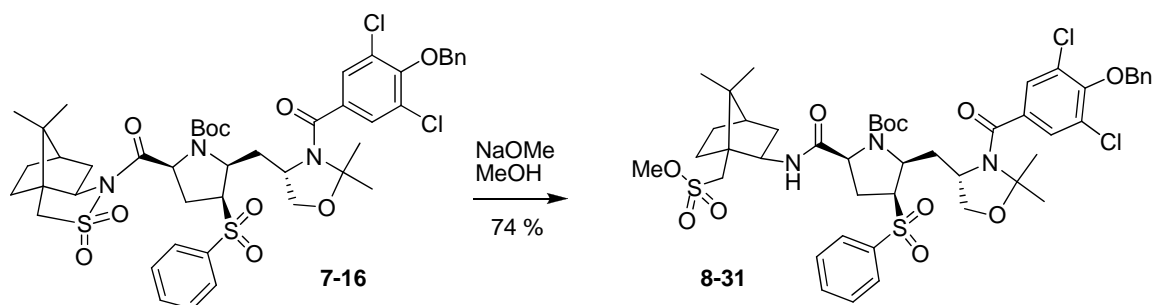
133.8 (CH(Ar)), 129.1 (CH(Ar)), 128.8 (C*(Ar)), 128.0 (CH(Ar)), 127.9 (CH(Ar)), 127.3 (CH(Ar)), 126.7 (CH(Ar)), 93.7 (NC*O), 80.2 (Boc), 74.4 (OBn), 66.8 (OCH₂), 62.0 (OMe), 57.7 (NCH), 57.2 (NCH), 56.5 (NCH), 51.6 (CHSO₂Ph) 35.8 (CH₂), 29.0 (CH₂), 27.4 (^tBu), 26.2 (Me), 23.0 (Me); HRMS (MALDI) *m/z* (%) for C₃₂H₃₅Cl₂N₂O₇S (MH⁺) calc. 661.1542, found 661.1579 HRMS (MALDI) *m/z* (%) for C₃₇H₄₃Cl₂N₂O₉S (MH⁺) calc. 761.2066, found 761.2005.



***tert*-Butyl (2*R*,4*S*,5*S*)-2-{[(4*S*)-3-{[(4*S*)-3-{[4-(Benzyloxy)-3,5-dichlorophenyl]carbonyl}-2,2-dimethyl-1,3-oxazolidin-4-yl]methyl}-3-(benzenesulfonyl)-5-[(10,10-dimethyl-3,3-dioxo-3 λ ⁶-thia-4-azatricyclo[5.2.1.0^{1,5}]decan-4-yl)carbonyl]pyrrolidine-1-carboxylate (7-16)**

To a solution of **7-14** (2.1 g, 2.49 mmol) in THF (19 mL) were added aq NaHCO₃ (943 mg, 11 mmol) in H₂O (19 mL) and di-*tert*-butyl-dicarbonate (1.068 g, 5.74 mmol) in THF (25 mL) at room temperature. After being stirred for 7 h, the THF was evaporated then the mixture was partitioned between sat'd aq NH₄Cl (100 mL) and EtOAc (5 × 50 mL). The reaction mixture was extracted with EtOAc. The organic layer was successively washed with water, brine, dried over MgSO₄, and concentrated in vacuo. The resulting residue was purified by silica gel chromatography using EtOAc/hexane

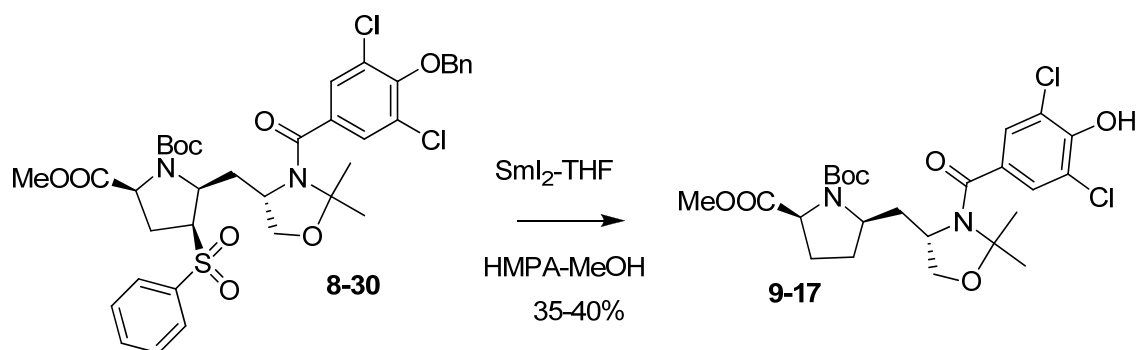
(1:3) as an eluant to yield 17 (2.11g, 90%) as slight yellow solid m.p. soften at 113-130 °C, liquidity (140-143 °C) R_f 0.5(1:1 hexanes/EtOAc); 0.96, NMR (DMSO, 90 °C) δ 7.78-7.36 (m, 10H, Ph), 7.52 (s, 2H, Ar), 5.09 (s, 2H, PhCH₂O), 4.63 (t, J = 8.8 Hz, 1H, COCH), 4.46 (d, J = 8.5 Hz, 1H, OCH₂), 4.50-4.34 (m, 1H, SO₂NHCH), 4.27 (5 Peaks, J = 6.5 Hz, 1H, PhSO₂CH), 4.03-3.95 (m, 2H, SO₂CHCH, OCH₂), 3.83-3.79 (m, 1H, CHCH₂O), 3.72 (d, J = 14.2 Hz, 1H, SO₂CH₂), 3.58 (d, J = 14.2 Hz, 1H, SO₂CH₂), 2.35-2.26 (m, 1H, CH₂CHSO₂Ph), 2.03-1.96 (m, 5H, CH₂CHSO₂Ph (1H), CH₂CHCH₂O (2H), 2H in sultam), 1.84-1.80 (m, 3H), 1.62 (s, Me), 1.57 (s, Me), 1.33 (s, 9H, ^tBu), 1.43-1.34 (m, 2H), 1.01 (s, Me), 0.91 (s, Me), ¹³C-NMR (DMSO, 90 °C) δ 169.0 (NCO), 163.6(NCO), 152.6 (Boc), 150.9 (C*(Ar)), 138.8(C*(Ar)), 135.7(C*(Ar)), 135.0(C*(Ar)), 133.8 (CH(Ar)), 129.1 (CH(Ar)), 128.8 (C*(Ar)), 128.0 (CH(Ar)), 127.2 (CH(Ar)), 126.7 (CH(Ar)), 93.7 (OCN), 80.2 (Boc), 74.4 (OBn), 64.1 (NCH), 61.4 (NCH), 58.7 (NCH), 57.1 (NCH), 56.6 (CHSO₂Ph), 51.7 (OCH₂), 48.5(C*), 47.0 (C*), 43.8 (CH), 37.3 (CH₂), 31.5 (CH₂), 27.6 (^tBu), 26.2 (Me), 25.4(CH₂), 23.1 (Me), 19.9 (CH₂), 19.0 (CH₂) HRMS (MALDI) m/z (%) for C₄₆H₅₆Cl₂N₃O₁₀S₂ (MH⁺) calc. 944.2784, found 785.7914 (-Boc, -MeCMe, -H₂O)



***tert*-Butyl (2*R*,4*S*,5*S*)-2-[[*(4S)*-3-[[*(4S)*-3-[[4-(Benzyloxy)-3,5-dichlorophenyl]carbonyl]-2,2-dimethyl-1,3-oxazolidin-4-yl]methyl]-3-(benzenesulfonyl)-5-({1-**

**[(methoxysulfonyl)methyl]-7,7-dimethylbicyclo[2.2.1]heptan-2-yl}carbamoyl)
pyrrolidine-1-carboxylate 8-31**

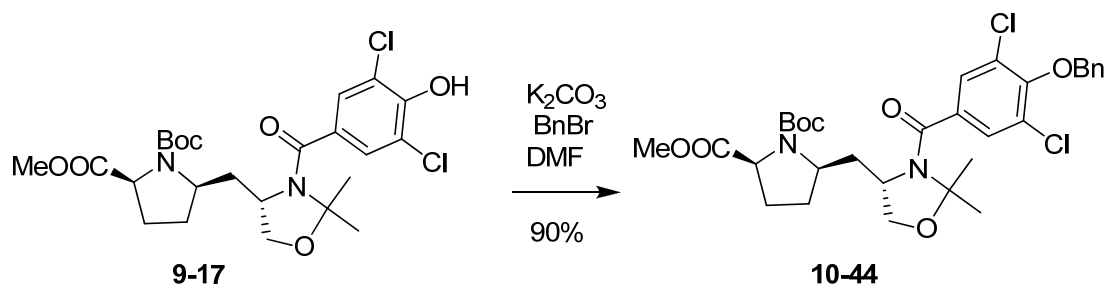
To the solution of **7-16** (1.857g, 1.969 mmol) in MeOH (30 mL), was added the newly prepared solution of Na (93 mg) in MeOH 10 mL) at 0 °C. The mixture was stirred for 0.5 h at 0 °C. Evaporated MeOH, the mixture was partitioned between sat'd aq NH₄Cl (100 mL) and DCM (5 × 50mL). The combined organic layers were washed with water (2 × 60 mL) and brine (60 mL), dried over MgSO₄, filtered and concentrated under reduced pressure. The crude cycloadducts were purified by flash chromatography and gave **8-31** (1.46g, 74%). m.p. soften at 139 °C, liquidity at 150 °C, decompose at 155 °C. R_f0.32 (1:1 hexanes/EtOAc); $[\alpha]_D^{25} = -14.16$ (*c* 1.21, CHCl₃). ¹H-NMR (DMSO, 75 °C) δ 7.84-7.32 (m, 10H, Ph), 7.54 (s, 2H, Ar), 5.09 (s, 2H, PhCH₂O), 4.54-4.40 (m, 1H, CHCH₂O), 4.40-4.16 (m, 1H, SO₂CHCH), 4.16-3.97 (m, 3H, COCH, CHSO₂, NCHCH₂O), 3.92 (dd, *J* = 5.2, 8.3 Hz, 1H, OCH₂), 3.88-3.82 (m, 1H, SO₂NCH), 3.79 (s, OMe), 3.55-3.50 (m, NH), 3.14 (s, 2H, SO₂CH₂); 2.15-1.90 (m, 5H, CH₂CHSO₂, CH₂CHNCH₂O, 1H at sultam), 1.79-1.65 (m, 4H), 1.64 (s, Me), 1.57 (s, Me), 1.41-1.30 (m, 1H), 1.35 (s, 9H, ^tBu), 1.19-1.09 (m, 1H), 0.91 (s, Me), 0.90 (s, Me); ¹³C-NMR (DMSO, 75 °C) δ 170.1 (NCO), 163.6 (NCO), 153.0 (Boc), 150.9 (C*(Ar)), 138.9, 135.8, 135.2, 133.8, 129.2, 128.9, 128.1, 127.5, 126.7, 93.7 (NC*O), 79.9 (Boc), 74.5 (OBn), 66.9, 58.8, 57.4, 57.0, 56.4, 55.4, 48.8, 47.8, 47.2, 44.1, 37.8, 35.9, 30.9, 27.6 (^tBu), 26.3 (Me), 26.1 (CH₂), 23.0 (Me), 20.4 (Me), 19.4 (Me) HRMS (MALDI) *m/z* (%) for C₄₇H₆₀Cl₂N₃O₁₁S₂ (MH⁺) calc. 976.3046, found 976.3034.



1-*tert*-Butyl 2-methyl (2*S*,5*R*)-5-{[(4*S*)-3-[(3,5-dichloro-4-hydroxyphenyl)carbonyl]-2,2-dimethyl-1,3-oxazolidin-4-yl]methyl}pyrrolidine-1,2-dicarboxylate (9-17)

To the solution of SmI_2 (0.1 M, 6 mL) and MeOH (60 μl) was added 8-29 (57 mg, 0.075 mmol). HMPA (0.2 mL) was added dropwise. The mixture was stirred at rt for 20-30 min, quenched with aqueous NH_4Cl (2 mL) and the THF removed under reduced pressure. HCl (aq) (0.1 N, 6 mL) was added at 0 °C to dissolve the solid. The solution was then extracted with EtOAc (3 \times 30 mL). The organic fraction was then washed with (3 \times 50 mL) brine, dried over MgSO_4 and the solvent was removed under reduced pressure. The crude desulfonylation products were purified by flash chromatography (1:1 Hexane : EtOAc) to give **9-17** (14mg, 35%). m.p. soften at 64 °C, liquid 72-74 °C, R_f 0.22 (5:2 hexanes/EtOAc); $[\alpha]_D^{25} = +67.5$ (c 0.39, CHCl_3). $^1\text{H-NMR}$ (DMSO, 90 °C) δ 7.45 (s, 2H, Ar), 4.06 (t, $J = 8.1$ Hz, 1H, CHCO), 4.03 (d, $J = 8.2$ Hz, 1H, CH_2O), 3.95-3.84 (m, 1H, OCH_2CH), 3.87 (d, $J = 8.2$ Hz, 1H, CH_2O), 3.62 (s, OMe), 3.52-3.42 (m, 1H, $\text{NCHCH}_2\text{CHNBoc}$), 2.06-1.93 (m, 2H, CH_2CHCO , $\text{CH}_2\text{CHNCH}_2\text{O}$), 1.79-1.65 (m, 1H, $\text{CH}_2\text{CH}_2\text{CHCO}$), 1.61 (s, Me), 1.54 (s, Me), 1.44-1.13 (m, 2H, CH_2CHCO , $\text{CH}_2\text{CHNCH}_2\text{O}$), 1.34 (s, 9H, ^tBu), 0.97-0.84 (m, 1H, $\text{CH}_2\text{CH}_2\text{CHCO}$); $^{13}\text{C-NMR}$ (DMSO, 90 °C) δ 172.4 (CO_2Me), 163.8 (NCO), 152.4 (Boc), 149.7 ($\text{C}^*(\text{Ar})$), 130.4

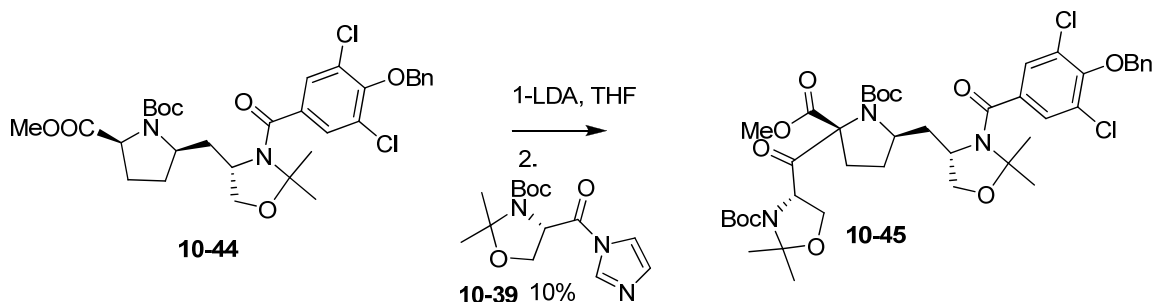
(C*(Ar)), 126.2 (CH(Ar)), 122.0 (C*(Ar)), 94.0 (NC*O), 78.9 (Boc), 66.5 (OCH₂), 58.8 (OMe), 56.0 (NCH), 55.1 (NCH), 51.3 (NCH), 38.0 (CH₂), 28.00 (CH₂), 27.6 (^tBu), 27.4 (CH₂), 26.1 (Me), 23.1(Me) HRMS (MALDI) *m/z* (%) for C₂₄H₃₃Cl₂N₂O₇ (MH⁺) calc. 531.1665, found 531.1528.



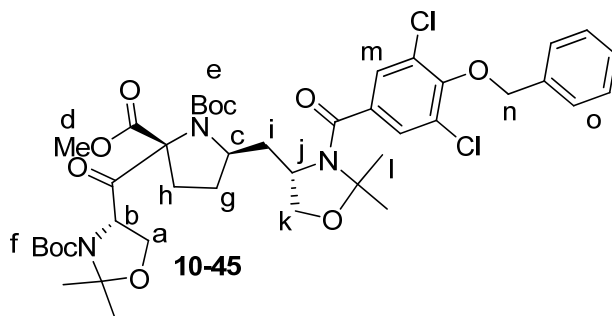
1-*tert*-Butyl 2-methyl (2*S*,5*R*)-5-{[(4*S*)-3-{[4-(benzyloxy)-3,5-dichlorophenyl]carbonyl}-2,2-dimethyl-1,3-oxazolidin-4-yl]methyl}pyrrolidine-1,2-dicarboxylate (10-44)

A mixture of **9-17** (39 mg, 0.073 mmol), benzyl bromide (14.8 μ L, 1.24eq), and K₂CO₃ (17.2 mg, 1.24 eq) in DMF (0.3 mL) was stirred for 10 h at room temperature and then diluted with EtOAc (10 mL) and water (10 mL). The organic layer was separated, washed with water (8 \times 10 mL) and brine (20 mL) and dried (Na₂SO₄) and concentrated in vacuo. The crude products were purified by flash chromatography and gave **10-44** (41 mg, 90%) as a white film. *R*_f 0.73, (Et₂O); ¹H-NMR (DMSO, 90 °C) δ 7.62 (s, 2H, Ar), 7.53-7.36 (m, 5H, Ph), 5.04 (s, 2H, OBn), 4.07(t, *J* = 7.5 Hz, CHCO), 4.04 (d, *J* = 8.5 Hz, 1H, CH₂O), 3.89 (d, *J* = 8.5 Hz, 1H, CH₂O), 3.91-3.80 (m, NCHCH₂O), 3.62 (s, OMe), 3.52-3.41 (m, 1H, NCHCH₂CHNBoc), 2.08-1.98 (m, 1H, CH₂CHCO), 2.03 (ddd, *J* = 3.8, 8.5, 16.1 Hz 1H, CH₂CHCH₂O), 1.79-1.66 (m, 1H, CH₂CH₂CHCO), 1.62 (s, Me), 1.56 (s, Me), 1.47-1.22 (m, 2H, CH₂CHCO, CH₂CHNCH₂O), 1.34 (s, 9H, ^tBu), 0.94-0.76 (m, 1H, CH₂CH₂CHCO); ¹³C-NMR (DMSO, 90 °C) δ 172.4 (CO₂Me), 163.3

(NCO), 152.4 (Boc), 150.7 (C*(Ar)), 135.5 (C*(Ar)), 135.4(C*(Ar)), 128.6(C*(Ar)), 128.1(CH(Ar)), 128.0 (2) (CH(Ar)), 126.8 (CH(Ar)), 94.1 (OC*N), 78.9 (Boc), 74.6 (OBn), 66.5 (OCH₂), 58.9 (OMe), 56.0 (NCH), 55.1 (NCH), 51.3 (NCH), 38.2 (CH₂), 28.2 (CH₂), 27.8 38.2 (CH₂), 26.1 (Me), 23.0 (Me); HRMS (MALDI) *m/z* (%) for C₃₁H₃₉Cl₂N₂O₇ (MH⁺) calc. 621.2129, found 563.1614 (-42-18)



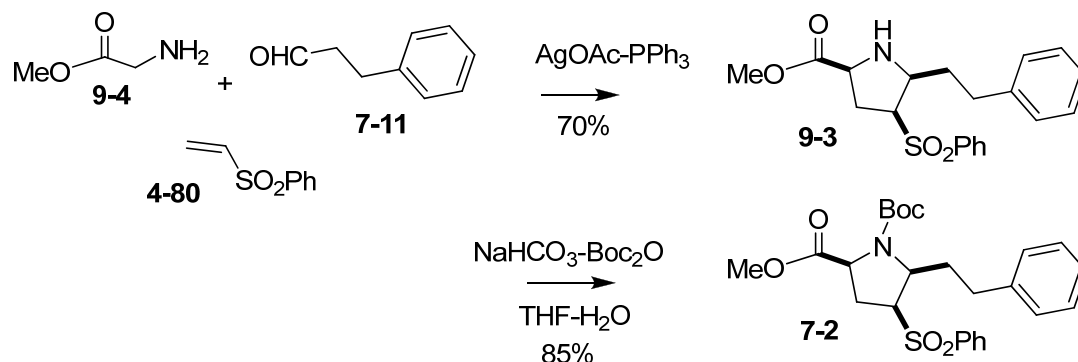
1-*tert*-Butyl 2-methyl (2*R*,5*R*)-5-{[(4*S*)-3-{[4-(benzyloxy)-3,5-dichlorophenyl]carbonyl}-2,2-dimethyl-1,3-oxazolidin-4-yl]methyl}-2-{[(4*S*)-3-[(*tert*-butoxy)carbonyl]-2,2-dimethyl-1,3-oxazolidin-4-yl]carbonyl}pyrrolidine-1,2-dicarboxylate (10-45)



To a dry, 50 mL, three-necked round-bottomed flask were added dry tetrahydrofuran (7.68 mL) and diisopropylamine (0.9 mL, 7.68 mmol). The solution was then cooled to below -70 °C (dry ice-acetone bath). To the THF solution, was added 2.79 mL (6.98 mol) of 2.5 M butyllithium in hexane dropwise. After the addition was complete, the solution is stirred at -78 °C for an additional 1h at 0 °C. To a dry, 50 mL,

Chapter 11: Experimental

three-necked round-bottomed flask was added **10-44** (36 mg, 0.0579 mmol) and THF (5 mL). While stirring at -78 °C 1 M lithium diisopropylamide (LDA) (63 μ L, 0.086 mmol, 1.5 eq) was added dropwise. After stirring at -78 °C for 2h, the reaction flask and its contents were warmed to 0 °C. A solution of **10-39** (1.5 eq) was slowly added to the vigorously stirring yellow-pink enolate solution at 0 °C. After 2h, 10 mL of a saturated aqueous ammonium chloride solution was added to the vigorously stirring mixture at -10 °C. At this point stirring was discontinued, the cooling bath was removed, and the partially frozen mixture was allowed to warm to room temperature. The contents of the reaction flask were introduced into a separatory funnel and 20 mL of DCM was added to the flask. The layers were shaken and then separated, and the aqueous phase was extracted again with a further 20 mL of DCM. The combined organic phase was washed with 20 mL of water and 20 mL of saturated brine and then dried over magnesium sulfate. After removal of the drying agent by filtration the solvents were removed under reduced pressure to give the residue. prep-TLC separation gave 4.4 mg (10%) of **10-45** along with **10-44** (36%). ¹H-NMR (DMSO, 90 °C) δ 7.65-7.39 (m, 7H, Ar, Ph), 5.05 (s, 2H), 4.12-3.98 (m, 4H), 3.94-3.82 (m, 2H), 3.64-3.42 (m, 4H), 2.08-1.88 (m, 2H), 1.62 (s, Me), 1.55 (s, Me), 1.39-1.14 (m, 20H, 2 Boc), 0.90-0.77 (m, 2H). MS (CI) *m/z* (%) for C₄₂H₅₆Cl₂N₃O₁₁⁺ (MH⁺) calc. 848.3292, found 848.6, 791.8



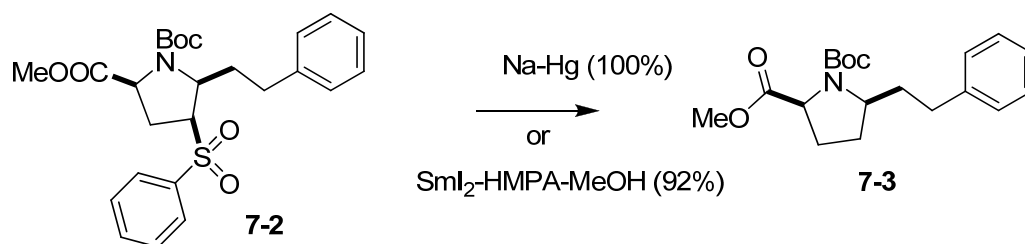
Methyl (2*S*,4*S*,5*S*)-4-(benzenesulfonyl)-5-(2-phenylethyl)pyrrolidine-2-carboxylate (9-3)

To a stirred mixture of glycine (0.37 mmol, 1.1 equiv) and AgOAc (5 mol %) and PPh₃ (10%) in dry THF (1 mL) was added aldehyde **7-11** (0.33 mmol, 1.0 eq) followed by phenyl vinyl sulfone (3.0 equiv) at room temperature. The reaction was stirred in the dark under Ar for the 5h, at which point the mixture was partitioned between saturated aq NH₄Cl (5 mL) and DCM (4 × 10 mL). The combined organic layers were dried over Na₂SO₄, filtered, and concentrated under reduced pressure. Flash chromatography purification gave 86 mg (70%) of endo product along with 8.6mg (7%) exo product. The major compound was converted to Boc protected product: ¹H-NMR (CDCl₃, rt) δ 7.83-7.08 (m, 10H, Ph), 3.92 (t, J = 8.1Hz, 1H, CHCO), 3.60 (ddd, J = 4.6, 5.8, 9.1 Hz, 1H), 3.30 (ddd, J = 4.6, 5.8, 10.0 Hz, 1H), 2.74 (ddd, J = 5.4, 8.9, 14.0 Hz, 1H, CH₂Ph), 2.57 (ddd, J = 4.7, 7.9, 13.8 Hz, 1H, CH₂Ph), 2.63-2.53 (m, 1H, CH₂CHCO), 2.27 (br, NH), 2.17 (ddd, J = 8.1, 9.6, 14.3Hz, 1H, CH₂CHCO), 1.84-1.65 (m, 2H, CH₂CH₂Ph); ¹³C-NMR (CDCl₃, rt) δ173.6 (CO₂Me), 141.2 (C*(Ar)), 138.2, 134.1, 129.6, 128.7, 128.6, 128.5, 126.2, 68.5 (OMe), 59.5 (NCH), 59.4 (NCH), 52.5 (CHSO₂), 37.8 (CH₂), 33.1 (CH₂), 31.9 (CH₂) HRMS (MALDI) m/z (%) for C₂₀H₂₄NO₄S (MH⁺) calc. 374.1426, found 374.1208

1-tert-Butyl 2-methyl (2*S*,4*S*,5*S*)-4-(benzenesulfonyl)-5-(2-phenylethyl)pyrrolidine-1,2-dicarboxylate (7-2)

To a solution of **9-3** (86 mg, 0.23 mmol), in THF (19 mL) were added aq NaHCO₃ (39 mg, 0.46 mmol) in H₂O (1 mL) and di-tert-butyl-dicarbonate (69 mg, 0.37 mmol) in THF 2 mL) at room temperature. After being stirred for 7h. the THF was evaporated then

the mixture was partitioned between sat'd aq NH₄Cl (100mL) and EtOAc (5 × 50mL). The reaction mixture was extracted with EtOAc. The organic layer was successively washed with water, brine, dried over MgSO₄, and concentrated in vacuo. The resulting residue was purified by silica gel chromatography to yield **7-2** (76 mg, 70%) as a white solid, m.p. 62-94 °C, R_f 0.19 (3:1 hexanes/EtOAc); ¹H-NMR (DMSO, 90 °C) δ 7.92-7.15 (m, 10H, Ph), 4.39-4.33 (m, 1H, CHCHSO₂Ph), 4.33 (t, *J* = 8.8 Hz, 1H, COCH), 4.20 (dt, *J* = 9.9, 6.9 Hz, 1H, SO₂CH), 3.70 (s, OMe), 2.87-2.63 (m, 2H, CH₂Ph), 2.30 (t, *J* = 9.3 Hz, 2H, CH₂CHCO), 2.24-2.12 (m, 1H, CH₂CH₂Ph), 1.97-1.84 (m, 1H, CH₂CH₂Ph), 1.38 (s, 9H, ^tBu); ¹³C-NMR (DMSO, 80 °C) δ 171.9 (CO₂Me), 152.8 (Boc), 141.9 (C*(Ar)), 139.0 (CH(Ar)), 133.7 (CH(Ar)), 129.2 (CH(Ar)), 128.0 (CH(Ar)), 127.9 (CH(Ar)), 127.7 (CH(Ar)), 127.4 (CH(Ar)), 79.6 (Boc), 62.5 (OMe), 57.3 (NCH), 51.7 (NCH), 32.9 (CH₂), 32.0 (CH₂), (CH₂), 28.8 (CH₂), 28.7 (CHSO₂Ph), 27.6 (^tBu); HRMS (MALDI) *m/z* (%) for C₂₅H₃₂NO₆S (MH⁺) calc. 474.1950, found 474.1917

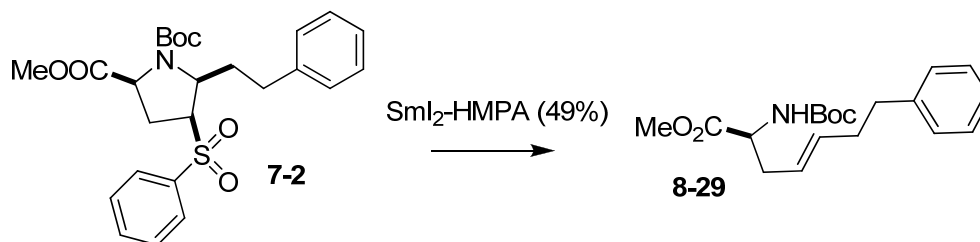


1-*tert*-Butyl 2-methyl (2*S*,5*S*)-5-(2-phenylethyl)pyrrolidine-1,2-dicarboxylate (**7-3**)

To a solution of **7-2** (55.6 mg) in methanol (4 mL) at 0 °C was added Na₂HPO₄ (42.6 mg 0.0898mmol) and sodium amalgam (5%, 160 mg). The reaction mixture was stirred vigorously for 2 h-11h at 0 °C. The reaction mixture was decanted and the flask rinsed with ether (100 mL). The organic layer was washed with H₂O (2 × 10 mL), dried

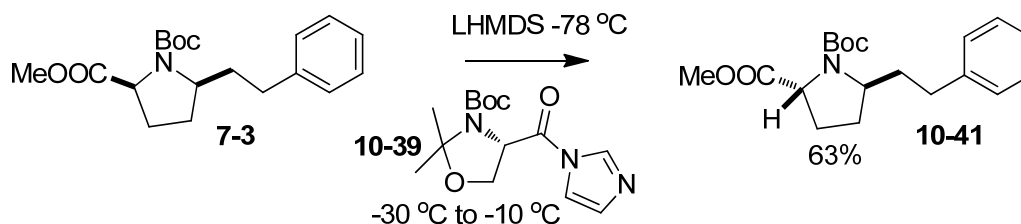
(MgSO₄), filtered, and concentrated. The crude oil was purified by chromatography (hexanes/EtOAc 10: 1) to give **7-3** (41 mg, 100%).

Alternatively: To the solution of SmI₂ (0.1 M, 4 mL) and MeOH (60 μL) was added **7-2** (34 mg, 0.071 mmol). HMPA (0.2 mL) was added dropwise. The mixture was stirred at rt for 20-30 min then quenched with NH₄Cl (2 mL). The THF was removed under reduced pressure. HCl (aq) (0.1 N, 6 mL, 0 °C) was added at 0 °C, to dissolve the solid. The solution was extracted with EtOAc (3 × 10 mL). The combined organic phase was washed with water (3 × 10 mL) and brine (50 mL), dried over MgSO₄ and the solvent was removed under reduced pressure. The crude desulfonylation products were purified by flash chromatography (6:1 Hexane: EtOAc) to give **7-3** (22 mg, 92%) as a yellow oil. R_f 0.28 (8:1 hexanes/EtOAc); ¹H-NMR (DMSO, 90 °C) δ 7.29-7.12 (m, 5H, Ph), 4.21 (t, *J* = 7.7 Hz, 1H, CHCO), 3.88-3.77 (m, CH), 3.64 (s, OMe), 2.70-2.52 (m, 2H, CH₂Ph), 2.21-2.12 (m, 1H, CH₂CHCO), 2.11-1.99 (m, 1H, CH₂CH₂Ph), 1.99-1.82 (m, 2H, CH₂CH₂CHCO,), 1.77-1.56 (m, 2H, CH₂CH₂CHCO, CH₂CH₂Ph), 1.35 (s, 9H, ^tBu); ¹³C-NMR (DMSO, 90 °C) δ 172.8 (CO₂Me) 152.8 (Boc), 141.6, 127.8, 127.7, 125.2, 78.5 (C*-Boc), 59.1 (OMe), 57.5 (NCH), 51.2 (NCH), 35.4 (CH₂), 31.7 (CH₂), 28.8 (CH₂), 27.6 (^tBu); HRMS (MALDI) *m/z* (%) for C₁₉H₂₈NO₄ (MH⁺) calc. 334.2018 found 234.1414.



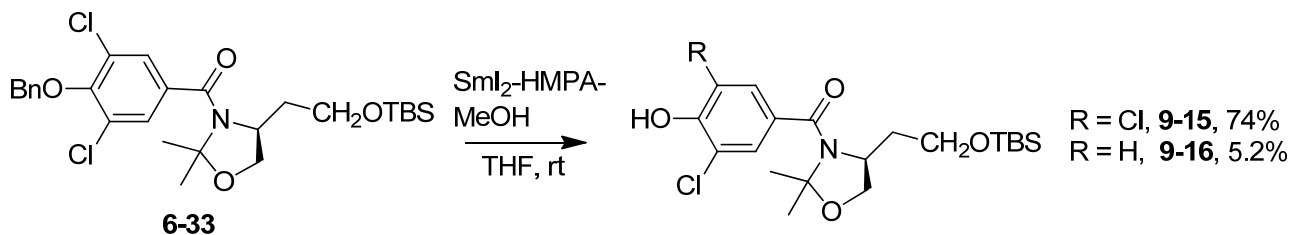
Methyl (2S,4E)-2-[[*tert*-butoxy)carbonyl]amino]-7-phenylhept-4-enoate (8-29)

To the solution of SmI_2 in THF (0.1 M, 4 mL) was added 7-2 (34.65 mg, 0.073 mmol). HMPA (0.4 mL) was added dropwise. The mixture was stirred at rt for 5 min then quenched with NH_4Cl (aq) (2 mL). The THF was removed under reduced pressure. HCl (aq) (0.1 N, 6 mL, 0 °C) was added at 0 °C to dissolve the solid. The solution was extracted with EtOAc (3×10 mL). The combined organic phase was washed with water (3×10 mL) and brine (50 mL), dried over MgSO_4 and the solvent was removed under reduced pressure. The crude desulfonylation products were purified by flash chromatography (6:1 Hexane: EtOAc) to give **8-29** (12 mg, 49%) as an oil. R_f 0.285 (8:1 hexanes/EtOAc); $^1\text{H-NMR}$ (CDCl_3 , rt) δ 7.32-7.15 (m, 5H, Ph), 5.56 (td, $J = 6.5, 15.4$ Hz, 1H, $\text{CHCHCH}_2\text{CH}_2$), 5.30 (td, $J = 7.3, 15.2$ Hz, 1H, CHCH_2CH_2), 5.0 (d, $J = 7.7$ Hz, NH), 4.36-4.26 (m, 1H, CHCO), 3.72 (s, OMe), 2.67 (dd, $J = 6.6, 8.5$ Hz, 2H, CH_2CHCO), 2.47-2.41 (m, 2H, CH_2Ph), 2.32 (q, $J = 7.3$ Hz, 2H, $\text{CH}_2\text{CH}_2\text{Ph}$), 1.45 (s, 9H, ^tBu).

**1-*tert*-Butyl 2-methyl (5S)-5-(2-phenylethyl)pyrrolidine-1,2-dicarboxylate (10-41)**

A dry, 50 mL, three-necked round-bottomed flask is charged with 7-3 (36 mg, 0.0579 mmol) and THF (5 mL). The stirrer is started at -78 °C and to this THF solution was added 1 M lithium diisopropylamide (LDA) (63 μL , 0.086 mmol, 1.5 eq) dropwise. With stirring at -78 °C for 2h, the reaction flask and its contents were warmed to 0 °C. A

solution of **10-39** (1.5 eq) was slowly added to the vigorously stirring yellow-pink enolate solution at 0 °C. After 2h, 10 mL of a saturated aqueous ammonium chloride solution was added to the vigorously stirring, -10 °C reaction mixture. At this point stirring was discontinued, the cooling bath was removed, and the partially frozen mixture is allowed to warm to room temperature. The contents of the reaction flask were introduced into a separatory funnel, 20 mL of DCM was added to the flask, the layers were shaken and then separated, and the aqueous phase was extracted again with 20 mL of DCM. The combined organic phase was washed with 20 mL of water and 20 mL of saturated brine and then dried over magnesium sulfate. After removal of the drying agent by filtration, the solvents were removed with a rotary evaporator at aspirator pressure to give the residue. prep-TLC separation gave 4.4 mg (10%) of **10-45** along with **10-41** (36%). (2R,5S)-1-tert-butyl 2-methyl 5-phenethylpyrrolidine-1,2-dicarboxylate. Yellow oil, R_f 0.29 (3:1 hexanes/EtOAc); $^1\text{H-NMR}$ (DMSO, 90 °C) δ 7.29-713 (m, 5H, Ph), 5.48-5.41 (m, 1H, COCH), 3.90-3.76 (m, 1H, CHCH_2), 2.70-2.51(m, 2H, CH_2Ph), 2.22-1.92 (m, 3H, $\text{COCHCH}_2\text{CH}_2$, PhCH_2CH_2), 1.87-1.61 (m, 3H, $\text{COCHCH}_2\text{CH}_2$, PhCH_2CH_2); $^{13}\text{C-NMR}$ (DMSO, 90 °C) δ 173.07 (CO_2Me), 152.9 (Boc), 142.6 ($\text{C}^*(\text{Ar})$), 128.9, 128.8, 126.3, 80.2 (O^tBu), 59.1 (OMe), 58.8 (NHCH), 52.8 (NHCH), 35.1 (CH_2), 32.8 (CH_2), 32.4 (CH_2), 28.6 (^tBu), 28.0 (CH_2); HRMS (MALDI) m/z (%) for $\text{C}_{19}\text{H}_{28}\text{NO}_4$ (MH^+) calc. 334.2018 found 334.2350.



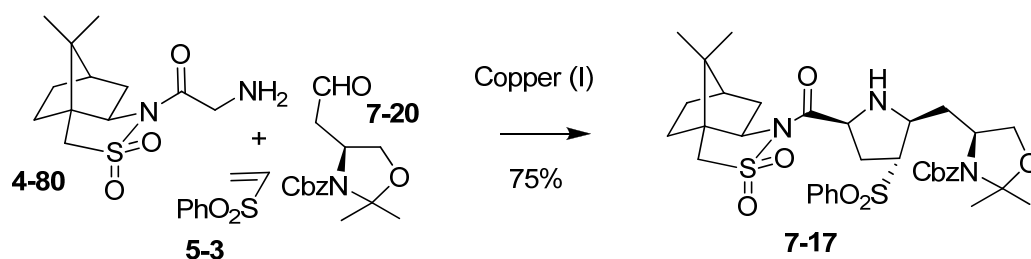
4-{{(4S)-4-{2-[(tert-butyldimethylsilyl)oxy]ethyl}-2,2-dimethyl-1,3-oxazolidin-3-yl}carbonyl}-2,6-dichlorophenol (9-15)

To the solution of SmI₂ in THF (0.1 M, 6 mL) was added **6-33** (39.9 mg, 0.074) and methanol (60 μL), and HMPA (0.2 mL) was added dropwise. The mixture was stirred at rt for 20 min then quenched with NH₄Cl (aq) (2 mL). The THF was removed under reduced pressure and HCl (aq) (0.1 N, 6 mL) was added at 0 °C to dissolve the solid. The solution was extracted with EtOAc (3 × 10 mL). The combined organic phase was washed with water (3 × 10 mL) and brine (50 mL), dried over MgSO₄ and the solvent was removed under reduced pressure. The crude desulfonylation products were purified by flash chromatography (6:1 Hexane: EtOAc) and gave **9-15** (24.4mg, 74%), **9-16** (1.6 mg, 5.2%). **9-15** m.p. 138-141 °C, R_f 0.80 (1:1 hexanes/EtOAc); [α]²⁵_D = +19.79 (*c* 0.195, CHCl₃). ¹H-NMR (DMSO, 70 °C) δ 10.41 (br, OH), 7.57 (s, 2H, Ar), 4.22-4.13 (m, 2H, OCH₂CHN), 3.97-3.91 (m, 1H, OCH₂CHN), 3.51 (dd, *J* = 5.8, 7.0 Hz, 2H, CH₂OTBS), 1.76-1.51 (m, 2H, CH₂CH₂OTBS), 1.72 (s, 3H), 1.64 (s, 3H), 0.87 (s, 9H, ^tBu), 0.02 (s, 3H), 0.00 (s, 3H); ¹³C-NMR (DMSO, 70 °C) δ 164.0 (NCO), 149.9 (C*(Ar)), 130.4 (C*(Ar)), 126.4 ((CH(Ar))), 121.8 (C*(Ar)), 93.9 (OC*N), 63.3 (OCH₂), 59.2 (NCH), 55.7 (NCH), 36.2 (CH₂), 26.3 (Me), 25.4 (^tBu), 23.2 (Me), 17.4 (Me) HRMS (MALDI) *m/z* (%) for C₂₀H₃₂Cl₂NO₄Si (MH⁺) calc. 448.1478, found 448.1290.

4-{{(4S)-4-{2-[(tert-Butyldimethylsilyl)oxy]ethyl}-2,2-dimethyl-1,3-oxazolidin-3-yl}carbonyl}-2-chlorophenol (9-16)

[α]²⁵_D = +15.46 (*c* 0.37, CHCl₃). ¹H-NMR (CDCl₃, rt) δ 7.52 (d, *J* = 1.9 Hz, 1H, Ar), 7.35 (dd, *J* = 8.5, 1.9 Hz, 1H, Ar), 7.08 (dd, *J* = 8.1 Hz, 1H, Ar), 4.30-4.14 (m, 1H,

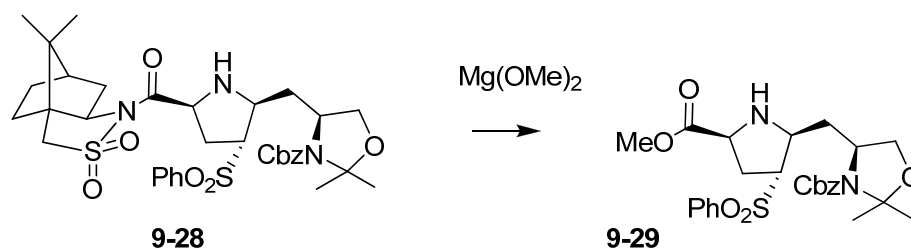
OCH₂CHN), 4.16 (dd, *J* = 8.9, 5.4 Hz, 1H, OCH₂CHN), 4.01 (dd, *J* = 8.9, 2.3 Hz, 1H, OCH₂CHN), 3.58-3.43 (m, 2H, CH₂OTBS), 1.81 (s, 3H), 1.71 (s, 3H), 1.86-1.60 (m, 2H, CH₂CH₂OTBS), 0.88 (^tBu), 0.02 (Me), 0.00 (Me). ¹³C (DMSO, 70 °C) δ 170.7 (NCO), 163.6 (NCO), 151.0 (C*(Ar)), 133.70 (CH(Ar)), 129.2 ((CH(Ar)), 128.6 (C*(Ar)), 127.9 (CH(Ar)), 127.7 (CH(Ar)), 126.9 (CH(Ar)), 94.1 (OCN), 74.5 (OCH₂), 67.5 (NCH), 67.2 (OCH₂), 63.9 (NCH), 59.2 (NCH), 56.7 (NCH), 56.5 (CHSO₂Ph), 51.9 (CH₂SO₂Ph), 48.2 (C*), 46.9 (C*), 43.9 (CH), 39.9 (CH₂), 37.3 (CH₂), 32.7 (CH₂), 31.5 (CH₂), 26.1 (CH₃), 25.4 (CH₂), 23.3 (CH₃), 20.0 (CH₃), 19.0 (CH₃); HRMS (MALDI) *m/z* (%) for C₂₀H₃₃ClNO₄Si (MH⁺) calc. 414.1867, found 414.1932.



4-[[[(2*S*,4*R*,5*S*)-4-(Benzenesulfonyl)-5-[[[(4*S*)-3-benzyloxycarbonyl-2,2-dimethyl-1,3-oxazolidin-4-yl]methyl]pyrrolidin-2-yl]carbonyl]-10,10-dimethyl-3λ⁶-thia-4-azatricyclo[5.2.1.0^{1,5}]decane- 3,3-dione (7-17)

The catalyst was prepared by stirring the copper salt (Cu(MeCN)₄PF₆ or CuOAc, 5 mol %) and bisphosphine ligand (dppb or dppf, 5 mol %) in DMSO (6 mL/mmol aldehyde) at rt for 1 h. To this mixture was added aldehyde **7-20** (138.5 mg, 0.5 mmol), glycyl sultam (178 mg, 0.65 mmol), and dipolarophile **5-3** (252 mg, 1.5 mmol). After stirring at rt for 3 h, the mixture was quenched with the addition of NH₄Cl (sat), then partitioned between satd NH₄Cl and DCM. The combined organic layers were washed with brine, dried over MgSO₄, filtered and the solvent removed under vacuum to give the

crude product. Flash chromatography separation gave 262 mg (75%) of pale yellow solid **7-17**. R_f 0.25 (1:1 hexane/EtOAc); $[\alpha]_D^{25} = -7.56$ (c 0.185, CHCl_3). $^1\text{H-NMR}$ (DMSO 90°C) δ 7.58 (s, 2H, Ar), 7.77-7.35 (m, 10H, Ph), 5.00 (s, 2H, OBn), 4.07-3.96 (m, 3H, COCHNHCH , CHCH_2O), 3.92-3.89 (m, 1H, OCH_2CH), 3.77 (t, $J = 6.7$ Hz, CHNSO_2), 3.74 (d, $J = 14.2$ Hz, 1H, CH_2SO_2), 3.58 (d, $J = 14.2$ Hz, 1H, CH_2SO_2), 3.23-3.10 (m, CHSO_2), 2.64-2.51 (m, NH), 2.32 (ddd, $J = 5.0, 8.0, 11.0$ Hz, 1H, CH_2CHCO), 2.30-2.18 (m, 1H, $\text{CH}_2\text{CHCH}_2\text{O}$), 1.92-1.68 (m, 7H, CH_2CHCO , $\text{CH}_2\text{CHCH}_2\text{O}$, 5H in sultam), 1.60 (s, Me), 1.53 (s, Me), 1.43-1.37 (m, 1H), 1.22-1.20 (m, 1H), , 0.92 (s, Me), 0.89 (s, Me) ^{13}C (DMSO, 70°C) δ 171.8, 164.6, 152.1, 138.6, 136.1, 134.8, 130.2, 129.0, 128.9, 127.9, 95.2, 75.6, 68.6, 68.3, 65.0, 60.3, 57.7, 57.6, 53.0, 49.2, 48.0, 45.0, 41.0, 38.4, 33.8, 32.6, 27.2, 26.5, 24.3, 21.0, 20.1 HRMS (MALDI) m/z (%) for $\text{C}_{35}\text{H}_{46}\text{N}_3\text{O}_8\text{S}_2$ (MH^+) calc. 700.2726, found 700.2269.

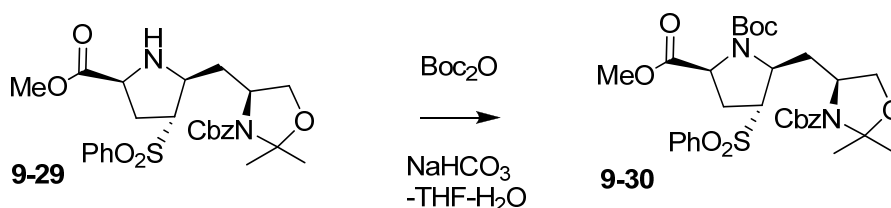


Benzyl (4S)-4-[(2S,3R,5S)-3-(benzenesulfonyl)-5-(methoxycarbonyl)pyrrolidin-2-yl]methyl}-2,2-dimethyl-1,3-oxazolidine-3-carboxylate (9-29)

The same procedure was used as for **8-28**.

The mixture of Mg (780 mg) in MeOH was refluxed for 3h. To the resulting solution of Mg(OMe)_2 , was added **9-28** (3.28 g, 4.695 mmol) at 0°C . The mixture was stirred for 8h from 0°C to rt. Evaporated MeOH, the mixture was partitioned between sat'd aq NH_4Cl (100 mL) and DCM ($5 \times 50\text{mL}$). The combined organic layers were

washed with water (2 × 60 mL) and brine (60 mL), dried over MgSO₄, filtered and concentrated under reduced pressure. The crude cycloadducts were purified by flash chromatography and gave **9-29** (2.05g, 85%) R_f 0.16 (PE/EtOAc); ¹H-NMR (DMSO 90 °C) δ 7.56 (s, 2H, Ar), 7.80-7.35 (m, 10H, Ph), 5.02 (s, 2H, OBn), 4.07-3.98 (m, 2H, NCHCH₂O), 3.92-3.86 (m, 1H, OCH₂CHN), 3.57 (s, OMe), 3.55 (t, *J* = 7.8 Hz, CHCO), 3.23-3.09 (m, 2H, SO₂CHCHN), 2.19-2.09 (m, 1H, CH₂CHCO), 1.94-1.83 (m, 1H, CH₂CHCO), 1.81-1.53 (m, 2H, OCH₂CHN), 1.59 (s, Me), 1.52 (s, Me) ¹³C (DMSO 90 °C) δ 172.1 (CO₂Me), 163.6 (NCO), 151.1 (C*(Ar)), 133.7 (CH(Ar)), 129.2 (CH(Ar)), 128.4 (C*(Ar)), 127.9 (CH(Ar)), 127.8 (CH(Ar)), 127.7 (CH(Ar)), 126.9 ((CH(Ar)), 94.1 (OC*N), 74.5 (OBn), 67.2 (OCH₂), 67.1 (OMe), 58.7 (NCH), 56.5 (NCH), 56.3 (NCH), 51.3 (CHSO₂Ph), 40.3 (CH₂), 31.3 (CH₂), 26.3 (Me), 23.3 (Me).



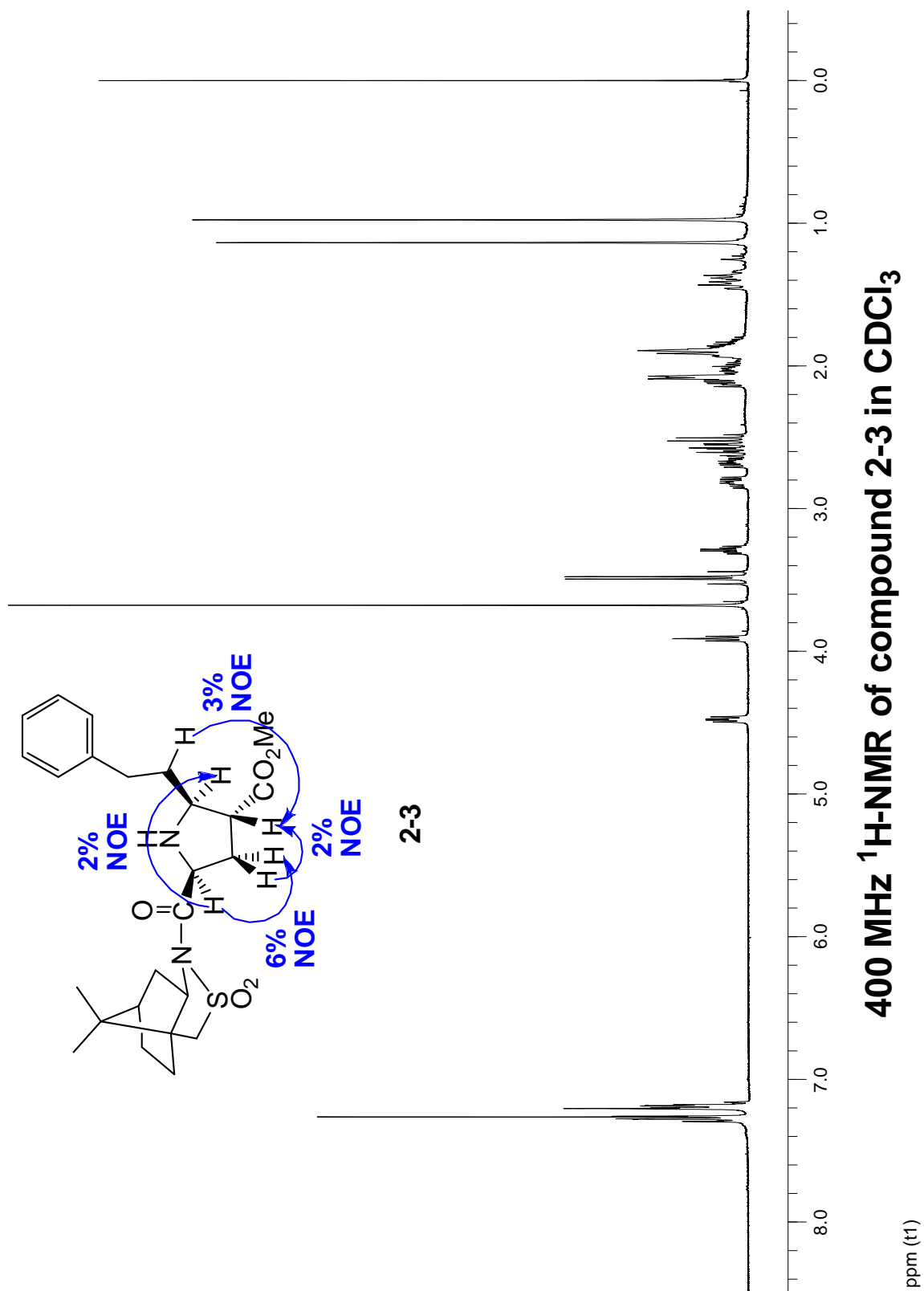
1-tert-Butyl 2-methyl (2*S*,4*R*,5*S*)-4-(benzenesulfonyl)-5-[[*(4S)*-3-[(benzyloxy)carbonyl]-2,2-dimethyl-1,3-oxazolidin-4-yl]methyl]pyrrolidine-1,2-dicarboxylate (9-30**)**

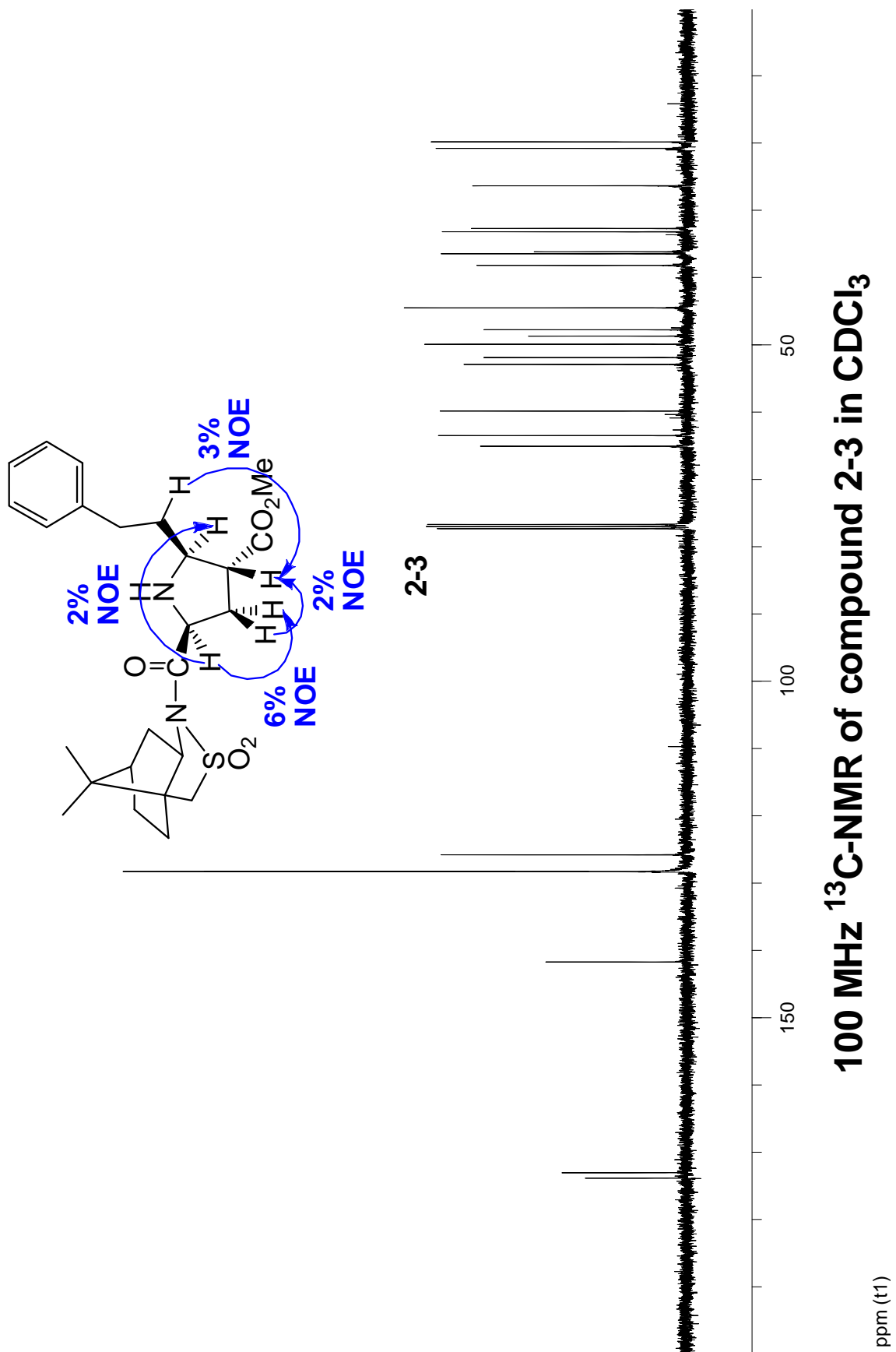
To a solution of **9-29** (118 mg, 0.23 mmol), in THF (19 mL) were added NaHCO₃ (39 mg, 0.46 mmol) in H₂O (1 mL) and di-tert-butyl-dicarbonate (69mg, 0.37 mmol) in THF (2 mL) at rt. After stirring for 7h the THF was evaporated, sat'd aq NH₄Cl (100mL) was added and the mixture was extracted with EtOAc (5 × 50mL). The organic layer was washed with water then brine, then dried over MgSO₄, and concentrated in vacuo. The resulting residue was purified by silica gel chromatography to yield **9-30** (99 mg,

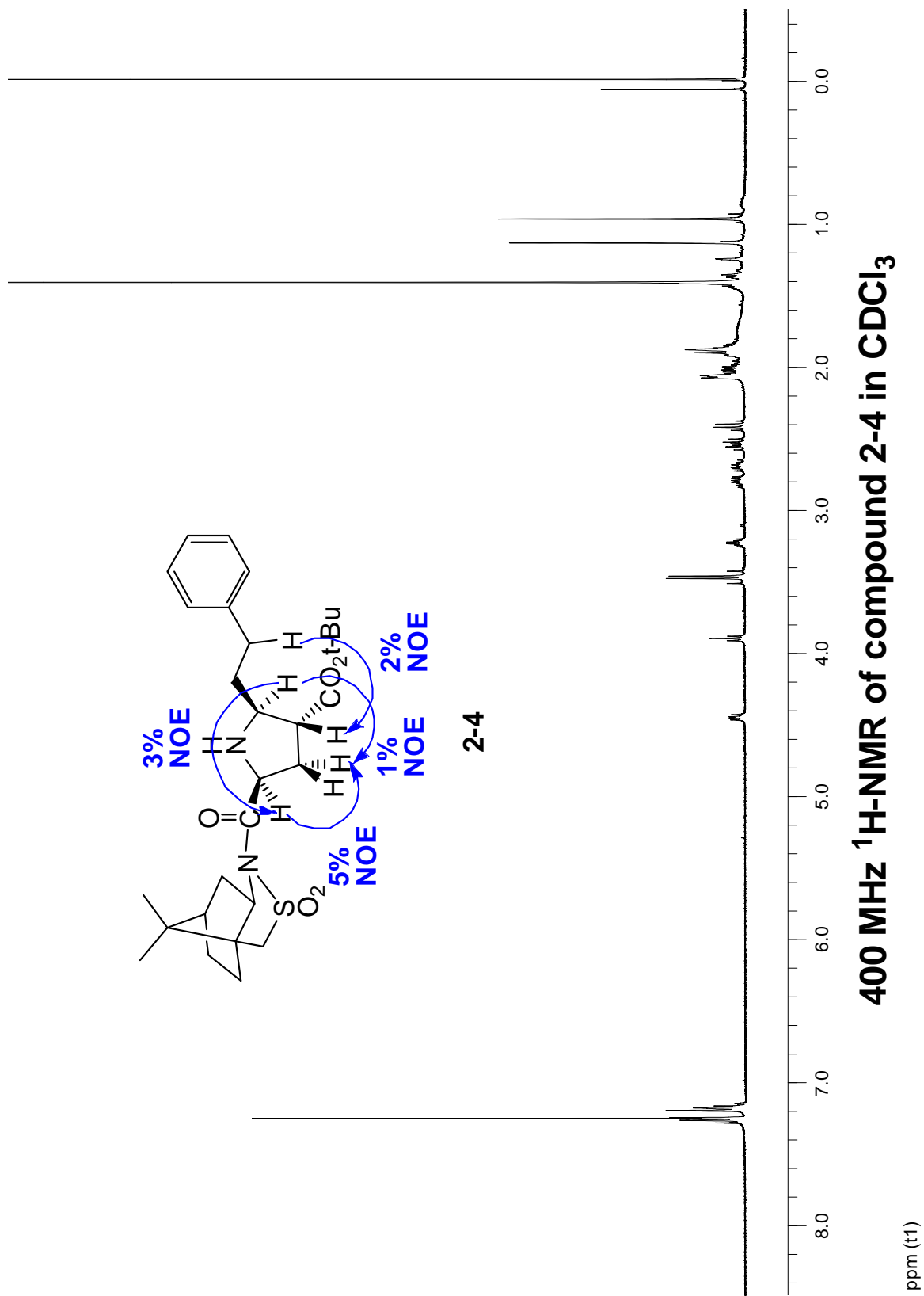
Chapter 11: Experimental

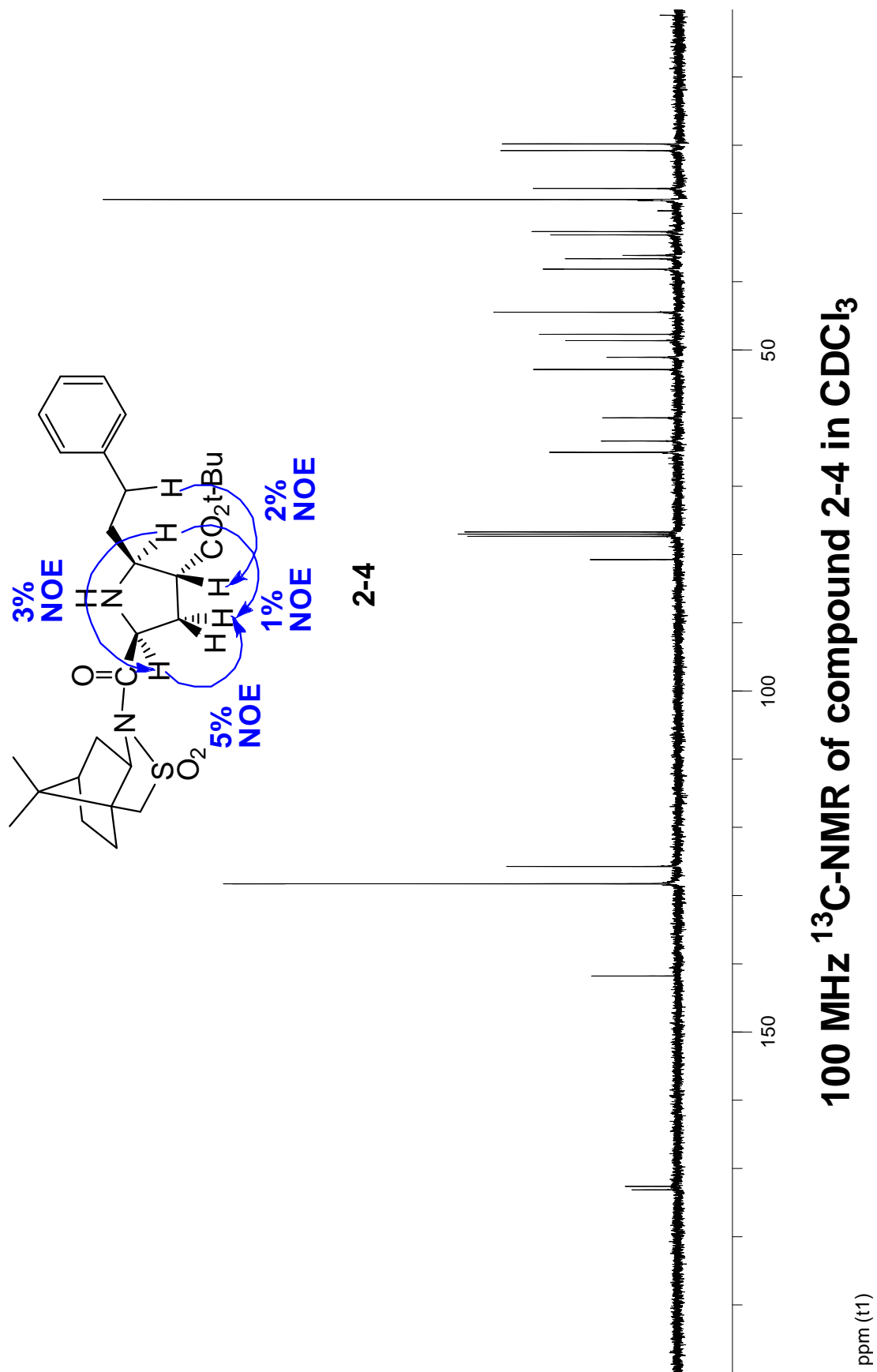
70%) as slightly yellow solid. R_f 0.32 (2:1 hexane/EtOAc); $[\alpha]_D^{25} = +27.9$ (c 2.45, CHCl_3). $^1\text{H-NMR}$ (DMSO 90 °C) δ 7.80-7.39 (m, 10H, Ph), 5.04 (s, 2H, OBn), 4.10-3.96 (m, CHCHSO_2), 3.91-3.86 (m, NCHCH_2O), 3.89 (dd, $J = 8.5, 5.2$ Hz, NCHCH_2O), 3.82-3.79 (m, COCH), 3.80 (d, $J = 8.5$, Hz, NCHCH_2O), 3.64 (s, OMe), 2.88-2.84 (m, CHSO_2), 2.56 (dd, $J = 14.6, 8.5$ Hz, NCHCH_2CHN), 2.01-1.91 (m, 2H, CH_2CHCO , NCHCH_2CH), 1.59 (s, Me), 1.53 (s, Me), 1.42-1.26 (m, 1H, CH_2CHCO), 1.33 (s, 9H, tBu); ^{13}C (DMSO 90 °C) δ 171.3 (CO2Me), 163.2 (NCO), 151.9 (Boc), 150.9 (C*(Ar), 134.2 (CH(Ar)), 129.4 ((CH(Ar)), 128.8 (C*(Ar), 128.0, 127.9 (2), 126.7, 94.2 (OC*N), 74.6 (OBn), 65.9 (OCH₂), 57.8, 56.0, 55.6, 51.7, 38.2 (CH₂), 27.5 (Boc), 26.2 (Me), 23.1 (Me) (NCH), 56.3 (NCH), 51.3 (CHSO₂Ph), 40.3 (CH₂), 31.3 (CH₂), 26.3 (Me), 23.3 (Me) HRMS (MALDI) m/z (%) for $\text{C}_{31}\text{H}_{41}\text{N}_2\text{O}_9\text{S}$ (MH^+) calc. 617.2533, found 617.2512.

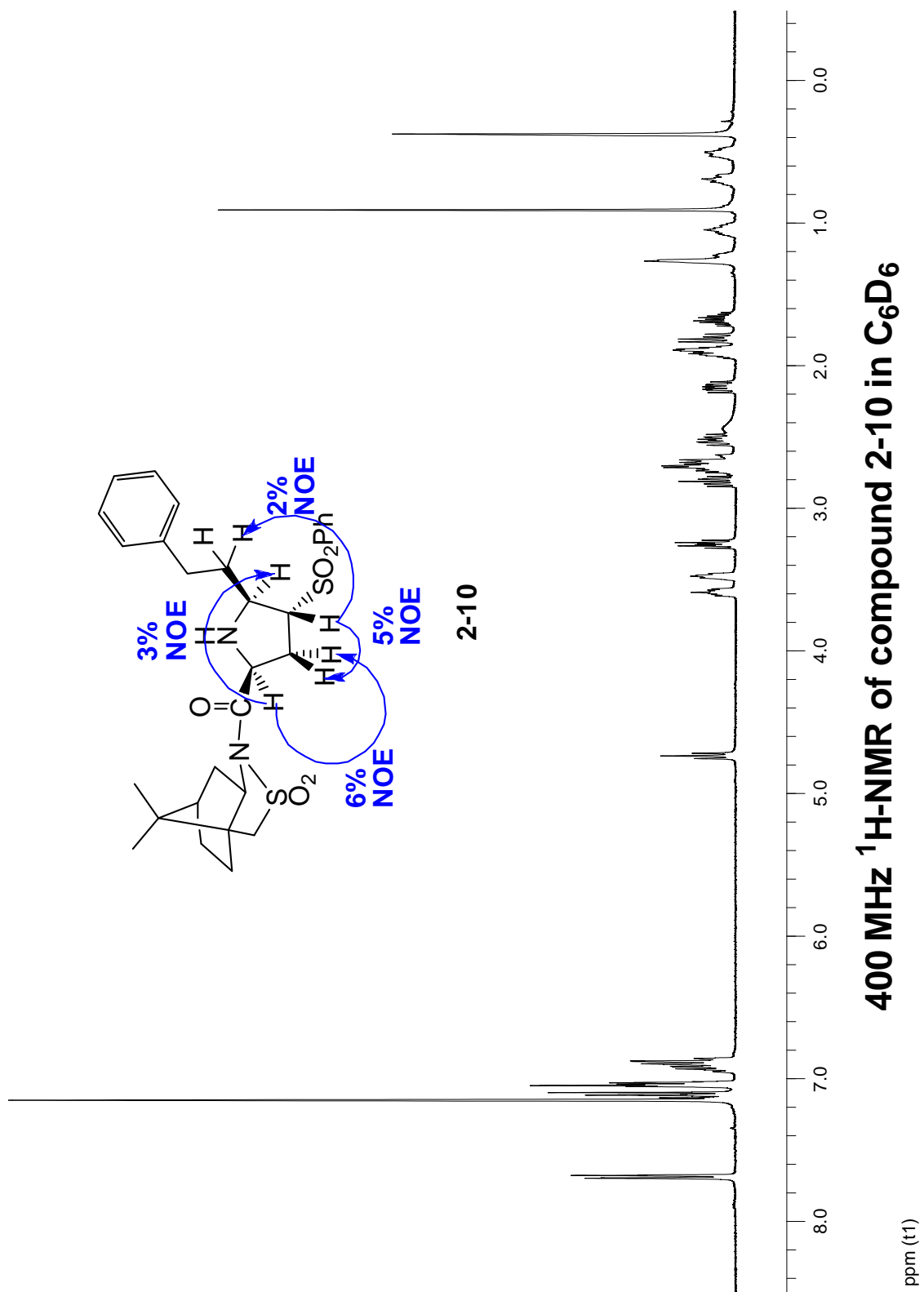
Appendix A

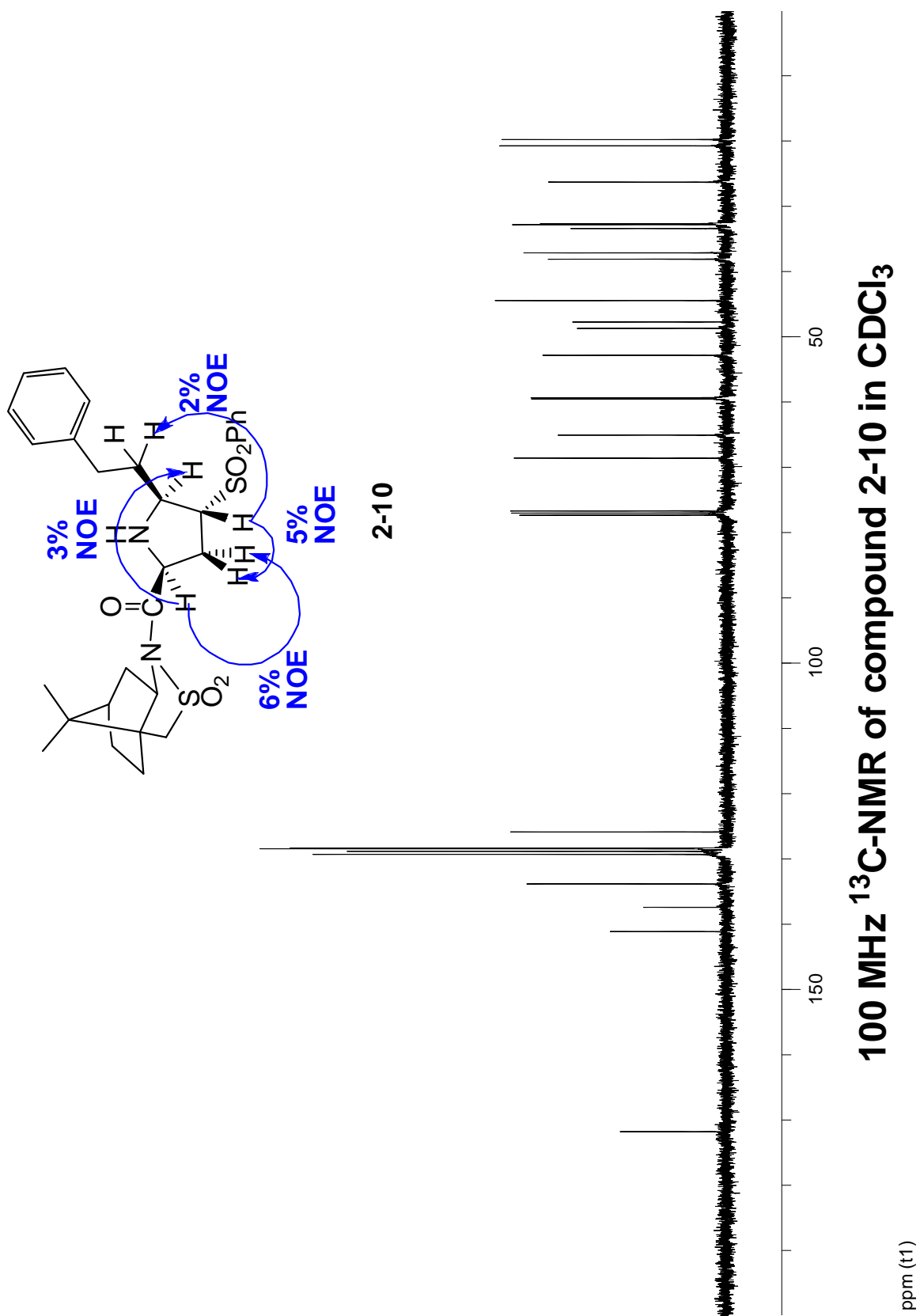


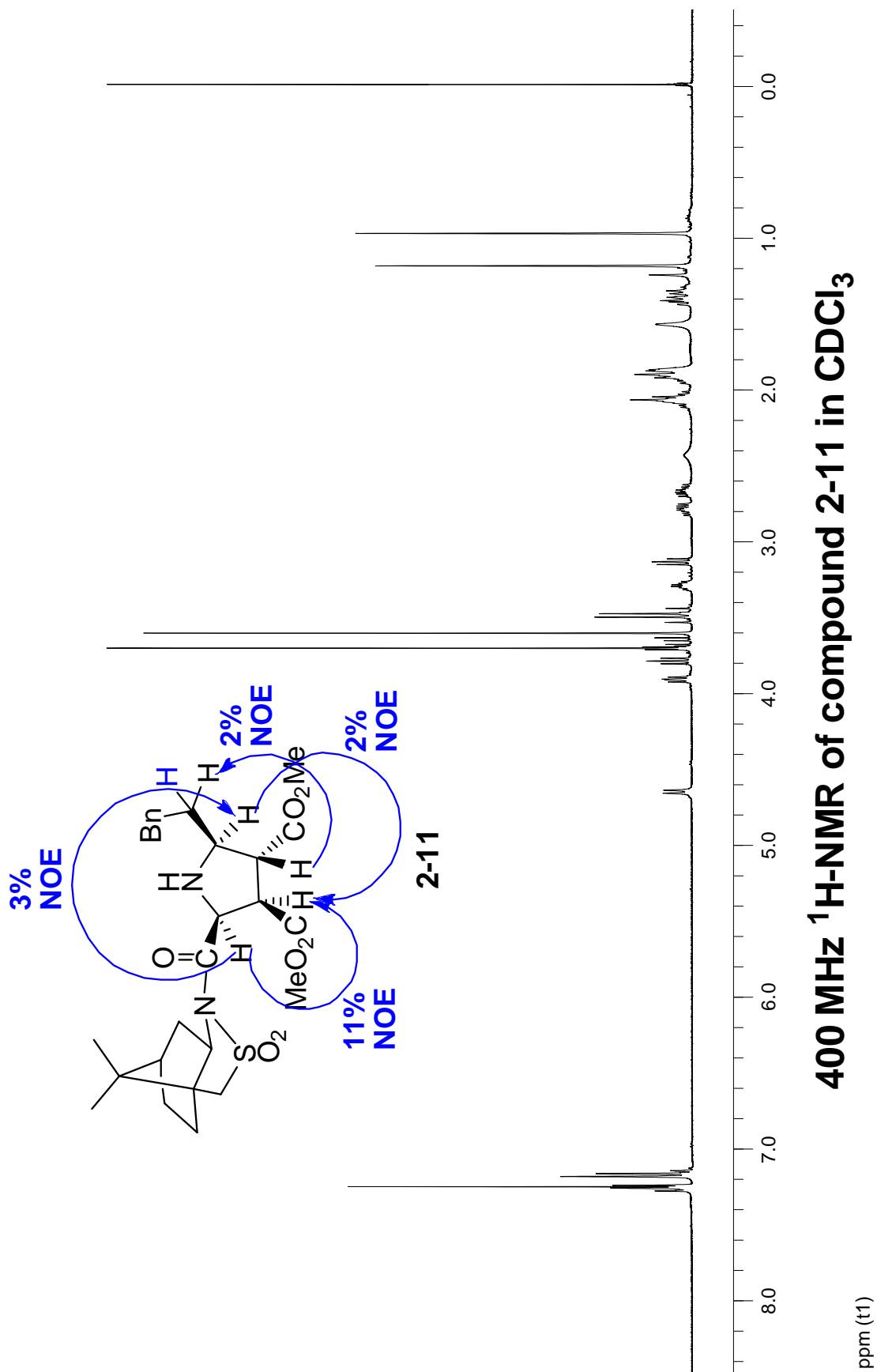


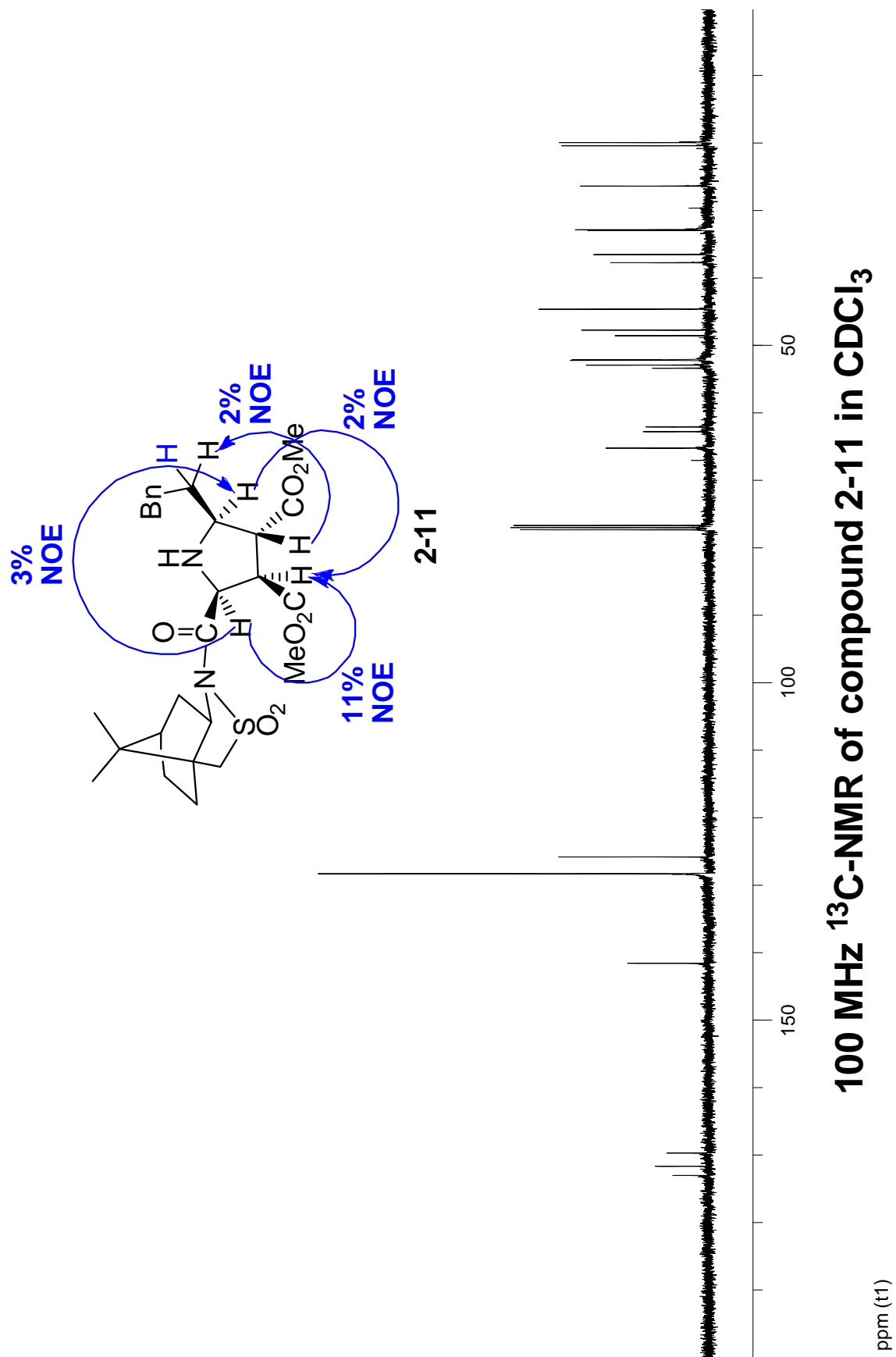


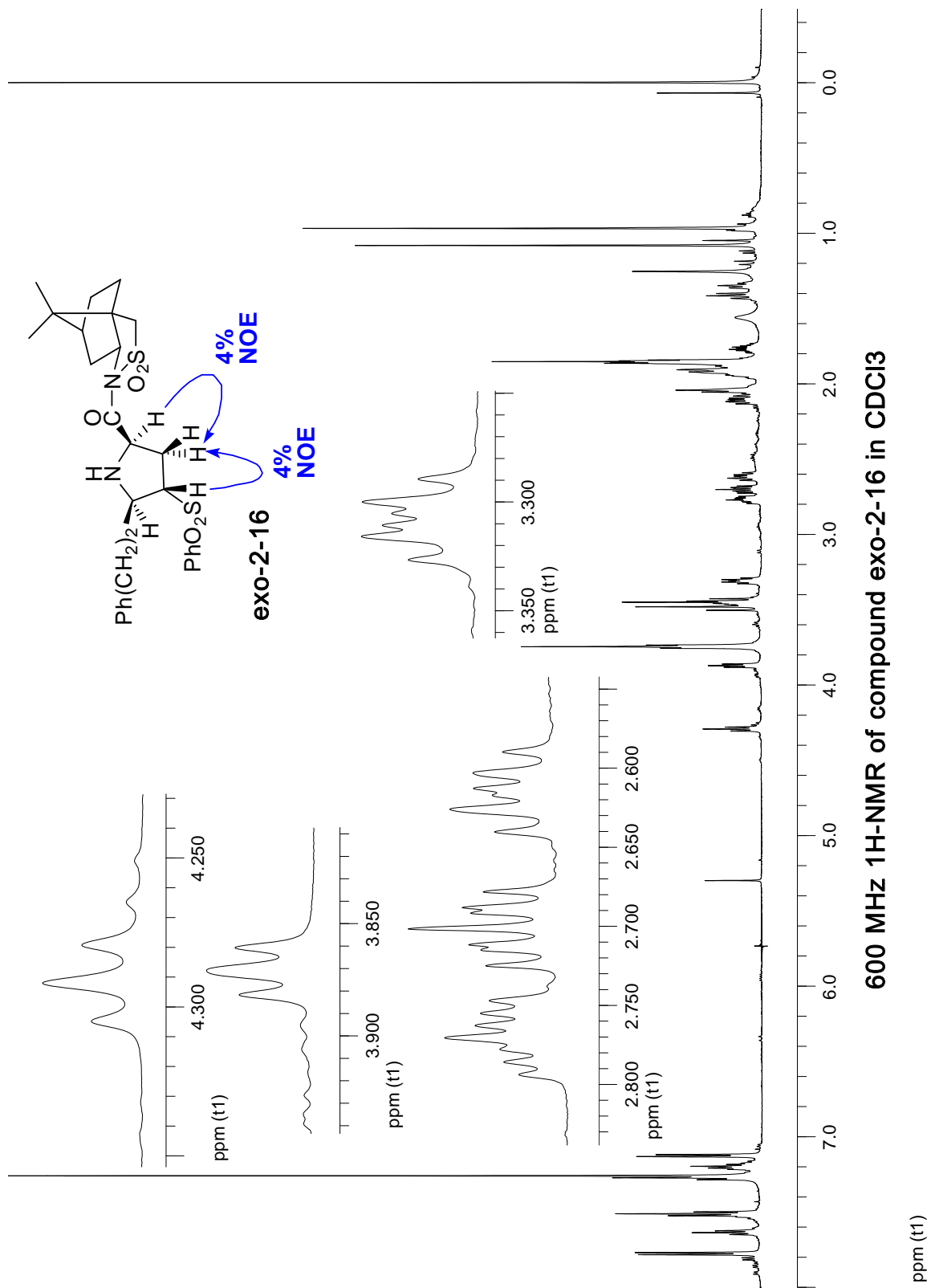


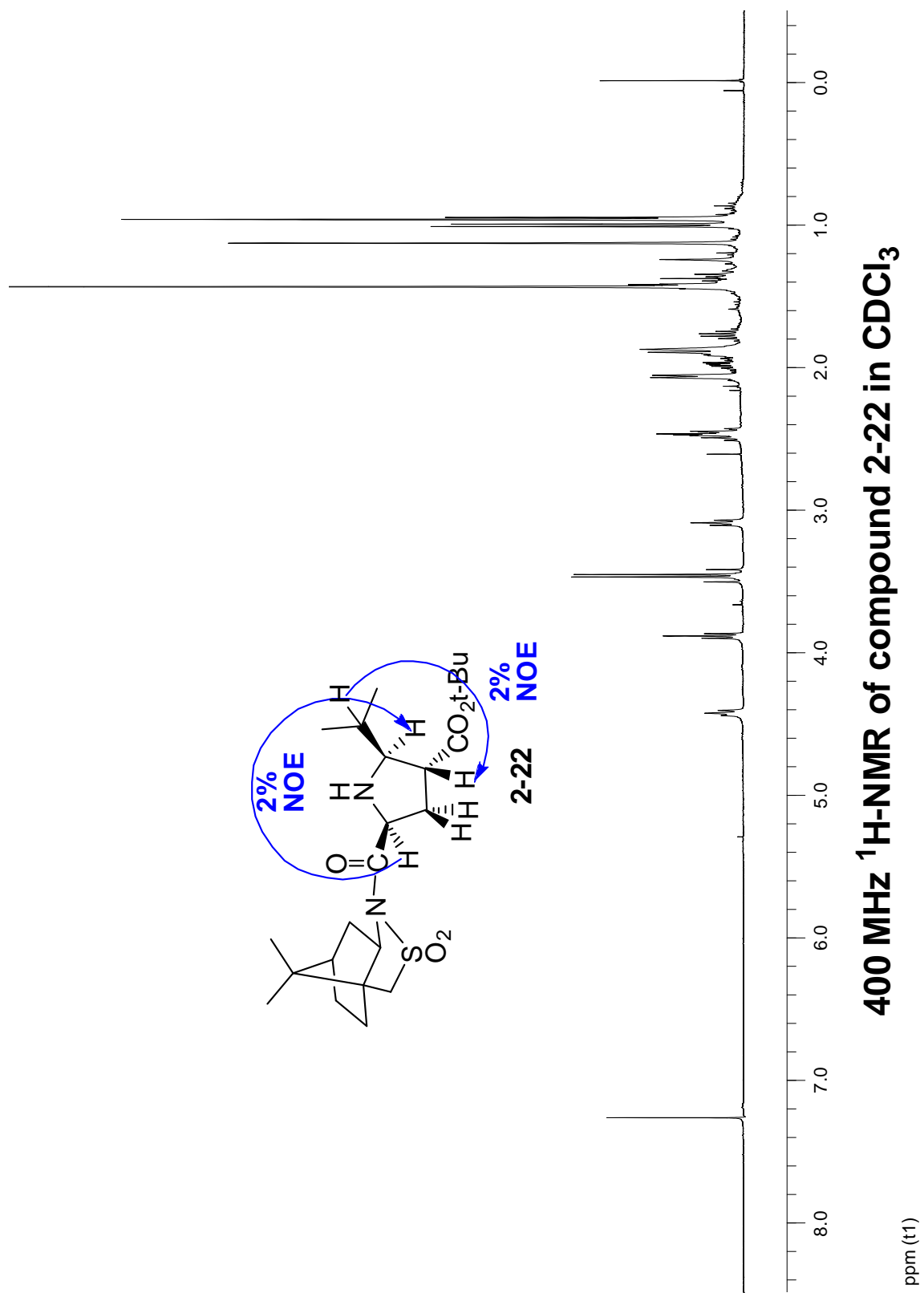


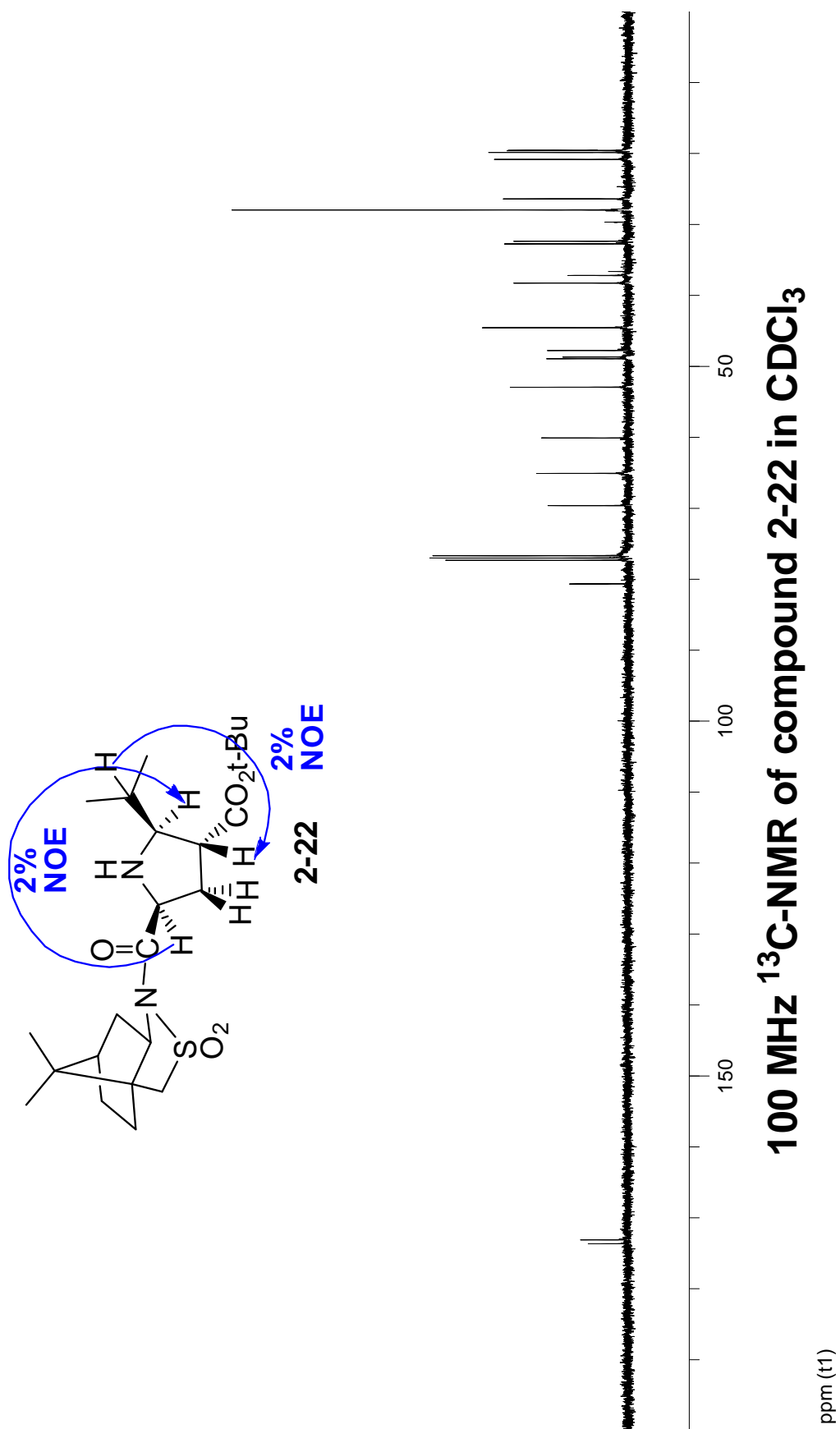


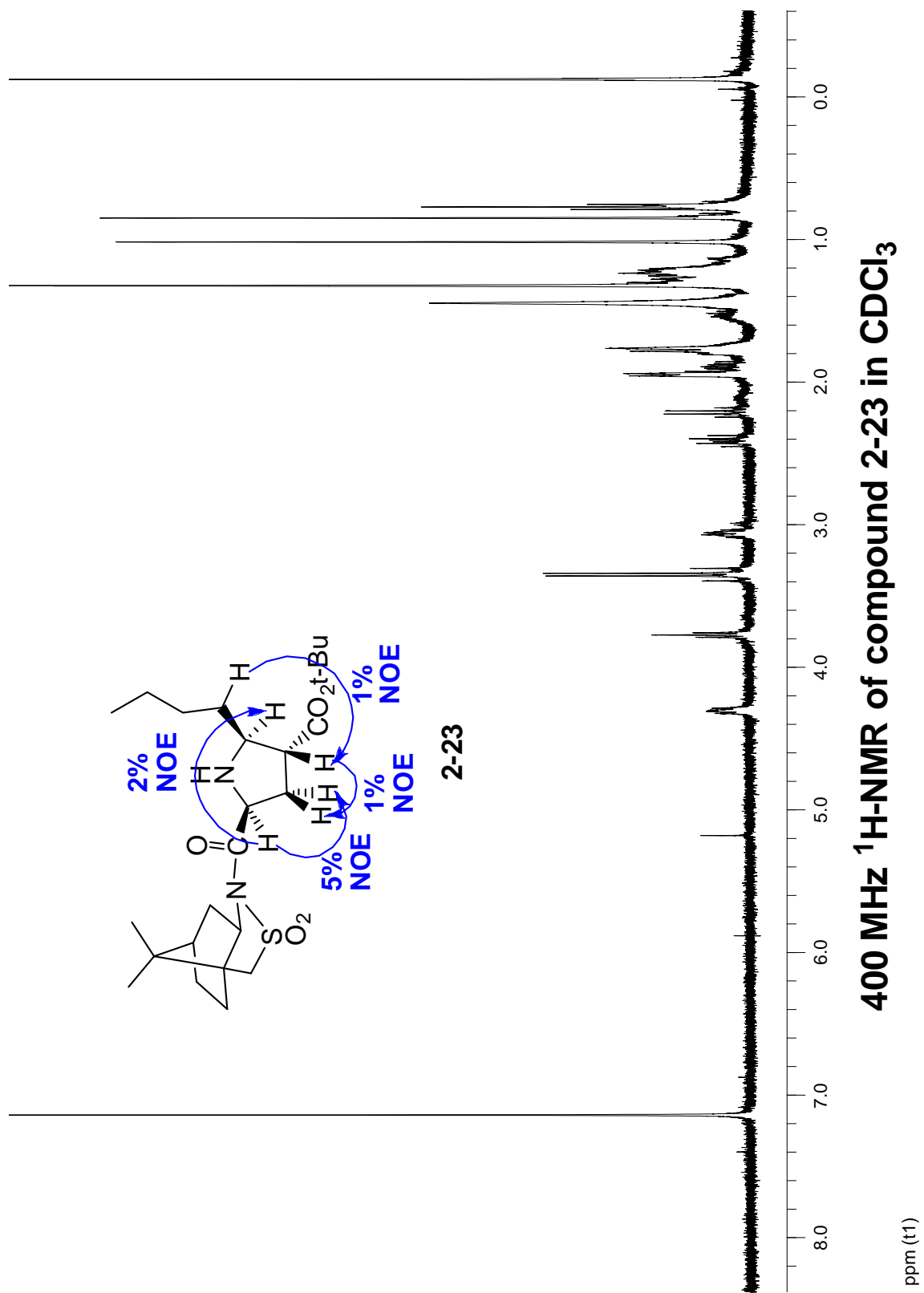


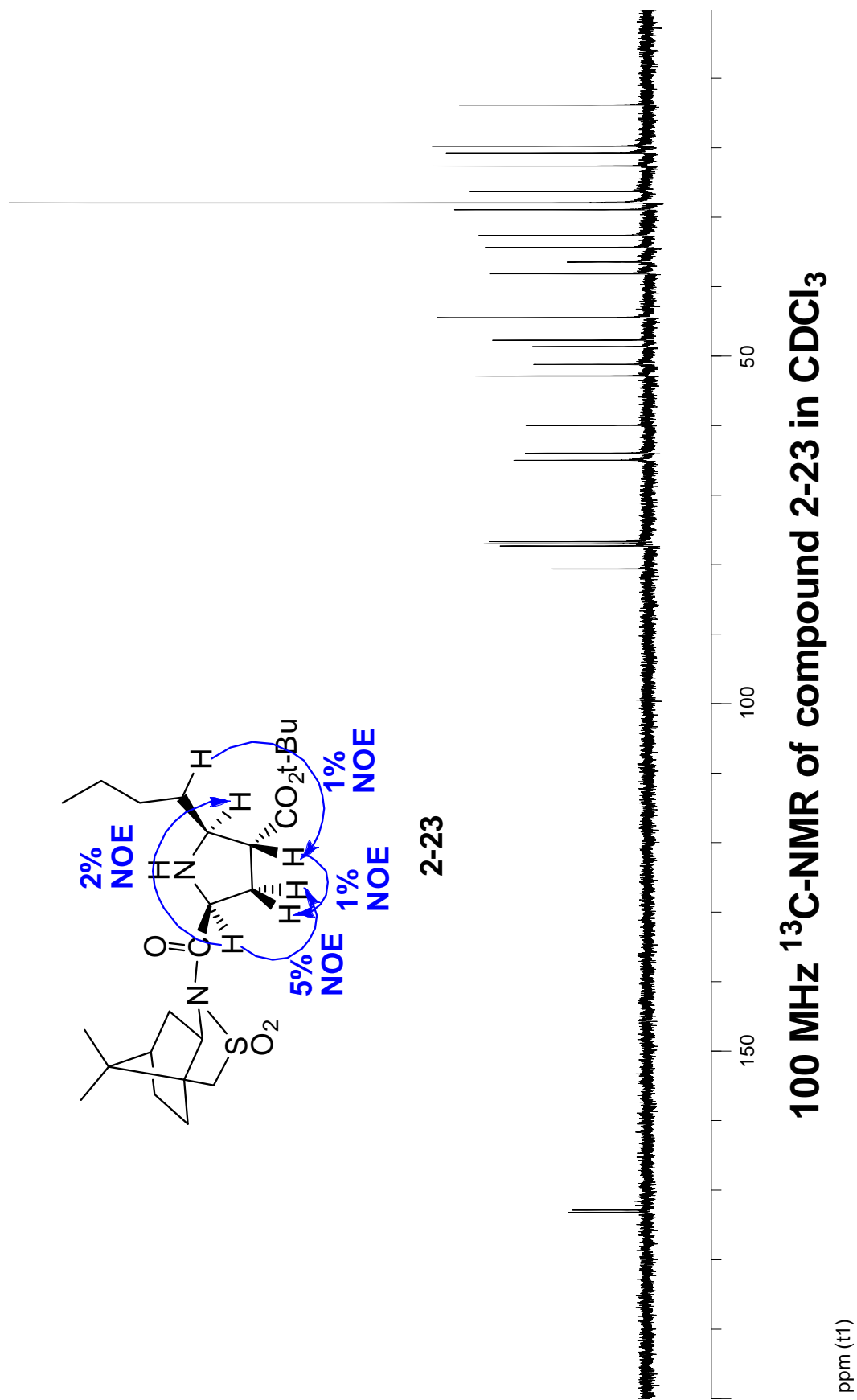


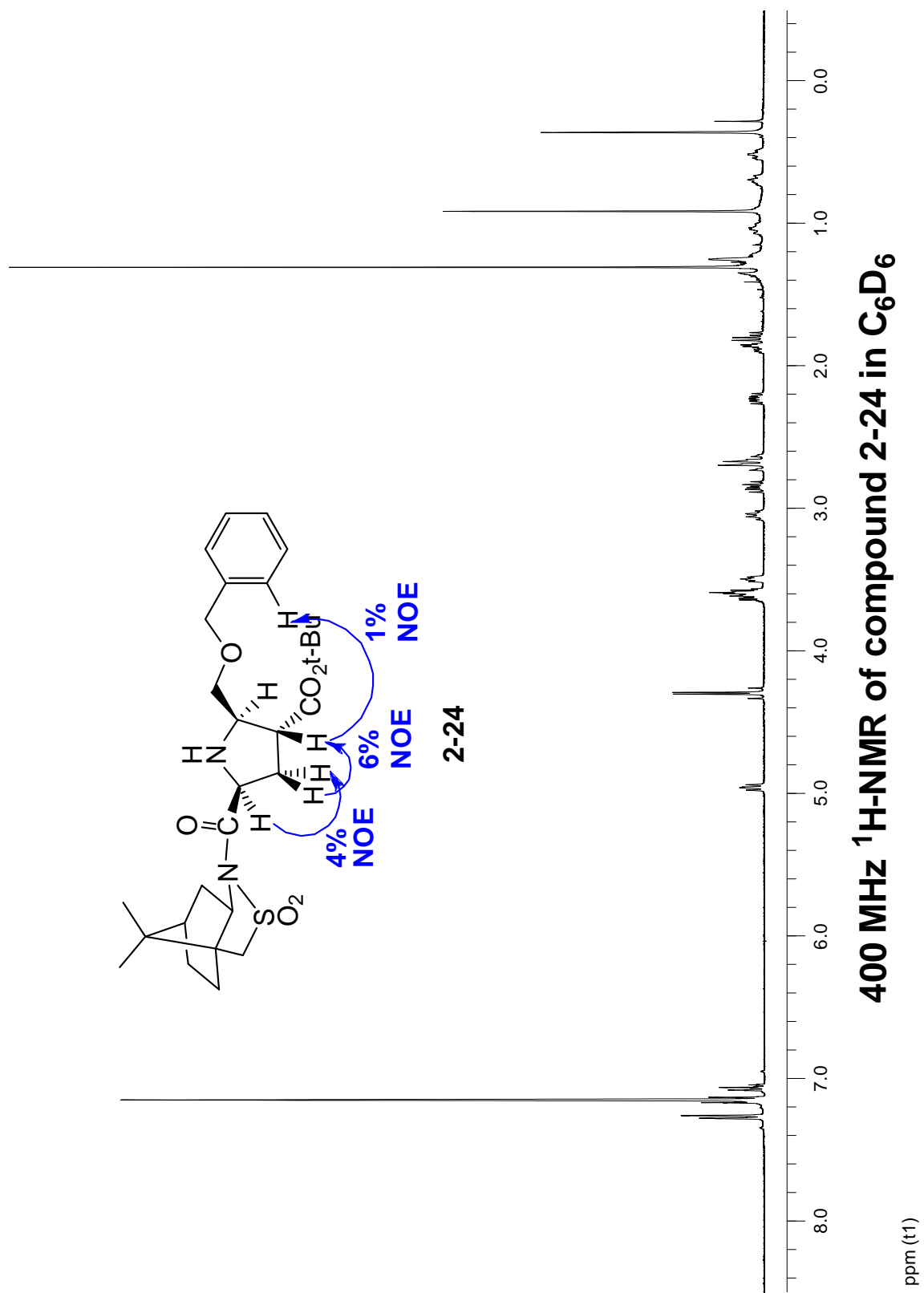


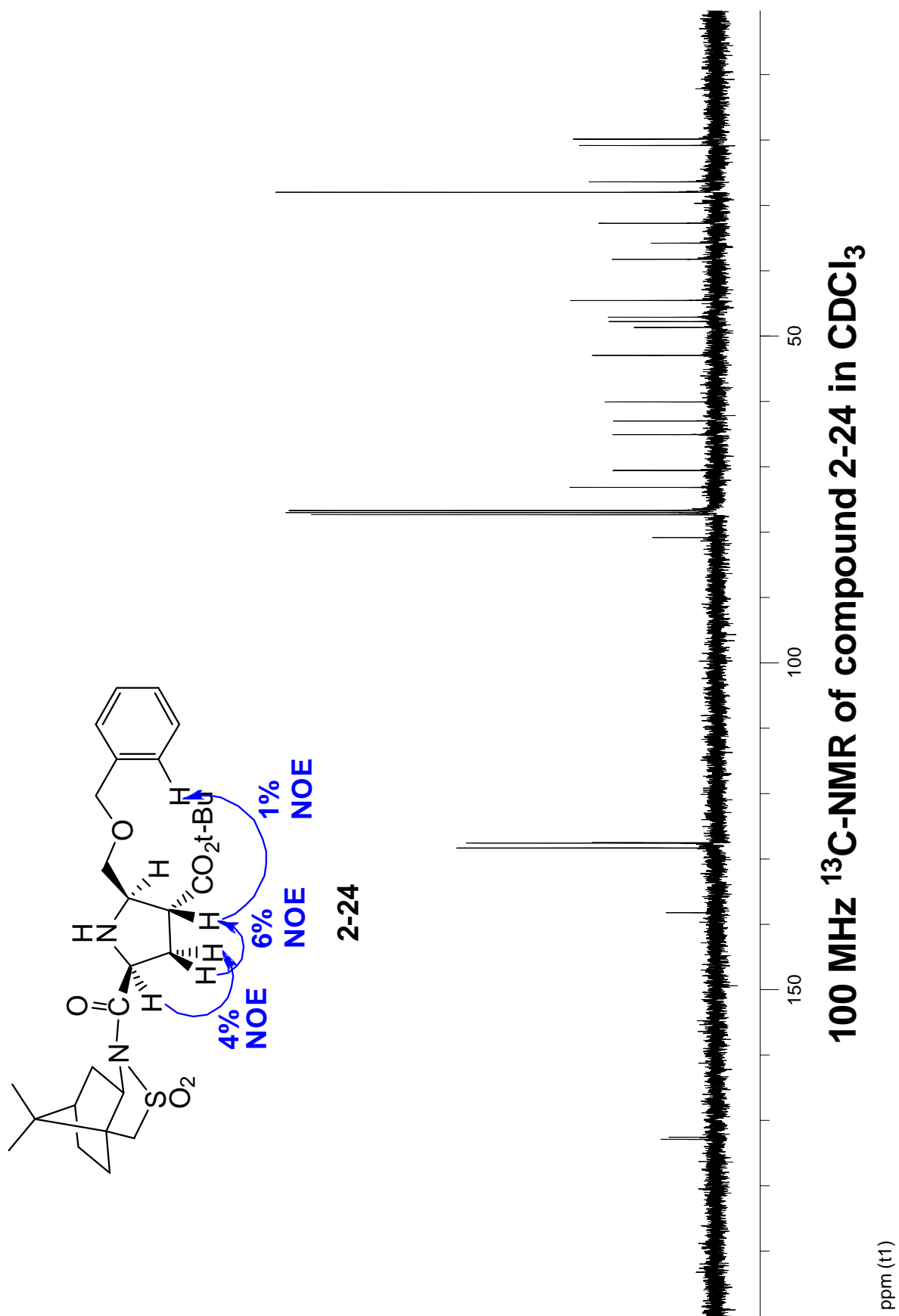


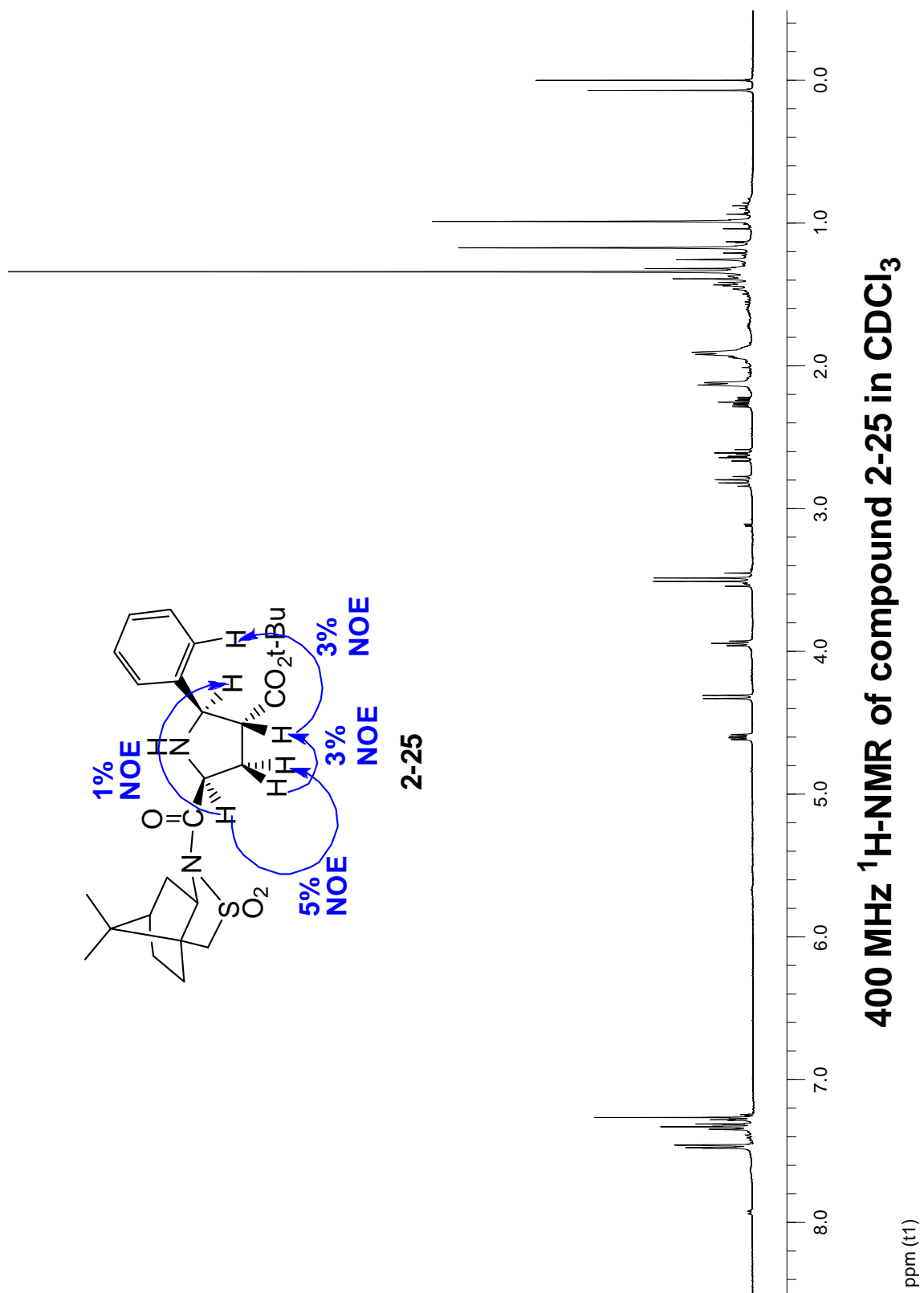


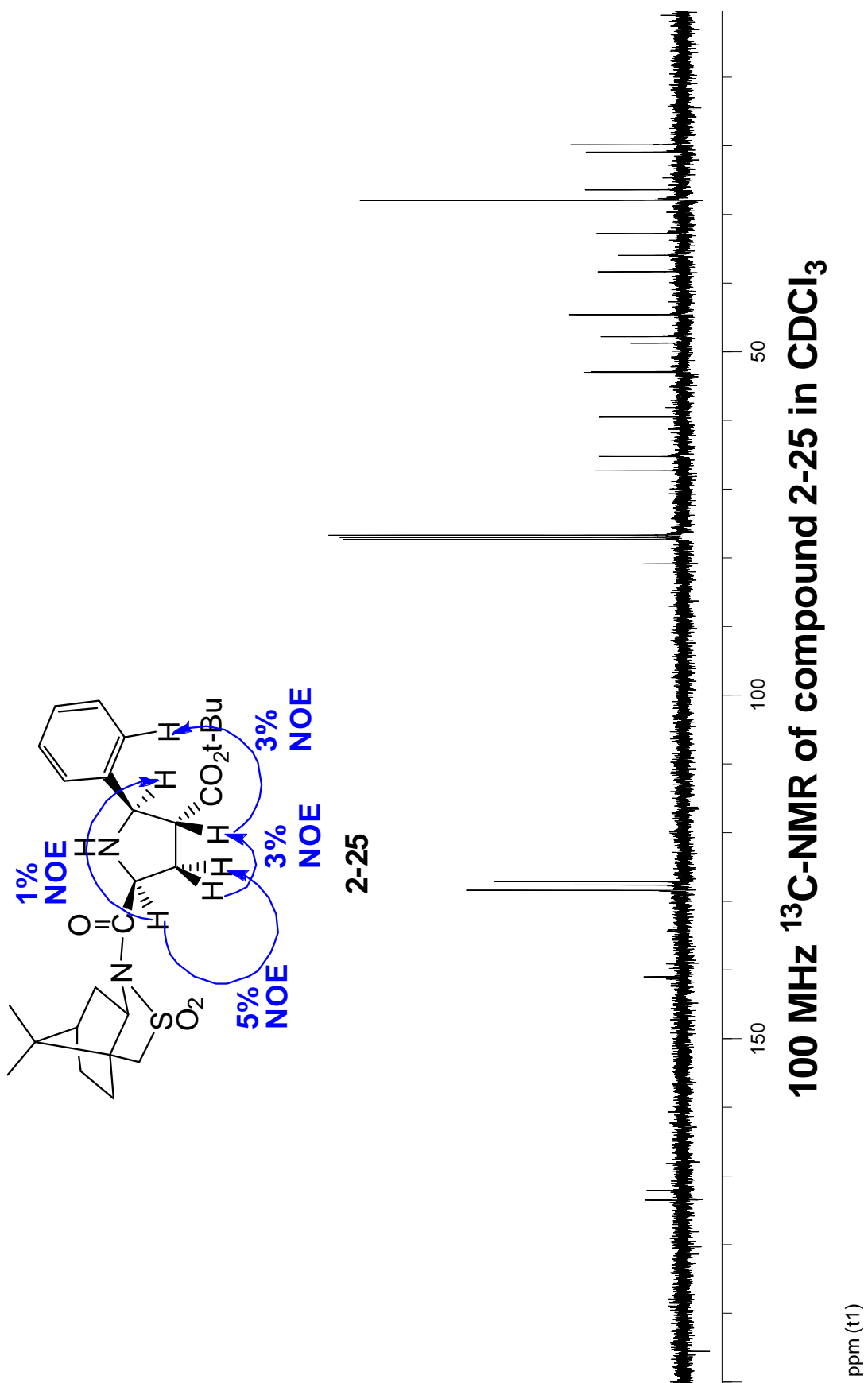


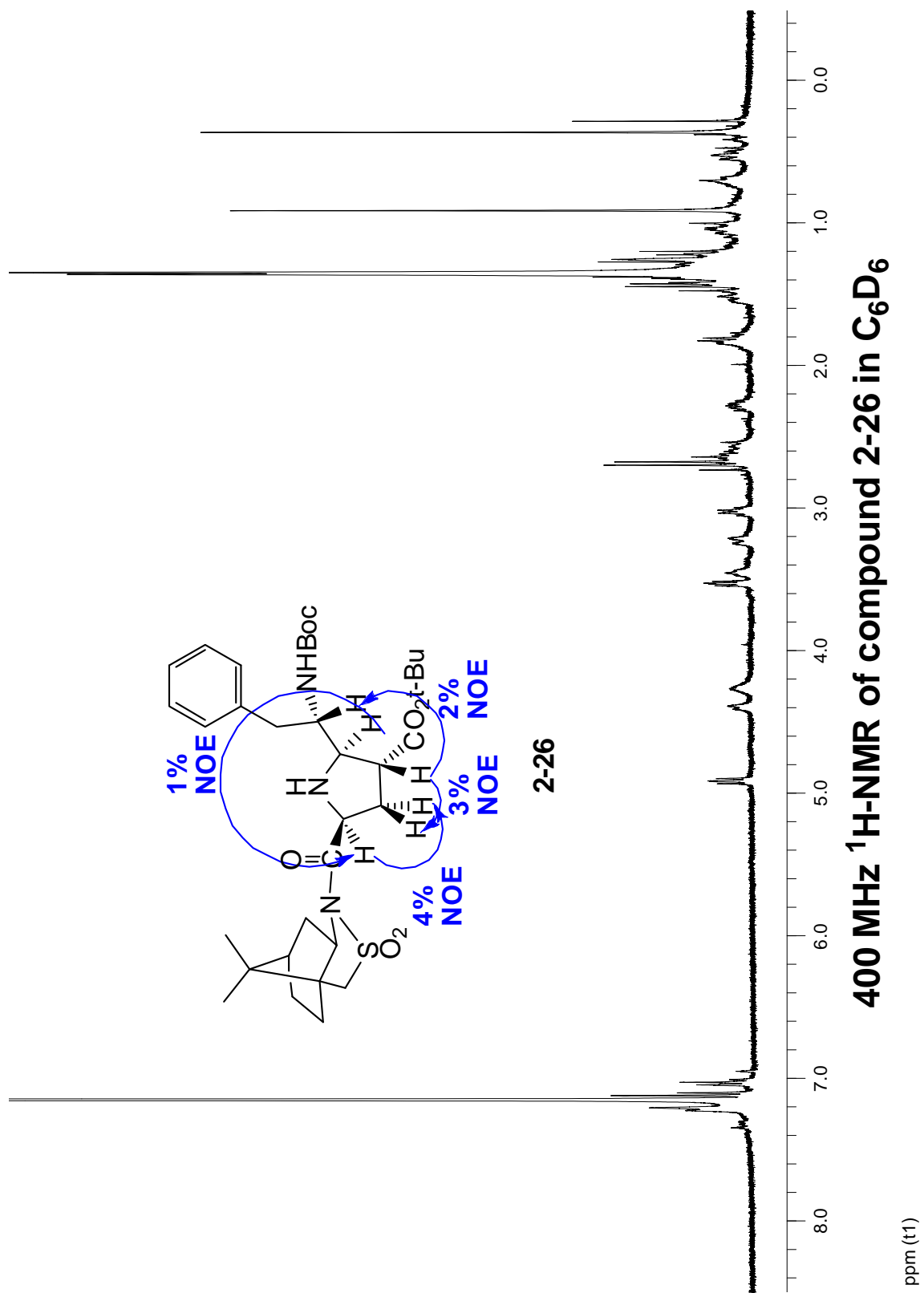


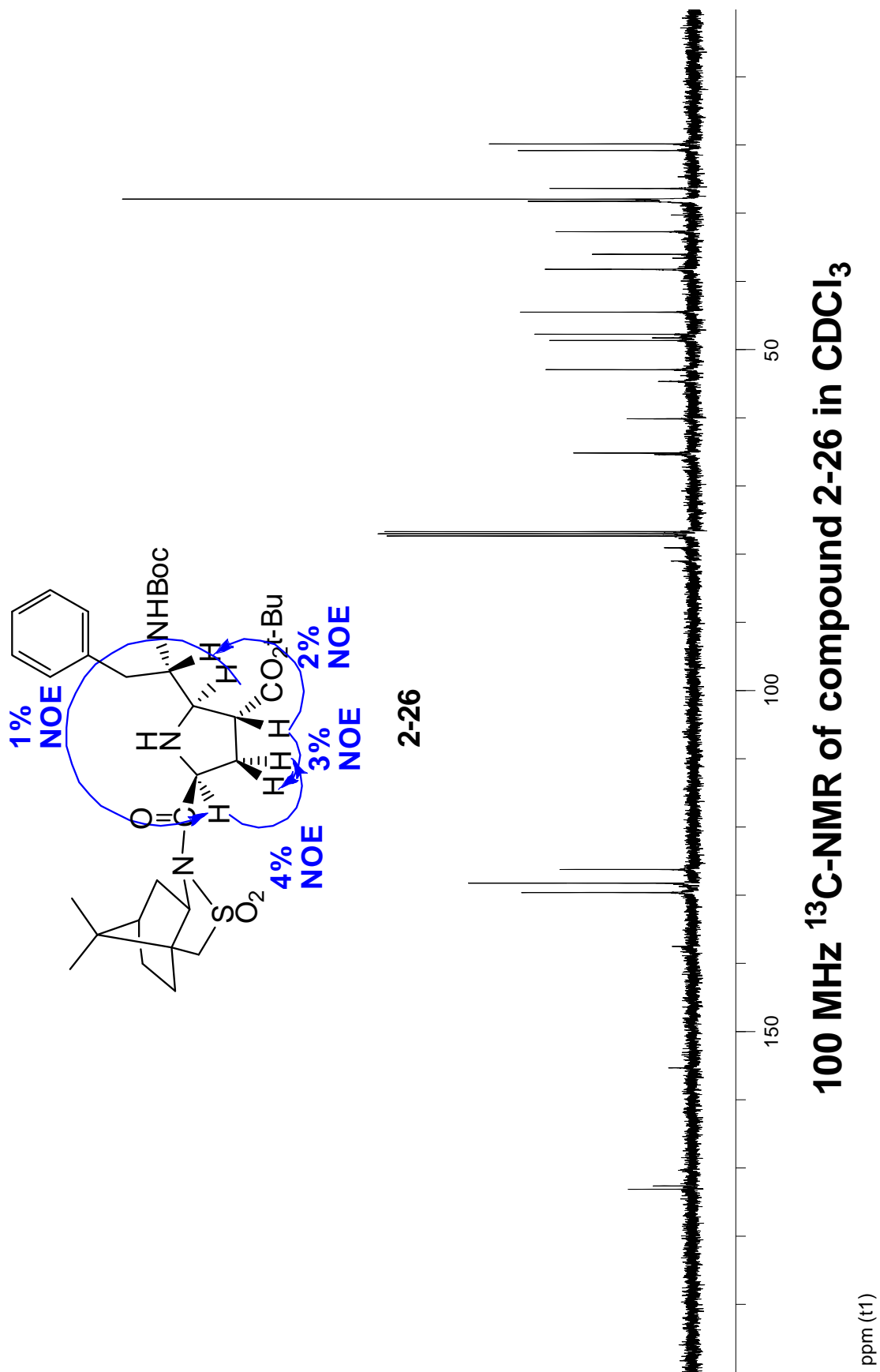


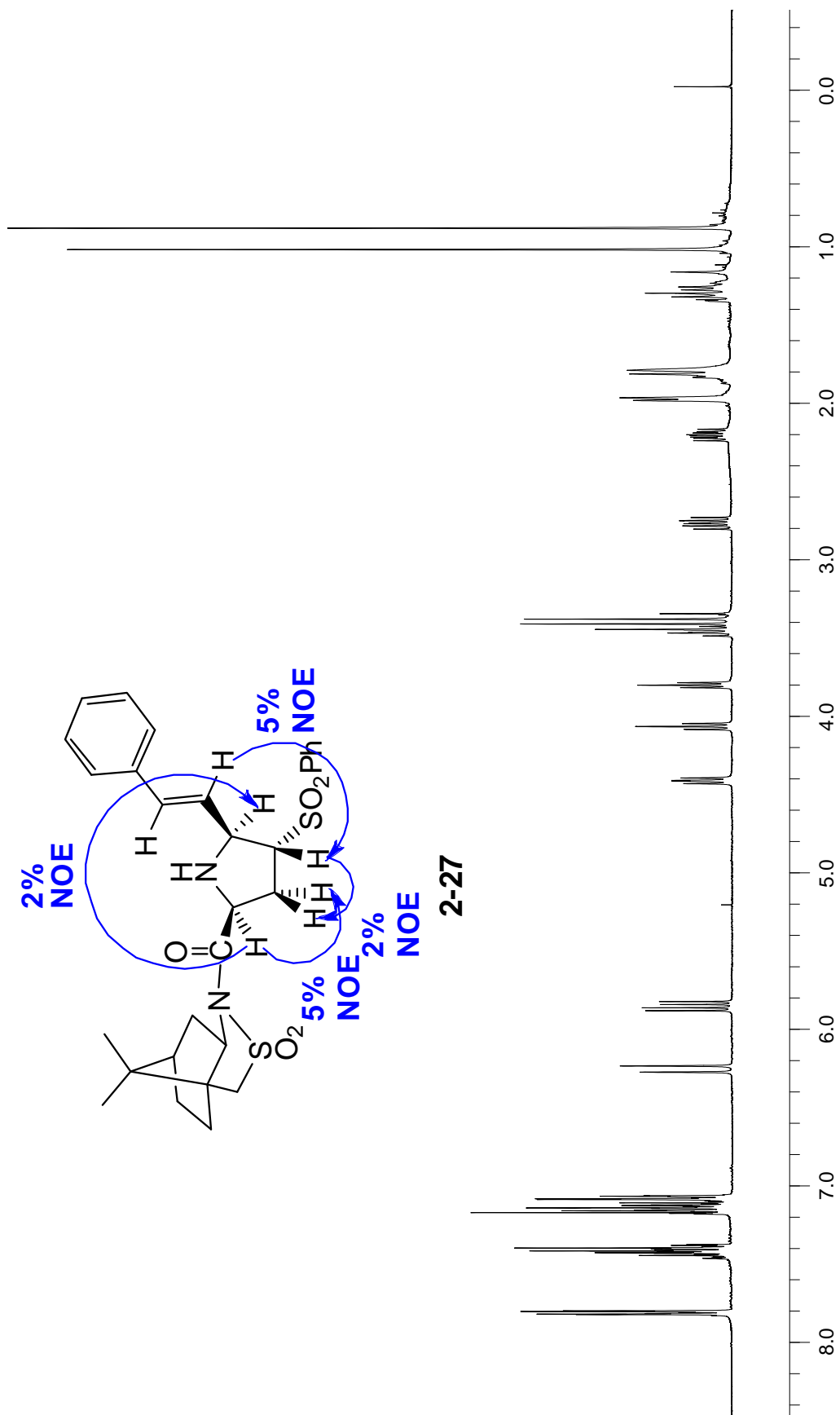


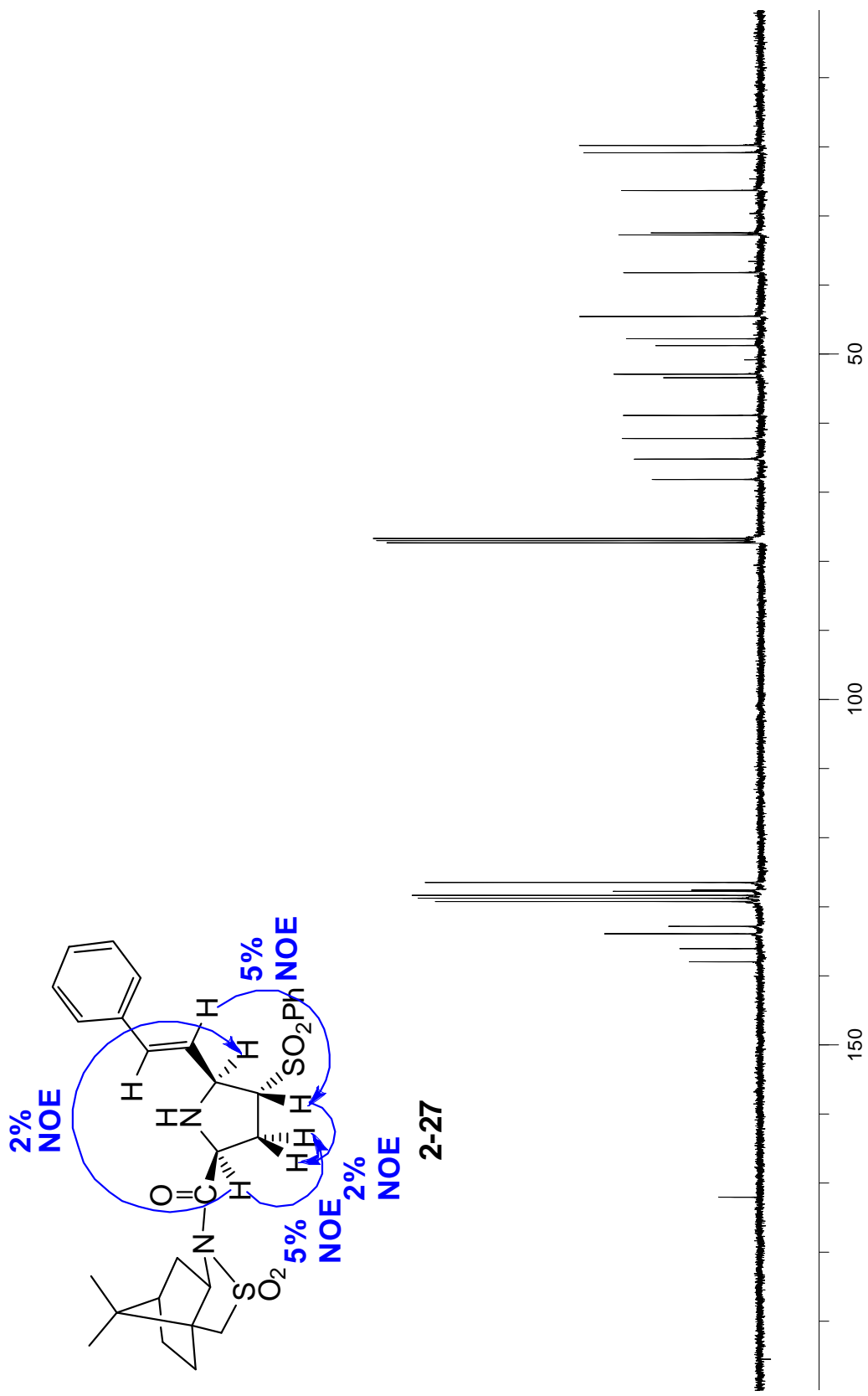


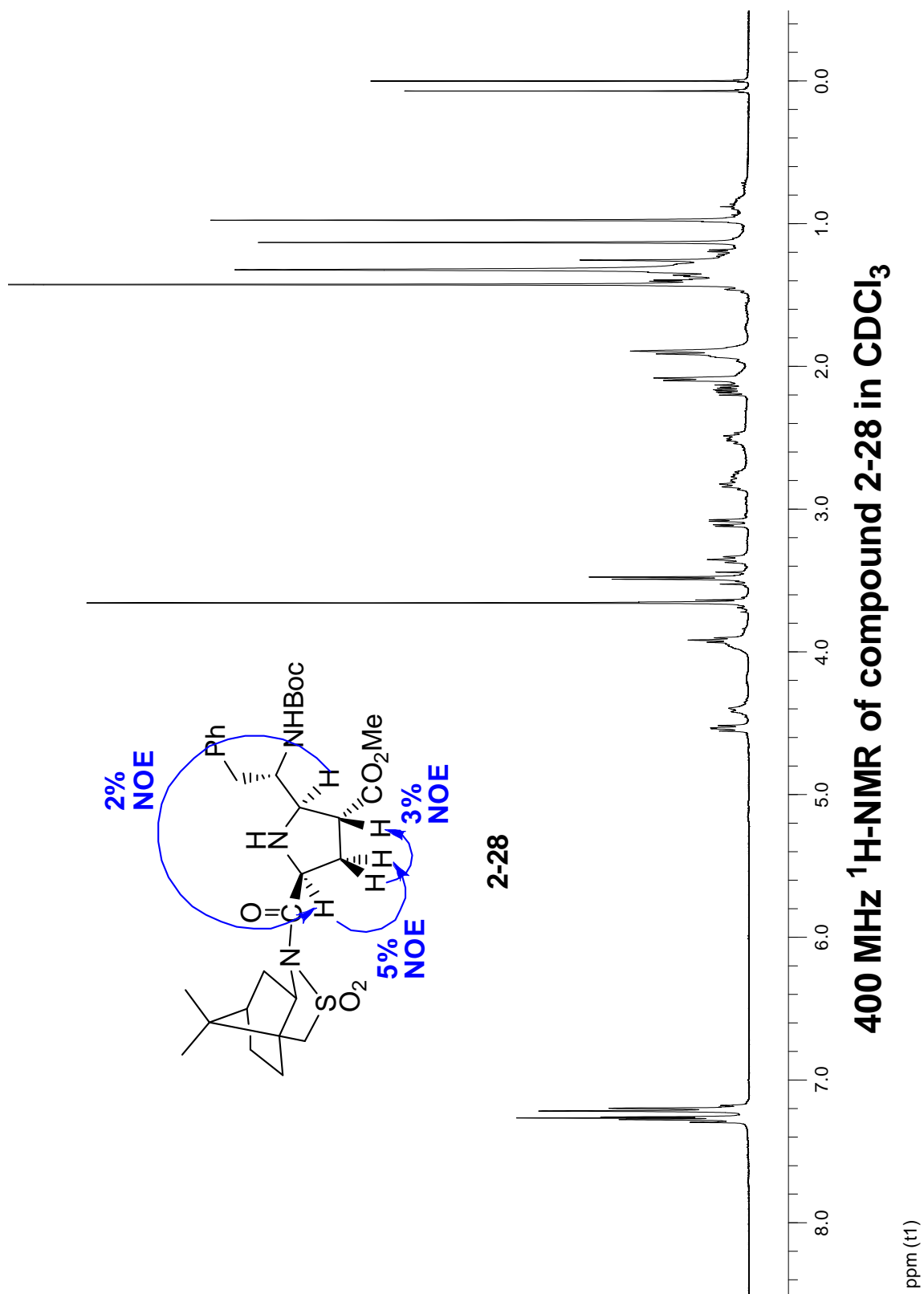


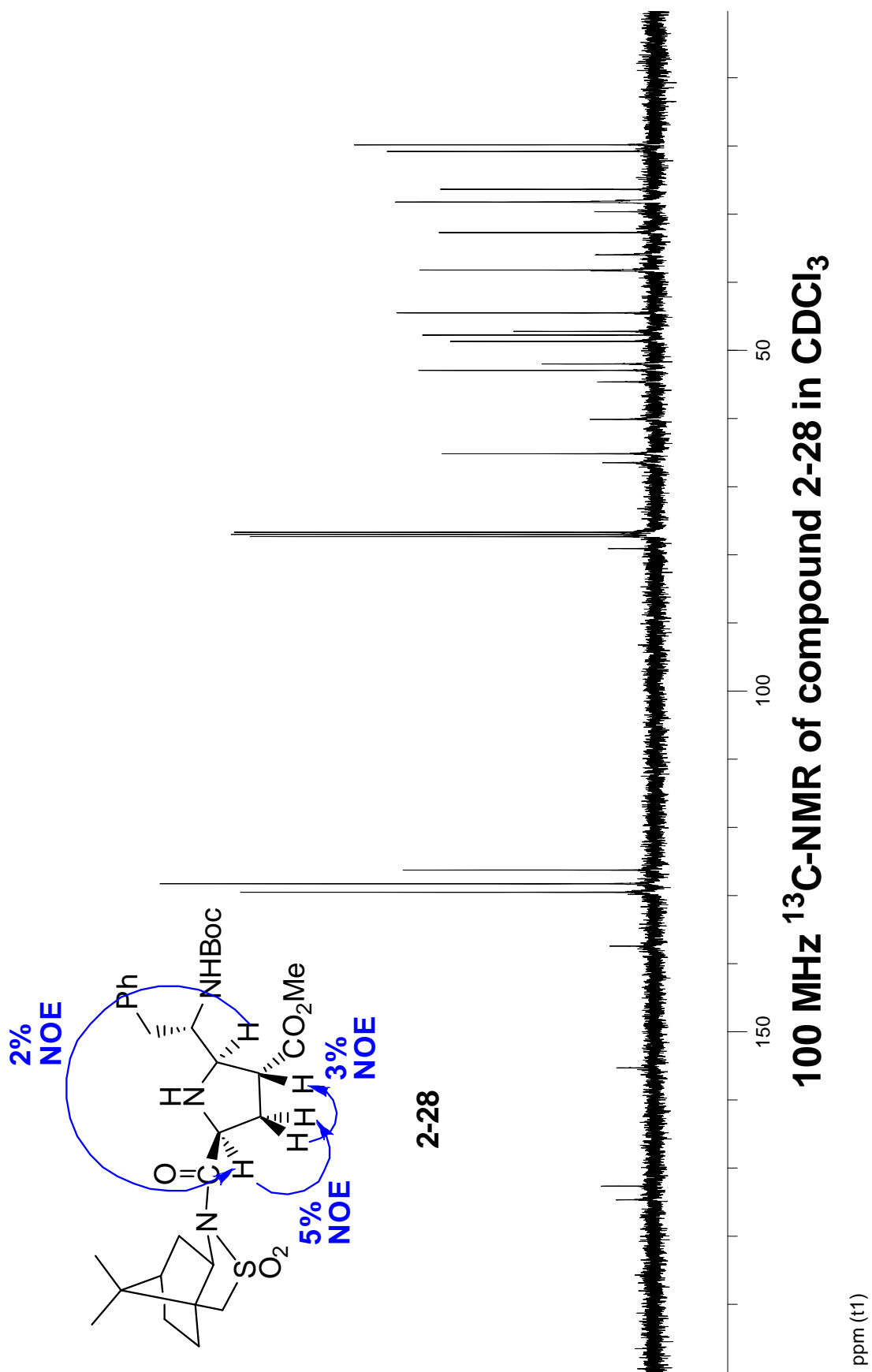


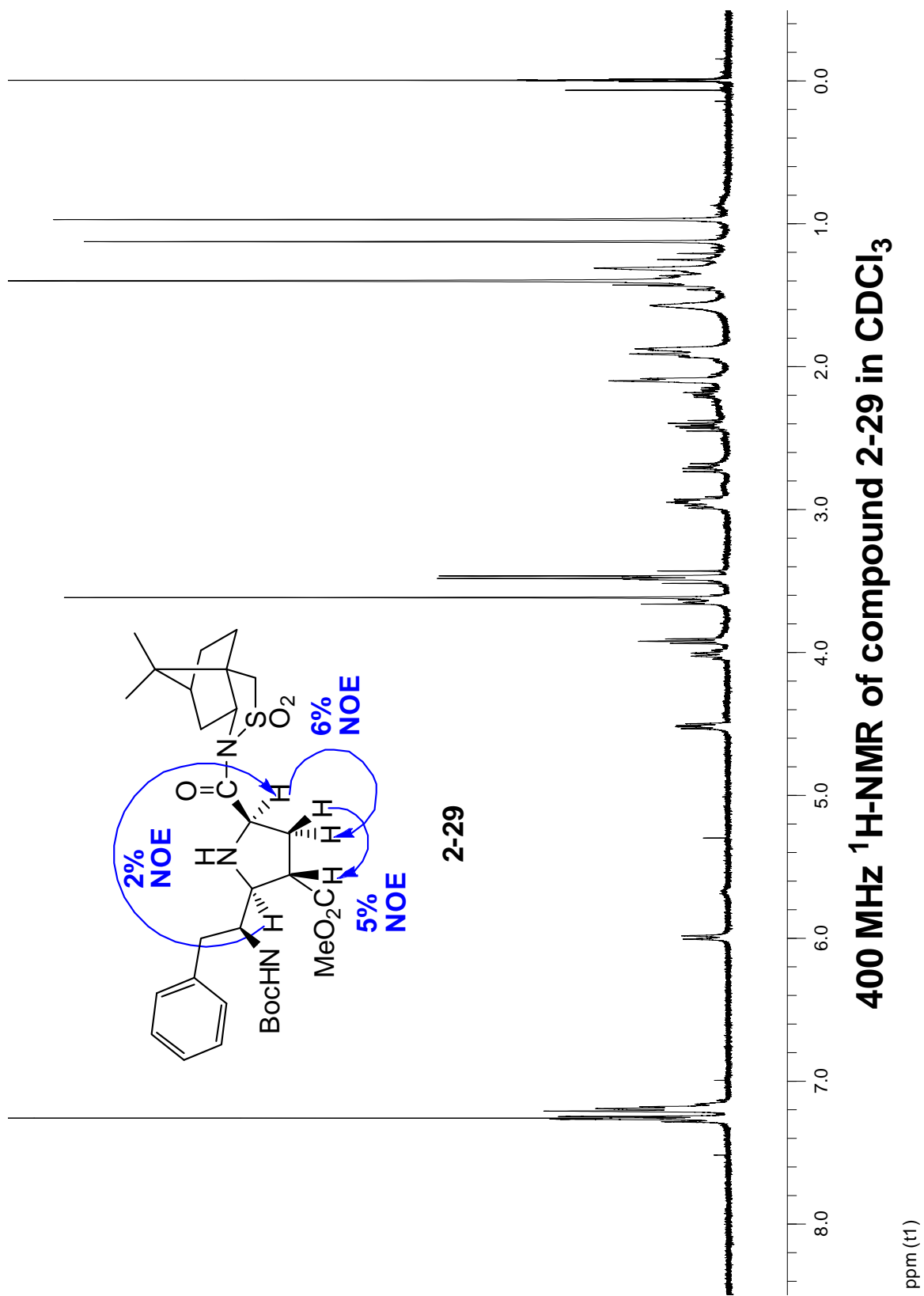


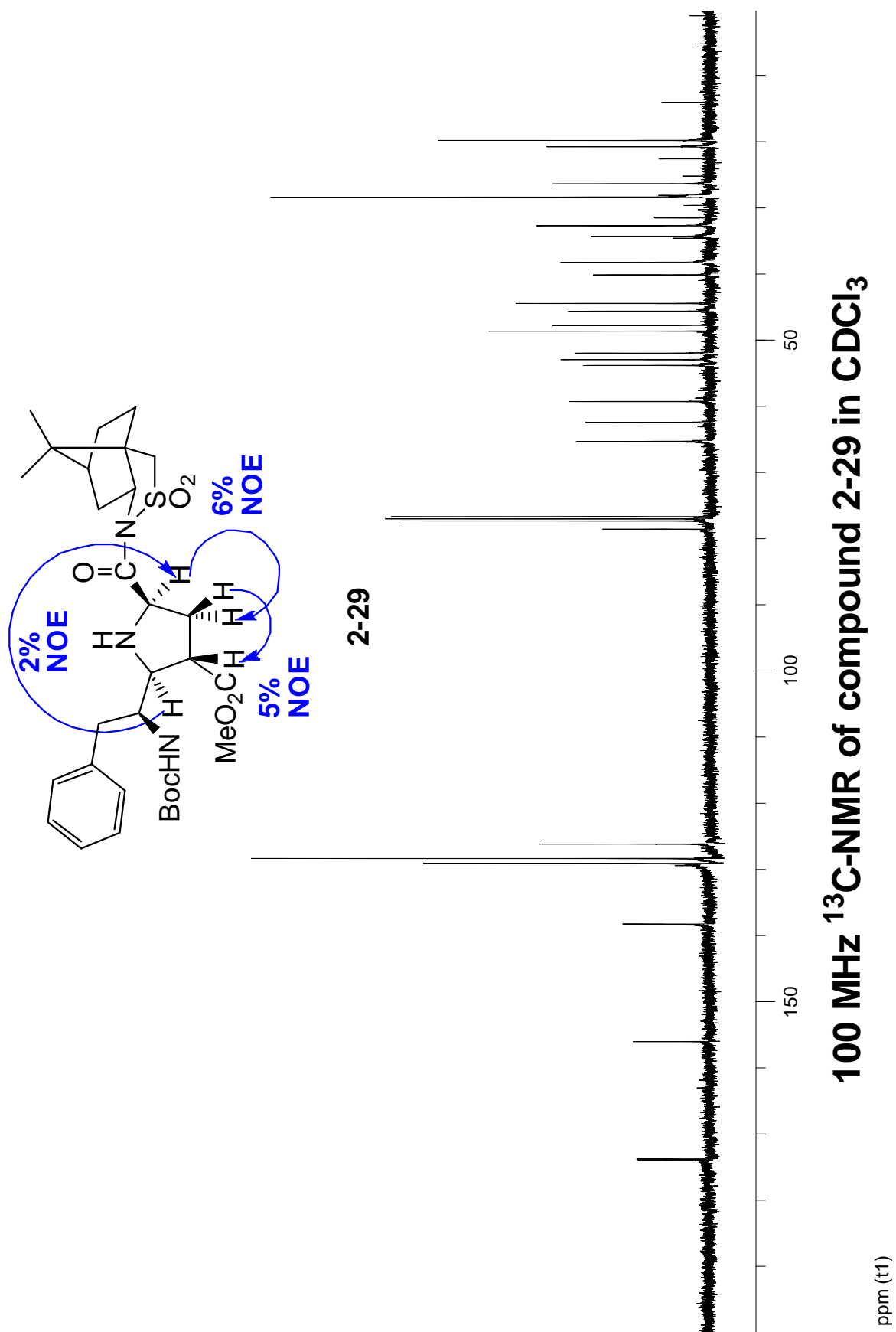


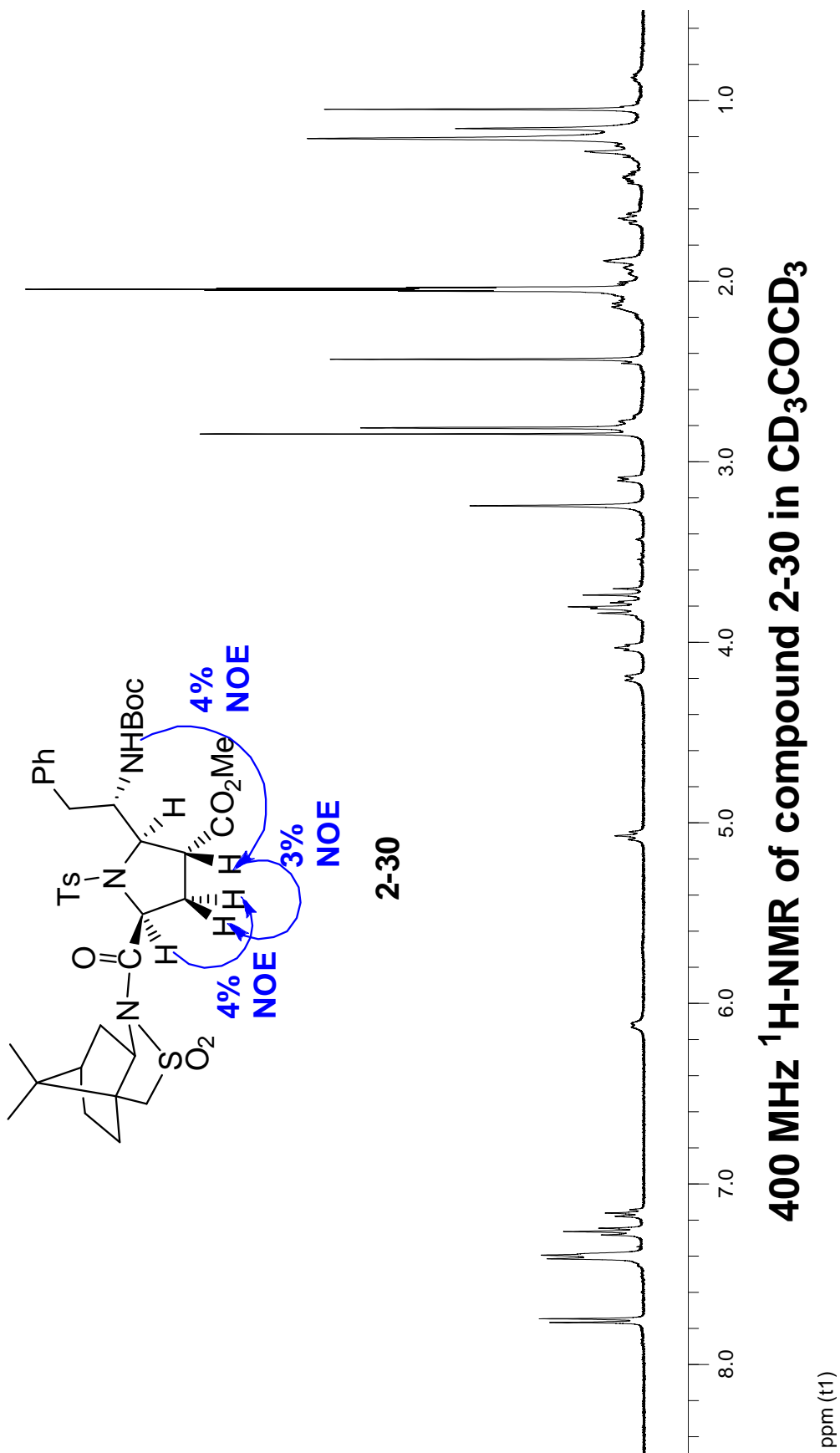


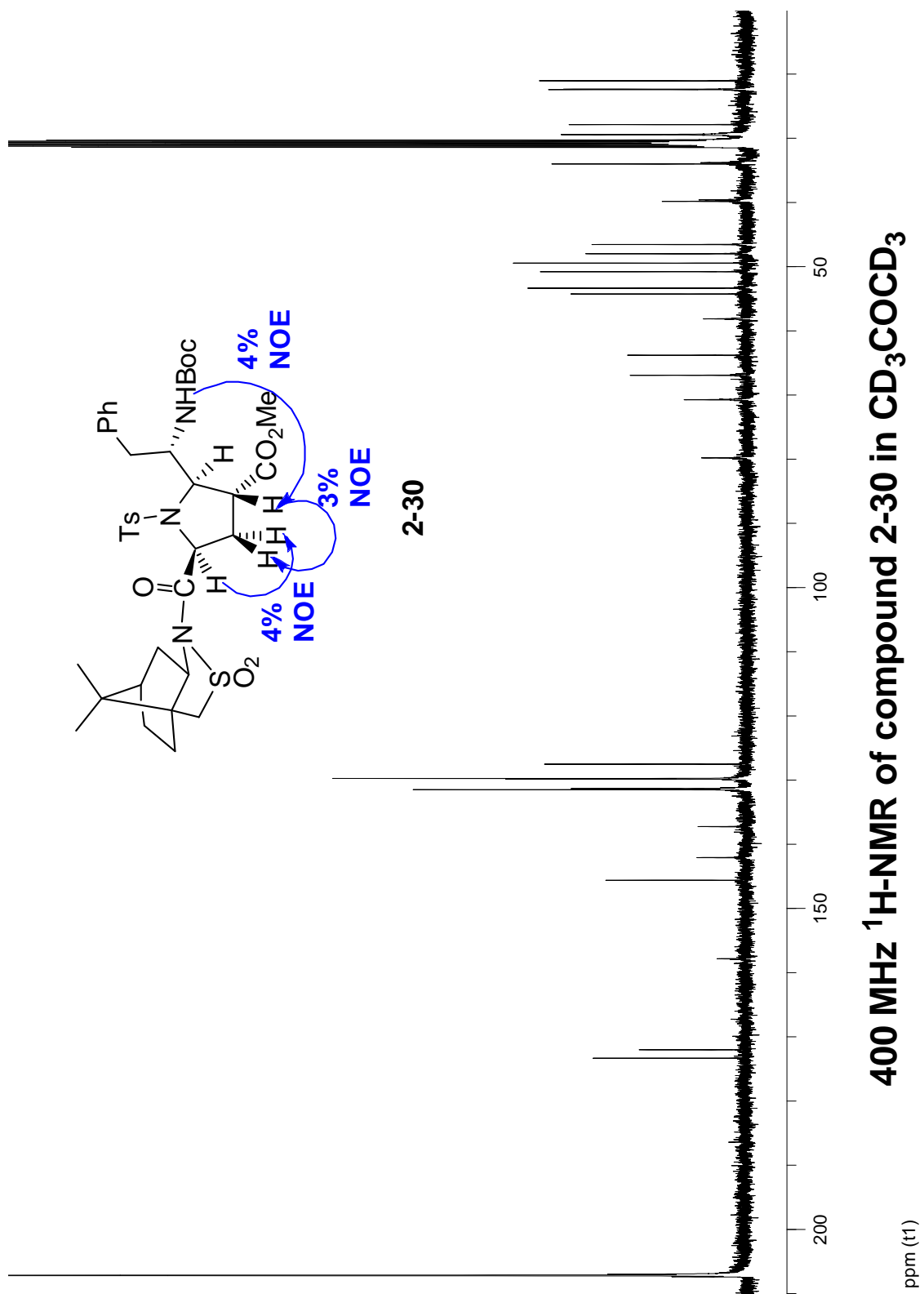


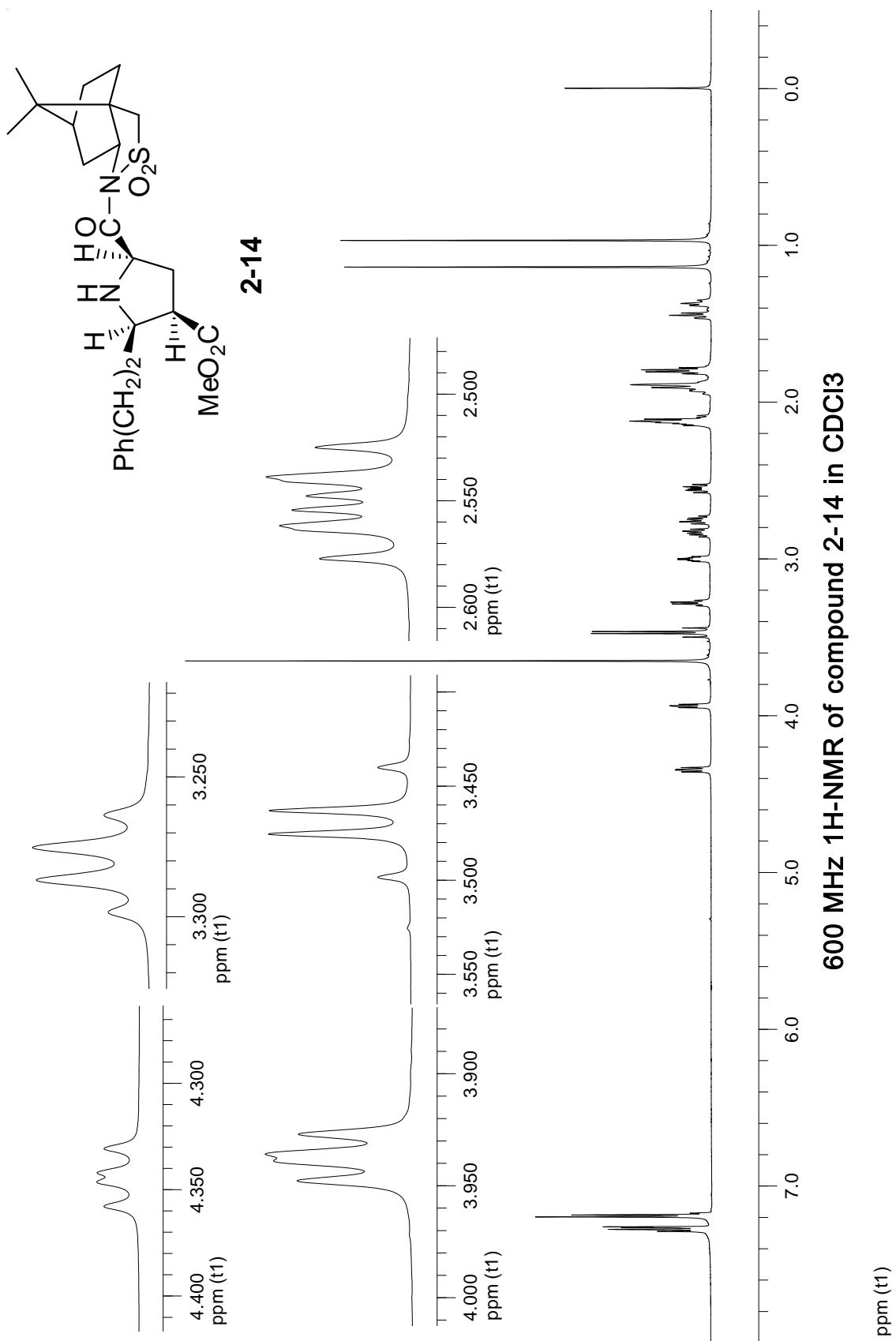


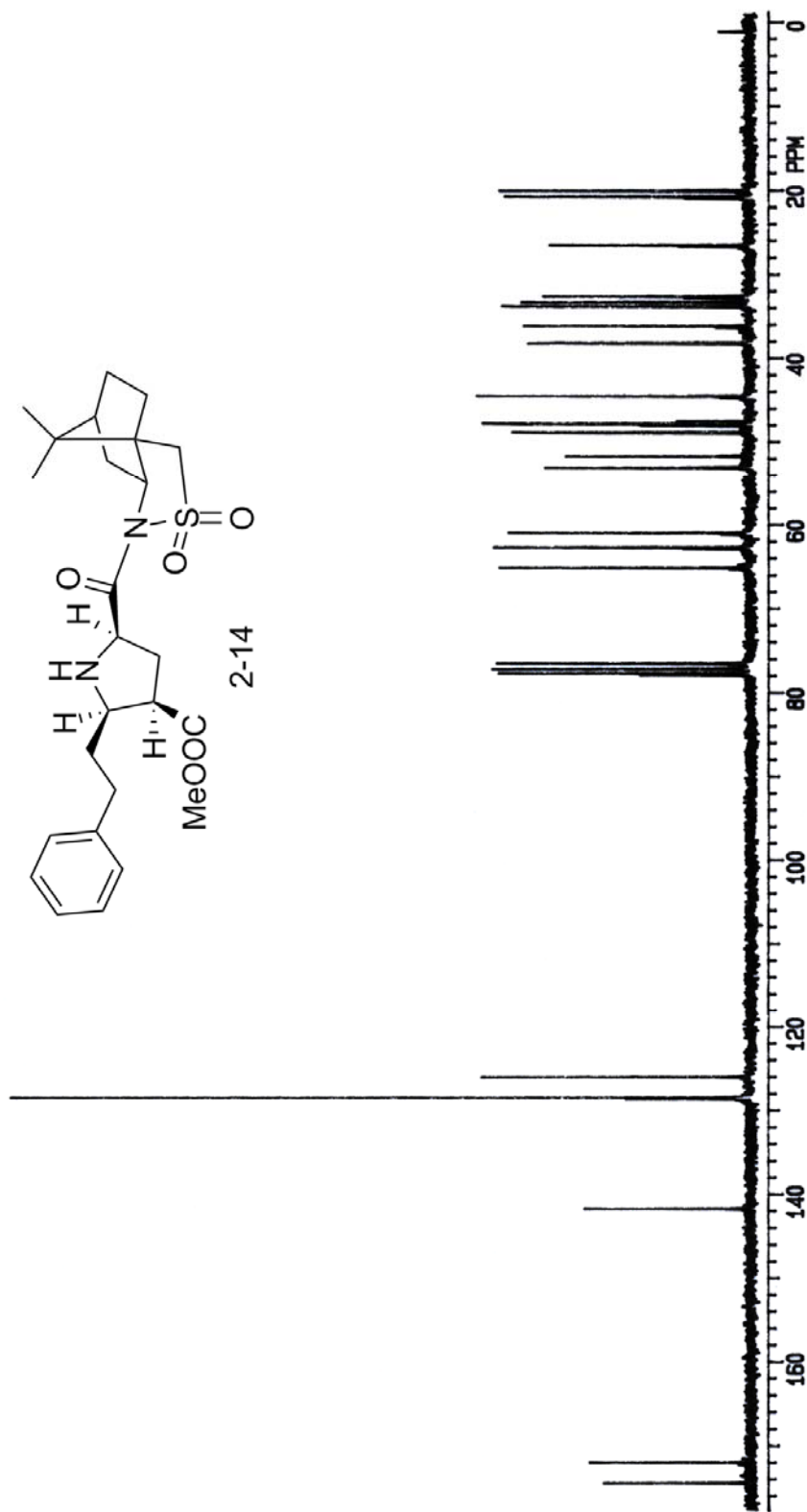


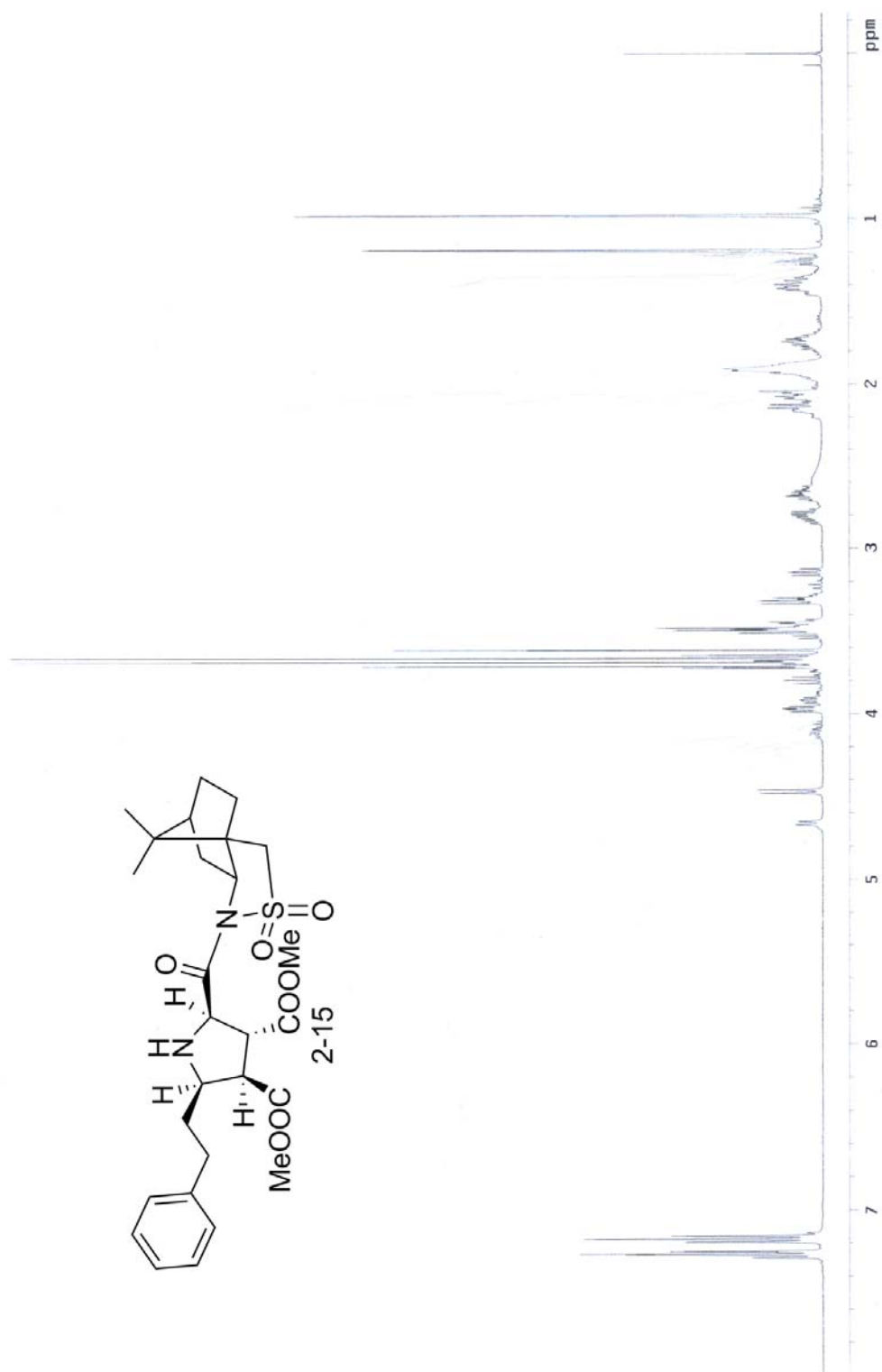


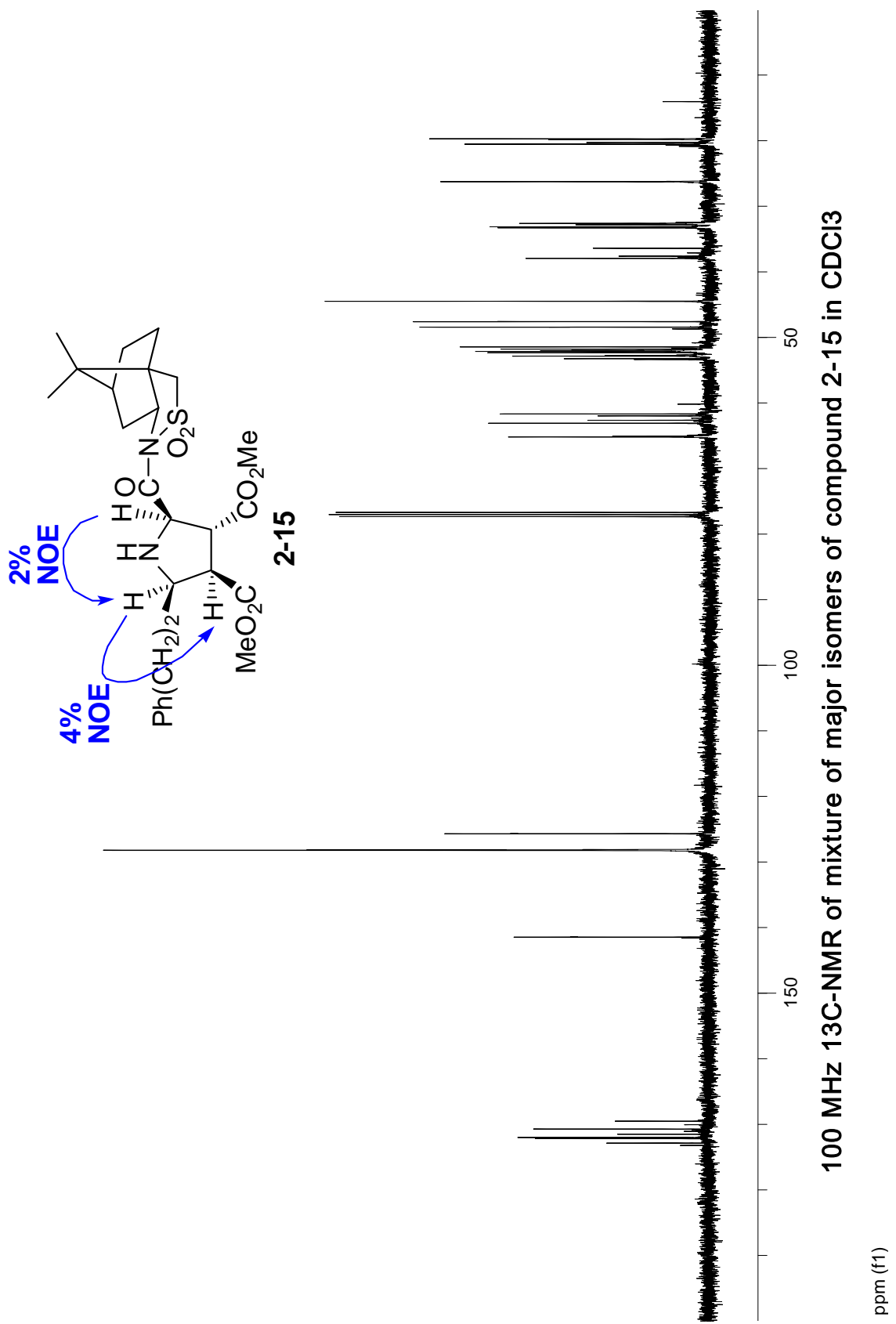


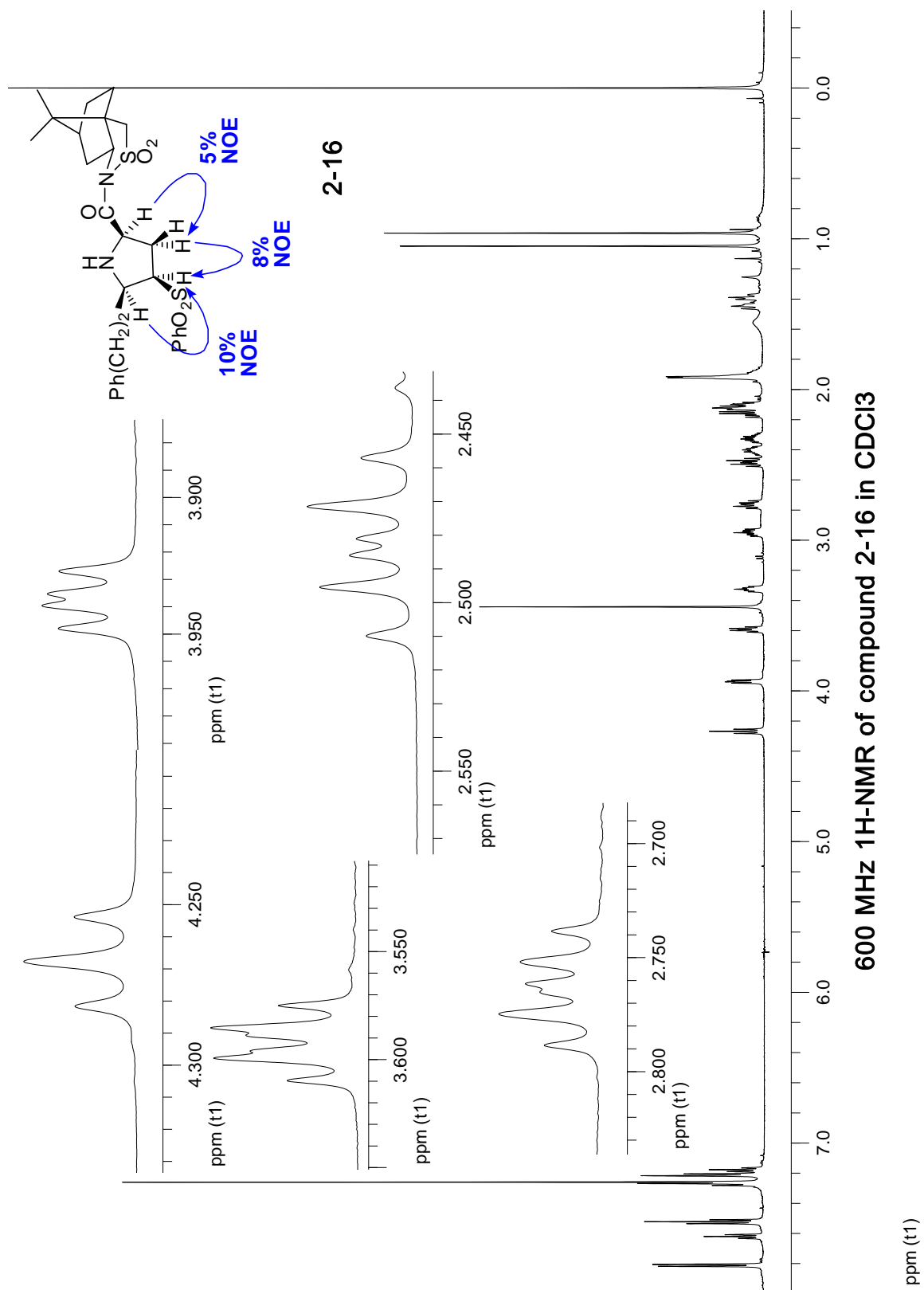


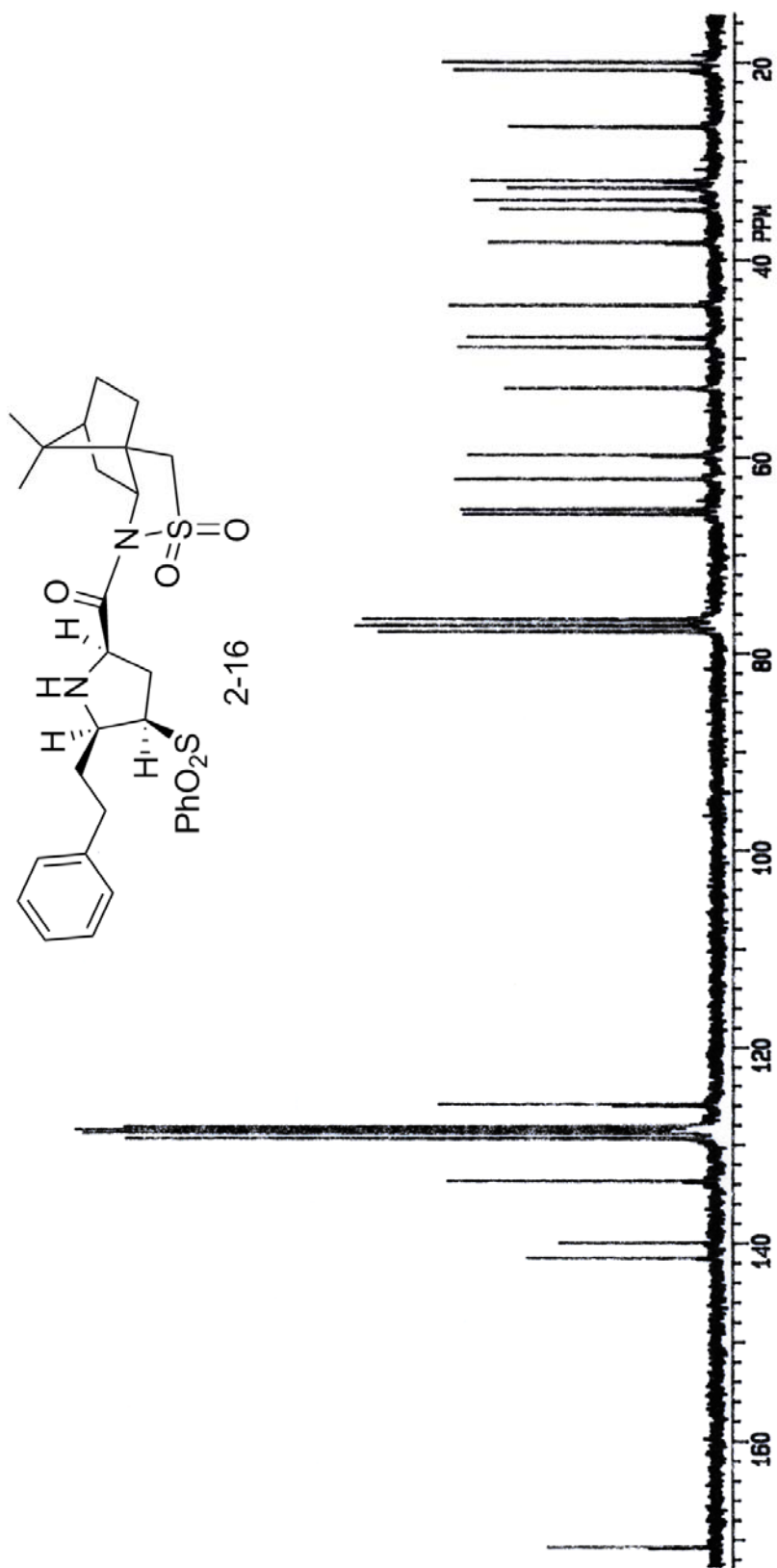


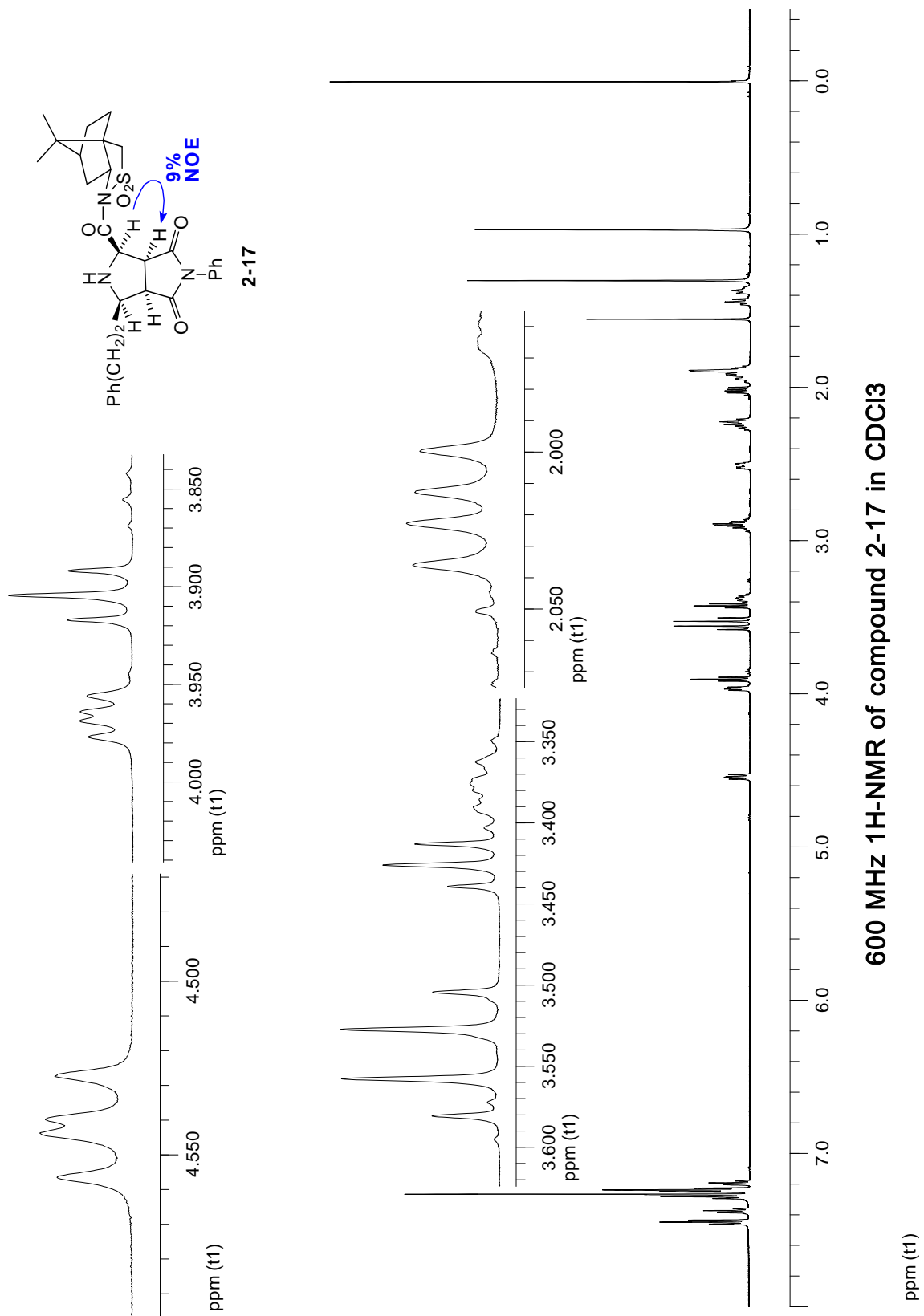
50 MHz ¹³C-NMR of compound 2-14 in CDCl₃

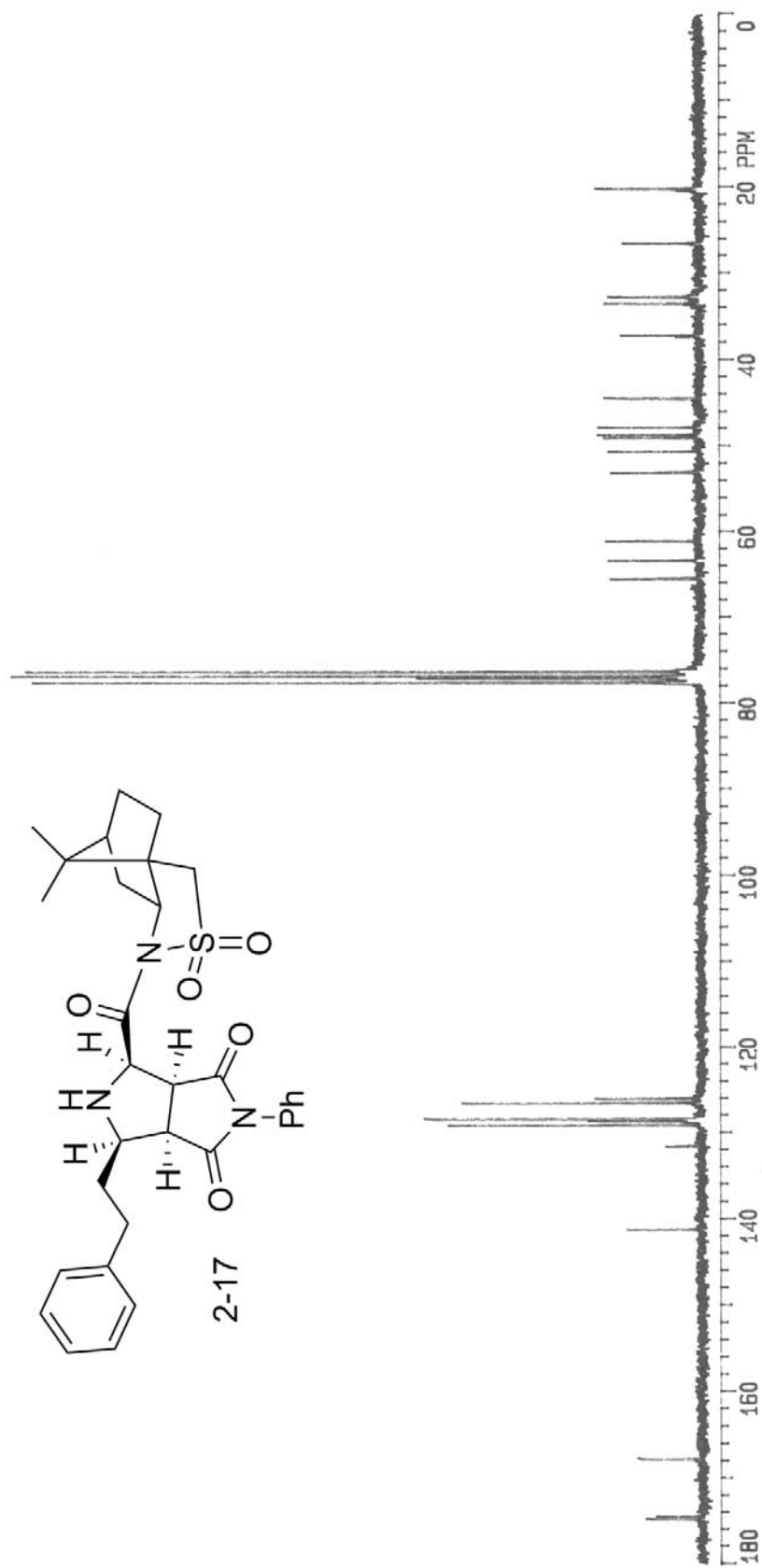
400 MHz ¹H-NMR of mixture of major isomers of compound 2-15 in CDCl₃

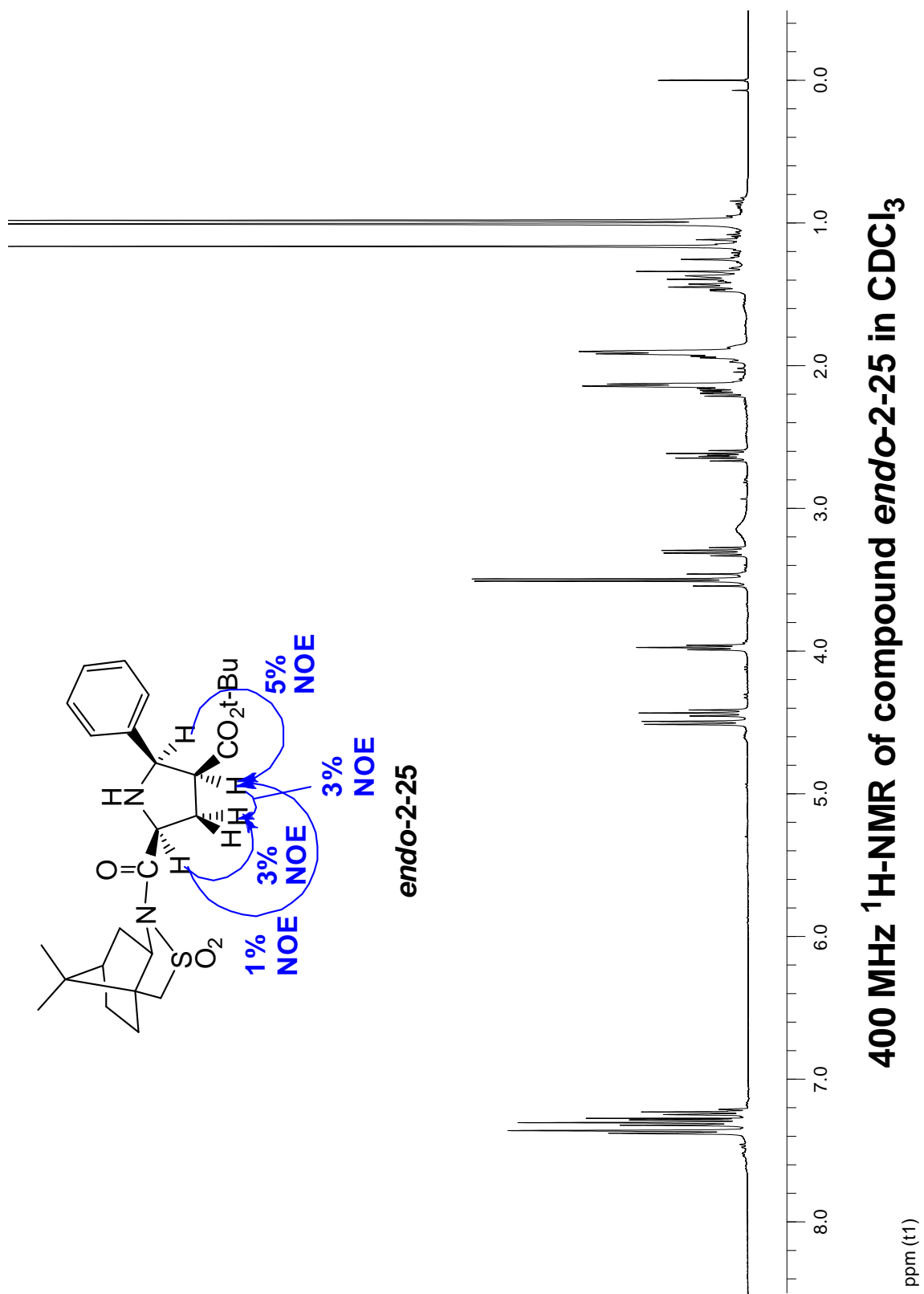


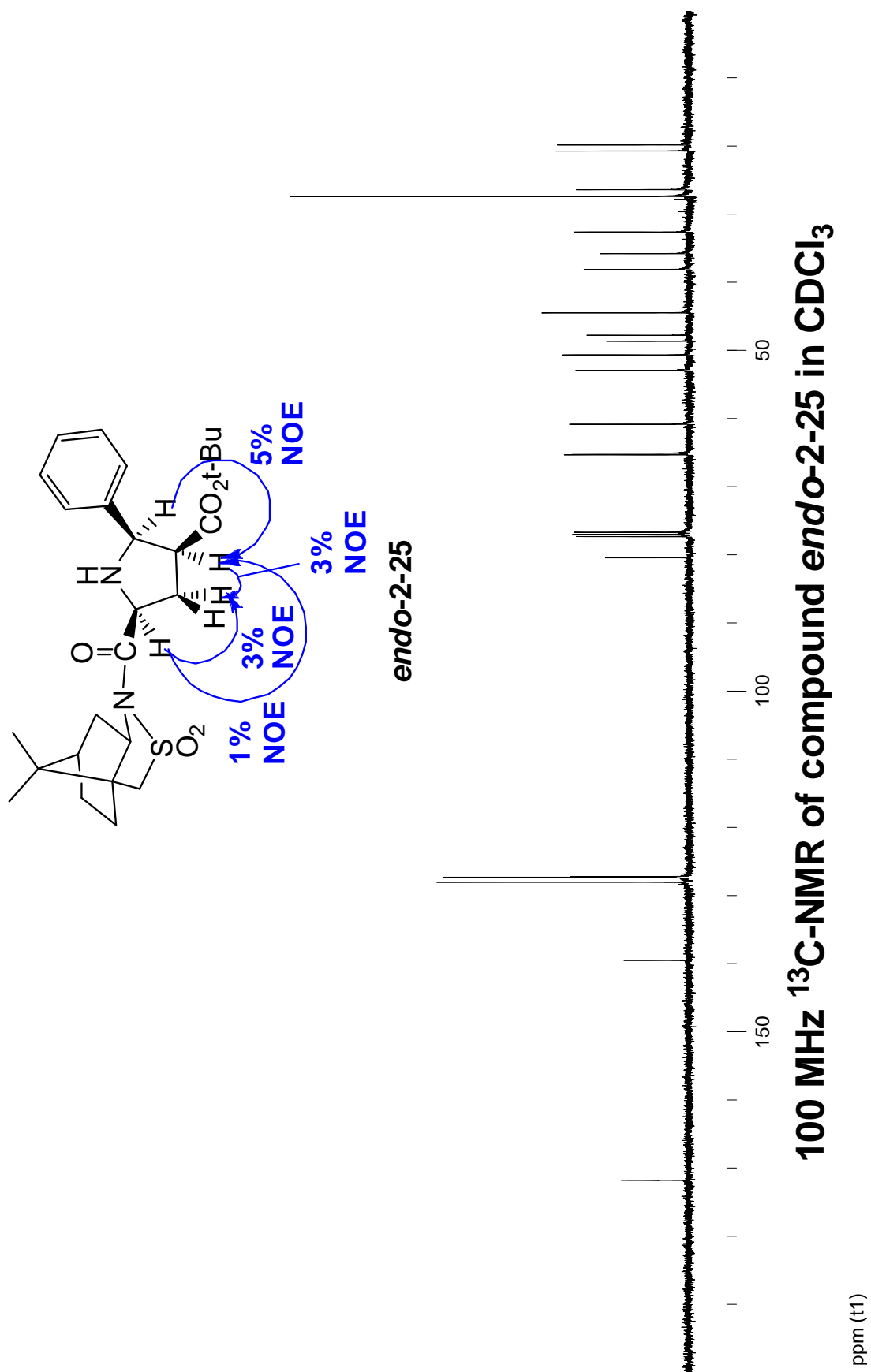


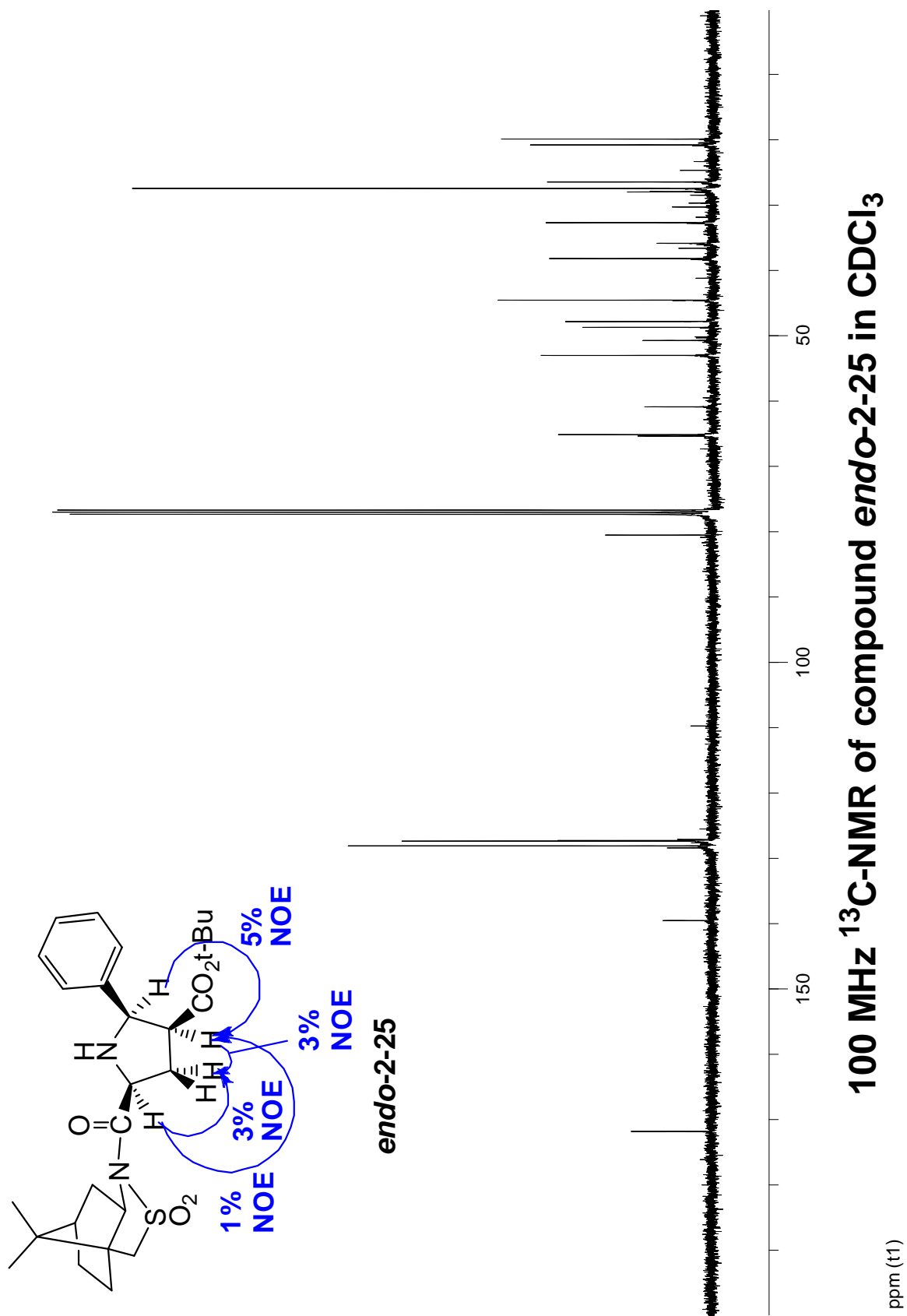
50 MHz ¹³C-NMR of compound 2-16 in CDCl₃



50 MHz ¹³C-NMR of compound 2-17 in CDCl₃

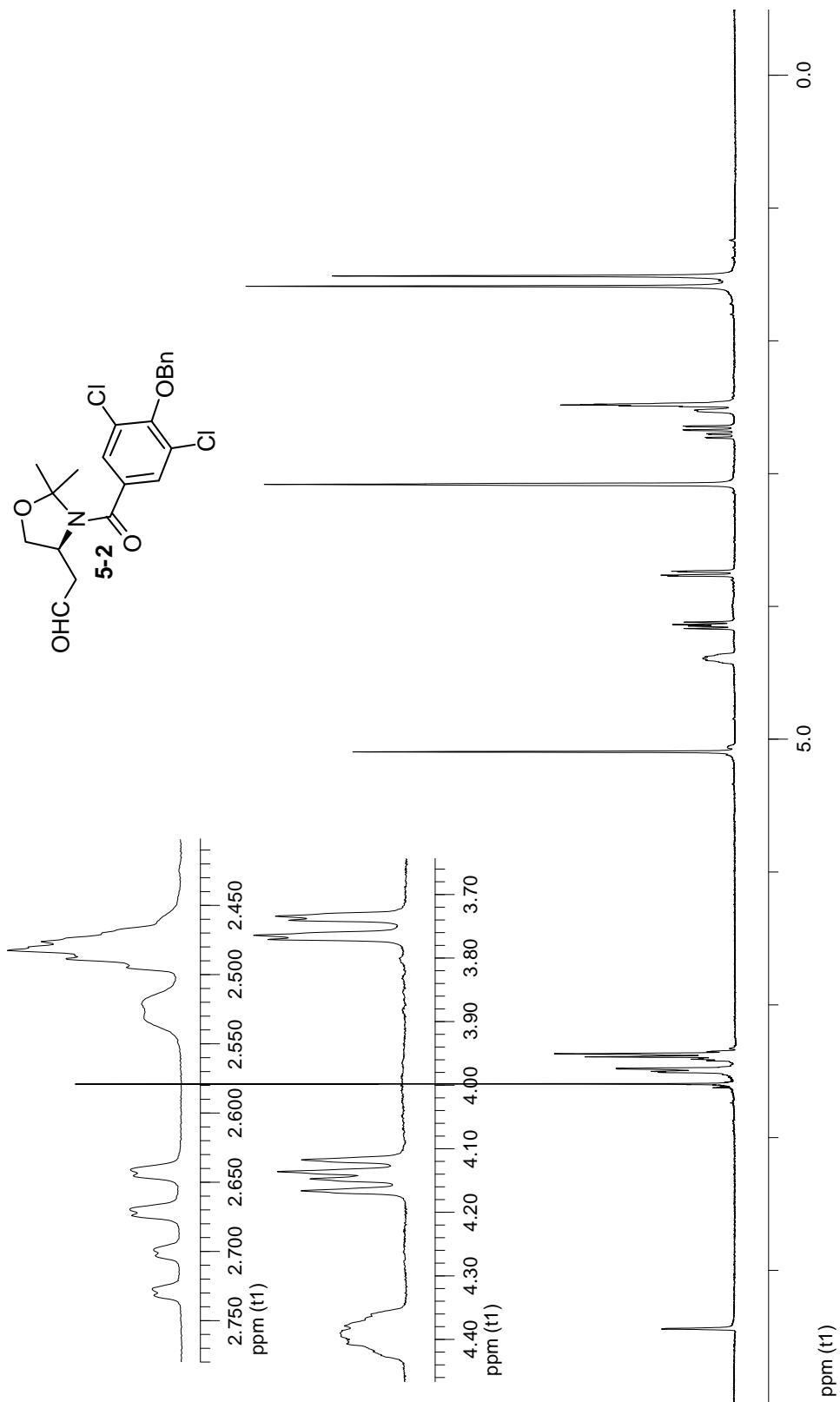


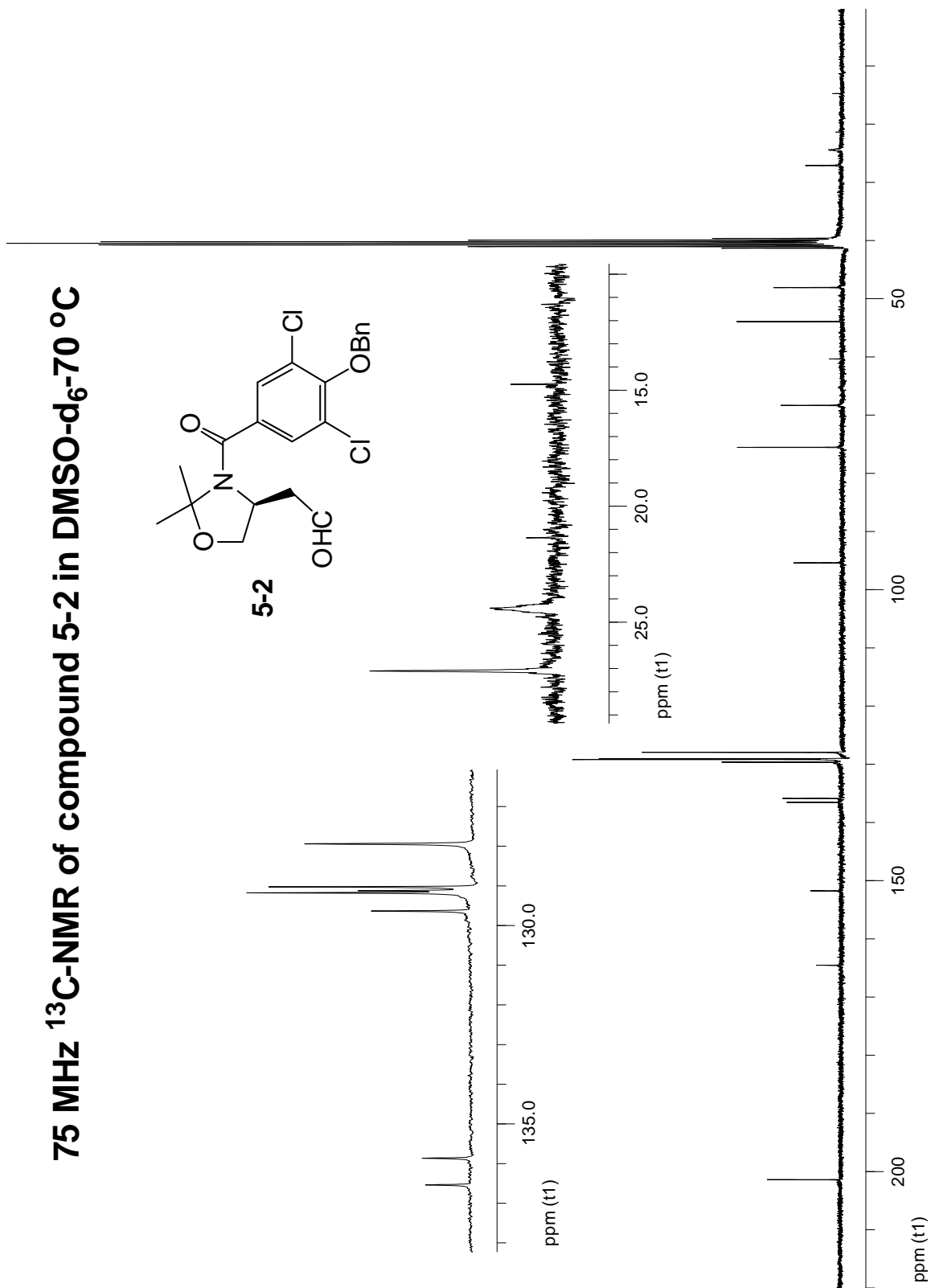
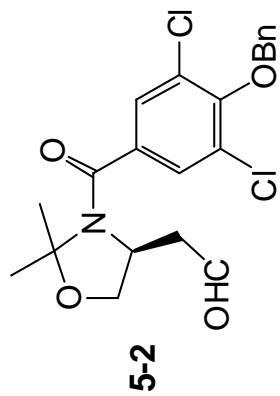


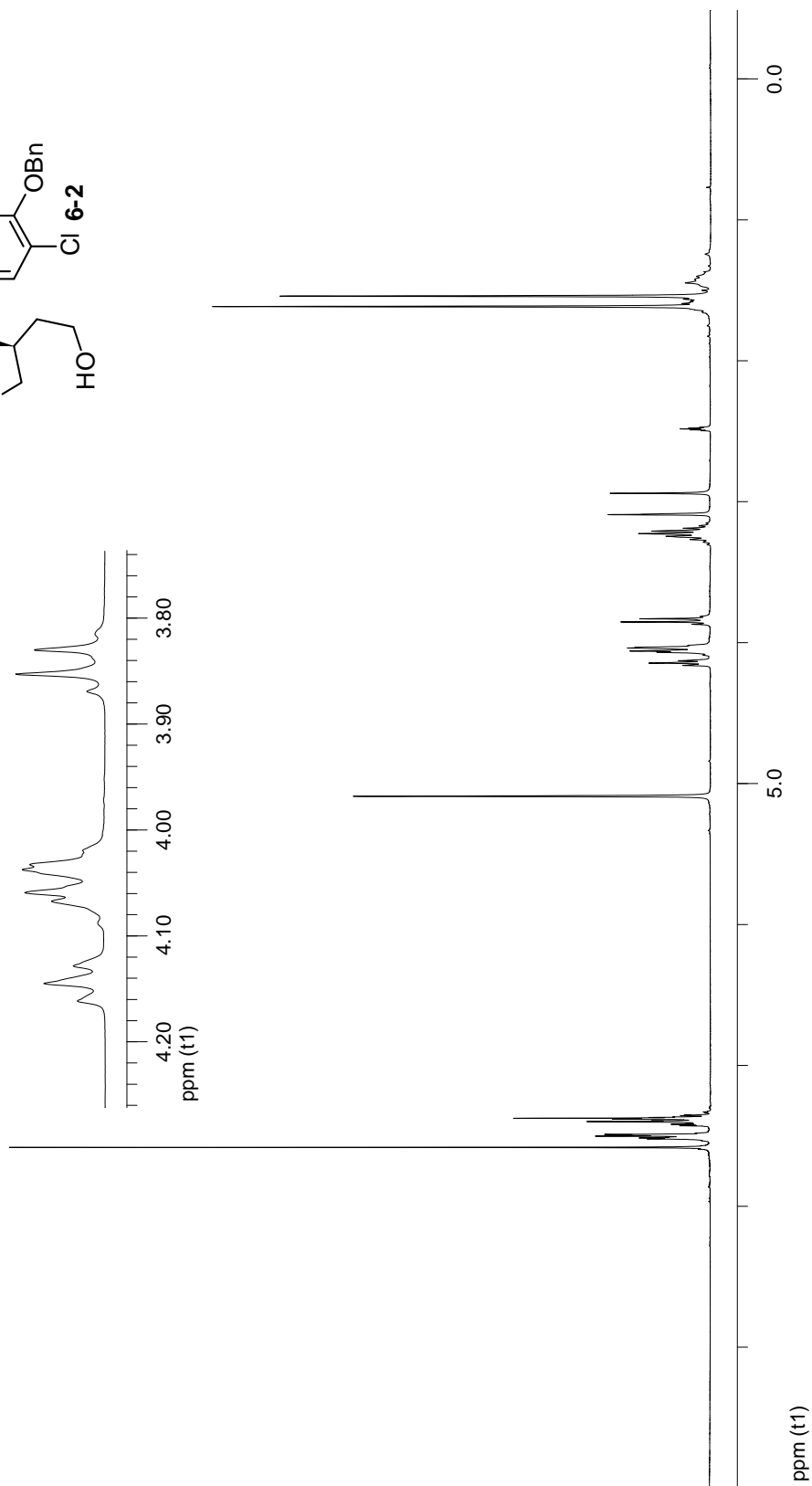
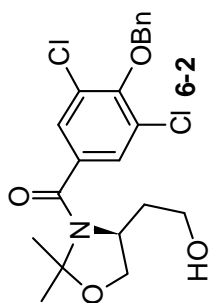


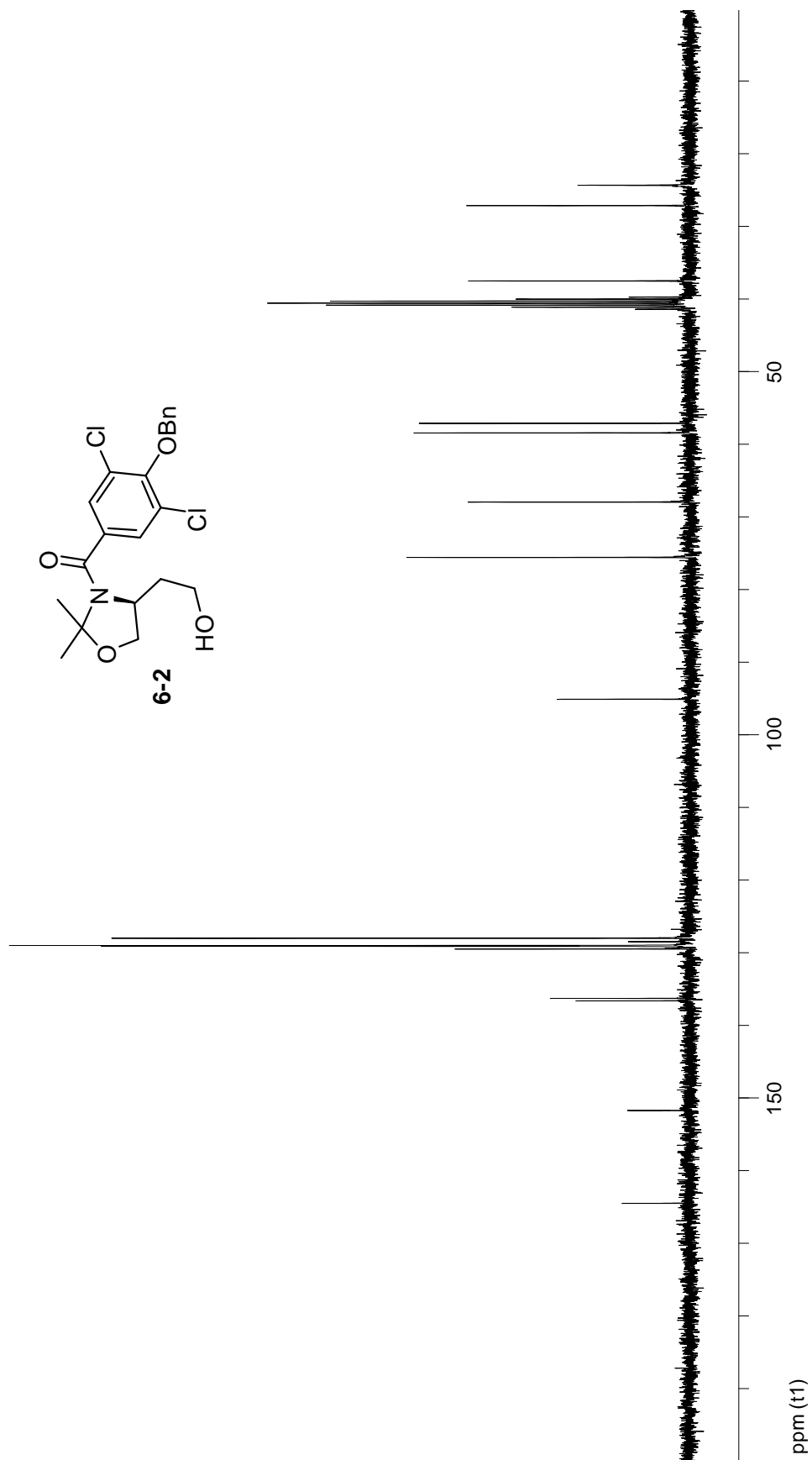
Appendix B

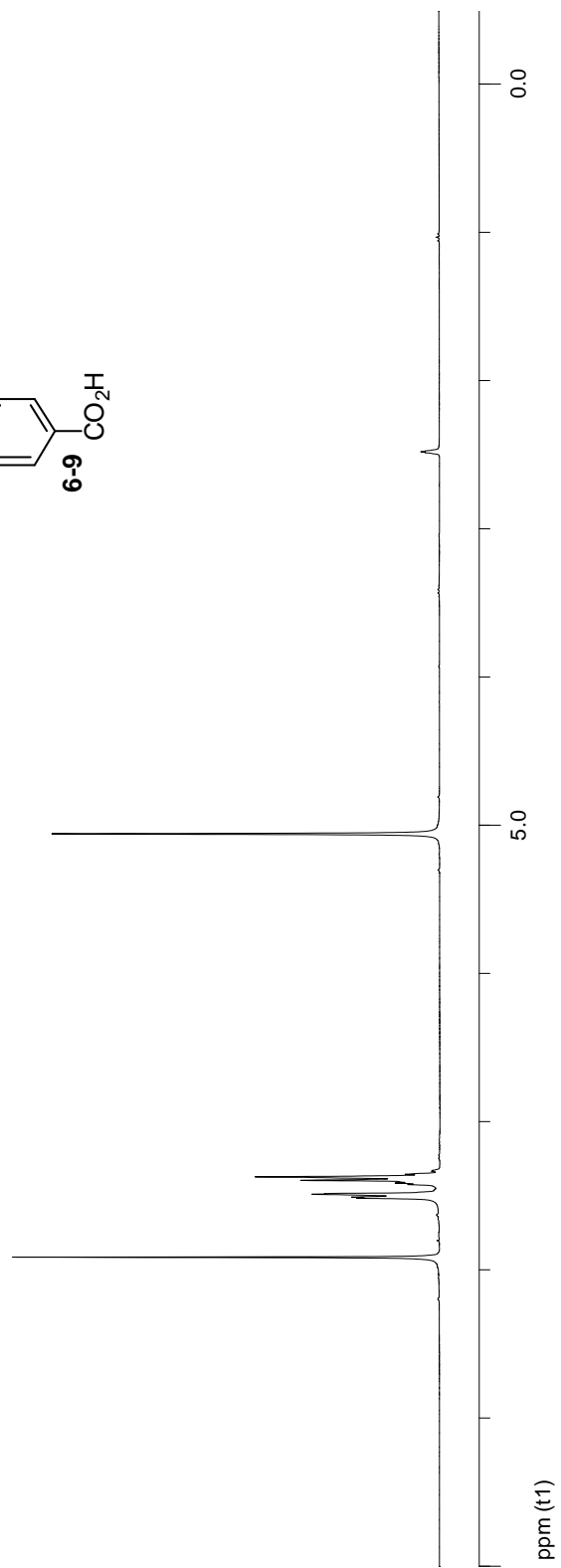
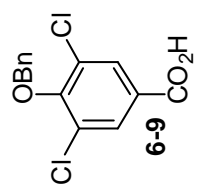
300 MHz ¹H-NMR of compound 5-2 in DMSO-d6 at 70 °C

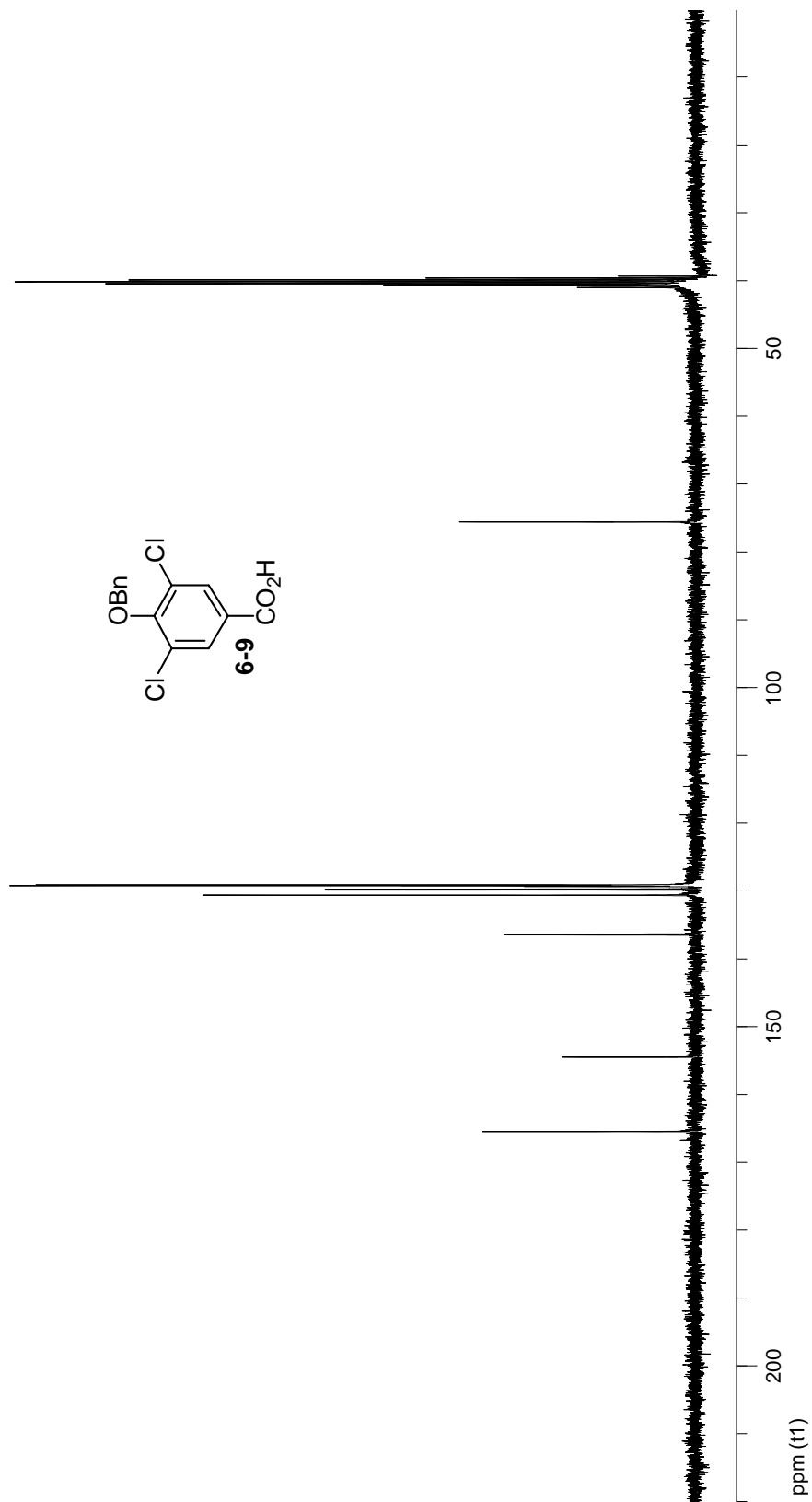


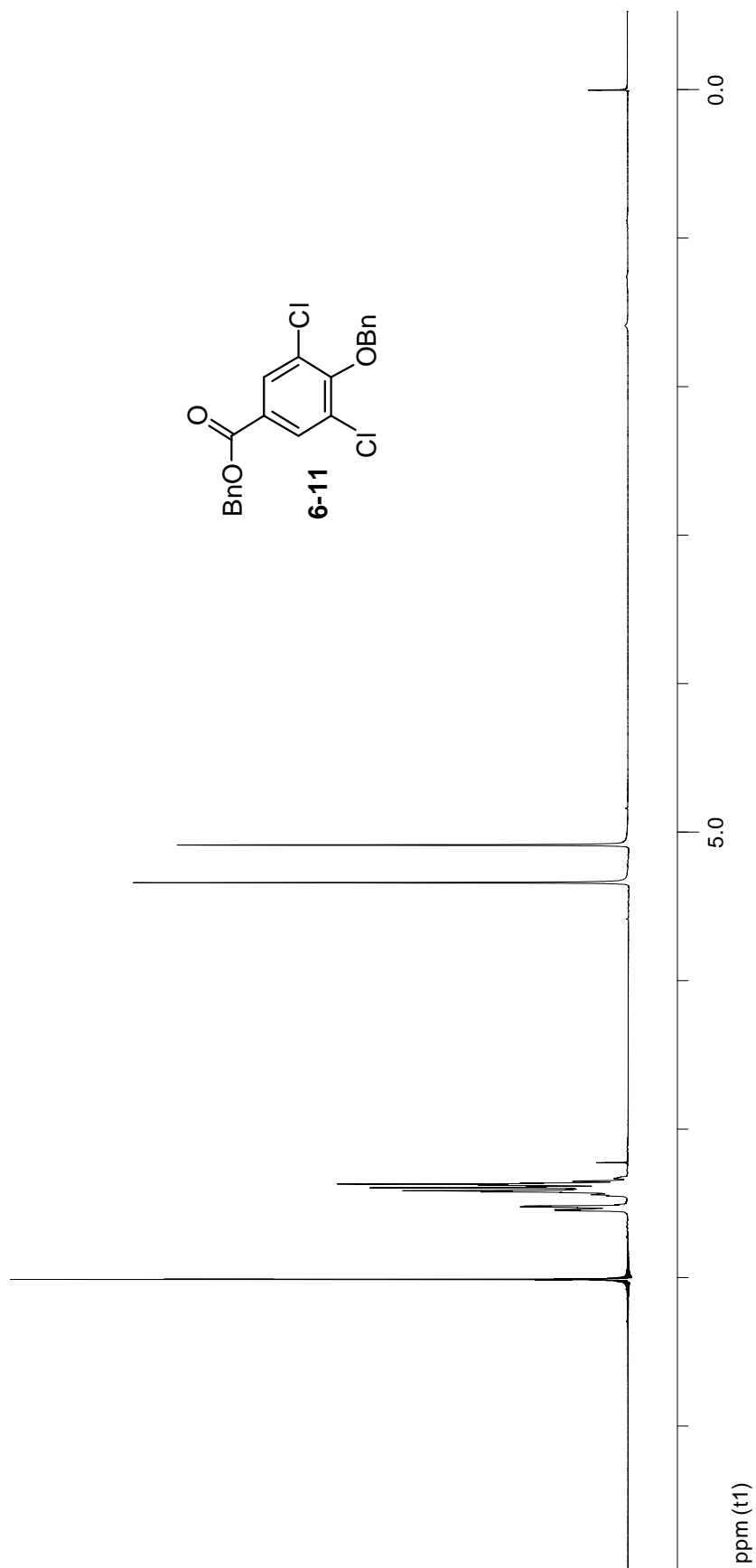
75 MHz ^{13}C -NMR of compound 5-2 in DMSO-d_6 -70 °C

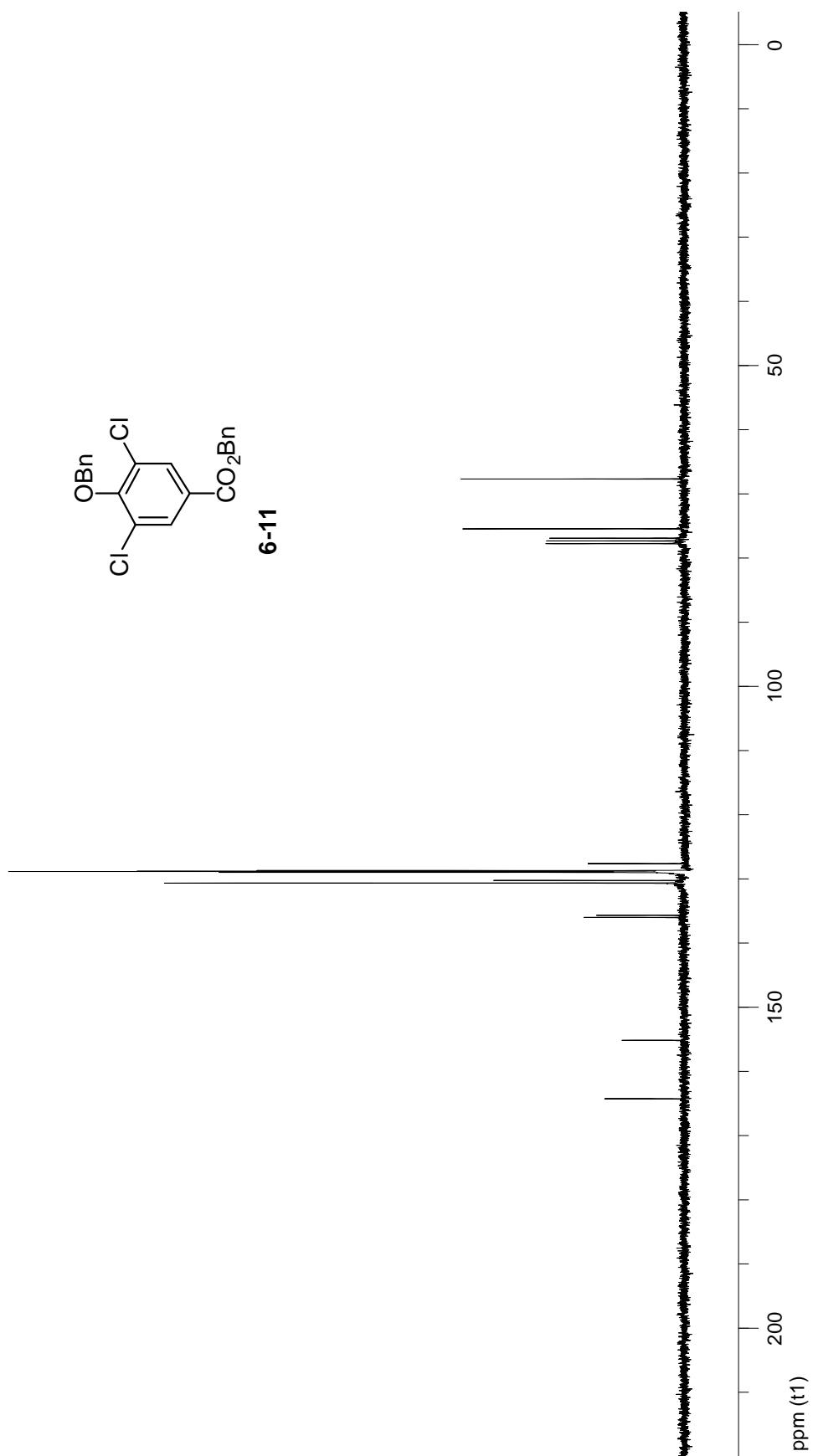
300 MHz $^1\text{H-NMR}$ of compound 6-2 in DMSO- d_6 at 90 $^\circ\text{C}$ 

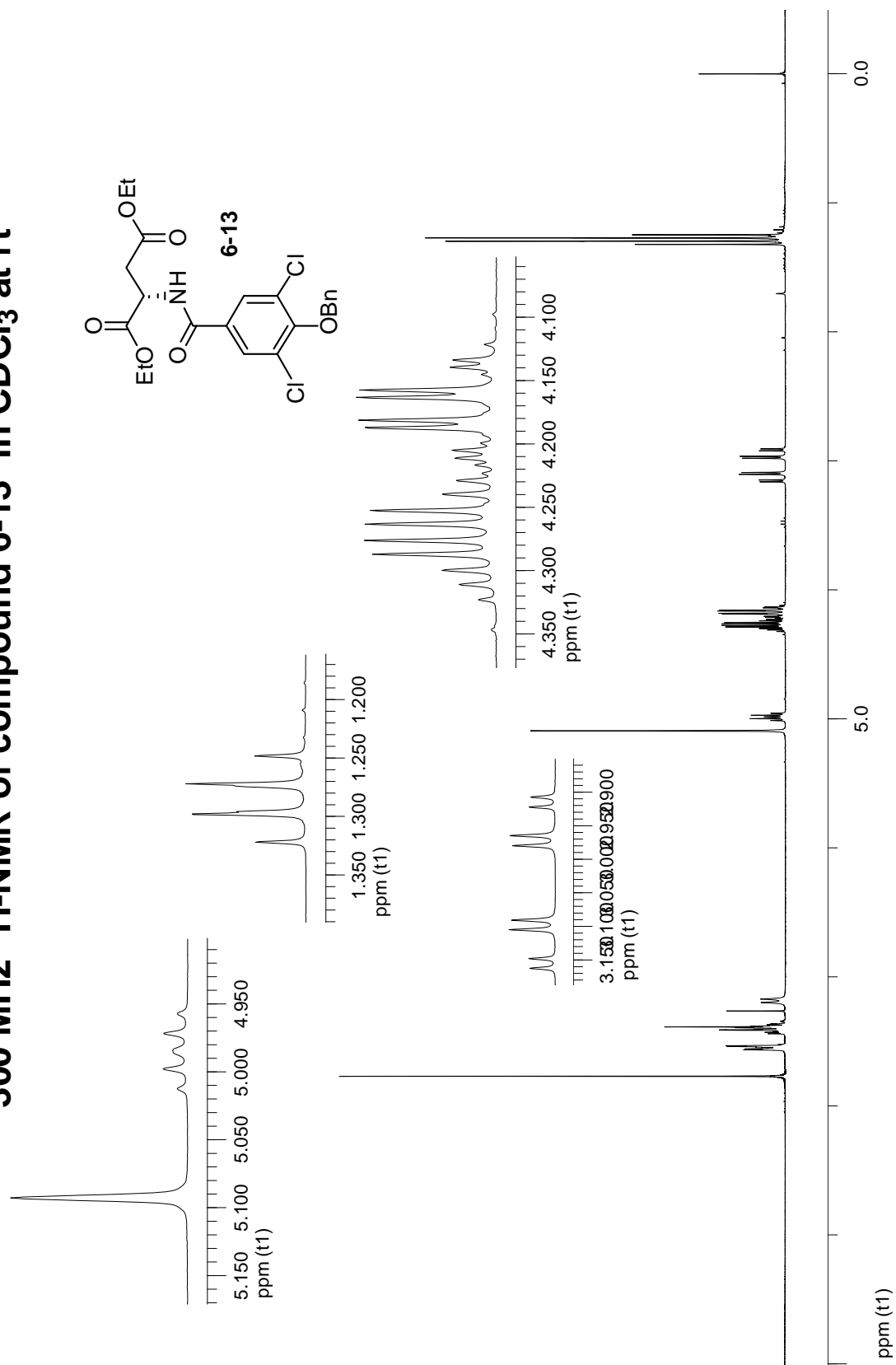
75 MHz ^{13}C -NMR of compound 6-2 in DMSO- d_6 at 90 °C

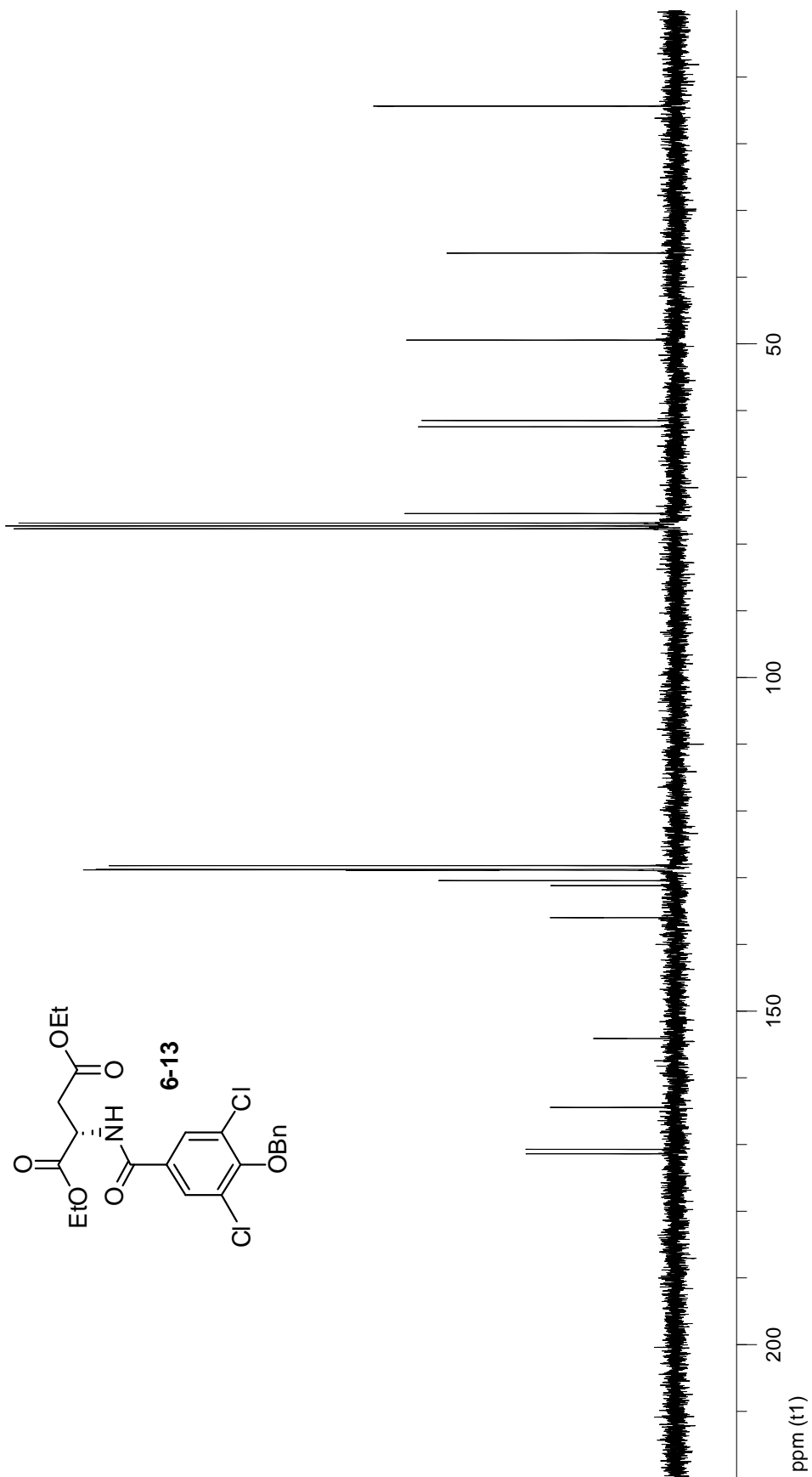
300 MHz $^1\text{H-NMR}$ of compound 6-9 in DMSO-d_6 at rt

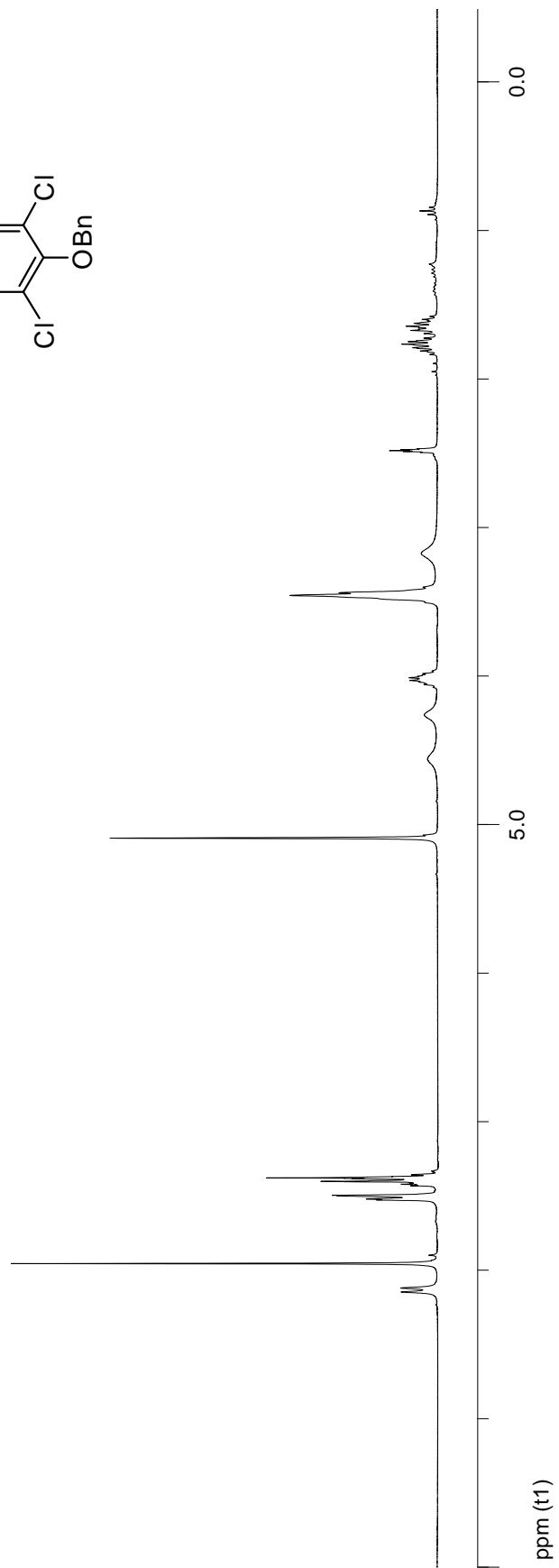
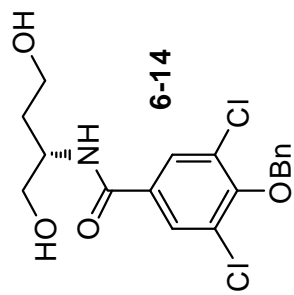
75 MHz ^{13}C -NMR of compound 6-9 in DMSO-d₆ at rt

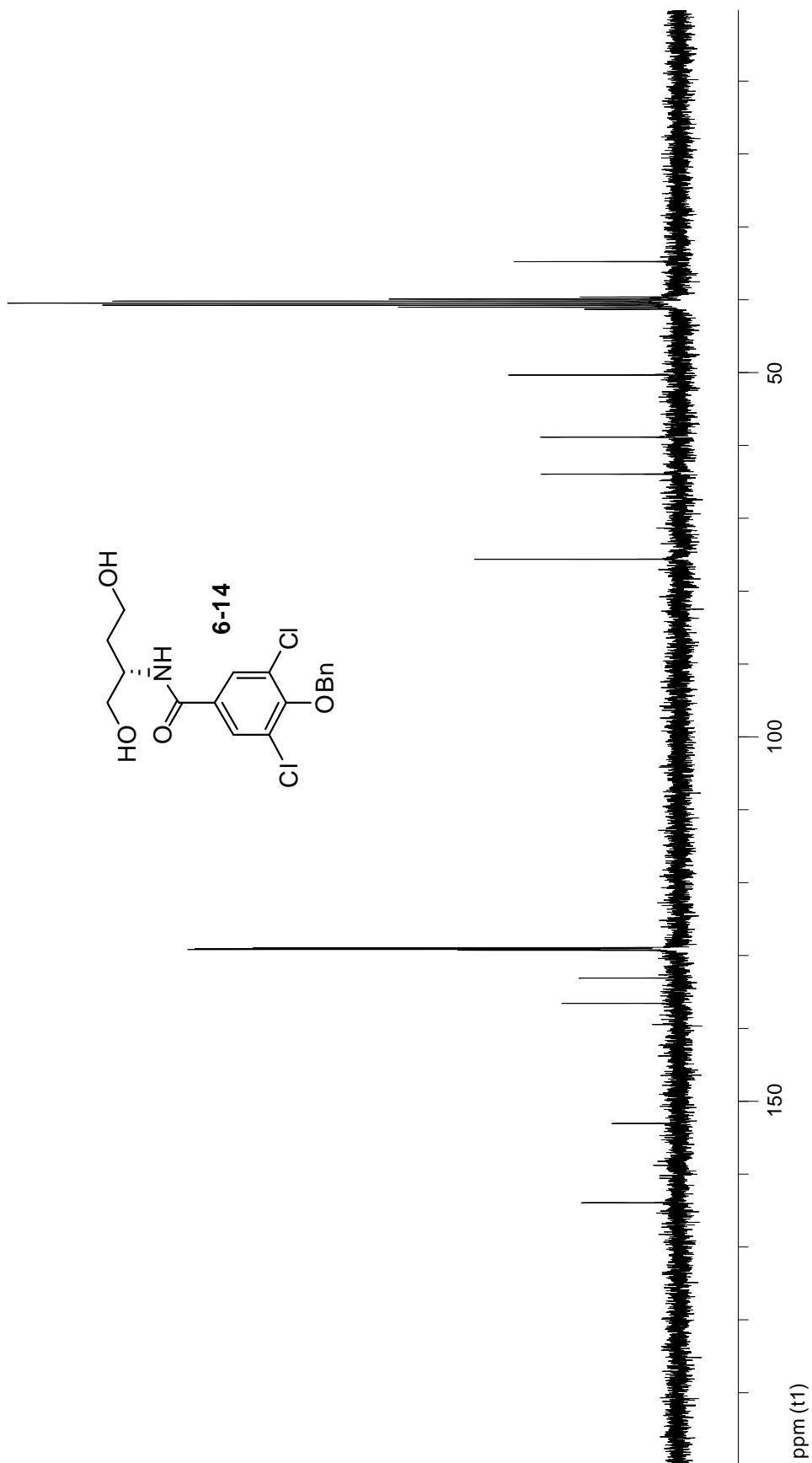
300 MHz $^1\text{H-NMR}$ of compound 6-11 in CDCl_3 at rt

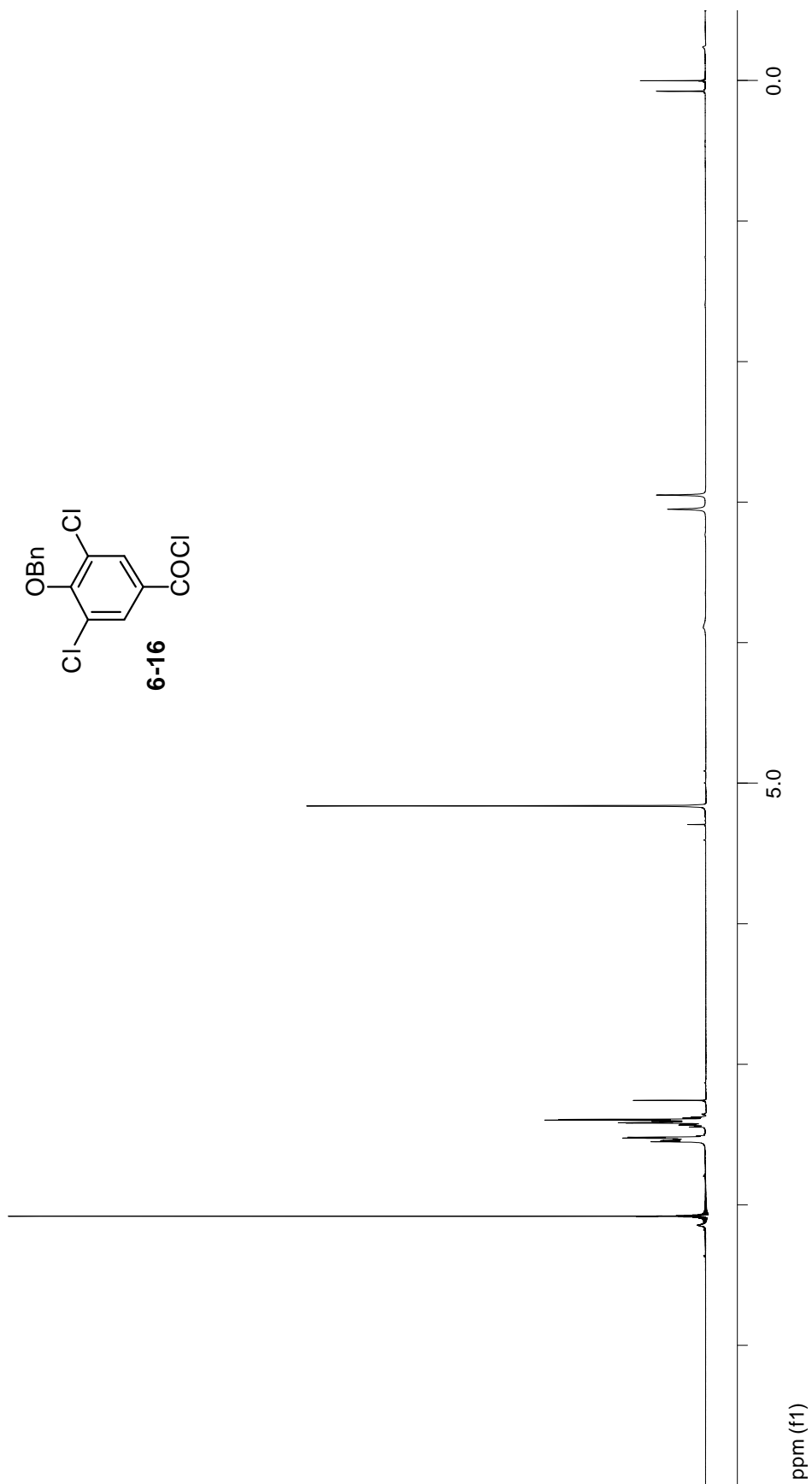
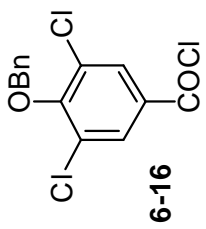
75 MHz ^{13}C -NMR of compound 6-11 in CDCl_3 at rt

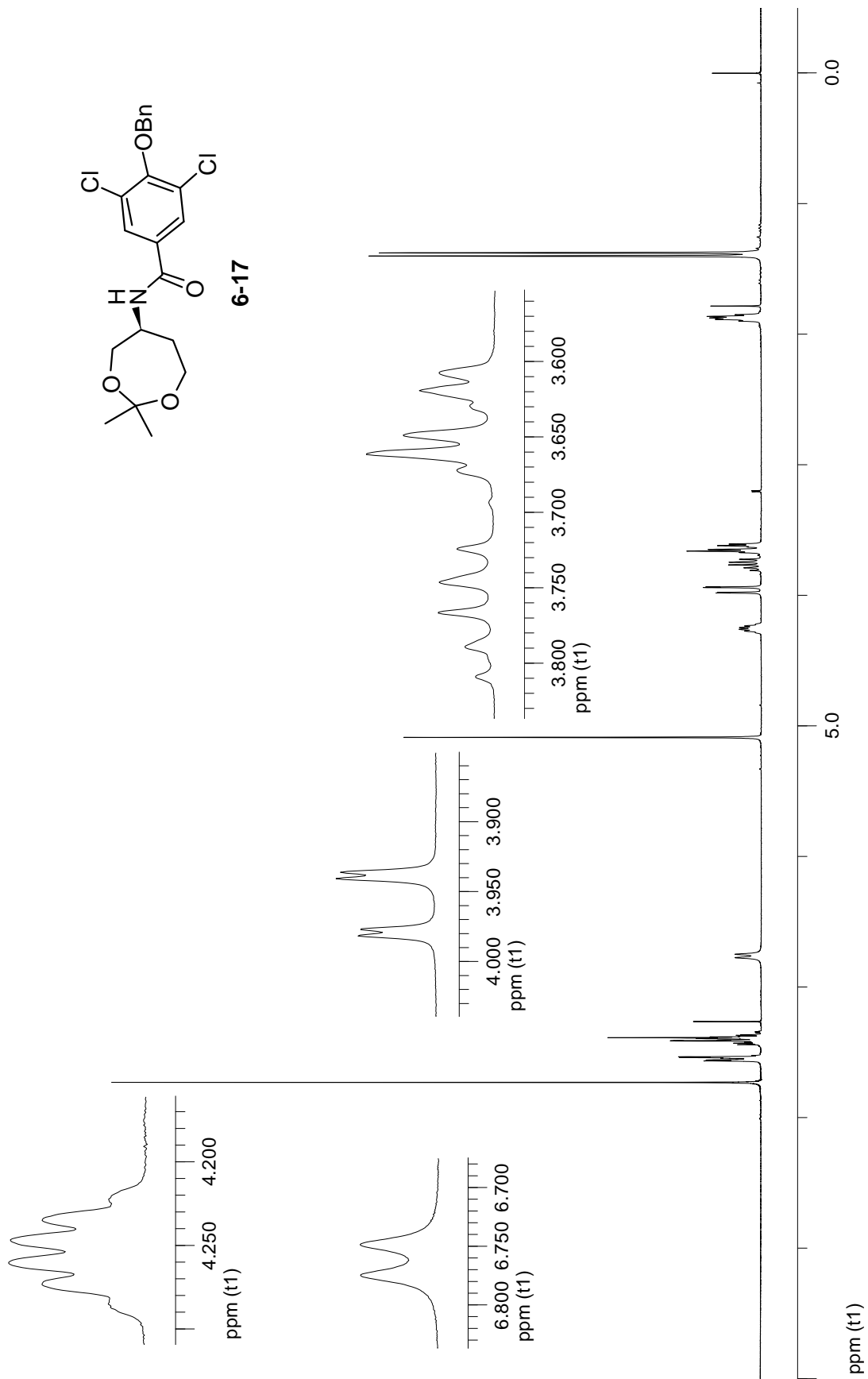
300 MHz ¹H-NMR of compound 6-13 in CDCl₃ at rt

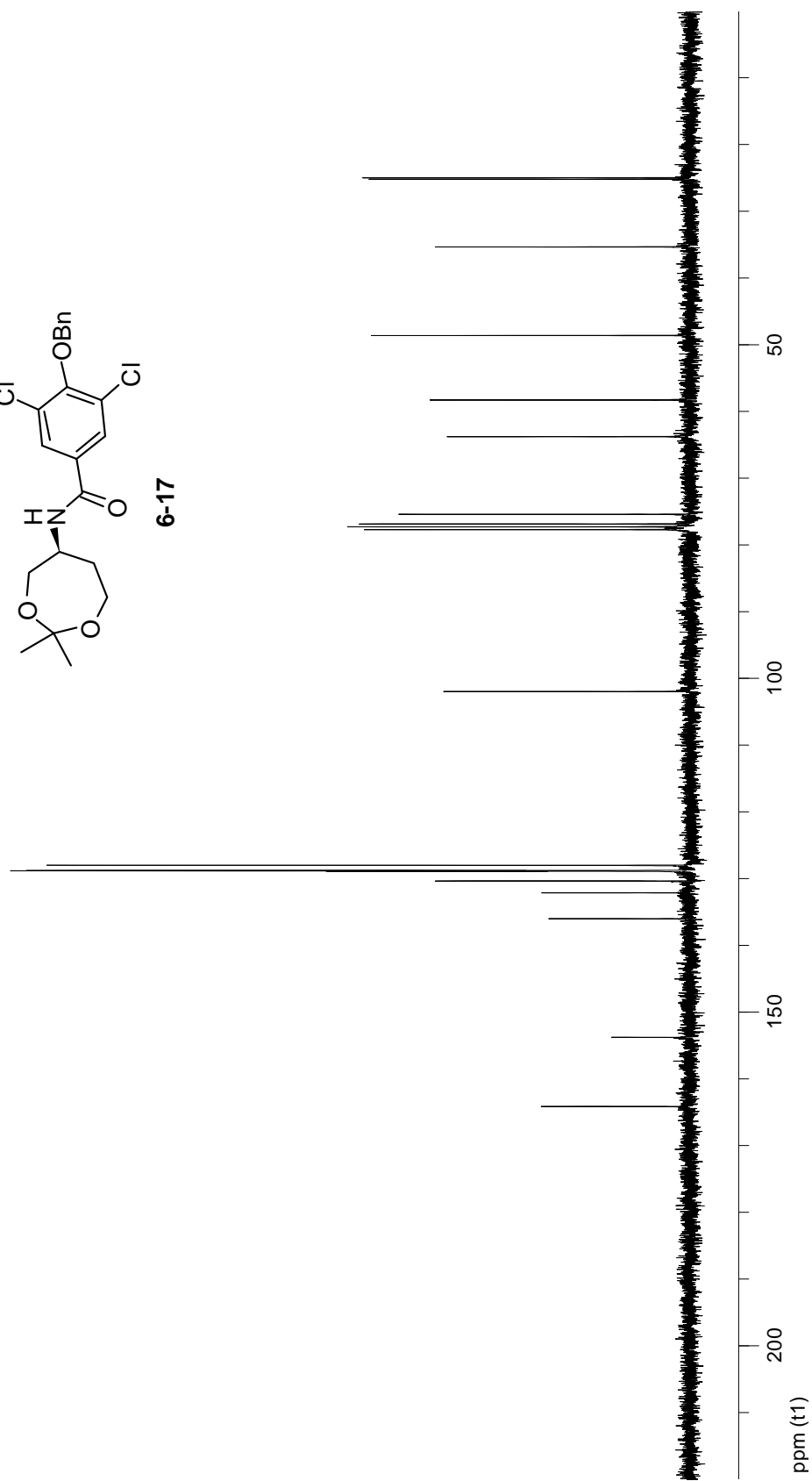
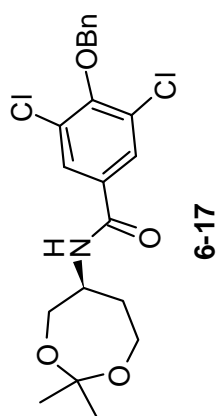
75 MHz ^{13}C -NMR of compound 6-13 in CDCl_3 at rt

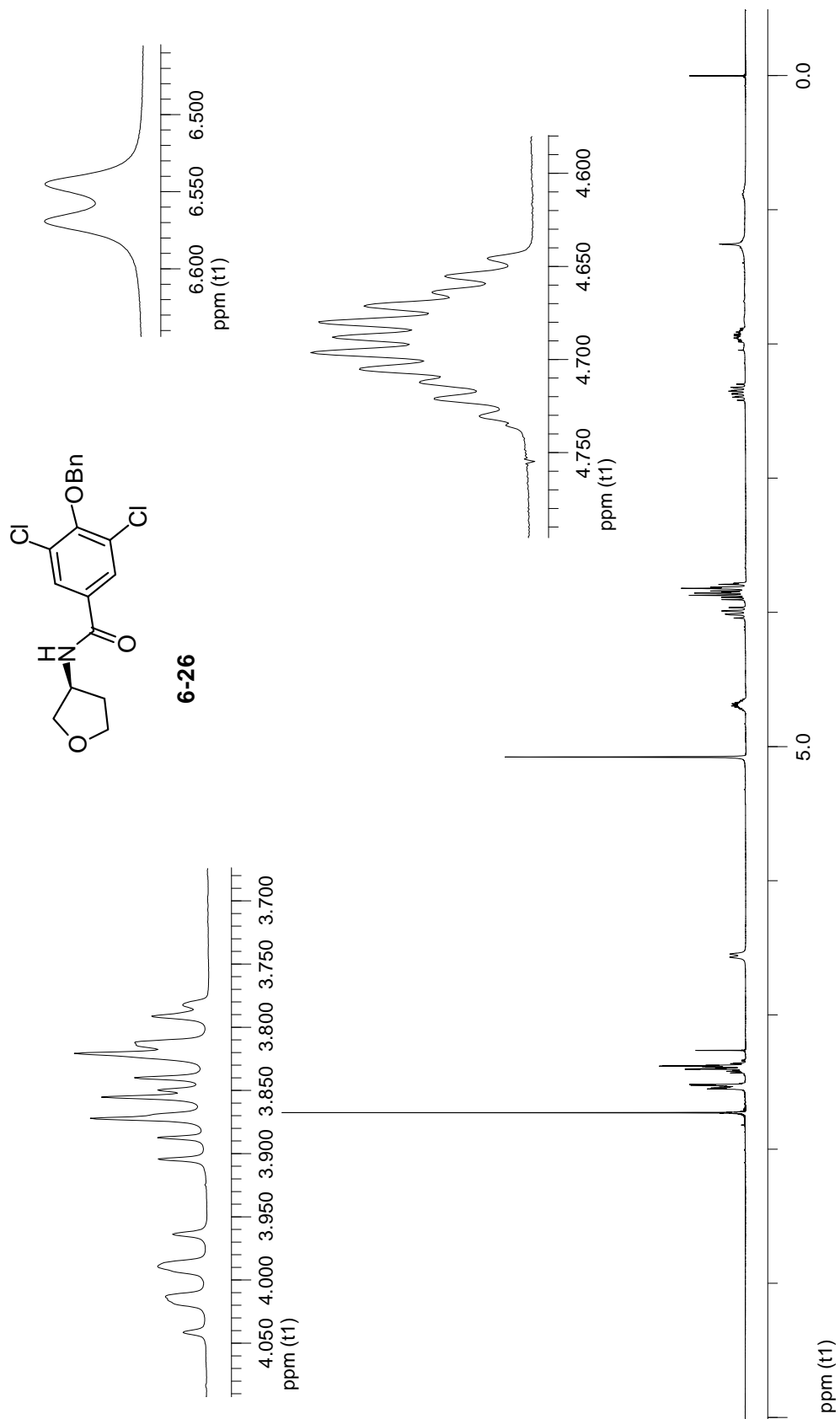
300 MHz $^1\text{H-NMR}$ of compound 6-14 in DMSO-d_6 at 90 °C

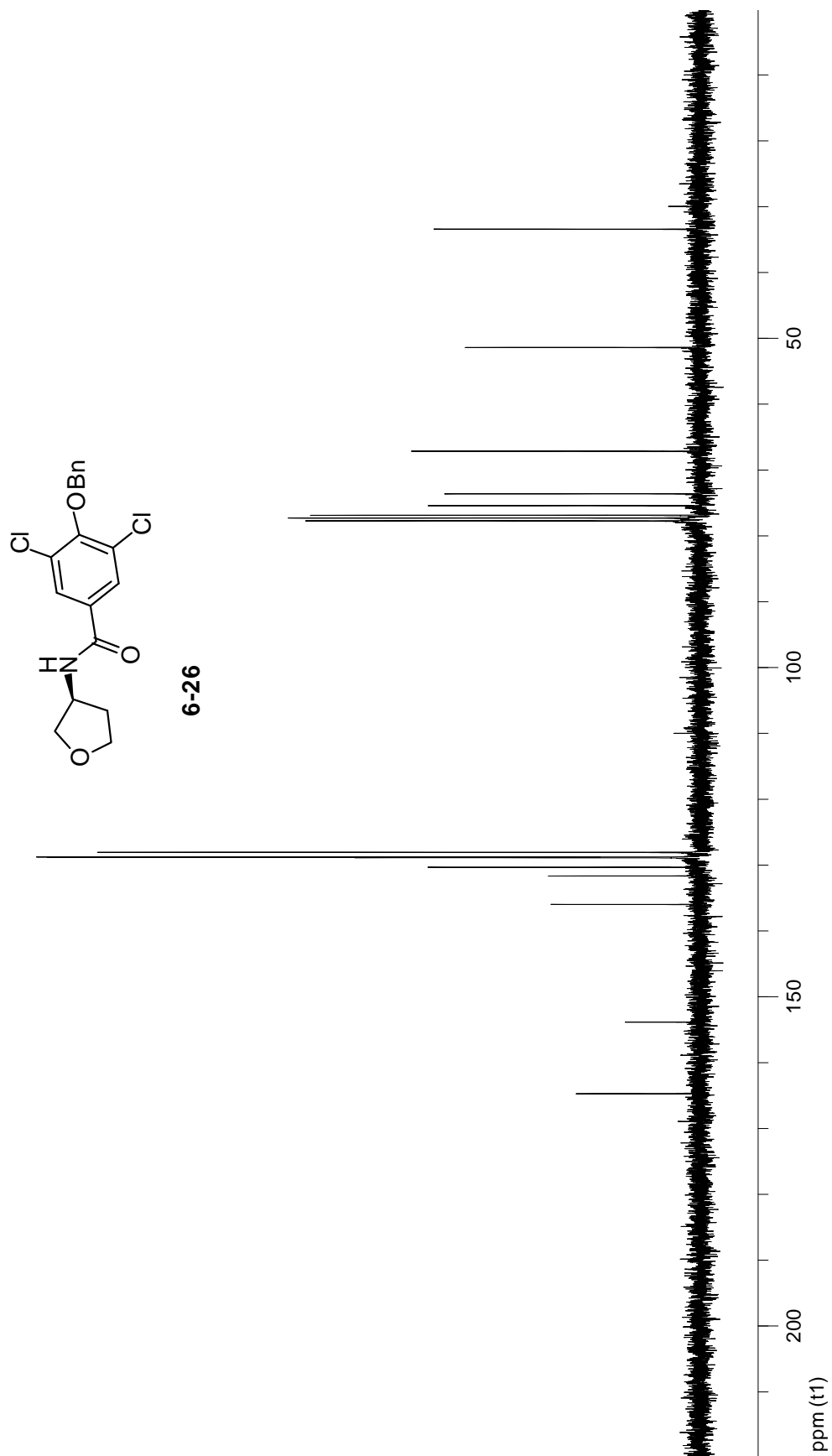
75 MHz ^{13}C -NMR of compound 6-14 in DMSO-d₆ at 70 °C

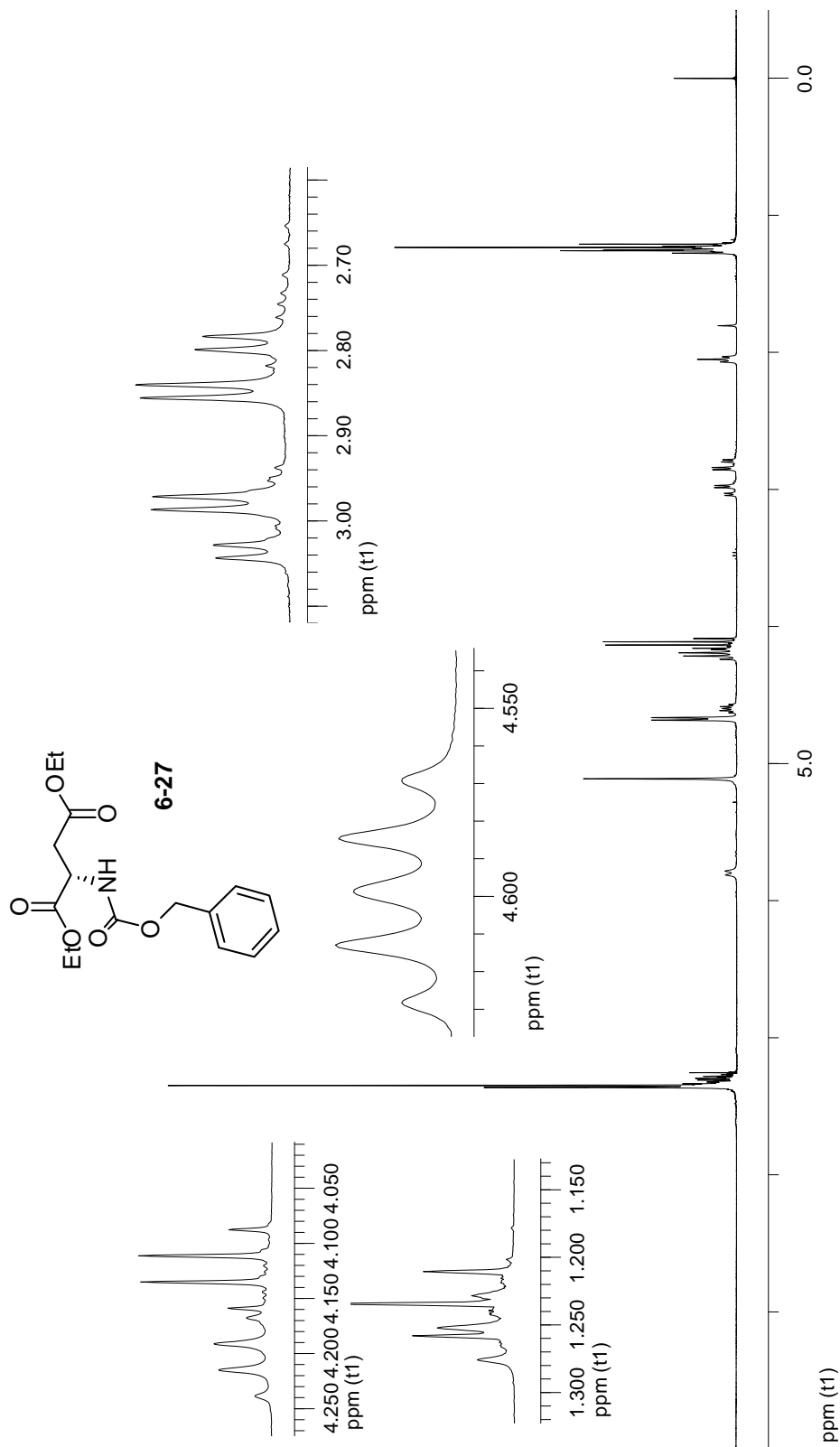
300 MHz $^1\text{H-NMR}$ of compound 6-16 in CDCl_3 at rt

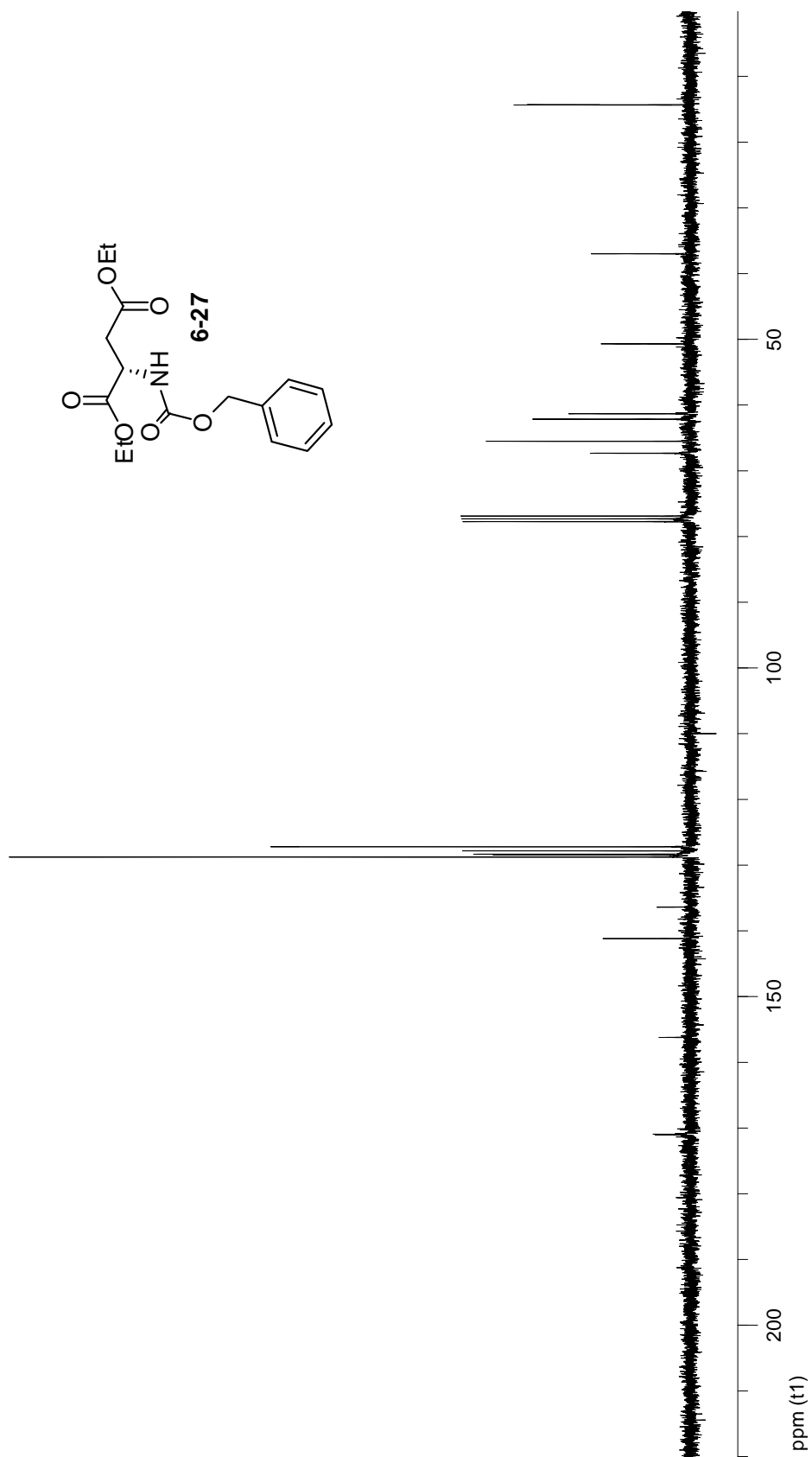
300 MHz $^1\text{H-NMR}$ of compound 6-17 in CDCl_3 at rt

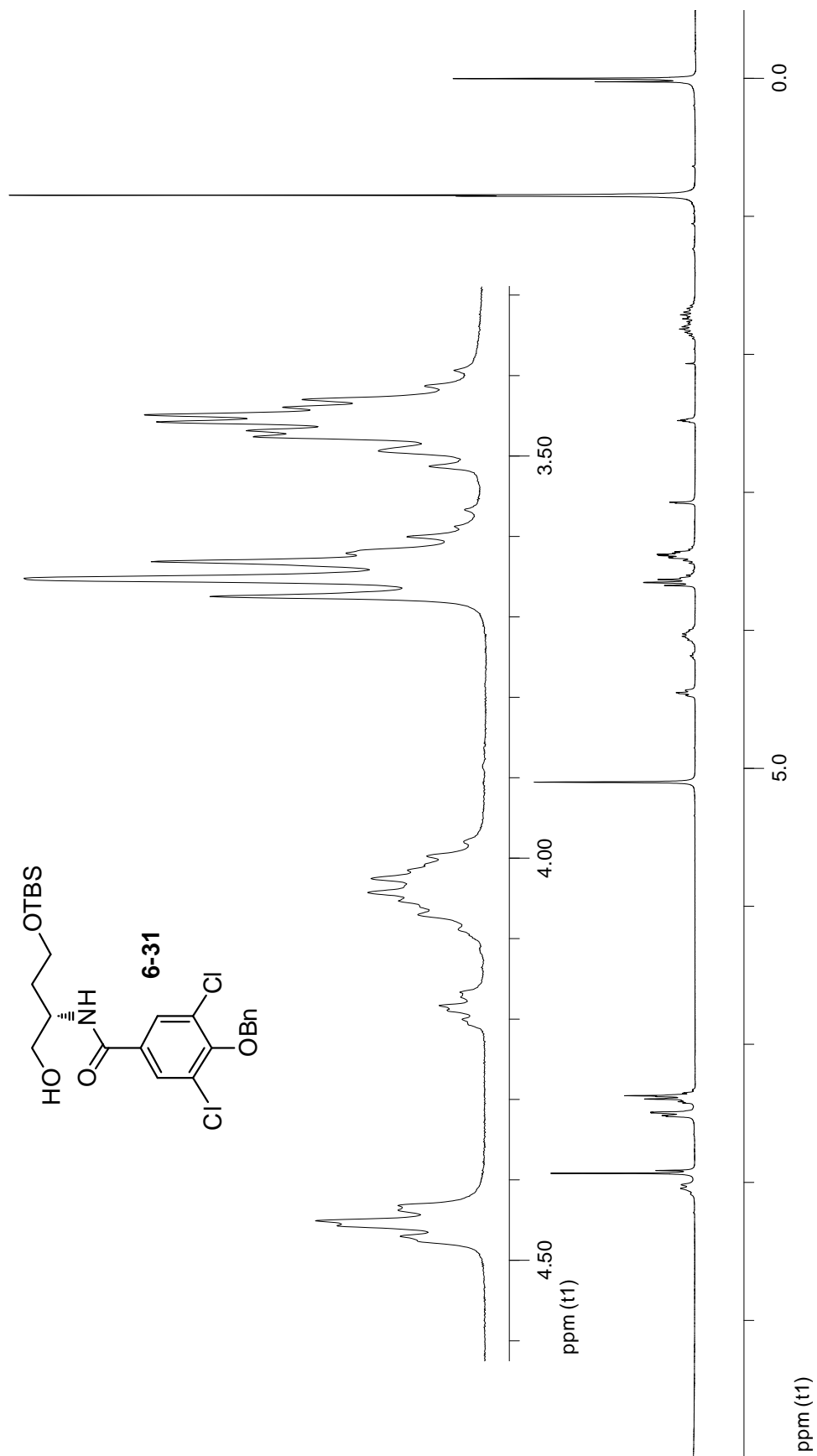
75 MHz ^{13}C -NMR of compound 6-17 in CDCl_3 at rt

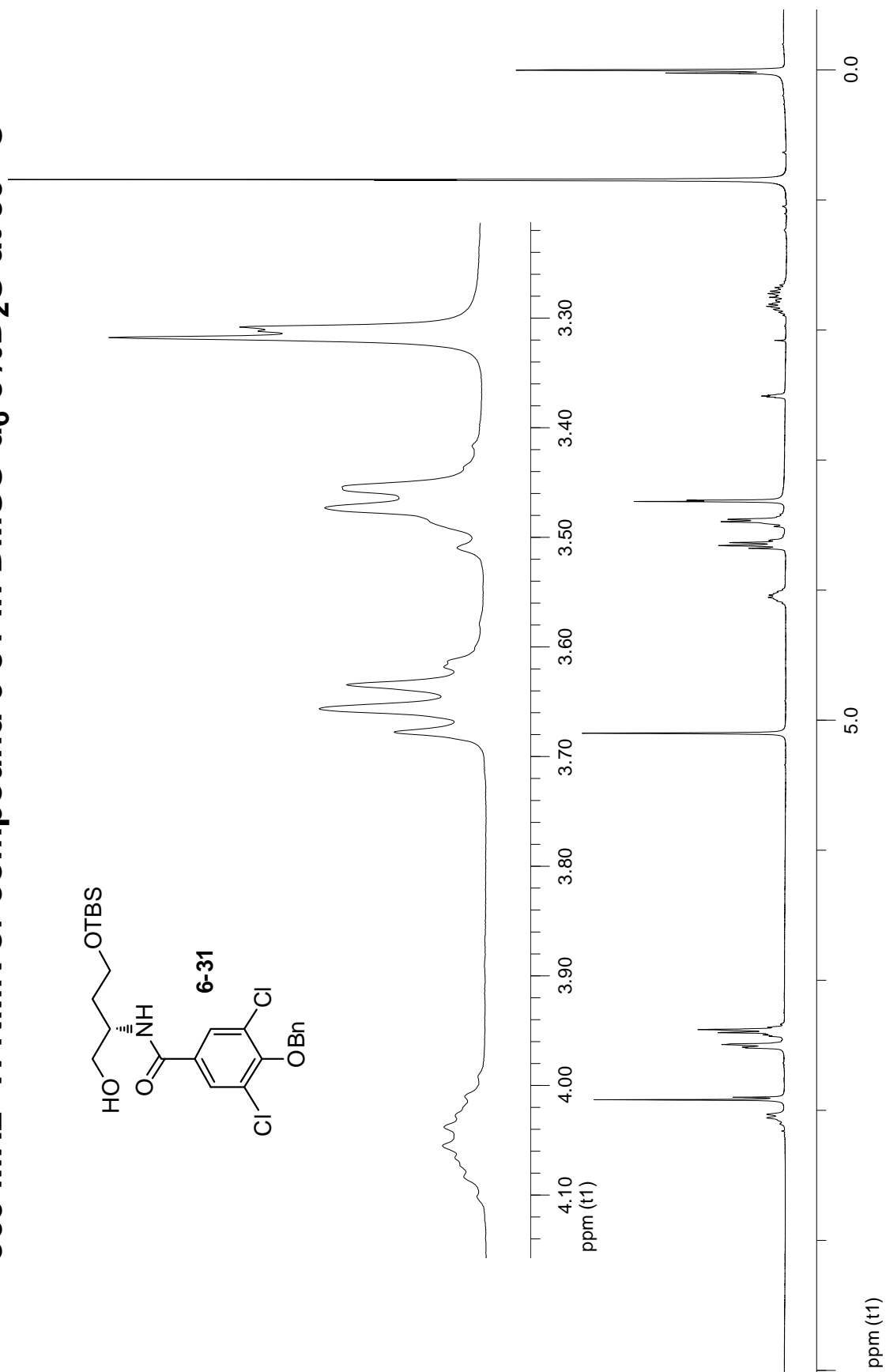
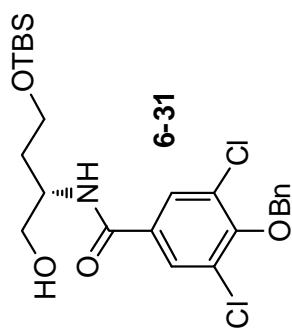
300 MHz $^1\text{H-NMR}$ of compound 6-26 in CDCl_3 at rt

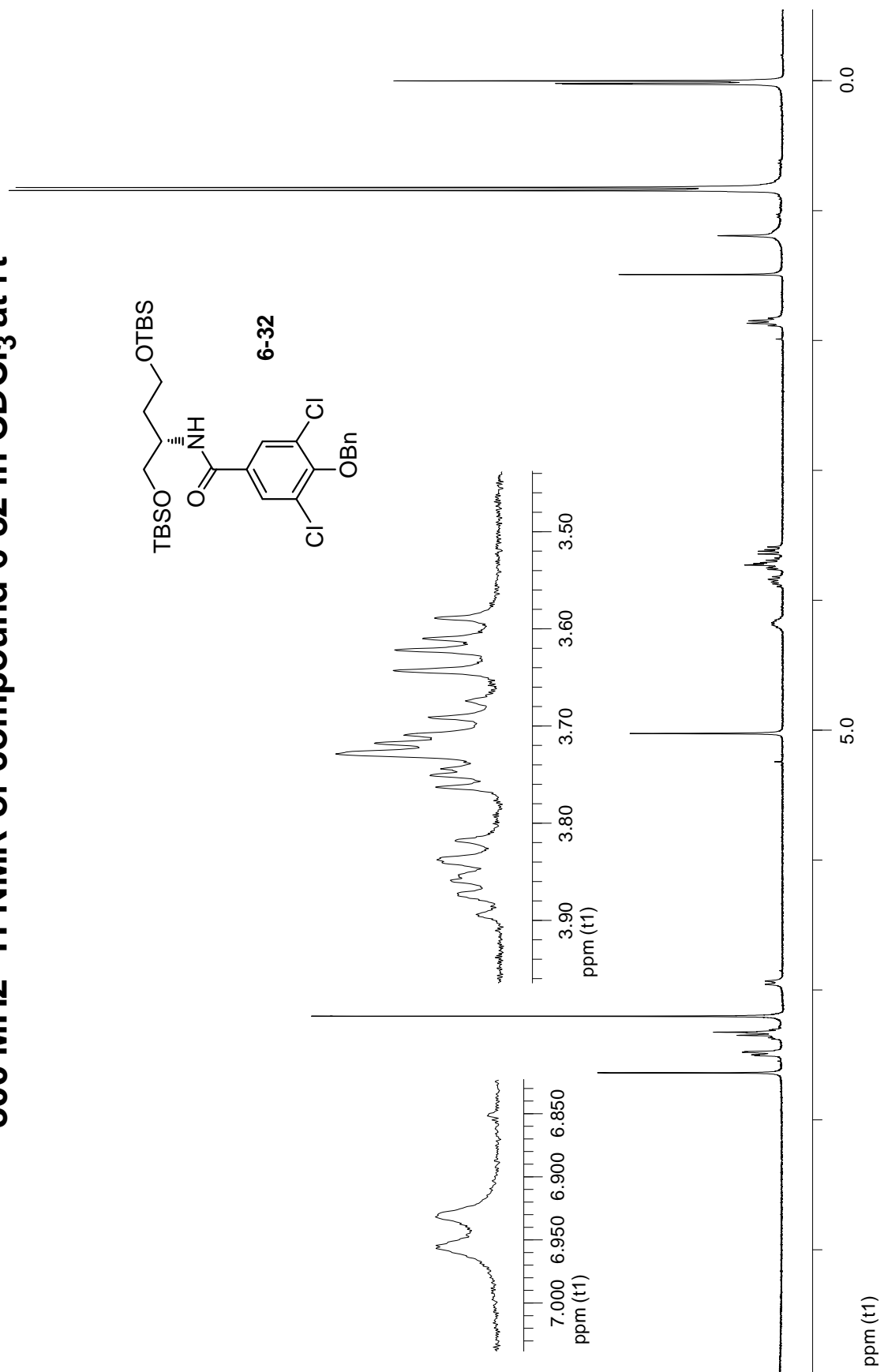
75 MHz ^{13}C -NMR of compound 6-26 in CDCl_3 at rt

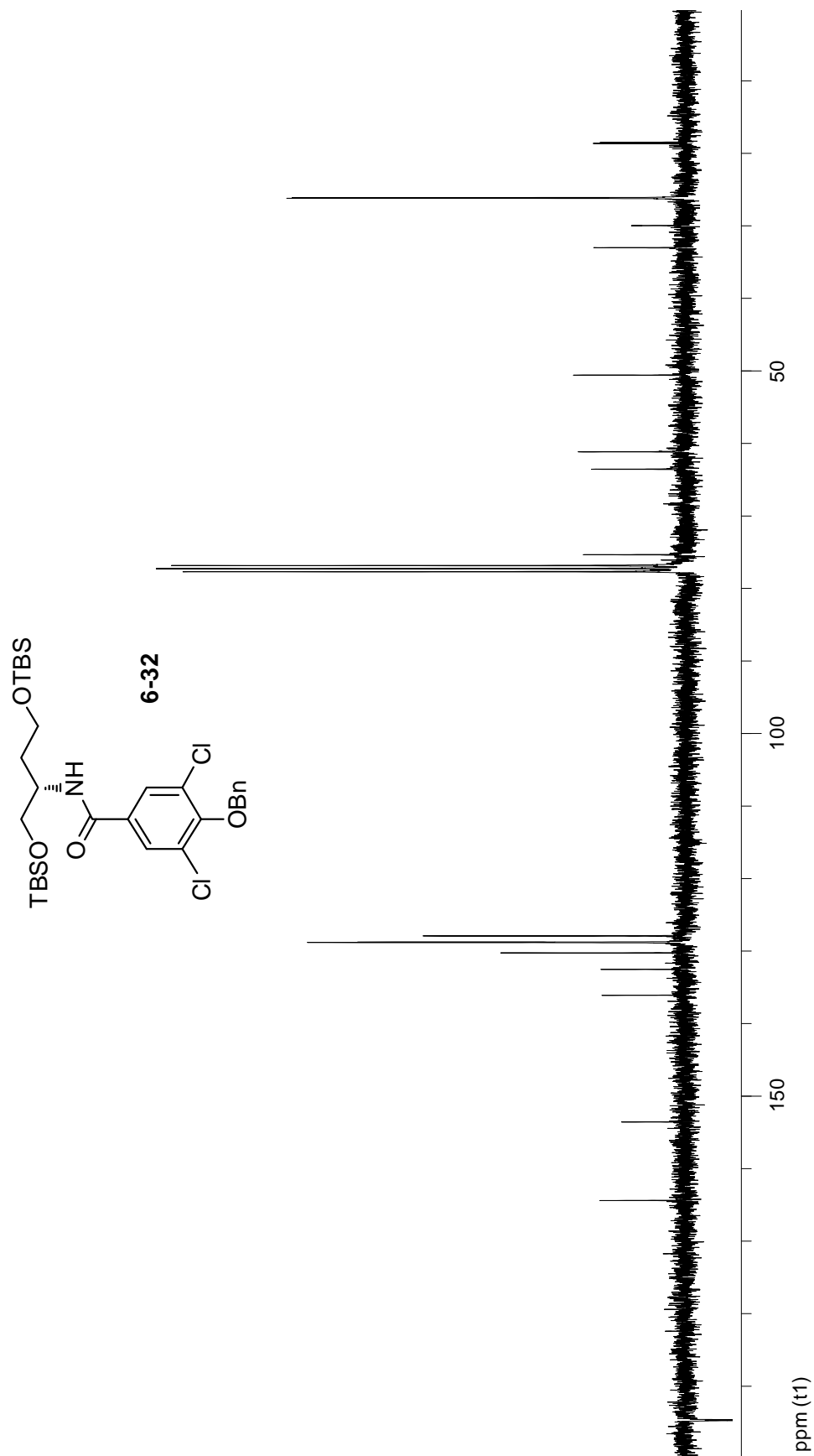
300 MHz $^1\text{H-NMR}$ of compound 6-27 in CDCl_3 at rt

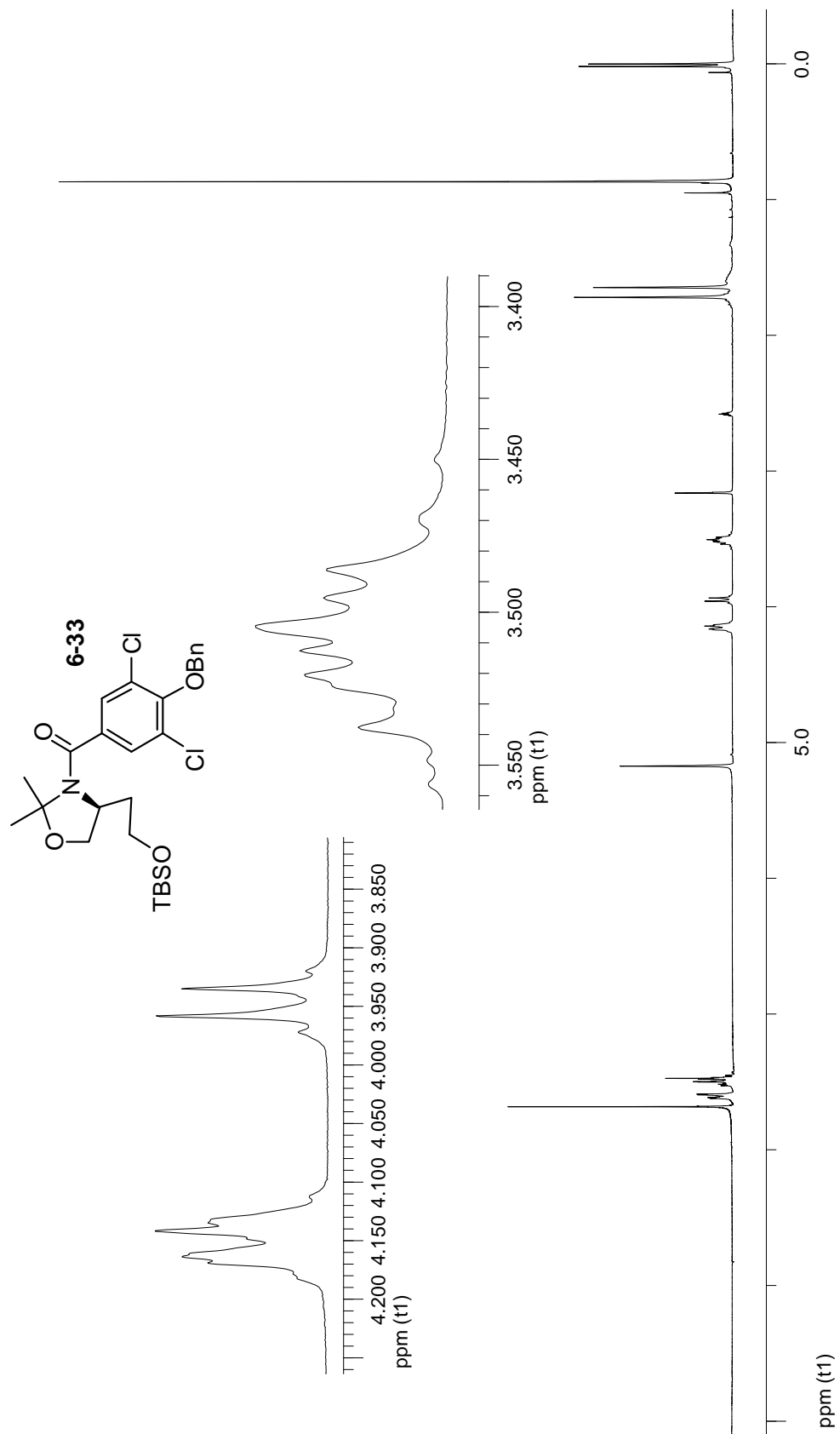
75 MHz ^{13}C -NMR of compound 6-27 in CDCl_3 at rt

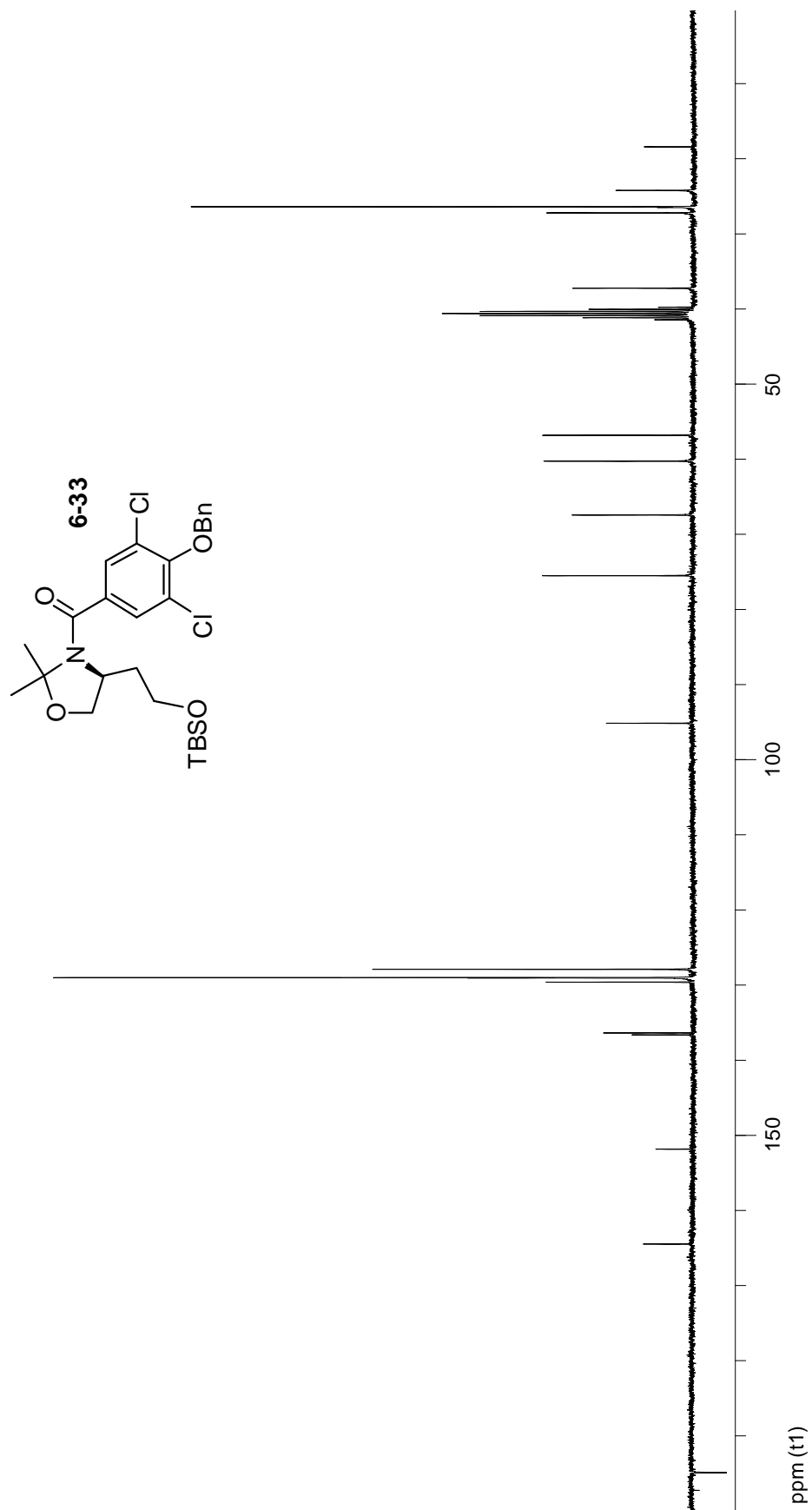
300 MHz $^1\text{H-NMR}$ of compound 6-31 in DMSO-d_6 at 90 $^\circ\text{C}$ 

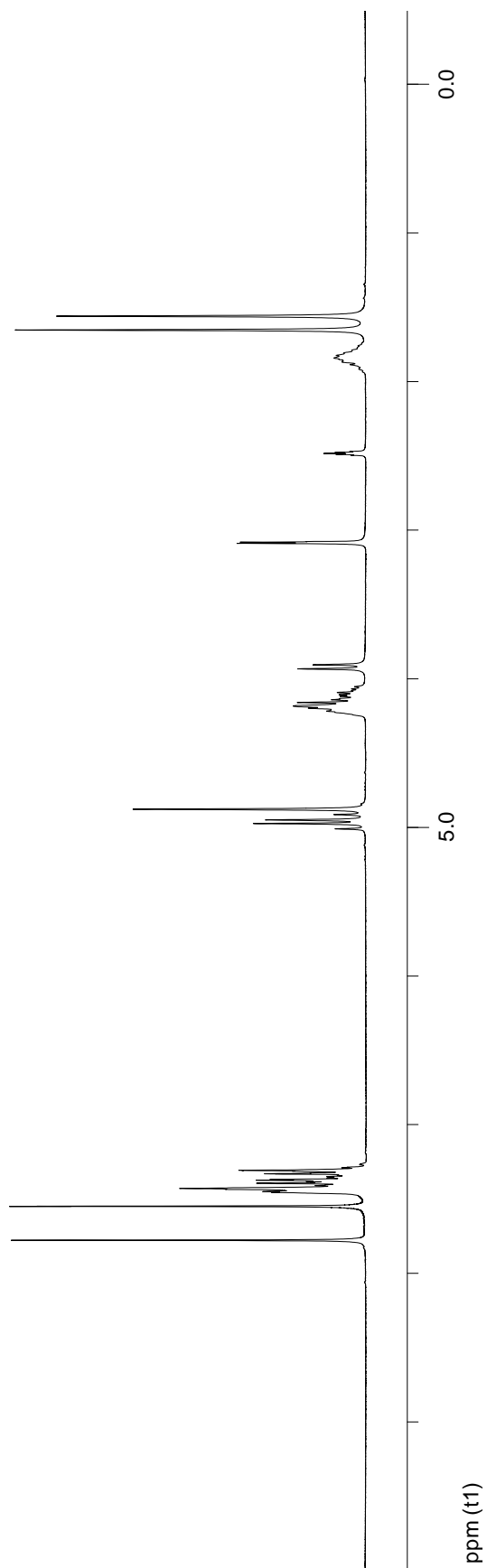
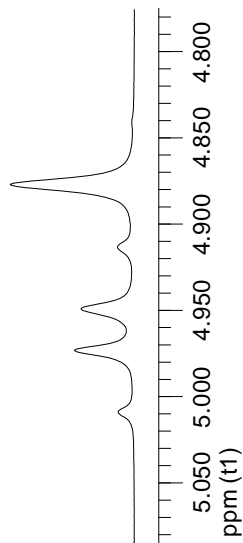
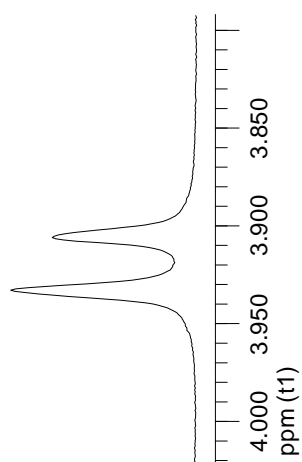
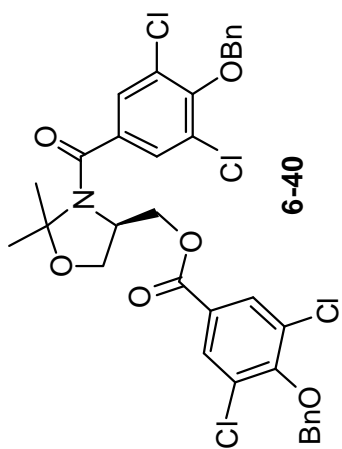
300 MHz $^1\text{H-NMR}$ of compound 6-31 in DMSO-d_6 -5% D_2O at 90 $^\circ\text{C}$ 

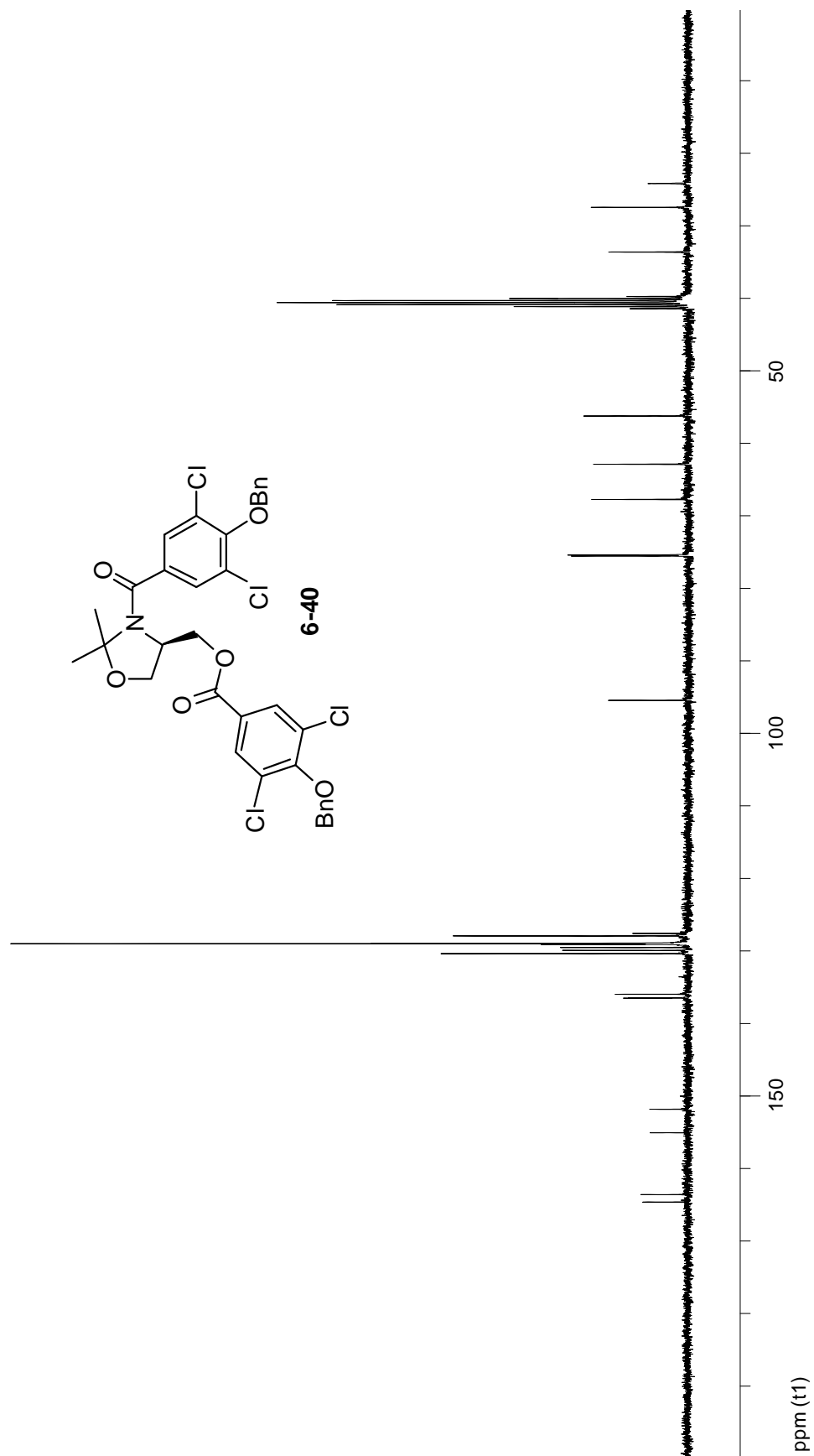
300 MHz $^1\text{H-NMR}$ of compound 6-32 in CDCl_3 at rt

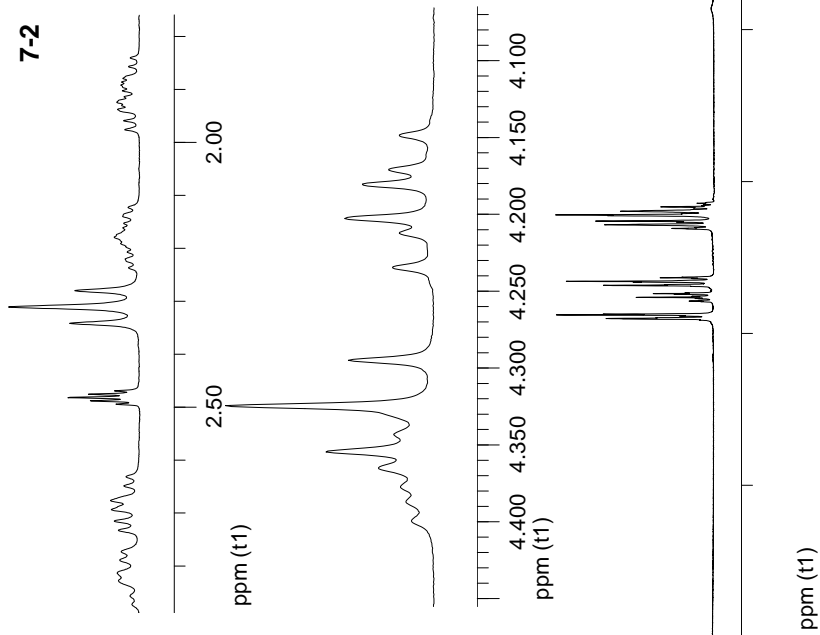
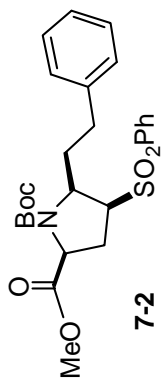
300 MHz $^1\text{H-NMR}$ of compound 6-32 in CDCl_3 at rt

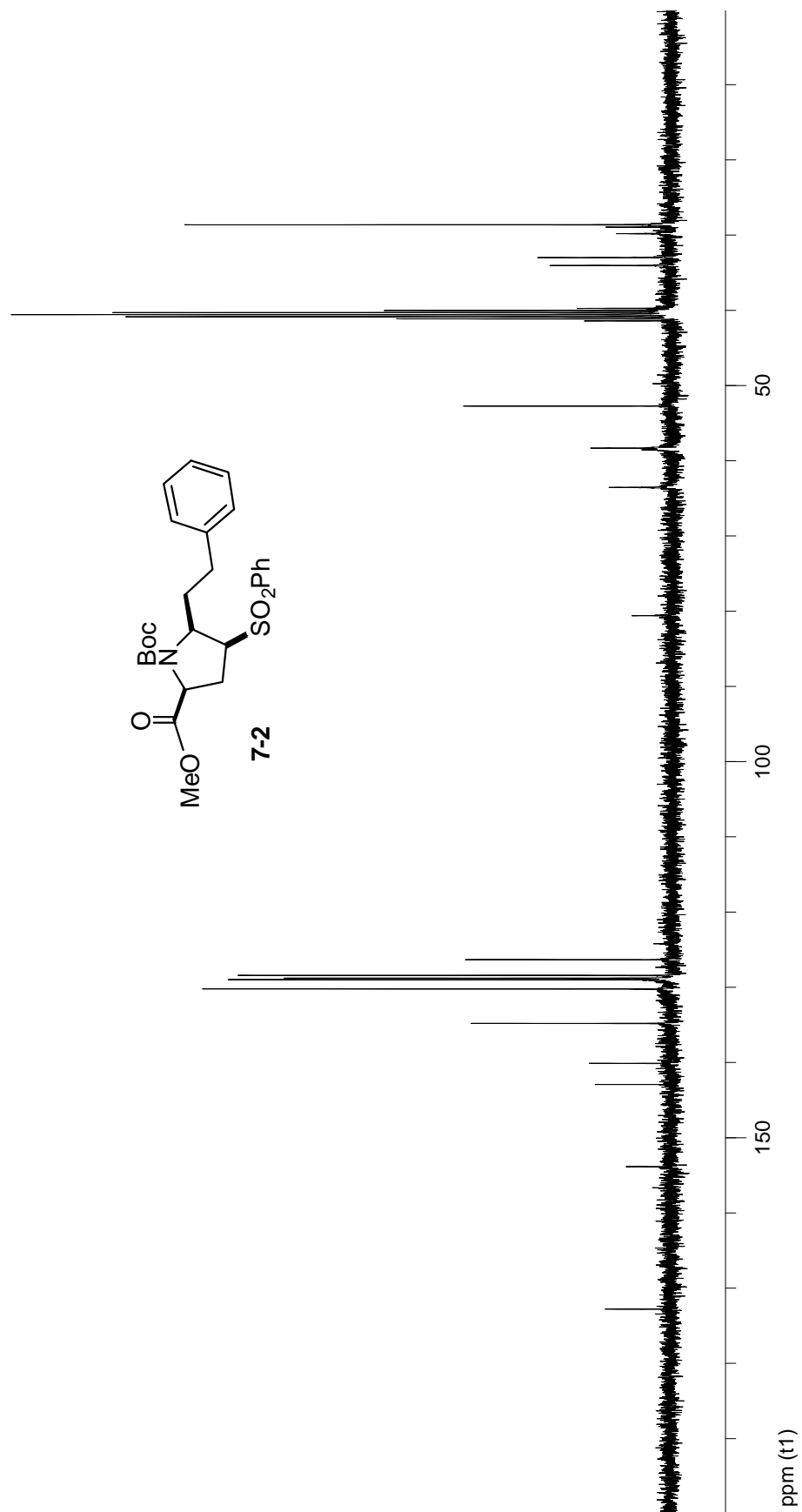
300 MHz $^1\text{H-NMR}$ of compound 6-33 in DMSO-d_6 at 90°C 

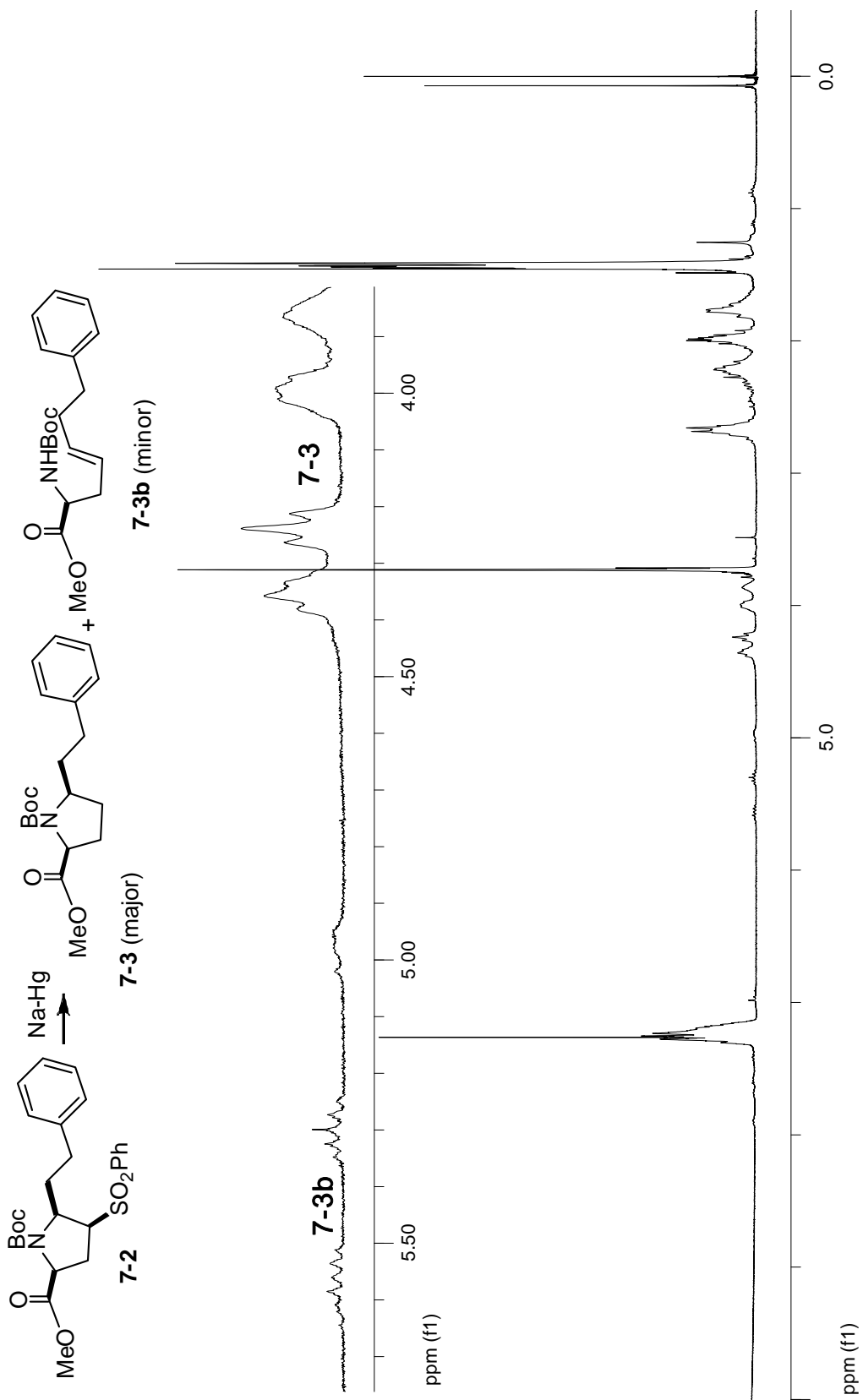
75 MHz ^{13}C -NMR of compound 6-33 in DMSO-d₆ at 90 °C

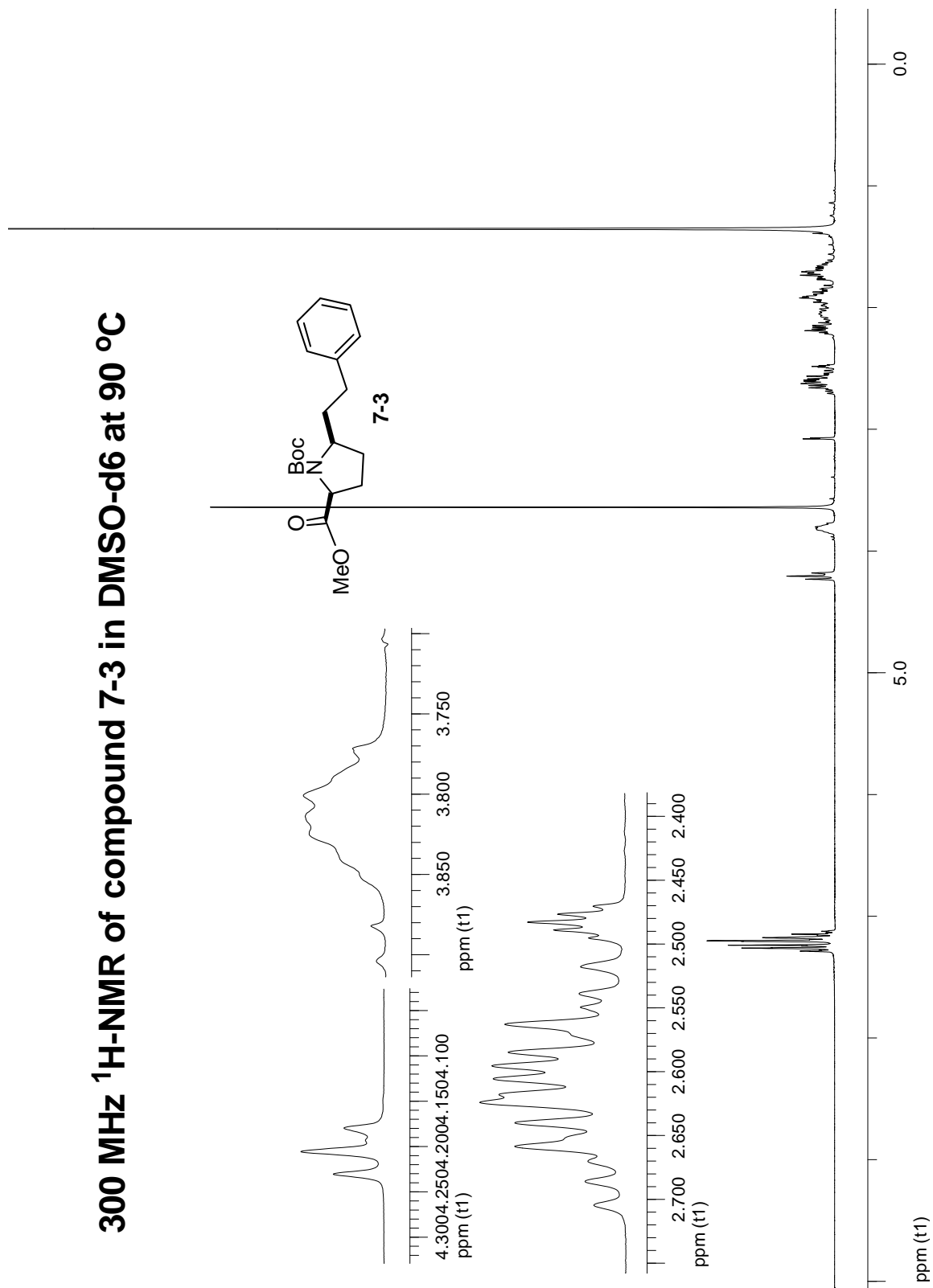
300 MHz ¹H-NMR of compound 6-40 in DMSO-d₆ at 90 °C

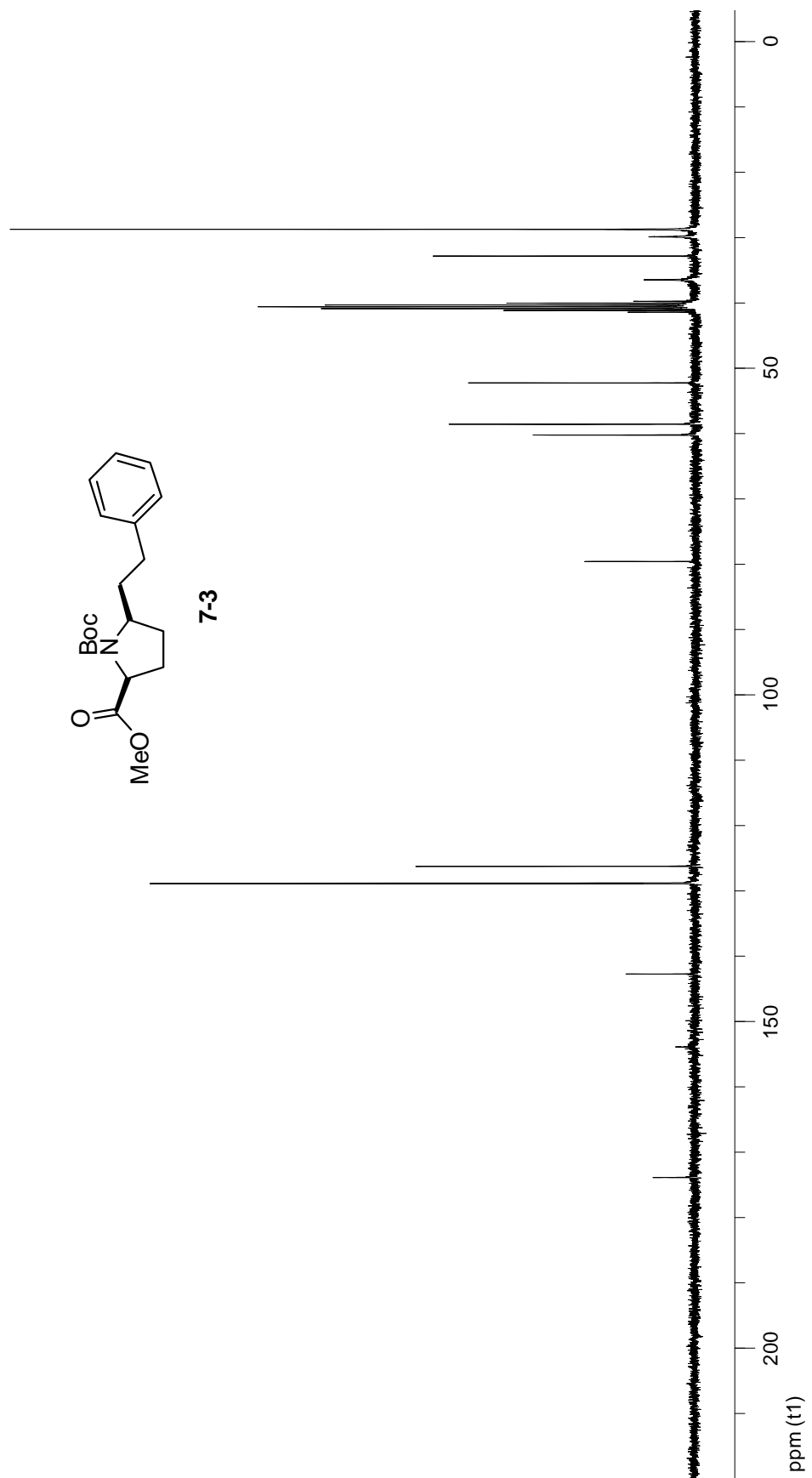
75 MHz ^{13}C -NMR of compound 6-40 in DMSO-d₆ at 90 °C

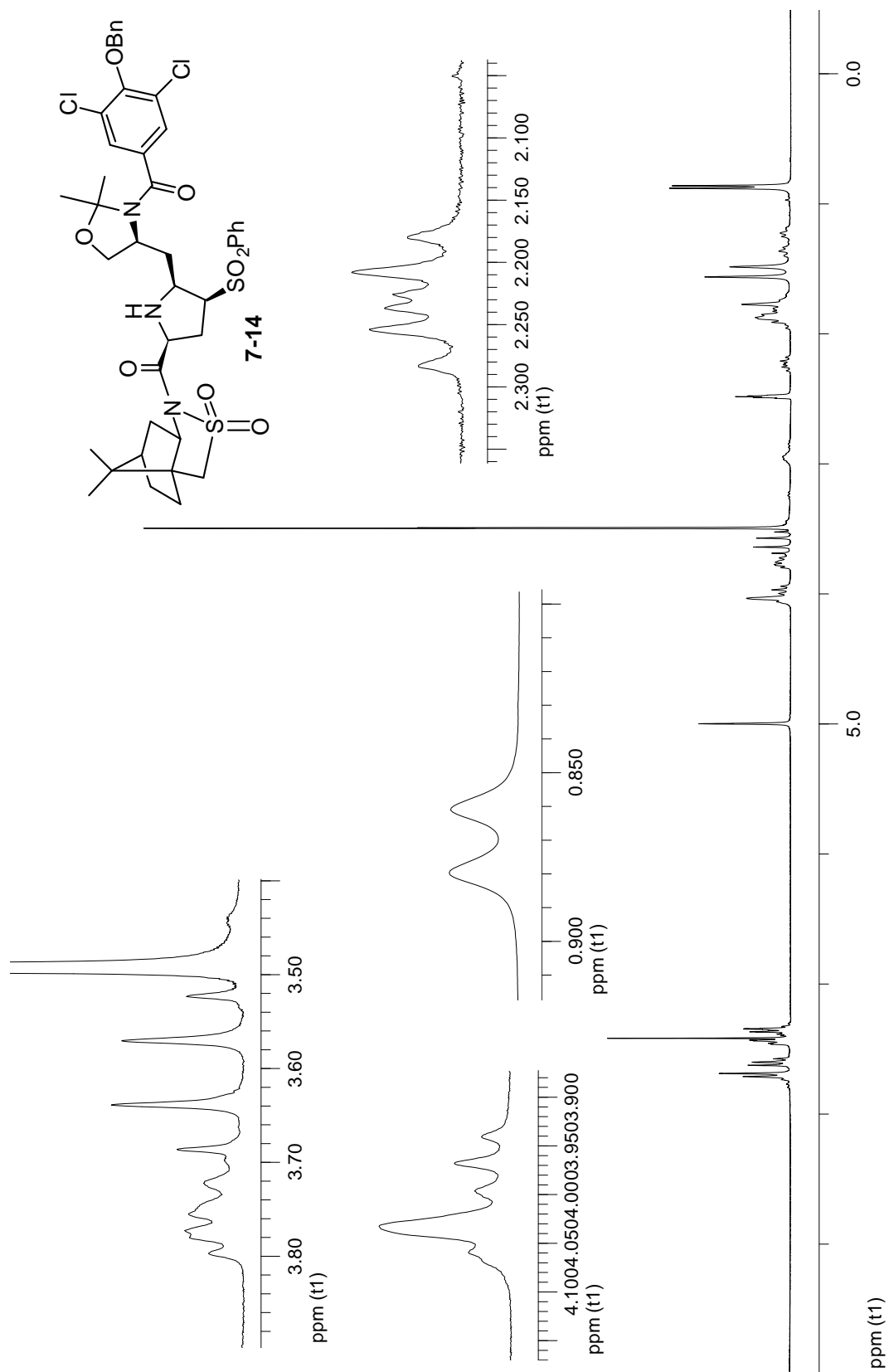
300 MHz $^1\text{H-NMR}$ of compound 7-2 in DMSO-d6 at 90 °C

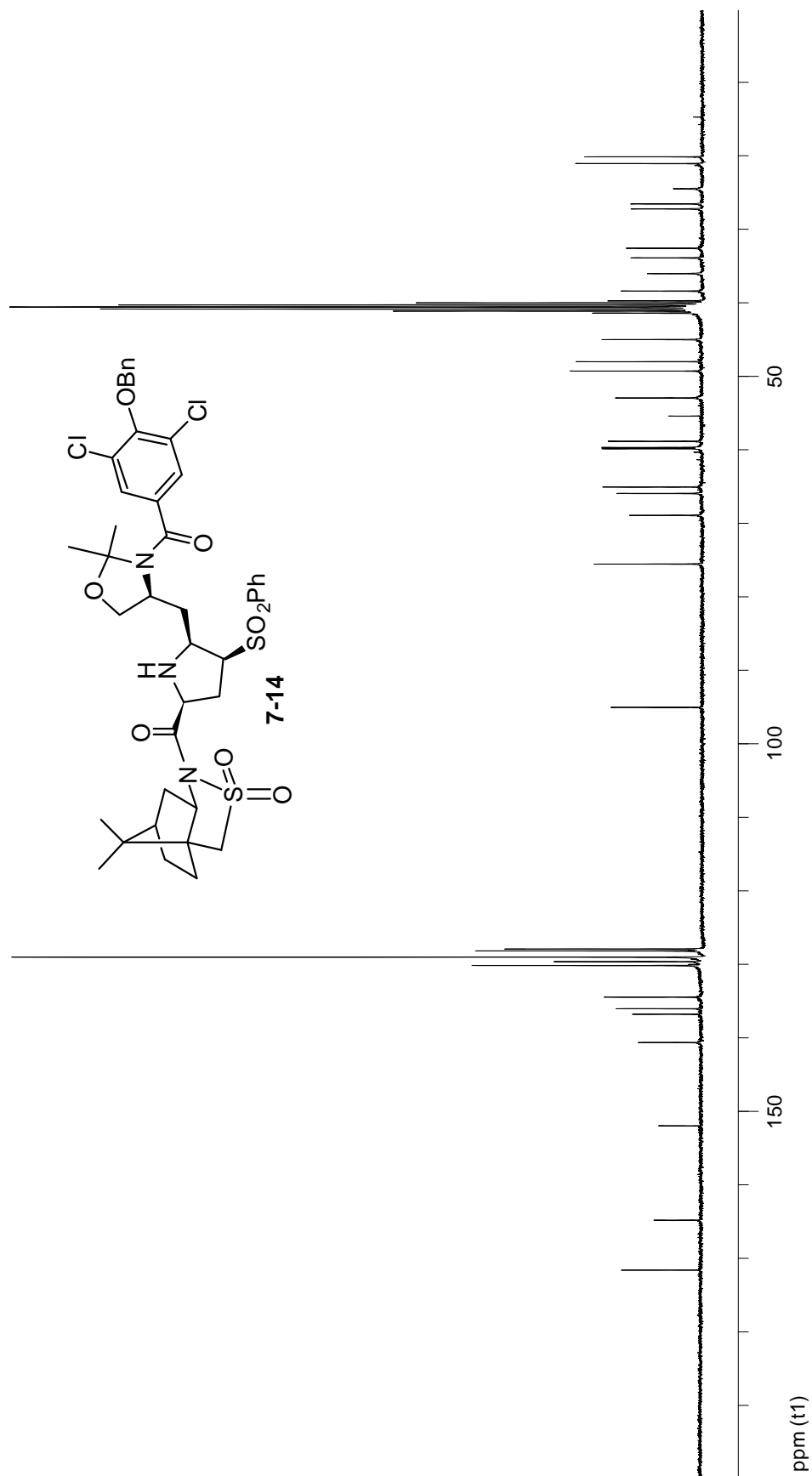
300 MHz $^1\text{H-NMR}$ of compound 7-2 in DMSO-d_6 at 90 °C

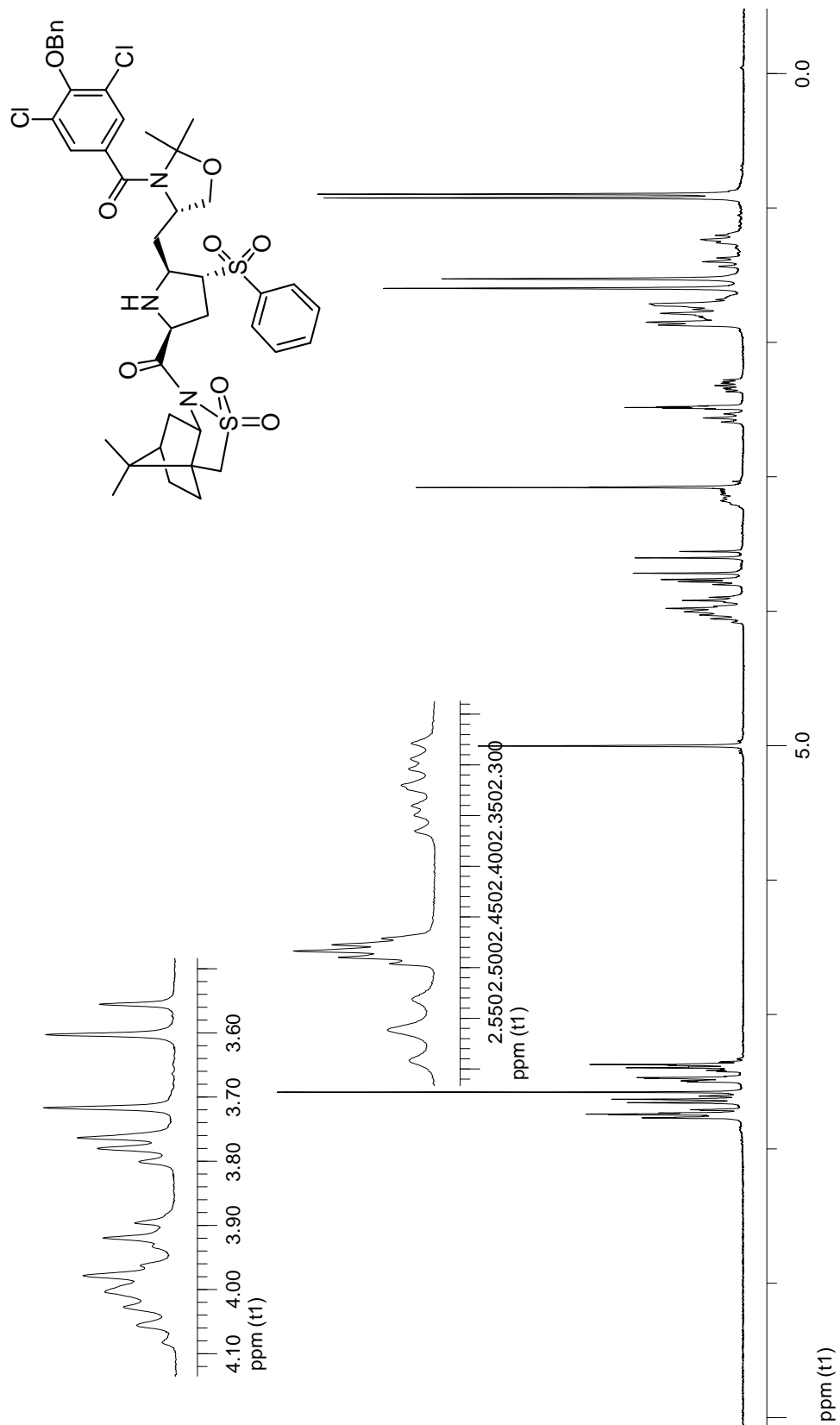
300 MHz $^1\text{H-NMR}$ of crude desulfonation with 7-2 in CDCl_3 at rt

300 MHz $^1\text{H-NMR}$ of compound 7-3 in DMSO-d_6 at $90\text{ }^\circ\text{C}$ 

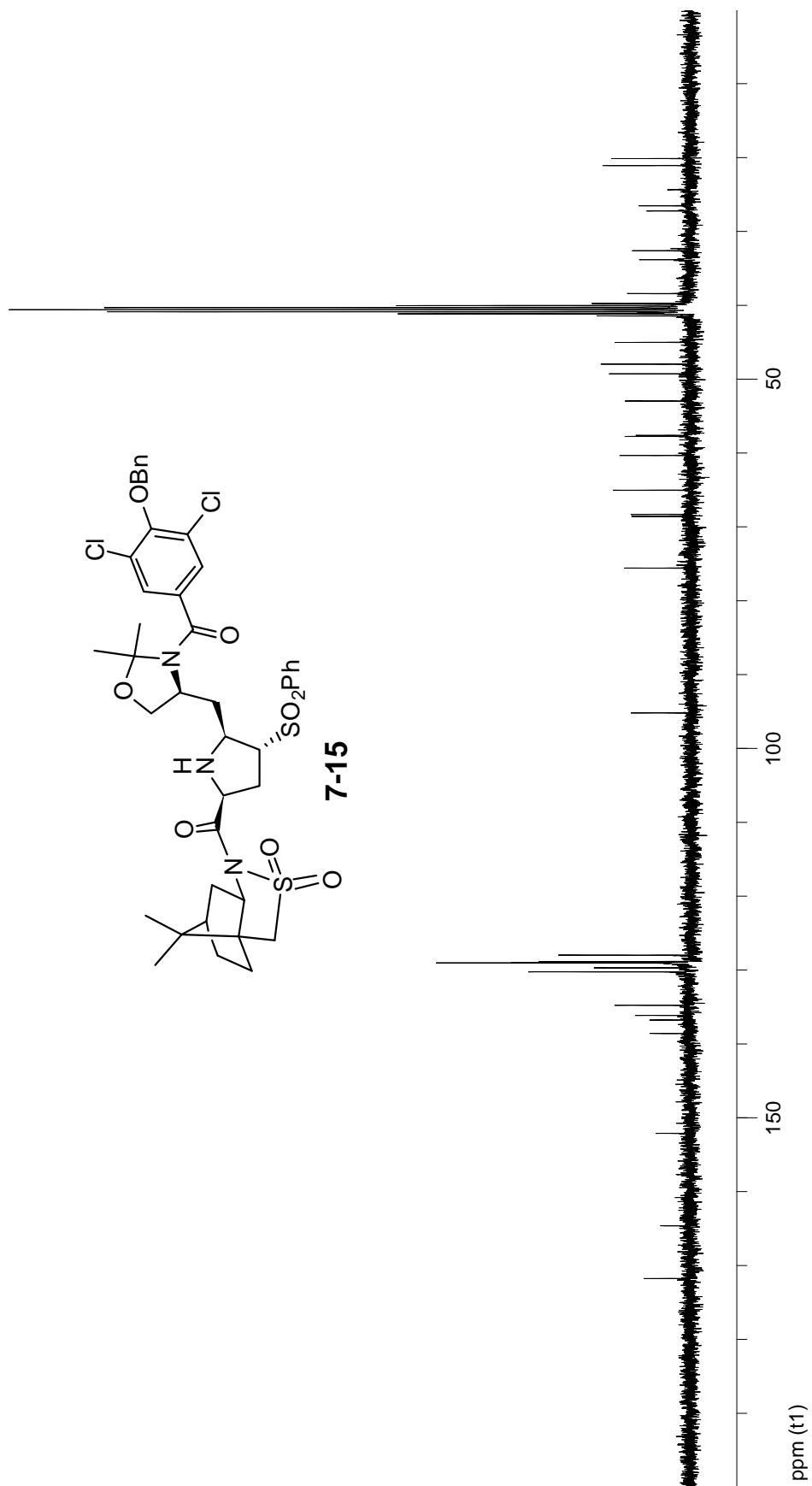
75 MHz ^{13}C -NMR of compound 7-3 in DMSO-d₆ at 90 °C

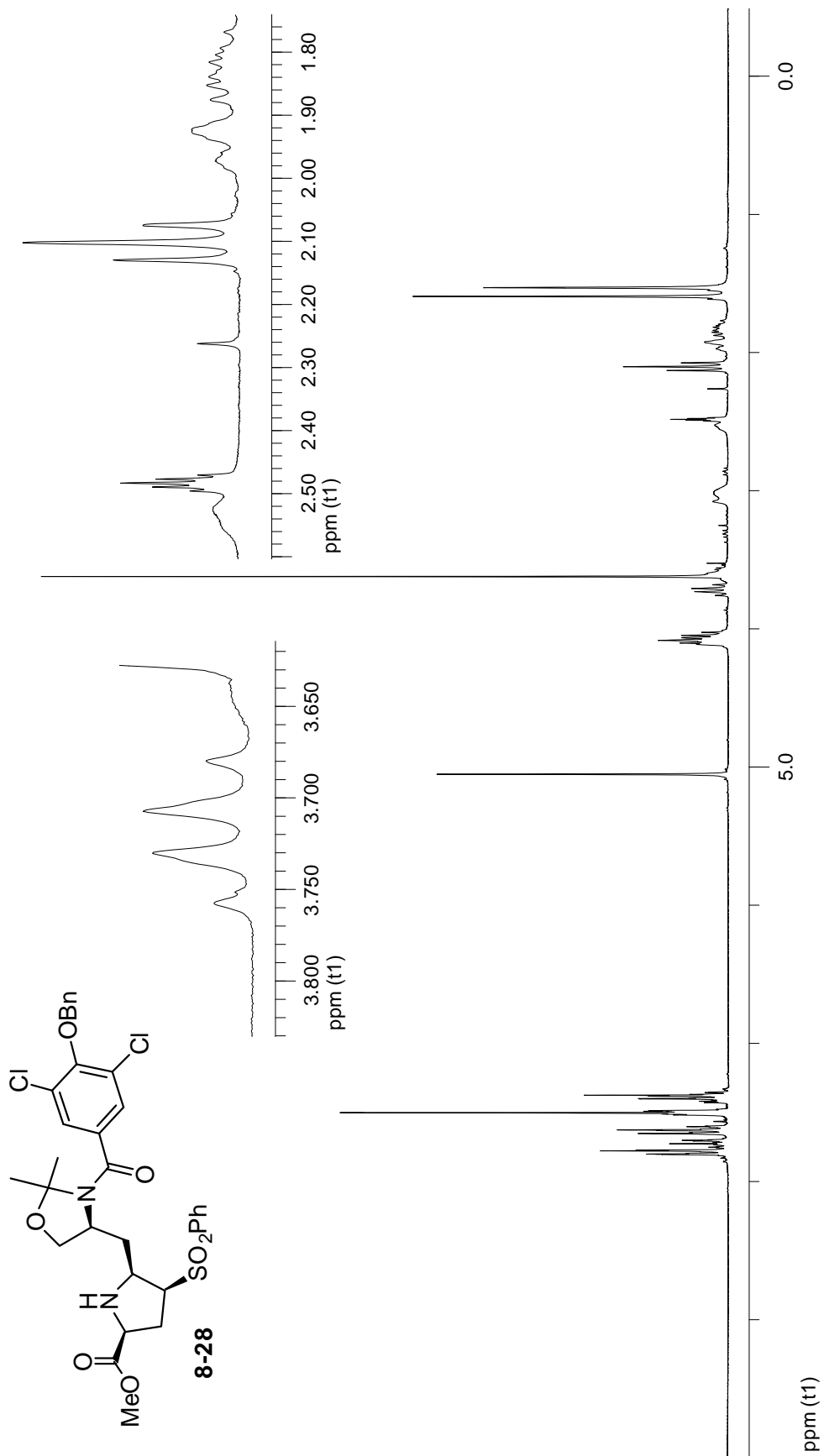
300 MHz $^1\text{H-NMR}$ of compound 7-14 in DMSO-d_6 -5% D_2O at 70 °C

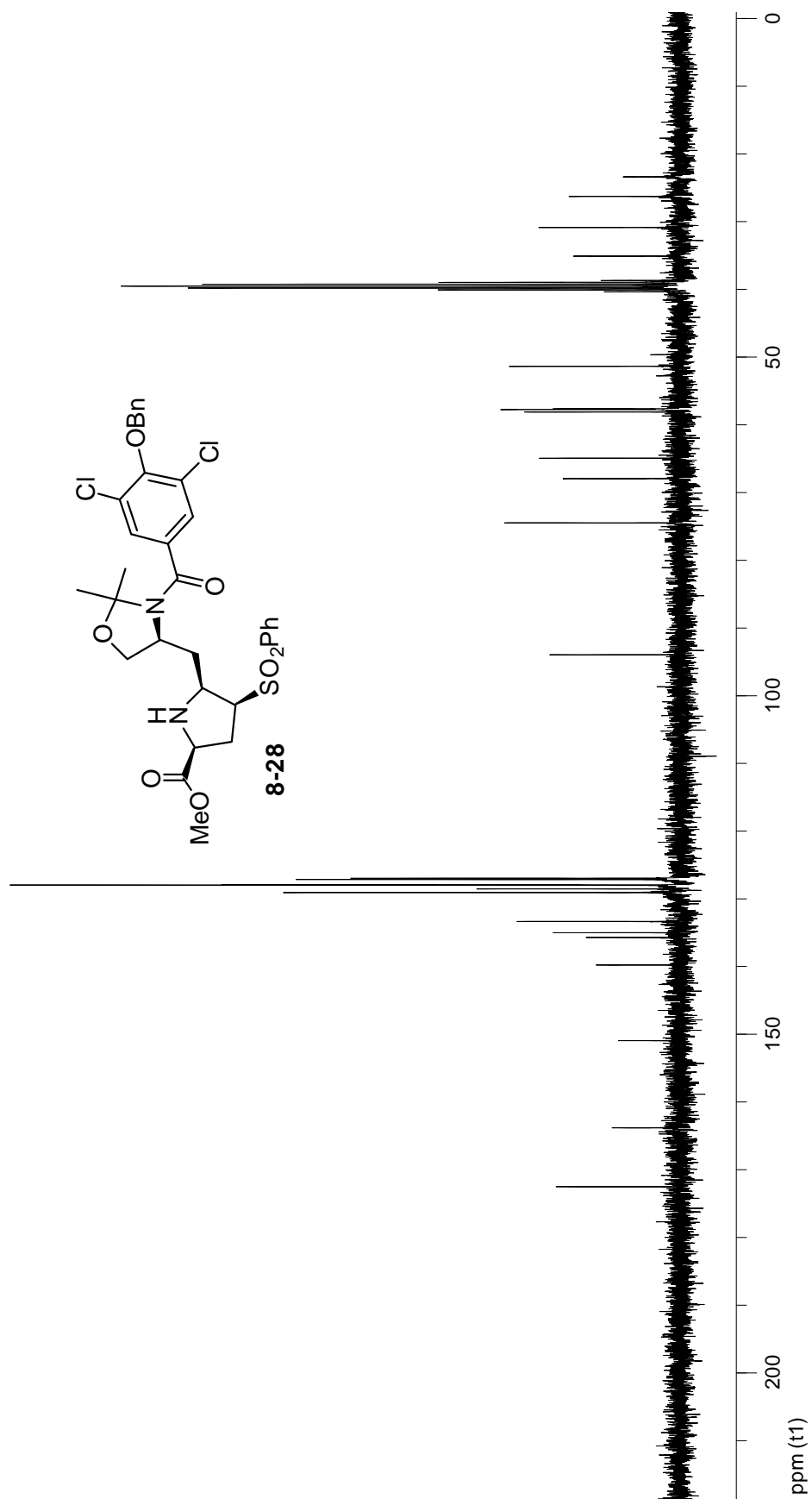
75 MHz ^{13}C -NMR of compound 7-14 in DMSO-d₆ at 90 °C

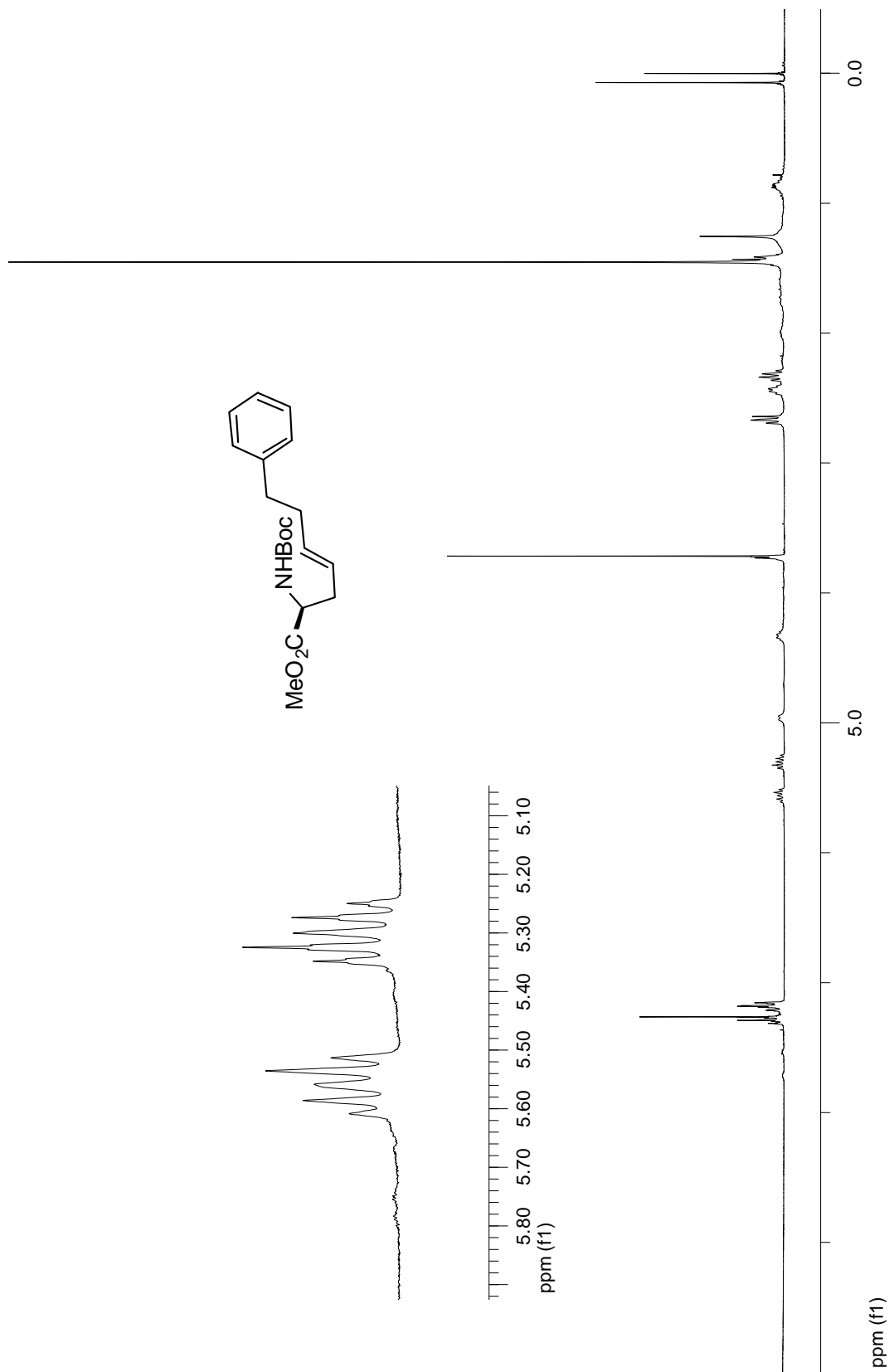
300 MHz $^1\text{H-NMR}$ of compound 7-15 in DMSO-d_6 -90 °C

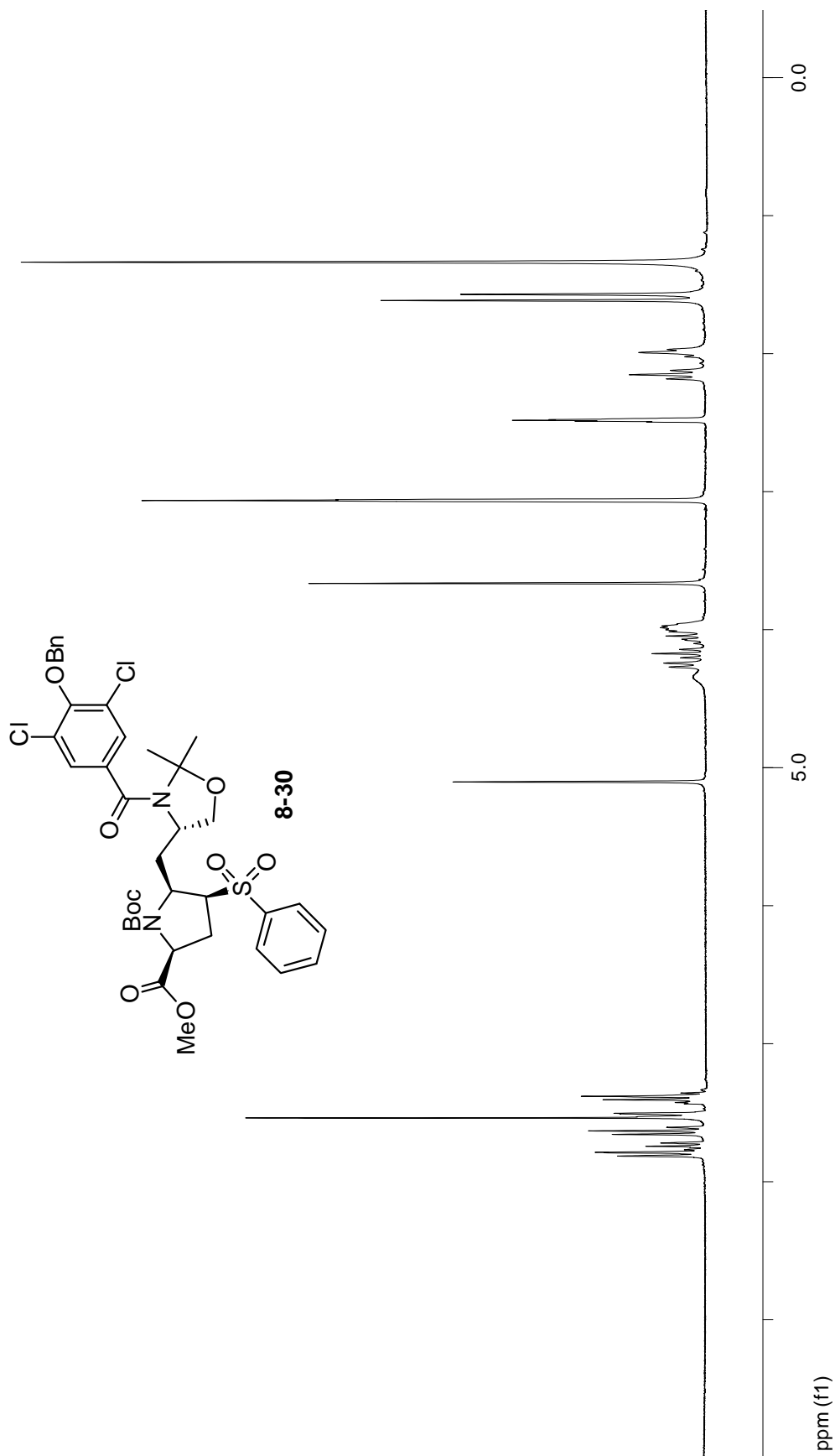
75 MHz ^{13}C -NMR of compound 7-15 in DMSO-d_6 -5% D_2O -90 °C

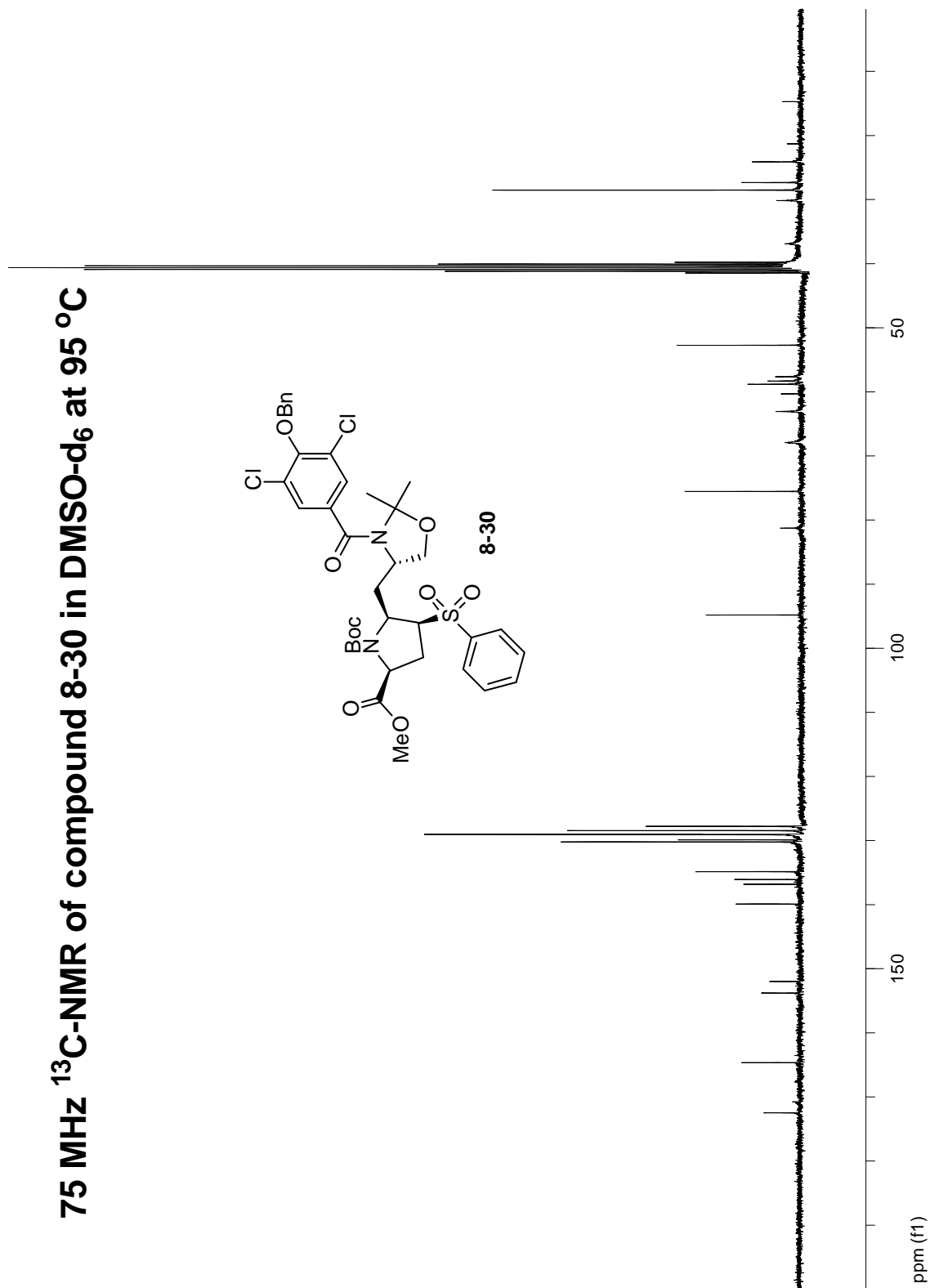
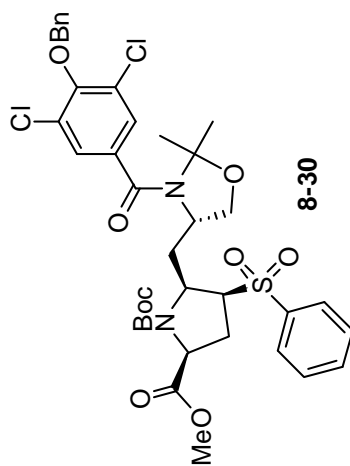
75 MHz ^{13}C -NMR of compound 7-15 in DMSO- d_6 -90 °C

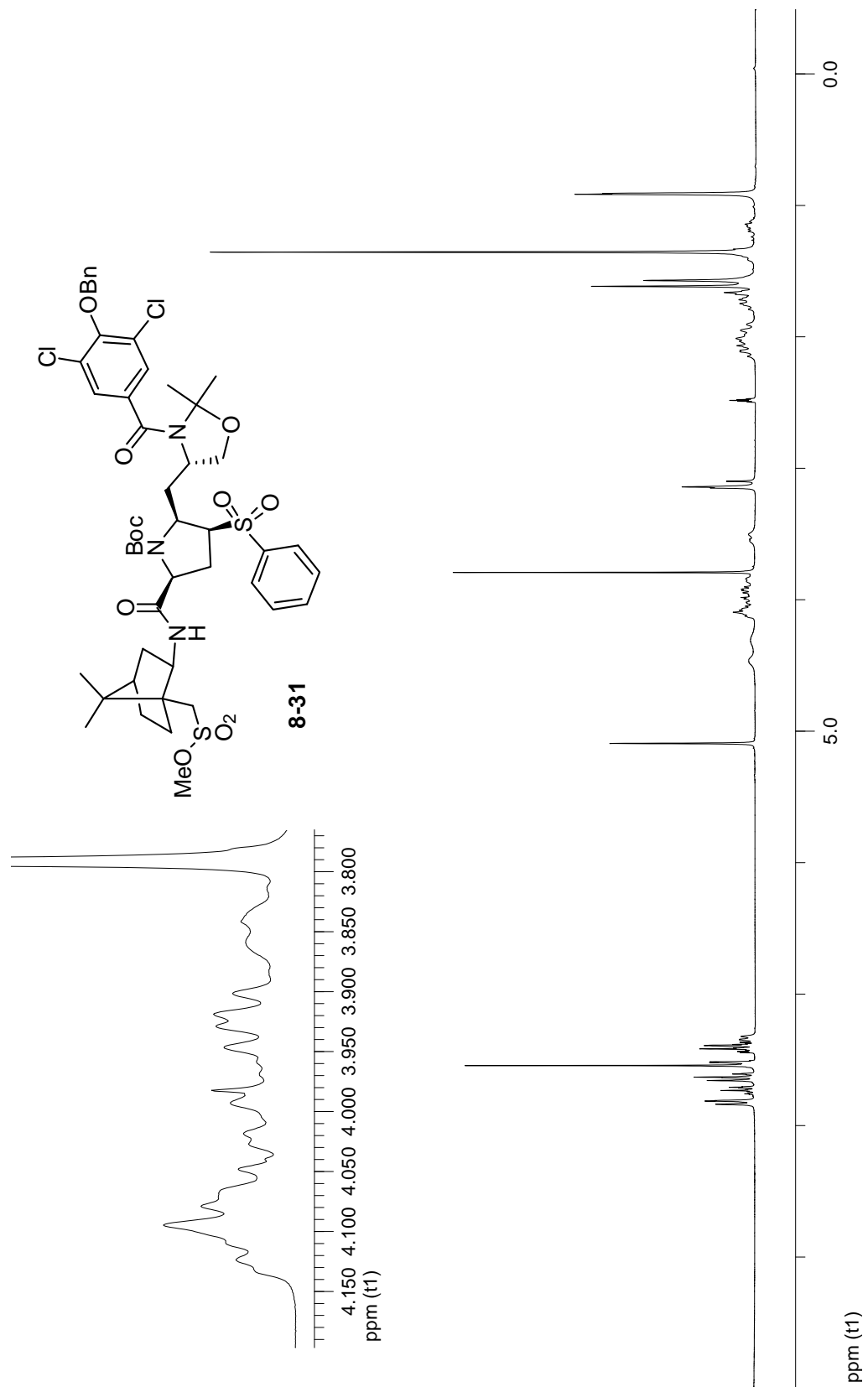
300 MHz $^1\text{H-NMR}$ of compound 8-28 in DMSO-d_6 -90 °C

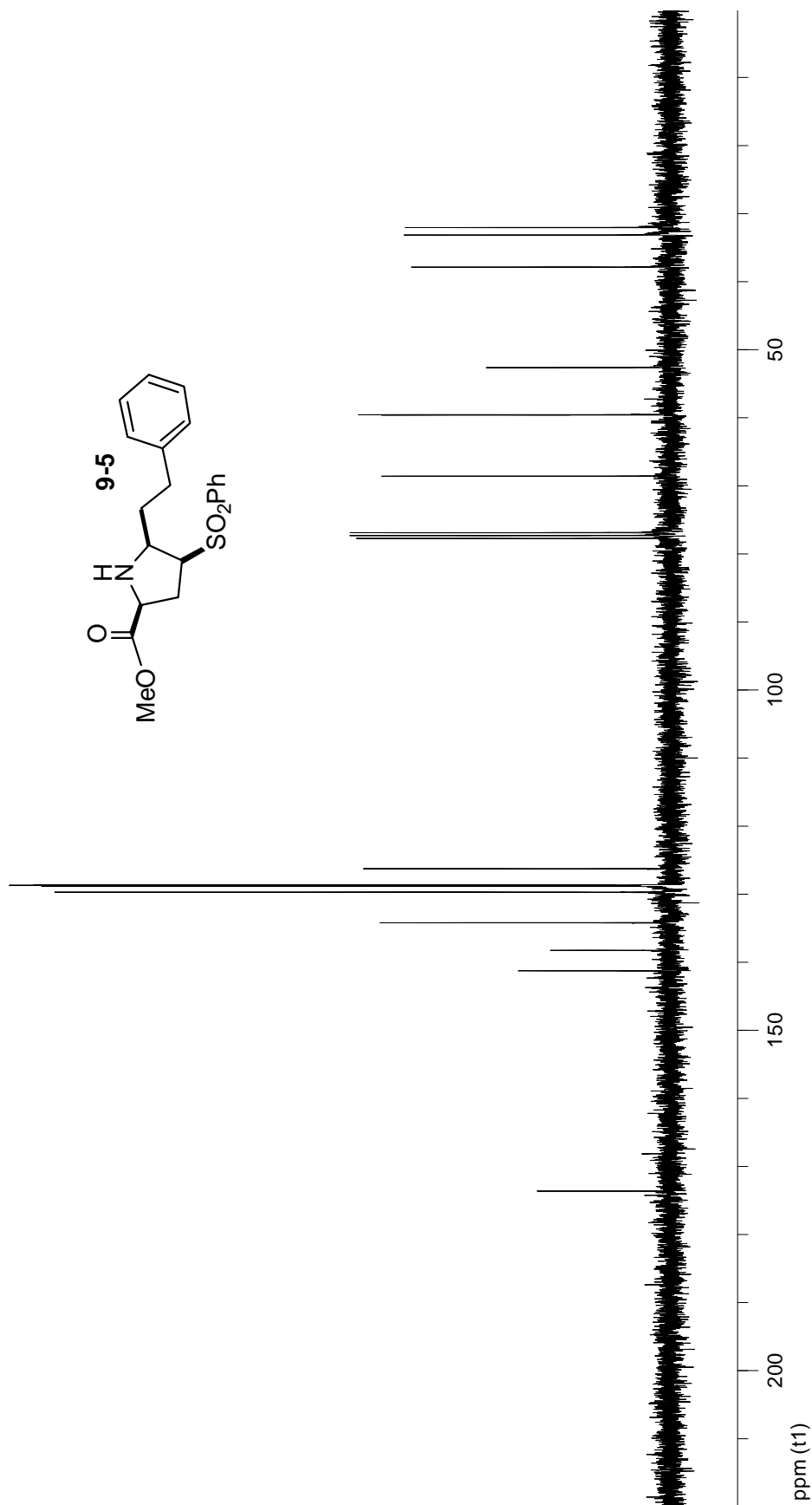
75 MHz ^{13}C -NMR of compound 8-28 in DMSO-90 °C

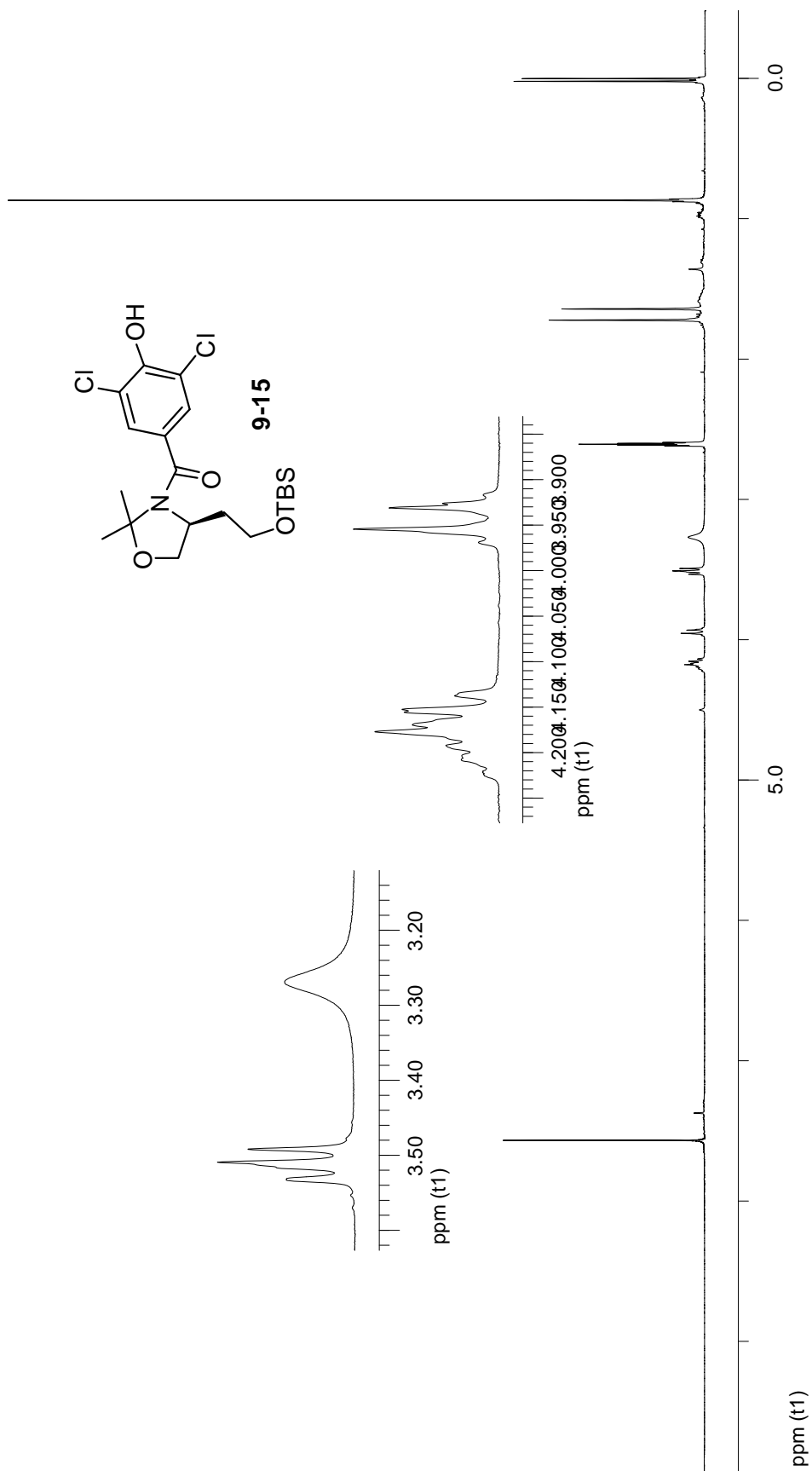
300 MHz $^1\text{H-NMR}$ of compound 8-29 in CDCl_3 at rt

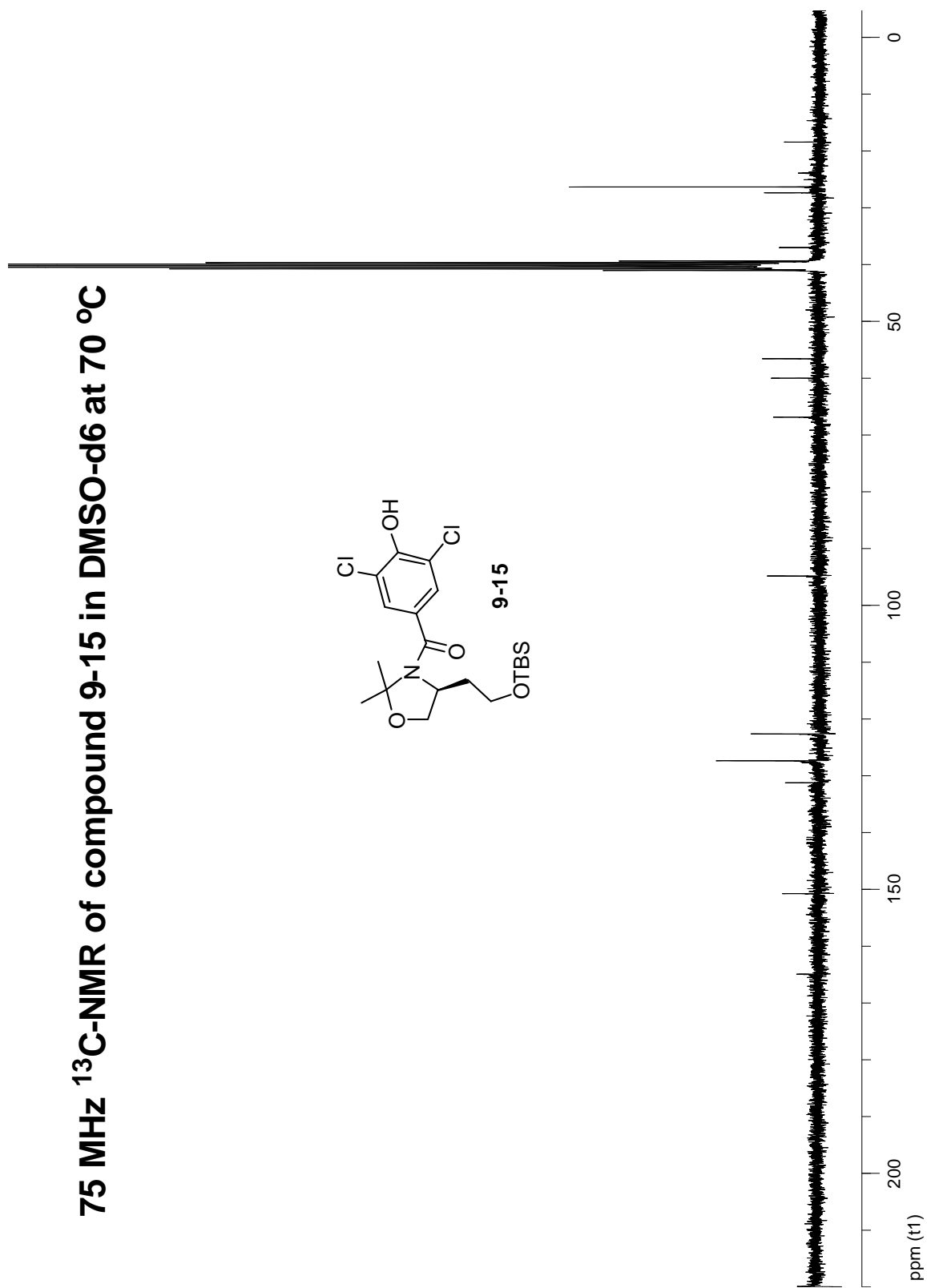
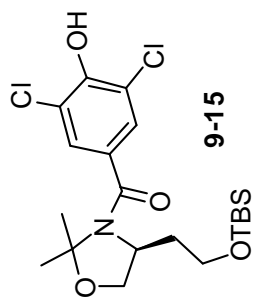
300 MHz $^1\text{H-NMR}$ of compound 8-30 in DMSO-d_6 at 95 $^\circ\text{C}$ 

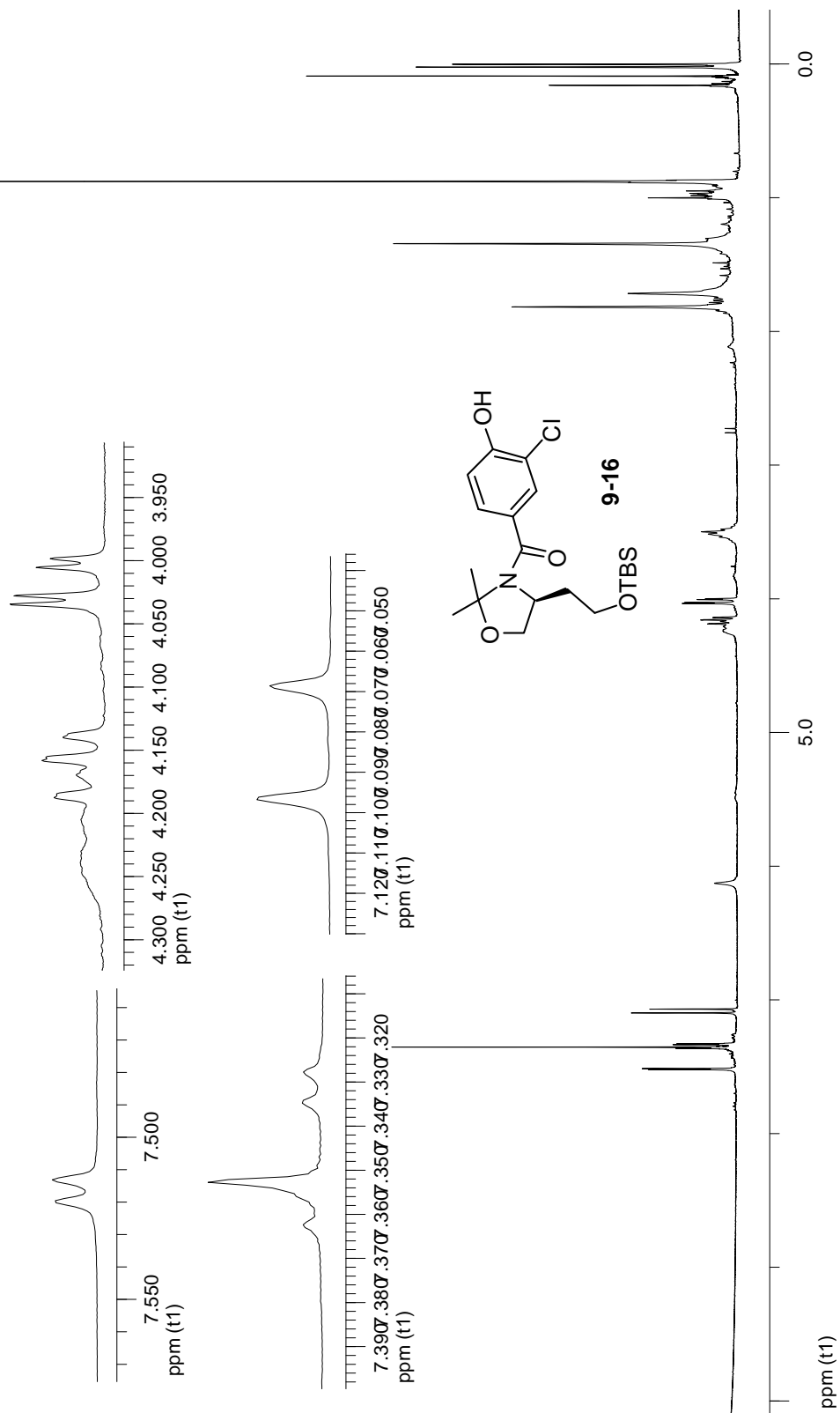
75 MHz ^{13}C -NMR of compound 8-30 in DMSO-d_6 at 95 °C

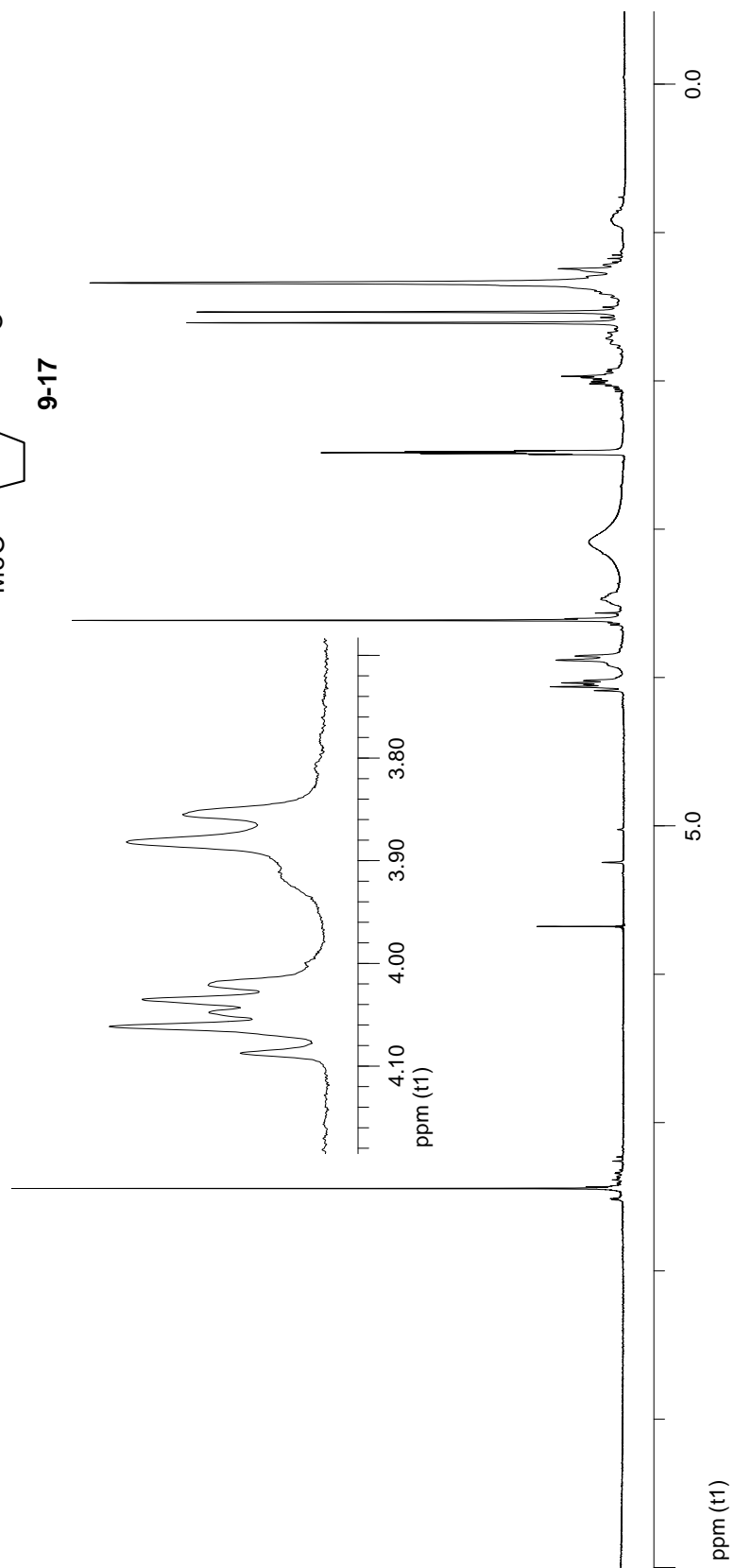
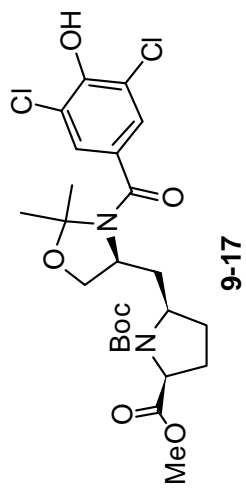
300 MHz $^1\text{H-NMR}$ of compound 8-31 in DMSO-d_6 at 75 $^\circ\text{C}$ 

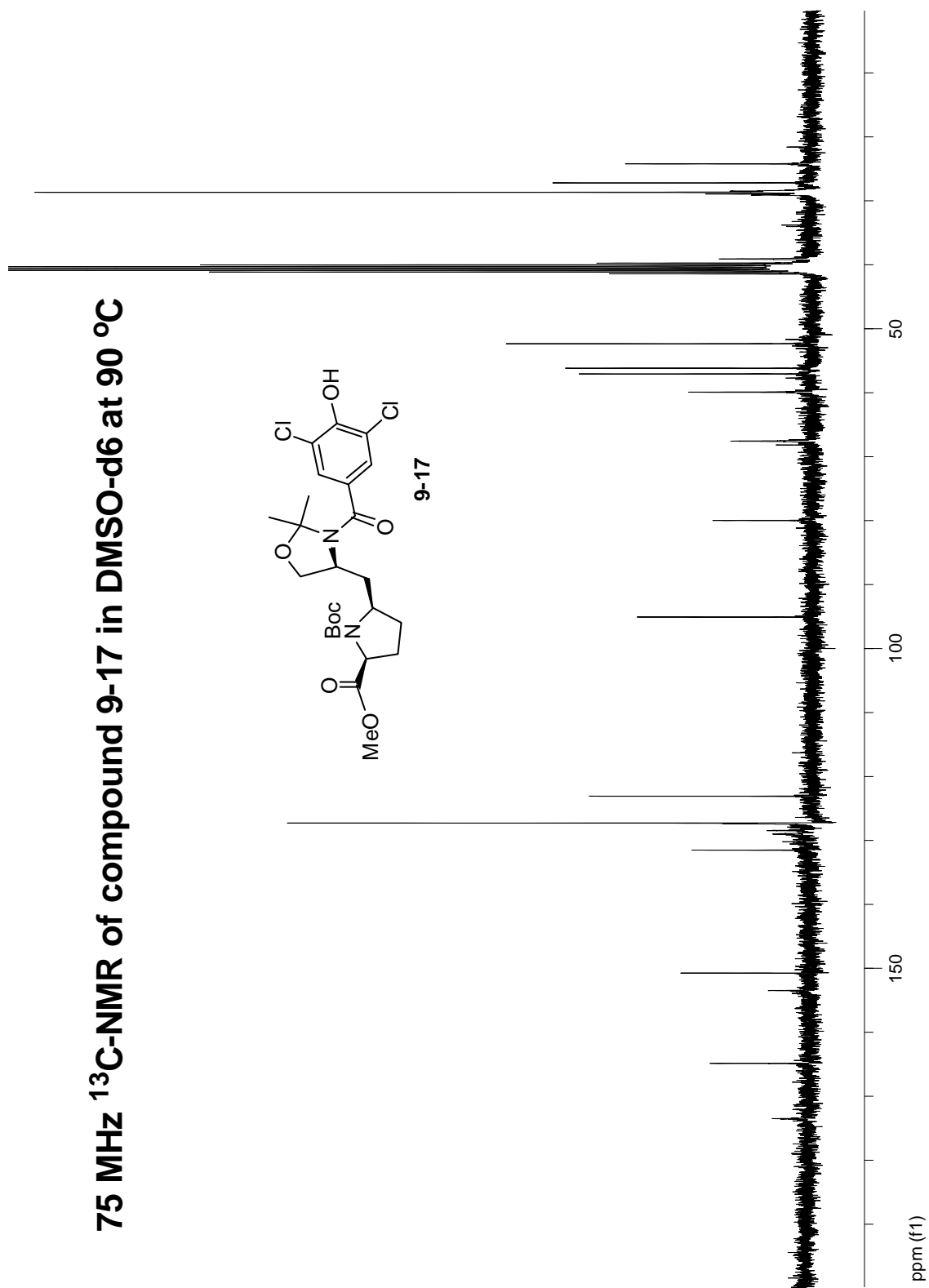
75 MHz ^{13}C -NMR of compound 9-5 in CDCl_3 at rt

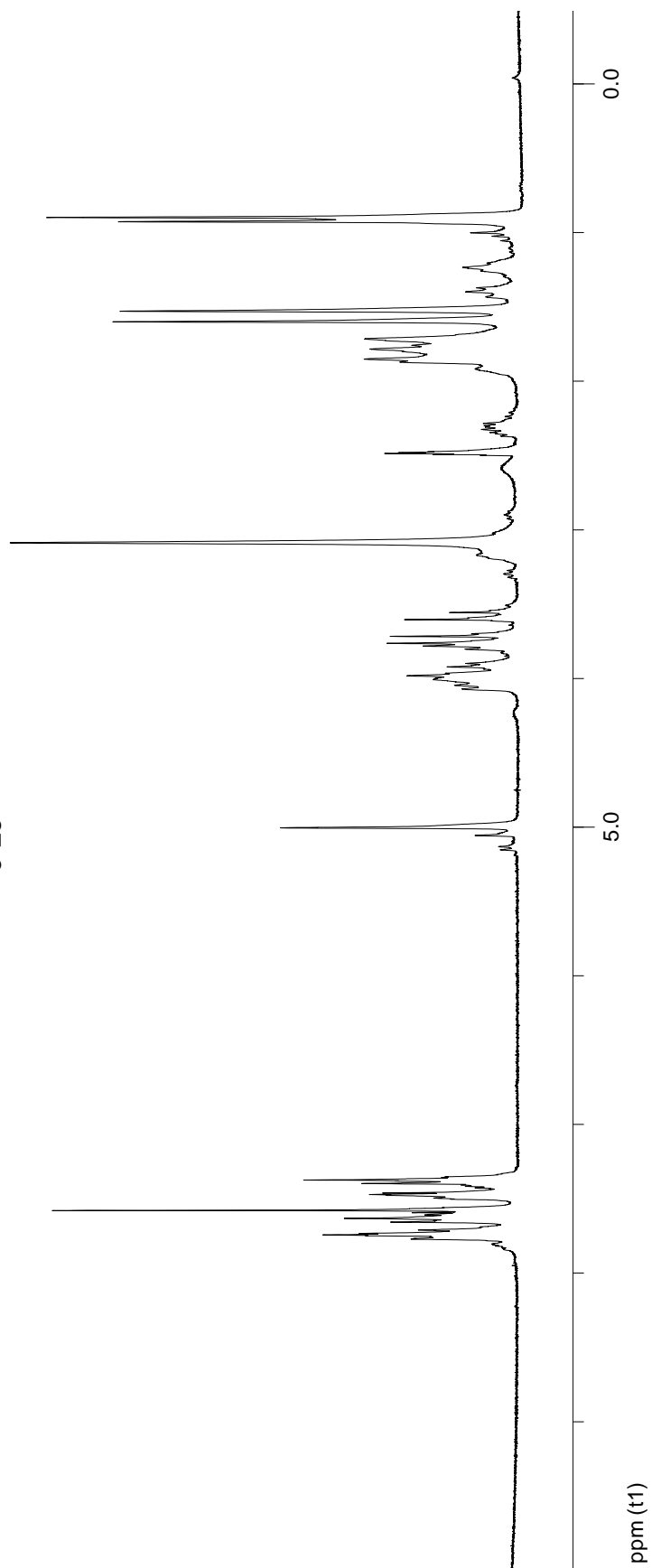
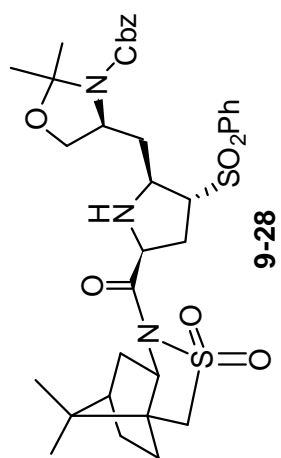
300 MHz ¹H-NMR of compound 9-15 in DMSO-d₆ at 70 °C

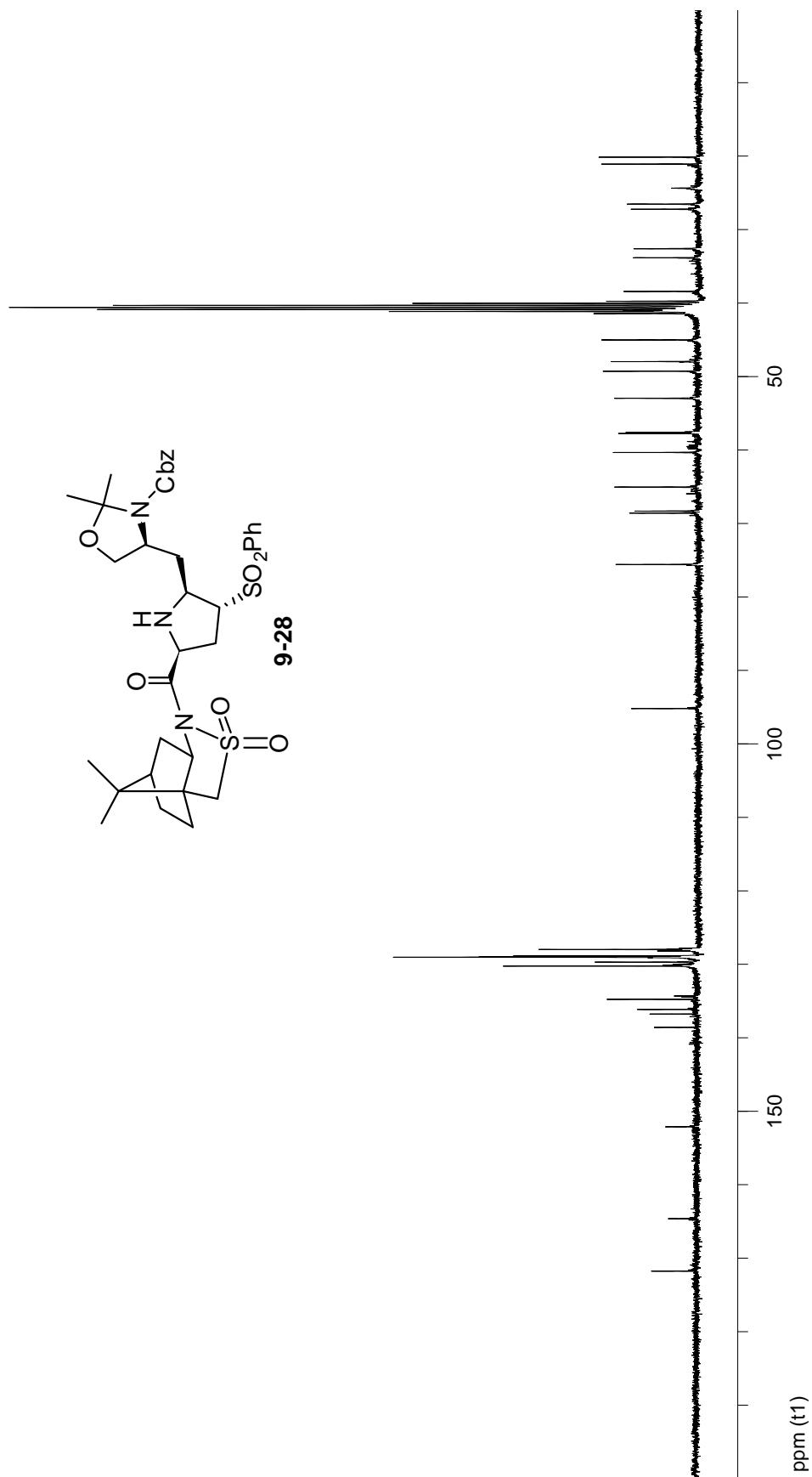
75 MHz ^{13}C -NMR of compound 9-15 in DMSO-d₆ at 70 °C

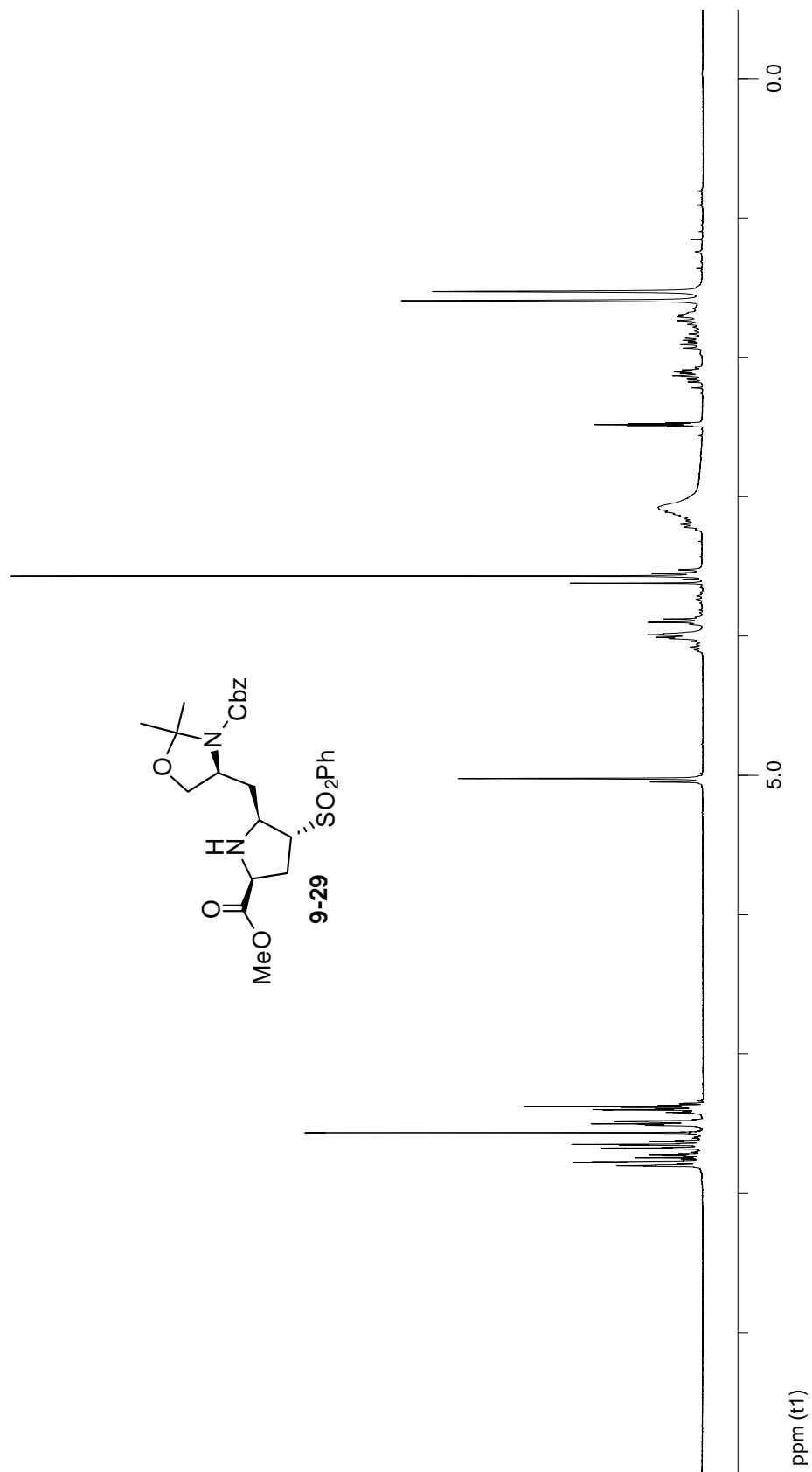
300 MHz $^1\text{H-NMR}$ of compound 9-16 in CDCl_3 at rt

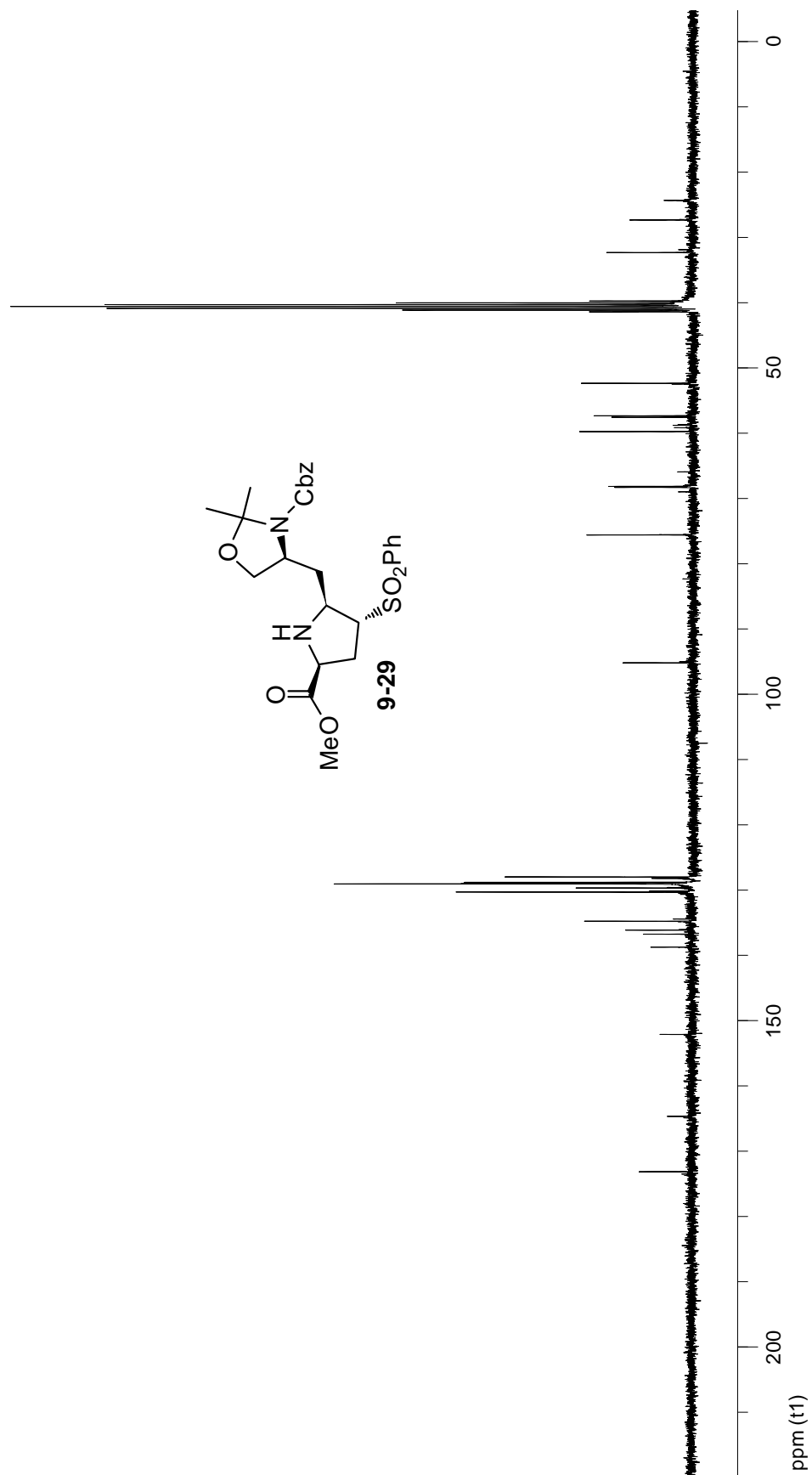
300 MHz $^1\text{H-NMR}$ of compound 9-17 in DMSO-d₆ at 90 °C

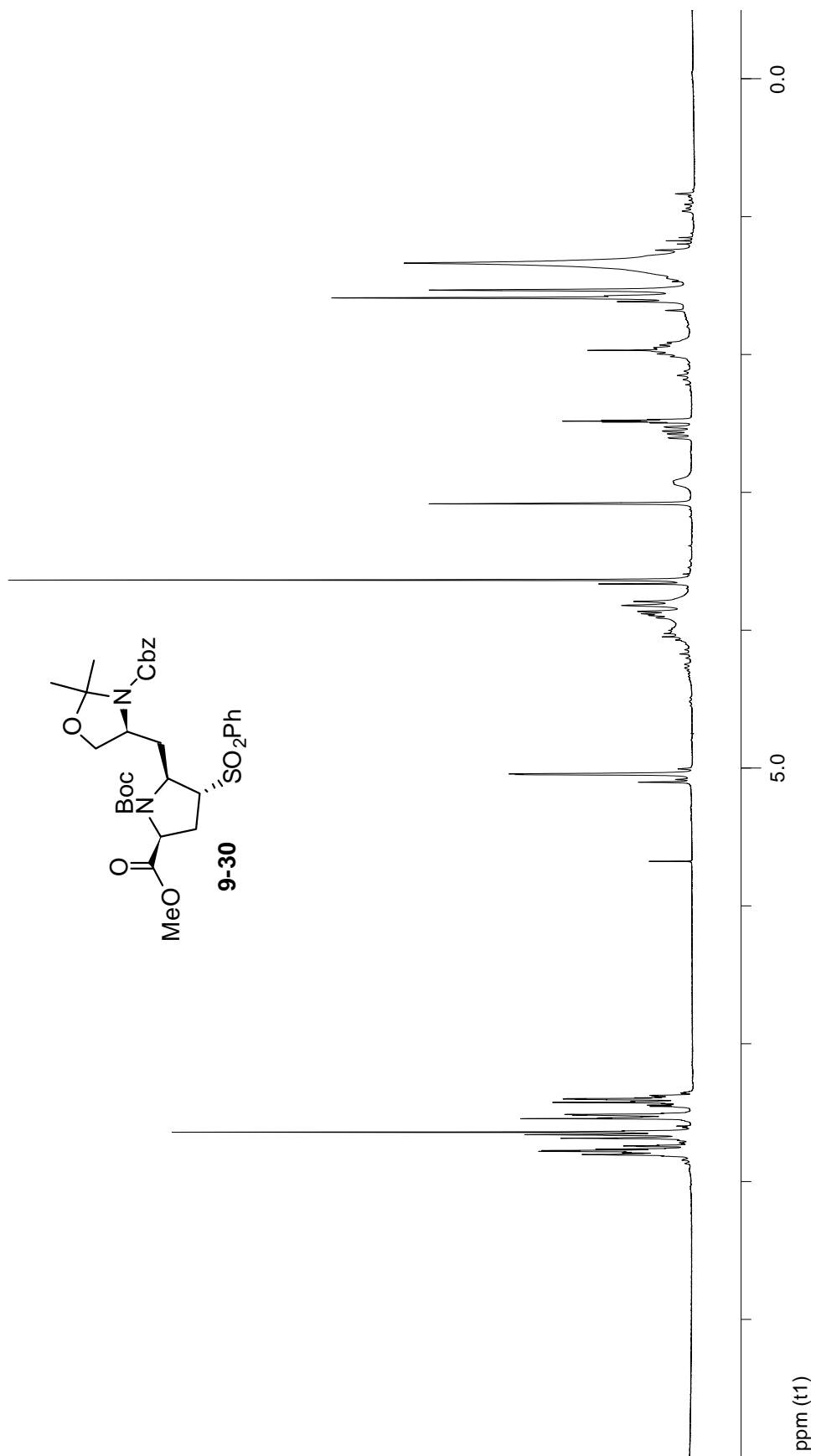
75 MHz ^{13}C -NMR of compound 9-17 in DMSO-d₆ at 90 °C

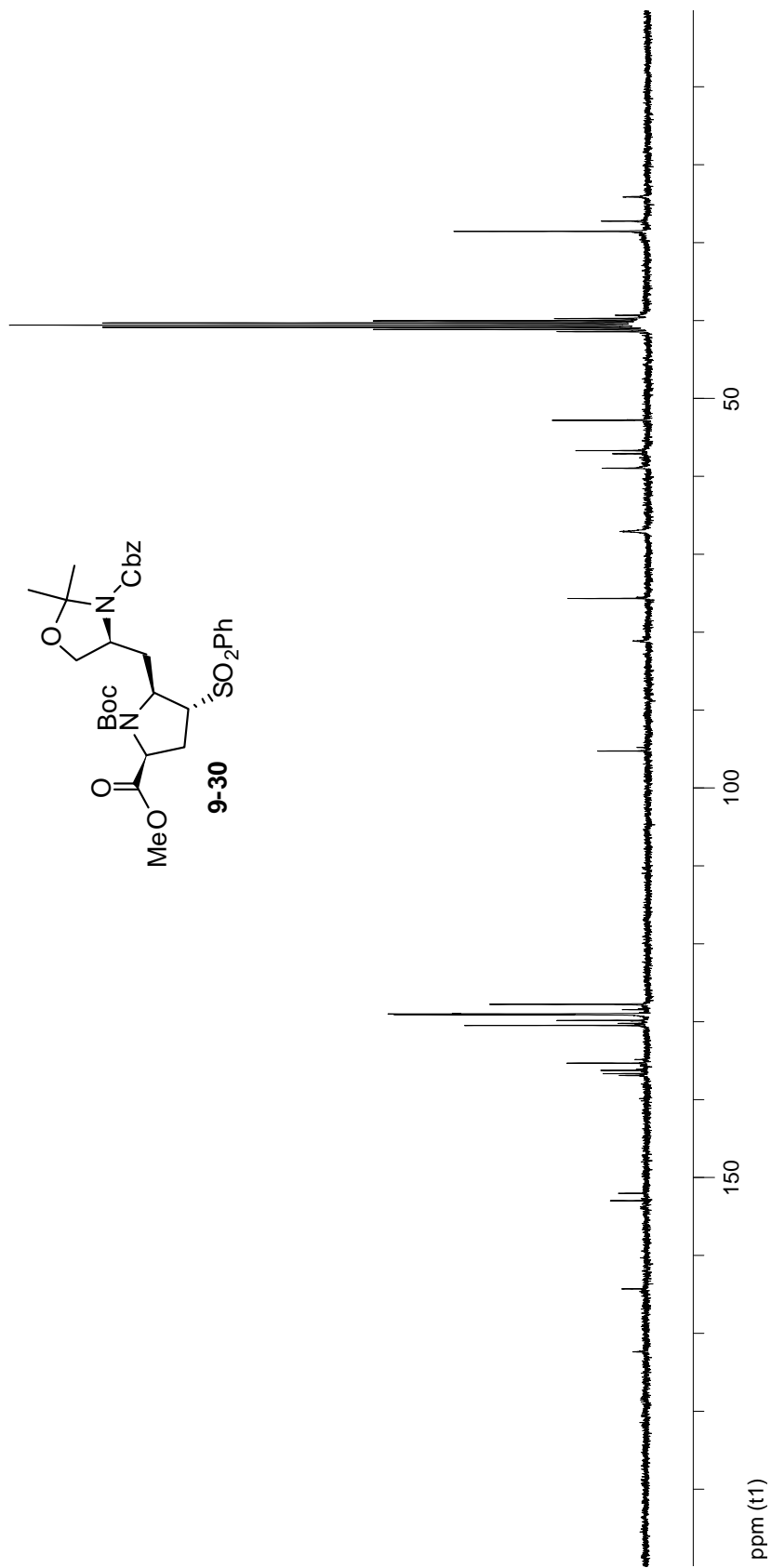
300 MHz $^1\text{H-NMR}$ of compound 9-28 in DMSO-d₆ at 90 °C

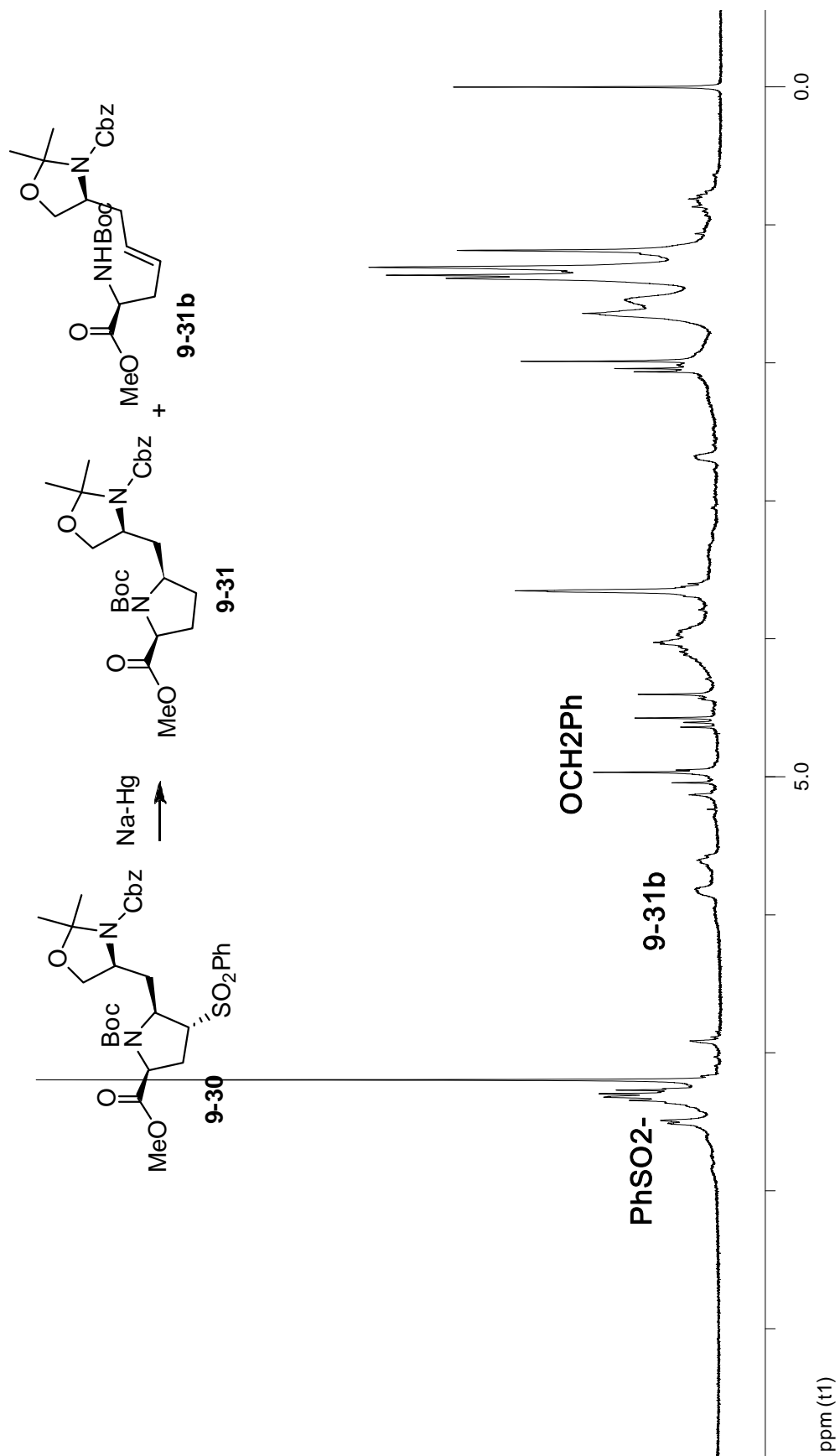
75 MHz ^{13}C -NMR of compound 9-28 in DMSO-d₆ at 90 °C

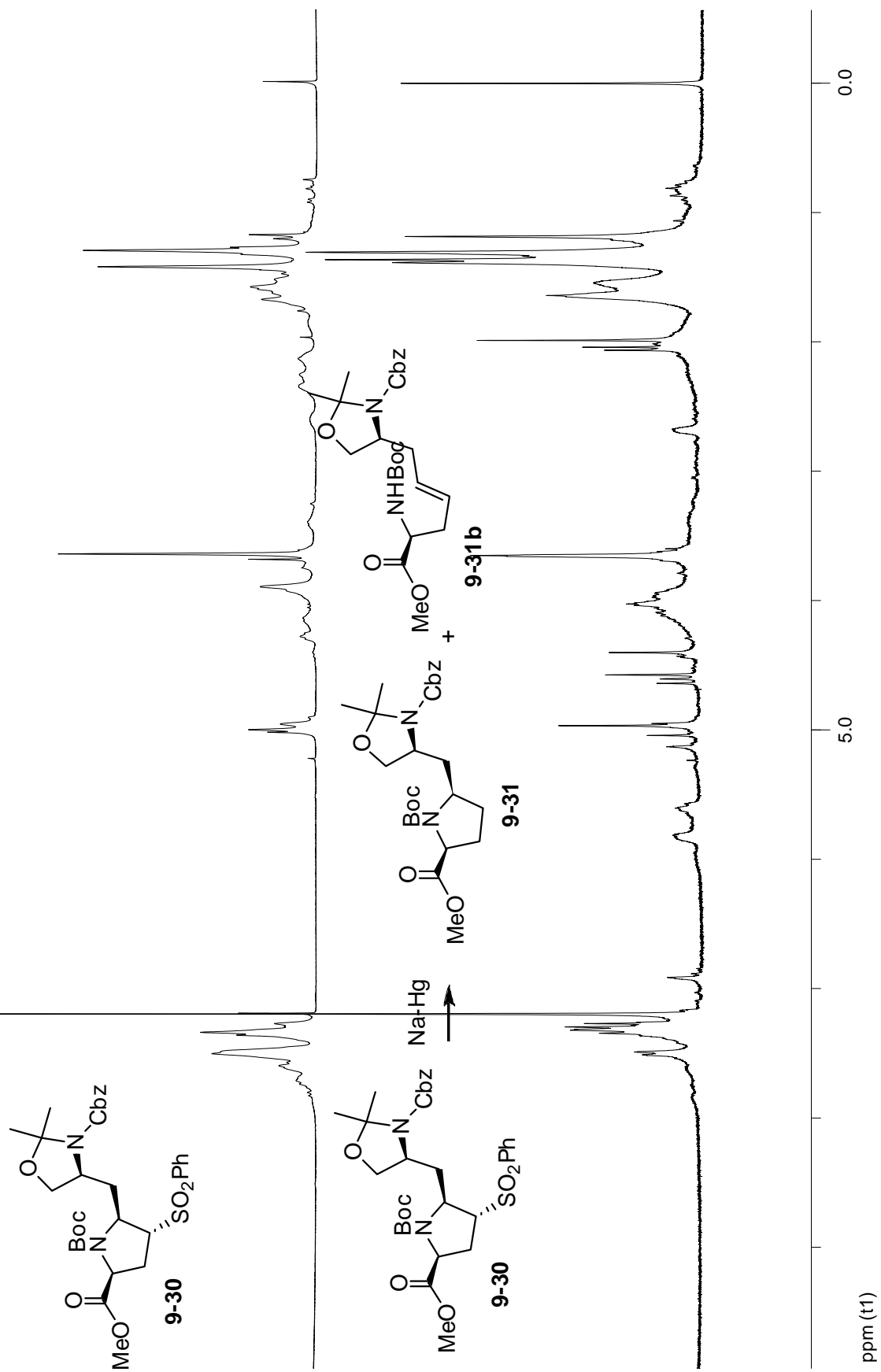
75 MHz ^{13}C -NMR of compound 9-29 in DMSO-d6 at 90 °C

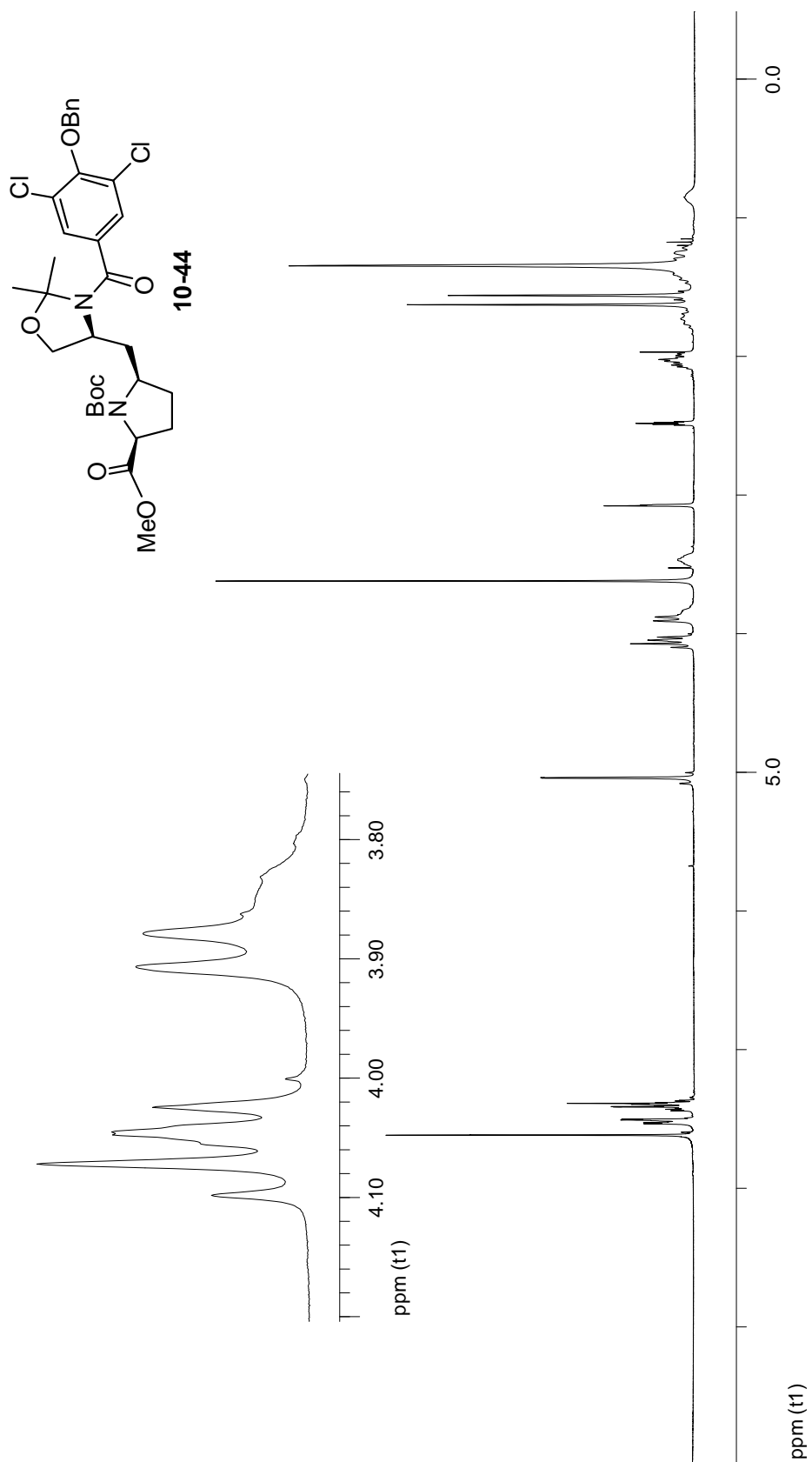
75 MHz $^1\text{H-NMR}$ of compound 9-29 in DMSO-d_6 at $90\text{ }^\circ\text{C}$ 

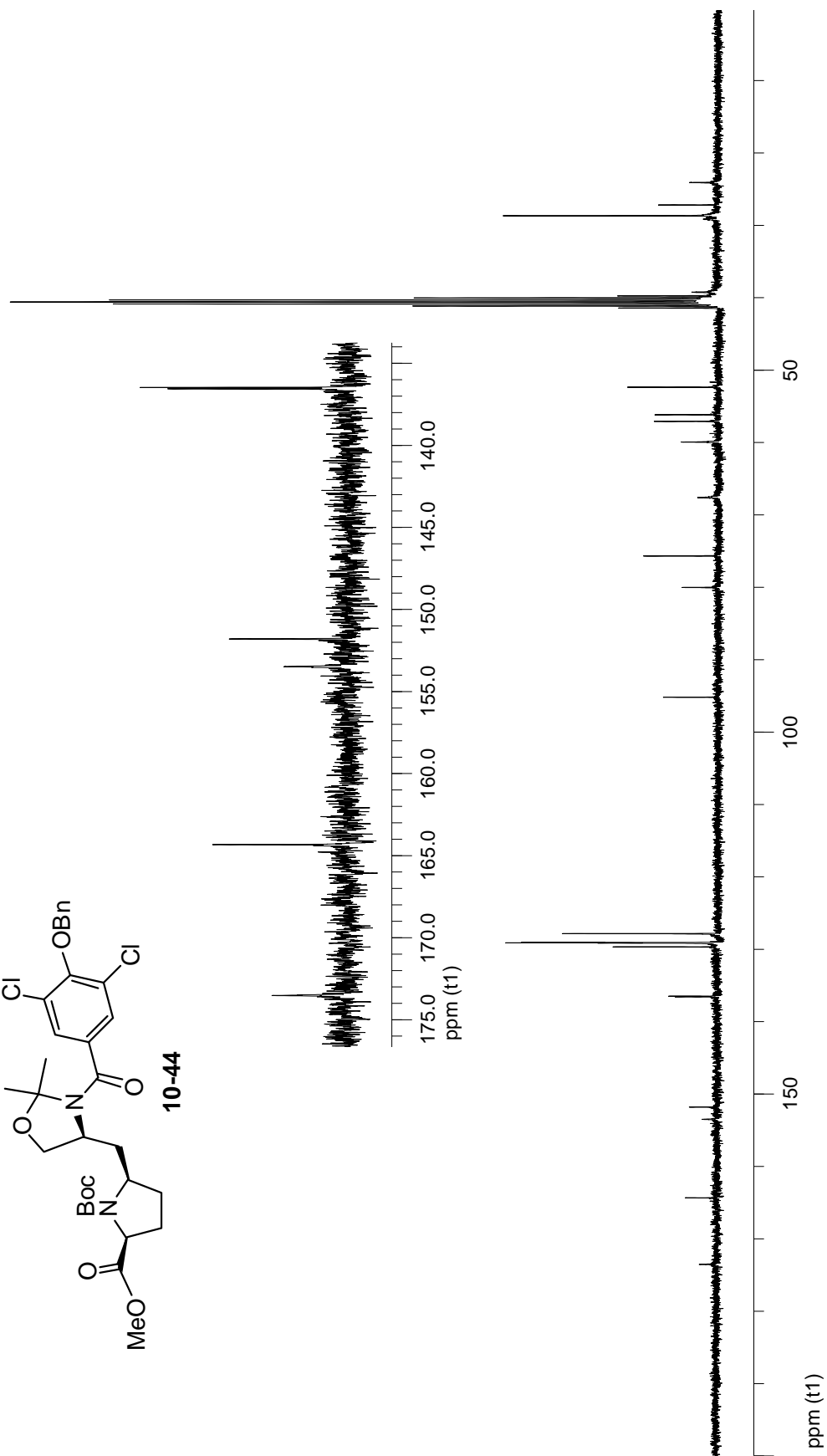
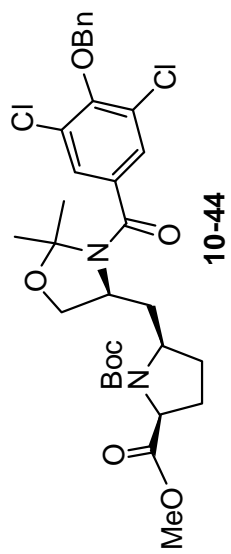
300 MHz $^1\text{H-NMR}$ of compound 9-30 in DMSO-d_6 at 90 $^\circ\text{C}$ 

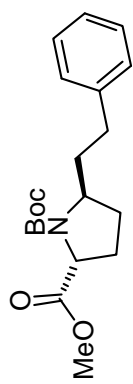
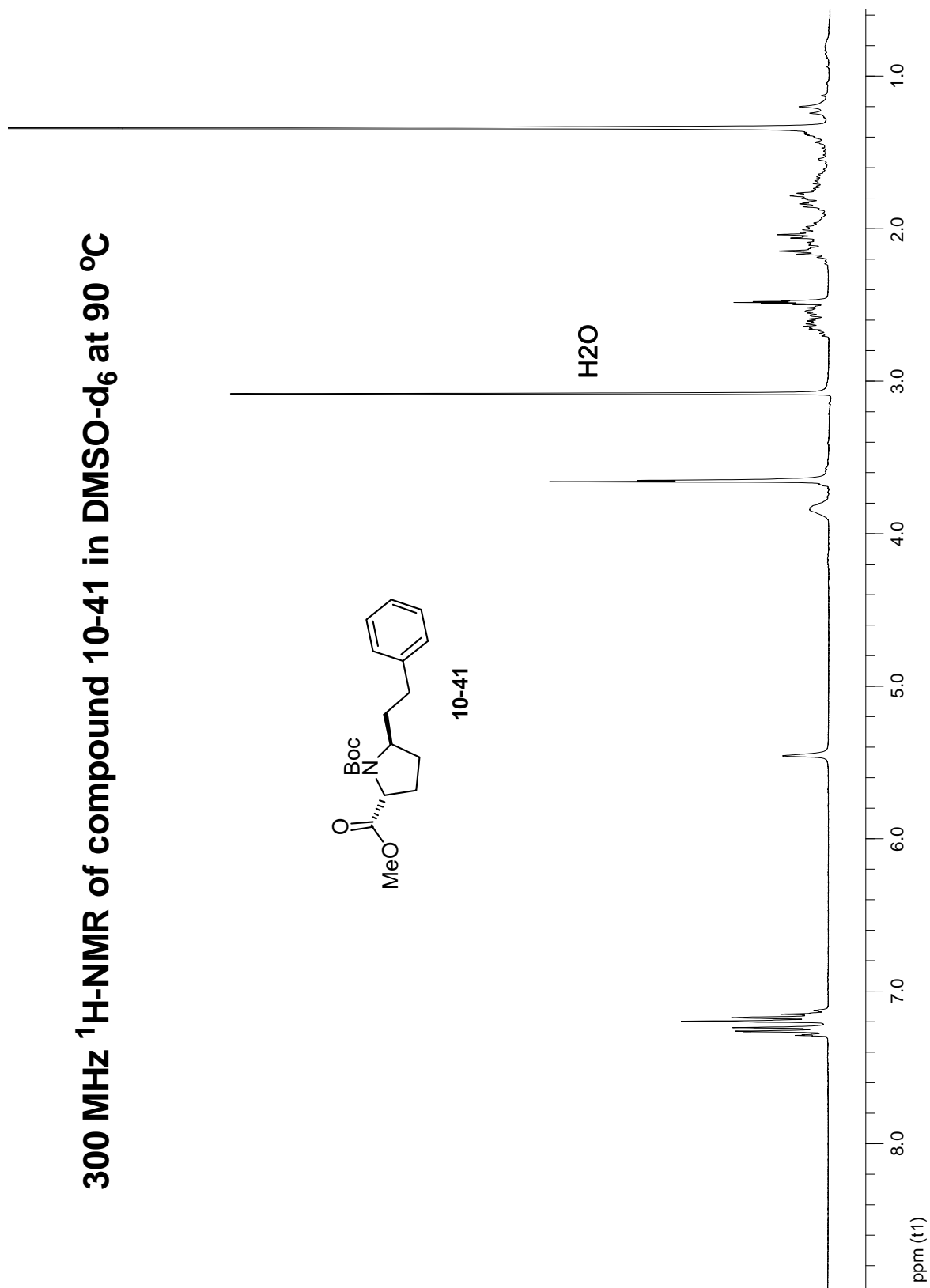
75 MHz ^{13}C -NMR of compound 9-30 in DMSO-d₆ at 90 °C

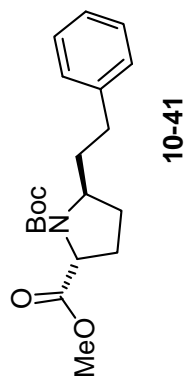
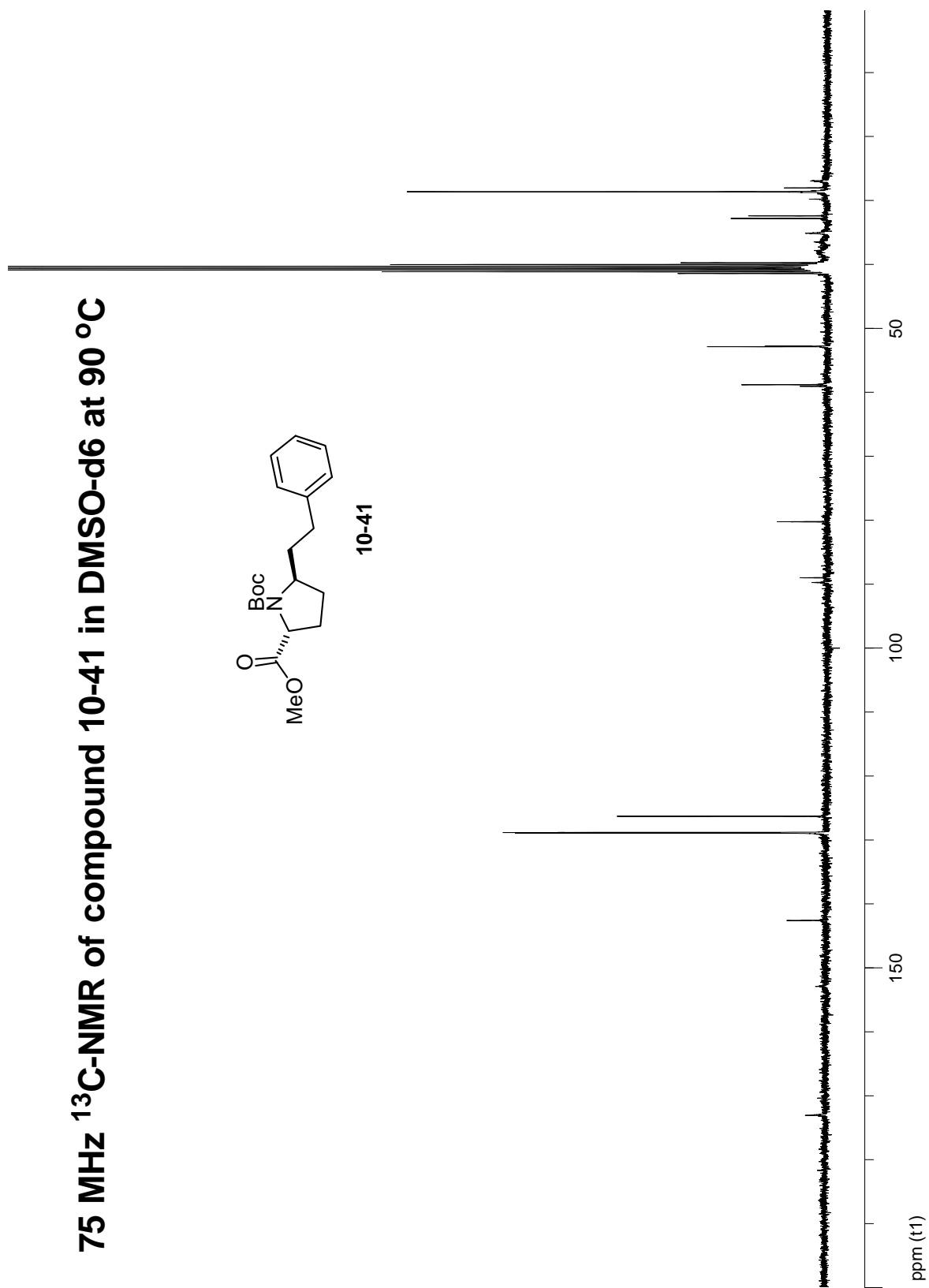
300 MHz $^1\text{H-NMR}$ of crude desulfonation of 9-30 in CDCl_3 at rt

300 MHz $^1\text{H-NMR}$ of 9-30 and its crude desulfonation in CDCl_3 at rt

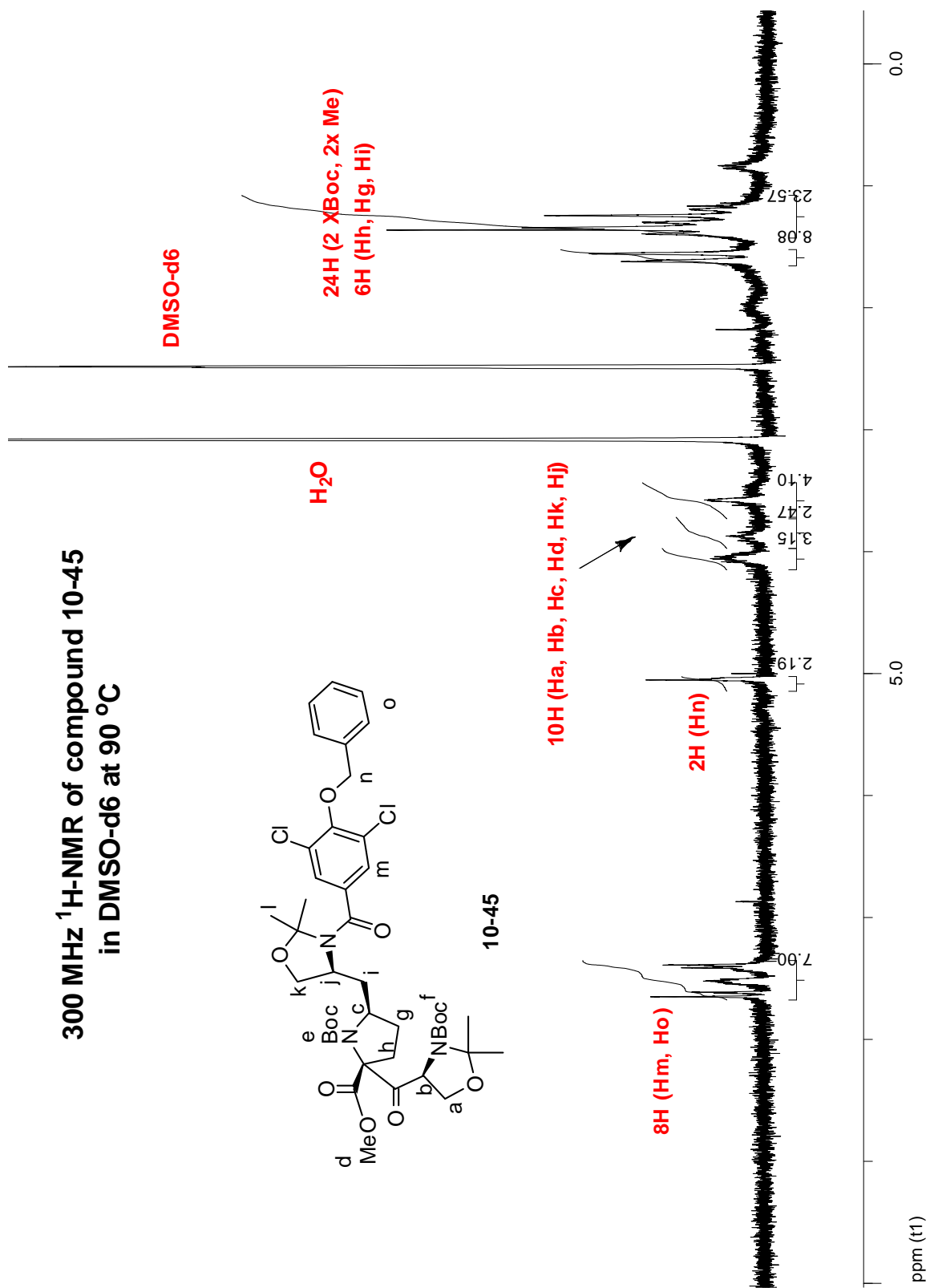
300 MHz $^1\text{H-NMR}$ of compound 10-44 in DMSO-d_6 at 90 $^\circ\text{C}$ 

75 MHz ^{13}C -NMR of compound 10-44 in DMSO-d₆ at 90 °C

300 MHz $^1\text{H-NMR}$ of compound 10-41 in DMSO-d_6 at 90 $^\circ\text{C}$ **10-41**

75 MHz ^{13}C -NMR of compound 10-41 in DMSO-d₆ at 90 °C**10-41**

300 MHz $^1\text{H-NMR}$ of compound 10-45
in DMSO-d6 at 90 °C



Bibliography

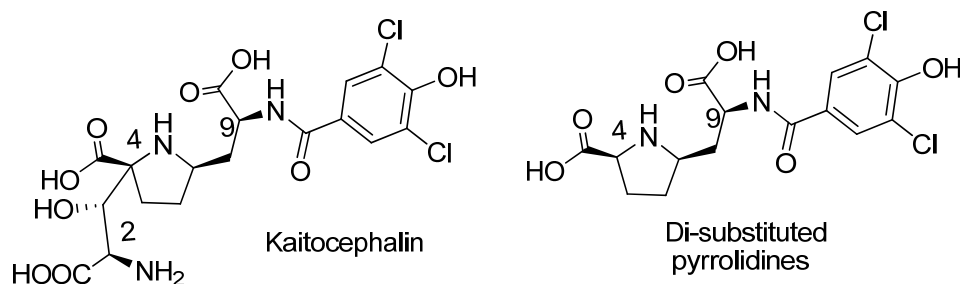
1. (a) Pyne, S. G.; Davis, A. S.; Gates, N. J.; Nicole, J.; Hartley, J. P.; Kindsay, K. B.; Machan, T.; Tang, M. *Synlett* **2004**, 2670. (b) Cheng, Y.; Huang, Z.-T.; Wang, M.-X. *Curr. Org. Chem.* **2004**, 8, 325. (c) Notz, W.; Tanaka, R.; Barbas, C. F., III *Acc. Chem. Res.* **2004**, 37, 580. (d) Felpin, F.-X.; Lebreton, J. *Eur. J. Org. Chem.* **2003**, 3693. (e) Pearson, W. H.; Soy, P. *Synlett* **2003**, 903.
2. (a) *Enantioselective Organocatalysis*; Dalko, P. I., Ed.; Wiley-VCH: Weinheim, Germany, **2007**. (b) *Asymmetric Organocatalysis*; Berkessel, A., Groger, H, Eds.; Wiley-VCH: Weinheim, Germany, **2005**.
3. For some reviews, see: (a) Kanemasa, S. *Synlett* **2002**, 1371. (b) Gothelf, K. V.; Jørgensen, K. A. *Chem. Rev.* **1998**, 98, 863. (c) Pichon, M.; Figadere, B. *Tetrahedron: Asymmetry* **1996**, 7, 927. (d) Grigg, R. *Chem. Soc. Rev.* **1987**, 16, 89. (e) Pearson, W. H.; Stoy, P. *Synlett* **2003**, 903; Grigg, R.; Sridharan, V. In *Advances in Cycloaddition*; Curran, D. P., Ed.; JAI Press: Greenwich, CT, **1993**; Vol. 3, p 161. (f) Kanemasa, S. *Synlett* **2002**, 9, 1371. (g) Padwa, A.; Price, A. T. *J. Org. Chem.* **1998**, 63, 556.
4. Laha, J. *Letters in Organic Chemistry*, **2007**, 4, 550; Gothelf, A.; Gothelf, K.; Hazell, R.; Jørgensen, K. A. *Angew. Chem. Int. Ed.* **2002**, 41, 4236; Dogan, Ö, Koyuncu, H.; Philip Garner, P.; Bulut, A.; Youngs, W. J.; Panzner, M. *Org. Lett.*, **2006**, 8, 4687; Wei Zeng, W.; Zhou, Y. *Org. Lett.* **2005**, 7, 5055; Silvia Cabrera, S.; Arrayás, R.; Juan C. Carretero, J.; *J. Am. Chem. Soc.* **2005**, 127, 16394; Chen, C.; Li, X.; Schreiber S. J. *Am. Chem. Soc.* **2003**, 125, 10174; Garner, P.; Kaniskan, H. Ü. *Tetrahedron Lett* **2005**, 46, 5181; James M. Longmire, J. M.; Wang, B.; Zhang X.; *J. Am. Chem. Soc.* **2002**, 124, 13400; Stohler, R.; Wahl, F.; Pfaltz, A. *Synthesis* **2005**, 1431; Tsuge, O.; Shuji Kanemasa, S.; Yoshioka, M., *J. Org. Chem.* **1988**, 53, 1384; Cooper, D.; Grigg, R.; Hargreaves, S.; Kennewell, P.; Redpath, J. *Tetrahedron*, **1995**, 51, 7791; Barbara Schnell, B.; Bernardinelli, G.; Kündig E.; *Synlett* **1999**, 3, 348; Alemparte, C.; Blay, G.; Jørgensen, K. *Org. Lett.*, **2005**, 7, 4569; Knöpfel, T.; Aschwanden, P.; Takashi Ichikawa, T.; Watanabe, T.; Carreira, E.; *Angew. Chem. Int. Ed.* **2004**, 43, 5971; Garner, P.; Kaniskan, H. Ü.; Hu, J.; Youngs, W. J.; Panzner, M. *Org. Lett.* **2006**, 8, 3647; Dogan, Ö.; Öner, I.; Ülkü, D.; Arici, C. *Tetrahedron: Asymmetry* **2002**, 13, 2099; Grigg, R.; Thornton-peett, M.; Xu, J.; Xu, L. *Tetrahedron*: **1999**, 55, 13841
5. Gao, W.; Zhang, X.; Raghunath, M. *Org. Lett.*, **2005**, 7, 4241
6. (a) Longmire, J. M.; Wang, B.; Zhang, X. *J. Am. Chem. Soc.* **2002**, 124, 13400; (b) Allway, P.; Grigg, R. *Tetrahedron Lett.* **1991**, 32, 5817 (c) Grigg, R. *Tetrahedron: Asymmetry* **1995**, 6, 2475-2486; (d) Chen, C.; Li, S.; Schreiber, S. L. *J. Am. Chem. Soc.* **2003**, 125, 10174.
7. Gothelf, A. S.; Gothelf, K. V.; Hazell, R. G.; Jørgensen, K. A. *Angew. Chem., Int. Ed.* **2002**, 41, 4236-4238.
8. (a) Oderaotoshi, Y.; Cheng, W.; Fujitomi, S.; Kasano, Y.; Minakata, S.; Komatsu, M. *Org. Lett.* **2003**, 5, 5043; Gao, W.; Zhang, X.; Raghunath, M. *Org. Lett.* **2005**, 7, 4241.

- Cabrera, S.; Arraya's, R. G.; Carretero, J. C. *J. Am. Chem. Soc.* **2005**, *127*, 16394. (b)
Cabrera, S.; Arraya's, R. G.; Marti'n-Matute, B.; Cossi'o, F. P.; Carretero, J. C. *Tetrahedron* **2007**, *63*, 6587; Marti'n-Matute, B.; Pereira, S. I.; Pen~a-Cabrera, E.; Adrio, J.; Silva, A. M. S.; Carretero, J. C. *Adv. Synth. Catal.* **2007**, *349*, 1714. Llamas, T.; Arraya's, R. G.; Carretero, J. C. *Org. Lett.* **2006**, *8*, 1795; Llamas, T.; Arraya's, R. G.; Carretero, J. C. *Synthesis* **2007**, 950; Shi, M.; Shi, J.-W. *Tetrahedron: Asymmetry* **2007**, *18*, 645; Yan, X.-X.; Peng, Q.; Zhang, Y.; Zhang, K.; Hong, W.; Hou, X.-L.; Wu, Y.-D. *Angew. Chem., Int. Ed.* **2006**, *45*, 1979.
9. Oderaotshi, Y.; Cheng, W.; Fujitomi, S.; Kasano, Y.; Minakata, S.; Komatsu, M. *Org. Lett.* **2003**, *5*, 5043.
10. Zeng, W.; Zhou, Y. M. *Org. Lett.* **2005**, *7*, 5055.
11. Yan, X.-X.; Peng, Q.; Zhang, Y.; Zhang, K.; Hong, W.; Hou, X.-L.; Wu, Y.-D. *Angew. Chem., Int. Ed.* **2006**, *45*, 1979.
12. Llamas, T.; Arraya's, R. G.; Carretero, J. C. *Org. Lett.* **2006**, *8*, 1795. Llamas, T.; Arraya's, R. G.; Carretero, J. C. *Synthesis* **2007**, 950.
13. Fukuzawa, S.; Oki, H. *Org. Lett.* **2008**, *10*, 1747.
14. Oderaotshi, Y.; Cheng, W.; Fujitomi, S.; Kasano, Y.; Minakata, S.; Komatsu, M. *Org. Lett.* **2003**, *5*, 5043; Gao, W.; Zhang, X.; Raghunath, M. *Org. Lett.* **2005**, *7*, 4241; Cabrera, S.; Arraya's, R. G.; Carretero, J. C. *J. Am. Chem. Soc.* **2005**, *127*, 16394. Cabrera, S.; Arraya's, R. G.; Marti'n-Matute, B.; Cossi'o, F. P.; Carretero, J. C. *Tetrahedron* **2007**, *63*, 6587; Llamas, T.; Arraya's, R. G.; Carretero, J. C. *Org. Lett.* **2006**, *8*, 1795. Llamas, T.; Arraya's, R. G.; Carretero, J. C. *Synthesis* **2007**, 950
15. Shi, M.; Shi, J.-W. *Tetrahedron: Asymmetry* **2007**, *18*, 645.
16. Garner, P.; Kaniskan, H. U. ; Hu, J.; Youngs, W. J.; Panzner, M. *Org. Lett.* **2006**, *8*, 3647.
17. Garner, P.; Kaniskan, H. U.; Hu, J.; Youngs, W. J.; Panzner, M. *Org. Lett.* **2006**, *8*, 3647.
18. Isleyen, A; Gonsky, C.; Ronald, R. C.; Garner, P. *Synthesis* **2009**, 1261.
19. Garner, P.; Dogan, O. ; Youngs, W. J.; Kennedy, V. O.; Protasiewicz, J.; Zaniewski, R. *Tetrahedron* **2001**, *57*, 71.
20. Garner, P.; Kaniskan, H. U.; Hu, J.; Youngs, W. J.; Panzner, M. *Org. Lett.* **2006**, *8*, 3647.
21. Gu, Y.; Xu, Y.; A. Krueger, C.; Madigan, D.; Sham, H. *Tetrahedron Lett.* **2002**, *43*, 955.
22. Belfaitah, A.; Isly, M.; Carboni, B.; *Tetrahedron Lett.* **2004**, *45*, 1969.
23. Garner, P.; Hu, J.; Parks, C.; Youngs, W. J.; Medvetz, D. *Tetrahedron Lett.* **2007**, *48*, 3867.
24. Paintner, F, F.; Gorler, K.; Voelter, W. *Synlett* **2003**, *4*, 522.

Bibliography

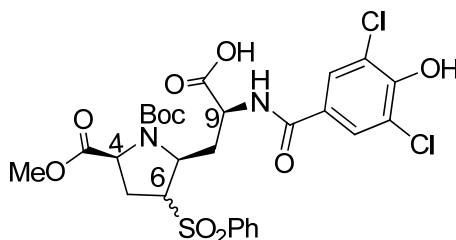
25. Shin-ya, K.; Kim, J.; Furihata, K.; Hayakawa, Y.; Seto, H. *Tetrahedron Lett.* **1997**, *40*, 7079.
26. (a) Brauner-Osborne, H.; Egebjerg, J.; Nielsen, E.; Madsen, U.; Krosgaard-Larsen, P. *J. Med. Chem.* **2000**, *43*, 2609. (b) Kozikowski, A. P. *Drug Design for Neuroscience*; Raven Press Ltd.: New York, **1993**; (c) Lee, J. M.; Zipfel, G. J.; Choi, D. W. *Nature* **1999**, 339 (supp), 47. (d) Parson, C. G.; Danyssz, W.; Quack, G. *Drug News Perspect.* **1998**, *11*, 523, and references therein.
27. Sheardown, M. J.; Nielsen, E. Q.; Hansen, A. J.; Jacobsen, P.; Honoré, T. *Science*, **1990**, *57*, 247.
28. Doble, A. *Pharmacol. Ther.* **1999**, *81*, 163.
29. Kobayashi, H.; Shin-ya, K.; Furihata, K.; Hayakawa, Y.; Seto, H. *Tetrahedron Lett.* **2001**, *42*, 4021.
30. Ohtani, I.; Kusumi, T.; Kashman, Y.; Kakisawa, H. *J. Am. Chem. Soc.* **1991**, *113*, 4092–4096.
31. Ma, D.; Yang, J. *J. Am. Chem. Soc.* **2001**, *123*, 9706.
32. Ma, D.; Yang, J. *J. Am. Chem. Soc.* **2002**, *124*, 6792.
33. Okue, M.; Kobayashi, H.; Shin-ya, K.; Furihata, K.; Hayakawa, Y.; Seto, H.; Watanabe, H.; and Kitahara, T. *Tetrahedron Lett.* **2002**, *43*, 857.
34. The data for synthetic compound 1: ¹H NMR (500 MHz, D₂O) δ 1.57 (m, 1H), 2.05 (m, 1H), 2.09–2.15 (m, 2H), 2.31 (dd, 1H, J = 6.7, 12.2 Hz), 2.36 (m, 1H), 3.61 (m, 1H), 3.81 (d, 1H, J = 4.3 Hz), 4.30 (d, 1H, J = 4.3 Hz), 4.33 (dd, 1H, J = 5.5, 9.2 Hz), 7.62 (s, 2H). [Lit. ¹H NMR (500 MHz, D₂O) δ 1.61 (m), 2.01 (m), 2.06 (m), 2.12 (m), 2.28 (ddd, J = 2.0, 6.0, 14.0 Hz), 2.41 (ddd, J = 6.0, 7.0, 14.5 Hz), 3.70 (m), 4.16 (brs), 4.35 (dd, J = 6.0, 8.0 Hz), 4.41 (brs), 7.62 (s, 2H).
35. Watanabe, H.; Okue, M.; Kobayashi, H.; and Kitahara, T. *Tetrahedron Lett.* **2002**, *43*, 861.
36. Kawasaki, M.; Shinada, T.; Hamada, M.; Ohfuné, Y. *Org. Lett.* **2005**, *7*, 4165–4167.
37. Vaswani, R.; and Richard Chamberlin, A. *J. Org. Chem.*, **2008**, *73*, 1661.
38. (a) Seebach, D.; Boes, M.; Naef, R.; Schweizer, W. B. *J. Am. Chem. Soc.* **1983**, *105*, 5390–5398; (b) Beck, A. K.; Blank, S.; Job, K.; Seebach, D.; Sommerfeld, T. *Org. Synth.* **1993**, *72*, 62–73.
39. Kawasaki, M.; Namba, K.; Tsujishima, H.; Shinada, T.; Ohfuné, Y. *Tetrahedron Lett.* **2003**, *44*, 1235–1238. (a) Moon, S.-H.; Ohfuné, Y. *J. Am. Chem. Soc.* **1994**, *116*, 7405–7406. (b) Namba, K.; Shinada, T.; Teramoto, T.; Ohfuné, Y. *J. Am. Chem. Soc.* **2000**, *122*, 10708–10709. (c) Ohfuné, Y.; Shinada, T. *Bull. Chem. Soc. Jpn.* **2003**, *76*, 1115–1129 and references therein.
40. Garner, P.; Kaniskan, H. U.; Hu, J.; Youngs, W. J.; Panzner, M. *Org. Lett.* **2006**, *8*, 3647; Garner, P.; Hu, J.; Parks, C.; Youngs, W. J.; Medvetz, D. *Tetrahedron Lett.* **2007**, *48*, 3867.

41. Álvarez-Corral, M; Muñoz-Dorado, M.; Rodríguez-García R. *Chem. Rev.* **2008**, *108*, 3174; Stanley, L. M.; and Sibi, M. P. *Chem. Rev.* **2008**, *108*, 2887; Kanemasa, S. *Synlett*, **2002**, *9*, 1371; Llamas, T.; Arraya's, R.; Carretero, J. C. *Org. Lett.*, **2006**, *8*, 1795; Berkom, L.; Kuster, J.; Kalmoua, F.; Gelder, R.; Scheeren, H. W. *Tetrahedron Lett.* **2003**, *44*, 5091–5093.
42. Llamas, T.; Arraya's, R. M.; Carretero J. C.; *Synthesis* **2007**, *6*, 950.
43. Postigo, A.; Kopsov, S.; Ferreri, C.; Chatgililoglu, C. *Org. Lett.*, **2007**, *9*, 5159-5162.
44. Yoshimitsu, T.; Fukumoto, N.; Tanaka, T. *J. Org. Chem.* **2009**, *74*, 696–702.
45. Kang, S.; Kang, S.; Lee, H.; Alan J. Buglass, A. *Chem. Rev.* **2005**, *105*, 4537.
46. Oppolzer, W; Moretti, R.; Thomi, S. *Tetrahedron Lett.*, **1989**, *30* 6009.
47. Botuha, C.; Haddad, M.; Larchevêque, M. *Tetrahedron: Asymmetry* **1998**, *9*, 1929.
48. Qian, K.; Nakagawa-Goto, K.; Yu, D.; Morris-Natschke, S.; Nitz, T.; Kilgore, N.; Allaway, G.; Lee, K. *Bioorganic & Medicinal Chemistry Letters*, **2007**, *17*, 6553.
49. Hayashi, T.; Konishi, M.; Fukushima, M.; Mise, T.; Kagotani, M.; Tajika, M.; Kumada, M. *J. Am. Chem. Soc.*, **1982**, *104*, 181.
50. Ribes, C.; Falomir, E.; Carda, M.; Marco, J. *Org. Chem.* **2008**, *73*, 7779.
51. Porte, A.; van der Donk, W.; Burgess, K. *J. Org. Chem.* **1998**, *63*, 5262.
52. Brown, D.; Cumming, J.; Nash, L. *PCT Int. Appl.* **2005**, 88
53. Paintner, F.; Allmendinger, L.; Bauschke, G.; Klemann, P.; *Org. Lett.* **2005**, *7*, 1423.
54. 10 mg of Na in 50 mL of MeOH.
55. 10 eq of Na, 1 g of Na in 50 mL of MeOH.
56. Rühl, T.; Böttcher, C.; Pumpor, K.; Hennig, L.; Sieler, J.; Burger, K. *Synthesis* **2004**, *18*, 3065.
57. The numbering system used is as the following:



58. Edmonds, D. J.; Johnston, D.; Procter, D. J. *Chem. Rev.* **2004**, *104*, 3371. Kagan, H. B. *Tetrahedron* **2003**, *59*, 10351.
59. Llamas, T.; Arraya's, R.; Carretero, J.; *Org. Lett.*, **2006**, *8*, 1795.
60. The numbering system is as the following:

Bibliography



61. Webster, R; Boing, C; Lautens, M. *J. Am. Chem. Soc.* **2009**, *131*, 444.
62. Chen, Y.; Li, Y. *PCT Int. Appl.* **2008**, *50*, CAN 149:576309.
63. Garner, P.; Kaniskan, H. U^{••}; Hu, J.; Youngs, W. J.; Panzner, M. *Org. Lett.* **2006**, *8*, 3647.
64. Kumaraswamy, G.; Padmaja, M.; Markondaiah, B.; Jena, N; Sridhar, B; Kiran, M. J. *Org. Chem.* **2006**, *71*, 337.
65. Paquette, L.; Kiinzer, H.; Green, K.; v.; Ottorino De Lucchi, O.; Licini, G.; Pasquato, L.; Valle, G. *J. Am. Chem. Soc.* **1986**, *108*, 3453-3460.
66. Clark, R; Pearson, W. *Org. Lett.*, **1999**, *1*(2), 349-351.
67. Berry, M.; Craig, D.; Jones, P., Rowlands, G. *Chem. Commun.*, **1997** 2141.
68. Doi, T.; Iijima, Y.; Takasaki, M.; Takahashi, T.; *J. Org. Chem.* **2007**, *72*, 3667.
69. Das, I.; Pathak, T.; *Org. Lett.*, **2006**, *8*, 1380.
70. Yu, S.; Pu, X.; Cheng, T.; Wang, R.; Ma, D. *Org. Lett.*, **2006**, *8*, 3179.
71. Mauleon, P.; Carretero, J.; *Chem. Commun.*, **2005**, 4961.
72. Prasad, E.; Flowers II, R.; *J. Am. Chem. Soc.* **2005**, *127*, 18093.
73. Zhai, H.; Parvez, M.; Back, T. *J. Org. Chem.*, **2007**, *72*, 3853.
74. Das, I.; Pathak, I. *Org. Lett.* **2006**, *8*, 1303.
75. Woo, L.; Bubert, C.; Sutcliffe, O.; Smith, A.; Chander, S.; Mahon, M.; Purohit, A.; Reed, M.; Potter, B. *J. Med. Chem.* **2007**, *50*, 3540.
76. Corey, E. J.; Gross, A. *Tetrahedron Lett.* **1984**, *25*, 495.
77. Ma, D.; Yang, J. *J. Am. Chem. Soc.* **2001**, *123*, 9706; Okue, M; Kobayashi, H; Shinya, K.; Furihata, K.; Hayakawa, Y.; Seto, H.; Watanabe, H.; and Kitahara, T. *Tetrahedron Lett.* **2002**, *43*, 857; Watanabe, H.; Okue, M.; Kobayashi, H.; and Kitahara, T. *Tetrahedron Lett.* **2002**, *43*, 861; Vaswani, R.; and Richard Chamberlin, A. *J. Org. Chem.*, **2008**, *73*, 1661.
78. Kim, H; Yoo, D; Choi, S.; Chung, Y.; Kim, Y. *Tetrahedron: Asymmetry* **2008**, *19*, 1965.
79. Dodd, J. H.; Hershenson, F. M.; Hicks, J. L.; Butler, D. E.; Lewis, E. P.; Huang, C. C. *J. Labelled Compd. Radiopharm.* **1986**, *23*, 415.
80. Gu, Y.; Xu, Y.; A. Krueger, C.; Madigan, D.; Sham, H. *Tetrahedron Lett.* **2002**, *43*, 955.

Bibliography

81. Lakanen, J.; Pegg, A. E.; Coward, J. K. *J. of Med. Chem.* **1995**, 38(14), 2714-27.
82. Kawasaki, M.; Shinada, T.; Hamada, M.; Ohfuné, Y. *Org. Lett.* **2005**, 7, 4165-4167.
83. Lakanen, J.; Pegg, A. E.; Coward, J. K. *J. of Med. Chem.* **1995**, 38(14), 2714-27.